WILSON & WILSON'S

COMPREHENSIVE ANALYTICAL CHEMISTRY

EDITED BY

D. BARCELÓ

VOLUME 48

PASSIVE SAMPLING TECHNIQUES IN ENVIRONMENTAL MONITORING

EDITED BY

R. GREENWOOD

G. MILLS

B. VRANA

CONTRIBUTORS TO VOLUME 48

Rocío Aguilar-Martínez
Department of Analytical Chemistry, University Complutense of Madrid, Ciudad Universitaria, 28040 Madrid, Spain
Ian Allan
School of Biological Sciences, University of Portsmouth, King Henry I Street, Portsmouth PO1 2DY, UK
David A. Alvarez
US Geological Survey, Columbia Environmental Research Center, 4200 New Haven Road, Columbia, MO 65201, USA
Damia Barceló
Department of Environmental Chemistry, IIQAB-CSIC, Jordi Girona 18-26, 08034 Barcelona, Spain
Michael E. Bartkow
National Research Centre for Environmental Toxicology (ENTOX), University of Queensland, Coopers Plains, Queensland 4108, Australia
Per-Anders Bergqvist
Environmental Chemistry, Department of Chemistry, Umeå University, SE-901 87 Umeå, Sweden
Kees Booij
Royal Netherlands Institute for Sea Research, P.O. Box 59, 1790 AB Texel, The Netherlands
Stephanie Bopp
European Commission – DG Joint Research Centre, Institute for Environment and Sustainability, T.P. 300, via E. Fermi 1, 21020 Ispra, Italy
Yong Chen
Department of Chemistry, University of Waterloo, Waterloo, Ont., Canada N2L 3G1
William Davison
Environmental Science Department, Lancaster University, Lancaster LA1 4YQ, UK
Jacqueline Gehrhardt
Department of Cell Toxicology, UFZ - Helmholtz Centre for Environmental Research, Permoserstr. 15, 04318 Leipzig, Germany
Dominic T. Getting
Environment Agency, Frimley, Camberley, Surrey GU16 7SQ, UK

Rosalinda Gioia
Department of Environmental Science and Centre for Chemicals Management, Lancaster University, Lancaster LA1 4YQ, UK
Jon P. Goddard
Environment Agency, Frimley, Camberley, Surrey GU16 7SQ, UK
Todd Gouin
University of Toronto at Scarborough, Department of Physical and Environmental Sciences, 1265 Military Trail, Toronto, ON, Canada, M1C 1A4
Peter Grathwohl
Center of Applied Geoscience, University of Tübingen, Sigwartstr. 10, 72076 Tübingen, Germany
Anthony Gravell
Environment Agency National Laboratory Service, Furnace, Llanelli, Carms SA15 4EL, UK
Richard Greenwood
School of Biological Sciences, University of Portsmouth, King Henry I Street, Portsmouth PO1 2DY, UK
Tom Harner
Science & Technology Branch, Environment Canada, 4905 Dufferin Street, Toronto, Ont., Canada M3H 5T4
James N. Huckins
USGS Columbia Environmental Research Center (CERC), 4200 New Haven Road, Columbia, MO 65201, USA
Kevin C. Jones
Department of Environmental Science and Centre for Chemicals Management, Lancaster University, Lancaster LA1 4YQ, UK
Tammy Jones-Lepp
US Environmental Protection Agency, Office of Research and Development, 944 E. Harmon, Las Vegas, NV 89119, USA
Graham A. Mills
School of Pharmacy and Biomedical Sciences, University of Portsmouth, White Swan Road, Portsmouth PO1 2DT, UK
Gregory Morrison
Water Environment Transport, Chalmers University of Technology, Gothenburg SE-412 96, Sweden
Jochen F. Müller
National Research Center for Environmental Toxicology, University of Queensland, 39 Kessels Rd, Coopers Plains, Queensland 4108, Australia

Jacek Namieśnik
Department of Analytical Chemistry, Chemical Faculty, Gdańsk University of Technology, 11/12 Narutowicza Str, 80-952 Gdańsk, Poland
Carl E. Orazio
U.S. Geological Survey, Columbia Environmental Research Centre (CERC), 4200 New Haven Rd., Columbia, MO 65201, USA
Gangfeng Ouyang
School of Chemistry and Chemical Engineering, Sun Yat-sen University, Guangzhou 510275, China
Albrecht Paschke
Department of Ecological Chemistry, UFZ – Helmholtz Centre for Environmental Research Leipzing-Halle, Permoserstrasse 15, 04318 Leipzig, Germany
Heidrun Paschke
Department of Groundwater Remediation, UFZ – Helmholtz Centre for Environmental Research Leipzig-Halle, Permoserstrasse 15, 04318 Leipzig, Germany
Janusz Pawliszyn
Department of Chemistry, University of Waterloo, Waterloo, Ont., Canada N2L 3G1
Jimmie D. Petty
US Geological Survey, Columbia Environmental Research Center, 4200 New Haven Road, Columbia, MO 65201, USA
Peter Popp
Department of Analytical Chemistry, UFZ – Helmholtz Centre for Environmental Research Leipzig-Halle, Permoserstrasse 15, 04318 Leipzig, Germany
Philippe Quevauviller
European Commission, DG Environment, Brussels
Kristin Schirmer
Department of Cell Toxicology, UFZ – Helmholtz Centre for Environmental Research, Permoserstr. 15, 04318 Leipzig, Germany
Gerrit Schüürmann
Department of Ecological Chemistry, UFZ – Helmholtz Centre for Environmental Research Leipzig-Halle, Permoserstrasse 15, 04318 Leipzig, Germany
Foppe Smedes
Ministry of Transport, Public Works and Water Management, National Institute for Coastal and Marine Management/RIKZ, P.O. Box 207, 9750 AE Haren, The Netherlands

B. Scott Stephens
Greenhouse and Agriculture Team, Australian Greenhouse Office, Department of Environment and Heritage, GPO Box 787, Canberra 2601 Act, Australia
Frank Stuer-Lauridsen
DH Water & Environment I, Agern Allé 5, DK-2970 Hørsholm, Denmark
Anna-Lena Sunesson
Department of Work and the Physical Environment, National Institute for Working Life, P.O. Box 7654, SE-907 13 Umeå, Sweden (old address)
County Council of Väster botten, 901.89 Umeå, Sweden (present address)
Branislav Vrana
School of Biological Sciences, University of Portsmouth, King Henry I Street, PO1 2DY Portsmouth, UK
Don A. Vroblesky
U.S. Geological Survey, 720 Gracern Road, Suite 129, Columbia, SC, USA
Kent W. Warnken
Environmental Science Department, Lancaster University, Lancaster LA1 4YQ, UK
Hansjörg Weiß
imw—Innovative Measurement Techniques Dr. Weiss, Wilhelmstr. 107, 72074 Tübingen, Germany
Luise Wennrich
Leibniz-Institute of Surface Modification, Permoserstrasse 15, 04318 Leipzig, Germany
Bożena Zabiegała
Department of Analytical Chemistry, Chemical Faculty, Gdańsk University of Technology, 11/12 Narutowicza Str, 80-952 Gdańsk, Poland
Audrone Zaliauskiene
ExposMeter AB, Nygatan 15, SE-702 11 Örebro, Sweden
Hao Zhang
Environmental Science Department, Lancaster University, Lancaster LA1 4YQ, UK

WILSON AND WILSON'S

COMPREHENSIVE ANALYTICAL CHEMISTRY

VOLUMES IN THE SERIES

Vol. 1A	Analytical Processes
	Gas Analysis
	Inorganic Qualitative Analysis
	Organic Qualitative Analysis
	Inorganic Gravimetric Analysis
Vol. 1B	Inorganic Titrimetric Analysis
	Organic Quantitative Analysis
Vol. 1C	Analytical Chemistry of the Elements
Vol. 2A	Electrochemical Analysis
	Electrodeposition
	Potentiometric Titrations
	Conductometric Titrations
	High-Frequency Titrations
Vol. 2B	Liquid Chromatography in Columns
	Gas Chromatography
	Ion Exchangers
	Distillation
Vol. 2C	Paper and Thin Layer Chromatography
	Radiochemical Methods
	Nuclear Magnetic Resonance and Electron Spin Resonance Methods
	X-Ray Spectrometry
Vol. 2D	Coulometric Analysis
Vol. 3	Elemental Analysis with Minute Sample
	Standards and Standardization
	Separation by Liquid Amalgams
	Vacuum Fusion Analysis of Gases in Metals
	Electroanalysis in Molten Salts
Vol. 4	Instrumentation for Spectroscopy
	Atomic Absorption and Fluorescence Spectroscopy
	Diffuse Reflectane Spectroscopy
Vol. 5	Emission Spectroscopy
	Analytical Microwave Spectroscopy
	Analytical Applications of Electron Microscopy
Vol. 6	Analytical Infrared Spectroscopy
Vol. 7	Thermal Methods in Analytical Chemistry
	Substoichiometric Analytical Methods
Vol. 8	Enzyme Electrodes in Analytical Chemistry
	Molecular Fluorescence Spectroscopy
	Photometric Titrations
	Analytical Applications of Interferometry

Volumes in the series

Vol. 9	Ultraviolet Photoelectron and Photoion Spectroscopy Auger Electron Spectroscopy Plasma Excitation in Spectrochemical Analysis
Vol. 10	Organic Spot Tests Analysis The History of Analytical Chemistry
Vol. 11	The Application of Mathematical Statistics in Analytical Chemistry Mass Spectrometry Ion Selective Electrodes
Vol. 12	Thermal Analysis Part A. Simultaneous Thermoanalytical Examination by Means of the Derivatograph Part B. Biochemical and Clinical Application of Thermometric and Thermal Analysis Part C. Emanation Thermal Analysis and other Radiometric Emanation Methods Part D. Thermophysical Properties of Solids Part E. Pulse Method of Measuring Thermophysical Parameters
Vol. 13	Analysis of Complex Hydrocarbons Part A. Separation Methods Part B. Group Analysis and Detailed Analysis
Vol. 14	Ion-Exchangers in Analytical Chemistry
Vol. 15	Methods of Organic Analysis
Vol. 16	Chemical Microscopy Thermomicroscopy of Organic Compounds
Vol. 17	Gas and Liquid Analysers
Vol. 18	Kinetic Methods in Chemical Analysis Application of Computers in Analytical Chemistry
Vol. 19	Analytical Visible and Ultraviolet Spectrometry
Vol. 20	Photometric Methods in Inorganic Trace Analysis
Vol. 21	New Developments in Conductometric and Oscillometric Analysis
Vol. 22	Titrimetric Analysis in Organic Solvents
Vol. 23	Analytical and Biomedical Applications of Ion-Selective Field-Effect Transistors
Vol. 24	Energy Dispersive X-Ray Fluorescence Analysis
Vol. 25	Preconcentration of Trace Elements
Vol. 26	Radionuclide X-Ray Fluorecence Analysis
Vol. 27	Voltammetry
Vol. 28	Analysis of Substances in the Gaseous Phase
Vol. 29	Chemiluminescence Immunoassay
Vol. 30	Spectrochemical Trace Analysis for Metals and Metalloids
Vol. 31	Surfactants in Analytical Chemistry
Vol. 32	Environmental Analytical Chemistry
Vol. 33	Elemental Speciation – New Approaches for Trace Element Analysis
Vol. 34	Discrete Sample Introduction Techniques for Inductively Coupled Plasma Mass Spectrometry
Vol. 35	Modern Fourier Transform Infrared Spectroscopy
Vol. 36	Chemical Test Methods of Analysis
Vol. 37	Sampling and Sample Preparation for Field and Laboratory
Vol. 38	Countercurrent Chromatography: The Support-Free Liquid Stationary Phase

Volumes in the series

Vol. 39	Integrated Analytical Systems
Vol. 40	Analysis and Fate of Surfactants in the Aquatic Environment
Vol. 41	Sample Preparation for Trace Element Analysis
Vol. 42	Non-destructive Microanalysis of Cultural Heritage Materials
Vol. 43	Chromatographic-mass spectrometric food analysis for trace determination of pesticide residues
Vol. 44	Biosensors and Modern Biospecific Analytical Techniques
Vol. 45	Analysis and Detection by Capillary Electrophoresis
Vol. 46	Proteomics and Peptidomics New Technology Platforms Elucidating Biology
Vol. 47	Modern Instrumental Analysis

Contents

Preface

The quality of the environment is recognised as a high priority across the world, and some key anthropogenic pollutants have been recognised as having a global impact. As a result, some international monitoring networks are being established, and progress in this area is particularly well developed for mapping air quality. Where water bodies cross national boundaries, there is a similar need for mapping environmental quality and, for comparable, representative data on pollutant loads and trends. A number of countries have been proactive in setting-up international agreements, and establishing national legislation to improve the quality of the whole environment. In order to succeed, it is necessary to obtain reliable information that is comparable between laboratories, is representative of environmental quality and will underpin risk assessments and decisions on remedial actions. The environmental and economic cost of incorrect responses based on poor information could be high. There is therefore an urgent requirement to develop robust, and cost-effective strategies and technologies to provide the large amount of reliable information needed by legislators, regulators and managers with responsibility for environmental quality. Much emphasis has been placed on the analytical chemical aspects of measuring pollutant levels in discrete samples but less attention has been paid to the underpinning sampling procedures despite the very much larger uncertainties associated with this crucial phase of the monitoring process. Acquisition of representative data is problematic, especially where levels of pollutants (anthropogenic and natural) vary in time and space. It would be expensive and difficult to obtain the extra data needed using only the routine methods (e.g. active air sampling, spot or grab sampling for water and sediments) that are currently employed in monitoring programmes. There is now a range of methods and tools that can provide more representative measurements of the quality of the major divisions (air, water, soil and sediments) of the environment. One promising approach is passive sampling. Passive samplers can be

deployed for extended periods, from days to months, and yield time-weighted average concentrations of pollutants to which they have been exposed. This technology has great potential because of the simplicity of the principles underlying its function, and structure. In contrast to active samplers, passive samplers have no moving parts and do not require a power source for their operation, and are relatively inexpensive. In addition, these devices can be deployed in almost any environmental condition, thus making them ideal for ecological monitoring even in remote areas.

Several types of passive sampler are commercially available and some are under commercial development. The use of passive samplers in monitoring the quality of ambient air, and workplace exposures to potentially harmful compounds, is well recognised and accepted. There are established standards and official methods for the use of these devices, and these form part of legal frameworks. In addition, world-wide monitoring networks have been set up using passive air monitors to follow the movement of persistent anthropogenic organic pollutants across the globe. The application of passive sampling in monitoring water quality is some way behind the situation for air, and the technologies available for monitoring soils and sediments are even further from recognition. Although the technologies are widely available for these matrices, they have still not been adopted in legislation. Water quality legislation is still firmly grounded in the use of infrequent spot or grab or bottle samples to measure levels of pollutants to use in comparisons with environmental quality standards. The appropriateness of this approach is now being questioned as the need for representative data is being recognised. The cost of obtaining representative data using classical methods is high, and this is stimulating an urgent consideration of possible alternative methods.

Some of the prerequisites for the adoption of passive monitoring within legal frameworks are clear demonstrations of the performance and validity of the method, and the development of recognised national and international standards for the technology. Most passive samplers work in a similar manner, and the aims of this book are to provide in a single volume a unifying account of the available technologies, their performance characteristics, and a source of information for practitioners in research, and potential end users. The contributors have provided a thorough account of the state-of-the-art of passive monitoring in air, water, soils and sediments. This book brings together a significant body of work on passive sampling, the performance of the various manifestations of this technology in the field and laboratory

and highlights the underpinning physicochemical models that describe the behaviour of these systems in the various divisions of the environment. All passive samplers behave according to the same physicochemical principles, and the underlying theory unifies this field of study. However, in this book the samplers that function in the main divisions of the environment have been allocated to different sections in order to make the book easier to use when looking for specific types of application.

This text aims to provide a useful source of information that is currently dispersed across a range of journals, patents, conference presentations and technical reports. The target audience includes researchers in environmental monitoring, analytical chemists, environmental toxicologists and those employed in regulatory and enforcement bodies (including national environment agencies, and health and safety bodies), and water companies. It is hoped that it will stimulate further discussions and help in the initiation of new research opportunities, and increase the adoption of these technologies in national and international monitoring programmes.

The editors wish to thank the authors of the chapters for their timely and erudite contributions.

Richard Greenwood
Graham Mills
Branislav Vrana

Series editor's preface

My opening sentence to the preface of a previous and complementary book in the series, volume 37, *Sampling and Sample Preparation Techniques for Field and Laboratory*, edited by J. Pawłiszyn and published in 2002, said: ''Many will agree that sampling and sample preparation are key parts of the analytical process. The reliability of analysis is based on the sampling process, storage and preservation of samples, isolation of the analytes, the clean-up and the final determination. From all these operations, sampling and sample preparation still determine the overall analysis time and are the real bottleneck''.

This sentence is fully applicable to the present book, *Passive Sampling Techniques in Environmental Monitoring*, edited by R. Greenwood, G. Mills and B. Vrana. Experts in the field recognize the great potential of passive samplers versus grab sampling methods. Passive samplers can be deployed for extended periods, from days to months, and yield time-weighted average concentrations of pollutants to which they have been exposed. So, the environmental information obtained is considerably higher than that obtained from conventional grab sampling.

The present volume brings together the theoretical and practical aspects of this area and it is certainly timely since the available data are dispersed across a range of journals, patents, conference presentations and technical reports. The volume is organized into four main sections covering air sampling, water sampling, soil/sediment, biomonitoring and bioassays. The major passive sampling devices used for air and water are described in detail, such as the semi-permeable membrane or solid-phase microextraction devices (SPMD or SPME, respectively). The book also addresses the issues of biomimetic sampling devices and the combination of bioassays with passive samples, a very useful approach to tackle one of the most challenging issues in environmental analysis: the correlation between the observed contamination levels with toxicants, the so-called Toxicity Identification Evaluation (TIE).

Overall, this book is an important problem-solving toolbox in environmental analysis, addressing one of the key parts of the whole analytical protocol: the sampling and sample preparation issue. It can be recommended to experts in the field and also to newcomers, since it has all the ingredients to interest a broad audience of scientists involved in environmental monitoring.

Finally, I would like to thank all the contributors for their time and efforts in preparing this excellent and useful book on passive sampling. My specials thanks are dedicated to the three editors, colleagues from various European Union projects and friends for more than 10 years, who were very open to my suggestion that they would be the most appropriate scientists to edit the present book. Congratulations for compiling this excellent work!

D. Barceló
Department of Environmental Chemistry, IIQAB-CSIC
Barcelona, Spain

Foreword

The development of legislation to protect different environmental compartments, i.e. air, water, sediments and soil, has been very active in both the USA and Europe within the last decade. Now that legislation is entering into force, action programmes are being designed—or are already implemented—which *inter alia* requires a sound evaluation of the chemical and biological quality of environmental media, as well as the identification of possible pollution trends. These programmes cannot be effectively established without representative and reliable monitoring data. In other words, effective monitoring of environmental quality is essential to underpin the legislative frameworks. For example, it is particularly difficult to assess the quality of water bodies where levels of pollutants can fluctuate in time as well as spatially depending on the nature of pressures present. This variability also holds for air, sediments and soil, and it encompasses possible (bio)chemical transformations of metals and organic compounds through different environmental pathways (e.g. volatilisation, changes in speciation, mobilisation, etc.). The successful implementation of strategies to improve the quality of the environment will thus depend on the availability and quality of information needed by managers and decision-makers. In this respect, there is an urgent need for the development and validation of cost-effective technologies and methodologies that could be adopted widely for routine monitoring of key environmental matrices that are covered by the legislation. Spot or grab sampling provides only a snapshot of the situation at the instant of sampling, and fluctuations associated with episodic events could be missed, or conclusions could be drawn on the basis of transitory high levels or absence of pollutants. The cost of incorrect information could be very high and there is therefore a need for improved integrating methodologies that can provide a complimentary approach to existing quality monitoring systems. However, monitoring tools will be useful only if they are

affordable, reliable and produce data that are of comparable quality between times and locations.

The range of promising tools responding to needs for integrated monitoring of various environmental media is expanding, and includes well-tried methods such as passive sampling techniques. Many of these are under development, and have the potential to be included in the set of useful tools in the toolbox available to those responsible for monitoring and improving environmental quality under the various legislative frameworks. This is particularly important in light of large-scale monitoring programmes such as the ones carried out in Europe under different EU-wide legislation, e.g. the Directive on Ambient Air and the related Clean Air for Europe (CAFE) programme, the Water Framework Directive (including water, sediment and biota monitoring), and the forthcoming Soil and Marine Framework Directives (presently under development by the European Commission). In the USA, the Clean Air and Clean Water Acts have similar aims of safeguarding the environment and the health of citizens, and similar requirements for monitoring, and this reflects a worldwide trend towards increasing governmental vigilance. This book, *Passive Sampling Techniques in Environmental Monitoring*, examines the properties of these methods and their applicability and potential contribution in monitoring air, water and sediment/soil for trace metals and organic compounds. Since there are major ongoing developments in this field at European level and in the USA, this book will provide a timely and valuable source of information for those involved in environmental management at all levels. The book is edited by prominent scientists and authored by internationally recognised experts in this very specific analytical sector.

Philippe Quevauviller
European Commission, DG Environment
Brussels

Chapter 1

Theory of solid phase microextraction and its application in passive sampling

Yong Chen and Janusz Pawliszyn

1.1 INTRODUCTION

Solid phase microextraction (SPME) was developed to address the need for rapid sampling/sample preparation, both in the laboratory and on-site (in the field where the investigated system is located) [1]. It presents many advantages over conventional analytical methods by combining sampling, sample preparation, and direct transfer of the analytes into a standard gas chromatograph (GC), thus minimizing analyte losses due to multi-step processes. Since its introduction in the early 1990s [2], SPME has been applied successfully to the sampling and analysis of environmental, food, pharmaceutical, and forensic samples [3]. More recently it has been used in passive sampling of air and water. Figure 1.1 shows the schematic of the first SPME device, which was implemented by incorporating coated fibres into a microsyringe [2]. The metal rod, which serves as the piston in a microsyringe, is replaced with stainless steel microtubing with an inside diameter (i.d.) slightly larger than the outside diameter (o.d.) of the fused silica rod. Typically, the first 5 mm of the coating is removed from a 1.5 cm long fibre, which is then inserted into the microtubing. High temperature epoxy glue is used to mount the fibre permanently. The coated fibre can be moved into and out of a stainless steel needle that serves the purposes of protecting the fibre when not in use and guiding it into the injector. The needle can also serve as a time-weighted average (TWA) passive sampling device in which the coating is kept inside the needle during sampling. This contrasts with conventional SPME, in which the coating is extended outside the needle and exposed directly to target analytes

Comprehensive Analytical Chemistry 48
R. Greenwood, G. Mills and B. Vrana (Editors)
Volume 48 ISSN: 0166-526X DOI: 10.1016/S0166-526X(06)48001-6

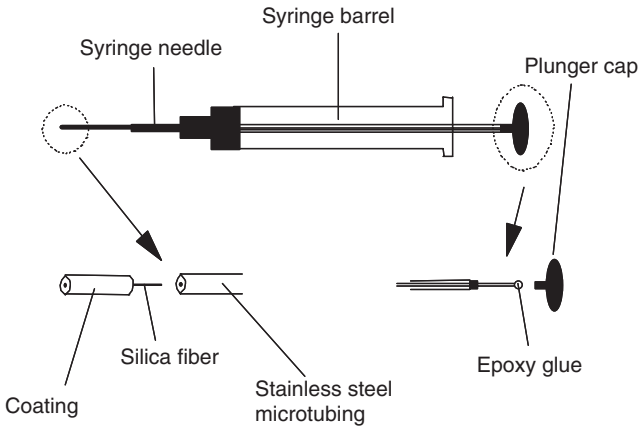

Fig. 1.1. The custom-made SPME device based on the Hamilton 7000 series syringe.

from a number of matrices, and the analytes then reach equilibrium with the coating.

Several different coatings are commercially available, including polydimethylsiloxane (PDMS), polyacrylate (PA), PDMS/divinylbenzene (PDMS/DVB), and Carboxen. The PDMS and PA coatings are a nonporous, amorphous polymeric phase whereas the PDMS/DVB and Carboxen are predominantly porous polymeric phases. Analyte uptake on PDMS and PA is by absorption whereas it is adsorptive for PDMS/DVB and Carboxen.

The use of SPME devices is very simple. When the plunger is depressed, the fibre is extended outside the needle and exposed to the sample matrix. After a certain amount of extraction time, the fibre is withdrawn into the needle. The needle is then introduced into the hot injector of a GC, where the analytes are thermally desorbed from the coating (Fig. 1.2). The analytes then pass into the GC column for separation and quantification.

At this point, it should be emphasized that one of the major advantages of SPME is that all of the sorbed analytes are analysed. In addition, no solvent vehicle is used with SPME; background noise from the solvent is therefore absent. Narrower peak widths are also obtained, thus increasing the overall analytical efficiency. Other quite important advantages are that the SPME sampling system is fully reusable and that when an SPME coating is analysed it is immediately available for a subsequent sampling session (the coating is clean). SPME is also readily amenable to field portability and automation [4].

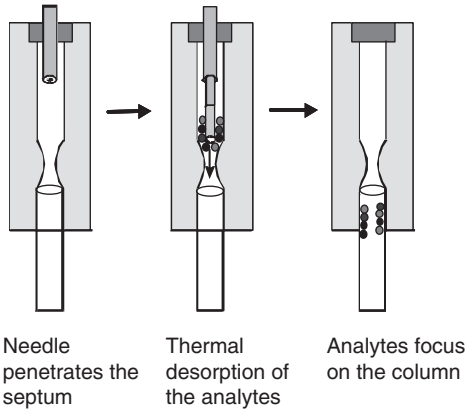

Fig. 1.2. Thermal desorption of the analytes from an SPME fibre in a GC injector.

Simplicity and convenience of operation make SPME an alternative to more established techniques for a number of applications. In some cases, the technique facilitates unique investigations. The most visible advantages of SPME exist at the extremes of sample volumes. Because the setup is small and convenient, coated fibres can be used to extract analytes from very small samples. For example, SPME devices are used to probe for substances emitted by a single flower bulb during its life span [3]. Since SPME does not often extract target analytes exhaustively, its presence in a living system should not result in significant disturbance [5]. In addition, the technique facilitates the measurement of speciation in natural systems, since the presence of a minute fibre, which removes small amounts of analyte, is not likely to disturb the chemical equilibrium in a system. It should be noted, however, that the fraction of analyte extracted increases as the ratio of coating to sample volume increases. Complete extraction can be achieved for small sample volumes when distribution constants are reasonably high. This observation can be important if exhaustive extraction is required. It is very difficult to work with small sample volumes using conventional sample preparation techniques. Also, SPME allows rapid extraction and transfer to an analytical instrument. These features result in an additional advantage when investigating intermediates in a system. Another advantage is that this technique can be used for studies of the distribution of analytes in a complex multiphase system [6], and allows for the speciation of different forms of analytes in a sample [7].

1.2 CALIBRATION IN SOLID PHASE MICROEXTRACTION

In SPME, a small amount of the extracting phase associated with a solid support is placed in contact with the sample matrix for a predetermined time (Fig. 1.3).

To date, there are several approaches to calibration developed for SPME, as shown in Fig. 1.4. Equilibrium extraction is the most

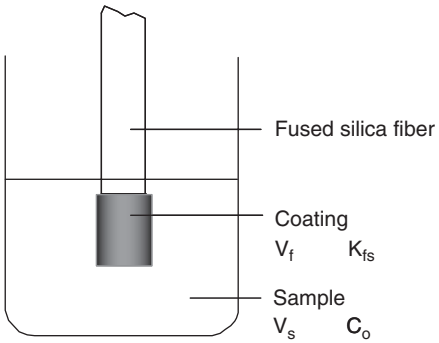

Fig. 1.3. Microextraction with SPME. V_f, volume of fibre coating; K_{fs}, fibre/sample distribution coefficient; V_s, volume of sample; C_0, initial concentration of analyte in the sample.

Calibration in SPME

- Equilibrium extraction : $n = \dfrac{K_{fs}V_fV_S}{K_{fs}V_f+V_s}C_0$
- Exhaustive extraction : $n = V_sC_0$
- Pre-equilibrium extraction : $n = [1-\exp(-at)]\dfrac{K_{fs}V_fV_S}{K_{fs}V_f+V_s}C_0$
- First-order reaction rate constant : $v(n/t) = K^*C_0$
- Diffusion :
  - Grab sampling : various empirical mass transfer correlations
  - Standards in the extraction phase
  - Time–weighted average sampling : Fick's First Law of Diffusion

Fig. 1.4. Various calibration methods in SPME.

frequently used method. When a sample volume is very small, exhaustive extraction might occur in SPME and can be used for calibration. To shorten long equilibrium extraction times, and/or address the displacement effects that occur when porous coatings are used, extraction can be interrupted before equilibrium, and calibration is still feasible if the extraction conditions are kept constant. While performing derivatization on the SPME fibre, when the reaction is the rate-limiting step, the first-order reaction rate constant can be used for calibration. The last approach, the diffusion-based calibration method, is very important for field sampling. This method eliminates the use of conventional calibration curves. Fast on-site analysis and long-term monitoring are thus possible.

1.2.1 Equilibrium extraction

If the extraction time is long enough, a concentration equilibrium is established between the sample matrix and the extraction phase. The equilibrium conditions can be described by Eq. (1.1), according to the law of mass conservation, if only two phases, for example, the sample matrix and the fibre coating, are considered [8]:

$$C_0 V_s = C_s^{\infty} V_s + C_f^{\infty} V_f \tag{1.1}$$

where C_0 is the initial concentration of a given analyte in the sample, V_s is the sample volume, V_f is the fibre coating volume, C_s^{∞} is the equilibrium concentration of analyte in the sample, C_f^{∞} is the equilibrium concentration of analyte in the fibre. The fibre coating/sample matrix distribution coefficient K_{fs} is defined as

$$K_{fs} = \frac{C_f^{\infty}}{C_s^{\infty}} \tag{1.2}$$

Combining Eqs. (1.1) and (1.2), rearrangement results in

$$n = \frac{K_{fs} V_f V_s}{K_{fs} V_f + V_s} C_0 \tag{1.3}$$

where n is the number of moles extracted by the coating. Equation (1.3) indicates that the amount of analyte extracted onto the coating (n) is linearly proportional to the analyte concentration in the sample (C_0), which is the analytical basis for quantification using SPME.

Equation (1.3), which assumes that the sample matrix can be represented as a single homogeneous phase and that no headspace is present in the system, can be modified to account for the existence of

other components in the matrix, by considering the volumes of the individual phases and the appropriate distribution constants [1].

In addition, when the sample volume is very large, i.e. $V_s \gg K_{fs}V_f$, Eq. (1.3) can be simplified to

$$n = K_{fs}V_f C_0 \tag{1.4}$$

which points to the usefulness of the technique for field applications. In this equation, the amount of extracted analyte is independent of the volume of the sample. In practice, there is no need to collect a defined sample prior to analysis, as the fibre can be exposed directly to the ambient air, water, production stream, etc. The amount of extracted analyte will correspond directly to its concentration in the matrix, without being dependent on the sample volume. When the sampling step is eliminated, the whole analytical process can be accelerated, and errors associated with analyte losses through decomposition or adsorption on the sampling container walls will be prevented.

Equation (1.4) also implies another important quantification method for field sampling using SPME. That is, by knowing the distribution coefficient, the concentration of analyte can be determined by the amount of the analyte on the fibre under extraction equilibrium. In other words, quantification is possible without external calibrations. This is a very desirable feature for field analysis, because external calibrations slow down the analytical process, and introduce additional errors. One of the applications of this approach is the determination of parameters like total petroleum hydrocarbons (TPH) in air [9].

1.2.2 Exhaustive extraction

As mentioned above, when the sample volume is very small, and the distribution coefficient is very large, such as sampling of semi-volatile organic compounds (semi-VOCs) in small volumes of a sample matrix, or sampling of VOCs in small volumes of a sample matrix using a cold fibre [10], V_s is far smaller than the product of $K_{fs}V_f$, and Eq. (1.3) can be simplified to

$$n = V_s C_0 \tag{1.5}$$

This implies that all analytes in the sample matrix are extracted onto the fibre coating.

Calibration for exhaustive extraction is very simple, as suggested by Eq. (1.5). However, it is not often used in SPME because of the small volume of the extraction phase. Only when the volume of sample matrix

is small and the distribution coefficient is very large is it possible to extract all analytes onto the fibre coating. Development of the cold fibre device provides an opportunity to perform exhaustive extraction [10,11]. Simultaneous heating of the sample matrix and cooling of the fibre coating significantly increases the distribution coefficient, facilitates release of analytes from the matrix, and accelerates the extraction process. When the volume of the sample is small, exhaustive extraction could occur. Another interesting method to obtain the total amounts of a set of analytes in the sample matrix is multiple SPME [12,13], in which the sample is repeatedly extracted with the fibre. This enables extrapolation to the total amounts of the analytes from just a few extractions, even without exhaustive extraction of the analytes in the sample matrix.

1.2.3 Pre-equilibrium extraction

When an SPME fibre is exposed to the sample matrix, transportation of the analyte from the sample matrix to the fibre coating occurs. The time to reach the extraction equilibrium, ranging from minutes to hours, is dependent on the agitation conditions, the physicochemical properties of analytes and the fibre coating, and the physical dimensions of the sample matrix and the fibre coating. The amount of analyte extracted onto the fibre coating is at a maximum when the equilibrium is reached, thus achieving highest sensitivity. If sensitivity is not a major concern of analysis, shortening the extraction time is desirable. In addition, the equilibrium extraction approach is not practical for solid porous coatings due to the displacement effect at high concentrations. For these circumstances, the extraction is stopped and the fibre is analysed before equilibrium is reached.

The kinetics of absorption of analytes onto a liquid fibre coating is described as follows [14]:

$$n = [1 - \exp(-at)]\frac{K_{\mathrm{fs}}V_{\mathrm{f}}V_{\mathrm{s}}}{K_{\mathrm{fs}}V_{\mathrm{f}} + V_{\mathrm{s}}}C_0 \tag{1.6}$$

where t is the extraction time, and a is a time constant, representing how fast an equilibrium can be reached.

When the extraction time is long, Eq. (1.6) becomes Eq. (1.3), characterizing equilibrium extraction. If the extraction equilibrium is not reached, Eq. (1.6) indicates that there is still a linear relationship between the amount (n) of analyte extracted onto the fibre and the analyte

concentration (C_0) in the sample matrix, if the agitation, the extraction time, and the extraction temperature remain constant.

1.2.4 Calibration based on first-order reaction rate constant

The main challenge in organic analysis is polar compounds. They are difficult to extract from environmental and biological matrices and difficult to separate on the chromatographic column. Derivatization approaches are frequently used to address these challenges. Figure 1.5 summarizes various derivatization techniques that can be implemented in combination with SPME [15]. Some of the techniques, such as direct derivatization in the sample matrix, are analogous to well-established approaches used in solvent extraction. With the direct technique, the derivatizing agent is first added to the sample vial. The derivatives are then extracted by SPME and introduced into the analytical instrument.

Because of the availability of polar coatings, the extraction efficiency for polar underivatized compounds is frequently sufficient to reach the sensitivity required. Occasionally, however, there are problems associated with the separation of these analytes. Good chromatographic performance and detection can be facilitated by in-coating derivatization following extraction. In addition, selective derivatization to analogues containing high detector response groups will result in enhancement of the sensitivity and selectivity of detection. Derivatization in the GC injector is an analogous approach, but it is performed at high injection port temperatures.

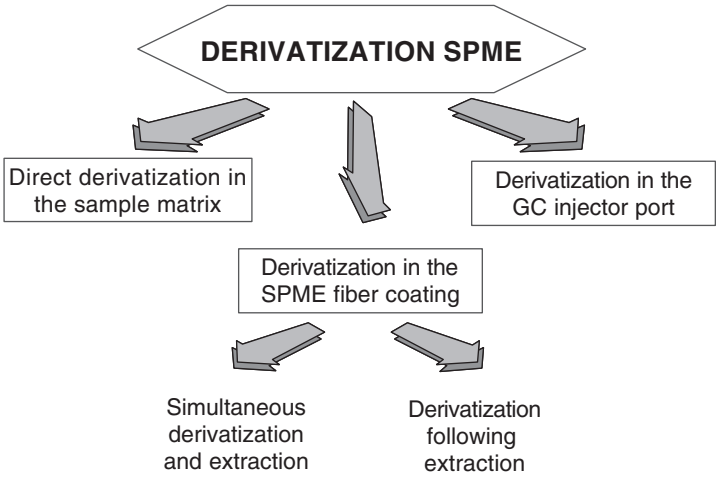

Fig. 1.5. SPME derivatization techniques.

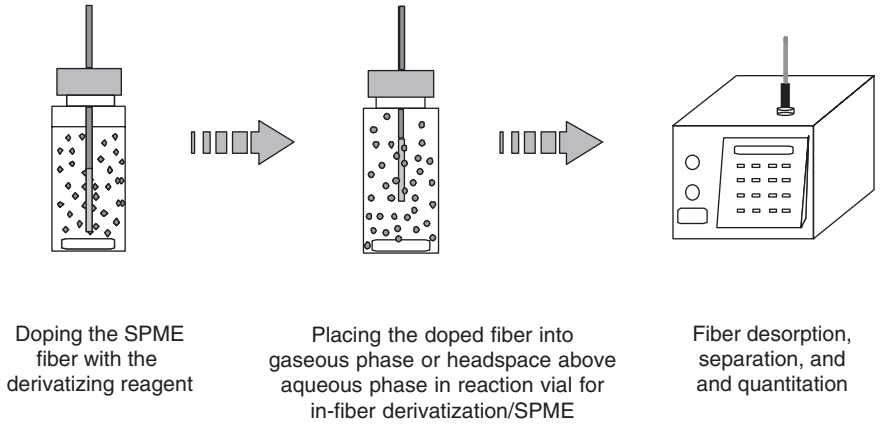

Fig. 1.6. In-coating derivatization technique with fibre doping method.

The most interesting and potentially very useful technique is simultaneous derivatization and extraction, performed directly in the coating. This approach allows for the high efficiencies and can be used in remote field applications. The simplest way to execute the process is to dope the fibre with a derivatization reagent and subsequently expose it to the sample (Fig. 1.6). The analytes are then extracted and simultaneously converted to analogues that possess a high affinity for the coating. This is no longer an equilibrium process, since derivatized analytes are collected in the coating as long as the extraction continues.

It is emphasized that if the sorbent is almost completely coated with a derivatizing reagent before its exposure to the analyte, a reaction between the approaching gaseous analyte and the sorbed derivatizing reagent is more likely to occur. This is especially true for short exposure times. When the reaction is the rate-limiting step, the reaction rate v (weight/time) is proportional to the concentration of gaseous analyte (C_0) and the rate constant of the reaction between the derivatization reagent and the analyte [16]:

$$v\left(\frac{n}{t}\right) = K^* C_0 \tag{1.7}$$

Therefore, quantitative analyses of an unknown analyte concentration (C_0) is possible using an empirically determined constant K^* and Eq. (1.7).

This simple and efficient approach is limited to low-volatility derivatizing reagents. The approach can be made more general by chemically attaching the reagent directly to the coating. The chemically

bound product can then be released from the coating, either by a high temperature in the injector, light illumination, or a change of the applied potential. The feasibility of this approach was recently demonstrated by synthesizing standards bonded to silica gel, and which were then released during heating. This approach allowed for solvent-free calibration of the instrument [17].

In addition to using a chemical reagent, electrons can be supplied to produce redox processes in the coating and convert analytes to more favourable derivatives. In this application, the rod and the polymeric film must have good electrical conductivity. A similar principle has been used to extract amines onto a pencil 'lead' electrode [18]. The use of conductive polymers, such as polypyrrole, will introduce additional selectivity of the electrochemical processes associated with the coating properties [19].

1.2.5 Calibration based on diffusion

1.2.5.1 Diffusion

Diffusion is the random movement of a chemical substance in a material system consisting of two or more components, from an area of higher chemical potential of the diffusing substance in the given phase towards an area of lower chemical potential [20]. Two mathematical methods are often used to formulate the transport by diffusion [21,22]. The first, referred to as a *mass transfer model*, relates the net flux J to the occupation density difference between two adjacent subsystems, A and B:

$$J = -h(C_B - C_A) \tag{1.8}$$

Fluxes J are usually expressed as mass per unit area and per time (ng cm^{-2} s^{-1}), and the concentration C as mass per volume (ng cm^{-3}). Then the constant (mass transfer coefficient h) in the flux expression must have the dimension of a velocity (cm s^{-1}). The second model, the *gradient-flux law*, is considered to be more fundamental. One well-known example of the gradient-flux law is Fick's first law, which relates the diffusive flux of a chemical to its concentration gradient and to the molecular diffusion coefficient:

$$J_z = -D\frac{dC}{dz} \tag{1.9}$$

where D is molecular diffusivity, and dC/dz is the spatial gradient of C along the Z direction. The molecular diffusivity (or molecular diffusion coefficient) D has the dimension (cm^2 s^{-1}), and depends on the

properties of the diffusing chemical as well as on those of the medium through which it moves.

Equation (1.10) is often referred to as Fick's second law of diffusion, and can be readily derived from Fick's first law of diffusion:

$$\frac{\partial C}{\partial t} = D\frac{\partial^2 C}{\partial z^2} \tag{1.10}$$

Fick's second law states that the local concentration change with time, due to a diffusive transport process, is proportional to the second spatial derivative of the concentration. As a special case, consider a linear concentration profile along the z-direction $C(z) = a_0 + a_1 z$. Since the second derivative of $C(z)$ of such a profile is zero, diffusion leaves the concentrations along the z-direction unchanged. In other words, a linear profile is a steady-state solution of Eq. (1.10).

The relationship between the flux of a property and the spatial gradient of a related property called a gradient-flux law is typical for an entire class of physical processes, in which some physical quantity such as mass or energy or momentum or electrical charge is transported from one region of a system to another. For example, heat flows through the bar from the high-temperature reservoir to the low-temperature reservoir. Another example is the transport of the electrical charge through a conductor by the application of an electrical potential difference between the ends of the conductor. Table 1.1 lists some physical processes obeying the gradient-flux law [23].

TABLE 1.1
Physical processes that obey the gradient-flux law

Physical process	Law	Equation	Variables
Molecular diffusion	Fick	$J_z = -D\frac{dC}{dz}$	J: Mass flux C: Concentration D: Diffusion coefficient
Conduction of heat	Fourier	$J_z = -\kappa\frac{dT}{dz}$	J: Heat flux T: Temperature κ: Thermal conductivity
Electric conductivity	Ohm	$J_z = -k\frac{dV}{dz}$	J: Electrical current flux V: Voltage K: Electric conductivity

The similarity of molecular diffusion and conduction of heat and electric conductivity is interesting and important. The former analogue provides the possibility of translation of various empirical correlations established for heat transfer to diffusion mass transfer, especially for the cases of ill-defined diffusion zones, such as the analogue of heat transfer from bulk to a rod, to mass transfer from bulk to a fibre. Conduction of heat has been extensively studied due to industrial demands. The heat transfer literature is immense, far greater than the mass transfer literature. Mass transfer research may thus benefit from the vast resources of heat transfer research.

The latter analogue between molecular diffusion and electric conductivity provides insight for the design of samplers based on diffusion. Figure 1.7 shows the schematic of conduction of electricity through two resistances, r_1 and r_2, and the schematic of mass diffusion through two tubes. The current through the two resistances can be expressed as

$$I = \frac{V_1}{r_1} = \frac{V_2}{r_2} = \frac{V}{r} \tag{1.11}$$

where I is in units of C s^{-1}, $r = r_1 + r_2$, and $r_1 = Z_1/k_1A_1$, $r_2 = Z_2/k_2A_2$, z_1 and z_2 are the length of the resistances of r_1 and r_2, respectively, A_1 and A_2 are the cross-sectional area of the resistances of r_1 and r_2, respectively, k_1 and k_2 are the electric conductivity of the resistances of r_1 and r_2, respectively, V_1 and V_2 are voltage drops along the resistances of r_1 and r_2, respectively, and total voltage $V = V_1 + V_2$.

Analogously, the mass flow diffusion through tube 1 and tube 2 can be expressed as

$$\frac{n}{t} = \frac{\Delta C_1}{Z_1/D_1A_1} = \frac{\Delta C_2}{Z_2/D_2A_2} = \frac{\Delta C}{Z/DA} \tag{1.12}$$

where n/t is mass flow in units of ng s^{-1}, ΔC_1 and ΔC_2 are concentration drops in tube 1 and 2, respectively, z_1 and z_2 are the length of tube 1 and

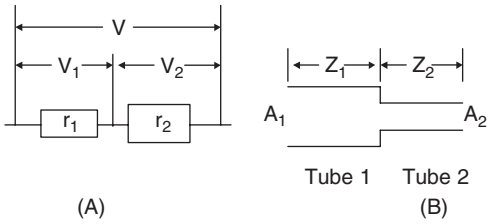

Fig. 1.7. (A) Schematic of conduction of electricity through two resistances r_1 and r_2, and (B) schematic of mass diffusion through two tubes.

tube 2, respectively, and A_1 and A_2 are the cross-sectional area of tube 1 and tube 2, respectively. Correspondingly, Z_1/D_1A_1 and Z_2/D_2A_2 are the mass transfer resistances in tube 1 and tube 2, and the overall mass transfer resistance is

$$\frac{Z}{DA} = \frac{Z_1}{DA_1} + \frac{Z_2}{DA_2} \tag{1.13}$$

Equation (1.13) has some important implications. Firstly, the mass transfer resistance is proportional to the diffusion length, and inversely proportional to the diffusion coefficient and the cross-sectional area of the diffusion zone. Secondly, the mass transfer resistances are additive. Further, when one mass transfer resistance is significantly larger than the other, the contribution from the small resistance is negligible. In other words, the larger resistance controls the overall mass transfer rate. The mass transfer can be predicted by knowing the larger resistance, and the change of the small resistance does not change the overall mass transfer rate significantly. This conclusion is very important for designing passive samplers.

1.2.5.2 Diffusion-based rapid SPME

There is a substantial difference between the performance of liquid and solid coatings. With liquid coatings, the analytes partition into the extraction phase, in which the molecules are solvated by the coating molecules. The diffusion coefficient in the liquid coating enables the molecules to penetrate the entire volume of the coating, within a reasonable extraction time if the coating is thin (see Fig. 1.8a). With solid sorbents (Fig. 1.8b), the coating has a glassy or a well-defined crystalline structure, which, if dense, substantially reduces the diffusion coefficients within the structure. Within the time of an experiment, therefore, sorption occurs only on the pores of a solid phase and after long extraction times, compounds that exhibit a poor affinity towards the phase are frequently displaced by analytes that bind more strongly or those that are present in the sample at high concentrations. This is due to the limited surface area available for adsorption. If this area is substantially occupied, competition occurs and the equilibrium amount extracted can vary with the concentrations of both the target and other analytes [24]. In an extraction with liquid phases, partitioning between the sample matrix and extraction phase occurs. Under these conditions, equilibrium extraction amounts vary only if the bulk coating properties are modified by the extracted components; this occurs only when the amount extracted is a substantial proportion (a few percent) of the

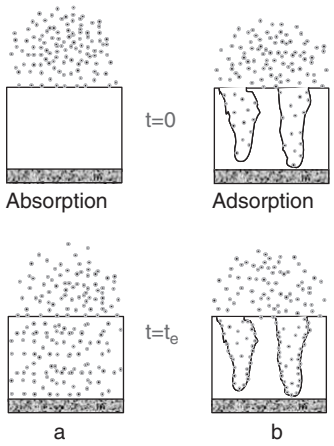

Fig. 1.8. Extraction using absorptive (a) and adsorptive (b) extraction phases immediately after exposure of the phase to the sample ($t = 0$) and after completion of the extraction ($t = t_e$).

extraction phase, resulting in a possible source of nonlinearity. This is rarely observed, because extraction/enrichment techniques are typically used for the analysis of trace contaminants.

One way to overcome this fundamental limitation of porous coatings in a microextraction application is through the use of an extraction time that is much less than the equilibration time. Thus the total amount of analytes accumulated by the porous coating is substantially less than the saturation value. When such experiments are performed, not only is it critical to control the extraction times precisely, but convection conditions must also be controlled because they determine the thickness of the diffusion layer. One way of eliminating the need to compensate for differences in convection is to normalize (use consistent) agitation conditions. The short-term exposure measurement has the advantage that the rate of extraction is defined by the diffusivity of analytes through the boundary layer of the sample matrix, and thus the corresponding diffusion coefficients, rather than by distribution constants. This situation is illustrated in Fig. 1.9 for a cylindrical geometry of the extraction phase dispersed on the supporting rod.

The analyte concentration in the bulk of the matrix can be regarded as constant when a short sampling time is used and there is a constant supply of analyte as a result of convection. The volume of the sample is much greater than the volume of the interface and the extraction process does not affect the bulk sample concentration. In addition, adsorption binding is frequently instantaneous and essentially irreversible.

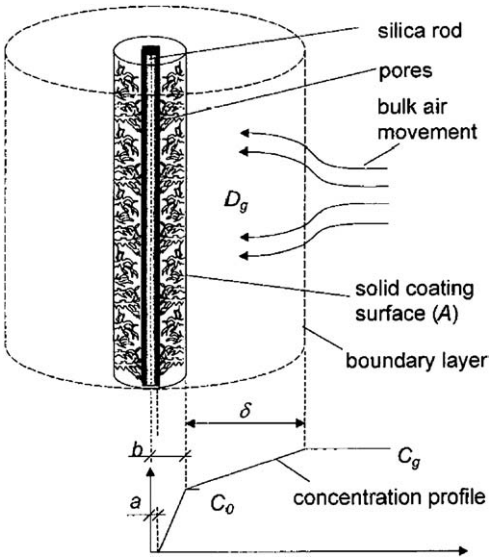

Fig. 1.9. Schematic diagram of the diffusion-based calibration model for cylindrical geometry. The terms are defined in the text.

The solid coating can be treated as a 'perfect sink' for analytes. The analyte concentration on the coating surface is far from saturation and can be assumed to be negligible for short sampling times and relatively low analyte concentrations. The analyte concentration profile can be assumed to be linear from C_g to C_0. The relationship between the mass of the extracted analyte and the sampling time can be described [25] by the following equation:

$$n(t) = \frac{B_3 A D_g}{\delta} \int_0^t C_g(t)dt \tag{1.14}$$

where n is the mass of analyte extracted (ng) in a sampling time (t), D_g is the gas-phase molecular diffusion coefficient, A is the outer surface area of the sorbent, δ is the thickness of the boundary surrounding the extraction phase, B_3 is a geometric factor, and C_g is the analyte concentration in the bulk of the sample. It can be assumed that the analyte concentration is constant for very short sampling times and, therefore, Eq. (1.14) can be further reduced to

$$n(t) = \left(\frac{B_3 D_g A}{\delta}\right) C_g t \tag{1.15}$$

It can be seen from Eq. (1.15) that the mass extracted is proportional to the sampling time, D_g for each analyte, and the bulk sample concentration and inversely proportional to δ. This is consistent with the fact that an analyte with a greater D_g will cross the interface and reach the surface of the coating more quickly. Values of D_g for each analyte can be found in the literature or estimated from physicochemical properties. This relationship enables quantitative analysis. As mentioned above, non-reversible adsorption is assumed. Equation (1.15) can be modified to enable the estimation of the concentration of analyte in the sample for rapid sampling with solid sorbents:

$$C_g = \frac{n\delta}{B_3 D_g A t} \tag{1.16}$$

where the amount of extracted analyte (n) can be estimated from the detector response.

The thickness of the boundary layer (δ) is a function of the sampling conditions. The most important factors affecting δ are the geometric configuration of the extraction phase, the sample velocity, temperature, and D_g for each analyte. The effective thickness of the boundary layer can be estimated for the coated fibre geometry by the use of Eq. (1.17), an empirical equation adapted from the heat transfer theory [1]:

$$\delta = 9.52\left(\frac{b}{Re^{0.62} Sc^{0.38}}\right) \tag{1.17}$$

where Re is the Reynolds number $= 2u_s b/v$, u_s is the linear sample velocity, v is the kinematic viscosity of the matrix, b is the outside radius of the fibre coating, and Sc is the Schmidt number $= v/D_s$. The effective thickness of the boundary layer in Eq. (1.17) is a surrogate (or average) estimate and does not take into account changes of the thickness that can occur when the flow separates, when a wake is formed, or when both occur. Equation (1.17) indicates that the thickness of the boundary layer will decrease with increasing linear sample velocity. Similarly, when the sampling temperature (T_s) increases, the kinematic viscosity decreases. Because the kinematic viscosity term is present in the numerator of Re and in the denominator of Sc, the overall effect on δ is small. Reduction of the boundary layer and an increased rate of mass transfer for the analyte can be achieved in

two ways—by increasing the sample velocity and by increasing the sample temperature. Increasing the temperature will, however, reduce the efficiency of the solid sorbent (reduce K). As a result, the sorbent coating might not be able to adsorb all of the molecules reaching its surface and it might, therefore, stop behaving as a 'perfect sink' for all of the analytes.

Further developments were made to provide accurate estimates of analyte concentrations using diffusion-based rapid SPME, and to this end a new mass transfer model was proposed [26] and this is illustrated in Fig. 1.10. When an SPME fibre is exposed to a fluid sample whose motion is normal to the axis of the fibre, the fluid is brought to rest at the forward stagnation point from which the boundary layer develops with increasing x under the influence of a favourable pressure gradient. At separation point, downstream movement is checked because fluid near the fibre surface lacks sufficient momentum to overcome the pressure gradient. In the meantime, the oncoming fluid also precludes flow back upstream. Boundary layer separation thus occurs, and a wake is formed in the downstream, where flow is highly irregular and can be characterized by vortex formation. Correspondingly, the thickness of the boundary layer (δ) is minimum at the forward stagnation point. It increases with the increase of x and reaches its maximum value right after separation point. In the rear of the fibre where a wake is formed, δ again decreases.

Instead of calculating δ, the average mass transfer coefficient was used to correlate the mass transfer process. According to Hilpert

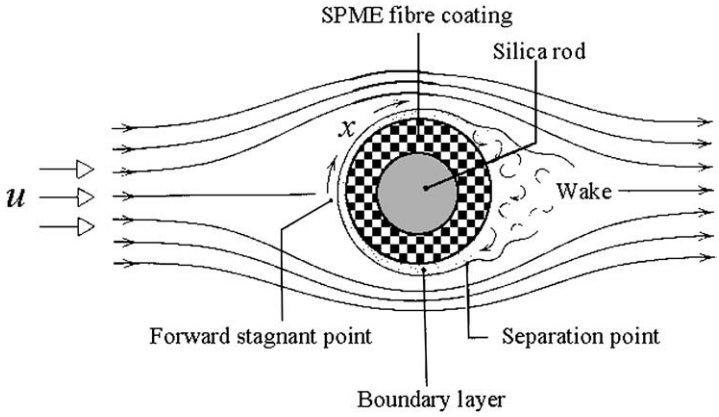

Fig. 1.10. Schematic of rapid extraction with an SPME fibre in cross flow.

[27,28], the average Nusselt number $\overline{Nu}$ can be calculated by the following equation:

$$\overline{Nu} \equiv \frac{\bar{h}d}{D} = ERe^{m}Sc^{1/3} \tag{1.18}$$

where $\bar{h}$ is average mass transfer coefficient, d is the outside diameter of the fibre, D is diffusion coefficient, Re is the Reynolds number, and Sc is the Schmidt number. Constants E and m are dependent on Reynolds number and are listed in Table 1.2 [28].

Once $\bar{h}$ is known, the amount of extracted analytes dn during sampling period dt can be calculated by the following equation:

$$dn = \bar{h}A \int_{0}^{t} (C_{\text{bulk}} - C_{\text{sorbent}})dt \tag{1.19}$$

where A is the surface area of the fibre, C_{bulk} is bulk analyte concentration, and C_{sorbent} is analyte concentration at the interface of the fibre surface and samples of interest. If the sorbent is highly efficient towards target analytes and also is far away from equilibrium, C_{sorbent} is assumed to be zero. Under constant bulk analyte concentration, integration of Eq. (1.19) results in

$$n = \bar{h}AC_{\text{bulk}}t \tag{1.20}$$

Inspection of Eq. (1.20) shows that the product of $\bar{h}A$ has the units of $\text{cm}^3\ \text{s}^{-1}$, which corresponds to the sampling rate, while the product of $\bar{h}C_{\text{bulk}}$ is the mass flux (ng $\text{cm}^{-2}\ \text{s}^{-1}$) towards the fibre.

Rearrangement of Eq. (1.20) results in

$$C_{\text{bulk}} = \frac{n}{\bar{h}At} \tag{1.21}$$

TABLE 1.2
Constants of Eq. (1.18) for the fibre in cross flow

Re	E	m
1–4	0.989	0.330
4–40	0.911	0.385
40–4,000	0.683	0.466
4,000–40,000	0.193	0.618
40,000–250,000	0.027	0.805

Equation (1.21) indicates that the concentration of samples can be determined by the mass uptake n onto an SPME fiber during sampling period t upon $\bar{h}$ is estimated from Eq. (1.18).

The main advantage of these methods is that quantification is diffusion based. In other words, no calibration curves or internal standards are needed. This is a very desirable feature, especially for field sampling. However, quantification requires a constant flow of the sample matrix. The sample velocity must be known and controlled. In cases where the sample velocity is changing, and/or it is difficult, if not impossible, to determine or control, on-site analysis using these methods is challenging.

To calibrate the agitation conditions of the matrix, the use of internal standards is useful (also see the use of performance reference compounds in Chapters 7 and 9). Internal standardization and standard addition are important calibration approaches that are very effective when quantifying target analytes in complex matrices. They compensate for additional capacity or activity of the sample matrix. However, such approaches require delivery of the standard. This is incompatible in some sampling situations, such as with on-site or in vivo investigations. This approach is also not practical for conventional exhaustive extraction techniques, since the extraction parameters are designed to facilitate complete removal of the analytes from the matrix. However, in microextraction a substantial portion of the analytes remains in the matrix during the extraction and after the equilibrium is reached. This suggests that the standard could be added to the investigated system together with the extraction phase. 'Stepwise SPME' was thus developed for field sampling/sample preparation, in which an internal standard was preloaded onto a fibre for calibrating the extraction of hydrocarbons in the field air, and monitoring the loss of extracted analytes during the transportation and storage of samplers [29]. In 'stepwise SPME', a Carboxen fibre, a 'zero sink' for both the internal standard and the target analytes, was used, which minimized the loss of the internal standard during short sampling durations. Therefore, no information about the convection conditions of the sample matrix could be obtained. To calibrate the convection conditions of the sample matrix, desorption of standards from the fibre to the sample matrix is necessary.

Absorption of an analyte onto an SPME liquid coating fibre is theoretically described with the following equation [14]:

$$n = n_0[1 - \exp(-at)] \tag{1.22}$$

where n is the amount of the extracted analyte, and n_0 is the amount of analyte loaded onto a fibre at equilibrium. Equation (1.22) shares the same format as Eq. (1.23) describing desorption of an analyte from an SPME liquid coating fibre [30]:

$$\frac{Q}{q_0} = \exp(-at) \tag{1.23}$$

where q_0 is the initial amount of analyte loaded on the fibre coating, and Q is the amount of analyte remaining on the fibre after exposure to the sample matrix for sampling time t. The constant a in Eqs. (1.22) and (1.23) has the same definition. In other words, the value of constant a should be the same for both the absorption and the desorption of analyte under the same experimental conditions (sample bulk velocity and temperature). This implies the isotropy of the absorption and the desorption of an analyte onto and from an SPME fibre, which can be demonstrated by rearranging Eq. (1.22) (absorption) into

$$\frac{n}{n_0} = 1 - \exp(-at) \tag{1.24}$$

The left side of Eq. (1.23) represents the fraction of the analyte remaining on the fibre after desorption time t, while the left side of Eq. (1.24) represents the fraction of the analyte absorbed on the fibre after absorption time t. When constant a has the same value for the absorption and the desorption, the sum of Q/q_0 (desorption) and n/n_0 (absorption) should be 1 at any desorption/absorption time.

The simultaneous absorption of toluene and desorption of deuterated toluene (d-8) proved the isotropy of the absorption and the desorption of an analyte onto and from an SPME fibre (Fig. 1.11) [30]. An important implication of this is that if the behaviour of either absorption or desorption is known, the behaviour of the other will also be understood. The application of this conclusion is clear. To determine the concentration of an analyte in a sample matrix, a certain amount of isotopically labelled analogue is loaded onto an SPME liquid coating fibre. Then, the fibre is exposed to the sample matrix for a certain time period, during which a part of the isotopically labelled analogue is desorbed from the fibre and a certain amount of the analyte is absorbed onto the fibre. The value n_0 can be obtained using the isotropic relationship ($Q/q_0+n/n_0 = 1$), by knowing the initial amount (q_0) of the isotopically labelled analogue loaded onto the fibre, the amount (Q) of

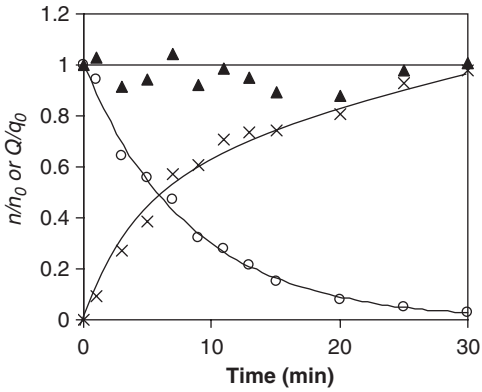

Fig. 1.11. The isotropy of absorption and desorption in SPME. Simultaneous absorption of toluene (×) and desorption of deuterated toluene (d-8) (○) onto and from a 100-μm PDMS fibre into water of 0.25 cm s^{-1} at 25°C. (▲) represents the sum of Q/q_0 and n/n_0.

the isotopically labeled analogue remaining on the fibre, and the amount (n) of analyte absorbed on the fibre after sampling time t. Since n_0 is expressed as $(KV_fV_s/(KV_f+V_s))C_0$, the concentration of the analyte (C_0) can readily be determined.

1.2.5.3 Time-weighted average passive sampling

Consideration of different arrangements of the extraction phase is beneficial. For example, extension of the boundary layer by a protective shield that restricts convection would result in a TWA measurement of the analyte concentration. A variety of diffusive samplers has been developed based on this principle. One system consists of an externally coated fibre with the extraction phase withdrawn into the needle (Fig. 1.12).

When the extraction phase in an SPME device is not exposed directly to the sample, but is contained within a protective tubing (a needle) without any flow of sample through it, diffusive transfer of analytes occurs via the static sample (gas phase or other matrix) trapped in the needle. This geometric arrangement provides the basis of a very simple method, capable of generating a response proportional to the integral of the analyte concentration over time and space (when the needle is moved through space) [31]. Under these conditions, the only mechanism of analyte transport to the extracting phase is diffusion through the matrix contained in the needle.

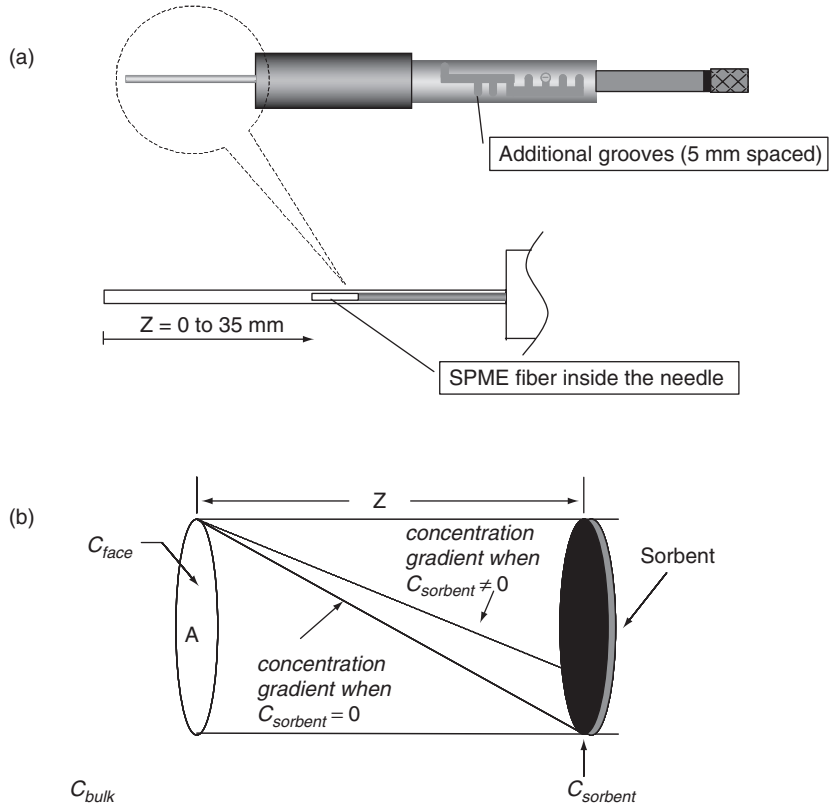

Fig. 1.12. Use of SPME for in-needle time-weighted average sampling. (a) Adaptation of commercial SPME manual extraction holder. (b) Schematic.

The basic process of analyte uptake by the SPME passive sampler can be described by Fick's first law of diffusion (Eq. (1.9)), where J, defined as dn/Adt, describes the flux of the analyte:

$$\frac{dn}{Adt} = -D\frac{dc}{dZ} \tag{1.25}$$

where dn is the amount of the analyte passing through a cross-sectional area A during a sampling period dt. dn is proportional to the linear concentration gradient in the sampler (dc/dZ) and the analyte diffusion coefficient D. For a given sampler, both the cross-sectional area A and the diffusion path length Z are constant. When sampling reaches the steady state:

$$\frac{dc}{dZ} = \frac{\Delta C}{Z} = \frac{C_{\text{sorbent}} - C_{\text{face}}}{Z} \tag{1.26}$$

If the sorbent has a large capacity and strong affinity for target analytes, acting as a zero sink, C_{sorbent}, the concentration of the analyte at the sorbent/gas interface, is negligible. Under these circumstances, Eq. (1.26) reduces to

$$\frac{dc}{dZ} = \frac{-C_{\text{face}}}{Z} \tag{1.27}$$

If C_{face}, the analyte concentration at the opening, is equal to C_{bulk} (the bulk analyte concentration), which is true when the sampled matrix is well agitated, then

$$\frac{dc}{dZ} = \frac{-C_{\text{bulk}}}{Z} \tag{1.28}$$

Substituting Eq. (1.28) into Eq. (1.25), we obtain, after rearrangement:

$$dn = \frac{AD}{Z} C_{\text{bulk}} dt \tag{1.29}$$

Because the dimensions of the expression AD/Z are $\text{cm}^3\ \text{min}^{-1}$, it is defined as a formal sampling rate R:

$$R = \frac{AD}{Z} \tag{1.30}$$

This definition indicates that the sampling rate, R, is proportional to the cross-sectional area, A, and the analyte diffusion coefficient, D, and inversely proportional to the diffusion path length, Z. Combining Eqs. (1.29) and (1.30) yields the following equation:

$$dn = RC_{\text{bulk}} dt \tag{1.31}$$

and after integration of both sides over time, Eq. (1.31) reduces to

$$n = R \int_{t_1}^{t_2} C_{\text{bulk}} dt \tag{1.32}$$

which describes the passive sampler response to a transient concentration of an analyte as a function of time. For a constant analyte concentration, Eq. (1.32) reduces to

$$n = RC_{\text{bulk}} t \tag{1.33}$$

or

$$R = \frac{n}{C_{\text{bulk}} t} \tag{1.34}$$

Equation (1.34) indicates that the rate of uptake of analyte mass by the passive sampler (n/t) is directly proportional to the sampling rate of the sampler (R) and the bulk analyte concentration.

According to Eq. (1.30), the sampling rate, R, will be a constant for a given analyte and passive sampler, and can be determined theoretically. Sometimes, however, it is difficult to determine R theoretically, especially when the diffusion coefficient is not available. In these circumstances Eq. (1.36) indicates that an empirical approach can be used. The mass loading, n, is determined during a sampling period, t, at a constant concentration C_{bulk}. When R is determined, it can be used to quantify the unknown analyte concentrations by use of the following equation:

$$C_{\text{bulk}} = \frac{n}{Rt} \tag{1.35}$$

it is in this way that the SPME device can be used practically as a passive sampler (Fig. 1.13) [32].

It should be emphasized that Eq. (1.35) is valid only when the amount of analyte extracted onto the sorbent is a small fraction (below the RSD of the measurement, typically 5%) of the equilibrium amount for the lowest concentration in the sample. To extend integration times, the coating can be placed further into the needle (larger Z, Fig. 1.14) [32], the opening can be reduced by placing an additional orifice over the needle (smaller A), or a higher capacity sorbent can be used. The first two solutions will result in low measurement sensitivity. Increasing the sorbent capacity is a more attractive proposition. It can be

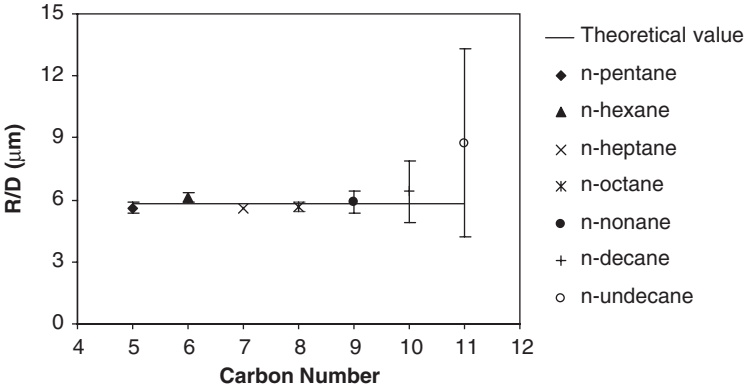

Fig. 1.13. Plot of the dependence of experimental and theoretical R/D on the carbon number of each analyte for the CAR/PDMS-75 fibre ($Z = 1.47$ cm).

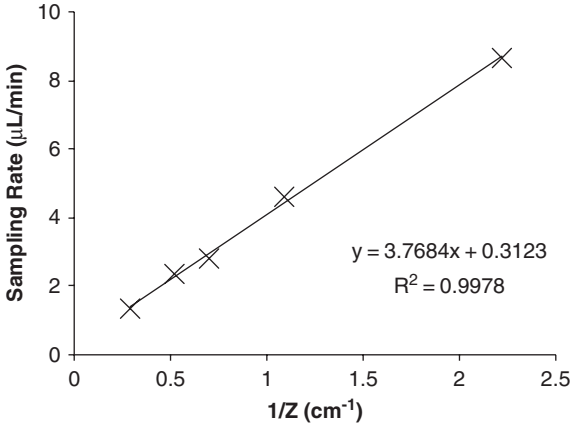

Fig. 1.14. Relationship between sampling rate and diffusion path length.

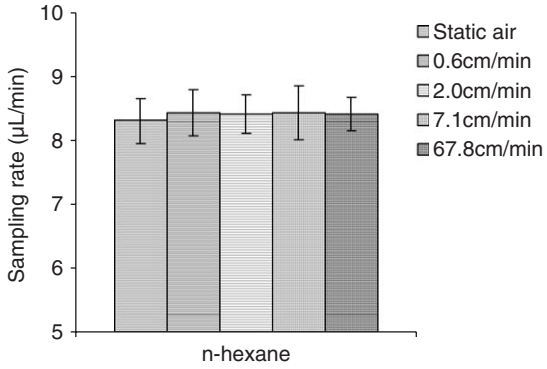

Fig. 1.15. Relationship between face velocity and sampling rate ($Z = 0.45$ cm).

achieved either by increasing the volume of the coating or by changing its affinity for the analyte. Because increasing the coating volume would require an increase in the size of the device, the optimum approach to increasing the integration time is to use sorbents characterized by large distribution constants. If the matrix filling the needle is something other than the sample matrix, an appropriate diffusion coefficient should be used in Eqs. (1.29) and (1.30).

In the system described, the length of the diffusion channel can be adjusted to ensure that mass transfer in the narrow channel of the needle controls overall mass transfer to the extraction phase, irrespective of the convection conditions (Fig. 1.15) [32]. This is a very desirable feature of TWA sampling, because the performance of this device is

independent of the flow conditions in the system investigated. This is difficult to ensure for high surface area membrane permeation-based TWA devices, such as, for example, a passive diffusive badge [33] and semipermeable membrane devices [34]. For analytes characterized by moderate-to-high distribution constants, mass transport is controlled by the diffusive transport in the boundary layer. The performance of these devices therefore depends on the convection conditions in the investigated system [35].

1.2.5.4 SPME field sampler

To facilitate the use of SPME for field sampling, a new field sampler was designed and tested [36]. The structure incorporated a commercialised fibre assembly to make the sampler more universal and to achieve inter-fibre reproducibility. The first requirement for a field sampler is that the fibre needle must be sealed. Teflon is soft and provides good sealing of the needle. It also is an inert material that minimizes adsorption of analytes released from the fibres and contamination from the environment. The Teflon cap should be attached to the SPME field sampler because a loose cap could be easily lost and would be difficult to find in the field. The cap should be easily replaceable if it becomes worn or is heavily contaminated. The next requirement is that the fibre needle must be protected. The needle shields the fibre, allows for introduction of the fibre into an injection port, and provides a diffusion channel for TWA sampling. Fibre protection is necessary throughout the sampling/sample preparation, storage, and transportation period due to the risk of operator injury and fibre damage. The third requirement is that the field sampler should be user-friendly, for acceptance in the industry as an alternative to existing methodologies. For example, a pen-like device would be easy to deploy and transport. The last requirement is that the field sampler should be amenable to automation, which requires that the physical dimensions of the field sampler be small, and the use of the device involves only a few simple movements.

Figure 1.16 shows the schematic of the new field sampler. Parts (a) and (b) are two cylinders with matching male and female screws. The needle of the fibre assembly (c) can be put through the central hole of part (a), whose inner diameter is slightly larger than the outside diameter, until the fibre assembly sits on part (a). Holding part (a) with the fibre assembly on it, the hub of the fibre assembly passes through the central hole of part (b) from the female screw end. Tightly screwing part (a) and (b), the fibre assembly is fixed to the holder. The hub of the

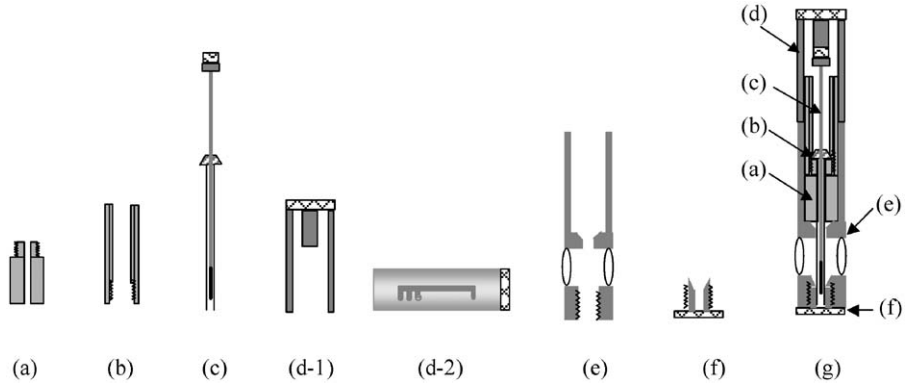

Fig. 1.16. Schematic of the new SPME field sampler (g). Parts (a) and (b) are the fibre holders. Part (c) is a commercialised fibre assembly. Part (d-1) is the cross view of the adjustable cylinder, and Part (d-2) is the side view of the adjustable cylinder. Part (e) is the protecting shield. Part (f) is a replaceable teflon cap.

fibre assembly can be connected to the inner pistol of part (d-1) by a screw. Part (d) can move along the fibre holder consisting of part (a) and (b). By controlling the position of part (d-2), the fibre can be positioned inside the needle for storage, transportation, or TWA sampling, or outside the needle for fibre injection, or rapid/short-term sampling. Part (e) is a protecting shield. The upper part of the protecting shield can hold and move along the fibre holder. Three sideholes are milled in the middle part of the shield, providing windows for analytes to access the fibre coating. The lower part of the shield is used to support the Teflon sealing cap (f). The Teflon cap can be easily replaced in the case of bad sealing or heavy contamination. Configuration (g) is the schematic of the final SPME field sampler that resembles a large pen. The overall dimensions of the field sampler are 137 mm $\times$ 13 mm. The prototype field sampler is larger than the final goal for the design, because this field sampler is designed for commercialised fibres. Since the dimensions of the SPME fibres can be decreased significantly, it can be expected that future SPME field samplers will be smaller.

The field sampler is very easy to use and the operation is schematically shown in Fig. 1.17. Configuration (a) is the field sampler in the status of standby, storage, or transportation. To use the sampler, first, unlock the protecting shield (part (e) in Fig. 1.16), pull the shield outward until it stops and is locked at the sampling position (b). Second, unlock the adjustable cylinder (part (d) in Fig. 1.16), adjust and lock the adjustable cylinder so that the fibre can be positioned further inside the

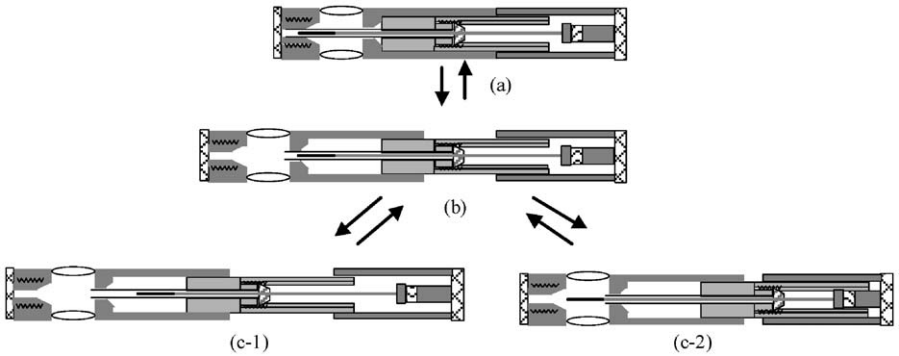

Fig. 1.17. Operation of the new SPME field sampler. (a) The status of standby, storage, or transportation. (b) The status when the protecting shield is pulled outward and locked at the sampling position. (c-1) The model for TWA sampling, and (c-2) the model for grab sampling.

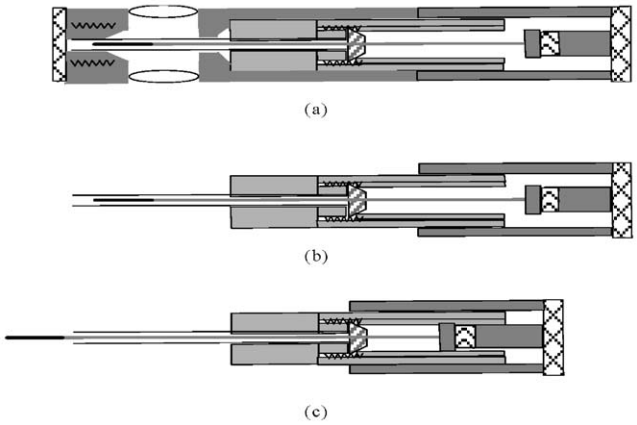

Fig. 1.18. Introduction of the fibre into a GC injector. (a) The fibre is protected, (b) the protecting shield is removed, (c) exposure of the fibre.

needle for TWA sampling (c-1), or exposed completely outside the needle for rapid/short-term sampling (c-2). After sampling, restore and lock the position of the adjustable cylinder (b), then restore and lock the protecting shield (a). When the sampler is transported to a laboratory, unlock the protection shield, and remove it from the sampler (Fig. 1.18b). The needle can then be introduced into the injection port of a GC for desorption (Fig. 1.18c).

The sampler is versatile and user-friendly. The SPME fibre can be positioned precisely inside the needle for TWA sampling, or exposed

completely outside the needle for rapid sampling. The needle is protected within a shield at all times hereby eliminating the risk of operator injury and fibre damage. A replaceable Teflon cap is used to seal the needle to preserve sample integrity. A preliminary field sampling investigation has demonstrated the validity of the new SPME device for field applications.

REFERENCES

1 J. Pawliszyn, *Solid Phase Microextraction — Theory and Practice*, Wiley-VCH, New York, 1997.
2 C.L. Arthur and J. Pawliszyn, *Anal. Chem.*, 62 (1990) 2145.
3 J. Pawliszyn (Ed.), *Applications of Solid Phase Microextraction*, RSC, Cambridge, UK, 1999.
4 L. Müller, T. Górecki and J. Pawlizsyn, *Fresenius J. Anal. Chem.*, 364 (1999) 610.
5 H.L. Lord, R.P. Grant, M. Walles, B. Incledon, B. Fahie and J. Pawliszyn, *Anal. Chem.*, 75 (2003) 5103.
6 J. Poerschmann, F.-D. Kopinke and J. Pawliszyn, *Environ. Sci. Technol.*, 31 (1997) 3629.
7 Z. Mester and J. Pawliszyn, *Rapid Commun. Mass Spectrom.*, 13 (1999) 1999.
8 D. Louch, S. Motlagh and J. Pawliszyn, *Anal. Chem.*, 64 (1992) 1187.
9 P. Martos and J. Pawliszyn, *Anal. Chem.*, 69 (1997) 206.
10 Z. Zhang and J. Pawliszyn, *Anal. Chem.*, 67 (1995) 34.
11 Y. Chen and J. Pawliszyn, *Anal. Chem.*, 78 (2006) 5222.
12 Q. Ezquerro, B. Pons and M.T. Tene, *J. Chromatogr. A*, 999 (2003) 155.
13 C.L. Arthur, L.M. Killam, K.D. Buchholz and J Pawliszyn, *Anal. Chem.*, 64 (1992) 1960.
14 J. Ai, *Anal. Chem.*, 69 (1997) 1230.
15 L. Pan and J. Pawliszyn, *Anal. Chem.*, 69 (1997) 196.
16 P. Martos and J. Pawliszyn, *Anal. Chem.*, 70 (1998) 2311.
17 P. Konieczka, L. Wolska, E. Luboch, J. Namiesnik, A. Przyjazny and J. Biernat, *J. Chromatogr. A*, 742 (1996) 175.
18 E.D. Conte and D.W. Miller, *J. High Resolut. Chromatogr.*, 19 (1996) 294.
19 J. Wu and J. Pawliszyn, *Anal. Chem.*, 73 (2001) 55.
20 T. Erdey-Gruz, *Transport Phenomena in Aqueous Solutions*, Wiley, New York, 1974.
21 E.L. Cussler, *Diffusion: mass transfer in fluid systems*, Cambridge University Press, New York, 1997.
22 R.P. Schwarzenbach, *Environmental Organic Chemistry*, Wiley, New York, 2003.

23 G.W. Castellan, *Physical Chemistry*, 2nd ed, Addison-Wesley Publishing Company, Massachusetts, 1971.
24 D. Ruthven, *Principles of Absorption and Adsorption Processes*, Wiley, New York, 1984.
25 H. Carslaw and J. Jaeger, *Conduction of Heat in Solid*, Clarendon Press, Oxford, 1986.
26 Y. Chen, J. Koziel and J. Pawliszyn, *Anal. Chem.*, 75 (2003) 6485.
27 R. Hilpert, *Forsch. Geb. Ingenieurwes.*, 4 (1933) 215.
28 J.G. Knudsen and D.L. Katz, *Fluid Dynamics and Heat Transfer*, McGraw-Hill, New York, 1958.
29 G. Xiong, Y. Chen and J. Pawliszyn, *J. Chromatogr. A*, 999 (2003) 43.
30 Y. Chen and J. Pawliszyn, *Anal. Chem.*, 76 (2004) 5807.
31 M. Chai and J. Pawliszyn, *Environ. Sci. Technol.*, 29 (1995) 693.
32 Y. Chen and J. Pawliszyn, *Anal. Chem.*, 75 (2003) 2004.
33 J. Koziel, Sampling and sample preparation for Indoor Air Analysis. In: J. Pawliszyn (Ed.), *Sampling and Sampling Preparation for Field and Laboratory*, Elsevier, Amsterdam, 2002.
34 J. Petty, C. Orazio, J. Huckins, R. Gale, J. Lebo, K. Echols and W. Cranor, *J. Chromatogr. A*, 879 (2000) 83.
35 B. Vrana and G. Schüürmann, *Environ. Sci. Technol.*, 36 (2002) 290.
36 Y. Chen and J. Pawliszyn, *Anal. Chem.*, 76 (2004) 6823.

Chapter 2

The use of different designs of passive samplers for air monitoring of persistent organic pollutants

Rosalinda Gioia, Kevin C. Jones and Tom Harner

2.1 INTRODUCTION

The United Nations Economic Commission for Europe (UN-ECE) and Convention on Long-Range Transboundary Air Pollution (CLRTAP) defined criteria that a chemical should meet to be classified as a persistent organic pollutant (POP), namely: (a) possess toxic characteristics, (b) be persistent in the environment, (c) tend to bioaccumulate in higher trophic levels and (d) undergo long-range atmospheric transport (LRAT). Information on the global distribution of POPs has increased during the last 20 years, due to their semi-volatility and persistence in the environment, which allows them to be transported over great distances [1]. As a result, these compounds have also been found in the Arctic and in the Antarctic [2–4] and have been shown to bioaccumulate and biomagnify in arctic animals such as whales, seals and polar bears, as well as humans [5–7]. Although the use of these compounds has been banned or restricted in most western industrialized countries, they remain ubiquitous in the environment.

It is generally assumed that the atmosphere can serve as a pathway for the delivery of these pollutants to water and terrestrial surfaces. Many factors control the air concentration of POPs such as primary and secondary emissions, advection and loss processes. Figure 2.1 is a conceptual diagram of input and loss mechanisms controlling atmospheric concentrations. Primary emissions of POPs to the atmosphere are characterized by leakage of a chemical directly from sources, while secondary sources involve volatilization of a chemical from an environmental reservoir such as soil or water bodies. Environmental loss processes include OH-radical degradation in the atmosphere,

Comprehensive Analytical Chemistry 48
R. Greenwood, G. Mills and B. Vrana (Editors)
Volume 48 ISSN: 0166-526X DOI: 10.1016/S0166-526X(06)48002-8

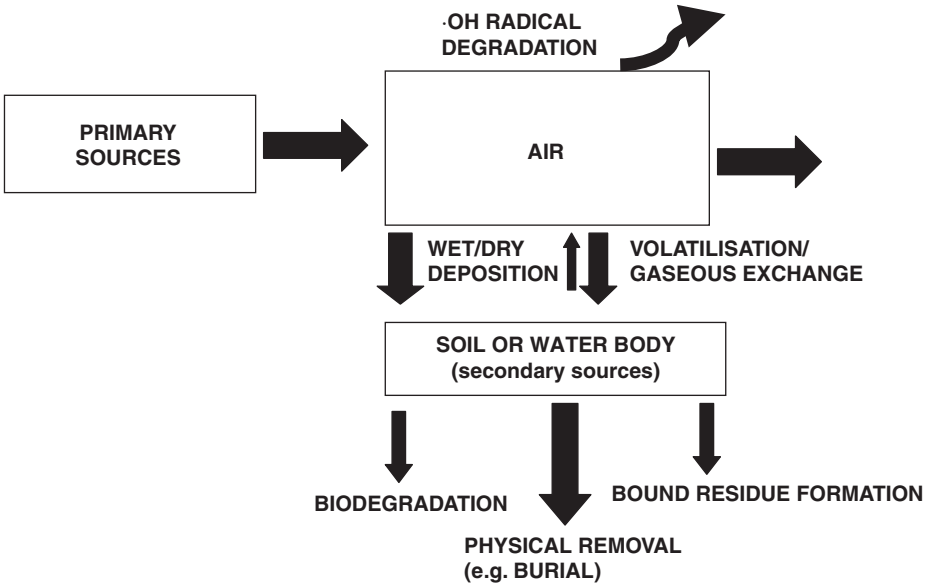

Fig. 2.1. Conceptual diagram of input and loss mechanisms controlling atmospheric concentrations of POPs. (Adapted from Ref. [8].)

biodegradation and physical removal processes (e.g. burial in deep ocean water and soil). These factors vary spatially and temporally due to differences in ambient temperature and physical/chemical properties of the chemicals. There is then the need to monitor the spatial and temporal variation in concentration of POPs in the atmosphere, in order to have a better knowledge of factors that control their concentration, fate and transport in the environment.

Wania and Mackay [9] suggested that POPs can undergo LRAT, with more volatile compounds being transported and condensing in colder regions and less volatile compounds depositing in warmer regions close to sources. The effect of this would be a relative enrichment of the more volatile compounds in colder (polar) areas over time. Criteria for global fractionation behaviour of chemicals depend on various physical–chemical properties and other processes such as deposition, volatilization and seasonal fluctuation. Two major scenarios can lead to global fractionation: (1) after being released by primary sources, a chemical is deposited near or far from sources depending on its physical/chemical properties. In this case, the environmental reservoir will act as a sink and absolute amounts will be expected to decrease with distance from source areas (primary sources dominate); (2) re-emission from

environmental reservoir will control the air concentration. In this case, the fractionation will become more important over time and the concentration of some chemicals can increase with latitude (secondary sources dominate).

Many investigators have found evidence of the global fractionation theory but uncertainties about whether environmental reservoirs act as sources or sinks and whether primary or secondary sources are controlling the levels of POPs in the environment [8–15] remain. Resolving these questions requires simultaneous measurements on global/regional scales over long periods at remote sites far from potential source areas.

2.2 THE CONTEXT: WHY DEVELOP PASSIVE AIR SAMPLING TECHNIQUES FOR POPS?

Conventional high-volume air samplers have been extensively used to measure levels of POPs in the atmosphere. However, they provide only a snapshot of the atmospheric concentrations of pollutants that is limited to the period of sampling. The most common active sampling method uses a pump to draw the air through a sampling module. This usually consists of a glass or quartz fibre filter (GFF and QFF types) where the particle phase is sampled and an adsorbent such as polyurethane foam (PUF) or XAD-resin where vapour species are retained. They are expensive, require the use of electrical power to work and can be operated only by qualified personnel. It is therefore often not cost effective to deploy them in remote areas. Additionally, there are sampling artefacts associated with active air sampling. Gas-phase compounds can adsorb to the filter and be falsely described as particle-bound species. Conversely, particle-bound species can desorb from the filter and be misascribed as vapour-phase components.

Many multinational and national air sampling networks, such as the joint Canada–US, Integrated Atmospheric Deposition Network (IADN), the New Jersey Atmospheric Deposition Network (NJADN) in the US and the Toxic Organic Micro Pollutants Survey (TOMPS) in the UK, operated on behalf of the UK Department of the Environment, Food and Rural Affairs (Defra), have used high-volume air samplers for long-term and time-integrated atmospheric sampling. Data from these networks have been of tremendous value for assessing the behaviour of POPs in the environment. However, these networks use just a few sites because of the aforementioned costs associated with the deployment

and use of active air samplers. For example, in the UK, the TOMPs air monitoring network uses only six sites nationally, while other pollutants, such as NO_x and ozone, are routinely sampled at tens to hundreds of locations nationally/regionally, using much cheaper sampling techniques, such as passive sampling diffusive tubes. There is therefore an incentive to develop more versatile and cost-effective sampling techniques to ensure compliance and provide baseline data.

Some major developments driving the development of passive sampling devices (PAS) for POPs are:

1. Under the Stockholm Convention on POPs, implemented through the United Nations Environment Programme (UNEP), signatory countries must conduct source inventories, identify ongoing sources and provide environmental monitoring evidence that ambient levels of POPs are declining. Developing countries, in particular, require cost-effective and simple approaches that can operate in the absence of power. They may lack the money to buy equipment (both sampling and analytical), to build the laboratories, to train their personnel and to finance the regular monitoring campaigns. PAS offer the opportunity to solve several of these problems, in the short term. Such inexpensive and easy-to-handle devices also offer the option of shipping samplers and filters for exposure, and returning the filters for final analysis. In addition, a 'Global Monitoring Network' is being designed, with the objective of establishing baseline trends at global background sites [16,17].
2. In the European Union, an air quality standard is to be adopted for polycyclic aromatic hydrocarbons (PAHs), because of health concerns over the carcinogenic properties of this compound class [18]. There has been much discussion over the limit to be adopted, because of concerns over exceedances, even in rural areas where coal/wood is used for space heating, or near roadsides. Air quality standards for 1,4-butadiene have also been proposed, and limits for POPs may follow in the future. Once an air quality standard is adopted, there will be the requirement for local authorities to test for compliance.
3. Attention is focused on occupational and indoor exposure to airborne POPs, because this can be an important source to workers and the general public. PAS can be used to sample indoor air unobtrusively, helping to identify sources/hotspots.
4. National environment agencies increasingly need to identify 'less obvious' diffusive sources of POPs, as they seek to reduce

emissions further, now that many primary sources have been/are becoming better controlled. PAS can be used to conduct 'screening/reconnaissance surveys', and are sensitive to site-/source-specific compound fingerprinting. They can therefore be used to help identify sources, and be used to help direct/target cost-effective active air sampling campaigns.

5. There is considerable interest in mapping the ambient distribution of POPs, to support national/international air monitoring networks and to yield input data for regional distribution models. Studies have been conducted to demonstrate the feasibility of such 'national' or 'continental scale' measurement/modelling programmes, by preparing and supplying PAS to be deployed simultaneously across large areas—even at the continental and global scale [19–21]. The samplers are then 'harvested', sealed and returned to the laboratory for analysis, data interpretation and modelling.
6. Besides their obvious usefulness for monitoring, mapping and source identification, PAS can also serve as tools in scientific investigations, by, for example, recording changes in atmospheric POP concentration and composition along environmental gradients (e.g. urban–rural; latitudinal; altitudinal; chiral signatures).
7. PAS techniques are particularly suited to complement and serve in the evaluation of compartmental multimedia fate and transport models, such as those exemplified by the fugacity approach [22]. Like these models, PAS are specifically designed, and therefore most appropriate, for persistent organic chemicals [23], and tend to provide information on the long-term average conditions in the atmosphere and ignore variability on a shorter timescale. Passive samplers have not yet reached a stage of maturity, which would allow the measurement of volumetric air concentrations with an accuracy approaching that of active samplers. The progress towards quantitative calibration notwithstanding, the strength of PAS lies in their ability to provide compositional information, such as parent/metabolite ratios, chiral signatures [20,21] and congener compositions of complex mixtures, such as the PCBs [24]. As long as the chemicals being compared are not approaching equilibrium between sampler material and atmospheric gas phase, even changes in PAS uptake kinetics with wind speed—as has been observed for some sampler designs—will not affect the relative abundance of isomers, enantiomers and congeners. Incidentally, multimedia fate and transport models are also much better suited

to predict compositional and relative information than absolute concentrations, because the latter depend on knowledge of the absolute emission rate, which for POPs is hardly ever known with high precision and accuracy [23].

2.3 WHAT APPROACHES CAN BE USED?

As just indicated, there are considerable incentives to develop passive air sampling techniques. These should be simple to use, cheap, versatile and capable of being deployed in many locations concurrently. Passive samplers can be designed and calibrated, to allow reliable estimates of air concentrations to be made, or to allow semiquantitative comparisons of the levels and patterns of POPs. Several designs are possible and, indeed, desirable. For example, it would be useful to have samplers to integrate ambient concentrations over timescales as short as hours/days or as long as weeks/months/years. The shorter timescales facilitate studies of contaminant dispersal, fluxes and transport processes and can provide data for dispersion/transport modelling. Longer timescales would allow source/sink regions to be identified and underlying trends in ambient levels to be investigated. Workers in the field have therefore been involved in development/deployment of a 'suite' of passive sampling designs and tools. The type, design and deployment can be varied.

Vegetation and leaves of plants such as pine needles have been used in the past to determine the spatial distribution of POPs in the atmosphere [25,26]. The green parts of higher plants are covered by a hydrophobic epicuticular wax that sorbs hydrophobic compounds, such as POPs, from the surrounding air. However, there are many problems associated with the use of vegetation as passive samplers, namely: (a) the same species of plant needs to be used during a study, which becomes very difficult in latitudinal studies where species can vary spatially. Not all species of plants have the same capacity to sample POPs, so it becomes challenging to find a suitable species at every location in studies at the national or continental scale. Further, plants grow over time and their capacity and ability to sample POPs can change even for short-term studies. Vegetation can act as a sink for POPs, but under certain atmospheric conditions, might shift over to a net source for re-emission of POPs into the atmosphere. The knowledge of the air/vegetation equilibrium is essential in order to understand this process.

The lack of standardization of vegetation as a passive sampler has led efforts to develop a more reproducible and cost-effective passive

sampling technique. Much effort has been made to improve existing technologies and design new procedures for passive sampling in the last few years. These designs, such as semipermeable membrane devices (SPMDs), PUF, XAD-2 resin and polymer-coated glass samplers (POGs) have been applied to long-term and short-term studies in several parts of the world to monitor the global fractionation and LRAT of POPs in the atmosphere. Different passive sampling technologies have been tested, calibrated and improved, depending on the analytes of interest and the length of the studies.

Kinetic uptake by passive samplers has been described in Chapter 6. In brief, when an analyte comes in contact with the passive sampler gas-phase compounds partition into the sampling medium during an uptake phase and, if the exposure time is long enough, approach equilibrium, which is in turn a function of temperature. Uptake of POPs in the linear region has been shown to be air-side controlled and thus a function of the air-side mass transfer coefficient, k_A [27]. Calibration tests are required to determine the sampling rate (R_S, volume of air sampled per unit time) during the linear uptake. The sampling rate (R_S) can be calculated as follows:

$$R_S = \frac{U}{C_{air}} \tag{2.1}$$

where R_S is the sampling rate, U is the slope of the plot of mass of analyte sampled N_{PAS} against time and C_{air} is the atmospheric concentration (C_{air}, mass per unite volume) during the calibration period and it should remain constant. During deployment time t of PAS, the mass (N_{PAS}) sequestered by PAS can be measured and the air concentration will be estimated as follows:

$$C_{air} = \frac{N_{PAS}}{(R_S \times t)} \tag{2.2}$$

When uptake has departed from the linear region and compounds are approaching equilibrium, Eq. (2.2) can lead to an underestimation of the air concentration. Therefore, in order to correct the uptake for nonlinearity the following model is used:

$$C_{air} = \frac{C_{PAS}}{K_{PAS-A}(1 - e^{-kt})} \tag{2.3}$$

where k is the dissipation rate constant that can be calculated from the sampling rate R_S and K_{PAS-A}. K_{PAS-A} is the PAS-air partition

coefficient, but measured values for K_{PAS-A} are often not available. It has been shown that K_{PAS-A} for many types of sampling devices is proportional to the *n*-octanol-air partition coefficient, K_{oa} [27,28]. Therefore it seems reasonable to relate K_{PAS-A} to K_{oa}.

The linear uptake sampling approach requires that the R_S values are identical at different sites. However, R_S values are also affected by environmental factors, principally wind speed. Ockenden *et al*. [24] found that values for R_S were greater in winter than in summer, after using SPMDs deployed in Stevenson screen boxes. This could have been the result of the decreased temperature, which increases the analyte affinity for lipid rather than the air or the increased wind speed in winter. The use of the chamber to buffer the flow of air and protect them from photodegradation has been shown to normalise uptake rates for PAS deployed at different locations. Additionally, isotopically labeled (i.e. non-native) permeation/performance reference compounds (PRCs) or more properly called depuration compounds (DCs) can be added to the PAS, so that loss (itself a function of wind speed) can be measured and used as a correction factor (also see Chapter 6).

2.4 THE CHOICE OF SAMPLER DESIGNS: FEATURES, ADVANTAGES AND POTENTIAL PROBLEMS

Passive air samplers can collect airborne species by gaseous diffusion, sorption and permeation. The capacity and time to reach equilibrium can be varied by the choice of sampler type, storage medium and size. The total capacity of the sampler at equilibrium also differs between compounds; generally, lighter POPs with low K_{oa} are expected to reach equilibrium faster, while heavier POPs with high K_{oa} are expected to be sampled during linear uptake. High/medium capacity PAS can be used for long-term studies (month/years) because the time to reach equilibrium will be longer, while low capacity PAS can be utilized for short-term studies (days). Sampling can therefore be conducted in the *kinetic* or *equilibrium* sampling mode, and through knowledge of the uptake rates and equilibrium partition coefficients (and their temperature correction factors, and the ambient conditions) air concentrations can be derived/estimated from the measured mass of a given POP on the PAS. A list of passive sampling devices with the description of their use, advantages and disadvantages is shown in Table 2.1.

Many POPs are found predominantly in the gas phase—in which case the general principles described above apply. However, some POPs

TABLE 2.1

Summary of applications, advantages and disadvantages of air sampling methodologies

Sampler type	Applications	Advantages	Disadvantages	Key references
POG	Short-term kinetic sampling (days/weeks) or equilibrium sampling	Low capacity, flexible, simple and fast to prepare; simple clean-up methodology; ability to manipulate equilibrium partitioning by varying the film thickness of EVA	Environmental factors not well understood, e.g. wind speed and temperature	[33–35]
PUF disk	Short–long term integrative kinetic sampling (weeks–months)	Medium–large capacity, cheap and easy to deploy, high spatial resolution and simple analytical clean-ups. Potential to use DCs to achieve site-specific sampling rates	Method not fully evaluated. Calibration studies for all compounds still needed to better understand environmental factors	[27,44]
SPMD	Long-term integrative kinetic sampling (weeks–years)	Large capacity, well-understood sampler; high spatial resolution, PRCs can correct for different sampling rates between sites	Complicated analytical clean-up, membrane and lipid may deteriorate over time following long exposure, affecting sampling rate	[36,39,43]
XAD-2 resin	Long-term integrative kinetic sampling (weeks–years)	Very large capacity; operates in the linear uptake phase, controlled by molecular diffusion and independent from wind velocity. Applicable to low to high volatility POPs	Field calibration studies are needed in order to understand which environmental factors have influence on the sampling rate. Potential XAD handling problems and contamination of blanks	[40]

are almost exclusively present on aerosols at ambient temperatures; this is a potential confounding factor since ultrafine particles (<100 nm) move through the atmosphere much like gases, and adhere to and become trapped by the sampler. It is not clear whether passive samplers are able to sample quantitatively the atmospheric particle phase and to what extent. Although several studies suggest that PAS

may be able to trap the particle phase of the atmosphere, the process leading to particle sampling is not well understood and further work is needed to allow detection of particle-associated species [24,29–31].

2.4.1 Low-capacity sampling: polymer-coated glass

POGs consist of a thin film of ethylene vinyl acetate (EVA, Elvax 40 W, Du Pont, Canada) coated onto the inside and outside surfaces of a hollow glass cylinder. They can be simply prepared in the laboratory by dissolving 4–8 g of EVA pellets in 200–400 mL of dichloromethane. Glass cylinders are then dipped into the coating solution. Once removed, dichloromethane evaporates and a microlayer of EVA is left on the glass surface. Designs typically have a surface area between 280 and 300 cm^2. The uptake of POPs is based on absorption of the compound into the polymeric phase, which in this case is EVA. These samplers therefore have a large surface area to mass ratio. Harner *et al*. [33] reported a mass of 0.0015–0.0033 g of EVA and a surface area of about 300 cm^2.

There has been an increasing need to develop a passive air sampler capable of sampling POPs over shorter timescales to facilitate studies of contaminant dispersal, fluxes, transport processes and occupational exposure. Interesting possibilities are being developed for short-term passive samplers operating on the principle that POPs from the gas-phase partition from the air onto the samplers of 'low capacity' reaching equilibrium with the sampler. Wilcockson and Gobas [32] originally developed EVA-coated samplers to measure the chemical fugacities in fish tissue and other solid substrates. The high surface-to-volume ratio allows rapid equilibration of (hours/days) of target analytes, while varying the surface area/coating thickness give the opportunity to vary the sensitivity and sampling time for different analytes and to meet different study objectives [33].

POGs have been tested and calibrated for indoor and outdoor studies, in which uptake rates, sampler designs and efficiency of sampling POPs have been discussed [33–35]. They approach equilibrium partitioning described by the K_{eva-a} partition coefficient and it is temperature dependent [33]. Uptake has been described for several PCB congeners (18, 28, 52, 49, 101, 118, and 153) under 'wind' (4 m s^{-1}) and 'no wind' conditions and with varying the thickness of the EVA film. The time to reach equilibrium under windy condition is shorter than under 'no wind' conditions, while increasing the thickness of the EVA results in a longer time to reach equilibrium. Since the uptake is

sensitive to wind speed, it is necessary to use sheltered chambers to dampen the effect of the wind for outdoor studies.

Farrar *et al*. [34,35] carried out a field calibration and deployment study with rapidly equilibrating thin-film passive air samplers of ca. 1-μm thickness. Results showed that time to reach equilibrium can vary between a few hours to ca. 20 days for PCB-18 and PCB-138, respectively. DCs were also used to estimate depuration rates, confirming that lighter PCBs displayed substantial losses over periods of few hours. This study demonstrated that POGs have the potential to be used as sensitive and dynamic PAS.

The flexibility, combined with the simple and fast preparation and clean-up methodology makes POGs useful for exposure studies with indoor air and potentially also for flux studies. The opportunity to manipulate equilibrium partitioning by varying the film thickness of EVA makes POGs good passive sampler devices to study complex environmental processes that affect POP sources and cycling. Although, POGs show a good potential for environmental investigations, further research and improvements are required. For example, the chambers have been shown to be effective for a wind speed of 4 m s^{-1}; however, effects of higher wind speeds need to be investigated. The effect of temperature of K_{eva-a} also needs further investigation.

2.4.2 Medium-capacity sampling devices: polyurethane foam disks

PUF disks are the same sampling medium as used in active air sampling to capture the gas-phase component of the air. Studies have usually been performed with disks 14 cm diameter × 1.35 cm thick. They have surface area of 365 cm^2, mass of 4.40 g, volume of 207 cm^3, density of 0.0213 g cm^{-3} and effective thickness of 0.567 cm, respectively [27]. PUF disks are particularly attractive as sampling devices, because they are cheap, do not require a trained operator to be handled and can be used to sample air over periods of several weeks/months. These are convenient sampling intervals for many ambient monitoring programmes. Shoeib *et al*. [27] have tested PUF disks as PAS and calibrated them against active samplers. PUF disks sample in the range of ~2.5–5 m^3 per day when operating in the kinetic mode [27]. Obviously, the time to reach equilibrium depends on the compound. Lighter PCBs and hexachlorobenzene (HCB) are likely to reach equilibrium within ~8 weeks, while heavier PCBs take several months [27].

PUF disks are deployed in sheltered chambers, as shown in Chapter 6, Fig. 6.4, made of stainless steel. The upper and lower steel bowl are put

together in a way that still allows the air to circulate inside the chamber. The chamber protects the sampling media from dry and wet deposition and from UV sunlight radiation, and dampens the high wind speeds, all of which may affect the measured uptake rate of the target compounds. With appropriate instrumental detection limits and low blank levels, many classes of POPs can be detected, following exposure periods of weeks in ambient air. For example, a deployment time of 6–8 weeks will yield the equivalent of 150–200 m^3 air sampled. With low sample blanks, this is sufficient to survey many POPs.

The widespread application of PUF disks at local, regional, continental and global scale has demonstrated that they can provide useful information on spatial and temporal variability of air concentration of POPs. It is desirable to operate PUF disks in the linear uptake phase so it is important to understand the interrelationship between equilibration time, sampler thickness and K_{puf-a} (analogous to K_{PAS-A} in Eq. (2.3)). In order to apply the sampling rates estimated for PCBs by Harner *et al*. [17], it is recommended that PUF disks are deployed in a sheltered chamber to avoid wind effects, deposition and UV radiation.

Further research is needed to improve the accuracy and the versatility of these sampling devices. For example direct measurements of K_{puf-a} as a function of temperature are required. Additionally, it is not known to what degree PUF disks are able to sample particle-bound species in the atmosphere.

2.4.3 High-capacity sampling devices: semipermeable membrane devices and XAD-2 resin

SPMDs have been designed by the U.S. Geological Survey (USGS) and consist of a low density lay flat polyethylene membrane containing a thin film of the synthetic lipid triolein (1,2,3 tri[*cis*-9-octadecenoyl] glycerol). Vapour-phase chemicals in the atmosphere permeate the membrane of the SPMD and become concentrated in the triolein, where they are retained. During sampler exposure, some methyl oleate and oleic acid (triolein primary lipid impurities) can slowly diffuse through the membrane and create a sticky surface on the exterior of the SPMD, where particles may adhere [29]. Although many uncertainties still remain, studies performed by Ockenden *et al*. [12,24], Lohmann *et al*. [29] and Söderström *et al*. [30,31] suggested that analytes associated with particles such as PAHs and polychlorinated dibenzo-*p*-dioxins and -furans (PCDD/Fs) can desorb from particles, permeate the membrane and be sequestered by the SPMD. It is then appropriate to remove the particles

from the surface of the SPMD before recovering the analyte sequestered. The most widely accepted laboratory procedure to do so is rinsing the surface with organic solvent before the sample is processed [12].

SPMDs have been extensively used to monitor PCB concentrations in water [36]. After observing abnormally high concentrations in field and laboratory control blanks, Petty *et al*. [37] demonstrated in a laboratory study that SPMDs are suitable for passively sampling the vapour phase of nonpolar organic compounds. Since 1993, SPMDs have been used to determine the atmospheric concentration of organic contaminants in remote and densely populated areas [12,24,38,39]. These devices provide the opportunity for short- and long-term time-integrated sampling and have shown to have a relatively high capacity for retaining POPs and a long linear uptake range. Ockenden *et al*. [24] have shown that the less volatile PCB congeners with five or more chlorine atoms can reach equilibrium after years/decades, while the more volatile PCB congeners can reach equilibrium in 2–3 years. The capacity of triolein is large, allowing detection of trace organic compounds. The large capacity of triolein allows POPs to be sampled in the uptake phase longer, even though there is a huge range of physical/chemical properties between classes of POPs.

The disadvantages of SPMDs are the complicated analytical clean-up and the need for further calibration studies in order to compare the data from previous studies and have a better understanding of the key controlling variables on the sampling rate. It has been suggested that SPMDs sample a small portion of the particle from the atmosphere. The process leading to particle sampling by SPMDs is not well understood and further work is needed to allow detection of particle-associated species. The 'leaking' of oils out of membrane over time, and the presence of 'two sampling phases', triolein and membrane, add to the complications of interpreting data.

XAD-2 resin was calibrated and implemented as a passive air sampler by Wania *et al*. [40], in response to the growing need for inexpensive and simple monitoring of POPs in the atmosphere. This passive sampling technique is based on sorption of the gaseous species to the sampling resin XAD-2, a styrene–divinyl benzene copolymer. As for PUF disks, the resin is routinely used as a sampling medium in conventional high-volume air samplers. The resin is placed in a container, which is in turn placed in a protective sampling shelter with an opening at the bottom. The sampling container is a long cylinder made of fine stainless steel mesh, held in shape by two end caps [40]. The entire cylinder is filled up with XAD-2 resin as sampling media (ca. 60 mL of

wet resin). The shelter is designed to protect the resin from wind speed, precipitation and deposition of coarse particles, and to ensure no wind speed effects.

Field calibration studies performed by Wania *et al*. [40] showed that XAD-2 resin has a high capacity for POPs and that sorption of gaseous compounds to the resin is not moisture, temperature or wind speed dependent (when deployed in the shelter). Therefore, sampling rates and efficiency of the sampler are not affected by these environmental variables. In this study, 42 passive samplers were deployed for varying periods of time up to 1 year at three field locations in the Laurentian Great Lakes and the Canadian High Arctic, alongside high-volume air sampler. Most of the investigated POPs were detectable after a 1-month deployment and did not reach equilibrium after a 1-year deployment. However, the study suggests that a minimum of 3-month deployment is required or the amounts accumulated will be very close to the limit of detection.

The study conducted by Wania *et al*. [40] calculated the uptake sampling rates of some of the organochlorine pesticides (OCs) and PCBs. The estimated air concentrations were compared with the annual mean concentration from the IADN network, which uses conventional high-volume air samplers. Passive sampler concentrations were in good agreement with those from the high-volume air samplers, with the exception of α-endosulfan. However, Wania *et al*. [40] suggested that XAD-2 resin can be used to derive at least semiquantitative information of POPs in the atmosphere and are suitable for the measurement of long-term average air concentrations of POPs in remote regions. Field calibrations by Wania *et al*. [40] have been found to differ between sampling sites. Reasons for this are not well known; it has been demonstrated that sampling rates are independent of wind speed and relative humidity. Temperature may be the cause, but this should be further investigated.

2.5 CASE STUDIES AND APPLICATIONS OF PAS FOR POPS

2.5.1 POGs: case studies and applications

The first and only application of the field deployment of POGs under ambient conditions was by Farrar *et al*. [34,35], where POGs were deployed at various heights of the CN Tower in Toronto, Canada. The study aimed to investigate the vertical distribution of selected POPs (PCBs, PAHs and OCs) in the atmospheric boundary layer of an urban

area. The study indicated the potential for rapid, low-volume sampling for POPs in ambient air. It was found that PAHs levels declined sharply with height, with the street-level urban environment being a major source of these compounds. PCBs were found to decline with the height but less strongly, compared with PAHs. The variations in concentrations with different heights demonstrated the dynamic sources and atmospheric mixing of POPs. By using a 1-μm film thickness of EVA, uptake rate during the kinetic phase is 3 m^3 per day for a range of compounds. This means that in 1-week exposure 21 m^3 of air can be retained in 9.4 mg of EVA, assuming the sampler is still in the uptake phase. The detection limit of 1 pg μL^{-1} injected in the gas chromatography column can be achieved for PCBs and OCs. The analytical sensitivity is theoretically able to detect between 10 and 25 picogram per concentrated sampler extract. However, the future challenge to deploy POGs successfully for ultralow level analysis is to optimise a procedure to reduce the blank signal.

2.5.2 SPMDs: case studies and applications

Monitoring of the local/regional and continental atmospheric distribution of PCBs, HCB, polybrominated diphenyl ethers (PBDEs) and PAHs using SPMDs has only recently been achieved. The spatial and temporal variations of these compounds in Norway and the UK were measured by the deployment of SPMDs at 11 sites for 2 years between 1994 and 1996 [24], 1998 and 2000 [13], 2000 and 2002 [14] and 2002 –and 2004 [15]. SPMDs were collected and re-deployed at sites every 2 years in summer. This monitoring network is useful to look for evidence of LRAT and to find evidence of the global fractionation theory. All sites were carefully selected far from sources. Data for PCBs, HCB, PBDEs and some OCs have been measured from 1998 to 2004.

In all sampling periods, sequestered amounts of the lighter PCBs are similar, while the heavier PCBs decrease with increasing latitude. For instance, the contribution of tri- and tetra-PCBs increases with latitude and decreases with increasing temperature, while the contribution of hexa-, hepta- and octa-PCBs shows the opposite. These results from 1994 through 2004 are consistent with the global fractionation theory. Furthermore, comparing the PCB levels among different campaigns (1994–1996, 1998–2000, 2000–2002 and 2002–2004), there is no significant difference in percentage decline between congeners and no extremely marked variation with latitude. This leads to the conclusion that PCB air concentrations at the continental scale are still controlled

by primary emissions rather than secondary emissions from environmental reservoirs. With three sampling intervals it has also been possible to have a first estimate of the clearance rates of PCBs in the atmosphere. Clearance rates ranged from 2.2 to 6.9 years for all congeners and locations [15]. This is a further support to the hypothesis that primary emissions still dominate in European background air.

Latitudinal distribution and fractionation for PBDEs have been estimated for the sampling campaign 2000–2002 and 2002–2004 [14,15]. Results showed that the lighter PBDEs decreased with increasing latitude. This is the opposite of what was observed for PCBs, where the sequestered amounts of heavier congeners decrease with increasing latitude, which is usually related to distance from sources. In a modelling study, Wania and Dugani [41] suggested that lower brominated congeners have an LRAT potential comparable to that of PCBs, whereas the highly brominated congeners were predicted to have a low potential to reach remote areas. PBDE congeners are heavier than their PCB analogues. However, the C–Br bond in PBDEs is weaker than the C–Cl bond in PCBs. For example, tri-BDEs and hepta-CBs have a molar mass of approximately 400 g mol^{-1}, yet the tri-BDEs are predicted to be more volatile and more reactive by over an order of magnitude in air than the hepta-CBs.

SPMDs have also been applied in studies at regional/local scale. Lohmann *et al*. [29] deployed SPMDs at 19 sites in northwest England during November/December 1999 to test their efficiency as passive samplers for PCDD/Fs and PAHs. The study suggested that SPMD efficiently sample vapour-phase species in the atmosphere, while species partially or completely associated with particles were found to be sampled by the SPMD with poorer reproducibility. Sequestered PAH and PCDD/Fs amounts were compared with active monitoring data where available. Good agreement was found between the active and the passive samplers.

Söderström *et al*. [30] deployed SPMDs at six sites in and around Bangkok, Thailand for 3 weeks in March and April 2000 to investigate spatial and temporal variation in concentrations for PAHs. Significant differences among sites were found with the highest PAH concentration in urban sites, showing again that SPMDs are suitable for semiquantitative studies for PAHs. Söderström *et al*. [31] also deployed SPMDs in five European countries (Austria, the Czech Republic, Poland, Slovakia and Sweden), to see whether there are any spatial differences between Northern, Central and Eastern Europe for PAHs and nitro-PAHs. Air sampling was performed for 3-week periods, one in autumn 1999 and

one in the summer 2000 with the exception of Poland where 4-week samples were taken in winter 1999 and summer 2000. The levels measured in Eastern Europe (Czech Republic and Poland) were 10 times higher than the levels measured in Northern and Central (Sweden and Austria). The difference in concentration reflect the influence of local sources. Despite the fact that PAH and nitro-PAH air concentrations have not been measured by SPMDs prior to this study, results were in good agreement with atmospheric PAH concentration measurements across Europe by Jaward *et al*. [19] using PUF disks. Bartkow *et al*. [42] carried out a calibration study in Australia during April 2002 for 32 days in order to obtain SPMD sampling rates for 12 US EPA priority pollutant PAHs. The sampling rates calculated by Bartkow *et al*. ranged from 0.6 to 6.1 m^3 per day, showing that SPMDs can be used to estimate air concentration with reasonable accuracy.

SPMDs have also been used to measure HCB and PCBs in high mountain areas (Central Pyrenees, Catalonia, Spain) at three different altitudes above the sea level over a period of 1.5 years [43]. Atmospheric concentrations measured in this study were also in agreement with levels obtained by active volume air sampling, suggesting that SPMDs can be useful tools to monitor organochlorine compounds in mountain areas.

2.5.3 PUF disks: case studies and applications

The practical application and utility of PUF disks have been demonstrated at the local [44], regional [45,46], continental [19,47,48] and global scale [17] and also for indoor studies for PBDEs and polyfluorinated compounds (PFCs) [49,50,]. Harner *et al*. [44] have used PUF disks along with SPMDs to investigate urban–rural differences of PCBs and OCs. The results demonstrate that PUF disks and SPMDs are useful tools to acquire information integrated over selected time periods on spatial differences between rural and urban sites. This study, as well as other local studies conducted in Ontario, was able to highlight the differences in concentrations for PCBs, PBDEs and some pesticides, seasonal variations and sources/sinks [44,45,51]. Further regional studies employing PUF disks have been conducted on a north–south transect in Chile [48]. In most South American countries, there is still lack of information on air concentration of POPs, principally because of financial constraints. However, the use of a cheap and versatile sampling technique such that of PAS has made possible to acquire knowledge on potential sources and LRAT in this region.

The feasibility of coordinated sampling at the continental/regional scale has also been demonstrated by studies in Europe, North America, South America and Asia where data from PUF disks surveys have confirmed their efficacy in defining known source/background areas of POP contamination. Jaward *et al*. [19] carried out a study in 22 European countries, where PUF disks were deployed for a period of 6 weeks at remote/rural/urban locations. Samplers were analysed for a range of POPs, including PCBs, OCs, PBDEs, PAHs and polychlorinated naphthalenes (PCNs). PUF disks were prepared in one laboratory; sealed to prevent contamination; sent out by courier to volunteers participating in different countries; exposed for 6 weeks; collected; re-sealed; returned to the laboratory for analysis. Calculated air concentrations were in good agreement with those obtained by conventional active air sampling techniques. The geographical pattern of all compounds reflected suspected regional emission patterns and highlighted localized hotspots. The trends of PCBs and PBDEs are linked to urbanized source areas. The levels of α-HCH and HCB were relatively uniform throughout Europe, while the levels of γ-HCH and the DDT and DDE were higher in southern and eastern locations [19]. The study demonstrated that it is possible to map local, regional and global sources of POPs using passive air samplers and identify unknown sources.

The use of PUF disks has recently shed light on global distribution of POPs in places where data are sparse or not even available. For the first time, a large-scale passive air sampling survey was therefore conducted in Asia, specifically in China, Japan, South Korea and Singapore. PUF disks were deployed simultaneously at 77 sites, between 21 September and 16 November 2004, and analysed for PCBs, OCs and PBDEs. Elevated concentrations of PCBs, DDTs and HCB occurred at sites in China, higher than reported in a similar recent European sampling campaign. [47] Chlordane was highest in samples from Japan (which also had elevated levels of PCBs and DDTs) and was also elevated in some Chinese locations. In collaboration with IADN investigators in the Great Lakes basin, PUF disk samplers were deployed at 15 sites over four consecutive seasons during 2002–2003 [52]. This was the first study to show seasonality of POPs, especially for some currently used pesticides such as lindane and endosulfans. Probability density maps were constructed for each site for each of the 3-month sampling periods in order to highlight potential source–receptor relationships. This study demonstrated the use of DCs to obtain site-specific sampling rates. Like PRCs, DCs are added to the PUF disks prior to exposure. Unlike PRCs,

however, DCs solely account for loss of these labelled chemicals that is attributed to the airside mass transfer coefficient, which controls both uptake and loss of chemical from the PUF disk.

The ongoing Global Air Passive Sampling (GAPS) Study started in December 2004 with the aim of demonstrating the feasibility of using passive samplers for conducting global monitoring. This study will test the recent UNEP Guidance document for Global POPs Monitoring where passive air samplers were promoted. A second aim of the GAPS study is to produce seasonally integrated concentrations of POPs at background locations around the world. This will further help to develop global transport models for POPs and to evaluate their LRAT. PUF disks have already been deployed around the world since December 2004, but data are not available yet with ''First results from the GAPS study have recently been published [17].''

Over recent years PUF disks have been very useful in understanding if ship-based sampling has the potential to be a source of contamination for active air sampling on board. Many investigators have found evidence for the global distribution and cycling of POPs [53–55]. Ship-based air sampling is a convenient and elegant way to explore the global distribution of POPs. Samples can be collected from a variety of sampling sites in very short periods of time, while the ship is steaming along a transect. However, air sampling on the ship needs to be consistent and respectful of strict quality control measures in order to avoid contamination of air samples by emissions from the ship contamination and detect low levels of POPs in remote regions [56]. Therefore, passive air samplers (PUF disks) were deployed in different locations in and onboard of the RV Polarstern during two different sampling cruises (November 2003–January 2004 in the Atlantic and June–July 2004 in the Arctic region) to determine whether the ship has the potential to be a source of contamination. PCBs data resulting from the passive air samplers and active air sampling on board suggest that RV Polarstern can act as a clean ship for these compounds [57].

2.5.4 XAD-2 resin: case studies and applications

A large-scale network of 40 XAD-2 resin passive samplers was used to characterize better the atmospheric distribution of PCBs, PBDEs, OCs and HCB across North America [20,21,58]. This represents the largest latitudinal transect (from Central America to the Canadian Arctic) of simultaneous airborne measurements of major POPs. Passive samplers were deployed over the period of 1 year in 2000–2001. Once the

atmospheric concentrations of POPs were obtained, long-range atmospheric potential for those compounds was predicted with assessment models.

For OCs, the length of the study period helped in deciding whether the elevated concentrations were due to past or present use of these compounds. With conventional high-volume air samplers these episodes will be missing if they occur between sampling events. For example, chlordanes and *p*,*p*′-DDT displayed elevated concentrations in south-eastern United States and southern Mexico and Belize respectively, indicating that there are potential source regions.

Evidence of global fractionation was found for PCBs. Abundance of tri-PCBs homologue were relatively uniform in the atmosphere, while that of tetra-PCBs increases with increasing latitude and penta- and hexa-PCBs showed a decrease from tropical regions to the Arctic. PCB congeners with intermediate degrees of chlorination have greater LRAT potential while lower chlorinated PCBs tend to degrade faster and higher chlorinated tend to be removed by particle-bound deposition. The investigation also shed light on the distribution and fractionation of PBDE in the North American atmosphere. Lighter PBDEs congeners had similar LRAT potential to PCBs, but no shift in composition was observed. Contrary to PCBs, PBDEs concentrations were not associated with urban areas; elevated concentrations were also observed in rural and remote areas, probably due to the open burning of household waste [21,58].

Results by Shen *et al*. [21] demonstrated that XAD-2 resin could play a useful role in monitoring levels and distribution of POPs in the atmosphere. This study clearly demonstrates that once atmospheric concentrations are measured simultaneously at different locations covering a large range of latitude and longitude, model-derived indicators of LRAT potential and principal components analysis can shed light on the behaviour of these compounds in the atmosphere and their differences in distribution variation respectively.

2.6 FUTURE IMPROVEMENTS AND NEEDS FOR PAS FOR POPS

Often PAS are used in applications where information on the *relative amounts* or *patterns* of POPs is obtained, which can highlight spatial patterns and trends. This can be an extremely useful output and worthy goal. However, if PAS are to find favour as a ‘routine monitoring tool’, they will need to be used to derive an estimate of the ‘true’ air

concentration, within a certain known tolerance, in a reproducible and sensitive way. Currently, PAS techniques are generally believed to enable estimates of the 'true concentration' within a factor of 2–3. Workers in the field are therefore currently focusing on:

(a) better understanding sampler performance (e.g. reproducibility, robustness, ability to operate under different environmental conditions and calibration against active samplers);
(b) better understanding of the influence of environmental variables (i.e. wind speed, temperature, humidity; influence of particle-bound POPs; and photodegradation/stability of compounds);
(c) optimisation of sampler design, deployment device/housing design, sample location/frequency etc;
(d) best practice for preparation, pre-cleaning, PRC/DC spiking and loss correction.

Once these studies have reached fruition, clear recommendations can be given, to help those planning monitoring or research programmes, where passive sampling brings benefits. As we have seen in other fields, such as the now routine monitoring of gaseous pollutants with diffusion tubes, PAS can then be used widely and with confidence to address the research, monitoring and regulatory challenges ahead.

REFERENCES

1 UNECE, Protocol on persistent organic pollutants under the 1979 convention on long-range transboundary air pollution; United Nations Economic Commission for Europe (ECE/EB.Air/60), 1998.
2 T.F. Bidleman, L.M.M. Jantunen, P.A. Helm, E. Brorström-Lunden and S. Juntto, *Environ. Sci. Technol.*, 36 (2002) 539.
3 H. Hung, C.J. Halsall, P. Blanchard, H.H. Li, P. Fellin, G. Stern and B. Rosenberg, *Environ. Sci. Technol.*, 36 (2002) 862.
4 T. Harner, H. Kylin, T. Bidleman, C. Halsall, W.M.J. Strachan, L.A. Barrie and P. Fellin, *Environ. Sci. Technol.*, 32 (1998) 3257.
5 J.R. Kucklick and J.E. Baker, *Environ. Sci. Technol.*, 32 (1998) 1192.
6 C.J. Halsall, R. Bailey, G.A. Stern, L.A. Barrie, P. Fellin, D.C.G. Muir, B. Rosenberg, F.Ya. Rovinsky, E.Ya. Kononov and B. Pastukhov, *Environ. Pollut.*, 102 (1998) 51.
7 D.C.G. Muir, C.A. Ford, B. Rosenberg, R.J. Norstrom, M. Simon and P. Béland, *Environ. Pollut.*, 93 (1996) 219.
8 A.J. Sweetman and K.C. Jones, *Environ. Sci. Technol.*, 34 (2000) 863.
9 F. Wania and D. Mackay, *Ambio*, 22 (1993) 10.

10 F. Wania and D. Mackay, *Sci. Total Environ.*, 160/161 (1995) 211.
11 F. Wania and D. Mackay, *Environ. Sci. Technol.*, 30 (1996) 390A.
12 W.A. Ockenden, F.M. Jaward and K.C. Jones, *Sci. World*, 1 (2001) 557.
13 S.N. Meijer, W.A. Ockeneden, E. Steinees, B.P. Corrigan and K.C. Jones, *Environ. Sci. Technol.*, 37 (2003) 454.
14 F.M. Jaward, S.N. Meijer, E. Steinees, G.O. Thomas and K.C. Jones, *Environ. Sci. Technol.*, 38 (2004) 2523.
15 R. Gioia, E. Steinnes, G.O. Thomas, N.S. Meijer and K.C. Jones, *J. Environ. Monit.*, 8 (2006) 700.
16 United Nations Environment Programme UNEP (2003). Proceedings UNEP Workshop to develop a global POPs monitoring programme to support the effectiveness evaluation of the Stockholm Convention. Geneva, Switzerland, 24–27 March 2003.
17 K. Pozo, T. Harner, F. Wania, D.C.G. Muir, K.C. Jones and L.A. Barrie, *Environ. Sci. Technol.*, 40 (2006) 4867–4873.
18 European Commission, Ambient air pollution by polycyclic aromatic hydrocarbons (PAH). Position paper; Luxembourg, 2001.
19 F.M. Jaward, N.J. Farrar, T. Harner, A.J. Sweetman and K.C. Jones, *Environ. Sci. Technol.*, 38 (2004) 34.
20 L. Shen, F. Wania, Y.D. Lei, C. Teixeira, D.C.G. Muir and T.F. Bidleman, *Environ. Sci. Technol.*, 38 (2004) 965.
21 L. Shen, F. Wania, Y.D. Lei, C. Teixeira, D.C.G. Muir and T.F. Bidleman, *Environ. Sci. Technol.*, 39 (2005) 409.
22 D. Mackay, *Multimedia Environmental Models: The Fugacity Approach*, Lewis Publishers, Chelsea, MI, 2001.
23 F. Wania and D. Mackay, *Environ. Pollut.*, 100 (1999) 223.
24 W.A. Ockenden, A.J. Sweetman, H.F. Prest, E. Steinnes and K.C. Jones, *Environ. Sci. Technol.*, 32 (1998) 2795.
25 P. Tremolada, V. Burnett, D. Calamari and K.C. Jones, *Environ. Sci. Technol.*, 30 (1996) 3570.
26 H. Kylin and A. Sjodin, *Environ. Sci. Technol.*, 37 (2003) 2350.
27 M. Shoeib and T. Harner, *Environ. Sci. Technol.*, 36 (2002) 4142.
28 C.T. Chiou, *Environ. Sci. Technol.*, 19 (1985) 57.
29 R. Lohmann, B.P. Corrigan, M. Howsam, K.C. Jones and W. Ockenden, *Environ. Sci. Technol.*, 35 (2001) 2576.
30 H.S. Söderström and P.-A. Bergqvist, *Environ. Sci. Technol.*, 37 (2003) 47.
31 H.S. Söderström, J. Hajšlová, B. Siegmund, A. Kočan, M.W. Obiedzinski, M. Tysklind and P.-A. Bergqvist, *Atmos. Environ.*, 39 (2005) 1627.
32 J.B. Wilcockson and F.A.P.C. Gobas, *Environ. Sci. Technol.*, 35 (2001) 1425.
33 T. Harner, N.J. Farrar, M. Shoeib, K.C. Jones and F.A.P.C. Gobas, *Environ. Sci. Technol.*, 37 (2003) 2486.

34 N.J. Farrar, T. Harner, A. Sweetman and K.C. Jones, *Environ. Sci. Technol.*, 39 (2005) 261.
35 N.J. Farrar, T. Harner, M. Shoeib, A. Sweetman and K.C. Jones, *Environ. Sci. Technol.*, 39 (2005) 42.
36 J.N. Huckins, G.K. Manuweera, J.D. Petty, D. Mackay and J.A. Lebo, *Environ. Sci. Technol.*, 27 (1993) 2489.
37 J.D. Petty, J.L. Zajicek and J.N. Huckins, *Chemosphere*, 27 (1993) 1609.
38 H.F. Prest, L.A. Jacobson and J.N. Huckins, *Chemosphere*, 30 (1995) 1351.
39 W.A. Ockenden, H.F. Prest, G.O. Thomas, A.J. Sweetman and K.C. Jones, *Environ. Sci. Technol.*, 32 (1998) 1538.
40 F. Wania, L. Shen, Y.D. Lei, C. Teixeira and D.C.G. Muir, *Environ. Sci. Technol.*, 37 (2003) 1362.
41 F. Wania and C.B. Dugani, *Environ. Toxicol. Chem.*, 22 (2003) 1252.
42 M.E. Bartkow, J.N. Huckins and J.F. Muller, *Atmos. Environ.*, 38 (2004) 5983.
43 B.L. Van droodge, J.O. Grimalt, K. Booij, L. Camarero and J. Catalan, *Atmos. Environ.*, 39 (2005) 5195.
44 T. Harner, M. Shoeib, M. Diamond, G. Stern and B. Rosenberg, *Environ. Sci. Technol.*, 38 (2004) 4474.
45 T. Gouin, T. Harner, G.L. Daly, F. Wania, D. Mackay and K.C. Jones, *Atmos. Environ.*, 39 (2005) 151.
46 F.M. Jaward, A. Di Guardo, L. Nizzetto, C. Cassani, F. Raffaele, R. Ferretti and K.C. Jones, *Environ. Sci. Technol.*, 39 (2005) 3455.
47 F.M. Jaward, G. Zhang, J.J. Nam, A. Sweetman, J.P. Obbard, Y. Kobara and K.C. Jones, *Environ. Sci. Technol.*, 39 (2005) 8638.
48 K. Pozo, T. Harner, M. Shoeib, R. Urrutia, R. Barra, O. Parra and S. Focardi, *Environ. Sci. Technol.*, 38 (2004) 6529.
49 M. Shoeib, T. Harner, B.H. Wilford, K.C. Jones and J. Zhu, *Environ. Sci. Technol.*, 39 (2005) 6599.
50 B.H. Wilford, M. Shoeib, T. Harner, J. Zhu and K.C. Jones, *Environ. Sci. Technol.*, 39 (2005) 7027.
51 T. Gouin, D. Mackay, K.C. Jones, T. Harner and S.N. Meijer, *Atmos. Pollut.*, 128 (2004) 139.
52 T. Gouin, T. Harner, B. Blanchard and D. Mackay, *Environ. Sci. Technol.*, 39 (2005) 9115.
53 F.M. Jaward, J.L. Barber, K. Booij, J. Dachs, R. Lohmann and K.C. Jones, *Environ. Sci. Technol.*, 38 (2004) 2617.
54 R. Lohmann, P.A. Brunciak, J. Dachs, C.L. Gigliotti, E. Nelson, D. van Ry, T. Glenn, S.J. Eisenreich, J.L. Jones and K.C. Jones, *Atmos. Environ.*, 37 (2003) 959.
55 S. Lakaschus, K. Weber, F. Wania, R. Bruhn and O. Schrems, *Environ. Sci. Technol.*, 36 (2002) 138.

56 R. Lohmann, F.M. Jaward, L. Durham, J. Barber, W. Ockenden, K.C. Jones, R. Bruhn, S. Lakaschus, J. Dachs and K. Booij, *Environ. Sci. Technol.*, 38 (2004) 3965.
57 R. Gioia, R. Lohmann and K.C. Jones, *Sampling POPs in the Arctic: dealing with ship-based contamination*, Poster for the Academic Poster Session at Lancaster University, UK, 2005.
58 L. Shen, F. Wania, Y.D. Lei, C. Teixeira, D.C.G. Muir and X. Hang, *Environ. Pollut.*, 144 (2006) 434.

Chapter 3

Passive sampling in combination with thermal desorption and gas chromatography as a tool for assessment of chemical exposure

Anna-Lena Sunesson

3.1 THE APPLICABILITY OF PASSIVE SAMPLING FOR CHEMICAL EXPOSURE ASSESSMENT

Passive (diffusive) sampling is a useful tool for monitoring chemical exposure, because of its simplicity to use in the field, both for monitoring chemical compounds in ambient and indoor air and for assessment of occupational exposure. The sampling rates of diffusive samplers are much dependent on the sampler construction, but are normally lower than with active (pumped) sampling. This can be seen both as an asset and a limitation, depending on the question to be answered by the sampling procedure. When assessing occupational exposure, the levels of compounds to be collected are often high enough to use diffusive sampling also for short-time measurements. The passive sampler is convenient because there is no necessity for a pump and hence much less interference with a worker's ability to perform his/her work as normal. This makes the passive samplers very attractive for personal exposure assessment. In ambient and in non-occupational indoor air, the concentrations of various volatile organic compounds (VOCs) are usually very low, often in levels of $\mu g\ m^{-3}$ or even $ng\ m^{-3}$. To be able to passively collect a sufficient mass of the compound(s) for analysis of interest, longer sampling times are needed than what is attainable with active sampling. This can give a better description of the average composition of the ambient or indoor air than one or a few hours sampling time, which is common when performing pumped sampling. However, if the aim is to monitor fast, dynamic processes in ambient or indoor air, active sampling is preferred.

Comprehensive Analytical Chemistry 48
R. Greenwood, G. Mills and B. Vrana (Editors)
Volume 48 ISSN: 0166-526X DOI: 10.1016/S0166-526X(06)48003-X

For many years, passive samplers have been considered to offer an attractive, cost-effective alternative to active sampling [1–3]. Kauppinen has addressed the importance of cost-effective measurements and survey strategies as general recommendations for health surveillance [4]. Nothstein *et al.* compared the cost effectiveness as a function of the number of annual samplers, for five passive samplers and one active sampler (pumped charcoal tubes) [5]. Including costs for validations, sampling equipment and labour, the calculations indicated that, in general, the unit cost was lower for a passive sampler than for an active sampler. If the passive sampler is thermally desorbed and thereby can be reused, the price per analysis is even lower. As the costs for performing the measurements are reduced, more samples are allowed to be taken, thereby giving a better description of the exposure situation at, e.g., a workplace.

Passive samplers are user-friendly devices that can normally be operated by the user, thus enabling self-assessment of exposure (SAE) [6–9].

3.2 PASSIVE SAMPLING, BASIC THEORY

Passive sampling uses the principles of mass transport across a diffusion layer. Samplers utilising this concept received an increasing interest since the early 1970s, when the first mathematical treatment of the principles was published [10]. It was an attempt to identify and codify the factors controlling uptake rate, in the application of Fick's law of diffusion. These fundamental laws were stated by the German physiologist Adolf Eugene Fick in 1855 [11]. Further details on the theory of passive sampling are given in Chapters 2 and 6 of this book; here only the very simplest and most basic equations are given.

Fick's first law describes the diffusive flux (J), or rate of diffusion dn/dt, of a solute across an area A, as

$$J = \frac{dn}{dt} = -DA\frac{\partial c}{\partial x} \tag{3.1}$$

where dn is the amount of solute crossing an area A in time dt, and $\partial c/\partial x$ is the concentration gradient of the solute. D, the diffusion coefficient, gets the unit $m^2\ s^{-1}$.

For diffusion through a tube, the concentration gradient within the tube falls linearly (Fig. 3.1), and is given by

$$-\frac{dc}{dx} = \frac{C - C_0}{L} \tag{3.2}$$

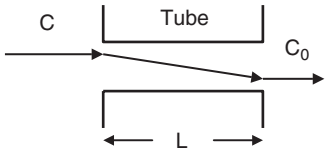

Fig. 3.1. Diffusion through tubes. Diffusion from concentration C to C_0 through a tube with length L.

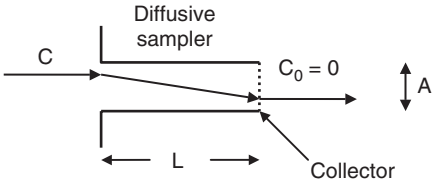

Fig. 3.2. Diffusion through tubes. Diffusion from concentration C to $C_0 = 0$ through a tube-type diffusive sampler with length L and cross-sectional area A.

where C_0 = concentration at the interface of the sorbent (g cm^{-3}), C = external concentration being sampled (g cm^{-3}) and L = length of diffusion path (cm).

The integrated Fick's first law then describes the rate of flow through the tube with

$$J = \frac{m}{t} = DA\frac{C - C_0}{L} \tag{3.3}$$

where m = mass transported (ng) and t = time (s).

A diffusive sampler has a collector (Fig. 3.2). The collector consists of an adsorbent (or a chemosorbent, i.e., a reagent coated on an adsorbent or filter that reacts with the compound to be sampled, forming a stabile derivative). If the concentration on the collector surface is zero ($C_0 = 0$), Fick's law is reduced to

$$\frac{m}{t} = DA\frac{C}{L} \tag{3.4}$$

The expression DA/L has the unit of cm^3 s^{-1} and represents what can be considered the sampling rate of the system (comparable to the pumped sampling rate in active sampling). As A and L are physical parameters associated with the sampler construction, the sampling rate is constant for a certain analyte and diffusive sampler (except for some minor and often negligible effects of temperature and pressure). The diffusion coefficient can be theoretically calculated and predicted

[12–15] and many manufacturers publish tables of calculated diffusion coefficients or sampling rates. It is, however, better to use sampling rates determined experimentally from dynamically generated test atmospheres, because effects of sorbent–analyte interactions and possible effects of concentration, time and wind velocity on the sampling rate can then be examined and taken into consideration.

3.3 SAMPLING RATES

The sampling rate of a chemical compound passively collected on an adsorbent depends on a number of factors. Choosing an adsorbent that can adsorb and desorb the compound of interest is a fundamental prerequisite for sampling, independent of whether the collection is performed by active or passive sampling. Presuming this is the case, the sampler design (especially the sampling area and the length of the diffusion path) has the most marked effect on the sampling rate. Other important factors exerting an influence on the sampling rate are the concentration of the collected compound and possibly effects of concentration gradients, temperature and pressure during sampling, humidity and air flow/turbulence. The wind velocity has a profound effect on sampling rates; at very low air flows the sampling rate can become unstable. For tube-type samplers (the most common samplers when thermal desorption (TD) is used for analysis), a minimum air movement of $0.01\,m\,s^{-1}$ is needed [16]. The sampling time can also affect the sampling rates, and often different sampling rates are used for a specific compound on an adsorbent depending on whether the sampling time is 8 h, 1 week or even longer. Laboratory determined sampling rates are recommended over theoretically calculated sampling rates. However, there are additional factors in ''real'' atmospheres that are difficult to simulate in laboratory experiments, such as the presence of interfering compounds, and realistic fluctuations in the factors influencing the sampling rate. It is therefore always valuable to perform field studies, where the passive sampler, packed with the selected adsorbent, is evaluated in parallel with some standard reference method. For environmental applications, the use of sampling rates determined only in the laboratory and not validated in the field has been concluded to be the main source of uncertainty [17].

3.4 STANDARDS FOR EVALUATION OF PASSIVE SAMPLERS

Several nationally and internationally approved standard methods relate to monitoring various VOCs in air. These standards give important

information on key issues to study or important guideline on the choice of sampling and analysis equipment etc. Many standards are written for specified applications, e.g., ambient indoor or workplace air, or for specific chemicals. The European Committee for Standardisation (CEN) has set standard protocols for testing and evaluation of passive samplers [18–21]. These protocols involve factors such as concentration, sampling time, relative humidity, face velocity, reverse diffusion and storage. None of these standards include TD analysis. There is a special CEN standard for diffusive sampling–TD–gas chromatography (GC) analysis of benzene in ambient air [22]. The International Standards Organisation (ISO) general standard ISO 16017 describes sampling and analysis of VOCs in ambient, indoor and workplace air by sorbent tube–TD–GC, part 1 for active and part 2 for diffusive sampling [23,24]. It also sets a standard protocol for evaluating the performance of diffusive samplers in workplace air [25]. ISO has published a specific standard for VOC sampling in indoor and test chamber air by sampling on Tenax^{TM} TA and subsequent TD–GC–MS/FID analysis, but that standard is for active sampling [26]. Standard protocols for collecting organic compounds on adsorbents for subsequent TD analysis are widely used, such as the US Environmental Protection Agency (EPA) methods for monitoring ambient air contaminants [27,28], the US National Institute of Occupational Safety and Health (NIOSH) methods for sampling VOCs in occupational environments [29] or the American Society for Testing and Materials (ASTM) methods for VOCs in air [30]. These methods are also, however, all based on active sampling approaches.

Much work on the combination of passive sampling and TD has been performed and published by the U.K. Health and Safety Executive (HSE) in their MDHS (Methods for Determination of Hazardous Substances) series. There is a number of methods for passive sampling–TD–GC analysis of specified compounds in that series. They have also published a protocol for evaluation of passive samplers [31]. MDHS 80 is a general and useful method for passive sampling–TD–GC analysis of VOCs in air, suitable for measurement of both individual compounds and mixtures of VOCs. It also includes sampling rates for a number of hazardous substances and adsorbents.

3.5 SAMPLER DESIGNS FOR PASSIVE SAMPLING–THERMAL DESORPTION ANALYSIS

There is a number of diffusion sampler designs on the market. For the combination of TD and diffusion sampling the various types of samplers

are much more limited. Utmost used for this purpose are tube-type samplers, often referred to as Perkin Elmer samplers, because that company was the first to produce and sell them commercially, after collaborative development with researchers. The first paper published addressing the advantage of a thermally desorbable and, without further treatment, reusable diffusion sampler was published by Brown *et al.* in 1981 [75]. Today, there are several companies selling these samplers. These are typically made of stainless steel, 90 mm × 6.3 mm O.D. × 5.0 mm I.D., with a cross-sectional area (A) of 19.3 mm^2 (Fig. 3.3). The sampler can be packed with various adsorbents, which are kept in place using stainless steel gauzes at both ends. The position of the gauze in the front (sampling) side has to be fixed to ensure a controlled and well-defined length of the diffusion path. For the most-used tube-type samplers specified above this length (L) is 15 mm. During sampling a tube-type sampler is equipped with a diffusion cap, consisting of a cap sealed to the tube with an "O"-ring and containing a gauze disc in its open end. Such caps are also available equipped with membranes, which prevent water from being sorbed on the adsorbent. Most applications and sampling rates published are, however, for samplers equipped with caps without membranes. The main advantage of tube-type samplers is that they can be automatically analysed, without any pre-treatment, and reused. A disadvantage is the small sampling surface area, which gives low sampling rates (often in the range of about 0.5–1 mL min^{-1}). Unless otherwise stated, the samplers discussed in this chapter belong to this class of stainless steel tube-type samplers.

Sampling rates for passive sampling on tube-type samplers have been determined for many compounds. In 1996, the HSE Committee on Analytical Requirements (CAR) Working Group 5 published a list of sampling rates compiled from various sources [33]. This list has been

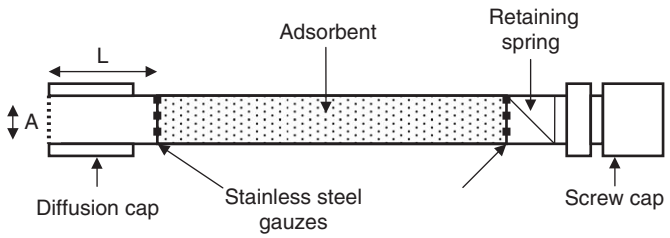

Fig. 3.3. Tube-type diffusive sampler (stainless steel). $L = 15$ mm, $A = 19.3$ mm^2. During sampling the tube is equipped with a diffusion cap. The back end is closed with a screw cap.

reproduced and is continuously updated by Markes International Limited and available on their website [34].

Other sampler designs that have recently been used in combination with TD are the SKC-Ultra sampler [35] and the Radiello sampler [35,36]. These sampler designs give substantially higher sampling rates, because of much larger diffusion areas. These much higher sampling rates allow shorter sampling times and/or sampling of atmospheres with lower concentrations of the analyte(s) of interest than conventional tube-type samplers.

The SKC-Ultra sampler is a badge sampler similar to the SKC 575-series. The cross-sectional area (A) is 21 mm in diameter and the diffusion path (L) is 15 mm.The major innovation of the SKC-Ultra sampler is that its back plate can be removed. The sampler can then be filled with a desired adsorbent, which after exposure can be poured out of the sampler into a tube for TD. The adsorbent has to be conditioned in a TD stainless steel tube before use. The Radiello sampler, developed in 1996 [37] consists of a stainless steel net coaxial cylindrical cartridge (60-mm long, 100 mesh hole size) filled with an adsorbent (about 530 mg) housed in a cylindrical diffusive body made of polycarbonate and micro-porous polyethylene (50-mm long and 16-mm diameter). The sorbent cartridge should be put in a stainless steel tube for TD and properly conditioned before use. The cartridge is stored and transported in the tube, and put in the radial diffusive body just prior to sampling. After exposure the cartridge is transferred into the stainless steel tube again. Sampling rates for radial diffusive samplers (Radiello) have been published for a number of compounds, and are typically in the range of 20–30 mL min^{-1} [38].

The fact that the adsorbent after exposure has to be transferred from the sampler into a tube for thermal analysis makes these sampler designs less convenient to handle than tube-type samplers that can be put directly in the thermal desorber. They also have to be repacked before reusing, which represents additional manual treatment compared to tube-type samplers. However, their much larger sampling rates can be of vital importance when sampling low concentrations or for short sampling times, and they are therefore likely to gain much interest in the coming years.

Other examples of laboratory-constructed samplers, made with the intention of increasing the sampling rate compared to tube-type samplers, have been published. Yamamoto *et al*. [39] developed a badge-type passive sampler based on the OVM 3500 (3 M) sampler cartridge. The sampler consists of a permeable membrane and an adsorbent disk

assembled in a disk-shaped plastic holder. They made an adsorbent disk for TD by packing Carbopack^{TM} B between two glass fibre filters and inserted it in the holder. After exposure, the disk was taken out and put in a specially constructed TD device, connected to a GC–MS. The method was validated in indoor and outdoor air and was found to be capable of measuring VOCs at sub-ppb levels for exposure periods of 2–8 h.

3.6 THERMAL DESORPTION

There are two major principles for desorbing collected compounds from adsorbent tubes for subsequent analysis by GC; solvent and TD. In solvent desorption, a known amount of solvent is added to the adsorbent, and the collected compounds are desorbed from the adsorbent into the solvent, e.g., by shaking. The technique has the major disadvantage that only a small fraction of the collected compounds can be used for the chromatographic analysis; the amount of solvent that can be injected on a GC is typically in the range of 1 μL, but the volume of solvent that has to be added to the adsorbent to desorb the collected compounds is in the magnitude of mL, resulting in about a 1000-fold dilution of the collected sample. Other disadvantages are that the analysis results in a big solvent peak, which may hide analytes of potential interest, and the solvent itself can impose a health hazard to the analyst.

When using TD, the collected analytes are desorbed by heating the tubes in a stream of an inert gas, which is further led to the GC in two stages, including a pre-concentration step. In the first stage, the compounds are desorbed from the adsorbent on which they have been collected. The time for this is normally set in the range of about 10 min.It is thereby not possible to lead the gas directly onto the GC column; the volume of desorption gas is too large and the long time for introduction of the compound onto the column would result in bad chromatography. Hence, a pre-concentration step is needed before the desorbed compounds are let into the chromatographic column. This pre-concentration step often involves a cold trap consisting of a glass tube packed with a suitable adsorbent, but other trapping designs, consisting of, e.g., fused silica capillaries, are used in some devices. The traps are cooled either electrically or by liquid cryo-focusing. In the cold trap, the desorbed analytes are re-adsorbed on a matrix that can be heated very rapidly, thus giving a rapid injection onto the chromatographic column. A part of the vapour is normally split after the trap but before the column (outlet split). This split can be set at low mL min^{-1} or

hundreds of mL min^{-1}, depending on the expected concentration of the sample. If the amount of collected sample is very high, a part of the vapour can be split after the primary desorption from the sample tube but before the cold trap (inlet split). The general principle of a two-stage TD is shown in Figs. 3.4 and 3.5.

The main advantage of TD is that all (or at least most of) the desorbed sample is transported to the column, resulting in a much higher sensitivity than with solvent desorption (if desirable only a minor fraction of the analyte can be injected on the column by splitting most of the desorbed sample before the column). Other advantages are the absence of a solvent peak or analytical interference from solvent artefacts, a possibility to reuse the sampler, no use of hazardous solvents and a minimum of handling to get the collected sample from the adsorbent onto the chromatographic equipment.

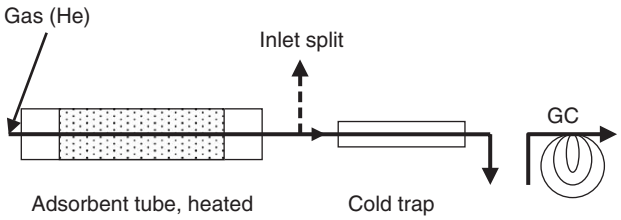

Fig. 3.4. Two-stage thermal desorption. Primary desorption. The adsorbent tube is heated in a stream of gas and the desorbed analytes are transferred to a cold trap, where they are re-collected. It is possible to split parts of the desorbed sample (inlet split).

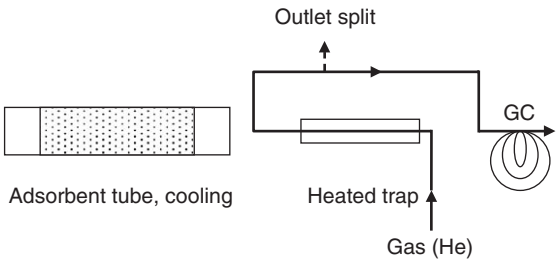

Fig. 3.5. Two-stage thermal desorption. Secondary desorption. The trap is rapidly heated in a stream of gas and the trapped analytes are transferred to the chromatographic column. The direction of the desorption gas flow is reverse that of the trap gas flow. Parts of the sample are usually split (outlet split) before the GC column.

There are also some limitations of the technique. Of course, the analytes of interest must be stable on the adsorbent and possible to desorb by heat. The selection of a suitable adsorbent is thereby most critical. TD cannot be used for compounds that are too unstable for conventional GC analysis. Inorganic gases can, with a few exceptions, not be analysed by TD. There is also an upper limit on how non-volatile the compounds can be; the technique is best investigated for VOCs, although also semi-VOCs, at least to some extent, can be analysed (this is partly depending on the analytical equipment). A general disadvantage of TD compared to solvent desorption has been that all sample is consumed in one analysis. It is not possible to re-analyse the sample if something fails during the analysis, or if it is desirable to analyse it under other analytical conditions. If the amount of collected sample is much higher than expected it can result in poor chromatography and an overloaded detector, which makes it impossible to correctly quantify the sample; it would have been necessary to split more of the sample before letting it into the GC. Correspondingly, a lower split can be needed if the collected amount is smaller than expected. Today, however, analytical equipment that can re-collect the sample that has been split after desorption and before entering the column is commercially available. Both the Markes' Unity^{TM} and the Perkin-Elmer TurboMatrix^{TM} 650 ATD allow sample split re-collection. If one does not have equipment with such facilities, it is wise to take at least duplicate samples, to have a spare sample if the analysis fails or if additional analyses are of interest.

If badge-type samplers (SKC-Ultra) or radial samplers (Radiello) are used, the adsorbent/diffusive sampling cartridge is put in a conventional stainless steel tube for TD before analysis, and analysed as conventional TD samplers. It is, however, important to take desorption time and flow into consideration when setting the parameters for TD of these samples. When performing diffusive sampling on tube-type samplers most of the analytes are adsorbed on the part of the adsorbent bed that is closest to the diffusion end of the tube. During desorption the flow direction through the tubes is reversed in relation to the direction of diffusion. This means that the adsorbed analytes in practice only pass a small part of the adsorbent bed during desorption. On the contrary, when the adsorbent is poured from the SKC-Ultra sampler or the Radiello cartridge is put into the tube for TD, the collected analytes are dispersed across the entire adsorbent surface inside the tube. Therefore, it might be necessary to increase desorption time and/or the desorption flow through the tube, compared with analysis of samples collected by

passive sampling on tube-type samplers, to ensure a complete desorption of the analytes.

3.7 ADSORBENTS

There are a large number of adsorbents available and many can be used in combination with TD. Selection of a suitable adsorbent for the analyte(s) of interest is one of the most important factors when developing a TD method. A strong adsorbent would generally give the best collection efficiency, but for best release during desorption a weak adsorbent is to be preferred. The choice of a suitable adsorbent for the purpose is therefore always a balance between these factors. A single adsorbent can never suit all compounds that could be desired to collect by passive sampling and analyse by TD–GC. In general, the more volatile the analyte in question, the stronger the adsorbent must be. But choosing the strongest possible adsorbent is not always the best alternative; a prerequisite is also that the adsorption is reversible by heating. Other necessary properties for making TD possible are that the adsorbent has a good thermal stability and is chemically inert. A low affinity for moisture and carbon dioxide is preferable, since these compounds are major constituents of air and might cause analytical problems if collected in large amounts.

The most commonly used adsorbent for TD is Tenax^{TM} TA, a polymer based on 2,6-diphenyl-*p*-phenyleneoxide, first described by van Wijk in 1970 [40]. It has been used in numerous studies and measurement activities over the years, both for assessment of workplace exposure, measurements in non-industrial indoor environments, sampling in ambient air and many other applications. It has been used both in studies of single compounds and for mixtures of analytes. Moisture is not retained by Tenax^{TM}, which is an important advantage of the adsorbent. Its major limitation is a poor retention for the most volatile compounds (a boiling point of 100°C is often considered an approximate guideline under which the adsorption of the compound on Tenax^{TM} is limited) and for alcohols and acids. The blank levels on Tenax^{TM} can be considered low for many applications, although there are a number of known oxidation products and other compounds present in the Tenax^{TM} blanks. Examples of such known artefacts are benzaldehyde, phenol, acetophenone, 2,6-diphenyl-*p*-benzoquinone and 2,6-diphenyl-*p*-hydroquinone [41,42].

Other much-used adsorbents are the Chromosorbs^{TM}, originally used as column packing material for chromatographic columns. Brown *et al.* [43] found Chromosorb^{TM} 106 (a cross-linked polystyrene

polymer) to be the best adsorbent for collection of a number of compounds, including benzene. One drawback of the Chromosorbs is their relatively low maximum desorption temperature, which makes them unsuitable for less volatile compounds. The blank levels are also considerably higher than for Tenax™ or carbon-based adsorbents, and this might cause problems when low concentrations of the compounds of interest are to be sampled and analysed. Although considered hydrophobic, it has a higher affinity for water than Tenax™, which might cause analytical problems when sampling under very humid conditions. If an FID is used, adsorbed water could, in a worst-case scenario, cause the flame in the detector to die and thereby ruin the analysis. One way to avoid such analysis failure for high-humidity samples might be to flush the tube with a small volume of helium before analysis (at room temperature). Flushing the tube in the reverse direction of sampling reduces the risk of losing the collected analytes.

Carbon-based adsorbents such as the graphitised carbon black adsorbent Carbopack™ B (similar adsorbents are Carbotrap™ or Carbograph™ 1TD) are also much used for TD. It has a higher surface area and exhibits higher adsorptive capacity than Tenax™ and is thermally stable at higher temperatures. It is often used for sampling the same kind of compounds that are sampled on Tenax™. Some studies have, however, shown an increased risk of breakdown on Carbopack™ B than on Tenax™, e.g., for terpenoid structures [77]. Carbopack™ C (similar to Carbotrap™ C and Carbograph™ 2TD) is a weaker adsorbent suitable for less volatile compounds. During recent years, another carbon-based adsorbent, Carbopack™ X, with high capacity for very volatile organic compounds (from C_3 to C_4), has been used and investigated [35,44–46]. It has been shown to be able to collect compounds such as 1,3-butadiene, which is of interest both in workplace and ambient air monitoring [35,45,46]. An adsorbent with a similar analyte range is Carbograph™ 5TD.

Porapak™ N is specifically designed for volatile nitriles, but is also stated to be suitable, e.g., pyridine and volatile alcohols (from ethanol). It has a comparatively low maximum desorption temperature and high artefacts levels. Porapak™ Q can be used for a wider range of volatiles, including oxygenated compounds, but has lower maximum desorption temperature and higher artefacts levels than Tenax™ and the carbon-based adsorbents.

For the most volatile compounds, various molecular sieves can be used as adsorbents. Molecular sieves do, however, have several drawbacks. They are hydrophilic, which makes them unsuitable to use in

humid conditions. They have high blank levels and are also easily and irreversibly contaminated by higher boiling compounds. Carbosieve™ SIII, Spherocarb™ and Unicarb™, which can be used for sampling many very volatile compounds, have been reported to have lower artefacts than the traditional molecular sieves. For all these adsorbents, and in particular for the molecular sieves, diffusive caps equipped with membranes to prevent water adsorption can be recommended.

Many adsorbents can be bought in several mesh sizes. A smaller mesh size gives a larger surface area, but also increases the risk of leakage of adsorbent through conventional sorbent retaining gauzes. This leakage might not be so much a sampling problem as an analysis problem, since leakage of small adsorbent particles into the desorption device can cause analytical problems in terms of leaking tubes that will not be desorbed. The carbon-based adsorbents are friable, which might also cause analytical problems. If such problems occur one way to at least partly overcome this can be to put a small amount of silanised glass wool in the back end (but *not* in the end that is open for passive sampling!) of the sampler. The most commonly used mesh sizes for TD is 20–40 or 60–80 mesh.

3.8 ANALYTICAL EQUIPMENT FOR THERMAL DESORPTION

There are several different analytical devices for automatic TD commercially available. Some devices are constructed for single tube desorption only. To perform larger studies, multiple tube desorption devices are most convenient. Perkin Elmer made the first multiple tube desorber, ATD 50, which was later developed into ATD 400. Today, Perkin Elmer offers a family of thermal desorbers with varying features, the TurboMatrix™ thermal desorbers, of which most models are 50-tube auto-samplers. The most advanced of them, the TurboMatrix™ 650 ATD, can re-collect the amount of sample vapour that is split in the outlet split mode. The sample can be re-collected either on the same or a new tube in the same tube magazine. Markes International Limited sells the Unity™ thermal desorber, which can be combined with their Ultra™ multi-tube auto-sampler for 100 tubes. With two Ultra™ auto-samplers (an Ultra™ 50:50 system) a quantitative re-collection of both inlet and outlet split for up to 100 tubes is possible. The Unity™ alone re-collects the sample from one tube. Gerstel sells the thermal desorber TDS-2, which can be combined with the auto-sampler TDS A for 20 sample tubes. All these devices are two-stage thermal desorbers, with electrically cooled secondary traps. Such traps offer practical advantages

over capillary cryo-focusing systems, in terms of eliminating the use of liquid cryogen consumption and having a low risk of ice formation, which can block the sample flow path through the trap.

3.9 APPLICATIONS USING PASSIVE SAMPLING–THERMAL DESORPTION–GAS CHROMATOGRAPHY FOR EXPOSURE ASSESSMENT; EXAMPLES AND TRENDS

Passive sampling in combination with TD–GC analysis was first applied to workplace monitoring. There are a large number of such applications published over the years, monitoring various VOCs. Passive sampling for occupational hygiene measurements have mostly concerned 8-h (full-shift) sampling, but there are also many examples of shorter sampling periods. Industrial monitoring usually involves comparatively high levels of the compounds to be sampled, and despite sampling rates in the range of 0.5 mL min^{-1} the TD technique is sensitive enough to facilitate sampling times often as short as 15–30 min. This can be valuable to monitor the exposure during short periods involving different work tasks. Workplace air monitoring will most certainly continue to be an important field for passive sampling–TD–GC analysis. It is well known that occupational exposures vary both within and between workers in a given occupational group [47,48]. A high variability implies the need for many measurements, thus it must be possible to collect data inexpensively. Passive sampling–TD–GC analysis fulfils the requirements to be a valuable tool for this purpose.

Another area in which passive sampling–TD–GC can be applied is monitoring chemical exposure in non-industrial indoor air [49–52]. Indoor air is a complex matrix to monitor; it contains a large number of various chemical compounds and the levels are low. This complexity makes it difficult if the aim is to correctly identify and quantify as many compounds as possible. ISO has published standards for sampling of VOCs in indoor air, both on general aspects of sampling strategy [53] and a standard for passive sampling of indoor/ambient/workplace air and subsequent TD-GC analysis [24]. Although sampling rates are reported for a number of compounds they are usually determined for occupational levels and 8-h sampling time. When performing passive sampling in non-industrial indoor air, significantly longer sampling times are usually needed to collect enough material for analysis. Published sampling rates might hence not be valid for these applications. Furthermore, for a majority of the compounds that would be collected when sampling in indoor air, there are no sampling rates published at all. Consequently, passive

sampling–TD–GC analysis of indoor air samples can often be considered semi-quantitative. It is common to quantify all compounds as toluene (toluene equivalents), and as sampling rates are unknown for many compounds semi-quantitative values can be obtained by using, e.g., the sampling rate for toluene for all compounds. Sampling rates for toluene for environmental monitoring have been published for various time periods, up to several weeks, and can be used for this purpose also in indoor air. Semi-quantitative values can be used, e.g., when comparing patterns of VOCs in problem and non-problem buildings, provided the samples have been compiled and treated the same way for all samples [52].

Multivariate methods for evaluation of complex VOC data, such as TD–GC–MS data from samples collected in non-industrial indoor air, have been shown to be a promising tool for evaluation of such samples [52,54,55,76]. These data evaluation techniques, which have been thoroughly described in the literature [56–61,76] are likely to gain much more attention in the future when it comes to questions such as classifications of problem and non-problem buildings and to track the possible sources for such problems. New analytical techniques, which make it possible to lock retention times and to make safer mass spectra interpretations, are now commercially available and these methods are still undergoing further development and refinement. This opens up the possibilities for more stable and reliable data and much less manual data pre-treatment than is necessary today when evaluating this kind of complex data. More importantly, however, this also facilitates analysing samples under stabilized conditions in different laboratories and to merge datasets from several laboratories into larger databases. Provided a number of other factors is fulfilled, relating to issues such as standardisation of classifications of problem and non-problem buildings, sampling procedures etc., it would be possible to get a large number of samples that could be evaluated by multivariate techniques. That opens possibilities for much better classifications and investigations of factors contributing to, e.g., health problems in buildings, factors that are generally valid for a large number of buildings.

An area gaining increasing interest using passive sampling–TD–GC techniques is environmental monitoring and assessing exposure of the general public to pollutants. Environmental monitoring implies sampling and analysis of trace levels. Passive sampling–TD–GC analysis is in many ways ideal for this purpose. However, the fact that the concentrations to be measured are low, the atmospheric conditions are very variable, places many demands on how to use the technique. The topic of environmental sampling is further treated in Chapters 2 and 6 of this book.

3.10 POSSIBLE LIMITATIONS/SOURCES OF ERROR WHEN USING PASSIVE SAMPLING–THERMAL DESORPTION–GAS CHROMATOGRAPHY

The risk of losses of sampled material due to back-diffusion (reverse diffusion) is an important problem that must not be overlooked when performing passive sampling. Especially for longer sampling times (many days/weeks), significant losses may occur.

Several studies have shown passive sampling rates that decrease over time [62]. This is caused by concentration gradients in the adsorbent bed. If the adsorbent layer closest to the orifice is saturated with the analyte, it acts as an additional diffusion barrier, which decreases the sampling rate compared to the initial or ideal rate. This leads to an underestimated air concentration of the analyte collected by the passive sampler. Attempts at theoretically calculating and adjusting for such effects have been published [62]. When diffusive sampling rates are experimentally determined the investigated sampling time should cover the time interval that is to be used later, to take time effects into consideration. Often different sampling rates are used for, e.g., sampling during 1 and 2 weeks.

Over the years, a large number of studies have compared active and passive sampling in the field, especially for monitoring various organic solvents in occupational environments. The results from these studies vary; some studies show no difference between active and passive sampling [32], while other studies indicate significant differences between the two sampling methods. Passive sampling has been reported to result in higher [63] as well as lower [64] levels of the analysed compounds. In a field validation of tube-type (Perkin Elmer) samplers for collection of monoterpenes in saw mills, Sunesson *et al.* [65] found a good agreement between active sampling on charcoal and diffusive sampling on Chromosorb^{TM} 106 for stationary samples, but the personal samples taken by diffusive sampling were lower (for Chromosorb^{TM} 106 on average 75% and for Tenax^{TM} TA 60% of the terpene levels received on charcoal) than the pumped samples. Terpene containing particles, which would be caught by active but not passive sampling, was suggested as one possible explanation to this 25% discrepancy. Another suspected reason for the discrepancy was that the construction of the diffusive sampler could have some limitations in its ability to correspond to the rapidly changing atmospheres the workers were exposed to. Such effects have been observed for various diffusive sampler designs, particularly when short concentration pulses occur [66]. A laboratory test was performed to elucidate

whether or not a rapidly changing atmosphere would have an impact on the uptake of the diffusive samplers where the terpene levels were varied between 5 and 600 mg m^{-3} in 30-min periods for in total 8 h. The agreement between pumped samples on charcoal and diffusive samples on Chromosorb^{TM} 106 was excellent, and it was concluded that the tube construction seems to be able to respond also to large fluctuations in concentrations of the compounds to be sampled.

Chien *et al.* [64] performed side-by-side active and passive sampling of various organic solvents in field studies in several occupational settings. Pumped sampling on charcoal was used as the active method and collection on Tenax^{TM} TA in tube-type diffusive samplers was the passive method. For all investigated compounds except for xylenes, statistically significant differences were obtained, especially for area sampling. The passive sampling–TD method gave lower concentrations in most cases. Possible causes for these discrepancies were discussed and presented as:

1. Influences from environmental factors. The sampling rates were determined in well-controlled environments and effects from various conditions encountered in the field and the potential interactions among them may not have been properly addressed. Air movements may occasionally have been too low to ensure proper diffusion behaviour.
2. The sampling rates are not unique. Between-system and within-system variations of sampling rates have been reported, and there are always uncertainties in the determined sampling rates.
3. Influences from non-theoretical adsorptive behaviour, which causes sampling rates to reduce over time and become non-constant. Tube-type samplers are more sensitive to this effect than badge-type samplers, because of their larger path-to-area ratio.
4. Interference from competitive adsorption among co-existing chemicals. Sampling rates are usually established in ''clean'' atmospheres, and possible effects of co-existing chemicals are thereby not taken into consideration. The atmospheres in which the compound of interest is collected in the field can, however, be of very varying compositions, and it would not be practically possible to experimentally adjust for a large number of interferences when determining sampling rates. Therefore field validations are important to find possible interaction effects and other factors contributing to sampling rates that differ from those determined in well-controlled laboratory atmospheres.

5. Contribution from aerosols. Passive samplers are in general designed to collect gases and vapours. So are many of the alternatively used active samplers for collection of organic compounds in air; e.g., the ''golden standard'' imposing pumped sampling on charcoal mainly collects gases and vapours and only to a minor extent aerosols. However, the active sampler, with a sampling rate of typically hundreds of mL min^{-1}, is more likely to collect aerosols than a diffusive sampler with a sampling rate of about 1 mL min^{-1}. If a considerable proportion of the analyte is present as aerosols, the active sampler would result in higher concentrations than the passive sampler. For a badge-type diffusive sampler (3M#3520) a contradictory effect of aerosols was proposed; aerosols settled on the passive sampler and the subsequent vaporization of the analyte (in this case styrene) was suggested to be the major contribution to the higher levels found by passive sampling in that study [63].

3.11 SELF-ASSESSMENT OF EXPOSURE

Passive samplers, easily worn on the lapel of the worker's shirt, are a prerequisite for self-assessment of exposure (SAE) [6–9]. Several attempts to involve workers or the general public in collecting exposure data have been published [6–8,67–73]. In these studies, the measurement procedures were delegated, to varying degrees, to the individual. In the studies by Liljelind *et al.* [6–8] members of the working population were required to perform personal measurements of the chemical exposure at their workplaces themselves, with only a short oral and written instruction. Their measurements were compared with samples taken by an occupational hygienist, to determine possible bias associated with SAE. The participating workers also personally received their results after each measurement. Furthermore, the workers and the management were also interviewed. Two issues were principally tested in the implementation of the self-assessment procedure; if the individual worker would develop a favourable attitude to the procedure, and what factors might influence the workers' and managers' readiness to perform measurements. [6,7]. The samplers used in these studies were tube-type passive samplers. Sunesson *et al.* have summarised the experiences from using this sampler as a tool for SAE in applications in occupational settings [9]. The most important conclusions are given below.

A passive sampler has to have some key features to be an effective tool for SAE. The sampler design has to be well suited for personal

sampling, in order to be practical, safe and reliable. It must be able to be stored both before and after sampling without risk of loss of analytes or contamination. Furthermore, analysis by TD is ideal for self-assessment studies, since the samplers are analysed without any time-consuming sample pre-treatment. Tube-type stainless steel samplers, packed with a suitable adsorbent, can fulfil these requirements.

Practically, the samplers can be put in a chest pocket or on the lapel of a shirt. The worker should open them at the start of the work shift and close them at the end of the shift. In some industries, workers occasionally wear respirators, and this must then be handled somehow in the sampling procedure. The ideal thing would be to wear the samplers inside the respirator, but this is usually not practically possible. If the samplers are worn outside the respirator, the worker can be requested to close the passive monitors during these periods and to record the time the samplers have been closed.

One critical part of the sampling procedure using tube-type samplers for diffusive sampling is to ensure a correct diffusion gap by putting the diffusion cap in the right position during sampling. The cap has to be pressed down as far as possible, but the construction can cause a resistance when putting the caps on and thereby a risk of not getting the cap as far down on the tube as it should be. Therefore, it is important to instruct people how to put the diffusion caps on correctly. If that is done, the studies by Liljelind *et al*. [7,8] showed that workers are able to handle the samplers as adequately as an expert; if there had been problems in handling the samplers this would have been revealed by large degrees of between sampler deviation, since each of the measurements was carried out using three sampling tubes in parallel. A comparison between the values of the tubes that had been handled by each worker himself/herself and the tubes that had been handled by the expert showed no difference in the distribution of the coefficients of variance between the tubes [6,9].

Further evaluation of the reliability of SAE was done by comparing exposure data (from benzene-exposed tanker drivers and styrene and monoterpene exposed industry workers) collected by self and expert assessments. The expert (an occupational hygienist) employed the same diffusive samplers and procedure that had been recommended for SAE, except that the expert was the one who chose the sampling day, handled the samplers and registered observations during the work shift. With one minor exception (in one out of six styrene handling factories), no statistically significant differences between self and expert assessments were observed. Thus, the results indicate that the workers themselves

are able to collect consistent and unbiased exposure data by employing currently state-of-the-art passive samplers, in this case tube-type samplers for subsequent TD analysis.

The workers and the managers of the companies participating in the SAE studies were also interviewed, to get more knowledge about the method as a general tool for exposure assessment. The questions concerned, among other things, the instructions given on performing the measurement and the presentation of the individual results after each measurement, to determine whether they were easy to understand or not. Other questions concerned the workers' and managers' opinions about SAE as a method for exposure control, if the measurements had caused any change in their work behaviour and the sustainability of the SAE programme [6,9,74]. A conclusion was that SAE demands not only a user-friendly sampler but also participating workers and managements. Basing an exposure-monitoring programme purely on voluntary measurements by workers is unlikely to succeed in establishing a long-term assessment programme. To make SAE a sustainable part of the companies' work environment programmes, a strong organisational support seems to be needed. If that is achieved, self-assessment of chemical exposure by using passive samplers in the industry in general and in small- and medium-sized enterprises in particular has several advantages and a potential of providing a strong tool for control and improvement of the work environment.

3.12 PRACTICAL CONSIDERATIONS

3.12.1 Selecting a suitable adsorbent for the analytes of interest

There are two obvious and basic issues that determine the selection of adsorbents for passive monitoring. The first is to find an adsorbent that quantitatively retains the analyte(s) to be collected, without significant losses due to back diffusion for the sampling time that is of interest. Secondly, the analytes have to be quantitatively desorbed from the adsorbent. Quite often more than one adsorbent could be considered suitable for the given application. If well-validated data on sampling rates are available for one adsorbent, it saves much time to choose that adsorbent, compared to perform own evaluations of sampling rates. If trace levels are to be collected, the level of artefacts on the adsorbent is also a key issue.

When sampling a mixture of compounds with various volatilities it is sometimes necessary to use more than one adsorbent. The different

adsorbents should be packed in different tubes, appropriately conditioned and exposed simultaneously in parallel. The analysis parameters have to be adjusted individually for the different adsorbents. Multisorbent tubes, containing several adsorbents packed in series in the tube, with increasing adsorption strength from the sampling end, are not recommended for diffusive sampling.

3.12.2 Minimising artefacts

Samplers should always be stored and handled in as clean environments as possible, to minimise the levels of artefacts that are collected/built up on the adsorbent. Minimising artefacts is very important when performing passive sampling for subsequent TD analysis, and in particular when sampling trace levels (e.g., in non-industrial indoor environments or for environmental applications). Conditioned or sampled tube-type samplers should always be equipped with 0.25-in. brass Swagelok-type screw caps fitted with polytetrafluoroethylene (PTFE) ferrules for storage. These should be tightened by hand plus an additional quarter turn using a wrench or a similar tool. However, if the tubes get cold (either during transportation or because they are put in a refrigerator) they have to be further re-tightened to be really tight. Normally, it is better to store the tubes at room temperature than in a refrigerator, both because the screw caps get loose when the tubes get cold (because of difference in thermal properties of brass and stainless steel) and because the air in refrigerators is often contaminated. If it can be expected that the tubes might get cold during, e.g., transportation, the capped tubes should be cooled and then further re-tightened before they are shipped. As an extra security to avoid contamination when monitoring trace levels, the capped tubes can be wrapped in uncoated aluminium foil and/or put in a sealed, uncoated glass or metal container during storage and transportation. A small amount of charcoal can be kept in the storage container to minimise the levels of trace organic compounds in the storage air.

The samplers should always be conditioned before use. The conditioning temperature should be higher than the desorption temperature, but one has to make sure that the maximum temperature of the adsorbent is not exceeded. Conditioning is done in a stream of inert gas, and care should be taken to flush the tubes long enough to eliminate all oxygen in the tube before heat is applied, to prevent the formation of oxidation products. After conditioning, the tubes (or at least a selection of the tubes) should be desorbed under analytical conditions to ensure

that the levels of artefacts are low enough for the sampling activity they are to be used for.

The outside of the sampling tubes should be kept as clean as possible. The tubes or caps should never be marked, e.g., with pens or sticky labels; every tube has an individual identification tag imprinted on it. If other physical labels for some reason have to be attached to the sample, they have to be affixed on the samplers without any glue and the label material should be as low emitting as possible.

3.12.3 Blank samples

Blank samples should be used and analysed for all kinds of sampling campaigns. They should be prepared simultaneously and in the same way as the samplers to be used for monitoring. Often, both laboratory and field blanks should be analysed. Laboratory blanks are kept in the laboratory after conditioning and are analysed to control tube conditioning, possible blank build-up etc. Even more important is the use of field blanks. They should be transported with the tubes used for monitoring, and treated at the sampling site just as the samplers used for monitoring, except for the sampling itself. They provide important information, e.g., on possible artefacts due to handling, storage and transportation of the samplers. It is advisable to analyse blank tubes in the same analytical sequence as the sample tubes.

3.12.4 Personal (individual) exposure assessment

When performing personal sampling, the sampling tube should be put in the breathing zone of the person. In practise, this is usually accomplished by putting the tubes in, e.g., a breast pocket or on the lapel of a shirt. Care must be exercised to make sure that no clothes or other objects somehow cover the diffusion cap and thereby restrict the diffusion area.

If workers or the general public are to handle the tubes themselves during sampling (self-assessment) it is very important to instruct the people how to put on the diffusion caps correctly, to ensure a correct length of the diffusion path. It is also important to give instructions on how to close the tubes subsequent to sampling termination.

The back end of the sampling tube is closed with Swagelok screw caps also during sampling. For personal sampling, and especially if several samples are taken in parallel, it could be worth buying aluminium screw caps for that end of the tube. Aluminium caps are

more expensive than brass caps, but they make the tubes considerably lighter to carry.

3.13 CONCLUDING REMARKS AND FUTURE PERSPECTIVES

Passive sampling in combination with TD–GC is in many aspects an ideal method for exposure assessment. It is easy to handle both during sampling and analysis and its simplicity and sensitivity makes it very useful for large surveys in both workplace, indoor and environmental applications. The general public and workers can, if given proper instructions, perform the sampling procedure themselves in a correct way. This is ideal also for, e.g., monitoring workplace air in small enterprises, which often do not have access to own trained personnel to perform the monitoring procedure. Many compounds that are today collected and analysed by active sampling–solvent desorption could be monitored using passive sampling–TD. When more sampling rates are published for various VOCs the passive sampling–TD technique is likely to become even more popular.

The utmost used sampler for passive sampling–TD analysis today is stainless steel tube-type samplers. They are likely to keep their popularity, but new, alternative sampler designs constructed to give a considerably higher sampling rate are likely to gain much interest in the future.

REFERENCES

1 V.E. Rose and J.L. Perkins, *Am. Ind. Hyg. Assoc. J.*, 43 (1982) 605.
2 M. Harper and C.J. Purnell, *Am. Ind. Hyg. Assoc. J.*, 48 (1987) 214.
3 A. Berlin, R.H. Brown and K. Saunders (Eds.), *Diffusive Sampling—An Alternative Approach to Workplace Air Monitoring*, Royal Society of Chemistry, London, 1987.
4 T. Kauppinen, *Scand. J. Work Environ. Health*, 22 (1996) 401.
5 G.L. Nothstein, R.M.A. Hahne and M.W. Spence, *Am. Ind. Hyg. Assoc. J.*, 61 (2000) 64.
6 I.E. Liljelind, PhD Thesis, Umeå University, Sweden, 2002.
7 I.E. Liljelind, A. Strömbäck, B.G. Järvholm, J.-O. Levin, B.L. Strangert and A.-L. Sunesson, *Appl. Occup. Environ. Hyg.*, 15 (2000) 195.
8 I.E. Liljelind, S.A. Rappaport, J.-O. Levin, A. Strömbäck, A.-L.K. Sunesson and B.G. Järvholm, *Scand. J. Work Environ. Health*, 27 (2001) 27.

9 A.-L. Sunesson, J.-O. Levin, M. Sundgren, I. Liljelind and A. Petterson-Strömbäck, *J. Environ. Monit.*, 4 (2002) 706.
10 E.D. Palmes and A.F. Gunnison, *Am. Ind. Hyg. Assoc. J.*, 34 (1973) 78.
11 A. Fick, *Pogg. Ann.*, 94 (1855) 59.
12 E.N. Fuller, P.D. Schettler and J.C. Giddings, *Ind. Eng. Chem.*, 58 (1966) 19.
13 G.A. Lugg, *Anal. Chem.*, 40 (1968) 1072.
14 N. van den Hoed and O.L.J. van Asselen, *Ann. Occup. Hyg.*, 35 (1991) 273.
15 E. Nordstrand and J. Kristensson, *Am. Ind. Hyg. Assoc. J.*, 55 (1994) 935.
16 UK Health & Safety Executive: MDHS 80: Volatile Organic Compounds in Air—Laboratory Method Using Diffusive Solid Sorbent Tubes, Thermal Desorption and Gas Chromatography. HSE, London, UK, 1995.
17 B. Tolnai, A. Gelencsér, C. Gál and J. Hlavay, *Anal. Chem. Acta*, 408 (2000) 117.
18 EN 838: European Standard Protocols for Diffusive Samplers. European Committee for Standardization (CEN) (1995).
19 EN 13528-1: Ambient air quality—Diffusive samplers for the determination of concentration of gases and vapours—Part 1: General requirements. European Committee for Standardization (CEN) (2003).
20 EN 13528-2: Ambient air quality—Diffusive samplers for the determination of concentration of gases and vapours—Part 2: Specific requirements and test methods. European Committee for Standardization (CEN) (2003).
21 EN 13528-3: Ambient air quality—Diffusive samplers for the determination of gases and vapours—Part 3: Guide for the selection, use and maintenance. European Committee for Standardization (CEN) (2003).
22 EN 14662-4 (2005)
23 ISO 16017-1 (2003)
24 ISO 16017-2 (2003)
25 25 ISO 16107 (1999)
26 ISO 16000-6 (2004)
27 US Environmental Protection Agency: TO-1, Method for the Determination of Volatile Organic Compounds in Ambient Air Using Tenax Adsorption and Gas Chromatography/Mass Spectrometry (GC/MS). EPA, Washington DC, 1984.
28 US Environmental Protection Agency: TO-17, Determination of Volatile Organic Compounds in Ambient Air Using Active Sampling onto Sorbent tubes. EPA, Washington DC, 1997.
29 National Institute for Occupational Safety and Health: Method 2549: Volatile organic Compounds. In: *NIOSH Manual of Analytical Methods*, 4th ed. NIOSH, Washington DC, 1996.
30 ASTM Method D6196-03.

31 UK Health & Safety Executive: MDHS 27: Protocol for the Evaluation of Diffusive Samplers. HSE, Sheffield, U.K., 1994.
32 R.H. Brown, K.J. Saunders and K.T. Walkin, *Am. Ind. Hyg. Assoc. J.*, 48(9) (1987) 760.
33 *Diffusive Monitor* 8 (1996) 14–16.
34 Markes International Limited, Thermal desorption technical support, Note 1. http://www.markes.com
35 B. Strandberg, A.-L. Sunesson, K. Olsson, J.-O. Levin, G. Ljungqvist, M. Sundgren, G. Sällsten and L. Barregard, *Atmos. Environ.*, 29 (2005) 4101.
36 P. Bruno, M. Caputi, M. Caselli, G. de Gennaro and M. de Rienzo, *Atmos. Environ.*, 39 (2005) 1347.
37 V. Cocheo, C. Boaretto and P. Sacco, *Am. Ind. Hyg. Assoc. J.*, 57 (1996) 897.
38 Markes International Limited, Thermal desorption technical support, Note 42. http://www.markes.com
39 N. Yamamoto, T. Matsubasa, N. Kumagai, S. Mori and K. Suzuki, *Anal. Chem.*, 74(2) (2002) 484.
40 R. van Vijk, *J. Chromatogr. Sci.*, 8 (1970) 418.
41 X.-L. Cao and C.N. Hewitt, *Environ. Sci. Technol.*, 28 (1994) 757.
42 P.A. Clausen and P. Wolkoff, *Atmos. Environ.*, 31 (1997) 715.
43 R.H. Brown, *Analyst*, 121 (1996) 1171.
44 K. Dettmer, Th. Knobbloch and W. Engewald, *Fresenius J. Anal. Chem.*, 366 (2000) 70.
45 N.A. Martin, D.J. Marlow, M.H. Henderson, B.A. Goody and P.G. Quincy, *Atmos. Environ.*, 37 (2003) 871.
46 N.A. Martin, P. Ducksworth, M.H. Henderson, D.J. Marlow and B.A. Goody, *Diffusive Monitor*, 14 (2003) 4.
47 H. Kromhout, E. Symanski and S.M. Rappaport, *Ann. Occup. Hyg.*, 17 (1993) 253.
48 S.M. Rappaport, H. Kromhout and E. Symanski, *Am. Ind. Hyg. Assoc. J.*, 54 (1993) 654.
49 V.M. Brown, D.R. Crump and D. Gardiner, *Environ. Technol.*, 13 (1992) 367.
50 V.M. Brown, D.R. Crump, D. Gardiner and C.F. Yu, *Environ. Technol.*, 14 (1993) 771.
51 B. Glas, J.-O. Levin, B. Stenberg, H. Stenlund and A.-L. Sunesson, *Anal. Environ. Epidemiol.*, 14(Suppl 1) (2004) S49.
52 A.-L. Sunesson, I. Rosén, B. Stenberg and M. Sjöström, *Indoor Air*, 16 (2006) 383.
53 ISO 16000-1 (2004).
54 J. Ten Brinke, S. Selvin, A.T. Hodgson, W.J. Fisk, M.J. Mendell, C.P. Koshland and J.M. Daisey, *Indoor Air*, 8 (1998) 140.

55 L. Pommer, J. Fick, J. Sundell, C. Nilsson, M. Sjöström, B. Stenberg and B. Andersson, *Indoor Air*, 14(1) (2004) 16.
56 L. Eriksson, E. Johansson, N. Kettaneh-Wold J. Trygg, C. Wikström, and S. Wold, Multi- and Megavariate Data Analysis—Principles and Applications, Umetrics AB, 2006.
57 J.E. Jackson, *A User's Guide to Principal Components*, Wiley, New York, 1991.
58 J.F. MacGregor and T. Kourti, *Control Eng. Practice*, 3 (1995) 403.
59 S. Wold, K. Esbensen and P. Geladi, *Chem. Intel. Lab. Syst.*, 2 (1987) 37.
60 S. Wold, M. Sjöström, L. Eriksson, PLS in Chemistry. In: P.v.R. Schleyer, N.L. Allinger, T. Clark, J. Gasteiger, P.A. Kollman, H.F. Schaefer III and P.R. Schreiner (Eds.), *The Encyclopedia of Computational Chemistry*, Wiley, Chichester, (1999, 2006).
61 S. Wold and M. Josefson, *Multivariate Calibration of Analytical Data.* In: R.A. Meyers (Ed.), *Encyclopedia of Analytical Chemistry*, Wiley, Chichester, 9710–9736.
62 S. Batterman, T. Metts and P. Kalliokoski, *J. Environ. Monit.*, 4 (2002) 870.
63 R.T. Dobos, *Appl. Occup. Environ. Hyg.*, 15 (2000) 673.
64 Y.-C. Chien, L.-J. Wu and J.-H. Lwo, *Appl. Occup. Environ. Hyg.*, 18 (2003) 368.
65 A.-L. Sunesson, M. Sundgren, J.-O. Levin, K. Eriksson and R. Carlson, *J. Environ. Monit.*, 1 (1999) 45.
66 D.L. Bartley, G.J. Deye and M.L. Woebkenberg, *Appl. Ind. Hyg.*, 2 (1987) 119.
67 D.P. Loomis, H. Kromhout, L.A. Peipins, R.C. Kleckner, R.I. Iriye and D.A. Savitz, *Appl. Occup. Environ. Hyg.*, 9 (1994) 49.
68 L. Saarinen, M. Hakkola, K. Pekari, K. Lappalainen and A. Aitio, *Intern. Arch. Occup. Environ. Health*, 71 (1998) 143.
69 S.M. Rappaport, M. Weaver, D. Taylor, L. Kupper and P. Susi, *Ann. Occup. Hyg.*, 43 (1999) 457.
70 P. Susi, M. Goldberg, P. Barnes and E. Stafford, *Appl. Occup. Environ. Hyg.*, 15 (2000) 26.
71 R. Lindahl, J.-O. Levin and B. Järvholm, In: *Proceedings of Indoor Air '99*, Vol. 4, (1999), 453pp.
72 P.P. Egeghy, R. Tornero-Velez and S.M. Rappaport, *Environ. Health Perspect.*, 108 (2000) 1195.
73 P.P. Egeghy, L. Nylander-French, K.K. Gwin, I.H. Picciotto and S.M. Rappaport, *Ann. Occup. Hyg.*, 46 (2002) 489.
74 A. Strömbäck-Pettersson, *Arbete och Hälsa*, 10 (2001) 67–68.
75 R.H. Brown, J. Charlton and K.J. Saunders, *Am. Ind. Hyg. Assoc. J.*, 42(12) (1981) 864.

76 S. Wold, C. Albano, W.J. Dunn, U. Edlund, K. Esbensen, P. Geladi, S. Hellberg, E. Johansson, W. Lindberg and M. Sjöström, *Multivariate Data Analysis in Chemistry*. In: B.R. Kowalski (Ed.), *Chemometrics: Mathematics and Statistics in Chemistry*, D. Reidel Publishing Company, Dordrecht, Holland, 1984.
77 A.-L. Sunesson, C.-A. Nilsson and B. Andersson, *J. Chromatogr. A*, 699 (1995) 203.

Chapter 4

Use of permeation passive samplers in air monitoring

Bożena Zabiegała and Jacek Namieśnik

4.1 INTRODUCTION

Passive sampling is now a well-established method to monitor pollution of air, especially indoor air [1–3]. Passive monitoring is generally characterized by the same accuracy as active monitoring, but an expensive sampling pump is not needed, which is very advantageous. Passive sampling offers considerable potential as a monitoring tool, especially for multi-point sampling over large, remote areas [2]. The only disadvantage of permeation passive samplers seems to be relatively low sampling rates, which requires long sampling times in environments with low pollutant concentrations and the necessity to calibrate passive samplers for each substance due to distinguishing membrane characteristics [4]. However, long sampling times at low concentrations can also be viewed as an advantage of the permeation passive sampling, as it makes it easy to determine time-weighted average (TWA) concentrations of analytes. In the overall assessment of the pollutant impact on human health, TWA concentrations are more useful than short-term concentrations, as they reflect the long-term exposure to these compounds. Permeation samplers, collecting gaseous pollutants at a rate controlled by permeation through a non-porous membrane, offer unique advantages, including effective moisture elimination and small sensitivity to air currents and temperature variations. In the case of indoor air quality measurements, they have the additional advantage of being much more acceptable by the inhabitants of the monitored areas compared to standard techniques based on dynamic sampling using sorption tubes.

Comprehensive Analytical Chemistry 48
R. Greenwood, G. Mills and B. Vrana (Editors)
Volume 48 ISSN: 0166-526X DOI: 10.1016/S0166-526X(06)48004-1

4.2 THEORY

Permeation passive samplers are taking samples of gaseous pollutants from the atmosphere, at a rate controlled by permeation through a membrane; they do not involve active movements of the air through the samplers. A schematic diagram of sample collection by a permeation passive sampler is shown in Fig. 4.1.

To collect analytes from an air sample, samplers are exposed to the ambient environment and they collect analyte molecules reaching the collecting medium following their permeation through a non-porous membrane [3,5]. The driving force for the molecular transport is the difference in chemical potential of the analyte on both sides of the barrier. This difference arises when analyte molecules are trapped by the collecting medium, which results in a concentration or vapour-pressure gradient across the barrier. An ideal collecting medium has 100% collection efficiency. As a consequence, analyte concentration near the surface of the medium is maintained close to zero during the entire sampling period [3].

Diffusional mass transfer across a membrane can be described by Fick's first law of diffusion [3,6–8]. The mass m, of the analyte transported by diffusion in time t, when the concentration gradient is linear and the collection efficiency is 100%, can be described by the following relationship:

$$m = Ut = \frac{SA}{l_{\mathrm{M}}} p_1 t \tag{4.1}$$

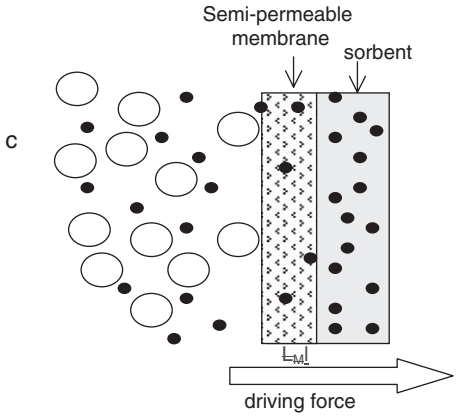

Fig. 4.1. Schematic diagram of sample collection by a permeation passive sampler (l_{M} is a membrane thickness and c is analyte concentration near the outer membrane surface).

where U is the diffusive transport rate ($\mathrm{mol\,s^{-1}}$), S is permeability coefficient of a given analyte ($\mathrm{cm^2/min}$), A is the cross-section area of the diffusion path ($\mathrm{cm^2}$), l_M is membrane thickness (cm) and p_1 is partial pressure of the analyte near the external membrane surface (Pa).

Partial pressure of the analyte at a given temperature can be easily converted to its mass concentration in air using the ideal gas law equation:

$$p_0 = \frac{n}{V}RT = aC_0 \tag{4.2}$$

where R is the universal gas constant ($\mathrm{J\,mol^{-1}\,K^{-1}}$), T is temperature (K), $a = RT/\mathrm{MW}$; MW is the molecular weight of the analyte ($\mathrm{kg\,mol^{-1}}$); C_0 is analyte concentration near the outer membrane surface ($\mathrm{kg^{-1}}$).

At a constant temperature, S, A, a and l_M are constants, and can be replaced by:

$$\frac{1}{k} = \frac{SAa}{l_\mathrm{M}} \tag{4.3}$$

where k is the so-called calibration constant. This constant describes the rate at which the analyte is collected from the air. In the passive sampling literature, the parameter $1/k$ is also referred to as a sampling rate S_R ($\mathrm{m^3\,s^{-1}}$). Thus, concentration of the analyte can be determined once m and t are known, using the relationship:

$$C_0 = \frac{mk}{t} \tag{4.4}$$

The response time of permeation passive samplers is determined by the rate of analyte transport through permeation barrier, which in turn, depends on the magnitude of the diffusion coefficient of the analyte in the material of the barrier (the semi-permeable membrane). For permeation passive sampler the response time is defined as:

$$t_\mathrm{R} = \frac{l_\mathrm{M}^2}{6S} \tag{4.5}$$

where t_R is the residence time (s) of a compound in the permeation zone.

If the membrane of permeation passive samplers is thin enough ($\sim$100 μm), the response time is typically in the order of seconds. Thus, it is negligibly small compared to overall sampling time (typically weeks).

Temperature is also an important parameter in permeation passive sampling. However, the effect of temperature on sampling rate is much smaller for permeation passive samplers than for diffusive samplers.

The temperature dependence of the permeability coefficient, S, can be described by the relationship:

$$S = S^0 \exp\left(-\frac{E_P}{RT}\right) \tag{4.6}$$

$$E_P = \Delta H + E_D \tag{4.7}$$

where S^0 is the standard permeability coefficient and E_P is the activation energy for permeation ($J\,mol^{-1}$), which is the sum of the heat of solution of the analyte in the membrane material (ΔH) ($J\,mol^{-1}$) and the activation energy for diffusion (E_D) ($J\,mol^{-1}$). Since E_D is typically small ($\leqslant 41.9\,kJ\,mol^{-1}$), either a very weak or virtually no temperature dependence of the sampling rate is usually observed in the ambient temperature range.

4.2.1 Membrane

In general, the membrane is a selective barrier that permits the separation of certain species by a combination of sieving and sorption diffusion mechanism. It can selectively separate components over a wide range of particle sizes and masses. In the case of permeation passive samplers, the non-porous membrane constitutes a diffusive barrier for analyte transport and defines the rate at which analyte molecules are collected at a given concentration, which is crucial for quantitative analysis [4,9]. The membrane of permeation passive samplers should eliminate or minimize the effect of external factors (such as the velocity of the sampled medium at the face of the sampler, humidity and temperature) on the sampling rate, thus, the material it is made of should meet specific requirements:

- It should be characterized by a high overall mass transfer coefficient for analytes of interest. The coefficient determines the concentration drop within the membrane. Permeation rates through a thick membrane made of the material characterized by a high mass transfer coefficient and through a thin membrane with a low coefficient can be quite close.
- It should be selective with respect to various compounds present in sampled air.
- It should be hydrophobic and hence poorly permeable for water vapour. In case of hydrophobic membranes, permeation rates do not depend on the humidity of the sampled air since water does not penetrate the membrane and hence it does not affect membrane

properties. Moreover, with very hydrophobic membranes, sorbents with high water affinity can be used to trap analytes without the risk of excessive water absorption.
- It should be homogenous so that permeation rates for samplers used in replicate measurements were not different.

Membranes are made of various polymer materials. Polydimethylsiloxane (PDMS) has been proven to have the best performance, therefore, is the material of choice for permeation passive samplers.

The process of permeation of analytes through a membrane can be described by a three-step solution-diffusion mechanism [10]:

- Sorption of the analyte on the surface of the membrane.
- Dissolution in the membrane material and diffusion of the dissolved analyte through the membrane. Dissolution is governed by the solubility of the analyte in the membrane material.
- Desorption of the analyte on the opposite side of the membrane. In order to extract effectively the analyte from the membrane into the sorption medium and to obtain high recoveries, the analyte distribution ratio between the membrane and the sorption medium should be small.

When analyte flux obeys Fick's law, permeability of a polymer is given by [7,10]:

$$P = \frac{Nl_{\mathrm{M}}}{p_0 - p_1} = \left(\frac{C_0' - C_1'}{p_0 - p_1}\right)\bar{D} \tag{4.8}$$

where N is the steady-state analyte flux through the polymer ($\mathrm{kg\,cm^{-2}.min}$), p_0 is analyte partial pressure near the outer surface of the membrane, p_1 is the analyte partial pressure near the inner surface of the membrane (Pa), C_0' is the analyte concentration in the polymer at the outer surface of the membrane (Pa), C_1' is its concentration in the polymer at the inner surface of the membrane and $\bar{D}$ is concentration-averaged diffusivity ($\mathrm{cm^2\,min^{-1}}$).

When p_1 is much lower than p_0 (which is normally the case for passive samplers, as the sorbent in the sampler should trap the analyte molecules quantitatively), the term in parentheses in e.g. Eq. (4.8) becomes C_0'/p_0, which is the analyte solubility coefficient S at pressure p_0. Consequently, Eq. (4.8) can be rewritten as:

$$P = S\bar{D} \tag{4.9}$$

At the same time, for rubbery polymers with liquid-like properties (such as PDMS), the term C'_0/p_0 is equivalent to Henry's law constant K_H of an analyte between polymer and air, which can be converted to the dimensionless Henry's constant K'_H:

$$K'_H\left(\equiv\frac{1}{K}\right)=K_H\frac{RT}{MW} \tag{4.10}$$

where K is the gas–membrane partition coefficient.

According to Eq. (4.9), the permeation rate is controlled by the combination of analyte solubility in the membrane material and its diffusivity within the membrane. The solubility at constant operating conditions (temperature, pressure and composition) is mainly a function of analyte condensability, which can be characterized for example by the normal boiling point temperature [10]. Diffusivity is inversely related to the size of the molecule. Larger molecules are typically more condensable, which leads to a trade-off in the overall magnitude of the permeability coefficient. However, the liquid-like matrix of PDMS has a poor ability to sieve molecules based on their size, therefore differences between the permeability coefficients of different molecules are mostly governed by the differences in their solubility in PDMS [10]. The solubility, in turn, determines the magnitude of the partition coefficient between the air and the membrane material. Consequently, permeability through the membrane is often described by the following equation [11]:

$$P=D_e\frac{K}{l_M} \tag{4.11}$$

where D_e is the effective diffusion coefficient of the analyte in the membrane material and K is the partition coefficient of the analyte between the membrane material and ambient air.

Often, effective diffusion coefficients of the analytes in the membrane material are unavailable; therefore, the analyte permeability has to be determined experimentally for each individual analyte (because the membrane of the permeation passive sampler has a well-defined surface area, the permeability is typically expressed through the calibration constant k—see Eq. (4.3)). This requirement constitutes the most important drawback of permeation passive samplers. Only target analytes, for which the calibration constants were determined in advance in model experiments, can be quantified using this technique.

4.3 DESIGN OF THE PERMEATION PASSIVE SAMPLER

Permeation passive samplers are most often badge type, although tube-type designs are also used. The badge design is dedicated by the need to have a large surface area of the membrane in order to achieve a high effective sampling rate. Air velocity has virtually no effect on the sampling rate of permeation passive samplers because permeability constants of analytes are several orders of magnitude lower than their diffusion coefficients in air (the resistance to mass transfer in the permeation membrane (l_M) is much higher than that in the stagnant boundary layer of air (l_B) at the surface of the sampler ($l_B/D_a \ll l_M/D_eK$). Consequently, analyte depletion in the vicinity of the sampler does not occur even in stagnant air. An example of badge-type permeation passive sampler using a bed of granulated sorbent as the collecting medium is a sampler designed at Gdansk University of Technology (GUT) [12,13]. The design is shown in Fig. 4.2. The GUT sampler is machined of polyamide. The sampler is equipped with PDMS membrane of 50-μm thickness (the sampling area of the permeation passive sampler is around 6 cm^2). Active carbon is used as the receiving phase (~300 mg of active carbon; 40–60 mesh, specific surface area of 1500 $m^2\,g^{-1}$).

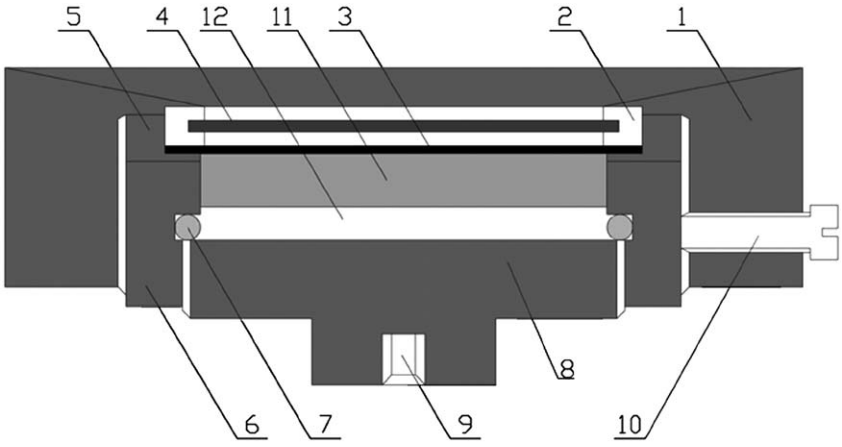

Fig. 4.2. Design of GUT permeation passive samplers. Key: 1, screw cap; 2, protective screen mount; 3, PDMS membrane of 50 μm thickness; 4, protective stainless steel screen; 5, washer; 6, main body; 7, O-ring; 8, plug; 9, opening for a screw-in holder; 10, set screw; 11, active carbon; 12, glass wool.

4.4 CALIBRATION OF GUT PERMEATION PASSIVE SAMPLERS

In order to relate the amount of analyte collected by a passive sampler to its TWA concentration in the air, the calibration constant of the sampler for a given analyte must be known. In addition, all parameters affecting the uncertainty of the final result such as temperature, humidity and air velocity should be defined. However, the uncertainty of determination of the analyte concentration by permeation passive samplers is affected mainly by the uncertainty in determination of calibration constants k. Parameters affecting the determination of the analyte concentration by permeation passive samplers are illustrated as a cause-and-effect diagram in Fig. 4.3 [14–16].

Consequently, calibration of the samplers is very important, as it determines the accuracy and reliability of further measurement results [12,13,17].

The membrane of the permeation passive sampler has a well-defined surface area, which is mandatory for quantitative measurements. The calibration constants k for target analytes can be determined from Eq. (4.4) by exposing the samplers to known, constant concentrations of these analytes in a standard gas mixture for known periods of time [12,13]. Each sampler has to be calibrated individually for each individual target compound, with replicate experiments carried out for each exposure time [9,12,16,18,19]. Assuming that the permeation rate of a given analyte through the membrane remains constant for a constant analyte concentration in the standard gas calibration mixture, the plots of the amount of analyte trapped by collecting medium vs. exposure time should be linear. The calibration constants k can be found from the reciprocals of the slopes of these lines (plotted individually for each compound) divided by the mean concentration of analyte in the gas calibration mixture. Examples of the calibration constants determined in model experiments for selected volatile organics belonging to four homologous series (n-alkanes, aromatics, n-alcohols and acetic acid esters of n-alcohols) are presented in Table 4.1.

4.5 DETERMINATION OF THE CALIBRATION CONSTANTS OF GUT PERMEATION PASSIVE SAMPLERS WITH SILICONE MEMBRANES BASED ON PHYSICO-CHEMICAL PROPERTIES OF THE ANALYTES

Air may contain a large number of organic compounds, and their composition may change over time [20–23]. Consequently, the need to

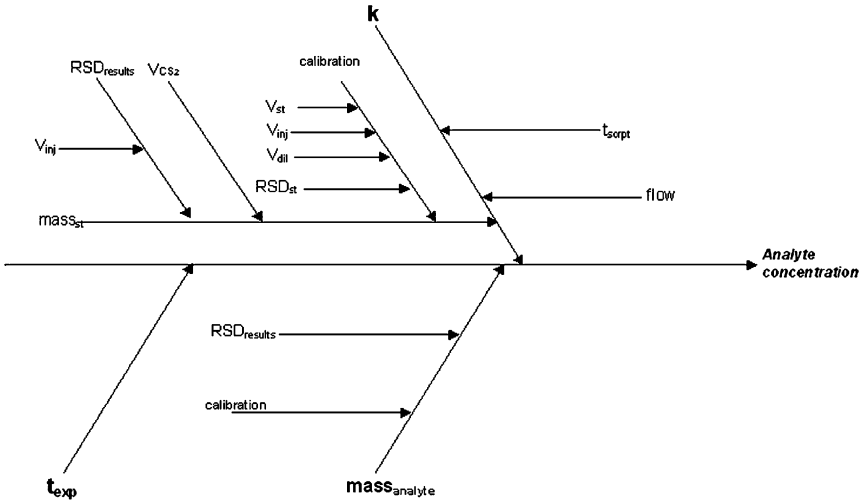

Fig. 4.3. The cause-and-effect diagram for the parameters affecting the determination of the analyte concentration in air by permeation passive samplers. k: calibration constant of the permeation passive sampler; $\text{mass}_{\text{analyte}}$: mass of the analyte trapped on the sorption bed of the passive sampler, determined chromatographically; t_{exp}: sampler exposure time; mass_{st}: chromatographically determined mass of analyte standards; flow: flow rate of the standard gas mixture; t_{sorpt}: exposure time of the passive sampler in the calibration chamber; $\text{RSD}_{\text{results}}$: relative standard deviation of the determination of analyte mass trapped on the sorption bed (depends on the uncertainty of the injection volume (V_{inj})), uncertainty of carbon disulfide volume (V_{CS2}) and the calibration of the GC–FID system (cal) (depends on the uncertainty of the injection volume (V_{inj}), uncertainty of the volume of the standard in the calibration mixture (V_{st}), uncertainty of the dilution of the calibration mixture (V_{dill}) and relative standard deviation of standard injection (RSD_{st})). Uncertainty of the mass of the analyte trapped by the passive samplers depends on the uncertainty of the calibration of the GC–FID system (cal) and the relative standard deviation of determination of the mass of the analyte trapped by the sorption bed ($\text{RSD}_{\text{results}}$). Reproduced from Ref. [16] with permission from Elsevier.

calibrate permeation passive samplers for each individual target compound is the single biggest obstacle in the widespread adoption of these samplers for air sampling. Experimental determination of the individual calibration constants k of permeation passive samplers is time-consuming and costly.

Equation (4.9) indicates that permeability of a compound through a polymeric membrane depends on the solubility and diffusivity of the chemical in the membrane material [10,13,16]. Since diffusivity in the PDMS polymer depends only weakly on the structure of a compound,

TABLE 4.1

Calibration constants k and the statistical parameters of the calibration curves (standard deviations of the regression coefficients of the calibration constant, the slope and the intercept (s_k, s_b and s_a) and the linear correlation coefficients r) ($y = bx+a$), where y is the amount of analyte trapped by collecting medium and x is exposure time

Compounds	$k \pm s_k$ (min mL^{-1})[a]	$b \pm s_b$ (min mL^{-1})	$a \times 10^{-3} \pm s_a$ (mL)	Correlation coefficient r ($n = 36$)
n-Pentane	0.217 ± 0.017	4.61 ± 0.17	−4.8 ± 2.3	0.989
n-Hexane	0.186 ± 0.013	5.36 ± 0.10	−1.2 ± 1.8	0.995
n-Heptane	0.172 ± 0.007	5.81 ± 0.17	5.9 ± 3.3	0.990
n-Octane	0.140 ± 0.014	7.13 ± 0.30	2.1 ± 5.4	0.976
n-Nonane	0.092 ± 0.009	10.9 ± 0.47	7.6 ± 7.3	0.999
n-Decane	0.056 ± 0.007	17.7 ± 0.66	−12 ± 12	0.980
n-Undecane	0.039 ± 0.005	25.9 ± 1.5	−10 ± 30	0.963
Benzene	0.168 ± 0.013	5.9 ± 0.18	−1.0 ± 3.5	0.999
Toluene	0.145 ± 0.009	6.90 ± 0.31	15.0 ± 6.0	0.978
Ethylbenzene	0.117 ± 0.009	8.56 ± 0.31	−1.3 ± 6.0	0.986
Butylbenzene	0.068 ± 0.006	14.7 ± 0.83	−4 ± 16	0.965
Methyl acetate	0.183 ± 0.020	5.46 ± 0.25	15.9 ± 9.4	0.971
Ethyl acetate	0.166 ± 0.009	6.03 ± 0.17	13.7 ± 6.8	0.986
Propyl acetate	0.127 ± 0.024	7.8 ± 0.52	50 ± 25	0.943
Butyl acetate	0.092 ± 0.016	10.9 ± 0.98	92 ± 47	0.883
n-Butanol	0.168 ± 0.022	5.95 ± 0.34	−8 ± 12	0.947
n-Pentanol	0.139 ± 0.019	7.19 ± 0.37	−13 ± 13	0.957
n-Hexanol	0.114 ± 0.010	10.3 ± 0.50	8 ± 18	0.962
n-Heptanol	0.098 ± 0.018	10.2 ± 1.1	97 ± 44	0.848
n-Octanol	0.054 ± 0.009	18.5 ± 1.6	140 ± 71	0.888

[a] $s_k = (s_b/b)k$.

permeability should be primarily determined by the solubility coefficient S, equivalent to Henry's law constant for analyte partitioning between air and the polymer. It is well known when considering partitioning between two phases that free energy of transfer of a molecule from one phase to the other changes consistently with incremental changes in the structure of the molecule. This observation forms the foundation of linear free energy relationships (LFER), to estimate *n*-octanol–water partition coefficients of chemicals from various physicochemical properties of the molecules [24]. We decided to use a similar approach to estimate the calibration constants of GUT permeation passive samplers equipped with thin PDMS membranes [13].

4.5.1 Number of carbon atoms

Addition of a certain fragment to a molecule should cause a consistent change in the free energy of transfer of this molecule between the two phases involved in partitioning. Consequently, in a homologous series of compounds, a unit change in the number of carbon atoms causes a constant change in the partitioning coefficient, thus also the calibration constant k. Figure 4.4 presents the relationships between the number of carbon atoms and the calibration constants k for GUT samplers for four families of organic compounds, including n-alkanes, aromatics, alcohols and esters [13]. The k value decreased linearly with increasing number of carbon atoms for all four series. The linear correlation coefficients (see Fig. 4.4) were generally very high.

The data presented in Fig. 4.4 clearly demonstrate that it is possible to predict the value of the calibration constant $\boldsymbol{k}$ for a member of a homologous series of compounds if the structure of the compound and the relationship between $\boldsymbol{k}$ and the number of carbon atoms for this series is known. The use of this approach should result in significant time and cost savings. The sampler can be calibrated using just two or three members of a homologous series, and the resultant correlation can be used to estimate the $\boldsymbol{k}$ values for any other member of the series, including compounds for which standards are unavailable.

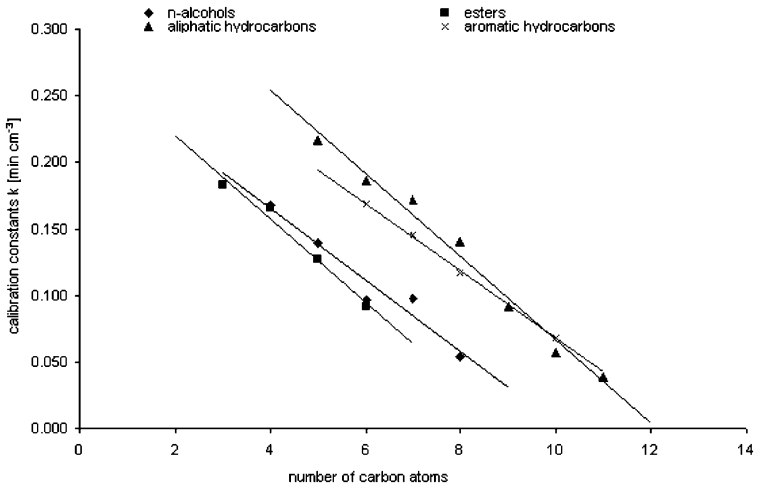

Fig. 4.4. Relationships between the number of carbon atoms in a homologous series of compounds and the calibration constants for the GUT permeation passive samplers equipped with PDMS membranes of 50 μm thickness.

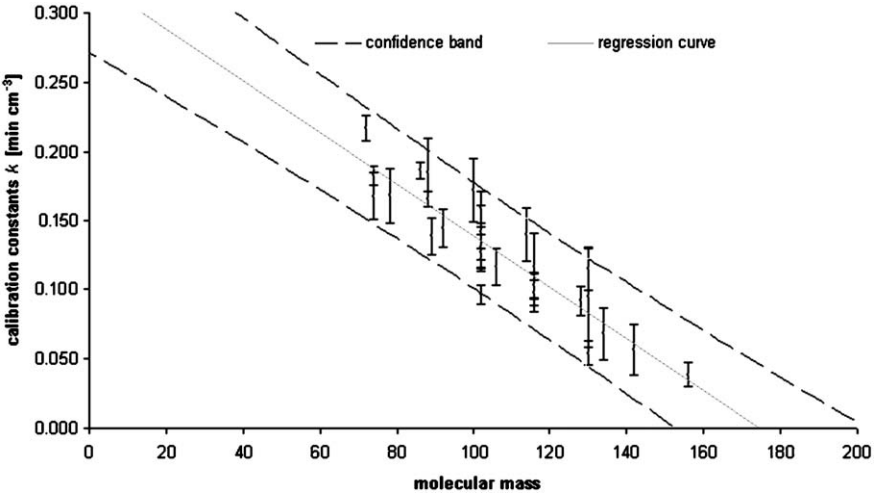

Fig. 4.5. Relationship between the molecular mass of a compound and the calibration constant for the GUT permeation passive sampler equipped with the PDMS membrane of 50 μm thickness. Equation of the regression line is $k = -0.00019x + 0.330$ ($r^2 = 0.824$), where x is molecular mass of the analyte.

4.5.2 Molecular mass

Physico-chemical properties of a compound, including its molecular weight and boiling point, are more closely related to the structure of a molecule than just the number of carbon atoms. Thus, they should be more useful when trying to predict the calibration constants for a broader range of compounds (not necessarily members of a homologous series).

Figure 4.5 presents the relationship between the molecular mass of a compound (for all four classes of compounds) and the calibration constant k [13]. In general, the relationship was linear, with a high value of the linear correlation coefficient ($r^2 = 0.824$). The confidence band of the calculated calibration constants is also plotted to help visualize the estimated range of values that an unknown compound might have [25,26]. It should be emphasized that for the relationship obtained, none of the compounds included in the study fell outside the 95% confidence band.

4.5.3 Boiling point temperature

Boiling point of a compound depends mostly on the strength of intermolecular interactions in the liquid phase, which are determined by the structure of a compound and the polarity of the functional groups

present in the molecule. The same factors affect the solubility of a compound in PMDS, therefore the calibration constant of a permeation passive sampler should be correlated to the boiling point of the analyte. Figure 4.6 shows the relationship between the experimentally determined calibration constants and the boiling points of the analytes [13]. Again, a linear relationship was obtained, with the linear correlation coefficient of $r^2 = 0.814$.

The results presented in Figs. 4.5 and 4.6 demonstrate that the calibration constant $\boldsymbol{k}$ of a permeation passive sampler can be estimated with reasonable accuracy from the molecular weight of a compound or its boiling point, without the need for experimental calibration for each individual compound. Also, the confidence band of the calculated calibration constants is plotted to help visualize the estimated range of values that an unknown compound might have. Again, none of the studied compounds fell outside the 95% confidence band.

The choice of one of the two descriptors (molecular weight or boiling point temperature) is somewhat arbitrary and depends on the nature of the compound. In fact, the best results were obtained by averaging the $\boldsymbol{k}$ values obtained by the two methods. Our experiments were carried out for analytes whose molecular weights ranged from 72 (*n*-pentane) to 156 (*n*-undecane) and the boiling points ranged from 36°C (*n*-pentane) to

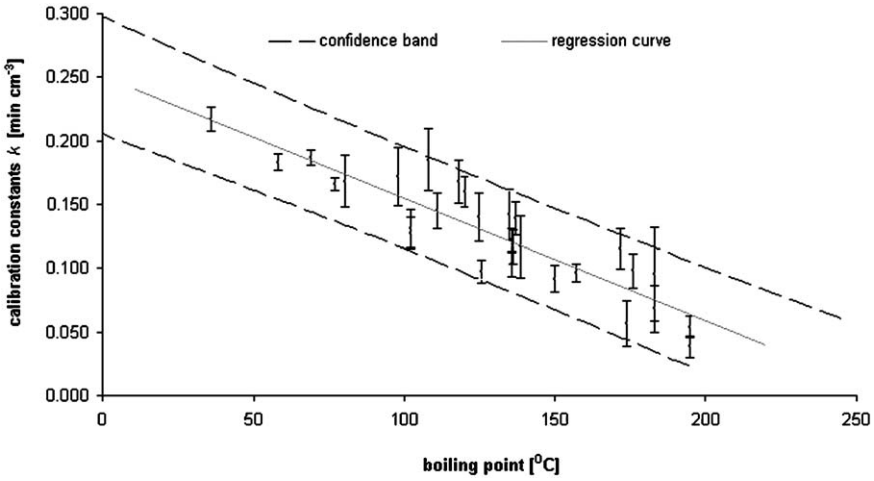

Fig. 4.6. Relationship between the boiling point of a compound and the calibration constant for the GUT permeation passive sampler equipped with the PDMS membrane of 50 μm thickness. Equation of the regression line is $k = -0.00096x + 0.250$ ($r^2 = 0.814$), where x is the boiling point temperature of the analyte.

183°C (butylbenzene). These ranges cover many organic compounds relevant to air analysis. The correlations established could probably be applied for compounds outside of these ranges, but care should be exercised when using this approach. The course of the regression line obtained for the relationship between the boiling point of a compound and the calibration constant of the passive sampler indicates that this regression can only be used for compounds whose boiling point is below 250°C.

4.5.4 Linear temperature-programmed retention index system

In field measurements, very often the identity of all compounds present in the sample is not known. The approaches proposed thus far cannot be used for obvious reasons for unknown analytes, which normally precludes even rough estimation of the total load of organics in the air when using permeation passive samplers. It would be very advantageous to be able to estimate the calibration constants for all compounds present in a sample. The knowledge of the calibration constants could then be used to quantify the unknown compounds provided that the response factors of the detector towards these compounds were known [13,16].

In the process of identification of organic compounds in complex mixtures, the use of retention indices is becoming more important [27]. This is a result of the outstanding stability of fused silica capillaries and the excellent reproducibility of the now available GCs [16]. Retention index (RI) is a measure of the retentiveness of a compound relative to straight (normal) chain hydrocarbons under given set of chromatographic conditions. In 1958, Kovats proposed the use of the homologous series of *n*-alkanes as retention markers [28]. The original Kovats retention index system was applicable to isothermal separations only. Since most separations in GC are carried out these days under temperature-programmed conditions, the linear temperature-programmed retention index system (LTPRI) proposed by Van den Dool and Kratz [29] is used much more often today. LTPRI of a substance is calculated according to the following formula:

$$\mathrm{LTPRI} = 100\left[\frac{t(\mathrm{A}) - t(n)}{t(n+1) - t(n)} + n\right] \tag{4.12}$$

where $t(\mathrm{A})$ is the retention time of the analyte, $t(n)$ is the retention time of the n-alkane eluting directly before the analyte, $t(n+1)$ is the retention time of the n-alkane eluting directly after the analyte and n is the number of carbon atoms in the n-alkane eluting directly before the analyte.

Martos *et al*. [30] demonstrated that LTPRI determined for a PDMS-coated capillary column could be used to estimate the partition coefficients of organic compounds between air and the PDMS coating of the SPME fibre. Since the solubility coefficient in Eq. (4.9) is essentially equivalent to the partition coefficient, there should also be a relationship between the LTPRI determined on PDMS-coated capillary columns and the calibration constant of a given compound for permeation passive samplers equipped with PDMS membranes. This relationship would not require the knowledge of the identity of the compound for the determination of its calibration constant.

The relationship between LTPRI and the calibration constant $\boldsymbol{k}$ is illustrated in Fig. 4.7 [13,16].

The relationship was linear, with the highest value of the linear correlation coefficient of the three correlations examined (molecular weight, boiling point and LTPRI). The regression equations obtained for all classes of compounds studied and the correlation coefficients are listed in Table 4.2.

Overall, the results confirmed the correlation between the calibration constants of GUT passive samplers equipped with PDMS membranes and LTPRI of the analytes on PDMS-coated GC columns. This correlation makes it possible to estimate the calibration constant of any analyte eluting within the LTPRI range examined (500–1100) from the

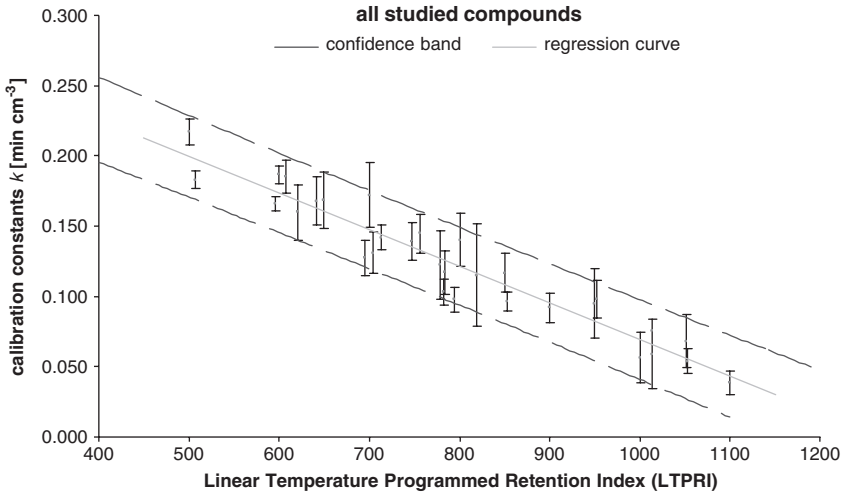

Fig. 4.7. The relationship between the LTPRI of analytes and the calibration constant for GUT permeation passive samplers equipped with PDMS membranes of 50 μm thickness. Equation of the regression line is $k = -0.000261(\text{LTPRI}) + 0.330$ ($r^2 = 0.914$). Reproduced from Ref. [16] with permission from Elsevier.

TABLE 4.2
Regression equations for each class of compounds, as well as for all compounds tested

Class of chemical compounds	Regression equations (k = $bx+a$), where x is LTPRI	Linear regression coefficient r^2
Aliphatic hydrocarbons	$k = -3.13 \times 10^{-4}x+0.379$	0.983
Aromatic hydrocarbons	$k = -2.53 \times 10^{-4}x+0.333$	0.998
Alcohols	$k = -2.47 \times 10^{-4}x+0.321$	0.943
Esters	$k = -3.15 \times 10^{-4}x+0.348$	0.980
Summary equation	$k = -2.61 \times 10^{-4}x+0.330$	0.914

regression line obtained for all analytes or (preferably) the regression line for the class of compounds to which the analyte belongs. The latter requires the use of mass spectrometry for analyte identification.

One way to determine whether the approach proposed might affect the accuracy of the determination of analyte concentration in the air is to examine the insignificance of the difference between the experimental ($\boldsymbol{k}_{\text{exp}}$) and the estimated ($\boldsymbol{k}_{\text{reg}}$) calibration constant. The following relationship is used for this purpose [31]:

$$|k_{\text{reg}} - k_{\text{exp}}| < 2\sqrt{u(k_{\text{reg}})^2 + u(k_{\text{exp}})^2} \tag{4.13}$$

where k_{exp} is the experimentally determined calibration constant, k_{reg} is the calibration constant estimated from the regression equation, u(k_{exp}) is the standard uncertainty of the determination of the experimental calibration constant k_{exp} calculated based on calibration curves and $u(k_{\text{reg}})$ is the standard uncertainty of the determination of the estimated calibration constant k_{reg} calculated based on the regression curve. When the above condition is fulfilled, the difference between the two values is smaller than the expanded uncertainty of determination of the two values; therefore, it is deemed insignificant. For all compounds studied, the condition defined by Eq. (4.13) was fulfilled, which means that the differences between the experimental and the estimated $\boldsymbol{k}$ values were statistically insignificant at 95% probability level. Figure 4.8 presents a comparison of the calibration constants obtained with the three methods (direct experimental determination, estimation from the regression line obtained for a given class of compounds and estimation from the regression line obtained for all analytes), including their expanded uncertainties (U), where U is defined as the standard

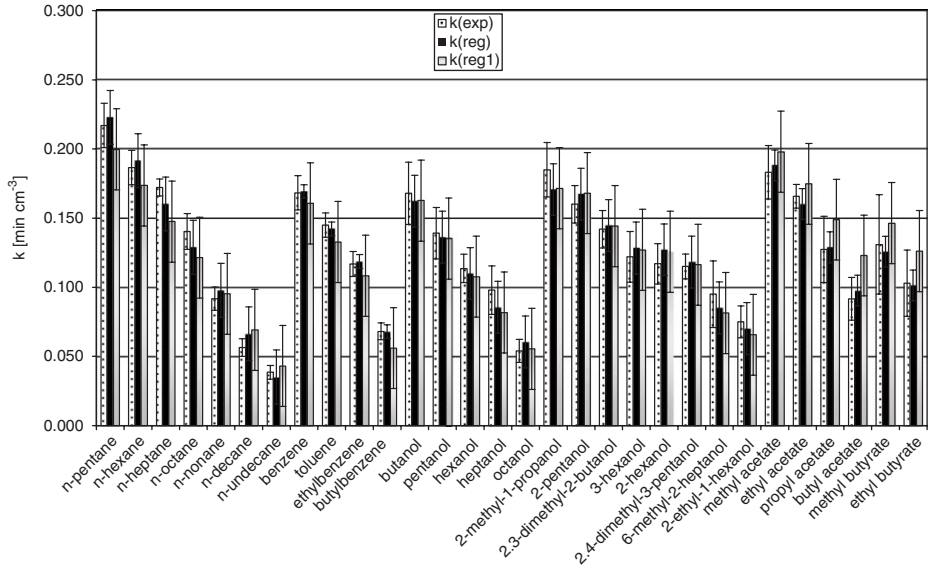

Fig. 4.8. A comparison of the calibration constants obtained with the three methods (direct experimental determination, estimation from the regression line obtained for a given class of compounds and estimation from the regression line obtained for all analytes), including their expanded uncertainties $U = ku(\boldsymbol{k})$; $k = 2$ for $P = 95\%$. Reproduced from Ref. [16] with permission from Elsevier.

uncertainty multiplied by coverage factor $\boldsymbol{k}$ for selected probability level (P): $U = ku(\boldsymbol{k})$; $k = 2$ for $P = 95\%$. It is clear when examining Fig. 4.8 that the k values obtained by any of the three methods fall within the expanded uncertainty ranges of the remaining methods.

The insignificance of the difference between $\boldsymbol{k}_{\mathrm{exp}}$ and $\boldsymbol{k}_{\mathrm{reg}}$ was also examined using the linear regression method [32–34]. Figure 4.9 presents the plot of $\boldsymbol{k}_{\mathrm{reg}}$ vs. $\boldsymbol{k}_{\mathrm{exp}}$.

For the difference between the two values to be insignificant, the dependence should be linear ($y = bx+a$), the line should pass through the origin of the coordinate system and the slope should be close to unity. In other words, the parameters used for the validation of the proposed approach to the estimation of the calibration constants of permeation passive samplers are the slope b and the intercept a. It was found that at the probability level $P = 95\%$ and for $f = n–2 = 28$ degrees of freedom, all of the above conditions were fulfilled ($t_{\mathrm{bcalc}}((1–b)/s_b) = 1.767 \leqslant t_{\mathrm{cr}} = 2.052$; $t_{\mathrm{acalc}}((a–0)/s_a) = 1.685 \leqslant t_{\mathrm{cr}} = 2.052$). Thus, the slope b and the intercept a were not significantly different from the expected values of $b_0 = 1$ for the slope and $a_0 = 0$ for the intercept,

which means that the differences between the estimated and the experimental calibration constants were statistically insignificant. It should be pointed out, however, that this approach does not take into account the uncertainties of determination of the individual

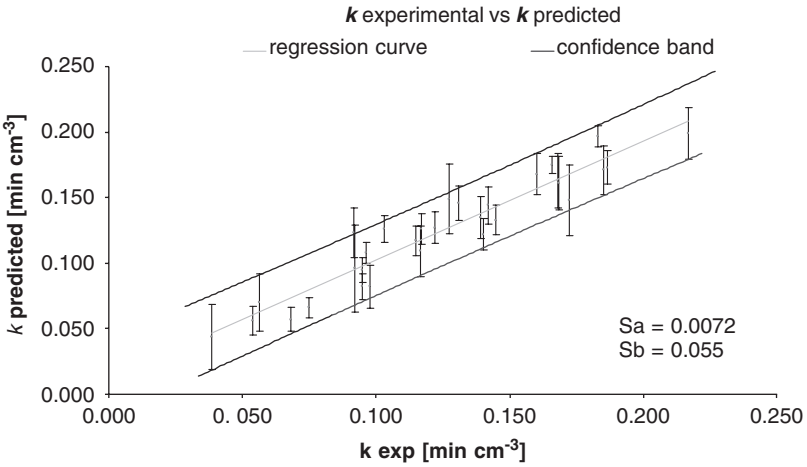

Fig. 4.9. The plot of k_{reg} vs. k_{exp}, used to examine the significance of the differences between the experimental and the estimated calibration constants. Reproduced from Ref. [16] with permission from Elsevier.

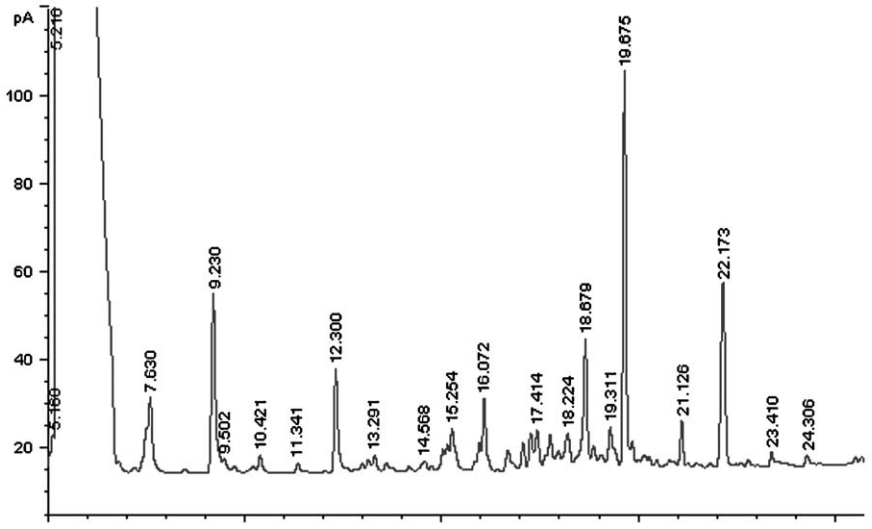

Fig. 4.10. An example of a chromatogram obtained for a real sample collected by GUT permeation passive sampler used in the study.

values—only the overall uncertainty is considered. In general, the examination of the significance of the differences between the experimental and the estimated calibration constants indicates that the results of air analysis with the use of permeation passive samplers should not differ with respect to accuracy irrespectively of the method of determination of the calibration constants of the samplers (experimentally determined or estimated from the LTPRI).

4.5.5 Application of GUT permeation passive samplers in indoor air analysis

An example of a chromatogram obtained for a sample of indoor air collected in an apartment in the city of Gdansk (Poland) by GUT permeation passive sampler is presented in Fig. 4.10. Table 4.3 shows the

TABLE 4.3

Concentrations of organic compounds presented in indoor air sample collected by GUT permeation passive samplers together with the retention times of the analytes, their LTPRI and the estimated calibration constants

Compound name	Retention time (RT)	LTPRI	k[a]	c (ng dm^{-3})[b]
Hexane	7.630	600	0.186	1.33
Benzene	9.230	658	0.168	3.05
Unknown	9.502	667	0.156	1.11
Heptane	10.421	700	0.172	0.15
Unknown	11.341	731	0.139	0.067
Toluene	12.300	764	0.145	1.49
Octane	13.291	800	0.140	0.11
Ethylbenzene	14.568	844	0.117	0.12
Unknown	15.254	868	0.104	0.31
Unknown	15.947	892	0.097	0.27
Unknown	16.072	897	0.096	0.58
Unknown	16.675	919	0.090	0.23
Heptanol	17.414	947	0.098	0.21
Unknown	18.224	978	0.075	0.35
Unknown	18.679	996	0.070	0.92
Unknown	19.311	1020	0.064	0.32
Unknown	19.675	1035	0.060	1.61
Octanol	19.867	1042	0.054	0.051
Unknown	21.126	1091	0.045	0.12
Unknown	22.173	1140	0.033	0.58

[a]Equation used for k values calculation for unknown compounds ($k = -0.000261(\text{LTPRI}) + 0.330$).
[b]Concentrations of indoor air pollutants: $c = k\text{m}/t$.

results obtained (concentrations of organic compounds) together with the retention times of the analytes, their LTPRI and the estimated calibration constants.

4.6 CONCLUSION

Passive sampling has numerous advantages. It is much cheaper and easier to use than active sampling; samplers can be deployed unattended for prolonged periods of time without the annoyance unavoidable in the case of active sampling. TWA concentrations can be determined using passive sampling without the need for averaging the results.

Permeation passive samplers compare very favourably to diffusive passive samplers. They are less sensitive to air currents. With the right membrane, they can eliminate problems related to changes in humidity. Finally, the sampling rate of permeation passive samplers depends very weakly on temperature. The single biggest obstacle in a wider acceptance of permeation passive samplers thus far has been the need to calibrate the samplers for each individual compound of interest. This limited the applicability of permeation passive samplers exclusively to target compound analysis. The approach proposed to predict calibration constants of permeation passive samplers based on physico-chemical properties of compounds/or their retention parameters eliminates this fundamental limitation of permeation passive sampling. The PDMS membrane used in this study assured high sampling rates. The samplers can be exposed to an unknown sample without the need to calibrate their response towards all analytes. Once the compounds present in the sample are identified, only the detector needs to be calibrated towards them.

The strong correlation found between the calibration constants (k) of permeation passive samplers equipped with PDMS membranes and LTPRI determined on PDMS-coated columns permit to conclude that the calibration constants for compounds, for which experimental determination of k has not been carried out, can be easily and reliably estimated based on the regression equations obtained. Thus, the correlation between LTPRI and the calibration constant of a permeation passive sampler makes it possible to use the latter as efficiently as sorption tubes, while preserving all the advantages of passive sampling, including low cost, simplicity, ease of deployment. The concentrations of unidentified analytes collected by the passive samplers can be estimated with the use of detectors with known, uniform response factors

for organic compounds (e.g. FID or atomic emission detector (AED)). When the analyte identity is known, the accuracy of the result can be further improved by calibrating the response of the detector towards this particular compound. This step would not differ from what would be done for a sample collected by any active method.

REFERENCES

1 B. Kozdroń-Zabiegała, J. Namieśnik and A. Przyjazny, *Indoor Environ.*, 4 (1995) 189.
2 J. Namieśnik, B. Zabiegała, A. Kot-Wasik, M. Partyka and A. Wasik, *Anal. Bioanal. Chem.*, 381 (2005) 279.
3 T. Górecki and J. Namieśnik, *Trends Anal. Chem.*, 21 (2002) 276.
4 N.C. van de Merbel, J.J. Hageman and U.A.Th. Brinkman, *J. Chromatogr.*, 634 (1993) 1.
5 K.D. Reiszner and P.W. West, *Sci. Technol.*, 7 (1973) 526.
6 E.D. Palmes and A.F. Gunnison, *Am. Ind. Hyg. Assoc. J.*, 34 (1973) 78.
7 L.B. Persson, G.M. Morrison, J.U. Friemann, J. Kingston, G. Mills and R. Greenwood, *J. Environ. Monitor.*, 3 (2001) 639.
8 S. Batterman, T. Metts, P. Kalliokoski and E. Barnett, *J. Environ. Monitor.*, 4 (2002) 361.
9 B. Zabiegała, B. Zygmunt, E. Przyk and J. Namieśnik, *Anal. Lett.*, 33 (2001) 361.
10 T.C. Merkel, V.I. Bondar, K. Nagai, B.D. Freeman and I. Pinnau, *J. Polym. Sci. B Polym. Phys.*, 38 (2000) 415.
11 G. Audunsson, *Anal. Chem.*, 58 (1986) 2714.
12 J. Namieśnik, T. Górecki, B. Kozdroń-Zabiegała and W. Janicki, *Indoor Air*, 2 (1992) 115.
13 B. Zabiegała, T. Górecki and J. Namieśnik, *Anal. Chem.*, 75 (2003) 3182.
14 K. Ishikawa, *Guide to Quality Control*, Asian Productivity Organization, Tokyo, 1982.
15 K. Ishikawa, *What Is Total Quality Control? The Japanese Way* [English translation by D.J. Lu], Prentice-Hall, Englewood Cliffs, NJ, 1985.
16 B. Zabiegała, M. Partyka, T. Górecki and J. Namieśnik, *J. Chromatogr. A.*, 1117 (2006) 19.
17 B. Kozdroń-Zabiegała, A. Przyjazny and J. Namieśnik, *Indoor Build. Environ.*, 5 (1996) 212.
18 B. Zabiegała, A. Przyjazny and J. Namieśnik, *J. Environ. Pathol. Toxicol. Oncol.*, 18 (1999) 47.
19 B. Kozdroń-Zabiegała, B. Zygmunt and J. Namieśnik, *Chem. Anal.*, 41 (1996) 209.
20 D.L. Heawner, W.T. Morgan and M.W. Ogden, *Environ. Intern.*, 21 (1995) 3.

21 B. Zabiegała, T. Górecki, E. Przyk and J. Namieśnik, *Atmos. Environ.*, 36 (2002) 2907.
22 J. Namieśnik, T. Górecki, B. Kozdroń-Zabiegała and J. Łukasiak, *Build. Environ.*, 27 (1992) 339.
23 B. Kozdroń-Zabiegała, J. Namieśnik and A. Przyjazny, *Indoor Environ.*, 4 (1995) 189.
24 R.P. Schwarzenbach, P.M. Gschwend and D.M. Imboden, *Environmental Organic Chemistry*, J. Wiley & Sons, Inc., New York, 1993.
25 J.N. Miller, *Analyst*, 116 (1991) 3.
26 K. Danzer and L.A. Currie, IUPAC, *Pure Appl. Chem.*, 70 (1998) 993.
27 H.J. Hübschmann, *Handbook of GC/MS: Fundamentals and Applicatio ns, 2001*, Wiley-VCH, Toronto, 2001.
28 E. Kovats, *Helv. Chim. Acta*, 41 (1958) 1915.
29 H. Van den Dool and P.D. Kratz, *J. Chromatogr.*, 11 (1963) 463.
30 P.A. Martos, A. Saraullo and J. Pawliszyn, *Anal. Chem.*, 69 (1997) 402.
31 B.W. Wenclawiak, M. Koch and E. Hadjicostas, *Quality Assurance in Analytical Chemistry. Training and Teaching*, Springer, New York, 2004.
32 L. Brüggemann and R. Wennrich, *Accred. Qual. Assur.*, 7 (2002) 269.
33 J.V. Loco, M. Elskens, C. Croux and H. Beernaert, *Accred. Qual. Assur.*, 7 (2002) 281.
34 K. Heydorn and T. Anglov, *Accred. Qual. Assur.*, 7 (2002) 153.

Chapter 5

Membrane-enclosed sorptive coating as integrative sampler for monitoring organic compounds in air

Peter Popp, Heidrun Paschke, Branislav Vrana, Luise Wennrich and Albrecht Paschke

5.1 INTRODUCTION

Membrane-enclosed sorptive coatings (MESCOs) are devices combining the advantages of passive sampling approaches with solvent-free preconcentration of organic contaminants from air, water or other matrices. The sampling materials are polymer-coated stir bars, solid-phase microextraction (SPME) fibres or pieces of polymer materials. In 2001, Vrana *et al*. [1] first described an integrative passive sampler for monitoring organic contaminants in water. The authors used a stir bar coated with polydimethylsiloxane (PDMS) as described by Baltussen *et al*. [2] for the enrichment of the contaminants. The PDMS-coated stir bar (''Twister'') is then thermally desorbed on-line into a capillary gas chromatograph coupled with mass selective detector (GC–MS) system. The MESCO used for the first investigations consisted of a stir bar enclosed in a dialysis membrane bag made from regenerated cellulose, filled with double distilled water and sealed at each end with Spectra Por enclosures. Another MESCO type used for passive sampling of analytes from water consists of a low-density polyethylene (LDPE) tubing heat-sealed at both ends and filled with PDMS fibres and an inner fluid [3].

Independently from the devices designed for passive sampling in water (described in Chapter 10 of this book) two types of MESCOs for the long-term monitoring of semi-volatile organic air pollutants were also developed. Type A consists of an LDPE membrane tubing with

Comprehensive Analytical Chemistry 48
R. Greenwood, G. Mills and B. Vrana (Editors)
Volume 48 ISSN: 0166-526X DOI: 10.1016/S0166-526X(06)48005-3

250 μm wall thickness enclosing a Twister (A1) or a silicone tubing (A2) [4], type B consists of heat-sealed LDPE membrane material with only 50 μm wall thickness enclosing a Twister (B1) or a silicone elastomer rod (B2) [5].

5.2 THEORY

The passive sampling devices described here consist of a hydrophobic solid receiving medium enclosed in an air-filled semi-permeable polyethylene membrane (Figs. 5.1 and 5.2).

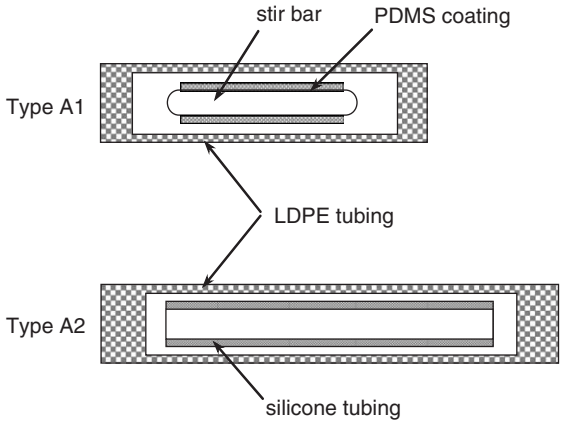

Fig. 5.1. Diagram of the MESCOs type A1 (stir bar) and A2 (silicone tubing).

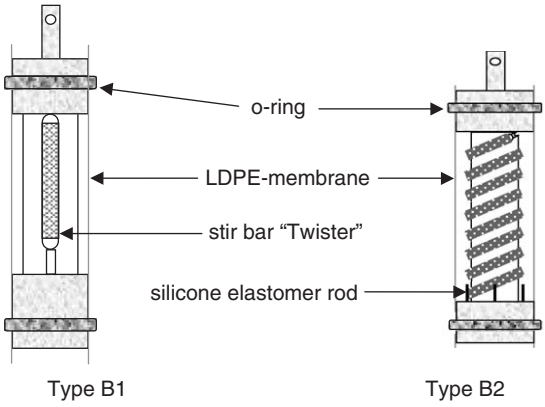

Fig. 5.2. Diagram of the MESCOs type B1 (stir bar) and B2 (silicone rod).

Huckins *et al*. [6] developed a theoretical model describing the uptake kinetics of organic compounds in water by passive samplers consisting of a triolein-filled polyethylene membrane. In a laboratory study investigating polychlorinated biphenyls (PCBs) in air, Petty *et al*. [7] demonstrated that this model was also applicable to air sampling. Vrana *et al*. [1] gave an overview of the theoretical aspects concerning the uptake of organic compounds in water by passive samplers consisting of a hydrophobic phase enclosed in a semi-permeable membrane based on the model mentioned above. This model is also applicable for the MESCOs of the type A and B. In the initial uptake phase (when the uptake is linear or integrative), the correlation between the concentration of the analyte in the receiving organic phase C_S and the concentration of the analyte in the gaseous phase C_{Air} is described by the following equation:

$$C_S = C_{S(0)} + C_{Air} k_O \left(\frac{A_S \alpha}{V_S}\right) t \tag{5.1}$$

where $C_{S(0)}$ is the concentration of analyte in the receiving organic phase at time $t = 0$, V_S is the volume of the receiving organic phase, k_O is the mass transfer coefficient, A_S is the membrane surface area, α is the pore area of the membrane as a fraction of the total membrane area and t is the time.

Equation (5.1) can be rewritten as

$$m_S = m_{S(0)} + C_{Air} R_S t \tag{5.2}$$

where m_S is the amount of analyte in the receiving organic phase, $m_{S(0)}$ is the amount of analyte in the receiving organic phase at $t = 0$ and R_S is the sampling rate of the passive sampler:

$$R_S = k_O A_S \alpha \tag{5.3}$$

According to Eq. (5.2) the sampling rate R_S can be determined in laboratory experiments at constant analyte concentrations C_{Air}. With regard to environmental air monitoring, the term C_{Air} represents the TWA concentration over the exposure time period. When the calibration parameter R_S is known, C_{Air} can be estimated from m_S, the amount of analyte received by the sampler:

$$C_{Air} = \frac{m_S - m_{S(0)}}{R_S t} \tag{5.4}$$

5.3 EXPERIMENTAL

5.3.1 Preparation and design of the MESCO samplers

The two types of MESCO samplers shown in Fig. 5.1 were prepared from LDPE membrane tubing (4.0 mm × 4.5 mm: wall thickness, 250 μm) enclosing a Twister bar (sampler type A1) or silicone tubing (outer diameter 3.6 mm; wall thickness 300 μm; length 80 mm; volume about 250 μL; sampler type A2), acting as the solid receiving medium. The Twister is a stir bar (length 10 mm) consisting of a glass-coated magnetic core with a layer of PDMS. The PDMS layer is 500 μm thick with a volume of about 24 μL. The Twister is produced by Gerstel (Mülheim/Ruhr, Germany). The length and effective membrane surface areas of the LDPE tubing are 20 mm/2.8 cm^2 (type A1) and 85 mm/12.0 cm^2 (type A2). The LDPE tubing with the receiving medium (stir bar or silicone tubing) inside were heat-sealed at each end.

Prior to use, the stir bars were placed into a vial containing 2 mL of a mixture of dichloromethane and methanol (1:1 v:v%) for at least 1 h. The solvent mixture was replaced and the procedure repeated. The stir bars were dried in a desiccator at room temperature and subsequently heated for 90 min at 250°C in a nitrogen flow of about 50 mL min^{-1}. To condition the silicone and LDPE tubing, these were placed into a vial containing 40 mL of *n*-hexane and shaken for about 15 h. The tubing was then dried in a desiccator at room temperature. The silicone tubing was also thermally conditioned in a manner similar to the stir bars (see above).

To prepare the MESCOs of the types B1 and B2 the membrane material (LDPE foil with a thickness of 50 μm) was cut into pieces and heat-sealed to form tubes. These membrane tubes can be used for both sampler types because their diameters are identical. The stir-bar sampler (Fig. 5.2, type B1) was designed so that the Twister (length 20 mm, volume 47 μL, thickness of the PDMS layer, 500 μm) is fixed between two aluminium parts. The membrane tube is pulled over the sampler and then attached with O-rings on both ends. The stir bar is installed (radially symmetrical) in the sampler and the distance between the receiving material and the membrane is 4.5 mm. The effective surface area of the membrane is 10.2 cm^2.

The second sampler of this type (Fig. 5.2, B2) contains a silicone elastomer rod (diameter: 1.0 mm) mounted in the spiral flute of the top part of the sampler acting as the receiving material. The end of the rod is fixed to the bottom part. The membrane tube is clamped with O-rings

to both ends of the sampler in the same way as type B1. The distance between membrane and silicone elastomer is 1.0 mm.The effective surface of the membrane surrounding the rod is 8.1 cm^2, the receiving surface of the rod is about 5 cm^2. The materials were purified as follows: the prepared tubing pieces were placed into a glass flask with *n*-hexane and agitated for 1 h using a horizontal shaker. The procedure was repeated with fresh solvent, the material was dried in a desiccator and then thermally conditioned for 8 h at 60°C.

The rod material was cut in pieces 158 mm long. The rods were shaken with a solvent mixture of dichloromethane and methanol (1:1 v:v%) for 2 h. This procedure was repeated after solvent exchange. The solvent-washed rods were dried and heated to 250°C overnight in a conditioning unit made by Gerstel, in which each of the pieces was enclosed in a glass tube purged by a nitrogen stream of 30 mL min^{-1}. Afterwards, the rod material was transferred into a vial wrapped with aluminium foil and stored at −18°C.

5.3.2 Chemicals

The test chemicals selected (Table 5.1) belong to different groups of semivolatile persistent organic pollutants: α-, γ- and δ-hexachlorocyclohexane (α-, γ- and δ-HCH), hexachlorobenzene (HCB), 2,4,4′-trichlorobiphenyl (PCB 28), 2,2′,5,5′-tetrachlorobiphenyl (PCB 52), 2,2′,4,5,5′-pentachlorobiphenyl (PCB 101) and fluoranthene (FLU). They were purchased from Promochem (Wesel, Germany). Table 5.1 also indicates which of these substances were used for the calibration of the sampler types A1, A2, B1 and B2.

5.3.3 Generation of the standard gas mixtures and calibration of the samplers

For the sampler calibration experiments two similar types of flow-through exposure chambers were used. The exposure chamber used for the determination of the sampling rates of the sampler types A1 and A2 is described by Wennrich *et al*. [4]. The experiments were performed in a flow-through exposure chamber made of glass with a volume of 21.5 L. An atmosphere with a constant contaminant concentration was established according to the procedure described by Hauk *et al*. [8]. Briefly, sea sand was mixed with a methanolic solution containing the relevant substances for 2 h in a rotary evaporator at ambient temperature. The solvent was then evaporated under vacuum and the loaded sand was

TABLE 5.1

Selected physicochemical properties of analytes investigated with the MESCO types A and/or B (molecular weight (M), sublimation pressure (P^{SV}), Henry's Law constant between air and water (H) and n-octanol/water partition coefficient (K_{OW}))

Compound[a]	M (g mol^{-1})	P^{SV} (mPa)	H^e (Pa m^3 mol^{-1})	log $K_{OW}{}^e$	MESCO type
α-HCH	290.83	6.3[b]	0.872	3.8	A, B
γ-HCH	290.83	2.8[b]	0.149	3.7	A, B
δ-HCH	290.83	4.5[b]	0.073	4.1	B
HCB	284.78	1.8[c]	131	5.5	A, B
PCB 28	257.55	16[d]	32	5.8	A, B
PCB 52	291.99	5.0[d]	48	6.1	A
PCB 101	326.44	1.6[e]	36	6.4	B
Fluoranthene	202.30	1.2[f]	1.04	5.2	A

[a]HCH, hexachlorocyclohexane; HCB, hexachlorobenzene; PCB, polychlorinated biphenyl congener.
[b]Ref. [14] (value at 25°C linear interpolated from the data).
[c]Ref. [15].
[d]Ref. [16].
[e]Ref. [17].
[f]Ref. [18].

filled into a glass column. An air flow was passed through the sand bed maintained at a temperature of 12°C. This contaminated air was mixed in the exposure chamber with a flow of purified air. The average temperature in the exposure chamber was 19°C and the air humidity was about 50%. In order to analyze the semi-volatile organic compound concentrations in the exposure chamber, a desorption tube filled with Tenax^{TM} TA sorbent was integrated in a bypass of the exhaust air flow of the exposure chamber. The loaded desorption tubes were stored in tube containers at 4°C in the dark until analysis using thermodesorption/GC–MS.

The system used for the calibration of the sampler types B1 and B2 was as described by Larsen *et al*. [9]. This system is easier to handle because no expensive conditioning is necessary. The standard gas mixtures were generated dynamically in a generator column (Fig. 5.3). Sea sand loaded with the test chemicals was placed in the flow-through cell. The procedure to prepare the sand was also performed according to the method of Hauk [8]. A U-formed glass tube (d) filled with 100 g contaminant loaded sea sand was placed in a thermostatic water bath with a temperature of 10°C. Approximately 22 mg of each component

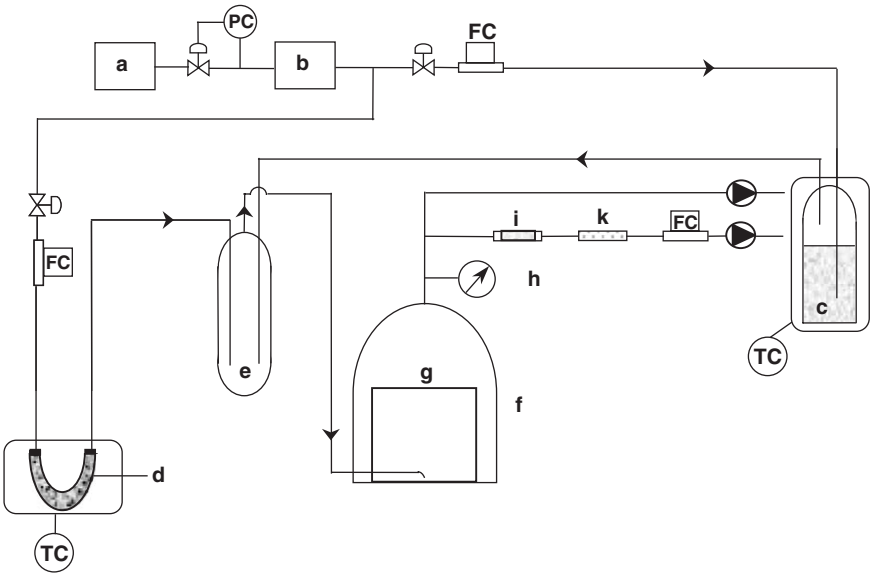

Fig. 5.3. Calibration device: FC, flow control; PC, pressure control; TC, temperature control; a, compressed air; b, purification system for air; c, washing bottle; d, glass column; e, mixing chamber; f, calibration chamber; g, stainless steel lattice; h, measure for humidity; i, Tenax^{TM} TA tube; k, glass column filled with blue silica-gel.

was adsorbed on the sand surface in the generator column. A purified compressed air flow (12 mL min^{-1}) was passed through the sand bed, purging the substances into the mixing chamber (e), where further dilution took place with the aid of an additional clean air flow of 15 L min^{-1}. Before reaching the mixing chamber, the dilution air was moisturized by continuously passing it through a temperature-controlled washing bottle (c) (12°C) filled with double distilled water.

A desiccator (volume 21.5 L) was used as calibration chamber (f). After the mixing step, the standard gas mixture was transferred to the bottom of the calibration chamber. A stainless steel lattice (g) was positioned inside the calibration desiccator at a height of 25 cm from the bottom, where the passive samplers were horizontally placed during exposure. Glass tubes were used for the connections between generator column, mixing chamber and exposure chamber.

The contaminated air in the calibration chamber flows out through an opening in the desiccator lid. The humidity in the exhaust air stream was measured with a Q hygrotemp 80 (Merck, Darmstadt, Germany) (h). A desorption tube filled with Tenax^{TM} TA (i) was installed in a

bypass of the exhaust air flow to determine analyte concentrations in the gas mixture. The analytes were accumulated from contaminated air flowing at 30–40 mL min^{-1}. The adsorption tubes were exposed for 6 h before the passive samplers were removed. After accumulation, the tubes were stored frozen at –18°C in a container wrapped with aluminium foil until thermodesorption/GC–MS analysis. The concentrations of the semi-volatile components in the chamber during exposure are shown in Table 5.2.

For the determination of sampling rates, the permeation samplers were positioned perpendicular to the flow direction in the calibration chamber. The average air humidity was 50.6%. The calibration device was installed in a room with a mean temperature of 28°C. After 72, 144, 216, 312 and 383 h two samplers of either type were removed, wrapped in aluminium foil and stored as described above.

5.3.4 Thermodesorption/GC–MS analysis

The semi-volatile compounds sorbed in the receiving phase of the samplers and enriched on Tenax^{TM} TA-filled desorption tubes were analysed using thermodesorption/GC–MS. The system used consisted of an Agilent Technologies 6890/5973N GC–MS system (Palo Alto, CA, USA) connected to a Gerstel TDSA thermodesorption device. The TDSA was operated under the following conditions: desorption temperature, 250°C; desorption time, 10 min; splitless (solvent vent mode); and helium flux, 100 mL min^{-1}. The temperatures of the two transfer lines (between the TDSA device and the cold injection system (CIS 4) and from the GC and MS ion source) were set at 250°C. The CIS was equipped with an empty liner to cryo-focus the analytes prior to transfer to the capillary column, and was cooled with nitrogen during thermodesorption. The following conditions were used for the cold injection system: during thermodesorption, temperature was set to –150°C, raised at 12°C s^{-1} to 250°C and held for 5 min; the injector was used in splitless mode with a time of 1.5 min. An HP-5 MS capillary column (30 m; 0.25 mm i.d.; 0.25 μm film thickness) (Agilent Technologies) was used with the following temperature programme: 50°C, 3 min isothermal, raised to 160°C at 15°C min^{-1}, raised at 3°C min^{-1} to 235°C, and then raised at 30°C min^{-1} to the final temperature of 280°C, held for 8 min. Helium was used as carrier gas with a linear velocity of 40 cm s^{-1} in constant flow mode. The single ion-monitoring (SIM) mode was selected for the detection of the analytes. Two characteristic target ions were chosen for each compound under consideration.

TABLE 5.2

Calibration data for the investigated MESCO samplers: average concentration (C_{Air}) of the analytes during exposure and relative standard deviation (RSD), comparison between slope, axis intercept, coefficient of correlation (r^2) and uptake rate (R_S)

Compound	C_{Air} (ng m^{-3})	RSD (%)	Slope (ng h^{-1})	Intercept (ng)	r^2	R_S (mL h^{-1})	Slope (ng h^{-1})	Intercept (ng)	r^2	R_S (mL h^{-1})
			Sampler A1				Sampler A2			
α-HCH	286	9.0	0.025	−1.16	1.00	88	0.180	−2.96	0.99	629
γ-HCH	561	10.8	0.058	−3.76	1.00	104	0.439	−18.2	0.99	783
HCB	63	8.2	0.007	−0.22	1.00	108	0.045	−0.98	0.99	719
PCB 28	70	8.0	0.023	−0.83	0.99	321	0.304	−8.16	0.98	4314
PCB 52	96	5.5	0.022	−1.33	0.98	231	0.334	−15.6	0.98	3468
FLU	16	17.7	0.001	−0.04	0.98	70	0.048	−1.99	0.96	3006
			Sampler B1				Sampler B2			
α-HCH	149	3.5	0.068	−1.02	0.97	454	0.077	0.47	0.98	519
γ-HCH	269	5.6	0.100	−0.02	0.96	372	0.137	2.93	0.99	511
HCB	282	12.1	0.025	−1.22	0.96	88	0.107	−3.77	0.99	379
PCB 28	109	5.9	0.060	−0.73	0.97	548	0.058	−0.15	0.98	537
PCB 52	171	3.6	0.208	−14.5	0.98	1216	0.091	−5.75	0.99	532
FLU	37	10.4	0.010	−0.87	0.94	263	0.010	−1.00	0.95	271

A six-point curve of the external calibration was used for the quantification of the substances sorbed on the receiving material. For this calibration, a 4 cm length plug of silanized glass wool in an empty thermodesorption glass tube was spiked with 1 μL of a methanolic calibration solution. The solvent was evaporated for 30 s in a nitrogen stream flowing at 30 mL min^{-1}. The spiked desorption tube was immediately transferred in the TDSA unit for analysis.

Freshly conditioned Tenax^{TM} tubes were used for the destination of the compounds in the standard gas atmosphere in the exposure chamber. The clean-up of the Tenax^{TM} tubes was the same as that used for the thermal conditioning of the rods (described above). Calibration was performed using conditioned Tenax^{TM} tubes spiked with 1 μL standard solution.

5.3.5 Field application

The MESCOs of the type A1 and A2 were tested for on-site monitoring in September–October 2001 in a highly polluted area—a disused waste dump for the chemical industry (Grube Antonie)—near Bitterfeld (Germany). The sampling devices were placed at four different locations. The samplers were hung vertically using stainless steel wires, 0.5 m above the ground, inside a box (stainless steel plate; diameter, 20 cm; height, 20 cm), open at the bottom and with perforated sides, to protect the samplers from rain and sunlight whilst allowing air to move over them. The passive samplers were deployed for 14 and 28 days. The average ambient temperature within this time period was 12.8°C.

The MESCOs of the types B1 and B2 were exposed in November 2002 at other site in the Grube Antonie. They were placed 0.9 m above the ground and protected against rain and solar radiation analogously to the samplers of the type A. The sampling periods were 7, 14 and 21 days. The average temperature was 5.5°C and the rainfall ranged between 0.0 and 13.0 mm over the sampling period.

5.4 RESULTS

5.4.1 Laboratory exposure experiments

The performance of the MESCOs described here (Figs. 5.1 and 5.2) for the long-term monitoring of SOCs was investigated by conducting exposure experiments with the flow-through exposure chambers described above. The concentrations in the exposure chambers were

between 16 ng m^{-3} (FLU) and 561 ng m^{-3} (γ-HCH) (see Table 5.2). The concentrations were constant throughout the whole exposure period. The reproducibility, given as the RSD values, was found in both exposure chambers $\leqslant$12.1% except FLU (17.7%), the compound with the lowest concentration.

In Fig. 5.4, the characteristic update curves of the analyte PCB 28 for the MESCOs A1, B1 and B2 are given. During the whole expose time of 15 days (sampler A1) and 16 days (samplers B1 and B2), respectively, the uptake of the pollutant was linear. The results of the linear regression are given in Table 5.2. The correlation coefficients (r^2) of the plots for the MESCOs A1 and A2 (use of the conditioned chamber) were in the range 0.96–1.00 and that of the plots for the MESCOs B1 and B2 (exposure chamber at room temperature) were in the range 0.94–0.99.

The sampling rates R_S were calculated using Eq. (5.2). The R_S (see Table 5.2) values are in the range 70–320 mL h^{-1} (sampler A1), 630–4300 mL h^{-1} (sampler A2), 90–1220 mL h^{-1} (sampler B1) and 270–540 mL h^{-1} (sampler B2). Compared with other common passive samplers, such as standard SPMDs [10] the R_S values of the samplers studied here are relatively low. For example, R_S values of standard SPMDs (450 cm^2 surface area) of 190 and 160 L h^{-1} were calculated for PCB 28 and PCB 52, respectively. This means that the sampling

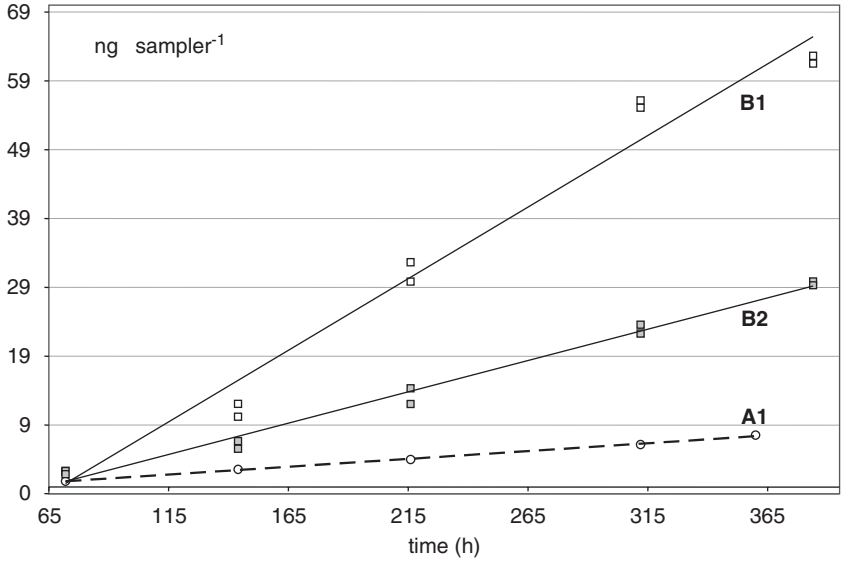

Fig. 5.4. Uptake profiles for PCB 28 by exposure of the MESCOs A1, B1 and B2 in the calibration atmosphere.

efficiency of the SPMDs is two or three orders of magnitude higher than that of the MESCOs described here, mainly due to the higher surface area of the SPMDs. However, the overall sensitivity of the four types of the MESCOs is sufficient because, in the case of these samplers, the total amount of analyte accumulated in the receiving medium is transferred to the GC–MS, whereas, in the case of SPMDs, only a small part of the extract is injected (commonly 1–2 μL, i.e. 1–2% of the analytes sampled) to avoid the potential contamination of the chromatographic system by impurities with higher molecular weights, such as lipids, still present in small quantities in the extracts following the clean-up.

5.4.2 Comparison of the different MESCO types

The MESCOs investigated in this study differ with regard to the membrane thickness (sampler type A: 250 μm, sampler type B: 50 μm), the area of the membrane (type A1: 2.8 cm^2, type A2: 12.0 cm^2, type B1: 8.1 cm^2, type B2: 10.2 cm^2) and the volume of the enclosed receiving medium (type A1: 24 μL, type A2: 250 μL, type B1: 47 μL, type B2: 125 μL).

The comparison of the two MESCOs of the type A shows that the enlargement of the surface area of the membrane by a factor of about four results in an increase in the R_S values by a factor of 7–15 (except FLU). The significantly increased R_S values of MESCO A2 are to be expected by the relationship between the surface area of the membrane and the uptake rate R_S. Accordingly when MESCO A2 is used, the average amounts of the analytes collected are approximately one order of magnitude higher than when using MESCO A1, resulting in an improved sensitivity. Additionally, the silicone tube-filled sampler is less expensive than the stir bar filled MESCO A1.

The effective membrane surfaces of the MESCOs of the type B differ insignificantly and the uptake rates of HCB, PCB 101, α-HCH and γ-HCH are comparable. The R_S values for δ-HCH are greater for the spiral-rod sampler, in contrast the uptake rate of PCB 28 for the stir-bar sampler is considerably larger.

The comparison of sampler types A1 and B1 (volume of the receiving phase of B1 is twice as large as that of A1 and the membrane surface of type B1 is also larger (factor 3.6)) shows that the R_S values of B1 for α-HCH, γ-HCH, HCB and PCB 28 measured with both sampler types are much higher.

As described by Vrana *et al*. [1] a negative intercept of the linear uptake curve can be interpreted as a lag-phase between the start of exposure and the penetration of analyte through the diffusion-limiting

membrane, i.e. the time required for the analyte to pass the membrane. This lag time for the MESCOs of the type B (50 μm membrane thickness) should be much shorter than for the MESCOs of the type A (250 μm membrane). The calculated lag times for the MESCOs A1 and A2 are in a range between 16 and 65 h. The lag-times for the MESCOs B1 and B2 calculated from the results of the exposure experiments differ much more so that for these samplers no reliable values exist. Further investigations are necessary.

5.4.3 On-site exposure experiments

The field exposure of the MESCO samplers A1 and A2 was performed according to the experimental conditions described above. To screen the site-relevant pollutants, one of the loaded samplers was analysed by TDSA/GC–MS with the MS operated in the scanning mode. Subsequently, the other loaded samplers were analysed in SIM mode (see Section 5.3), for selected relevant pollutants.

Results of this field study are given in Table 5.3. The accumulated amounts of analytes are listed for both types of sampler at an exposure

TABLE 5.3

Amounts of analytes accumulated in the receiving medium of the MESCO samplers of the type A (M_S in ng) exposed for 14 days on different sampling sites (S) in the area of the landfill ''Grube Antonie''

Compound[a]	Sampler A1				Sampler A2			
	S1	S2	S3	S4	S1	S2	S3	S4
∑TeCB	2.24	2.85	2.76	1.09	12.66	14.16	2.00	2.77
PeCB	0.82	0.79	1.19	0.50	4.33	3.61	0.86	1.19
HCB	0.71	0.68	0.74	0.67	2.54	1.70	1.63	2.62
α-HCH	57.2	220.8	63.4	22.4	599.3	2730.1	213.1	81.3
β-HCH	2.73	5.83	5.70	1.76	17.91	85.43	11.19	5.88
γ-HCH	14.80	9.43	8.32	1.33	33.4	66.28	8.42	8.65
o,*p*′-DDE	0.81	0.81	0.84	0.79	1.89	1.81	3.61	1.06
p,*p*′-DDE	0.81	0.80	0.83	0.79	2.71	1.92	5.58	1.34
o,*p*′-DDD	0.81	0.78	0.80	n.d.[b]	3.13	1.88	1.93	1.10
p,*p*′-DDD	0.78	n.d.	n.d.	n.d.	2.06	1.70	1.67	0.89
o,*p*′-DDT	1.67	1.65	1.66	n.d.	8.60	8.23	11.23	2.79
p,*p*′-DDT	n.d.	n.d.	n.d.	n.d.	3.56	2.98	3.89	1.84

[a]DDD, 1,1-dichloro-2,2-*bis*(chlorophenyl)ethane; DDE, 1,1-dichloro-2,2-*bis*(chlorophenyl)ethene; TeCB, tetrachlorobenzene; PeCB, pentachlorobenzene; for definition of other compounds, see text.
[b]n.d., not detected.

time of 14 days. As can be seen, large amounts of HCH isomers were enriched by the samplers. α-HCH was the main air pollutant in the area investigated. These findings correspond well with measurements in the Bitterfeld region performed with low volume samplers [11]. Additionally, higher chlorinated benzenes and DDX-compounds (DDE, DDD and DDT) were detected in significantly lower amounts compared to the HCHs. Comparison of the four sampling locations revealed significant differences in the air burden, especially for HCH isomers. Significantly higher amounts of pollutants were accumulated by sampler A2.

The sampling rates R_S determined for the two HCH isomers and HCB were used to calculate the time-weighted average (TWA) air concentrations C_{Air} of these pollutants according to Eq. (5.4). The C_{Air} values for the four sampling locations on the landfill ''Grube Antonie'' are listed in Table 5.4. The TWA concentrations in this polluted area were in the lower μg m^{-3} range for α-HCH and in the ng m^{-3} range for γ-HCH and HCB. These values in the order of magnitude correspond with concentrations calculated from measurements on the same landfill in 1999 using semi-permeable membrane devices [12].

The MESCOs of the type B1 and B2 were exposed at another place on the deposit ''Grube Antonie'' as described in Section 5.3. Here, tri- and tetrachlorobenzenes, pentachlorobenzene, HCB and the HCH isomers were identified as contaminants. As expected, the HCH isomers are the dominant pollutants. The quantified amounts listed in Table 5.5 are averages from triplicate determinations of samplers during the different exposure times and are given together with the relative standard deviations. The MESCOs of the type B1 (stir-bar samplers) varied between 0.8% and 19.4% and the MESCOs of the type B2 (spiral-rod samplers) varied between 2.3% and 26.3%. The higher deviations of the B2 samplers may be due to the longer contact with ambient air during handling. The rod is approximately 16 cm long but the heated

TABLE 5.4

Calculated time-weighted average (TWA) concentrations of pollutants in ambient air (C_{Air} in ng m^{-3}) for different sampling sites (S) of the landfill ''Grube Antonie'' using MESCO type A1

Compound	S1	S2	S3	S4
HCB	19.5	18.7	20.4	18.5
α-HCH	1935	7469	2146	757
γ-HCH	424	270	238	37.9

TABLE 5.5

Accumulated amounts: mean values of three MESCOs of the type B1 and B2 (M_S in ng) after different exposure times and relative standard deviation (RSD in %) in the field experiment

Compound[a]	Sampler B1						Sampler B2					
	7 days (ng)	RSD (%)	14 days (ng)	RSD (%)	21 days (ng)	RSD (%)	7 days (ng)	RSD (%)	14 days (ng)	RSD (%)	21 days (ng)	RSD (%)
∑TriCB	0.50	3.0	0.99	1.6	1.21	6.8	1.56	6.7	2.96	3.0	4.07	3.6
∑TeCB	0.64	0.8	1.20	2.7	1.76	6.5	1.57	5.8	2.80	4.3	4.94	3.6
PeCB	0.10	5.4	0.20	8.4	0.26	5.0	0.31	11.8	0.53	5.0	0.82	5.0
HCB	0.05	8.1	0.13	10.0	0.23	3.0	0.14	23.5	0.35	16.0	0.67	8.2
α-HCH	8.60	8.7	18.7	14.5	26.0	4.4	13.9	10.4	25.4	16.3	35.8	11.2
β-HCH	0.10	4.0	0.24	9.3	0.31	5.9	0.94	16.0	1.57	26.3	2.45	5.2
γ-HCH	2.51	8.3	5.60	19.4	7.11	4.9	3.31	22.6	7.32	4.8	11.4	8.4
δ-HCH	2.38	5.2	4.60	17.0	5.73	8.4	3.81	17.1	10.3	12.3	17.1	2.3

[a]TriCB, trichlorobenzene; TeCB, tetrachlorobenzene; PeCB, pentachlorobenzene.

zone of the thermodesorption unit is just 8 cm long, and so the silicone elastomer must be folded in the middle.

The results of linear regression analysis show that the amounts of different compounds accumulated per sampler versus time display a linear trend (see Ref. [5]).

5.5 CONCLUSIONS

The MESCOs for air sampling combine the benefits of a passive sampling system with those of analysing the accumulated analytes by thermodesorption/GC–MS, while avoiding the use of solvents and laborious and expensive sample preparation and clean-up steps. The passive sampling devices developed are small, robust and inexpensive. The receiving medium employed—stir bar, silicone tubing or silicone rod—can be reused after each deployment. The stable enveloping LDPE membrane (wall thickness 250 μm) makes the MESCOs of the type A robust for field experiments. On the other hand the thin LDPE film of the MESCOs of the type B reduces the lag-phase. The results of the measurements with both sampler types show that the uptake of PCBs and HCH is linear over some weeks. Moreover, the passive sampling technique can detect TWA air concentrations in the pg m^{-3} range and the passive samplers were successfully tested in a polluted area.

Finally it should be mentioned that the scope of the MESCOs is not restricted to field air monitoring. For indoor air analysis, typically performed under nearly stationary conditions it is possible to determine TWA concentrations of SVOCs (e.g. PCBs or polycyclic aromatic hydrocarbons) that are hardly to monitor with commercial devices at present.

Further investigations are needed to better estimate the reproducibility of this technique. In addition, the influence of relevant environmental conditions, e.g. temperature, humidity and air velocity, on the sampling rates must be studied in detail. For the adjustment of laboratory-derived sampling rates to concrete field conditions it could be helpful to determine on-site elimination rates of so-called performance reference substances [13] with which the MESCO sampling phases were preloaded before field deployment.

REFERENCES

1 B. Vrana, P. Popp, A. Paschke and G. Schüürmann, *Anal. Chem.*, 73 (2001) 5191.

2 E. Baltussen, P. Sandra, F. David and C. Cramers, *J. Microcolumn Sep.*, 11 (1999) 737.
3 B. Vrana, P. Popp, A. Paschke, B. Hauser, U. Schröter and G. Schüürmann, Patentschrift DE 100 42 073 C2, Deutsches Patent-und Markenamt München (2002).
4 L. Wennrich, P. Popp and C. Hafner, *J. Environ. Monit.*, 4 (2002) 371.
5 H. Paschke and P. Popp, *Chemosphere*, 58 (2005) 855.
6 J.N. Huckins, G.K. Manuweera, J.D. Petty, D. Mackay and J.A. Lebo, *Environ. Sci. Technol.*, 27 (1993) 2489.
7 J.D. Petty, J.N. Huckins and J.L. Zajicek, *Chemosphere*, 27 (1993) 1609.
8 H. Hauk, G. Umlauf and M.S. McLachlan, *Environ. Sci. Technol.*, 28 (1994) 2372.
9 B. Larsen, T. Bomboi-Mingarro, E. Brancaleoni, A. Calogirou, A. Cecinato, C. Coeur, I. Chatzianestis, M. Duane, M. Frattoni, J.L. Fugit, U. Hansen, V. Jacob, N. Mimikos, T. Hoffmann, S. Owen, R. Perez-Pastor, A. Reichmann, G. Seufert, M. Staudt and R. Steinbrecher, *Atmos. Environ.*, 31 (1997) 35.
10 W.A. Ockenden, H.F. Prest, G.O. Thomas, A. Sweetman and K.C. Jones, *Environ. Sci. Technol.*, 32 (1998) 1538.
11 P. Popp, L. Brüggemann, P. Keil, U. Thuss and H. Weiß, *Chemosphere*, 41 (2000) 849.
12 A. Paschke, B. Vrana, P. Popp and G. Schüürmann, *Environ. Pollut.*, 144 (2006) 414.
13 J.N. Huckins, J.D. Petty, J.A. Lebo, F.V. Almeida, K. Booij, D.A. Alvarez, W.L. Cranor, R.C. Clark and B.B. Mogensen, *Environ. Sci. Technol.*, 36 (2002) 85.
14 E.W. Balson, *Trans. Faraday Soc.*, 43 (1947) 54.
15 F. Wania, W.Y. Shiu and D. Mackay, *J. Chem. Eng. Data*, 39 (1994) 572.
16 L.P. Burkhard, A.W. Andren and D.E. Armstrong, *Environ. Sci. Technol.*, 19 (1985) 500.
17 J.W. Westcott and T.F. Bidleman, *J. Chromatogr. A*, 210 (1981) 331.
18 D. Mackay, W.Y. Shiu and K.C. Ma, *Illustrated Handbook of Physical-Chemical Properties and Environmental Fate of Organic Chemicals*, Vols. I, II, V, Lewis Publishers, Boca Raton, 1992.

Chapter 6

Towards quantitative monitoring of semivolatile organic compounds using passive air samplers

Michael E. Bartkow, Carl E. Orazio, Todd Gouin, James N. Huckins and Jochen F. Müller

6.1 INTRODUCTION

Semivolatile organic compounds (SOCs) include a range of potentially toxic pollutants which are distributed throughout the environment primarily via the atmosphere. Examples of SOCs include polycyclic aromatic hydrocarbons (PAHs), polychlorinated biphenyls (PCBs), polychlorinated dibenzodioxins (PCDDs), polychlorinated dibenzofurans (PCDFs), various pesticides and also emerging pollutants such as polybrominated diphenyl ethers (PBDEs). Many of these compounds have been implicated in causing a range of health problems in the immune, endocrine, nervous and reproductive systems of animals and humans [1]. The environmental management of SOCs is so important that an international treaty was successfully negotiated to reduce and eliminate the most persistent SOCs, classified as persistent organic pollutants or POPs [2]. This treaty was ratified by more than 50 countries in 2004.

Traditionally, the monitoring of SOCs in the atmosphere is undertaken using active air sampling systems. These sampling systems require a power supply to operate and are generally bulky and intrusive. Also, they cannot always be easily deployed where monitoring is required to gauge human exposure to SOCs, such as in city and industrial areas, workplaces and homes. Active samplers are also relatively expensive, and vulnerable to vandalism. This limits their use in large-scale monitoring programs. The need for alternative monitoring techniques has resulted in the development of passive samplers.

Comprehensive Analytical Chemistry 48
R. Greenwood, G. Mills and B. Vrana (Editors)
Volume 48 ISSN: 0166-526X DOI: 10.1016/S0166-526X(06)48006-5

Passive samplers provide a potentially cost-effective means of augmenting current monitoring programs. These samplers passively accumulate SOCs via diffusion and deposition from the air and therefore they do not require any external source of energy to operate. Depending on the design of the sampler and deployment chamber, these passive samplers are relatively simple to prepare and deploy in the field and can be placed at a range of sites inaccessible with standard active sampling equipment. Biotic passive samplers such as the leaves of plants have been used to monitor the spatial variability of SOCs (e.g. Refs. [3,4]). However, the variability and complexity of such biological matrices generally limits their use for quantitative monitoring.

In response to the need for a more reproducible and cost-effective monitoring technology, a range of abiotic passive air samplers is currently available, including semipermeable membrane devices (SPMDs), polyurethane foam (PUF) samplers, XAD resin based samplers, polymer-coated glass samplers (POGs), solid-phase microextraction fibres (SPMEs) and polyethylene-based samplers (PSDs) [5–10].

SPMDs were initially developed for monitoring organic pollutants in water [11]. SPMDs consist of two sampling phases, an outer low-density polyethylene membrane (LDPE) encasing a synthetic lipid material. They have been used as passive air samplers in a range of studies measuring the levels of PAHs, PCDD/Fs and PCBs [12–15]. The other samplers use one phase to collect pollutants and in particular, the PUF, XAD and POG samplers are being used in an increasing number of studies to passively sample SOCs in the atmosphere (e.g. Refs. [16–22]).

6.2 ESTIMATING AIR CONCENTRATIONS

Levels of organic pollutants in the atmosphere are subject to variability. For many semivolatile organics this variability in air concentration has been shown to be correlated with changes in emission source strength, air temperature and other meteorological factors. For instance, rain or snow can effectively scavenge semivolatiles from the atmosphere, lowering their air concentrations. Air masses that have moved over source areas before arriving at the sampling site can accumulate the contaminant in question, causing concentrations to become elevated. Consequently, depending on deployment duration, active air sampling may provide only a ‘snap shot’ of air concentrations at a given site. Passive air samplers allow a time-integrated air concentration to be determined. On this basis, active samplers may be useful in assessing how concentrations

of a substance may change in response to changing meteorological conditions or emission source strength, whereas the passive air sampler is well suited for monitoring changes in concentration from one period to another. The latter is useful in assessing whether or not levels of banned substances are declining as a result of regulatory activity.

In order to use passive air samplers to measure atmospheric concentrations of pollutants, calibration data are required. Calibration data include parameters such as sampling rates, sampler/air partition coefficients and loss rate constants [23]. These parameters are usually determined in the laboratory, at a reference site or *in situ*.

When using passive sampler data to estimate the air concentration of SOCs, investigators commonly assume that sampling follows first-order exchange kinetics. Thus, during the first stage of sampler uptake, chemicals are accumulated linearly relative to time. Later, as the outward flux of accumulated chemicals slowly increases, sampling moves into a curvilinear stage and eventually, sampling reaches an equilibrium stage where analyte uptake and loss fluxes are balanced (Fig. 6.1). Because the physicochemical properties of SOCs vary widely, the estimation of atmospheric concentrations from passive sampling data may require the use of all stages of this model. For example, if uptake remains in the linear phase (i.e. loss from the sampler is negligible) during an exposure, then the sampling rates that describe the extraction of chemicals from a certain volume of air over time (i.e. metre cube per day) are used along with the amount of pollutant quantified in the sampler to estimate air concentrations. Before quantitative determinations of atmospheric chemical concentrations from passive samplers

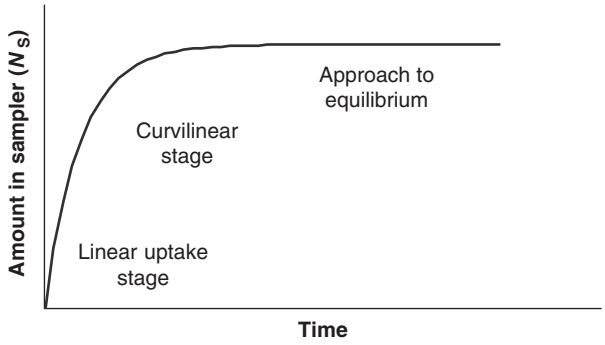

Fig. 6.1. Uptake curve for a passive air sampler showing the linear, curvilinear and equilibrium stages of analyte accumulation [23]. Reprinted from Ref. [23]. Copyright (2005), with permission from Elsevier.

are possible, investigators must have a high level of confidence that the model used for concentration extrapolations fits sampler exchange kinetics and that the calibration data used closely reflect actual *in situ* sampling rates.

A range of studies have made comparisons between air concentrations measured using passive and active samplers. Shen *et al*. [22] have used XAD-based passive air samplers to measure the air concentration of organochlorine pesticides throughout North America. These values compared reasonably well with recent measurements made using active sampling equipment in other studies. Work reporting ∑PBDE and ∑PCB air concentrations in Canada using PUF disks and active samplers have also shown good agreement [16,24]. Van Drooge *et al*. [25] reported good agreement between SPMDs and active samplers when measuring the air concentration of PCBs and HCB at sites in the Pyrenees, with many values comparing within a factor of 2. Jaward *et al*. [26] used PUF and active samplers to measure the air concentration of PCBs and HCB in Italian mountain air, also reporting that agreement was generally within a factor of 2. Further studies from North America have reported comparable measurements using PUF and active sampling data for hexachlorocyclohexane [27] (Fig. 6.2).

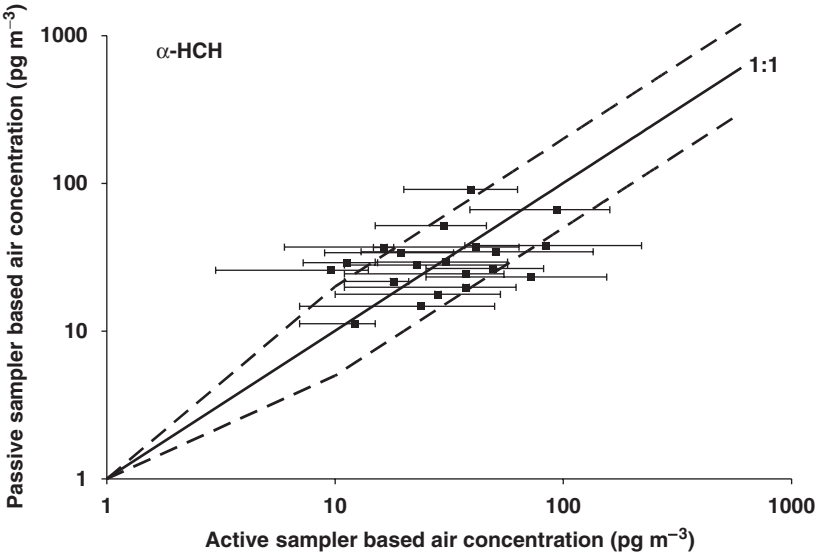

Fig. 6.2. Plot of alpha-HCH air concentrations measured using active and passive samplers at sites in Canada. The error bars indicate the maximum and minimum measurements made by the active samplers. The dashed lines represent where the two measures of air concentration vary by a factor of 2.

Bartkow *et al*. [28] showed that SPMDs could be used reproducibly to estimate air concentrations of various PAHs at an urban site in Brisbane, Australia. The difference between SPMD-derived air concentrations and those measured using active samplers was within a factor of 2. Jaward *et al*. [29] achieved similar results using PUF disks to estimate the air concentration of PAHs at four sites in the UK. The outliers reported by Jaward *et al*. [29] were from one site, and all other compared values were within a factor of 2. Both studies reported good estimates of PAH concentrations for the higher molecular weight compounds, which are predominantly associated with particles (Fig. 6.3).

The good agreement between passive sampler-based air concentrations and measurements made using active samplers for PAHs predominantly associated with particles is interesting. Models used to describe chemical exchange by passive samplers were developed to describe the uptake of vapour phase compounds which accumulate in the sampler by diffusion from the air via first-order kinetics. At this stage, it is unclear which processes dominate the uptake of predominantly particle-bound SOCs.

Bartkow *et al*. [28] suggested that the dominant uptake process for particle-bound PAHs (i.e. those with log *n*-octanol-air partition coefficients (K_{OA}s) > 9) sampled by SPMDs was via particle deposition. These

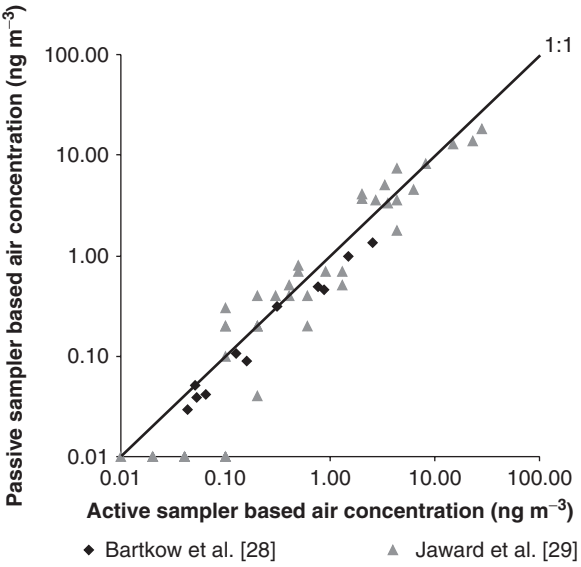

Fig. 6.3. Plot of various PAH air concentrations measured using active and passive samplers at sites in the UK and Australia.

results are useful for SPMDs; however, because the nature of the sampler surface will affect how particles are sampled, further work is required to characterize how particle-bound PAHs are accumulated by other samplers. For example, the SPMD membrane is non-porous but it usually develops a sticky external surface after being deployed in the field, whereas the surface of PUF disks is clearly porous. Furthermore, the design of the sampler chamber also plays a role in how much particle-bound material reaches the sampler surface. Preliminary reports from recent studies suggest that the bowl deployment chambers (Fig. 6.4) used in several studies actually stop a significant proportion of coarse particles from reaching the sampler surface [29].

Unless sampling sites experience very high wind velocities, the mechanism of particulate accumulation by samplers deployed in the bowl chambers (Fig. 6.4) is likely to be Brownian diffusion. Diffusion becomes the dominant mechanism of contact with surfaces only when particle diameters are $<0.3\,\mu m$. In the case of active samplers, the particulate fraction sampled by glass fibre filters is generally $\geqslant 0.3\,\mu m$ in diameter. The probability of fine particles ($<0.3\,\mu m$) sticking on a solid surface (e.g. the PUF sorbent) is generally controlled by local adhesive forces. In light of this information, it is surprising to find that the active sampler total concentrations (gas and particulate phases), of individual high molecular weight analytes, correspond well to the total

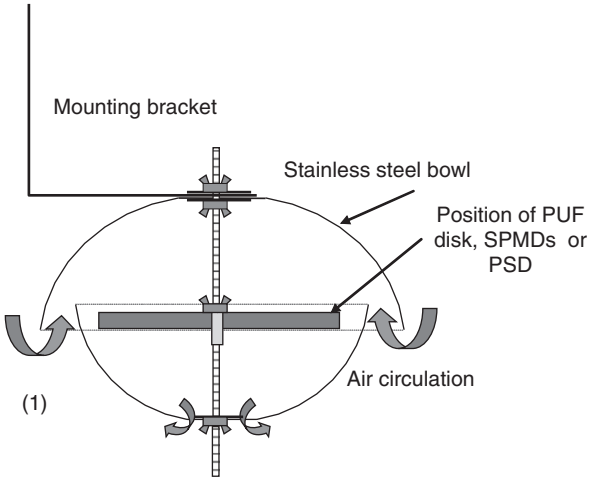

Fig. 6.4. Schematic representation of the bowl chamber (transparent side view). Adapted with permission from Ref. [15]. Copyright (2004) American Chemical Society.

concentrations (gas and particulate phases), of the same individual analytes, accumulated by passive samplers enclosed in protective deployment chambers.

Discrepancies between air concentrations measured using passive and active samplers at the same site can occur for various reasons. Firstly, if passive and active samplers are not deployed for the same periods, changes in air concentrations during these periods will obviously influence results. Particles can also affect results, particularly for SOCs such as PAHs and PBDEs, many of which are associated with particles in ambient air. However, certain environmental factors can also affect the performance of passive air samplers to a greater extent than active air samplers.

6.3 ENVIRONMENTAL FACTORS

The accumulation of many pollutants in passive air samplers is influenced by factors such as changes in wind speed and temperature. For example, for a range of SOCs the rate of chemical exchange between the sampler and atmosphere is governed by the effective thickness of the air-side boundary layer under laminar flow conditions. An increase in wind speed can reduce the effective thickness of the boundary layer, resulting in higher rates of exchange and increased sampling rates [7]. If samplers are exposed to different wind speeds at different sites then comparisons between sites can become confounded, unless the effect of wind is taken into consideration. Temperature significantly affects the sampler-air partition coefficient (K_{SA}) but only weakly affects SOC diffusion rates across the air boundary layer [6].

In order to account for such differences in environmental conditions between sites, Huckins *et al*. [30] have suggested the use of *in situ* performance reference compounds (PRCs) for SPMDs. PRCs are chemicals that do not occur at measurable concentrations in the environment, so their uptake into a passive sampler is negligible. The PRCs are introduced into a sampler prior to its deployment and their loss rates during an exposure are influenced by the same environmental factors that affect the uptake rates of the compounds of interest [30,31]. The loss of PRCs and uptake of target compounds are assumed to occur via isotropic exchange kinetics. Huckins *et al*. [30] showed that the loss of PRCs loaded into passive water samplers allowed *in situ* calibration of exchange kinetics reflecting exposure to different flow rates at different sites.

Experimentation has shown that the effect of wind speed on sampler performance can be detected using PRCs. Söderström and Bergqvist [32] tested the use of PRCs in SPMDs exposed to different wind speeds. In their study, the loss of PRCs from SPMDs increased with increasing wind speeds. Importantly, at very high wind speeds ($\sim$50 m s^{-1}) sampler-side limitation to chemical exchange was evoked and PRC losses were no longer proportional to wind speed. A similar study has also shown the influence of wind speed on the loss of PRCs from PUF disks [33]. Results from both studies showed that certain sampling chamber geometries effectively reduced the impact of high wind speeds on the analyte exchange rates of passive samplers.

The use of PRCs in SPMDs has also shown that photolysis of accumulated PAHs occurs without adequate shading. The potential for photolysis of analytes accumulated in passive samplers must be minimised to ensure that sampler concentrations can be related to environmental concentrations. When SPMDs were deployed with deuterated PAHs as PRCs, the loss rates of both PRCs were very high, indicating that degradation of the PRCs had occurred [28]. These samplers were deployed inside chambers which allowed reflected light to enter through the louvered sides and the open bottom of the chamber. PAHs have high molar absorptivities in the near ultraviolet region ($>$290 nm) and the major abiotic environmental degradation pathway is photolysis. Half-lives for PAH photolysis by sunlight are relatively short, ranging from 6 min to 5 h, depending on the molecular structure and the solvent. Since polyethylene membrane and the triolein, have UV cutoffs below 200 nm, the SPMD itself does not screen out wavelengths responsible for PAH photolysis.

In an earlier study, Orazio *et al*. [34] used a set of EPA Priority Pollutant PAHs as PRCs in SPMDs exposed to outdoor air. Some samplers were deployed in direct sunlight for 1.5 h and others were deployed for 1 week in mesh canisters (with and without foil shading). In another experiment, SPMDs were exposed for 2 min to direct sunlight to simulate a scenario where SPMDs were exposed to solar radiation during retrieval from the field. The photolysis of the PAHs was tracked by comparing the initial level (peak heights in the chromatogram) of PAHs in an unexposed SPMD with the level observed in the exposed SPMD. Partial shielding of the SPMD from sunlight was achieved by covering the top half of the horizontally hung canister with a foil tent. This blocked direct sunlight, and allowed only reflected sunlight to pass into the canisters and reach the SPMD. Nevertheless, several photosensitive PAHs were degraded. In SPMDs that were only protected by

the canister, PAHs were severely photodegraded. Photolysis was greatest in SPMDs exposed to direct sunlight for one and a half hours. The results of these deployments underscore the need for proper shielding of SPMDs from sunlight during air sampling. These tests show that photolysis of certain PAHs in passive samplers exposed to the atmosphere can occur in just 2 min of exposure to direct sunlight.

It is evident that the integrity of PAH sampling with passive air samplers can be compromised if samplers are exposed even briefly to sunlight during deployment, retrieval, processing and analysis. Care must be taken to transfer samplers without any sunlight exposure. Extreme care should be taken to avoid sunlight exposure when using perdeuterated PAHs as PRCs, as even partial photodegradation of PRCs would invalidate their use to derive *in situ* sampling rates of analytes.

Potentially, selected PRCs can be used to detect any photolysis of accumulated analytes in passive samplers. One such approach employs passive samplers spiked with highly photosensitive compounds, which have very low fugacity in the sampler matrix and act as reference standards for verifying photostability during exposures. This approach could become an integral part of the quality control for the use of passive samplers for atmospheric sampling.

Regardless of how PRCs are used to account for the effects of environmental factors on sampler performance, deployment chambers should still be used to ensure that the impacts of wind, light and dust particles are minimized. The chamber design used by Bartkow *et al*. [28] was shown to provide inadequate protection from incident light. This chamber consisted of a galvanized iron box (40 cm by 40 cm by 40 cm) with louvered sides and an open bottom. Preliminary results from recent work shows that even when a louvered plate is fitted into the base of the chamber, some photolysis of PAHs still occurs [35]. In the same study, the aluminium bowl sampler chambers were shown to provide more effective protection against photodegradation. This chamber can also be easily transported and deployed without being obtrusive.

6.4 CONCLUSIONS

An increasing number of studies are showing that passive air samplers can be used to measure the air concentration of various SOCs with reasonable reliability. In many cases, air concentrations measured using passive and active samplers are within a factor of 2 or better,

particularly when the samplers are co-deployed for the same period. Because active and passive sampling approaches differ significantly and quantification of analytes at trace or ultra-trace concentrations can increase the variability of measurements, this level of correspondence is promising. The need for passive samplers is underscored when we consider that active air samplers cannot be used, either for practical reasons or budgetary limitations, at a range of sites. For these reasons, passive air samplers are often the best choice for the monitoring of SOCs.

The use of PRCs holds considerable promise for assessing the effects of wind speed and temperature on passive sampler performance. However, further work is required to show that PRCs can be used to correct for photodegradation. Therefore, samplers should be deployed in appropriately designed passive sampling chambers to minimize the effects of sunlight and wind on sampler performance. Further studies aimed at examining particle deposition on passive sampler surfaces are required for a better understanding of the mechanisms controlling the accumulation of particle-bound SOCs. In summary, considerable progress has been made towards the development of passive samplers and associated methodologies that permits reliable near-quantitative determinations of airborne chemicals.

ACKNOWLEDGMENTS

Funding provided by an ARC SPIRT Linkage Grant, with industry support from Queensland EPA, Queensland Health Scientific Services and ERGO. Queensland Health provides funding for The National Research Centre for Environmental Toxicology.

REFERENCES

1 H. Vallack, D.J. Bakker, I. Brandt, E. Brostrom-Lunden, A. Brouwer, K.R. Bull, C. Gough, R. Guardans, I. Holoubek, B. Jansson, R. Koch, J. Kuylenstierna, A. Lecloux, D. Mackay, P. McCutcheon, P. Mocarelli and R.D.F. Taalman, Controlling persistent organic pollutants—what next? *Environ. Toxicol. Pharmacol.*, 6 (1998) 143.
2 UNEP 2001. Stockholm Convention on Persistent Organic Pollutants. United Nations Environment Programme: http://www.pops.int
3 P. Tremolada, V. Burnett, D. Calamari and K.C. Jones, Spatial distribution of PAHs in the U.K. atmosphere using pine needles, *Environ. Sci. Technol.*, 30 (1996) 3570.

4 H. Kylin and A. Sjodin, Accumulation of airborne hexachlorocyclohexanes and DDT in pine needles, *Environ. Sci. Technol.*, 37 (2003) 2350.
5 J.D. Petty, J.N. Huckins and J.L. Zajicek, Application of semipermeable membrane devices (SPMDs) as passive air samplers, *Chemosphere*, 27 (1993) 1609.
6 M. Shoeib and T. Harner, Characterization and comparison of three passive air samplers for persistent organic pollutants, *Environ. Sci. Technol.*, 36 (2002) 4142.
7 T. Harner, N.J. Farrar, M. Shoeib, K.C. Jones and F.A.P.C. Gobas, Characterization of polymer-coated glass as a passive air sampler for persistent organic pollutants, *Environ. Sci. Technol.*, 37 (2003) 2486.
8 F. Wania, L. Shen, Y.D. Lei, C. Teixeira and D.C.G. Muir, Development and calibration of a resin-based passive sampling system for monitoring persistent organic pollutants in the atmosphere, *Environ. Sci. Technol.*, 37 (2003) 1352.
9 M.E. Bartkow, D.W. Hawker, K.E. Kennedy and J.F. Müller, Characterizing uptake kinetics of PAHs from the air using polyethylene-based passive air samplers of multiple surface area-to-volume ratios, *Environ. Sci. Technol.*, 38 (2004) 2701.
10 H. Paschke and P. Popp, New passive samplers for chlorinated semivolatile organic pollutants in ambient air, *Chemosphere*, 58 (2005) 855.
11 J.N. Huckins, M.W. Tubergen and G.K. Manuweera, Semipermeable membrane devices containing model lipid: A new approach to monitoring the bioavailability of lipophilic contaminants and estimating their bioconcentration potential, *Chemosphere*, 20 (1990) 533.
12 R. Lohmann, B.P. Corrigan, M. Howsam, K.C. Jones and W.A. Ockenden, Further developments in the use of semipermeable membrane devices (SPMDs) as passive air samplers for persistent organic pollutants: Field application in a spatial survey of PCDD/Fs and PAHs, *Environ. Sci. Technol.*, 35 (2001) 2576.
13 W.A. Ockenden, B.P. Corrigan, M. Howsam and K.C. Jones, Further developments in the use of semipermeable membrane devices as passive air samplers: Application to PCBs, *Environ. Sci. Technol.*, 35 (2001) 4536.
14 S.N. Meijer, W.A. Ockenden, E. Steinnes, B.P. Corrigan and K.C. Jones, Spatial and temporal trends of POPs in Norwegian and UK background air: Implications for global cycling, *Environ. Sci. Technol.*, 37 (2003) 454.
15 F.M. Jaward, N.J. Farrar, T. Harner, A.J. Sweetman and K.C. Jones, Passive air sampling of PCBs, PBDEs, and organochlorine pesticides across Europe, *Environ. Sci. Technol.*, 38 (2004) 34.
16 T. Harner, M. Shoeib, M. Diamond, G. Stern and B. Rosenberg, Using passive air samplers to assess urban-rural trends for persistent organic pollutants. 1. Polychlorinated biphenyls and organochlorine pesticides, *Environ. Sci. Technol.*, 38 (2004) 4474.

17 K. Pozo, T. Harner, M. Shoeib, R. Urrutia, R. Barra, O. Parra and S. Focardi, Passive-sampler derived air concentrations of persistent organic pollutants on a north-south transect in Chile, *Environ. Sci. Technol.*, 38 (2004) 6529.
18 L. Shen, F. Wania, Y.D. Lei, C. Teixeira, D.C.G. Muir and T.F. Bidleman, Hexachlorocyclohexanes in the north American atmosphere, *Environ. Sci. Technol.*, 38 (2004) 965.
19 B.H. Wilford, T. Harner, J. Zhu, M. Shoeib and K.C. Jones, Passive sampling survey of polybrominated diphenyl ether flame retardants in indoor and outdoor air in Ottawa, Canada: Implications for sources and exposure, *Environ. Sci. Technol.*, 38 (2004) 5312.
20 N.J. Farrar, T. Harner, M. Shoeib, A. Sweetman and K.C. Jones, Field deployment of thin film passive air samplers for persistent organic pollutants: A study in the urban atmospheric boundary layer, *Environ. Sci. Technol.*, 39 (2005) 42.
21 N.J. Farrar, T.J. Harner, A.J. Sweetman and K.C. Jones, Field calibration of rapidly equilibrating thin-film passive air samplers and their potential application for low-volume air sampling studies, *Environ. Sci. Technol.*, 39 (2005) 261.
22 L. Shen, F. Wania, Y.D. Lei, C. Teixeira, D.C.G. Muir and T.F. Bidleman, Atmospheric distribution and long-range transport behaviour of organochlorine pesticides in North America, *Environ. Sci. Technol.*, 39 (2005) 409.
23 M.E. Bartkow, K. Booij, K.E. Kennedy, J.F. Müller and D.W. Hawker, Passive air sampling theory for semivolatile organic compounds, *Chemosphere*, 60 (2005) 170.
24 T. Gouin, T. Harner, G.L. Daly, F. Wania, D. Mackay and K. Jones, Variability of concentrations of polybrominated diphenyl ethers and polychlorinated biphenyls in air: Implications for monitoring, modeling and control, *Atmos. Environ.*, 39 (2005) 151.
25 B.L. Van drooge, J.O. Grimalt, K. Booij, L. Camarero and J. Catalan, Passive sampling of atmospheric organochlorine compounds by SPMDs in a remote high mountain area, *Atmos. Environ.*, 39 (2005) 5195.
26 F.M. Jaward, A. Di Guardo, L. Nizzetto, C. Cassani, F. Raffaele, R. Ferretti and K.C. Jones, PCBs and selected organochlorine compounds in Italian mountain air: The influence of altitude and forest ecosystem type, *Environ. Sci. Technol.*, 39 (2005) 3455.
27 T. Gouin, T. Harner, P. Blanchard and D. Mackay, Passive and active air samplers as complementary methods for investigating persistent organic pollutants in the Great Lakes basin, *Environ. Sci. Technol.*, 39 (2005) 9115.
28 M.E. Bartkow, J.N. Huckins and J.F. Müller, Field-based evaluation of semipermeable membrane devices (SPMDs) as passive air samplers of polyaromatic hydrocarbons (PAHs), *Atmos. Environ.*, 38 (2004) 5983.

29 F.M. Jaward, N.J. Farrar, T. Harner, A.J. Sweetman and K.C. Jones, Passive air sampling of polycyclic aromatic hydrocarbons and polychlorinated naphthalenes across Europe, *Environ. Toxicol. Chem.*, 23 (2004) 1355.
30 J.N. Huckins, J.D. Petty, J.A. Lebo, F.V. Almeida, K. Booij, D.A. Alvarez, W.L. Cranor, R.C. Clark and B.B. Mogensen, Development of the permeability/performance reference compound approach for in situ calibration of semipermeable membrane devices, *Environ. Sci. Technol.*, 36 (2002) 85.
31 K. Booij, H.M. Sleiderink and F. Smedes, Calibrating the uptake kinetics of semipermeable membrane devices using exposure standards, *Environ. Toxicol. Chem.*, 17 (1998) 1236.
32 H.S. Soderstrom and P.A. Bergqvist, Passive air sampling using semipermeable membrane devices at different wind-speeds in situ calibrated by performance reference compounds, *Environ. Sci. Technol.*, 38 (2004) 4828.
33 M.E. Bartkow, K.C. Jones, K. Kennedy, N. Holling, D. Hawker and J. Müller, Evaluation of performance reference compounds in PUF passive air samplers at different wind speeds, *Organohalogen Compounds*, 66 (2004) 139.
34 C.E. Orazio, S.A. Haynes, J.A. Lebo, J.C. Meadows, J.N. Huckins and J.D. Petty, Potential for photodegradation of contaminants during SPMD sampling, *23rd Annual National Meeting of the Society of Environmental Toxicology and Chemistry*, Salt Lake City, Utah, USA, 2002.
35 M.E. Bartkow, K.C. Jones, K.E. Kennedy, N. Holling, D.W. Hawker and J.F. Müller, Evaluation of performance reference compounds in polyethylene-based passive air samplers, *Environ. Pollut.*, 144 (2006) 365.

Chapter 7

Theory, modelling and calibration of passive samplers used in water monitoring

Kees Booij, Branislav Vrana and James N. Huckins

7.1 INTRODUCTION

Contaminant uptake by passive sampling devices (PSDs) can be seen as a multi-stage transport process. To illustrate the basic steps involved, we will first discuss contaminant uptake by a PSD that consists of a central sorption phase, surrounded by a membrane. For this exercise, we assume that the sampler is biofouled, and is contained within a protective cage (Fig. 7.1). Coming from the surrounding waters, analytes first have to enter the protective cage, where the motion of water may be reduced relative to the water outside the cage. Close to the biofouling layer, convective transport of analyte molecules is reduced more and more, until all transport takes place by molecular diffusion within the water boundary layer (WBL). When ventilating organisms are present, diffusion may be amended with convective currents that are set up by the organisms. After diffusion through the membrane, analytes are finally sorbed by the central sorption phase. This general picture may differ from case to case. For example, protective cages and biofouling layers may be absent, the membrane may act as the final sorption phase (e.g. various types of solid-phase microextraction devices (SPMEs), and low-density polyethylene (LDPE) and polydimethylsiloxane (PDMS) strip samplers), or the sampler may be equipped with additional phases between the membrane and the central phase (e.g. membrane-enclosed sorptive coating (MESCO) and Chemcatcher samplers).

A variety of models has been used over the past 15 years to better understand the kinetics of contaminant transfer to passive samplers. These models are essential for understanding how the amounts of absorbed contaminants relate to ambient concentrations, as well as for

Comprehensive Analytical Chemistry 48
R. Greenwood, G. Mills and B. Vrana (Editors)
Volume 48 ISSN: 0166-526X DOI: 10.1016/S0166-526X(06)48007-7

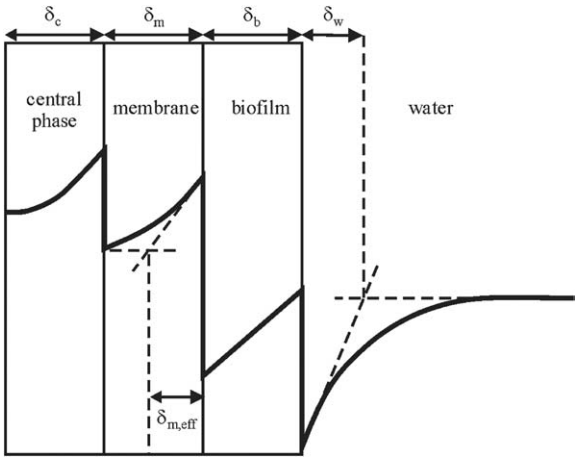

Fig. 7.1. Schematic representation of concentration profiles in a dual-phase PSD with exterior biofilm (i.e. the right half of a symmetrical sampler, or the whole cross section of a sampler with an impermeable boundary located to the left of the central phase). Dashed lines indicate how the effective thickness of the respective phases may be estimated (see Sections 7.5 and 7.6).

the design and evaluation of calibration experiments. Models differ in the number of phases and simplifying assumptions that are taken into consideration, such as the existence of (pseudo-) steady-state conditions, the presence or absence of linear concentration gradients within the membrane phase, the way in which transport within the WBL is modelled and whether or not the aqueous concentration is constant during the sampler exposure.

In the next sections, we will introduce the basic concepts and models used in the literature on passive samplers for the special case of triolein-containing semipermeable membrane devices (SPMDs). These can easily be extended to samplers with more or with less sorption phases. Then we will discuss the transport of chemicals through the various phases constituting PSDs. Finally, we will discuss the implications of these models for designing and evaluating calibration studies.

7.2 BASIC CONCEPTS AND MODELS FOR SPMDS

Mass-transfer coefficients (k_i) are frequently used to link the flux (j_i) through a phase (i) to the concentration difference ΔC_i between the end points of that phase

$$j_i = k_i \Delta C_i \tag{7.1}$$

Equation (7.1) is an expression of the notion that mass fluxes (j) are linearly proportional to a driving force (ΔC_i). The mass-transfer coefficient can be interpreted as a conductivity term, with the dimension of a velocity (e.g. cm day^{-1}). This approach has been followed to model contaminant uptake by a number of PSDs [1–7]. Huckins *et al*. [3] have applied this scheme for the case of contaminant uptake by triolein-filled SPMDs in the presence of biofouling, assuming that the fluxes at both sides of each interface are equal, and that local sorption equilibrium exists at the interfaces. In addition, these authors assumed that the ratios of space-averaged concentrations in the triolein and in the membrane phases are close to the triolein–membrane partition coefficient at all times. The latter assumption was confirmed for the case of SPMDs, by numerical integration of Fick's second law [8]. The differential equation that governs the uptake process can then be expressed as

$$\frac{dC_s}{dt} = \frac{Ak_o}{V_s}\left(C_w - \frac{C_s}{K_{sw}}\right) \tag{7.2}$$

where C_s and C_w are the volume-based contaminant concentrations in SPMD and in water respectively, V_s is the SPMD volume, A is the SPMD surface area, and K_{sw} is the SPMD–water partition coefficient. The K_{sw} equals the volume-averaged partition coefficient for the triolein phase (K_{Lw}) and the membrane (K_{mw}), as shown by Huckins *et al*. [9]

$$K_{sw} = \frac{V_m K_{mw} + V_L K_{Lw}}{V_m + V_L} \tag{7.3}$$

The overall mass-transfer coefficient k_o is given by

$$\frac{1}{k_o} = \frac{1}{k_w} + \frac{1}{K_b K_{bw}} + \frac{1}{k_m K_{mw}} \tag{7.4}$$

where k_w, k_b, k_m are the mass-transfer coefficients for the WBL, the biofilm and the LDPE membrane, and K_{bw}, K_{mw} are the biofilm–water and the membrane–water partition coefficients, respectively. Equation (7.4) is an expression of the fact that the total mass-transfer resistance ($1/k_o$) equals the sum of the resistances posed by the respective phases. Acknowledging that a mass-transfer coefficient equals the ratio of a diffusion coefficient and an effective phase thickness (δ), Eq. (7.4) can also be written as

$$\frac{1}{k_o} = \frac{\delta_w}{D_w} + \frac{\delta_m}{D_m K_{mw}} + \frac{\delta_b}{D_b K_{bw}} \tag{7.5}$$

Bartkow *et al*. [10] have accounted for the transport resistance posed by a protective cage that may surround SPMDs, by adding a term A/Q_v to the right-hand side of Eq. (7.4), where Q_v is the volume rate of water flow to the protective cage and A the surface area of the SPMD. These authors concluded, however, that this resistance can be neglected, except for some rather extreme cage designs.

For short exposure times, the concentration in the SPMD is much smaller than its equilibrium value (i.e. $C_s \ll K_{sw}C_w$), and Eq. (7.2) reduces to

$$dC_s \approx \frac{Ak_o}{V_s} C_w dt \tag{7.6}$$

which yields after integrating over time [3]

$$\int \mathrm{d}C_s \approx \frac{Ak_o}{V_s} \int C_w \mathrm{d}t = \frac{Ak_o}{V_s} C_{w,TWA} t \tag{7.7}$$

where $C_{w,TWA}$ is the time-weighted average (TWA) concentration in the water phase. Three names may be used to refer to the initial stage of the sampling process. When C_w is constant with time, the concentration of accumulated contaminants increases linearly with time. This stage of the uptake is therefore called the linear uptake stage. For scenarios where aqueous concentrations vary with time, the concentration in the SPMD is linearly proportional to the TWA concentration, and sampling is called time-integrative. Finally, because the rate of change of concentrations in the sampler is linearly proportional to the aqueous concentration, this initial sampling stage may be called kinetic sampling. An interesting aspect of Eq. (7.7) is that the product Ak_ot is equivalent to the apparent water volume extracted during the exposure time t. Hence, the product Ak_o can be viewed as an apparent water sampling rate (R_s)

$$R_s = k_o A \tag{7.8}$$

Because R_s represents the volume of water extracted per unit time, it forms a conceptual link between traditional batch water extraction methods and PSD-based methods. Equation (7.8) shows that water sampling rates are linearly proportional to the surface area of the sampler. For this reason, a comparison of sampling rates among different sampler designs only yields meaningful results when differences in surface area are taken into account.

For very long exposure times and a constant C_w, the concentration in the SPMD does not change with time, and Eq. (7.2) reduces to

$$C_w - \frac{C_s}{K_{sw}} = 0 \tag{7.9}$$

which merely is an expression that the concentration in the SPMD attains its equilibrium value ($C_s = K_{sw}C_w$). The corresponding sampling scenario is called equilibrium sampling.

A general solution to Eq. (7.2) for constant C_w is given by [4]

$$C_s = K_{sw}C_w[1 - \exp(-k_e t)] + C_0 \exp(-k_e t) \tag{7.10}$$

where C_0 is the concentration at $t = 0$, and the elimination rate constant (k_e) is given by

$$k_e = \frac{k_o A}{K_{sw}V_s} = \frac{R_s}{K_{sw}V_s} \tag{7.11}$$

Equation (7.10) shows that the uptake from the environment and the elimination of the initial amounts (found in the PSD fabrication controls) are additive. Subtraction of these levels can be problematic when the initial concentration is higher than, or about equal to, the equilibrium concentration. In that case, the concentrations in exposed samplers can be smaller than the concentrations observed in fabrication controls, and control subtraction would yield negative concentrations. Equation (7.10) also shows that the uptake and elimination process of a particular compound are characterised by the same k_e value. This observation is the basis of estimating *in situ* sampling rates from the dissipation rates of performance reference compounds (PRCs) (Section 7.9.4) [11].

When the initial concentration equals zero, Eq. (7.10) takes the form of the more familiar release equation [2]

$$C_s = K_{sw}C_w\left[1 - \exp\left(-\frac{R_s t}{K_{sw}V_s}\right)\right] \tag{7.12}$$

which in the short time limit reduces to the linear uptake equation

$$C_s = \frac{C_w R_s t}{V_s} \tag{7.13}$$

For the dissipation of PRCs that do not occur in the environment ($C_w = 0$) and that are spiked into the sampler prior to exposure, Eq. (7.10) reduces to the more familiar release equation [2]

$$C_s = C_0 \exp(-k_e t) \tag{7.14}$$

Aqueous concentrations can be calculated from the amounts (N_s) absorbed by the PSD, the *in situ* sampling rate of the compounds and their sampler–water partition coefficients, using the rearranged Eq. (7.12)

$$C_w = \frac{N_s}{K_{sw}V_s[1 - \exp(-R_s t/K_{sw}V_s)]} \tag{7.15}$$

For equilibrium samplers, the term in square brackets equals 1 to good approximation, and aqueous concentrations are calculated from

$$C_w \approx \frac{N_s}{K_{sw}V_s} \tag{7.16}$$

For kinetic samplers, operating in the linear uptake mode, the term in square brackets is approximately equal to $(R_s t)/(K_{sw}V_s)$, and aqueous concentrations can be calculated from

$$C_w \approx \frac{N_s}{R_s t} \tag{7.17}$$

The denominators in Eqs. (7.15)–(7.17) can be interpreted as the apparent water volume that is cleared of analyte during the exposure (Fig. 7.2). In the case of equilibrium sampling, this volume is limited by the sorption capacity of the sampler ($K_{sw}V_s$). For kinetic sampling, the apparently extracted water volume is limited by the sampling rate and the exposure time ($R_s t$).

7.3 MODEL APPLICATION TO OTHER PASSIVE SAMPLERS

The discussion in the previous section can easily be extended to other passive samplers that contain any number of sub-phases, provided that sorption equilibrium exists at the interfaces and that (pseudo-) steady-state conditions apply within the barriers between the water and the collection phase (i.e. the difference between the inward and outward fluxes for each intermediate phase should be relatively small). Equation (7.5) may then be generalised as [4]

$$\frac{1}{k_o} = \sum \frac{\delta_i}{D_i K_{iw}} \tag{7.18}$$

where the summation runs over all phases i. The evolution of the analyte amounts accumulated in the receiving phase (i.e. that part of the sampler that is actually extracted and analysed) is given by

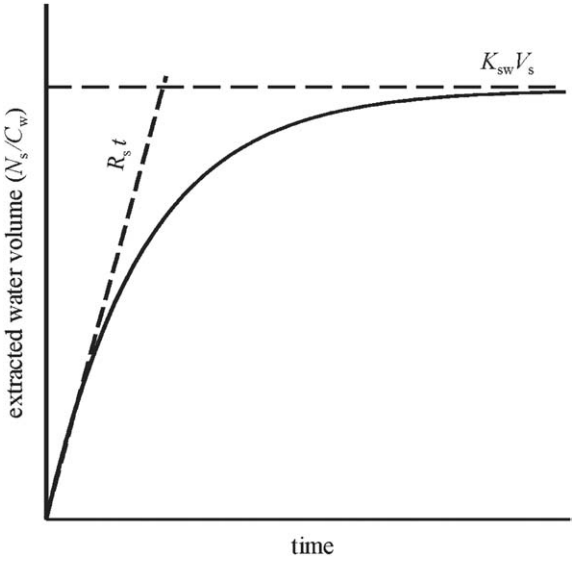

Fig. 7.2. Effectively extracted water volume as a function of time. For long exposure times the extracted volume is constrained by the sorption capacity of the PSD ($K_{sw}V_s$), and at short exposure times by the product of sampling rate and time ($R_s t$).

Eq. (7.12), where K_{sw} takes the general form

$$K_{sw} = \frac{\sum V_i K_{iw}}{\sum V_i} \tag{7.19}$$

and the sampler volume V_s equals the sum of the volumes of all the subphases that are analysed.

In the SPME literature, a slightly different (empirical) model is used to describe the sampler–water exchange kinetics [7,12]

$$\frac{dC_s}{dt} = k_1 C_w - k_2 C_s \tag{7.20}$$

This model is mathematically equivalent to Eq. (7.2), with $k_2 = (Ak_o)/(K_{sw}V_s)$ and $k_1 = K_{sw}k_2$.

7.4 VALIDITY OF THE MODEL ASSUMPTIONS

For the models above, it was assumed that linear concentration gradients exist in the membrane and in the central phase; that equilibrium exists at the interfaces; that molecular diffusion is the predominant

transport mechanism in the membrane with a diffusion coefficient that is independent of time and of concentration.

In the initial stages of the exposure, analytes have to penetrate the membrane to get to the central phase. The resulting time lag has been experimentally confirmed to be about 10 h for the uptake of PCB 52 by SPMDs [2]. A theoretical model for the mass flux through a plane sheet with constant concentration on both sides of the sheet predicts a lag time of [13]

$$t = \frac{\delta_{\mathrm{m}}^2}{6D_{\mathrm{m}}} \tag{7.21}$$

Diffusion coefficients differ widely among polymers. Values for benzene include $3 \times 10^{-9}\,\mathrm{m^2\,s^{-1}}$ in PDMS, $2 \times 10^{-12}\,\mathrm{m^2\,s^{-1}}$ in LDPE, $2 \times 10^{-16}\,\mathrm{m^2\,s^{-1}}$ in poly(methylacrylate) and $1 \times 10^{-19}\,\mathrm{m^2\,s^{-1}}$ in poly (vinylalcohol) [14,15]. For 100 μm thick membranes of these polymers Eq. (7.21) predicts lag times of 6 s, 14 min, 4 months, and 4 centuries, respectively, and these values are expected to increase with molecular size. Evidently, for WBL-controlled uptake, the analyte distribution within the membrane does not affect the uptake rates. Adopting an aqueous diffusion coefficient of $5 \times 10^{-10}\,\mathrm{m^2\,s^{-1}}$ and an effective boundary layer thickness of 30–300 μm (Section 7.5), lag times of 0.3–30 s may be expected for WBL-controlled uptake. However, when the membrane is discarded, and only the central phase is analysed, the lag time for membrane passage has to be accounted for, even in the case of WBL-controlled uptake.

Linear gradients in the membrane cannot exist when the membrane accumulates analytes, because in this case the flux into the membrane must be larger than the flux out of the membrane. By the same argument, linear gradients cannot exist in the central receiving phase either. The concentration gradient in the middle of the receiving phase (e.g. SPMD, MESCO equipped with a PDMS rod), or next to an impermeable wall (e.g. Chemcatcher, SPME) should be zero. (Otherwise, a discontinuity in the flux would occur.) Yet, the concentration gradient at the outer side of the central phase should differ from zero. (Otherwise, the central phase would not accumulate anything.) Again, for WBL-controlled uptake, the existence of non-linear gradients in the membrane or in the central phase does not invalidate the model, but for membrane-controlled uptake, this phenomenon may have to be accounted for. The non-linearity of concentration gradients can be assessed in terms of an effective phase thickness ($\delta_{\mathrm{i,eff}}$) as shown in Fig. 7.1 for the membrane phase. Using an analytical radial diffusion model for uptake by SPME

fibres, Louch *et al*. [16] showed that the effective membrane thickness deviates less than 20% from the actual membrane thickness for times that are larger than the lag time (Eq. (7.21)). Using numerical methods, Hofmans [8] obtained similar results for SPMDs.

The assumption that instantaneous equilibrium exists at the interfaces is likely to be met for the small mass-transfer rates encountered in passive sampling methods, particularly for rubbery polymers, which are characterised by short relaxation times [14].

Although diffusion coefficients in polymers have been shown to depend on diffusant concentration, this dependence is reported to be weak [14], and can probably be neglected in passive sampling because of the relatively low analyte concentrations encountered.

7.5 WATER BOUNDARY LAYER RESISTANCE

Exact models for mass transfer through the WBL exist only for some simple flow arrangements, such as the flow through ducts and pipes, and parallel flow along an absorbing flat plate [17–20]. Starting at the leading edge of the plate, the momentum of the water that is immediately adjacent to the plate is reduced due to surface friction. As the water moves along the plate, this retarded water layer in turn attenuates the momentum of the water layers at larger distance from the surface, which results in the development of a viscous sublayer, with a thickness that increases with distance downstream of the leading edge. Similarly, analytes are removed from a layer with a thickness that increases downstream, leading to the development of a concentration boundary layer. With increasing thickness of this layer, transport by eddy diffusion becomes increasingly important, since turbulent diffusion coefficients increase with increasing distance from the surface [19,21]. At large distances from the leading edge, a steady-state concentration profile is established that no longer depends on the distance along the plate. Equations for the short-plate limit (growing concentration boundary layers) and the long-plate limit (distance-independent concentration boundary layers) have been given by Opdyke *et al*. [22] for hydrodynamically smooth flows (i.e. flows along surfaces where the roughness elements are embedded in the viscous sublayer). The (surface averaged) mass-transfer coefficients for the short-plate limit are given by [22,23]

$$k_{\mathrm{w}} = 0.81 u_* \left(\frac{D_{\mathrm{w}}}{\nu}\right)^{2/3} \left(\frac{\nu}{u_* L}\right)^{1/3} \tag{7.22}$$

where ν is the kinematic viscosity of the water, L is the length of the plate, and u_* is the friction velocity, which is frequently used in the literature on hydrodynamics to parameterise the shear stress (τ)

$$u_* = \sqrt{\frac{\tau}{\rho}} \tag{7.23}$$

where ρ is the density of water. In turbulent flows, u_* can be interpreted as the characteristic eddy velocity relative to the main stream [24,25]. The friction velocity for an essentially laminar flow along a flat surface is related to the free-stream velocity (U) by [18]

$$u_*^2 = 1.328U^2\sqrt{\frac{\nu}{UL}} \tag{7.24}$$

Equation (7.24) is arranged so as to stress that it is dimensionally consistent (i.e. u_* has the same dimension as the main stream velocity U, and $\nu/(UL)$ is dimensionless). The transition from laminar to turbulent flow takes place at values of $UL/\nu > 4 \times 10^6$ when special precautions are taken to reduce the turbulence intensity of the main flow [17]. When no such precautions are taken, the transition to turbulent flow takes place at lower values, i.e. $UL/\nu > 350{,}000$ to 500,000, depending on the turbulence intensity of the main flow [17].

In the long-plate limit, the mass-transfer coefficients are given by [19,22]

$$k_{\mathrm{w}} = 0.08u_*\left(\frac{D_{\mathrm{w}}}{\nu}\right)^{2/3} \tag{7.25}$$

and u_* (for fully developed turbulent flow) may be estimated from the free-stream velocity by [18]

$$u_*^2 = 0.074U^2\left(\frac{\nu}{UL}\right)^{1/5} \tag{7.26}$$

For more complex scenarios, such as mass transfer for cylinders and packed bed reactors, empirical correlations have been established of the form [18,26]

$$\frac{\mathrm{Sh}}{\mathrm{ReSc}^{1/3}} = B\mathrm{Re}^{\mathrm{m}} \tag{7.27}$$

where the (dimensionless) Sherwood (Sh), Reynolds (Re) and Schmidt (Sc) numbers are defined by

$$\mathrm{Sh} = \frac{k_{\mathrm{w}}d}{D_{\mathrm{w}}} \tag{7.28}$$

$$\mathrm{Re} = \frac{ud}{v} \tag{7.29}$$

$$\mathrm{Sc} = \frac{v}{D_w} \tag{7.30}$$

where d is a conveniently chosen characteristic length scale and u a characteristic velocity. The constant B in Eq. (7.27) is of the order 1 and $m \approx -0.5$ (range -0.3 to -0.7). For the case of mass transfer to a cylinder with its main axis perpendicular to the flow, d equals the diameter of the cylinder, $B = 0.6$ and $m = -0.487$, which is valid for the range $100 < \mathrm{Re} < 3500$ and $1000 < \mathrm{Sc} < 3000$. It follows from Eq. (7.27) that mass-transfer coefficients are proportional to $D^{2/3}$ and to the flow velocity $U^{0.5}$.

Equations (7.22) and (7.25) could be used for passive samplers with a planar configuration. It should be realised, however, that in many situations, the flow near the sampler surface may vary in both time and space. The sampler may be mounted in a protective cage in a zigzag or twisted configuration, and the main flow may generate vortices when passing through ventilation holes or over sharp edges. Furthermore, the sampler surface may bend, twist or vibrate depending on flow velocity, angle of incidence, sampler material. In addition, the flow velocity may vary along the sampler surface, where even dead spots may exist as a result of the mounting pattern. Similarly complex hydrodynamics may exist around samplers with a cylindrical configuration. Despite the complexity of the hydrodynamics near passive samplers, some general conclusions remain, however. First, the number of variables in experiments on mass transfer through the boundary layer may be reduced by correlating the appropriate dimensionless numbers Sh, Re and Sc for a given sampler geometry. Second, a wide number of such empirical correlations from the engineering literature suggests that Sh typically is proportional to $\mathrm{Sc}^{1/3}$, indicating that k_w be proportional to $D^{2/3}$ [18,27]. This in turn indicates that the effective boundary layer thickness increases with increasing diffusion coefficient according to $\delta_w \sim D^{1/3}$. Third, the effective WBL thickness, though useful for visualising the extent to which the concentration gradient penetrates into the main flow, should not be misinterpreted as the thickness of physically unrealistic entities like a stagnant film or an unstirred boundary layer. Fourth, for a given geometry and flow, the k_w values for small samplers can be expected to be larger than for large samplers. Fifth, k_w increases with flow velocity, for a given PSD geometry, but its absolute value is difficult to predict.

TABLE 7.1

Sampling rates of 460 cm^2 SPMDs estimated for the case of laminar flow (Eq. (7.24)) in the short-plate limit (Eq. (7.22)) at parameter values $L = 10$ cm, $\nu = 10^{-6}\,m^2\,s^{-1}$, $D = 5 \times 10^{-10}\,m^2\,s^{-1}$

U (cm s^{-1})	Re	u_* (cm s^{-1})	u_*L/ν	k_w (μm s^{-1})	R_s (L day^{-1})
1	1000	0.2	200	2	7
10	10000	1.2	1200	6	22
100	100000	6.5	6500	18	70

As a check on how far the equations above help to understand sampling rates for boundary layer controlled uptake, we evaluated the case of 460 cm^2 SPMDs that are exposed to water flows of 1, 10 and 100 cm s^{-1} at 20°C, adopting an average stream length over the SPMD of 10 cm (i.e. somewhere between 2.5 and 91 cm), a kinematic viscosity of $10^{-6}\,m^2\,s^{-1}$ and a diffusion coefficient of $5 \times 10^{-10}\,m^2\,s^{-1}$. For these flow velocities, the group UL/ν equals 10^3, 10^4 and 10^5 respectively, which is below the transition to turbulence (see above). Estimating the friction velocity from Eq. (7.24) and k_w for the short-plate limit (Eq. (7.22)) yields sampling rates between 7 and 70 L day^{-1} (Table 7.1). These estimates are in fair agreement with observed sampling rates of 4–10 L day^{-1} at flow velocities $\leqslant$ 1 cm s^{-1} [9,28,29] and 100 L day^{-1} at 90 cm s^{-1} [30], but are higher than the values of about 5 L day^{-1} at 50 cm s^{-1} [29]. However, comparison of estimated and experimental sampling rates is hindered by the fact that reported flow velocities are usually calculated rather than measured.

7.6 MEMBRANE RESISTANCE

Two types of polymeric membranes have been used for passive samplers. Non-porous membranes include LDPE [3,5,6,31,32], polypropylene and polyvinylchloride [3,33], PDMS [3,33–35], polyimide [36], polyacrylate (PA) [37,38] and other non-polar polymers [38]. Microporous membranes include regenerated cellulose [4,39,40], polyethersulfone (PES) [41], polysulfone (PS) [32] and polyacrylamide hydrogel [42]. Some other membranes used are discussed by Stuer-Lauridsen [43] in an extensive review of passive sampling techniques. In some applications, the membrane is also the primary accumulation site of the analytes (Twister™ bars, LDPE strip samplers, SPME, silicone strip samplers). In other applications, the membrane is meant to separate a

sorption phase from the water (diffusive gradients in thin films (DGT), Chemcatcher, MESCO, SPMD) and to reduce the flux to the sorption phase.

The conductivity to mass transport through the membrane is given by

$$k_{\mathrm{m}}K_{\mathrm{mw}} = \frac{D_{\mathrm{m}}K_{\mathrm{mw}}}{\delta_{\mathrm{m}}} \tag{7.31}$$

where δ_{m} is the thickness of the membrane (Eq. (7.5)). Both D_{m} and K_{mw} are compound-dependent. The role of K_{mw} in Eq. (7.31) may be appreciated by considering that compounds with high membrane–water partition coefficients will have similarly high concentrations at the membrane side of the membrane–water interface. As a result, the concentration gradient over the membrane is elevated compared with that found for compounds with low K_{mw} values, and the steeper concentration gradient results in a larger flux through the membrane. Conversely, the selection of a membrane for which the target analytes have a low affinity (e.g. hydrophilic membranes for sampling hydrophobic compounds) results in an enhanced transport resistance posed by the membrane and to reduced sampling rates. Several examples of this effect have been reported. A comparison between solvent-filled cellulose and polyethylene membranes showed that the uptake rates of organochlorine pesticides by the samplers with cellulose membranes were lower by two orders of magnitude [40]. Similarly, the uptake kinetics of hydrophobic contaminants by the MESCO and Chemcatcher were greatly enhanced by replacing the hydrophilic membrane by polyethylene [5,6], and the uptake rates of the polar compounds diazinon, ethynylestradiol and atrazine by the polar organic chemical integrative sampler (POCIS) were much larger with PES membranes than with polyethylene or Nylon-66 membranes. The choice of membrane material has an effect not only on the sampling rates, but also on the flow sensitivity of the sampler. When the membrane resistance becomes smaller, rate control switches more to side of the WBL, which is by nature dependent on the hydrodynamic conditions at the membrane–water interface. Therefore, attempts to reduce the flow sensitivity of passive samplers by installing membranes that have lower partition coefficients for the analytes, automatically reduce the sampling rates. Conversely, membranes with high K_{mw} values enhance sampling rates but also increase the sensitivity of these samplers to changing flow conditions [5]. Whether or not reduced sampling rates are problematic, depends of course on the aqueous concentration levels,

the exposure time and the sensitivity of the analytical equipment. No general rule can be given, but in the light of the above, it seems unlikely that a flow-insensitive passive sampler can be developed that has sufficiently high sampling rates in all environments.

Estimating sampling rates of compounds for membrane-controlled uptake is hindered by the scarcity of data on diffusion coefficients, particularly for compounds of environmental interest. Diffusion coefficients (D_m) in LDPE have been collected from the engineering literature by Hofmans [8]. She proposed to model D_m as a function of molecular weight (M) according to

$$\begin{aligned} &\log D_m = -7.47 - 2.33 \log M \\ &n = 42, s = 0.44, 70 < M < 655 \end{aligned} \tag{7.32}$$

where D_m is in units of $m^2 s^{-1}$. Diffusion coefficients of PAHs in PDMS appear to be higher than in LDPE by about two to three orders of magnitude and D_m values of PAHs in polyoxymethylene are about one order of magnitude lower than in LDPE (Tatsiana Rusina, Research Center for Environmental Chemistry and Ecotoxicology, Masaryk University, Czech Republic, personal communication). These observations are consistent with the theory that diffusion coefficients increase with increasing segmental mobility and free volume fraction of the polymer [14,44,45], and decrease with increasing glass-transition temperature of the polymer [14].

A large volume of data on PDMS–water and PA–water partition coefficients of organic contaminants can be found in the SPME literature [12,38,46–49,50]. A smaller data set is available for the case of LDPE [30,45,51]. Available log K_{mw} values are shown in Fig. 7.3 as a function of log K_{ow}. Although the scatter is rather high, some general trends can be identified. Log K_{mw} values for LDPE are higher than for PDMS by 0.7 log units, on average. In the range $1 < \log K_{ow} < 4.5$, the log K_{mw} values for PA are 0.3 log units higher than those for LDPE, but this trend does not seem to persist in the higher log K_{ow} range. The log K_{mw} data could be modelled by

$$\begin{aligned} &\text{LDPE}: \quad \log K_{mw} = 1.057 \log K_{ow} - 0.72 \\ &(R^2 = 0.96, s = 0.28, n = 41) \end{aligned} \tag{7.33}$$

$$\begin{aligned} &\text{PDMS}: \quad \log K_{mw} = 1.060 \log K_{ow} - 1.39 \\ &(R^2 = 0.92, s = 0.36, n = 74) \end{aligned} \tag{7.34}$$

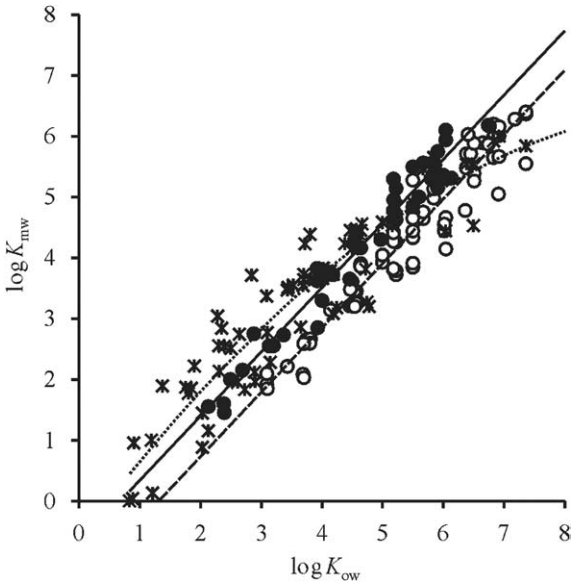

Fig. 7.3. Membrane–water partition coefficients and regression models for LDPE (filled circles, drawn line = linear fit), PDMS (open circles, dashed line = linear fit) and PA (asterisks, dotted line = quadratic fit).

$$\text{PA}: \quad \log K_{\text{mw}} = -0.0629 \log K_{\text{ow}}^2 + 1.341 \log K_{\text{ow}} - 0.62$$
$$(R^2 = 0.88, s = 0.50, n = 74) \tag{7.35}$$

The higher residual errors in the case of PA may be due at least partly to the relatively large number of K_{mw} values of polar compounds, for which K_{ow} is not a very good descriptor. The inclusion of polar interactions and hydrogen bonding appears to be appropriate in this case [12]. For membrane-controlled uptake, it can be expected that samplers that are equipped with a PDMS membrane have 20 times (1.3 log units) higher sampling rates than samplers with an LDPE membrane, i.e. the 0.7 log units lower partition coefficient for PDMS is more than offset by diffusion coefficients that are 2 log units higher. However, for WBL-controlled uptake no difference among membrane types can be expected. Applying Eqs. (7.31)–(7.33) to the case of membrane controlled uptake by 460 cm^2 SPMDs with a 85 μm LDPE membrane, yields sampling rates of 6 L day^{-1} for hexachlorocyclohexanes and 14 L day^{-1} for naphthalene. These estimates are larger than the experimental values of 2 L day^{-1} [28] and 0.9 L day^{-1} [9], respectively, which may be related to the uncertainities in the estimates of D_{m} and K_{mw}.

For membrane-controlled uptake, the slope of a log R_s versus log K_{mw} plot is expected to attain a value of about one, because $R_s \sim k_o \sim D_m K_{mw}$. In practice, somewhat smaller slopes are found, since D_m decreases with molecular size [12,30,50], Alternatively, since $k_e \sim K_{sw}^{-1}$ (Eq. (7.11)), membrane-controlled uptake can be identified when the slopes of log k_e versus log K_{mw} are about 0, or slightly smaller. These conditions are typically observed for compounds with log K_{mw} values <3.5 for SPME with PA fibres [12,50] and for compounds with log K_{ow} values <4.5 in sampling with SPMDs [3,33]. It should be noted, however, that the transition to WBL-controlled uptake depends not only on the properties of the analytes, but also on the hydrodynamic conditions at the membrane–water interface (Eq. (7.5)). Thus, in quiescent or highly turbulent conditions, the critical K_{mw} values for transition to WBL control may be lower or higher respectively [49,52].

7.7 BIOFOULING LAYER

The growth of bacterial mats, periphyton and even macrofauna can intuitively be expected to have a major impact on uptake rates [53]. Richardson *et al*. [54] observed that the amounts of organochlorine pesticides and PAHs, absorbed by SPMDs for which the membrane had been pre-fouled for 1–4 weeks were about 30–40% lower than the amounts absorbed by unfouled SPMDs. These reductions were higher for OCPs than for PAHs, but did not appear to be related to log K_{ow}. Similar reductions of phenanthrene uptake by pre-fouled SPMDs (26–39%) were reported by Ellis *et al*. [55]. Huckins *et al*. [3,11,56] reported that sampling rates of PAHs by pre-fouled SPMDs were smaller than for unfouled SPMDs by 30–70%. These authors reported a weak dependency of the sampling rate reduction with hydrophobicity, with the larger reductions occurring at the higher log K_{ow} end. Assuming that the biofouling layer can be modelled as a water layer with dispersed organic matter (i.e. similar to a layer of sediment), its conductivity for mass transport is given as [3]

$$k_b K_{bw} = \frac{\phi^2 D_w}{\theta \delta_b} \tag{7.36}$$

where ϕ is the porosity and θ the tortuosity of the diffusion pathways within the biofilm (i.e. the ratio of the actual diffusion path length and the thickness of the biofilm). Since both ϕ and θ are of order 1, Eq. (7.36) states that the biofilm behaves essentially like an immobilized water

layer, with a conductivity that is independent of the biofilm–water partition coefficient. As an example, we will apply this model to estimate the thickness of a biofouling layer that causes a reduction in the sampling rate of 460 cm^2 SPMDs from 5 to 2.5 L day^{-1}. Adopting a porosity of 0.9, a tortuosity of 2 and a D_w value of $5 \times 10^{-10}\,m^2\,s^{-1}$, a biofilm thickness of 160 μm can be calculated, which seems to be a reasonable value. It has been suggested by several authors that the use of PRCs allows to quantify the effects of biofouling on the *in situ* uptake rates [11,54], but to date the experimental evidence has not yet been presented in the peer-reviewed literature.

It appears that LDPE is more sensitive to biofouling than PES [41]. Attempts to inhibit biofouling by applying antifouling agents during SPMD deployments [31] have been unsuccessful [55]. Other examples of undesirable impacts of organisms in passive sampling are biodegradation of the regenerated cellulose membranes [6] and physical damage of SPMDs [54]. Although instances of severe biofouling have been reported [54,57], the associated sampling rate reduction seems to be limited to a factor of about 2.

7.8 OTHER INTERMEDIATE PHASES

Next to a central phase enclosed by a membrane phase, other phases have been incorporated as well. Wennrich *et al*. [6] studied the effect of water and air, enclosed between a central PDMS phase and an LDPE membrane, on the sampling rates of organochlorines and PAHs. They found that the air-filled samplers had up to 20 times higher sampling rates than the water-filled samplers, with the exception of β-HCH, γ-HCH and δ-HCH. Higher sampling rates may be expected if the mass-transfer conductivity of a layer of air is larger than that of a water layer of the same thickness, i.e. if

$$\frac{D_a K_{aw}}{D_w} > 1 \tag{7.37}$$

where D_a is the diffusion coefficient in air and K_{aw} the dimensionless Henry's law constant. Calculated ratios ($D_a K_{aw}/D_w$) ranged from 520 for HCB to 0.1 for β-HCH and δ-HCH. For compounds with K_{aw} values $>10^{-4}$, the effect of an unfavourable air–water partition coefficient is offset by a more favourable diffusion coefficient in air ($\sim 5 \times 10^{-6}\,m^2\,s^{-1}$) compared with that in water ($\sim 5 \times 10^{-10}\,m^2\,s^{-1}$). Similar observations have been made for a Chemcatcher sampler, equipped with a central compartment of C_{18}-coated silica and an LDPE membrane [5].

Replacing water by air as intermediate phase resulted in an increase in sampling rates up to a factor of 6. Decreasing sampling rates were observed for the 5-ring PAHs, which showed a decrease in sampling rate by a factor of 2–3 as a result of their very low K_{aw} values ($<3 \times 10^{-5}$). The use of 1-octanol as intermediate phase resulted in an approximately 20-fold increase in sampling rates compared with water as intermediate phase [5]. It should be noted again, however, that reducing the transfer resistances of the internal phases, enhances the relative importance of the mass-transfer resistance of the WBL (Eq. (7.5)), and hence the sensitivity of the sampler to changes in flow conditions.

7.9 CALIBRATION

7.9.1 Static exposure design

In the experimentally convenient static exposure scenario, passive samplers are exposed in a single volume of contaminated water. This method has been used in the past for determining bioaccumulation factors and uptake rates of contaminants by fish and mussels. The evolution of aqueous concentrations in the exposure water is given by [58–60]

$$C_w = \frac{C_{w0}\left\{1 + \frac{K_{sw}V_s}{V_w}\exp\left[-\left(1 + \frac{K_{sw}V_s}{V_w}\right)\frac{R_s t}{K_{sw}V_s}\right]\right\}}{1 + \frac{K_{sw}V_s}{V_w}} \tag{7.38}$$

where C_{w0} is the aqueous concentration at $t = 0$. The concentration in the sampler can be evaluated from the mass balance ($V_s C_s = V_w[C_{w0} - C_w]$)

$$C_s = \frac{C_{w0}K_{sw}\left\{1 - \exp\left[-\left(1 + \frac{K_{sw}V_s}{V_w}\right)\frac{R_s t}{K_{sw}V_s}\right]\right\}}{1 + \frac{K_{sw}V_s}{V_w}} \tag{7.39}$$

which reduces to Eq. (7.12) in the limit $V_w \to \infty$. With Eqs. (7.38) and (7.39) it is assumed that there are no competing sorption phases (equipment and particulate/dissolved organic matter) in the exposure system. In the short time limit, Eq. (7.38) may be approximated by

$$C_w = C_{w0}\left(1 - \frac{R_s t}{V_w} + \cdots\right) \tag{7.40}$$

and the concentration in the sampler may be approximated by

$$C_s = \frac{C_{w0} R_s t}{V_s} \left(1 - \frac{1}{2}\frac{R_s t}{V_w} - \frac{1}{2}\frac{R_s t}{K_{sw} V_s} + \cdots\right) \tag{7.41}$$

When the concentration in the sampler is much lower than its equilibrium value (i.e. $R_s t \ll K_{sw} V_s$), the third term between the parentheses in Eq. (7.41) may be neglected, and Eq. (7.41) reduces to

$$C_s = \frac{C_{w,TWA} R_s t}{V_s} \tag{7.42}$$

where $C_{w,TWA}$ is the TWA concentration during the exposure.

Static exposures have been used in the calibration of SPMDs and similar samplers [9,11,28,59,61] and also is the typical calibration scenario in SPME research [36,60,62]. Equilibration times obtained with static exposures are sometimes erroneously assumed to also apply to field exposures [59,61]. Equation (7.39) shows that the evolution of analyte concentrations in the samplers follows first-order kinetics, with a rate constant that is dependent on the water volume, among other factors. High rate constants can be found when the water volume is small compared with the sorption capacity of the sampler ($V_w \ll K_{sw} V_s$). In this case, the rate constant is approximately equal to R_s/V_w. However, the water volume in the field is essentially infinite ($V_w \gg K_{sw} V_s$), and the rate constant for the attainment of equilibrium equals $R_s/(K_{sw} V_s)$ in that case. The intuitive explanation of short equilibration times that may be observed in static exposure designs is that both the accumulation in the sampler and the depletion of the water favour the attainment of equilibrium [63]. By contrast, depletion of the water phase in the field is insignificant.

7.9.2 Static renewal design

In static renewal designs, the exposure water is refreshed batchwise [41,54]. This design may be used when static or continuous flow exposure designs are not an option. This may occur, for example, when a static exposure would result in an excessive depletion of the water phase, or when problems occur in maintaining stable aqueous concentrations during flow-through exposures. Aqueous concentrations should be measured at least at the beginning and at the end of each renewal period, in order to estimate their average. Uptake curves may be generated when it can be assumed that the amounts removed from the water are absorbed by the sampler (i.e. loss terms like evaporation

and wall sorption, as well as sorption on to dissolved/particulate matter can be neglected) and that the average aqueous concentrations do not vary greatly among renewals. Even then, the mathematical modelling of such data is not so easy, except for the case of kinetic sampling over the entire exposure period (Eq. (7.42)).

7.9.3 Continuous flow design

Continuous flow designs aim at preventing depletion of the water phase during the exposure by ensuring a constant supply of freshly contaminated water to the exposure chamber. As with the static and static renewal designs, sorption to dissolved/particulate matter should be negligible in order to prevent overestimating C_w. However, sorption to the equipment used in the exposure system has no detrimental effect, provided that the equipment has equilibrated with the water. Stable aqueous concentrations can be maintained during the entire exposure if the flushing rate (Q: volume per unit time) of the exposure chamber is much larger than the total sampling rate of all samplers [30]

$$Q \gg nR_s \tag{7.43}$$

where R_s is the sampling rate per sampler and n the total number of samplers in the exposure system. For example, an exposure system that contains five passive samplers that have a sampling rate for a particular compound of 4 L day^{-1} would require a flushing rate at the beginning of the experiment, that is much higher than 20 L day^{-1}. Such a set-up would therefore require a flushing rate of at least 100 L day^{-1} of water with dissolved organic carbon (DOC) levels that are low enough to ensure that contaminant sorption to DOC is insignificant. With the gradual removal of samplers during the experiment, the flushing rate may be reduced, provided that the hydrodynamic conditions in the exposure chamber can be kept constant, e.g. by additional stirring or by recirculation pumping. Because sampling rates are linearly proportional to the sampler surface, the use of smaller samplers may help to reduce the water demand. It should be realised in this case, however, that for WBL-controlled uptake the sampling rate may be a weak function of the sampler length (Eq. (7.22)).

Mixing of stock solutions in methanol or acetone is the most widely used method for preparing contaminated water needed in the exposure experiments [2,6,32], but generator column techniques based on C_{18}-coated silica [28,30] or permeation through a dialysis membrane [64] have also been used.

When constant aqueous concentrations can be maintained during the entire experiment, sampling rates and sampler–water partition coefficients may be obtained by curve fitting of Eq. (7.12). In case the extent of equilibrium attained is insufficient to estimate K_{sw}, the linear uptake equation (Eq. (7.13)) should be used. Decision methods for selecting the correct model are discussed elsewhere [28,65].

Slightly more complicated models should be used when aqueous concentrations are not sufficiently constant during the exposure. Suppose that the aqueous concentrations can be described by a second-order polynomial in time

$$C_w(t) = C_0 + C_1 t + C_2 t^2 \tag{7.44}$$

the solution to the differential equation (Eq. (7.2)) can be found as [66]

$$\frac{C_s}{K_{sw}} = \left(C_0 - \frac{C_1}{k_e} + \frac{2C_2}{k_e^2}\right)[1 - \exp(-k_e t)] + \left(C_1 - \frac{2C_2}{k_e}\right)t + C_2 t^2 \tag{7.45}$$

where k_e is given by Eq. (7.11). The solution for constant concentrations (Eq. (7.12)) and aqueous concentrations that vary linearly with time [30] can be seen to be special cases of Eq. (7.45).

7.9.4 *In situ* calibration

The evaluation of dissipation rate constants of PRCs has been used as a method for calibrating the uptake rates of PSDs *in situ* [2,11,65,67–69]. When PRCs are selected that do not occur in the environment in significant amounts (e.g. ^{13}C-labelled PCBs or perdeuterated PAHs), their dissipation rate constants can be estimated from the rearranged Eq. (7.14)

$$k_e = -\frac{\ln(C/C_0)}{t} \tag{7.46}$$

where C_0 is the PRC concentration at $t = 0$. Consequently, the sampling rate of this PRC can be obtained from the rearranged Eq. (7.11)

$$R_s = k_e K_{sw} V_s \tag{7.47}$$

PRCs can be used only if their dissipation rate is large enough to quantify the difference in PRC concentration at the beginning and at the end of the exposure. Analytical precision is the controlling factor in this case. For compounds with large dissipation rates, detection limits may be an issue. As a result, PRC-derived sampling rates can be obtained only for compounds that span a 1.5 log units wide range in log K_{ow}. In the case of SPMDs, this range spans log K_{ow} values between 4.5 and 6, but for PSDs

with smaller sorption capacities, these values may be shifted towards the higher K_{ow} end.

Extrapolation of PRC-based sampling rates to compounds with much lower log K_{ow} values is not so critical, because these compounds will have attained a substantial, if not complete, degree of equilibrium, and Eq. (7.15) is quite insensitive to uncertainties in sampling rates for this group of compounds. However, uncertainty exists on the question of how PRC-based sampling rates should be extrapolated to the high log K_{ow} range. Huckins *et al*. [11] defined the exposure adjustment factor (EAF) as the ratio of the (PRC-based) sampling rate in the field and the sampling rate of compounds with the same physicochemical properties obtained during laboratory calibration studies

$$\mathrm{EAF} = \frac{R_{s,field}}{R_{s,lab}} \tag{7.48}$$

These authors showed that the EAF is only a weak function of log K_{ow}, and that PRCs may be used to reduce the effect of exposure conditions on sampling rates from 3- to 10-fold to about 2-fold. The EAF approach has recently been generalised [3]. An alternative method of using PRC-based sampling rates to estimate R_s values of more highly hydrophobic compounds is based on the assumption that the conductivity of the WBL is proportional to $D_w^{2/3}$ [3,30,69]. Since D_w is a weak function of molecular size, R_s can be estimated from [3]

$$R_s = R_{sPRC}\left(\frac{V_{PRC}}{V}\right)^{0.39} \tag{7.49}$$

where V_{PRC} and V are the LeBas molar volumes of PRC and analyte respectively. The PRC should be subject to WBL-controlled kinetics, in this case. Experimental sampling rates for WBL-controlled uptake decrease much stronger with molecular size than indicated by Eq. (7.49), but this decrease may well be caused by the overestimation of concentrations of dissolved analyte, due to sorption to DOC [3,5,30]. However, to date, experimental proof of this assumption is not available.

7.10 CONCLUSION AND OUTLOOK

Considerable progress has been made in understanding the factors that control hydrophobic organic contaminant uptake by passive samplers.

- Transfer through the water boundary layer generally is the rate-limiting step for the uptake of highly hydrophobic compounds. As a

result, the sampling rates (R_s) for these compounds depend on the hydrodynamic conditions at the exposure site. Unfortunately, sampling rates for these compounds are difficult to estimate from the local flow velocities and turbulence intensities, and *in situ* calibration techniques based on the dissipation of performance reference compounds (PRCs) are necessary.

- Diffusion through the membrane is the rate-limiting step for compounds with low membrane–water partition coefficients (K_{mw}). Sampling rates for these compounds are only dependent on temperature, and sampling rates obtained in the laboratory can be applied in the field.
- Attempts have been made to eliminate the flow-dependency of sampling rates for highly hydrophobic compounds, by adding additional transport barriers in the sampler and by using more polar membranes. These attempts have been unsuccessful due to a dramatic drop in sampling rates, resulting in detectability problems.
- The dissipation of PRCs allows for estimating sampling rates *in situ*. This technique is hampered by the limited range of log K_{ow} values ($4.5 < \log K_{ow} < 6$) for which dissipation rate constants can be estimated. Model calculations are presently used to extrapolate PRC-based sampling rates into the high log K_{ow} range, but the experimental evidence in support of these models is scarce, and more research in this area is needed. In addition, reliable experimental values of the sampler–water partition coefficients for PRCs are still missing.

Much less is known about samplers for hydrophilic contaminants. The models that have been developed for hydrophobic samplers are useful for understanding the functioning of hydrophilic samplers as well, but some important differences between the sampling of hydrophobic and hydrophilic contaminants are worth noting. First, reliable K_{mw} values for hydrophilic contaminants are missing. Experimental K_{mw} values as well as models that can be used to predict these values from the contaminant's molecular properties are needed. Second, sorption of hydrophilic compounds to the membrane and the central sorption phase involves surface interactions and non-linear sorption isotherms. This may result in anisotropic exchange and competition for sorption sites. Third, the sampling rates that can be obtained for hydrophilic compounds are much lower than for hydrophobic substances, which results in high detection limits. Although a number of different membranes have been tested already, the selection of other membrane

types may yield somewhat higher sampling rates. Assessing these issues is a major challenge for the near future.

REFERENCES

1 G.L. Flynn and S.H. Yalkowsky, Correlation and prediction of mass transport across membranes I: Influence of alkyl chain length on flux-determining properties of barrier and diffusant, *J. Pharm. Sci.*, 61 (1972) 838.
2 J.N. Huckins, G.K. Manuweera, J.D. Petty, D. Mackay and J.A. Lebo, Lipid-containing semipermeable membrane devices for monitoring organic contaminants in water, *Environ. Sci. Technol.*, 27 (1993) 2489.
3 J.N. Huckins, J.D. Petty and K. Booij, *Monitors of Organic Chemicals in the Environment: Semipermeable Membrane Devices*, Springer, New York, 2006.
4 B. Vrana, P. Popp, A. Paschke and G. Schüürmann, Membrane-enclosed sorptive coating. An integrative passive sampler for monitoring organic contaminants in water, *Anal. Chem.*, 73 (2001) 5191.
5 B. Vrana, G. Mills, R. Greenwood, J. Knutsson, K. Svensson and G. Morrison, Performance optimisation of a passive sampler for monitoring hydrophobic organic pollutants in water, *J. Environ. Monit.*, 7 (2005) 612.
6 L. Wennrich, B. Vrana, P. Popp and W. Lorenz, Development of an integrative passive sampler for the monitoring of organic water pollutants, *J. Environ. Monit.*, 5 (2003) 813.
7 Y. Chen and J. Pawliszyn, Kinetics and the on-site application of standards in a solid-phase microextraction fiber, *Anal. Chem.*, 76 (2004) 5807.
8 H.E. Hofmans, *Numerical Modelling of the Exchange Kinetics of Semipermeable Membrane Devices*, MSc Thesis, Netherlands Institute for Sea Research, Den Burg, The Netherlands, 1998.
9 J.N. Huckins, J.D. Petty, C.E. Orazio, J.A. Lebo, R.C. Clark, V.L. Gibson, W.R. Gala and K.R. Echols, Determination of uptake kinetics (sampling rates) by lipid-containing semipermeable membrane devices (SPMDs) for polycyclic aromatic hydrocarbons (PAHs) in water, *Environ. Sci. Technol.*, 33 (1999) 3918.
10 M.E. Bartkow, K. Booij, K.E. Kennedy, J.F. Müller and D.W. Hawker, Passive sampling theory for atmospheric semivolatile organic compounds, *Chemosphere*, 60 (2005) 170.
11 J.N. Huckins, J.D. Petty, J.A. Lebo, F.V. Almeida, K. Booij, D.A. Alvarez, W.L. Cranor, R.C. Clark and B.B. Mogensen, Development of the permeability/performance reference compound approach for *in situ* calibration of semipermeable membrane devices, *Environ. Sci. Technol.*, 36 (2002) 85.
12 W.H.J. Vaes, C. Hamwijk, E.U. Ramos, H.J.M. Verhaar and J.L.M. Hermens, Partitioning of organic chemicals to polyacrylate-coated solid

phase microextraction fibers: Kinetic behavior and quantitative structure–property relationships, *Anal. Chem.*, 68 (1996) 4458.
13 J. Crank, *The Mathematics of Diffusion*, University Press, Oxford, 1957.
14 S.C. George and S. Thomas, Transport phenomena through polymeric systems, *Prog. Polym. Sci.*, 26 (2001) 985.
15 M. Saleem, A.A. Asfour and D. De Kee, Diffusion of organic penetrants through low density polyethylene (LDPE) films: Effect of size and shape of the penetrant molecules, *J. Appl. Polym. Sci.*, 37 (1989) 617.
16 D. Louch, S. Motlagh and J. Pawliszyn, Dynamics of organic compound extraction from water using liquid-coated fused silica fibers, *Anal. Chem.*, 64 (1992) 1187.
17 H. Schlichting and K. Gersten, *Boundary Layer Theory*, 8th ed., Springer-Verlag, Heidelberg, 2000.
18 R.B. Bird, W.E. Stewart and E.N. Lightfoot, *Transport Phenomena*, Wiley, New York, 1960.
19 B.A. Kader and A.M. Yaglom, Heat and mass transfer laws for fully turbulent wall flows, *Intern. J. Heat Mass Transfer*, 15 (1972) 2329.
20 B.P. Boudreau and N.L. Guinasso, The influence of a diffusive sublayer on accretion, dissolution, and diagenisis at the sea floor. In: K.A. Fanning and F.T. Manheim (Eds.), *The Dynamic Environment of the Ocean Floor*, Lexington Books, Toronto, 1982 Chapter 6.
21 J.S. Son and T.J. Hanratty, Limiting relation for the eddy difusivity close to a wall, *AICHE J.*, 13 (1967) 689.
22 B.N. Opdyke, G. Gust and J.R. Ledwell, Mass transfer from smooth alabaster surfaces in turbulent flows, *Geophys. Res. Lett.*, 14 (1987) 1131.
23 T.J. Hanratty and J.A. Campbell, Measurement of wall shear stress. In: R.J. Goldstein (Ed.), *Fluid Mechanics Measurements*, Hemisphere Publishing Corporation, New York, 1983 Chapter 11.
24 J.T. Davies, *Turbulence Phenomena*, Academic Press, New York, 1972.
25 V.G. Levich, *Physicochemical Hydrodynamics*, Prentice Hall, Englewood Cliffs, NJ, 1962.
26 J.G. Knudsen, H.C. Hottel, A.F. Sarofim, P.C. Wankat and K.S. Knaebel, Heat and mass transfer. In: D.W. Green and J.O. Maloney (Eds.), *Perry's Chemical Engineer's Handbook*, 7th ed., McGraw-Hill, New York, 1997 Chapter 5.
27 E. Worch, Eine neue Gleichung zur Berechnung von Diffusionskoeffizienten gelöster Stoffe, *Vom Wasser*, 81 (1993) 289.
28 B. Vrana and G. Schüürmann, Calibrating the uptake kinetics of semipermeable membrane devices in water: Impact of hydrodynamics, *Environ. Sci. Technol.*, 36 (2002) 290.
29 D.R. Luellen and D. Shea, Calibration and field verification of semipermeable membrane devices for measuring polycyclic aromatic hydrocarbons in water, *Environ. Sci. Technol.*, 36 (2002) 1791.

30 K. Booij, H.E. Hofmans, C.V. Fischer and E.M. van Weerlee, Temperature-dependent uptake rates of non-polar organic compounds by semipermeable membrane devices and low-density polyethylene membranes, *Environ. Sci. Technol.*, 37 (2003) 361.
31 J.N. Huckins, M.W. Tubergen and G.K. Manuweera, Semipermeable membrane devices containing model lipid: a new approach to monitoring the bioavailability of lipophilic contaminants and estimating their bioconcentration potential, *Chemosphere*, 20 (1990) 533.
32 J.K. Kingston, R. Greenwood, G.A. Mills, G.M. Morrison and L.B. Persson, Development of a novel passive sampling system for the time-averaged measurement of a range of organic pollutants in aquatic environments, *J. Environ. Monit.*, 2 (2000) 487.
33 J.N. Huckins, J.D. Petty, H.F. Prest, R.C. Clark, D.A. Alvarez, C.E. Orazio, J.A. Lebo, W.L. Cranor, and B.T. Johnson, A guide for the use of semipermeable membrane devices (SPMDs) as samplers of waterborne hydrophobic organic contaminants. API publication 4690. American Petroleum Institute, Washington, DC, 2002.
34 Z. Zhang, M.J. Yang and J. Pawliszyn, Solid phase microextraction, *Anal. Chem.*, 66 (1994) 845A.
35 E. Baltussen, P. Sandra, F. David and C. Cramers, Stir bar sorptive extraction (SBSE), a novel extraction technique for aqueous samples: Theory and principles, *J. Microcolumn Sep.*, 11 (1999) 737.
36 C.L. Arthur and J. Pawliszyn, Solid phase microextraction with thermal desorption using fused silica optical fibers, *Anal. Chem.*, 62 (1990) 2145.
37 H.A. Leslie, A.J.P. Oosthoek, F.J.M. Busser, M.H.S. Kraak and J.L.M. Hermens, Biomimetic solid-phase microextraction to predict body residues and toxicity of chemicals that act by narcosis, *Environ. Toxicol. Chem.*, 21 (2002) 229.
38 A. Paschke and P. Popp, Solid-phase microextraction fibre–water distribution constants of more hydrophobic organic compounds and their correlations with octanol–water partition coefficients, *J. Chromatogr. A*, 999 (2003) 35.
39 A. Södergren, Solvent-filled dialysis membranes simulate uptake of pollutants by aquatic organisms, *Environ. Sci. Technol.*, 21 (1987) 855.
40 D. Sabaliunas and A. Södergren, Uptake of organochlorine pesticides by solvent-filled cellulose and polyethylene membranes, *Ecotox. Environ. Safe.*, 35 (1996) 150.
41 D.A. Alvarez, J.D. Petty, J.N. Huckins, T. Jones-Lepp, D.T. Getting, J. Goddard and S.E. Manahan, Development of a passive, *in situ*, integrative sampler for hydrophilic organic contaminants in aquatic environments, *Environ. Toxicol. Chem.*, 23 (2004) 1640.
42 H. Zhang and W. Davison, Performance characteristics of diffusion gradients in thin films for the *in situ* measurement of trace metals in aqueous solution, *Anal. Chem.*, 67 (1995) 3391.

43 F. Stuer-Lauridsen, Review of passive accumulation devices for monitoring organic micropollutants in the aquatic environment, *Environ. Pollut.*, 136 (2005) 503.
44 D.R. Lloyd and T.B. Meluch, Selection and evaluation of membrane materials for liquid separations. In: D.R. Lloyd (Ed.), *Materials Science of Synthetic Membranes*, American Chemical Society, Washington, DC, 1985 Chapter 3.
45 G.W. Reynolds, J.T. Hoff and G.W. Gillham, Sampling bias caused by materials used to monitor halocarbons in groundwater, *Environ. Sci. Technol.*, 24 (1990) 135.
46 M.B. Heringa, D. Pastor, J. Algra, W.H.J. Vaes and J.L.M. Hermens, Negligible depletion solid-phase microextraction with radiolabeled analytes to study free concentrations and protein binding: An example with [^{3}H]estradiol, *Anal. Chem.*, 74 (2002) 5993.
47 H.A. Leslie, T.L. Ter Laak, F.J.M. Busser, M.H.S. Kraak and J.L.M. Hermens, Bioconcentration of organic chemicals: Is a solid-phase microextraction fiber a good surrogate for biota?, *Environ. Sci. Technol.*, 36 (2002) 5399.
48 P. Mayer, W.H.J. Vaes and J.L.M. Hermens, Absorption of hydrophobic compounds into the poly(dimethylsiloxane) coating of solid-phase microextraction fibers: High partition coefficients and fluorescence microscopy images, *Anal. Chem.*, 72 (2000) 459.
49 E.U. Ramos, S.N. Meijer, W.H.J. Vaes, H.J. Verhaar and J.L.M. Hermens, Using solid-phase miroextraction to determine partition coefficients to humic acids and bioavailable concentrations of hydrophobic chemicals, *Environ. Sci. Technol.*, 32 (1998) 3430.
50 E.M.J. Verbruggen, W.H.J. Vaes, T.F. Parkerton and J.L.M. Hermens, Polyacrylate-coated SPME fibers as a tool to simulate body residues and target concentrations of complex organic mixtures for estimation of baseline toxicity, *Environ. Sci. Technol.*, 34 (2000) 324.
51 L. Lefkovitz, E. Crecelius and N. McElroy, The use of polyethylene alone to predict dissolved-phase organics in the Columbia River. 17th annual meeting Society of Environmental Toxicology Chemistry, 17–21 November 1996, Washington, D.C.
52 K. Booij, J.R. Hoedemaker and J.F. Bakker, Dissolved PCBs, PAHs, and HCB in pore waters and overlying waters of contaminated harbor sediments, *Environ. Sci. Technol.*, 37 (2003) 4213.
53 H.-C. Flemming, G. Schaule, T. Griebe, J. Schmitt and A. Tamachkiarowa, Biofouling—the achilles heel of membrane processes, *Desalination*, 113 (1997) 215.
54 B.J. Richardson, P.K.S. Lam, G.J. Zheng, K.E. McClellan and S.B. De Luca-Abbott, Biofouling confounds the uptake of trace organic contaminants by semi-permeable membrane devices (SPMDs), *Mar. Pollut. Bull.*, 44 (2002) 1372.

55 G.S. Ellis, J.N. Huckins, C.E. Rostad, C.J. Schmitt, J.D. Petty and P. MacCarthy, Evaluation of lipid-containing semipermeable membrane devices for monitoring organochlorine contaminants in the Upper Mississippi River, *Environ. Toxicol. Chem.*, 14 (1995) 1875.
56 J.N. Huckins, J.D. Petty, H.F. Prest, J.A. Lebo, C.E. Orazio, R.W. Gale and R.C. Clark, Important considerations in semipermeable membrane devices (SPMDs) design, performance, and data comparability. 18th Annual Meeting of Society of Environmental Toxicology and Chemistry, 16 November, 1997, San Francisco, CA, USA.
57 H.F. Prest, B.J. Richardson, L.A. Jacobson, J. Vedder and M. Martin, Monitoring organochlorines with semi-permeable membrane devices (SPMDs) and mussels (*Mytilus edulis*) in Corio Bay, Victoria, Australia, *Mar. Pollut. Bull.*, 30 (1995) 543.
58 S. Banerjee, R.H. Sugatt and D.P. O'Grady, A simple method for determining bioconcentration parameters of hydrophobic compounds, *Environ. Sci. Technol.*, 18 (1984) 79.
59 Y.P. Xu, Z.J. Wang, R.H. Ke and S.U. Khan, Accumulation of organochlorine pesticides from water using triolein embedded cellulose acetate membranes, *Environ. Sci. Technol.*, 39 (2005) 1152.
60 W.H.J. Vaes, E.U. Ramos, H.J.M. Verhaar, W. Seinen and J.L.M. Hermens, Measurement of the free concentration using solid-phase microextraction: Binding to protein, *Anal. Chem.*, 68 (1996) 4463.
61 K.E. Gustafson and R.M. Dickhut, Distribution of polycyclic aromatic hydrocarbons in Southern Chesapeake Bay surface water: Evaluation of three methods for determining freely dissolved water concentrations, *Environ. Toxicol. Chem.*, 16 (1997) 452.
62 K.D. Buchholz and J. Pawliszyn, Optimization of solid-phase microextraction conditions for determinations of phenols, *Anal. Chem.*, 66 (1994) 160.
63 H.F. Prest, J.D. Petty and J.N. Huckins, Validity of using semipermeable membrane devices for determining aqueous concentrations of freely dissolved PAHs, *Environ. Toxicol. Chem.*, 17 (1998) 535.
64 G.F. Ouyang, Y. Chen and J. Pawliszyn, Flow-through system for the generation of standard aqueous solution of polycyclic aromatic hydrocarbons, *J. Chromatogr. A*, 1105 (2006) 176.
65 K. Booij, H.M. Sleiderink and F. Smedes, Calibrating the uptake kinetics of semi-permeable membrane devices using exposure standards, *Environ. Toxicol. Chem.*, 17 (1998) 1236.
66 R.C. Weast, *Handbook of Chemistry and Physics*, 64th ed., CRC Press, Boca Raton, FL, 1983.
67 H.F. Prest, W.M. Jarman, T. Weismuller, M. Martin and J.N. Huckins, Passive water sampling via semipermeable membrane devices (SPMDs) in concert with bivalves in the Sacramento/San Joaquin river delta, *Chemosphere*, 25 (1992) 1811.

68 B. Vrana, H. Paschke, A. Paschke, P. Popp and G. Schüürmann, Performance of semipermeable membrane devices for sampling of organic contaminants in groundwater, *J. Environ. Monit.*, 7 (2005) 500.
69 F. Verweij, K. Booij, K. Satumalay, N. van der Molen and R. Van der Oost, Assessment of bioavailable PAH, PCB and OCP concentrations in water using semipermeable membrane devices (SPMDs), sediments and caged carp, *Chemosphere*, 54 (2004) 1675.

Chapter 8

Tool for monitoring hydrophilic contaminants in water: polar organic chemical integrative sampler (POCIS) ☆

David A. Alvarez, James N. Huckins, Jimmie D. Petty, Tammy Jones-Lepp, Frank Stuer-Lauridsen, Dominic T. Getting, Jon P. Goddard and Anthony Gravell

8.1 INTRODUCTION

Global emissions of persistent bioconcentratable organic chemicals have resulted in a wide range of adverse ecological effects. Consequently, industry developed less persistent, more water soluble polar or hydrophilic organic compounds (HpOCs), which generally have low bioconcentration factors. However, evidence is growing that the large fluxes of these seemingly more environmentally friendly compounds (e.g., pesticides, prescription and non-prescription drugs, personal care and common consumer products, industrial and domestic-use chemicals, and their degradation products) into aquatic systems on a world-wide basis may be responsible for incidents of acute toxicity and sublethal chronic abnormalities [1–3]. These adverse effects include altered behavior, neurotoxicity, and severely impaired reproduction [4]. Furthermore, the presence of these HpOCs likely plays a major role in the endocrine disrupting effects of complex mixtures of chemicals present in aquatic environments [5,6]. In regard to physiological effects, pharmaceuticals are of particular concern because they are designed to elicit diverse pharmacological responses. Unfortunately,

☆Although the research described in this chapter has been funded in part by the United States Environmental Protection Agency through (IAG #DW14900401) to USGS-CERC, it has not been subjected to Agency review and, therefore, does not necessarily reflect the views of the Agency and no official endorsement should be inferred.

Comprehensive Analytical Chemistry 48
R. Greenwood, G. Mills and B. Vrana (Editors)
Volume 48 ISSN: 0166-526X DOI: 10.1016/S0166-526X(06)48008-9

the effects of this class of HpOCs on non-target, aquatic organisms are largely unknown.

The HpOCs enter aquatic systems through treated effluents from wastewater treatment plants (WWTPs), leaking septic tanks and sewage lagoons, direct environmental disposal of unused drugs, landfill leachates, and surface runoff. They are often present at low concentrations, posing problems with most traditional sampling and analytical procedures. Measurements of HpOCs in environmental waters generally require modifications of existing methods or development of new methods to improve detection limits. The fate of these contaminants during wastewater treatment and in the environment is largely unknown. However, some findings suggest that many of these chemicals survive treatment and some are returned to their biologically active form via deconjugation [7–11]. Of greater concern is a study showing that many of these chemicals also survive treatment in drinking water plants and are present in finished waters [12].

There has been considerable effort directed towards development of active sampling methods for HpOCs in water, but nearly all this research has centered on the use of solid-phase extraction (SPE) employing specially modified polymeric resins in either a cartridge or enmeshed in an inert membrane disk [13–16]. Although SPE is advantageous over earlier liquid–liquid extraction methods, it often requires the collection of large volumes of water to satisfy the detection limit requirements of commonly used analytical methods. In cases where bulk (or filtered) water samples are shipped to the laboratory, the preservation and transport of large volumes of water can be problematic. On the other hand, the use of on-site automated sampling systems can be costly and difficult to maintain.

Because nearly all traditional sampling methods provide data only at the moment of sampling, episodic events such as spills or stormwater runoff may not be detected. This problem is particularly relevant to HpOCs, as their residence times in riverine systems are generally lower than hydrophobic organic compounds (HOCs). However, transient but frequent occurrence of certain HpOCs in wastewater effluents may result in temporal changes in the habitat quality of receiving waters. Thus, there is a critical need for sampling and analytical methods capable of enhancing the detection and identification of HpOCs in an integrated manner, which in turn, provides highly relevant time-weighted average (TWA) concentrations. Without this type of methodological advancement, investigators face a daunting task in adequately assessing the environmental risks posed by this diverse class of chemicals.

Passive samplers offer an attractive alternative to traditional sampling methods. The success of small personal dosimeters, or passive monitors, in determining TWA exposure concentrations of organic vapors in occupational environments has contributed to the application of the same principle to dissolved organic contaminants in aquatic environments [17,18]. A wide variety of passive samplers has been developed to sample HOCs, volatile organic compounds, and labile metals [19]. Passive integrative (i.e., no significant losses of accumulated residues during the exposure period) samplers concentrate ultra-trace to trace levels of chemicals over prolonged sampling periods, generally resulting in much greater masses of sequestered chemicals than those recovered using grab sampling techniques. Consequently, the use of this approach results in increased analytical sensitivity and lower detection limits relative to those reported for most traditional methods. Furthermore, the use of passive integrative samplers enhances the probability of the detection of chemicals that rapidly dissipate or degrade.

8.2 FUNDAMENTALS OF POCIS

8.2.1 POCIS description and rationale

The classification of a compound as an HpOC is based on the presence of one or more polar functional groups (e.g., hydroxyls) or a significant molecular dipole moment. The *n*-octanol–water partition coefficient (K_{ow}) provides a convenient but somewhat arbitrary means of discriminating between HpOCs and HOCs. For example, volatile organic compounds may have relatively low K_{ow} values but they are generally non-polar. In this chapter, we use a log K_{ow} value of 3.0 as the cutoff point between HOCs and HpOCs However, it is important to have some overlap in the compounds sequestered by samplers for HOCs and HpOCs to ensure holistic sampling of organic contaminants.

Although a few passive sampling devices have been tested for HpOCs, the first sampler reported for this chemical class was the polar organic chemical integrative sampler or POCIS [20–25]. The POCIS has been shown to sample a wide variety of HpOCs as well as some HOCs with log K_{ow} values between 3.0 and 4.0. The POCIS consists of a disk-like configuration of a solid-phase sorbent or a mixture of sorbents sandwiched between two microporous polyethersulfone (PES) membranes. Unfortunately, PES is not amenable to heat sealing, therefore, rings are used to form a compression seal to prevent sorbent loss. Figure 8.1 depicts an array of POCIS supported on a threaded rod with an exploded view of

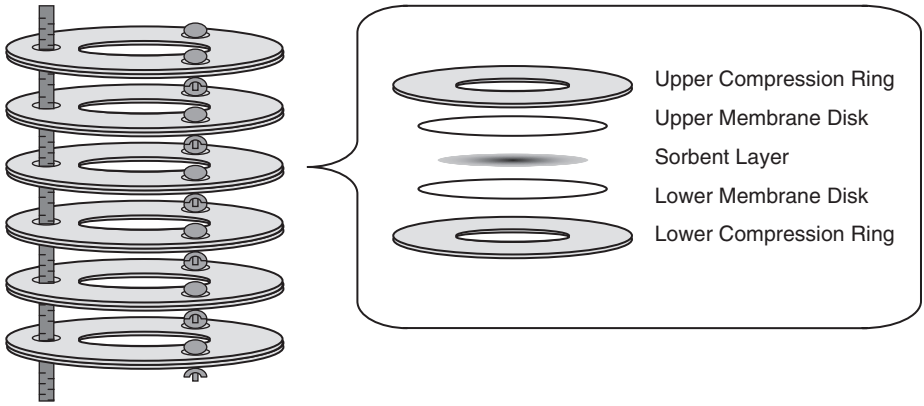

Fig. 8.1. An array of POCIS disks mounted on a support rod ready for insertion into a deployment canister. The inset is an exploded view of a single POCIS.

the ''membrane–sorbent–membrane sandwich'', which comprises the functional component of the sampler. The compression rings can be made of either a metallic or polymeric material (free of surficial or leachable contaminants) and a combination of thumb screws, bolts, nuts, or clips are used to secure the rings to the membranes.

The microporous PES membrane acts as a semipermeable barrier between the sorbent and the surrounding environment. It allows dissolved HpOCs to pass through to the sorbent, while particulates, microorganisms, and macromolecules with cross-sectional diameters greater than 100 nm are selectively excluded. Without the protection of the membrane, biofouling of POCIS sorbents is very likely during extended exposures (>2 weeks) in surface waters. Unlike the planar surfaces of PES or low-density polyethylene (i.e., membrane used for semipermeable membrane devices (SPMDs)), no effective methods are known for the direct removal of the biofilm-particulate phases from the surfaces of spherical or granular POCIS sorbents directly exposed to surface waters. Thus, the amounts of analytes accumulated in POCIS sorbents could not be distinguished from the amounts present in the biofilm-particulate phases, greatly complicating data interpretation. Fortunately, the PES membrane appears to resist biofouling much better than other polymeric materials commonly used in passive samplers and serves as an effective barrier to particle deposition eliminating these potential problems.

Upon deployment of POCIS, water rapidly permeates the pore structure of PES membrane and makes direct contact with the sorbents. The water-filled transport corridors through the PES membrane

are more tortuous than the linear structures of many microporous membranes. Based on mass per volume measurements and density information [20,23,26], the estimated volume of the hydrated pore structure is 76.5% of the total membrane volume. The average thickness of the hydrated PES membrane is approximately 130 μm.

For a typical POCIS disk used in field studies, the effective surface area of the membranes in contact with exposure waters is 41 cm^2 and the sorbent mass is ≈228 mg. Herein we define a standard POCIS as having a surface area to sorbent mass ratio of ≈180 cm^2 g^{-1}. Because the amount of chemical sampled is directly related to the surface area of the device, it is sometimes necessary or desirable to combine the extracts from the sorbents of multiple POCIS disks into a single sample to increase the mass of sequestered chemical for analysis or bioassay.

The POCIS is versatile in that the sorbents can be changed to target-specific chemicals or chemical classes. However, two types of sorbent systems are considered as standards for all POCIS field deployments to date. Because each sorbent system is better suited for specific classes or types of HpOCs, it is common to have both standard sorbents in POCIS deployed in a single protective canister. This configuration is designed to maximize the number of detectable HpOCs at sample sites. One sorbent system consists of the triphasic admixture of Isolute ENV+ polystyrene divinylbenzene resin (80% by weight) and Ambersorb 1500 carbon lightly dispersed on S-X3 Biobeads (20% by weight). Ambersorb 1500 is no longer commercially available; however, Ambersorb 572 is an equivalent substitute. Details regarding the triphasic admixture have been discussed by Alvarez [20,23]. This mixture has a higher capacity than many other sorbents evaluated and exhibits excellent concentration of waterborne HpOCs with efficient recovery of most pesticides, natural and synthetic hormones, and other wastewater-related contaminants. Because of its broad applicability, the triphasic admixture is considered to be the generic-sorbent configuration for HpOCs. The other standard POCIS configuration incorporates the Oasis HLB sorbent for optimum sequestering of pharmaceutical HpOCs. The use of the Oasis HLB configuration is necessary because many pharmaceuticals have multiple functional groups, which have a tendency to strongly bind to the carbonaceous component of the triphasic admixture, resulting in poor recoveries of some members of this class of compounds. Because Oasis HLB is a commonly used sorbent for the SPE-based sampling of pharmaceuticals and certain other HpOCs from water, considerable data exist on the recoveries of sorbed analytes. Furthermore, solvents used to recover chemicals from the Oasis HLB are

generally compatible with toxicity tests, precluding the need for rigorous solvent exchange.

8.2.2 Applicability of POCIS

Although the standard POCIS configurations will concentrate a wide range of HpOCs, they are not suitable for all environmental contaminants. Table 8.1 lists the chemical classes or selected compounds shown to concentrate in POCIS, but it is not all inclusive. For compounds with log K_{ow} values",4,0,4? > 3.0, POCIS may not perform as well as other passive samplers such as SPMDs. A graphical representation of the sampling characteristics of POCIS and SPMDs relative to their log K_{ow} values is depicted in Fig. 8.2. The normalized sampling rates for the POCIS are visibly less than those for the SPMDs. This difference is likely due to the additional aqueous transport resistance (relative to a SPMD) of the water-filled PES membrane. Clearly shown is the significant overlap in the types of chemicals sampled by the two devices. Therefore, the use of SPMDs and POCIS in concert should provide a better understanding of the full extent of organic chemical contamination.

8.3 THEORY AND MODELING

Accumulation of chemicals by passive samplers generally follows first-order kinetics, which is characterized by an initial integrative phase, followed by curvilinear and equilibrium partitioning phases. For all phases of uptake sampling rates (R_s; units of L or mL day^{-1}) and sorbent–water (sw) partition coefficients (K_{sw}; units of mL mL^{-1} or g^{-1}) are independent of exposure concentrations [27]. During the integrative phase of uptake, a passive sampling device acts as an infinite sink for contaminants, and assuming constant exposure concentrations, residues are accumulated linearly relative to time. Based on results to date, POCIS remains in the integrative phase of sampling during exposure periods of at least 30 days. An advantage of integrative samplers over equilibrium partition samplers is that TWA concentration of contaminants can be determined from sampler concentration data (assuming appropriate calibration data are available). Unlike samplers that rapidly achieve equilibrium (characterized by very high surface area to sorbent volume or mass ratios), chemical residues from episodic release events are retained by integrative samplers at the end of the exposure period. Thus, integrative samplers have very small analyte loss rates and times to reach equilibrium are very large.

TABLE 8.1
Classes or specific chemicals known to concentrate in POCIS

23 pharmaceuticals including
Acetaminophen
Azithromycin
Carbamazepine
Propranolol
Sulfa drugs (antibiotics)
Tetracycline antibiotics
2 illicit drugs (methamphetamine, MDMA)
Several natural and synthetic hormones
17β-Estradiol
17α-Ethynylestradiol
Estrone
Estriol
12 Triazine herbicides including
Atrazine
Cyanazine
Hydroxyatrazine
Terbuthylazine
Various polar pesticides including
Alachlor
Chlorpyrifos
Diazinon
Dichlorvos
Diuron
Isoproturon
Metolachlor
Various household and industrial products and degradation products including
Alkyl phenols (nonylphenol)
Benzophenone
Caffeine
DEET
Indole
Triclosan
Urobilin (fecal contamination marker)
Essentially, any compound with log $K_{ow} \leq 3.0$

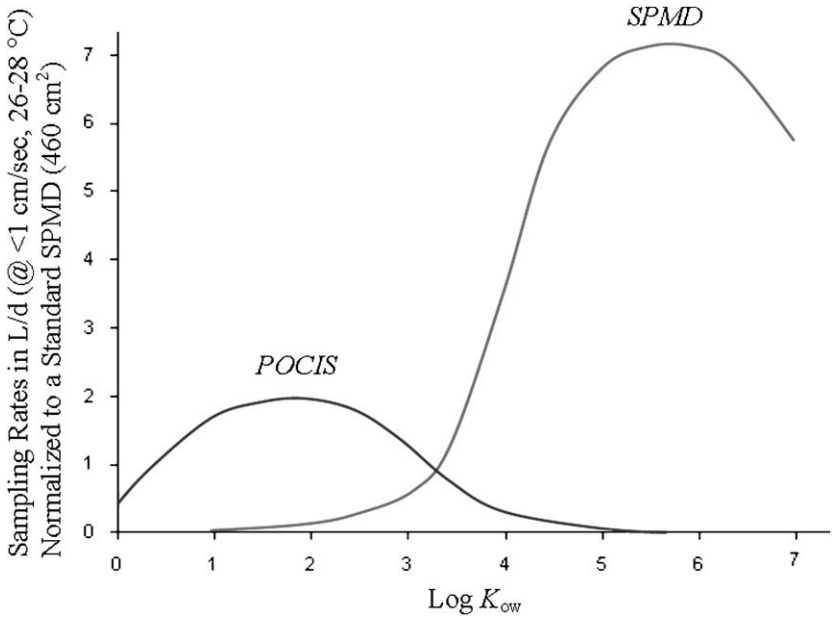

Fig. 8.2. Comparison of POCIS and SPMD sampling rates (normalized to 460 cm^2 surface area) for a wide range of organic chemical log K_{ow} values.

To derive reasonable estimates of ambient environmental concentrations of analytes from the concentrations in a passive sampler, three requirements must be met: (1) concentrations in the device must be proportional to environmental concentrations and the associated rate constants for chemical exchange and partition coefficients must be independent of ambient analyte concentrations; (2) calibration data (rate constants and partition coefficients) applicable to *in situ* conditions must be available for target compounds; and (3) the sampling process should not significantly reduce analyte concentrations in the medium sampled [27].

Laboratory experiments under turbulent conditions have shown that a number of pesticides (atrazine, diazinon, diuron, and isoproturon) and pharmaceuticals (azithromycin, fluoxetine, omeprazole, and levothyroxine) remain in the linear or integrative phase of residue accumulation up to 56 days [23,24]. Therefore, both laboratory and field data justify the use of a linear uptake model for the derivation of sampling rates and calculation of ambient water concentrations. Because curvilinear uptake has not been observed in POCIS exposures to HpOCs, it is unknown if the approach to equilibrium will follow first-order kinetics.

Huckins *et al*. [27] formulated the following equation for integrative (i.e., linear) sampling by a passive sampling device:

$$C_w = \frac{C_s M_s}{R_s t} \tag{8.1}$$

where C_w and C_s are the analyte concentration in the water and sorbent, respectively; M_s is the mass of the sorbent; and t is time in days. The formulation of R_s in Eq. (8.1) changes slightly depending on whether uptake is controlled by the external aqueous boundary layer (WBL) or the PES membrane. Under external WBL control, R_s is given by

$$R_s = \left(\frac{D_w}{\delta_w}\right) A \tag{8.2}$$

where D_w is the diffusion coefficient in water, δ_w is the effective thickness of the WBL, and A is the surface area of the sampling device. Under membrane control, R_s is given by

$$R_s = \left(\frac{D_m}{\delta_m}\right) K_{mw} A \tag{8.3}$$

where D_m is the diffusion coefficient in the membrane matrix, K_{mw} is the equilibrium membrane–water partition coefficient, and δ_m is the thickness of the hydrated membrane. Actually, mass transfer through the PES membrane is probably more complicated than the simple analogies used in Eq. (8.3) (diffusion through the membrane matrix alone) and Fig. 8.3 (diffusion through the water-filled pores alone), as is subsequently shown in Eq. (8.5). Use of Eq. (8.1) is considered valid from the time that steady-state flux into the sampler has been established to the time that sampler concentrations reach about half their equilibrium concentrations ($t_{1/2}$), which is defined by

$$t_{1/2} = \frac{0.693}{R_s / K_{sw} V_s} \tag{8.4}$$

Figure 8.3 illustrates most of the barriers to chemical uptake by the POCIS sorbent. In this example, we assume WBL control of uptake rates. Mass transfer of analytes into POCIS sorbents include the following steps: movement of HpOC solutes from the bulk water and diffusion through the WBL (note: the biofilm is not considered in this narrative), diffusion through the water-filled membrane pores and through the membrane matrix, and finally, diffusion through any WBLs associated with the inside surface of the membrane and sorbent

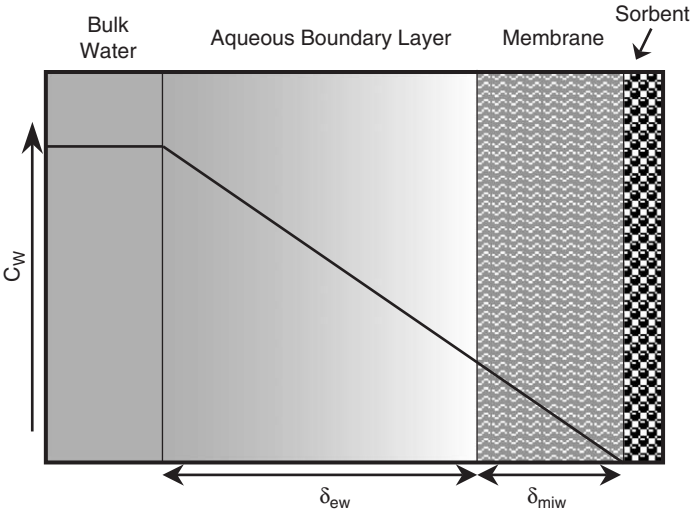

Fig. 8.3. Representation of the barriers to chemical uptake into the POCIS. The deltas (δ) represent the effective thickness of each region and the associated subscripts denote the region. The line shows the chemical concentration gradient in the water through each barrier.

particles. The resistance to mass transfer of any biofilm and the WBLs associated with the inside of the membrane and sorbent particles are not considered in Fig. 8.3. The resistance to mass transfer for all steps or barriers are assumed to be additive. Therefore, a fractional reduction in the resistance of any barrier will result in some increase in chemical uptake rate. However, for the same percentage reduction in individual barrier resistances, the greatest increase in sampling rate is achieved when the change occurs in the rate-limiting barrier (e.g., turbulent thinning of the WBL).

Mass transfer through the microporous PES membrane used in the POCIS may follow a biphasic pathway with solute transport through both the water-filled pores and the polymer matrix. Assuming steady state and no biofouling, the flux, or mass per unit time, of solutes through the membrane can be described as a weighted average of both water-filled pores and the polymer matrix pathways.

$$\frac{Q_o}{t} = C_w\left(\frac{D_{IS}A}{\phi_{IS}}\right) = C_w\left[\frac{D_m K_{mw} A(1-\theta)}{\phi_M} + \frac{D_{IM}A\theta}{\phi_{IM}}\right] = C_w\left(\frac{D_w A}{\delta_w}\right) \qquad (8.5)$$

where Q_o is the mass of chemical sampled by the POCIS sorbent; θ is the porosity factor, which we assume is 0.7 for PES membranes based

on hydrated membrane volume measurements; ϕ_M and ϕ_{IM} are the length of the diffusional pathways through the membrane matrix and the water-filled interstitial spaces in the membrane, respectively; D_{IM} is the diffusion coefficient in the membrane interstitial water, which we assume as $D_{IM} \approx D_W$; and D_{IS} and ϕ_{IS} are the diffusion coefficient and length of the diffusional pathway, respectively, for the WBL associated with the sorbent. This relationship assumes the sorbent acts as an infinite sink for sequestered chemicals. For compounds that are less than 400 Da, the main determinant in which pathway (i.e., interstitial water or membrane) is dominant is the magnitude of the K_{MW}. Unlike δ_m used in Eq. (8.3), the terms ϕ_M, ϕ_{IM}, and ϕ_{IS} include a tortuosity factor. For example,

$$\phi_{IM} = m_t \tau \tag{8.6}$$

where m_t is the hydrated membrane thickness and τ is the tortuosity factor.

Based on the studies to date, uptake rates of HpOCs with log K_{ow} values <3 are largely controlled by diffusion across the WBL at the external membrane surface [23]. This observation stems from the observed increase in chemical uptake with increased flow or turbulence in exposure water. At some point, increasing flow will thin the effective thickness of the external WBL enough to switch rate control to the water-filled membrane pores or to the membrane matrix. Under membrane control, an HpOC's sampling rate will not change due to further increases of flow at the membrane surface. Finally, environmental turbulence likely reduces the effective thickness of WBLs associated with POCIS sorbent particles, but this effect is not differentiated from the effect on the rate-limiting external WBL.

Sampling rates for selected chemicals have been determined using a static renewal scheme. Specific details regarding the calibration procedure have been described by Alvarez *et al.* [23]. Briefly, POCIS were exposed to the test chemicals in glass chambers containing 1 L of water fortified with test chemicals. Chemical concentrations were renewed daily during exposures to maintain relatively constant concentrations. The exposures were performed under both quiescent and turbulent conditions to measure effects of flow-turbulence on chemical uptake. The R_s for the individual analytes were determined by measuring the mass of analyte in POCIS at 7, 14, 28, and 56 days relative to the mean concentration of the analyte in water. Selected results of R_s values (L day^{-1}; 41 cm^2 POCIS) determinations are listed in Table 8.2.

TABLE 8.2
Sampling rates (R_s values) of POCIS (L day^{-1}; 41 cm^2 POCIS) under quiescent (non-stirred) and turbulent (stirred) conditions

Analyte	R_s from quiescent renewals (L day^{-1})	R_s from turbulent renewals (L day^{-1})
Herbicides		
Diuron[a]	0.011	0.100
Isoproturon[a]	0.034	0.200
Prescription pharmaceuticals		
Azithromycin[a]	0.048	0.270
Fluoxetine[a]	0.027	0.200
Levothyroxine[a]	0.021	0.120
Omeprazole[a]	0.016	0.068
Illicit drugs		
Methamphetamine	N/A[b]	0.089
MDMA	N/A[b]	0.170

Values reported are means ($n = 3$).
[a]Previously reported by Alvarez *et al.* [23].
[b]R_s was determined under turbulent conditions only.

8.4 STUDY CONSIDERATIONS

8.4.1 Use and processing

Figure 8.4 shows the general processing, enrichment, and fractionation scheme for POCIS samples. For transport to and from the laboratory and during sample storage, POCIS is stored frozen in solvent-rinsed airtight container, such as a metal paint can. At the onset of processing, the exterior of POCIS membranes is gently cleaned with a soft brush and running water to reduce the probability of contamination of sorbents with particulate matter. Care must be taken during this cleaning process not to damage the membrane. Then, the POCIS membranes are separated and the sorbent is transferred with a suitable solvent such as methanol into a glass, gravity-flow chromatography column plugged with glass wool. The sequestered chemicals are recovered from the sorbent using an optimized solvent elution scheme. The solution containing the targeted analytes is then reduced in volume by rotary evaporation, solvent reduction with a N_2 stream, or similar methods. Depending on the requirements of the analytical method, the sample may undergo further enrichment and fractionation. Afterwards, the

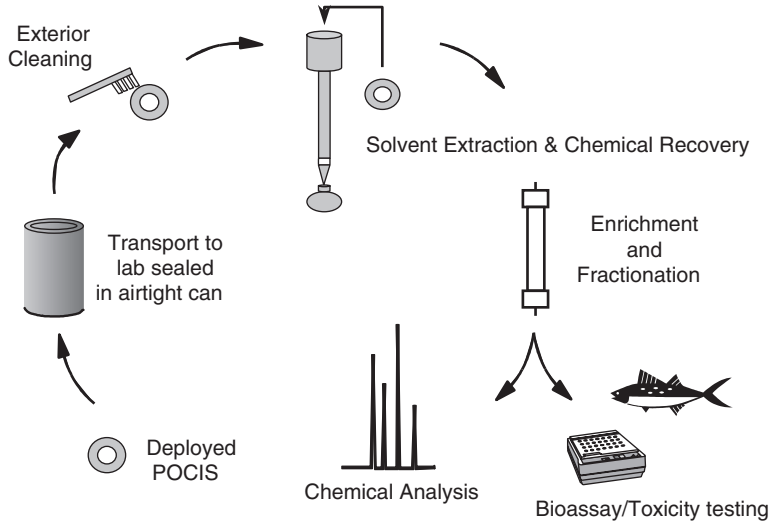

Fig. 8.4. General POCIS processing scheme.

POCIS extract is ready for analysis using common analytical instrumentation or for bioassay or toxicity testing.

Any instrumental technique suitable for quantification of the targeted analyte can be used by the analyst. Gas chromatography (GC) with an electron capture, nitrogen–phosphorus, or flame ionization detectors, GC–mass spectrometry, liquid chromatography (LC) with diode array detection, and LC coupled with mass spectrometry have been used for the analysis of POCIS extracts. Also, POCIS extracts have been subjected to various bioassay techniques including Microtox®, the yeast estrogen screen (YES), and the yeast androgen screen (YAS) to determine the toxicological significance of sequestered chemicals. Blank POCIS used for quality control purposes have not shown any matrix effects interfering with these techniques.

8.4.2 Data quality consideration

The POCIS approach is well suited as a screening tool for determining the presence/absence, sources, and relative amounts of chemicals (ranking) at the study sites. For projects requiring estimates of ambient HpOC concentrations, calibration data are needed for targeted chemicals. At the current state of the technology, sampling rates are available for only a limited number of HpOCs and site conditions.

However, in cases where R_s data are available, the agreement between estimated water concentrations and measurements by traditional water sampling methods has been quite good. For example, in the River Thames (United Kingdom) concentrations of the herbicides diuron and isoproturon derived from POCIS data and measured with traditional methods varied by a maximum of 1.7-fold, with only one exception [23].

The application of appropriate quality control (QC) procedures or criteria is a mandatory consideration in the use of any passive sampler. QC samples must address issues of analyte recovery, background in sampler components, and any contamination incurred during transport, deployment, retrieval, storage, processing, enrichment/fractionation, and analysis. These issues are typically addressed by the following types of QC samples: fabrication blanks, process blanks, reagent blanks, field blanks, matrix spikes, and procedural spikes. Fabrication blanks are POCIS that are constructed concurrently with the deployed POCIS, but are stored frozen in an inert atmosphere until processing of the entire sample set begins. Fabrication blanks account for interferences and/or contamination incurred from the POCIS components, laboratory storage, processing, and analysis. Process blanks are POCIS prepared just prior to initiation of the processing of exposed samplers and these, along with fabrication blanks, account for the analytical background. Reagent blanks consist of identical portions of all solvents used in the extraction of the POCIS. These blank sample extracts are carried along with the POCIS samples extracts through the entire analytical procedure and provide information on background due to laboratory reagents and procedures. Field blanks are POCIS samples that account for contamination during transport to and from study sites, and during deployment and retrieval of exposed POCIS. Field blanks are stored frozen in vapor-tight containers between the deployment and retrieval periods. Matrix spikes are used to determine the recoveries of the target compounds from the POCIS sorbents and to establish ''control limits'' for the analytical process. Procedural spikes can be used to determine the recovery of target compounds for an individual procedural step, multiple steps, or for the whole analytical process. Often, radiolabeled compounds (^{14}C- or ^{3}H-labeled) are used as procedural spikes to provide a rapid indication of the performance of an individual step. Because as many as seven types of spikes and blanks are used for POCIS sampling and analysis, the amount of QC samples required often ranges between 20 and 50% of the total number of samples. The exact percentage of QC used is dependent on project

goals, which should be determined during the developmental phase of a project.

8.5 CASE STUDIES

8.5.1 Application of POCIS for pharmaceutical monitoring in the United States

The usefulness of the POCIS for monitoring waterborne levels of pharmaceuticals and personal care products (PPCPs) was demonstrated in a collaborative effort between the US Geological Survey (USGS) and the US Environmental Protection Agency (US EPA). Methods were developed to use the pharmaceutical POCIS configuration to sample the prescription pharmaceuticals azithromycin (a common antibiotic), fluoxetine (an antidepressant), levothyroxine (used in thyroid replacement therapy), omeprazole (an anti-ulcer agent), and the illicit drugs, methamphetamine and MDMA (or Ecstasy). The field component of this study involved deploying the POCIS in the treated effluents of three municipal WWTPs located in Nevada, Utah, and South Carolina for 30 days during the summer of 2002. To determine seasonal differences in the presence and concentration of these chemicals, a second deployment was performed at the Nevada plant during the following winter.

Of the four prescription pharmaceuticals targeted for this study, only azithromycin was detected [24]. Azithromycin was detected in the effluents of each WWTP during the summer deployment at concentrations ranging from 15 to 56 $ng\,L^{-1}$. Comparison of the summer and winter deployments at the Nevada WWTP showed a 4-fold increase (15–66 $ng\,L^{-1}$) in the water concentration of azithromycin. This increase was not surprising due to the onset of the cold and flu season and the boost in antibiotic prescriptions.

The analysis of the POCIS for methamphetamine and MDMA resulted in the detection of both illicit drugs, albeit at different sites [24]. Methamphetamine was detected at the Nevada site during both the summer and winter samplings at concentrations of 1.3 and 0.8 $ng\,L^{-1}$, respectively. MDMA was measured in the effluent of the South Carolina WWTP at a concentration of 0.5 $ng\,L^{-1}$. These results were substantiated by reports on the production and usage of these drugs (US Drug Enforcement Agency).

In addition to the analysis of the targeted pharmaceuticals, other chemicals identified included the nonylphenol polyethoxylate and

alcohol polyethoxylate surfactants. Furthermore, the perfluorinated surfactants, perfluorooctanoic acid (PFOA) and perfluorooctane sulfonate (PFOS), used in the production of fire-fighting foams, fabric treatments, cosmetics, and many other consumer products were qualitatively identified POCIS extracts from each site at levels above associated controls [28].

In a related experiment, POCIS were deployed in a southern Nevada creek that was suspected to be impacted by leaking septic tanks from bordering housing developments. Analysis of the POCIS extracts revealed the presence of urobilin, a chemical marker for fecal contamination. Urobilin is a mammal-specific, breakdown product of hemoglobin, which is excreted in urine and feces and is known to be prevalent in human wastes [29]. Urobilin alone may not be a conclusive marker of human fecal contamination, however, the presence of urobilin along with human-use pharmaceuticals provides strong evidence implicating human sources.

8.5.2 Comparison of POCIS and traditional sampling for wastewater monitoring

In this USGS study, the POCIS sampling method was compared to a traditional water-column composite sampling method for the analysis of select HpOCs in wastewater [25]. The study area was a portion of Assunpink Creek near Trenton, NJ, USA. This watershed is predominantly agricultural in its headwaters and becomes heavily urbanized in its lower reaches. A major municipal WWTP, discharging about 10 million gallons of tertiary-treated effluent into the creek per day, is located near the center of the watershed. This creek is a tributary to the Delaware River, which is used further downstream as a source of drinking water for the city of Philadelphia and surrounding metropolitan areas. Two sites, approximately 110 m and 3.2 km downstream from the effluent discharge, were selected to determine the presence and potential transport of organic contaminants. At each site, POCIS were deployed for 54 days and water samples were taken at 14-day intervals using standard depth and width composite techniques. POCIS extracts and the water samples were sent to collaborating USGS laboratories for analysis of pharmaceuticals and other wastewater HpOCs using LC–MS and GC–MS.

Out of a total of 96 targeted analytes, 24 were identified in the water-column samples and 32 were isolated from the POCIS extracts. Chemicals identified in the POCIS included pharmaceuticals,

TABLE 8.3

Representative wastewater-related contaminants identified in POCIS extracts from a comparison study with traditional water sampling techniques

Pharmaceuticals	Fire retardants	Plasticizers
Acetaminophen	Fryol CEF	Diethylhexylphthalate*
Carbamazepine	Fyrol FR2	Triphenyl phosphate
Dehydronifedipine*	Tri(2-butoxyethyl)phosphate	
Diphenhydramine		Non-ionic detergent metabolites
Sulfamethoxazole	Miscellaneous	4-Cumylphenol*
Thiabendazole*	5-Methyl-1H-benzothriazole*	4-*tert*-Octylphenol*
	Anthraquinone	Nonylphenol, diethoxy*
Pesticides	Benzophenone	
Atrazine	Caffeine	Fragrances
DEET	Cotinine	3-Methyl-1H-indole*
Diazinon*	Tributyl phosphate	HHCB
Metolachlor	Triclosan	Indole
Pentachlorophenol*	Triethyl citrate	Methyl salicylate*
Prometon		Tonalide

Chemicals marked with an asterisk (*) were identified in POCIS extracts only.

pesticides, fire retardants, non-ionic detergent metabolites, fragrances, plasticizers, and other miscellaneous wastewater-related contaminants (Table 8.3). Analytes detected in traditional water-column samples were highly variable with 9–24 HpOCs in individual samples. These data suggest that the use of the POCIS integrative sampling approach provided a more holistic picture of transient WWTP-related HpOCs present in riverine systems than traditional grab sampling methods.

8.5.3 Application of POCIS for pesticide monitoring in Denmark

In 2002, POCIS (generic configuration) were used as part of a monitoring program in Storstrøms County, Denmark. The objective was to provide a time-integrated estimate of pesticide concentrations in the county's agricultural watersheds during spring and fall pesticide application and runoff periods. Three sites were selected including a reference stream with minimal agricultural activity, one stream directly impacted, and one stream indirectly impacted by agricultural practices. POCIS were deployed for periods of 1 month during the spring, summer and fall for a total of five deployments at each location.

Out of the 63 pesticides targeted for this study, 36 were found at quantifiable limits at least at one of the sites. Chemicals identified at all sites and all sampling periods include 2,6-dichlorbenzamide (BAM), bentazon, 4,6-dinitro-*o*-cresol (DNOC), ethofumesate, and *p*-nitrophenol. In more than 50% of the samples, 22 of the 36 quantified

pesticides were detected. At Sites 1 and 3, 14 and 20 pesticides, respectively, were present during all sampling periods.

In addition to the field sampling, tentative calibration data for the targeted pesticides were generated (Table 8.4). The generic POCIS configuration was exposed for 5 days in a 10 L glass chamber to 8 L of water fortified at 10 $\mu g\,L^{-1}$ of each pesticide. The water was replaced

TABLE 8.4
Tentative calibration data for selected pesticides

	R_s (L day^{-1})		R_s (L day^{-1})
2,4-D	0.092	Hexazinone	0.260
2,6-Dichlorbenzamide (BAM)	0.280	Hydroxyatrazine	0.100
Aldrin	0.032	Hydroxycarbofuran	0.006
Atrazine	0.240	Hydroxysimazine	0.054
Azinphos-ethyl	0.180	Ioxynil	0.112
Azinphos-methyl	0.178	Isodrin	0.034
Bentazon	0.092	Lenacil	0.340
Bromoxynil	0.102	Lindane	0.092
Carbofuran	0.026	Malathion	0.005
Chlorfenvinphos	0.200	MCPA	0.072
Chloridazon	0.240	Mechlorprop	0.122
Chlorsulfuron	0.106	Metabenzthiazuron	0.200
Clopyralid	0.020	Metamitron	0.220
Cyanazine	0.340	Metazachlor	0.260
DDE ($o,p'+p,p'$)	0.032	Metoxuron	0.240
DDT ($o,p'+p,p'$)	0.018	Metribuzin	0.168
Desethylatrazine	0.260	Metsulfuron-methyl	0.078
Desethylterbuthylazine	0.300	Mevinphos	0.060
Desisopropylatrazine	0.220	Parathion-ethyl	0.142
Dichlobenil	0.146	Parathion-methyl	0.122
Dichlorprop	0.116	Pendimethalin	0.260
Dichlorvos	0.006	Pirimicarb	0.300
Dieldrin	0.086	*p*-Nitrophenol	0.196
Dimethoate	0.220	Prochloraz	0.098
Dinoseb	0.110	Propachlor	0.240
4,6-Dinitro-*o*-cresol (DNOC)	0.090	Propiconazole	0.300
Endrin	0.094	Propyzamide	0.280
Ethofumesate	0.280	Simazine	0.220
Fenitrothion	0.090	Tebuconazole	0.240
Fenpropimorph	0.088	Terbuthylazine	0.280
Fluroxypyr	0.086		

Sampling rates (R_s) are presented as L day^{-1} for a standard 41 cm^2 generic configuration POCIS.

daily with freshly fortified water and the system was stirred to simulate a turbulent system.

In general, there is good agreement between the preliminary calibration data generated in this study and other data generated as part of time-integrated uptake studies [20,23] (D.A. Alvarez, unpublished data). However, since these values are representative of a single data point after a 5-day exposure period, extreme caution should be exercised when using these values. Previously reported data indicate that the uptake rates are slightly enhanced during the first few days of sampling [20]. Presoaking the POCIS prior to use has been shown to minimize this effect [20]. During a 28-day deployment, this burst effect in the first few days of sampling becomes negligible in the overall rate-determining linear uptake curve. Therefore, POCIS are typically not presoaked prior to deployment to eliminate logistic issues during transport and storage.

8.5.4 Application of POCIS for pharmaceutical monitoring in the United Kingdom

As part of an ongoing collaboration between the USGS and the Environment Agency of England and Wales (EA), POCIS were used in a reconnaissance study to determine the presence of pharmaceuticals in the effluent from WWTPs. A series of common antibiotic, anti-inflammatory, anti-analgesic, and anti-estrogen drugs were targeted in the effluent outfalls of three WWTPs. The samplers were deployed for 28 days over three successive months to measure any temporal differences in the presence and/or concentration of the targeted chemicals.

The POCIS (pharmaceutical configuration) were constructed and processed by the USGS, and the EA carried out the deployments and performed the instrumental analysis. Generally, the extracts were analyzed using a single quadrupole LC–MS, which was used to monitor two or three ions for each targeted compound. In most cases, the coefficient of variation (CV) of POCIS replicates for all surveys at all sample sites was less than $\pm 20\%$ and often less than $\pm 10\%$.

Quality control measures including recovery of the targeted chemicals from fortified POCIS sorbent and laboratory and field blanks were used in this study. The recovery of the targeted chemicals from the POCIS was generally greater than 95% (Table 8.5). Analysis of laboratory and field blanks did not indicate the presence of potentially interfering chemicals occurring from the POCIS matrix (Fig. 8.5).

TABLE 8.5

Pharmaceutical compounds in the effluent of British WWTPs

Chemical	Matrix % recovery	Site 1[a]		Site 2			Site 3		
		Survey 2	Survey 3	Survey 1	Survey 2	Survey 3	Survey 1	Survey 2	Survey 3
Acetaminophen	98 (2.5)[b]	<0.005	<0.005	<0.005	<0.005	<0.005	<0.005	<0.005	<0.005
Dextropropoxyphene	90 (2.3)	0.50 (6.9)	0.59 (22)	0.47 (26)	0.32 (15)	0.32 (3.3)	0.72 (10)	0.62 (12)	0.89 (9.3)
Diclofenac	95 (2.5)	0.48 (20)	0.41 (26)	2.0 (9.0)	0.82 (49)	1.8 (94)	2.9 (6.4)	1.9 (24)	0.61 (5.1)
Erythromycin	130 (18)	0.15[c]	0.15[c]	<0.005[c]	<0.005[c]	0.033[c]	0.10[c]	0.064[c]	<0.005[c]
Ibuprofen	99 (5.3)	<0.005	<0.005	<0.005	<0.005	<0.005	<0.005	<0.005	<0.005
Mefenamic acid	97 (7.4)	<0.005	<0.005	<0.005	<0.005	<0.005	<0.005	<0.005	<0.005
Propranolol	95 (2.2)	0.36 (3.8)	0.41 (20)	0.68 (36)	0.62 (14)	0.74 (2.0)	1.1 (7.1)	1.0 (2.5)	1.3 (7.3)
Sulfamethoxazole	95 (4.3)	<0.015	<0.015	0.17 (13)	0.16 (61)	0.19 (17)	<0.015	<0.015	<0.015
Tamoxifen	93 (0.8)	<0.005	<0.005	<0.005	<0.005	<0.005	<0.005	<0.005	<0.005
Trimethoprim	95 (2.8)	0.28 (7.7)	0.06 (10)	0.05 (59)	0.08 (26)	0.11 (10)	1.0 (5.1)	0.75 (7.5)	0.80 (8.0)

Recovery of targeted analytes from fortified matrix and concentrations in POCIS (pharmaceutical configuration) samples from each site are given. Results are presented at micrograms of chemical sequestered per POCIS. CVs are given in parenthesis ($n = 3$).

[a]Survey 1 POCIS from Site 1 were lost during deployment.

[b]Acetaminophen recovery from the fortified POCIS matrix performed at $n = 2$.

[c]Only one replicate from each survey was analyzed.

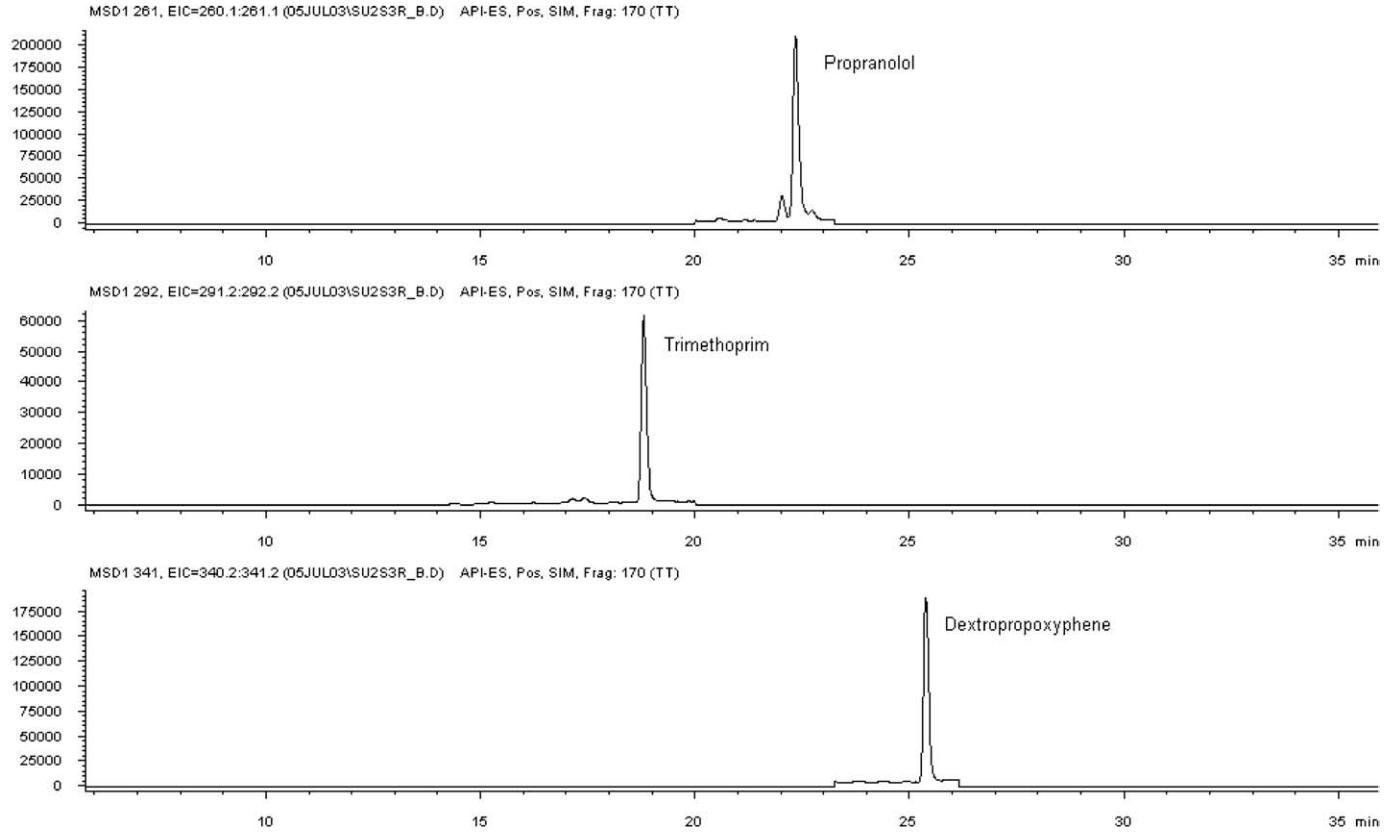

Fig. 8.5. Selected LC–MS extracted ion chromatograms for trimethoprim, propranolol and dextropropoxyphene in a POCIS extract from Site 3, Survey 2 (Replicate B) of the pharmaceutical reconnaissance in British WWTP effluents.

Analysis of erythromycin proved very difficult in the field deployed samples due to other closely eluting peaks with the same mass ion and also a weak confirmatory ion when using a single quadrupole LC–MS. Confirmation of the presence of erythromycin was performed using an ion trap LC–MS–MS. Identification of diclofenac was problematic in some of the field samples also requiring confirmation on the ion trap LC–MS–MS. Although the identity of the interfering chemicals was not determined, it appears they were sampled by the POCIS and not due to the sampler matrix. All analyses were performed on raw (no sample manipulation) extracts. It may have been possible to remove the interferences with the future development of cleanup and/or fractionation techniques for pharmaceuticals.

This study represents the first time POCIS was used for temporal environmental sampling. Examination of the data reveals that the concentrations of the pharmaceuticals detected remain relatively constant over the three sampling periods (Table 8.5). These findings support the claim by Daughton and Ternes [9] that although many PPCP are known to be relatively non-persistent, they maintain a fairly constant concentration due to a continuous input from human activities.

8.6 FUTURE RESEARCH CONSIDERATION

8.6.1 Development of the PRC approach in POCIS

Performance reference compounds (PRCs) are analytically non-interfering chemicals (e.g., deuterium- or ^{13}C-labeled compounds and native compounds not found in the environmental system of interest) that are added to a passive sampler prior to use [27]. PRCs are commonly used in partitioning-based passive samplers (e.g., SPMDs, low-density polyethylene strips, and silicone-based samplers) and they provide important information on how certain environmental conditions affect the rates of analyte uptake and loss.

Implicit in the PRC approach for passive samplers is the assumption that the overall uptake and release of targeted chemicals and PRCs are governed by first-order kinetics and that the sum of resistances to mass transfer across sampler associated barriers is equal in both directions [30]. These characteristics are commonly observed in the partitioning of residues between immiscible liquid phases and between certain nonpolar polymeric films (those with rubbery or liquid-like regions) and water or air. This assumption may not be valid for SPE sorbents because of the fundamental differences between solute partitioning and

adsorption phenomena. The adsorption of aqueous solute molecules on active surfaces results in a greater loss of kinetic energy than their partitioning into a liquid or liquid-like polymers, where chemical potential or fugacity is low. However, the capacity of a SPE sorbent for solutes is limited by its accessible surface area and the strength of the binding mechanism. The SPE resins (Oasis HLB and Isolute ENV+) and the activated carbon (Ambersorb 1500 or 572) sorbents used in POCIS have high porosities with pore sizes ranging from about 15 to 900 Å and high surface areas ranging from 800 to 1100 m^2 g^{-1}. A sorbent-specific combination of several types of attractive forces likely control HpOC solute retention or binding on the internal surfaces of POCIS sorbents, which include π–π cloud, electrostatic, lone pair, and hydrogen bonding. In cases where solutes are very large, adsorption is limited by molecular size exclusion. The accumulation of solutes by SPE sorbents is characterized by several types of adsorption isotherms, which describe the equilibrium relationship between sorbed molecules and those remaining in solution at a specific temperature. For example, the empirical Freundlich isotherm (typically the adsorption isotherm of choice for activated carbon or graphitic adsorbents) is given by

$$\frac{Q_o}{M_s} = kC_{We}^{1/n} \tag{8.7}$$

where M_s is the mass of the sorbent, k and n are constants, and C_{We} is the equilibrium concentration of the solute in the water. Huckins *et al.* [27] have pointed out that the uptake rates of residues by passive samplers must be independent of water concentration. Regardless of the type of isotherm characterizing an adsorbent, the linear or zero-order phase of uptake is independent of solute concentration. Several studies have shown that uptake of HpOCs by POCIS remains the linear phase for at least 50 days. This is not surprising in view of the relatively low sampling rates of POCIS (Fig. 8.2), the high sorption capacity (i.e., K_{sw} times M_s or V_s) of the sorbents used in POCIS, and the relatively low environmental concentrations of HpOCs. Because POCIS sorbents act as an infinite sink, the selection of a PRC with sufficient fugacity from POCIS is problematic.

An alternative to using PRCs incorporated in the POCIS is to use PRC containing SPMDs in conjunction with the POCIS. The fact that the uptake of chemicals targeted by both SPMDs and POCIS are under WBL controls suggests that this approach is feasible. For example, the differences between POCIS R_s values for nine analytes measured under quiescent and turbulent exposure conditions averaged 5.6-fold ($n = 9$)

with a CV of 32% indicating strong WBL control. Furthermore, differences in the polarity of organic analytes accumulated in SPMDs and POCIS have no relevance to equations used for the diffusion of aqueous solutes through the WBLs of POCIS and SPMDs.

To date, small SPMDs containing PRCs have been used by either placing the SPMD inside the POCIS deployment canister or by attaching a small SPMD holder to the outside of the POCIS canister. However, by fixing PRC-spiked SPMDs between POCIS compression rings and mounting the resulting disk similarly to POCIS disks in deployment canisters, the turbulence regime experienced by the SPMD disk should be about the same as adjacent POCIS disks. With the exception of the differences in biofouling between the POCIS and SPMD membranes, environmentally induced changes in the rates of PRC loss from SPMDs should reflect the changes in POCIS sampling rates. PRC-SPMD fixed to the outside of POCIS canisters provides only a means of adjusting relative differences in flow and temperature among sites.

Although attempts to use the classical PRC approach (i.e., spiking of PRCs into sorptive matrix of the sampler) for current POCIS configurations have been unsuccessful so far (D.A. Alvarez, unpublished data), research will continue in this area. Initial experiments have revealed that a silicone membrane disk may be a suitable alternative as a sorbent material for POCIS PRC determinations. Seven-day trials in microcosms containing 1 L of stirred water indicated that silicone disks fortified with ^{14}C diazinon lost up to 50% of the chemical to the surrounding water. Concurrent trials with the two sorbents commonly used in the POCIS showed less than 1% loss of ^{14}C diazinon to the water. Evaluation of the PRC-loaded silicone disks contained within the PES membranes is on-going.

8.6.2 Determination of sampling rate and kinetic data for chemicals of interest

As previously mentioned, the estimation of ambient water concentrations is dependent on the availability of R_s values for the chemicals of interest. Calibration studies to determine these R_s values and measurements of the membrane–water partition coefficient (K_{mw}) for chemicals over a range of K_{ow} values are necessary for an improved understanding of HpOC uptake by POCIS. Further understanding as to the transport of chemicals through the membrane, whether by partitioning into the polymer matrix or passage through the water-filled pore structure, will allow for models to be refined. The influence of

temperature on R_s also requires some investigation in regard to the duration of the linear uptake phase.

8.7 CONCLUSIONS

There has been a recent global awakening to the problems of emerging contaminants entering the environment due to human use and inadequate or improper waste treatment practices. These anthropogenic contaminants may include complex mixtures of pesticides, prescription and non-prescription drugs, personal care and common consumer products, agricultural, industrial, and domestic-use materials and the degradation products of these compounds. The development of the POCIS provides environmental scientists and policy makers a tool for assessing the presence and potential impacts of the hydrophilic component of these organic contaminants. To date, over 120 HpOCs have been identified in POCIS extracts.

The POCIS provides a means for determining the TWA concentrations of targeted chemicals that can be used in risk assessments to determine the biological impact of HpOCs on the health of the impacted ecosystem. Generating a sufficient number of samples to estimate TWA concentration by traditional methods may be logistically and financially imprudent as part of a regular monitoring program. Field studies have shown that the POCIS has advantages over traditional sampling methods in sequestering and concentrating ultra-trace to trace levels of chemicals over time resulting in increased method sensitivity, ability to detect chemicals with a relatively short residence time or variable concentrations in the water (i.e., chemical/biological degradation, sorption, dissipation), and simplicity in use.

Following a simple organic solvent extraction, the POCIS extracts are amenable to the same cleanup and fractionation schemes and analysis by standard instrumental techniques as samples originating from other matrices. POCIS extracts can also be tested using bioassays and can be used in organism dosing experiments for determining toxicological significance of the complex mixture of chemicals sampled.

The POCIS has been successfully used worldwide under various field conditions ranging from stagnant ponds to shallow creeks to major river systems in both fresh and brackish water. Estimation of ambient water concentrations is becoming possible with the addition of R_s data for a continually growing suite of chemicals. Due to the quality of the data obtained, ease of use, and broad applicability to both chemical and

biological assessments, the POCIS technique has the potential to become the standard for global water quality monitoring.

REFERENCES

1 B.W. Brooks, P.K. Turner, J.K. Stanley, J.J. Weston, E.A. Glidewell, C.M. Foran, M. Slattery, T.W. LaPoint and D.B. Huggett, *Chemosphere*, 52 (2003) 135.
2 A.B.A. Boxall, C.J. Sinclair, K. Fenner, D. Kolpin and S.J. Maund, *Environ. Sci. Technol.*, 38 (2004) 368A.
3 C.M. Flaherty and S.I. Dodson, *Chemosphere*, 61 (2005) 200.
4 A.R. Greenlee, T.M. Ellis and R.L. Berg, *Environ. Health Perspect.*, 112 (2004) 703.
5 T. Colborn, F.S. vom Saal and A.M. Soto, *Environ. Health Perspect.*, 101 (1993) 378.
6 W.V. Welshons, K.A. Thayer, B.M. Judy, J.A. Taylor, E.M. Curran and F.S. vom Saal, *Environ. Health Perspect.*, 111 (2003) 994.
7 C. Desbrow, E. Routledge, G. Brighty, J. Sumpter and M. Waldock, *Environ. Sci. Technol.*, 32 (1998) 1549.
8 B. Halling-Sørensen, S. Nors Nielsen, P. Lanzley, F. Ingerslev, H. Holten Lützhøft and S. Jørgensen, *Chemosphere*, 36 (1998) 357.
9 C. Daughton and T. Ternes, *Environ. Health Perspect.*, 107 (1999) 907.
10 X.-S. Miao, F. Bishay, M. Chen and C.D. Metcalfe, *Environ. Sci. Technol.*, 38 (2004) 3533.
11 O. Braga, G.A. Smythe, A.I. Schäfer and A.J. Feitz, *Environ. Sci. Technol.*, 39 (2005) 3351.
12 P.E. Stackelberg, E.T. Furlong, M.T. Meyer, S.D. Zaugg, A.K. Henderson and D.B. Reissman, *Sci. Total Environ.*, 329 (2004) 99.
13 D.F. Hagen, C.F. Markell, G.A. Schmitt and D.D. Blevins, *Anal. Chim. Acta*, 236 (1990) 157.
14 M.C. Hennion and V. Pichon, *Environ. Sci. Technol.*, 28 (1994) 567A.
15 C.E. Green and M.H. Abraham, *J. Chromatogr. A*, 885 (2000) 41.
16 N. Fontanals, M. Galià, P.A.G. Cormack, R.M. Marcé, D.C. Sherrington and F. Borrull, *J. Chromatogr. A*, 1075 (2005) 51.
17 W.K. Fowler, *Am. Lab.*, 14 (1982) 80.
18 American Conference of Governmental Industrial Hygienists (ACGIH), *Threshold Limit Values for Chemical Substances and Physical Agents and Biological Exposure Indices*, ACGIH, Cincinnati, OH, 1990.
19 J. Namieśnik, B. Zabiegala, A. Kot-Wasik, M. Partyka and A. Wasik, *Anal. Bioanal. Chem.*, 381 (2005) 279.
20 D.A. Alvarez, Ph.D. thesis: *Development of an Integrative Sampling Device for Hydrophilic Organic Contaminants in Aquatic Environments*, University of Missouri-Columbia, Columbia, MO, USA, 1999.

21 J.D. Petty, J.N. Huckins and D.A. Alvarez, *Device for Sequestration and Concentration of Polar Organic Chemical from Water*, US Patent No. 6 478 961, 2002.
22 J.D. Petty, J.N. Huckins, D.A. Alvarez, W.G. Brumbaugh, W.L. Cranor, T. Lieker, C. Rostad, E. Furlong and A. Rastall, *Chemosphere*, 54 (2003) 695.
23 D.A. Alvarez, J.D. Petty, J.N. Huckins, T.L. Jones-Lepp, D.T. Getting, J.P. Goddard and S.E. Manahan, *Environ. Toxicol. Chem.*, 23 (2004) 1640.
24 T.L. Jones-Lepp, D.A. Alvarez, J.D. Petty and J.N. Huckins, *Arch. Environ. Contam. Toxicol.*, 47 (2004) 427.
25 D.A. Alvarez, P.E. Stackelberg, J.D. Petty, J.N. Huckins, E.T. Furlong, S.D. Zaugg and M.T. Meyer, *Chemosphere*, 61 (2005) 610.
26 H. Saechtling, *International Plastics Handbook for the Technologist, Engineer and User*, 2nd ed., Oxford University Press, New York, NY, 1992.
27 J.N. Huckins, J.D. Petty, H.F. Prest, R.C. Clark, D.A. Alvarez, C.E. Orazio, J.A. Lebo, W.L. Cranor and B.T. Johnson, *A Guide for the Use of Semipermeable Membrane Devices (SPMDs) as Samplers of Waterborne Hydrophobic Organic Contaminants*, American Petroleum Institute (API), API publication number 4690, Washington, DC, USA.
28 C.R. Casey, L. Strattan, T.L. Jones-Lepp and D.A. Alvarez, *EPA Science Forum 2004*, Healthy Communities and Ecosystems, Washington, DC, 2004.
29 E. Collinder, G. Björnhag, M. Cardona, E. Norin, C. Rehbinder and T. Midtvedt, *Ecol. Health Dis.*, 15 (2003) 66.
30 J.N. Huckins, J.D. Petty, J.A. Lebo, F.V. Almeida, K. Booij, D.A. Alvarez, W.L. Cranor, R.C. Clark and B. Mogensen, *Environ. Sci. Technol.*, 36 (2002) 85.

Chapter 9

Monitoring of priority pollutants in water using Chemcatcher passive sampling devices

Richard Greenwood, Graham A. Mills, Branislav Vrana, Ian Allan, Rocío Aguilar-Martínez and Gregory Morrison

9.1 INTRODUCTION

In recent years, a number of alternative methods of monitoring water quality has been developed to complement and/or replace spot sampling methods that provide only an instantaneous estimate of the concentration of pollutants at the time and point of sampling. Amongst these alternative technologies are passive sampling devices that use a diffusion membrane to separate a receiving phase (with a high affinity for the pollutants to be monitored) from the aqueous environment.

Over the last decade, a range of low-cost passive sampling devices, incorporating a polymeric membrane and a sorbent receiving phase held in an inert plastic body, for monitoring polar contaminants (e.g. triazine pesticides), non-polar organic pollutants (e.g. polycyclic aromatic hydrocarbons (PAHs) and organochlorine pesticides (OCPs)), organometallic compounds (e.g. organotin compounds) and heavy metals (e.g. copper, lead, mercury and zinc) in aquatic environments has been developed in our laboratory. The performance of the sampling devices for the various groups of target analytes was optimised by an appropriate selection of combinations of various sorbent receiving phases and polymeric membranes.

9.2 CONCEPT OF CHEMCATCHER

The design of this passive sampling device was developed to provide a single low-cost sampler body that could house a range of combinations of receiving phases and diffusion membranes as appropriate for the

Comprehensive Analytical Chemistry 48
R. Greenwood, G. Mills and B. Vrana (Editors)
Volume 48 ISSN: 0166-526X DOI: 10.1016/S0166-526X(06)48009-0

wide range of classes of pollutants in the aquatic environment. Analytes permeate through the membrane, across a fixed diffusion gap to the receiving phase, where they are retained. Accumulation rates and selectivity are regulated by the choice of both the diffusion-limiting membrane and the solid-phase receiving material. One objective of this design was to overcome some of the problems associated with some of the other currently used passive sampling techniques. A range of solid-phase extraction materials bound to an inert polymeric disk matrix was used as a receiving phase for the accumulation of contaminants from water. This is advantageous as there is no risk of leakage or loss of receiving phase into the aquatic environment. The receiving phase consists of a chromatographic (for organic and organometallic analytes) or chelating (inorganic analytes) receiving phase separated from the aqueous environment by means of a diffusion membrane. These receiving phases have the advantage that they are relatively easy to extract to provide clean samples for chemical analysis.

9.2.1 Receiving phases

The accumulation of organic analytes by a passive sampler occurs as a result of absorption or adsorption of compounds from an unfavourable (bulk water phase) to a more favourable medium (receiving phase). The driving force of this process is determined by the difference between chemical potentials of an analyte in the two media. The Chemcatcher passive sampling system uses a receiving phase based on a solid sorbent immobilised in a polymeric matrix in the form of a disk, and this overcomes a number of problems associated with the use of liquid receiving phases. Not only is the system physically robust but because the receiving phase can be selected from a wide range of commercially available phases, there is potential for increasing the range of analytes sampled or for making the sampling system selective. Substances accumulate from the external aqueous environment into the receiving phase until equilibrium is achieved. This process is fully reversible for receiving phase materials based on sub-cooled liquids (e.g. low-density polyethylene (LDPE) or polydimethylsiloxane (PDMS)). However, sorption is often not fully reversible for solid sorbent materials.

In the simplest case, capacity of a receiving phase accumulating a chemical from water is defined as a product of its affinity for an analyte, given by its distribution coefficient between the receiving phase and water K_{DW}, and the volume of receiving phase V_D.

TABLE 9.1
Chemcatcher configurations for integrative sampling of various pollutant classes

Pollutant class	Receiving phase	Diffusion membrane
Hydrophobic organic compounds (log $K_{OW} > 3$)	C_{18} Empore^{TM} disk	Non-porous low-density polyethylene (LDPE)
Hydrophilic organic compounds (log $K_{OW} < 3$)	C_{18} Empore^{TM} disk	Microporous polysulfone (PS)
	SDB-RPS Empore^{TM} disk	Microporous polyethersulfone (PES)
Metals	Chelating Empore^{TM} disk	Microporous cellulose acetate (CA)
Mercury	Chelating Empore^{TM} disk	Microporous polyethersulfone (PES)
Organotin compounds	C_{18} Empore^{TM} disk	Microporous cellulose acetate (CA)

Empore^{TM} extraction disks were selected as convenient receiving phases for use in the Chemcatcher samplers. They are available as standard 47-mm diameter sorbent particle loaded disks. The particles are held together within an inert matrix made of polytetrafluoroethylene (PTFE) (90% sorbent: 10% PTFE, by weight). The variety of sorbent materials used in the Empore^{TM} disk technology enabled the selection of suitable receiving phases for all classes of pollutants under investigation, including polar and non-polar organic analytes, organometallic compounds and metals (Table 9.1). A further advantage is the availability of published extraction protocols for a number of analytes and a simple analyte elution with consistent recoveries. Moreover, procedures enabling the disks to be loaded (using procedures developed for solid-phase extraction) in a reproducible manner with internal standards or performance reference compounds (PRCs) by filtering an aqueous standard solution through the disk were developed [1].

9.2.2 Diffusion membranes

Two types of polymeric membranes have been tested for construction of Chemcatcher samplers; non-porous membranes including LDPE and

microporous membranes including glass fibre, nylon, polycarbonate, PTFE, polyvinylidenedifluoride (PVDF), cellulose acetate (CA), polysulfone (PS), polyethersulfone (PES) and regenerated cellulose. The membranes separate the sorption phase from the bulk water phase, and reduce the flux to the sorption phase. The membrane acts as a semi-permeable barrier between the receiving phase and the aqueous environment. The dissolved analytes can pass through to the receiving phase, while particulates, microorganisms and macromolecules with a size greater than the exclusion limit cannot permeate. Without the protection of the membrane, there is a risk of deterioration of the receiving phase disks in the aqueous environment due to biofouling. The criteria for selecting an optimum membrane for sampling a specific group of analytes have been discussed in Chapter 7.

The physical strengths, handling properties and chemical resistance of membrane materials were assessed during the initial evaluation. These tests were followed by accumulation studies of test analytes in prototype devices fitted with different membranes in a flow-through system. The latter studies were designed to determine the conductivity to mass transfer of membranes for a broad range of organic and organometallic pollutants and metal ions. Differences in conductivity of various membrane materials are shown in Fig. 9.1. In this first evaluation stage, optimum combinations of diffusion membrane/receiving phase systems were selected for a comprehensive evaluation, including calibration in the laboratory and testing in the field (Table 9.1).

PS and PES membranes were selected for sampler devices designed to sample polar organic pollutants ($\log K_{OW} < 3$) and mercury. These membranes have a high degree of physical strength and good antifouling properties, due to their low surface energy that prevents adsorption of macromolecules to the surface. Polar molecules readily diffuse through the 0.2-μm wide water-filled pores. In contrast, more hydrophobic compounds sorb to the polymer matrix of the membrane. Due to low diffusivity in the polymer matrix, conductivity of the membrane decreases dramatically with increasing hydrophobicity of sampled compounds. CA was selected as a material suitable for construction of Chemcatcher samplers for inorganic ions and organotin compounds, due to their optimum diffusion through the water-filled membrane pores, combined with negligible adsorption to the membrane material.

The non-porous LDPE allows permeation of hydrophobic analytes ($\log K_{OW} > 3$–4), due to the favourable combination of high membrane/water partitioning coefficients and membrane diffusivities for those compounds (see Chapter 7). On the other hand, the membrane has a

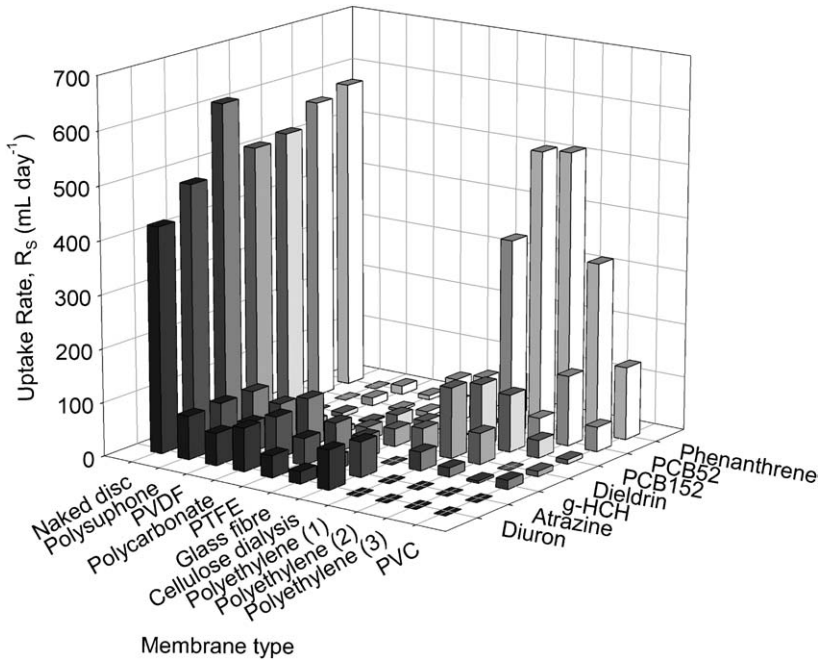

Fig. 9.1. The effect of diffusion membrane materials on the patterns of uptake of seven organic compounds. The exposure was performed at constant analyte concentration in water at 11°C in a flow-through tank. A 47-mm C_{18} Empore™ disk was used as receiving phase in all cases.

high resistance to mass transfer of more polar compounds and completely excludes the permeation of ions and molecules with effective diameter larger than 1 nm.This material was used in the Chemcatcher designed to sample non-polar organic pollutants.

9.2.3 Sampler body

9.2.3.1 Reusable sampler body prototype

The principles of Fickian diffusion state that the flux of a substance to the receiving phase is proportional to the surface area over which diffusion takes place and is inversely proportional to the diffusion path length. Therefore, if passive sampling obeys Fickian diffusion, the physical dimensions of the sampler body significantly affect the sampling rate for analytes. During the development phase, the design of the Chemcatcher body was optimised in terms of both construction materials and sampler geometry.

In the evaluation stage, PTFE was selected as a construction material for the sampler body. Its advantage is a low sorption capacity for most environmental pollutants. Moreover, PTFE is denser than water and is not buoyant in the sampled environment, making it easy to deploy this prototype in the field by suspending it from a wire or a string.

The system was constructed to fit a 47-mm Empore^{TM} disk as the receiving phase, with the chosen diffusion membrane material being laid directly on its surface. Both were supported by means of a 50-mm rigid PTFE backing plate (Fig. 9.2). The active surface area of the Chemcatcher sampler is 17.5 cm^2. To seal the sampler, a sleeve open at the back was screwed into place to hold the individual body sections together. In addition, a sealing plate allowed the system to be filled with water and sealed during storage and transport. Thus, the sampler body also acts as a container for storage and transport. The PTFE body could be reused several times, but only after a thorough cleaning involving a multi-step washing procedure.

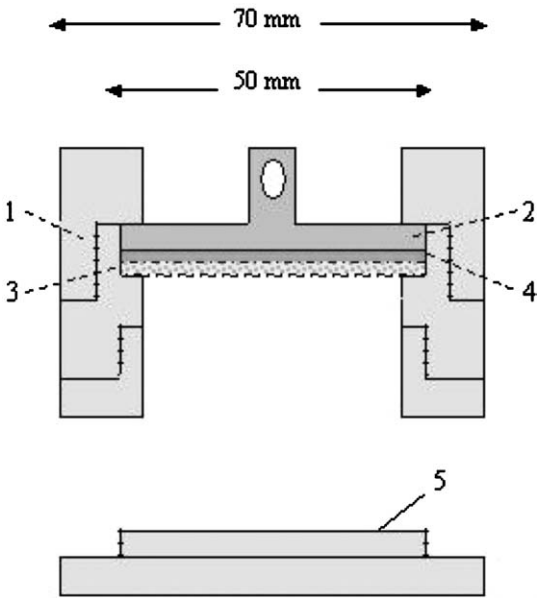

Fig. 9.2. Schematic diagram of the prototype Chemcatcher device, used during the sampler development. The PTFE body parts (components 1 and 4) support the receiving phase (component 2) and the diffusion membrane (component 3) and sealed them in place. The sampler is sealed by means of a screw cap (component 5) for storage and transport.

In the early stages of development [2], a protective steel mesh was used to protect the surface of the membrane. However, the use of a mesh was later abandoned, because it proved to accumulate particulate matter in the field and also to provide shelter for colonising organisms that cause fouling or degradation of the membrane.

9.2.3.2 Disposable sampler body prototype

In subsequent performance tests, the uptake kinetics of many analytes were shown to be controlled by diffusion in the aqueous boundary layer on the membrane surface. The resistance to mass transfer of the boundary layer depends on hydrodynamic conditions in the membrane vicinity. These are significantly affected by the construction geometry of the sampler body. The membrane and receiving phase of the first-generation Chemcatcher prototype were located inside a 20-mm deep depression in the sampler body. This sampler design effectively buffers the effect of fluctuating flow on the sampler performance. However, it also effectively reduces convective transport of analytes to the sampler membrane, causing reduced sampling rates (i.e. the rate at which the sampler accumulates chemicals). For an optimum sampler performance, high sampling rates are essential, especially for sampling non-polar chemicals, due to their extremely low concentrations in the water column. In order to increase sampling rates, the geometry of the body was further refined in the latest version of Chemcatcher body prototype by reducing the depth of the cavity to a minimum (Fig. 9.3). In comparison with the first-generation prototype, the second-generation sampler collects analytes with increased sampling rates. Tests showed that the sampling rate for non-polar compounds ($\log K_{OW} > 3$–4), which are accumulated under aqueous boundary layer control, was increased by a factor of 2. This provides improved sensitivity, but also increased variation of sampling rates in response to fluctuations in turbulence (water flow).

In the latest design, the Chemcatcher body is made of mouldable plastic materials. The body consists of three components (two body parts and a lid for storage and transport), which are clipped together (Fig. 9.3). This makes the sampler assembly and disassembly faster than it was in the first-generation prototype, where assembly was made using screw threads. This sampler body prototype was designed as a disposable device for a single field deployment. This removes difficulties connected with cleaning procedures and accompanying quality control measures required for use in trace analysis. The plastic material can be recycled.

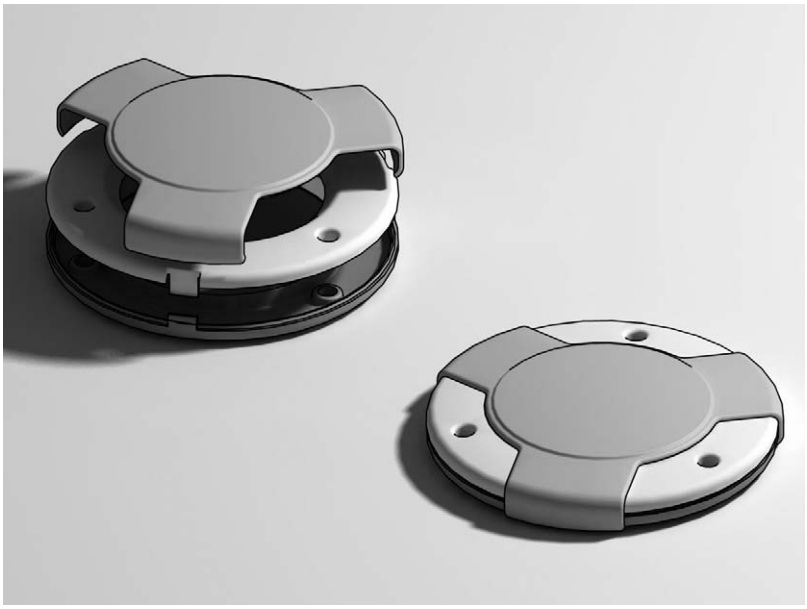

Fig. 9.3. Views of the disposable Chemcatcher sampler.

Depending on the nature (temperature, turbulence, presence of suspended solids) of the environment to be sampled and on the target analyte properties, a sampler design can be selected to provide an optimum performance.

9.3 THEORY

The general theory of passive sampling is described in Chapter 7, and this is applicable to the various Chemcatcher designs. In summary, mass transfer of a chemical into the sampler involves several diffusion and interfacial mass transport steps across the various barriers that may be present; i.e. the stagnant aqueous boundary layer, possibly a biofilm, the diffusion membrane, the inner fluid (liquid or gaseous) phase, and the receiving phase. In the initial stages of exposure, analyte uptake is expected to be linear or time-integrative after steady-state flux of chemicals into the sampler has been achieved [3,4]. Under these conditions, the amount of a chemical in the receiving phase is directly proportional to the product of the concentration in the surrounding water (C_W) and the exposure time (t). For practical purposes, uptake in

the linear phase can be described by

$$m_D(t) = m_0 + C_W R_S t \quad (9.1)$$

where m_D is the amount of analyte accumulated in the receiving phase, m_0 is the initial amount of analyte in the receiving phase, and R_S is the sampling rate of the system:

$$R_S = k_{ov} A \quad (9.2)$$

where k_{ov} (m s^{-1}) is the overall mass transfer coefficient and A (m^2) is the surface area of the membrane. The uptake of an analyte is linear and integrative approximately until the concentration factor of the sampler ($m_D(t)/C_W$) reaches half saturation. The sampling rate of an individual chemical can be determined experimentally under fixed conditions at constant analyte concentration. Under environmental conditions, when the water concentration changes during the exposure, the term C_W represents a time-weighted average (TWA) concentration during the deployment period.

9.4 CALIBRATION

The sampling rate depends on the physicochemical properties of the analyte, the environmental conditions and the sampler design. To enable measurement of TWA water concentrations of a range of pollutants, the Chemcatcher sampler was calibrated in flow-through tank studies under controlled conditions of temperature and water turbulence. Concentrations of the analytes in water (C_W) and the amounts accumulated in the receiving disk (m_D) were measured regularly during the exposure. In each experiment, passive samplers were exposed for up to 14 days in a constant concentration of analyte. Each factor (temperature and stirring speed (turbulence)) was tested at three levels. The calibration experiments were designed to characterise the effect of physicochemical properties, temperature and hydrodynamics on kinetic and thermodynamic parameters characterising the exchange of analytes between the sampler and water. So far, calibration data have been reported for the non-polar Chemcatcher [1,5] and calibration data for other Chemcatcher designs will be reported shortly [6,7].

9.5 SAMPLING OF HYDROPHOBIC ORGANIC CONTAMINANTS

Kingston *et al*. [2] designed one of the Chemcatcher prototypes for the sampling of non-polar organic compounds with log K_{OW} values greater

than 3. This system uses a 47-mm C_{18} Empore^{TM} disk as the receiving phase and a 35-μm thick LDPE diffusion membrane. The C_{18} Empore^{TM} disk has a very high affinity and capacity for the sampled hydrophobic organic pollutants. LDPE is a non-porous material, even though transient cavities with diameters approaching about 1 nm are formed by random thermal motions of the polymer chains. The thermally mediated transport corridors of the polyethylene exclude large molecules, as well as those that are adsorbed on sediments or colloidal materials such as humic acids. Only truly dissolved and non-ionised contaminants are sequestered.

Recently, the optimisation of this sampler design has been reported [8]. This involved the improvement of sampling characteristics including the enhanced sampling kinetics and precision by decreasing the internal sampler resistance to mass transfer of hydrophobic organic chemicals ($\log K_{OW} > 5$). This was achieved by adding a small volume of *n*-octanol, a solvent with high permeability (solubility × diffusivity) for target analytes, to the interstitial space between the receiving sorbent phase and the polyethylene diffusion membrane. The use of *n*-octanol as an interstitial phase resulted in an approximately 20-fold increase in sampling rates compared with those observed with water as the interstitial phase [8].

9.5.1 Calibration data

Calibration data for the non-polar Chemcatcher were obtained in laboratory experiments designed to measure the uptake of target analytes (sampling rate; R_S) and offloading of PRCs (elimination rate constants; k_e) at different combinations of temperature and hydrodynamic conditions in a full factorial design. The calibration data were gathered in order to determine the sampling parameters and to observe how they are affected by environmental conditions to enable a more precise measurement of TWA concentrations of non-polar priority pollutants in the field [1].

Over the range of controlled laboratory conditions (temperature and turbulence), the magnitude of R_S values of hydrophobic chemicals spanned over two orders of magnitude (i.e. from 0.008 L day^{-1} up to 1.380 L day^{-1}). The sampling rate is strongly affected by the physicochemical properties of the compounds. Among the non-polar priority pollutants, the highest sampling rates were observed for small, moderately hydrophobic compounds: anthracene, phenanthrene, fluoranthene and pyrene. The lowest sampling rates were measured for

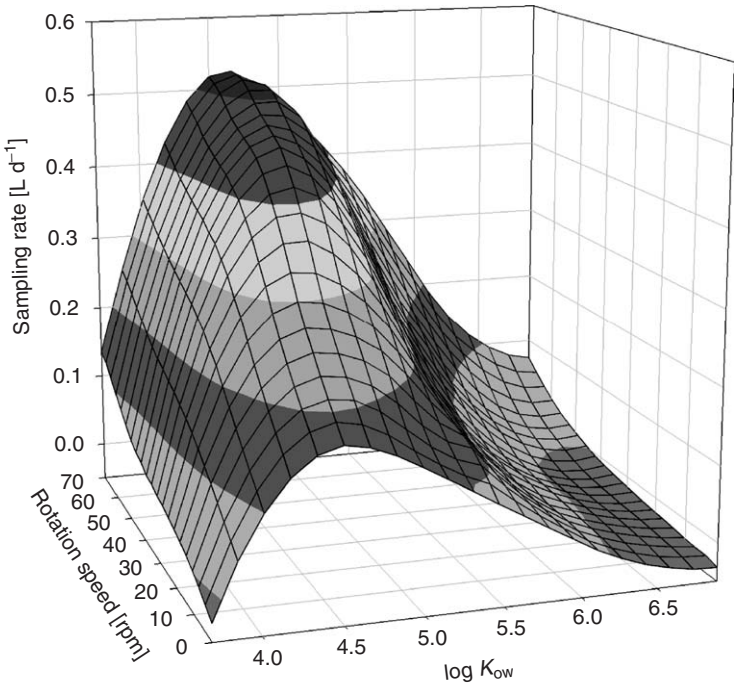

Fig. 9.4. Effect of water turbulence (expressed as rotation speed of a carousel device loaded with samplers) and log K_{OW} on the sampling rates for a range of non-polar organic compounds in the Chemcatcher at 11°C.

indeno[1,2,3-cd]pyrene, dibenz[a,h]anthracene and benzo[g,h,i]perylene; large and extremely hydrophobic compounds. The typical dependence of sampling rates on hydrophobicity is shown in Fig. 9.4.

Sampling rates increase with the increasing temperature, and the temperature dependence of the sampling rate R_S can be described by an Arrhenius-type equation. The mean activation energy for all of the hydrophobic analytes under investigation was 93 kJ mol^{-1}. This corresponds to an increase in sampling/offload rate of a factor of 5.2 over the temperature range 6–18°C. For comparison, Huckins *et al*. [9] calculated from the literature data available for semipermeable membrane devices (SPMDs) an average activation energy of 37 kJ mol^{-1}. Thus, the effect of temperature on the Chemcatcher uptake kinetics appears to be more significant than that on SPMD sampling rates.

With the exception of the moderately hydrophobic lindane (log $K_{OW} = 3.7$), a significant increase in sampling rate with increasing flow velocity was observed for all compounds under investigation (Fig. 9.4). This corresponds well with the theory of diffusion through two films in

series [10,11], which predicts a switch in the overall mass transfer to the aqueous boundary layer control for hydrophobic compounds. A similar effect of hydrodynamics has been observed and explained for SPMDs [12].

9.5.2 Performance reference compound concept

Figure 9.5 shows that for a range of environmental conditions (temperatures and water flow rates) there is a good correlation between uptake kinetics (sampling rate R_S) of analytes and offload kinetic parameters (elimination rate constant k_e) of their deuterated analogues (used as PRCs). This demonstrates isotropy of the uptake (absorption) onto and the offload (desorption) from the sampler for a range of hydrophobic analytes. Thus, the PRC concept can be applied to the measurement of *in situ* exchange kinetics in the field.

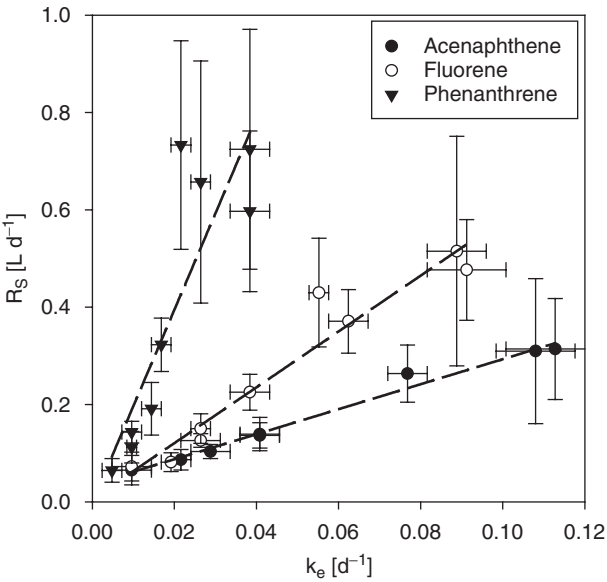

Fig. 9.5. The correlation between the sampling rates R_S of three polycyclic aromatic hydrocarbons and the elimination rate constants k_e of their perdeuterated analogues demonstrates the isotropic exchange kinetics for the non-polar Chemcatcher sampler variant. The data represent laboratory flow-through exposures performed at various combinations of water temperature and turbulence. Reproduced from Ref. [1] with permission from Elsevier.

9.5.3 Non-polar Chemcatcher/water distribution coefficients

Assuming isotropy of the exchange kinetics of the chemicals under investigation, and the validity of the model used to describe the kinetics, the value of the receiving phase water distribution coefficient K_{DW} can be calculated as the ratio of the absorption and desorption transport parameters for a particular compound (see also Chapter 7):

$$K_{DW} = \frac{R_S}{k_e V_D} \tag{9.3}$$

The experimental evidence indicates that K_{DW} values are not significantly affected by temperature in the range 6–18°C. This enables the derivation of an empirical equation to calculate the distribution coefficient K_{DW} of a compound between the non-polar Chemcatcher sampler and water using the *n*-octanol–water partition coefficient:

$$\log K_{DW} = 1.382 \ \log K_{OW} - 1.77 \quad (r = 0.97, s = 0.13, n = 31) \tag{9.4}$$

Huckins *et al.* [9] have shown that for SPMDs, the log K_{OW} versus log SPMD/water partition coefficient plot for compounds with log $K_{OW} > 5.0$ deviated from linearity. This phenomenon has also been observed for plots of log bioconcentration factor versus log K_{OW} [13]. It has not yet been demonstrated whether or not a deviation from linearity occurs for very hydrophobic compounds in the non-polar Chemcatcher.

9.5.4 Empirical uptake rate model

It is convenient to derive an empirical equation for the *in situ* estimation of sampling rates for use in the interpretation of results obtained with the Chemcatcher passive sampler in field studies. Huckins *et al.* [9,14] showed that for SPMDs, differences in exposure conditions cause sampling rates to be shifted by a constant factor for all compounds. A similar observation was made for the non-polar Chemcatcher. Log R_S versus log K_{OW} plots from all calibration studies for the Chemcatcher have very similar shapes, but show a varying offset for the different exposure conditions (combinations of water temperature and turbulence). A nonlinear regression analysis of log-transformed sampling rates R_S on a third-order polynomial function of log K_{OW} from all calibration studies enabled the derivation of an empirical model that can be used to calculate the sampling rate as a function of hydrophobicity.

This relationship is applicable within the range of log K_{OW} 3.7 to 6.8 and for a range of exposure conditions (temperatures between 6 and 18°C and water turbulence (stirring speeds from 0 to 70 rpm)):

$$\log R_S = P + 22.755\ \log K_{OW} - 4.061\ \log^2 K_{OW} + 0.2318\ \log^3 K_{OW}$$
$$(r = 0.92, s = 0.22, n = 134) \tag{9.5}$$

The relative ratios of sampling rates of any two compounds within the calibration range are constant for a broad range of exposure conditions. The knowledge of the parameter P is sufficient to characterise the effect of varying environmental conditions on the absolute magnitude of the sampling rates. The standard deviation of the fit (0.22 log units) corresponds to an uncertainty factor of approximately 1.7, which is relatively low considering the large differences in exposure conditions tested. Information on concentrations, that are accurate within a factor of 2, is still highly relevant for environmental risk assessment purposes.

9.5.5 Estimation of *in situ* TWA concentrations

An algorithm has been derived to calculate TWA water concentrations from the amounts of analytes accumulated in non-polar Chemcatcher samplers during field deployment [5]. This involves the characterisation of *in situ* exchange kinetics, using PRCs. The PRC elimination rate constant k_e is calculated using two points: amount of PRC in a sampler prior to and after a field exposure. Isotropic first-order exchange kinetics are assumed. Sampling rates R_S of PRCs are calculated using Eqs. (9.3) and (9.4). The PRC-derived sampling rates are then fitted to Eq. (9.5), using the exposure-specific effect P as the only adjustable parameter. The sampling rates of individual compounds are then estimated from Eq. (9.5) with the optimised value of parameter P. TWA concentrations of target analytes at the sampling site can be estimated from concentrations in the exposed samplers using the rearranged Eq. (9.1):

$$C_W = \frac{m_D(t) - m_{Df}}{R_S t} \tag{9.6}$$

where C_W represents the TWA water concentration during the deployment period, $m_D(t)$ is the analyte mass found in the sampler after field exposure, m_{Df} is the average mass of analyte found in the field blank, R_S is the estimate of the *in situ* sampling rate derived as described above and t equals exposure time.

9.6 SAMPLING OF HYDROPHILIC ORGANIC CONTAMINANTS

9.6.1 Integrative sampler

Kingston *et al.* [2] designed a Chemcatcher prototype for integrative sampling of polar organic compounds with log K_{OW} values lower than 3 over long exposure times. This system uses a 47-mm C_{18} Empore^{TM} disk as the receiving phase and a 100-μm thick PES diffusion membrane. The C_{18} Empore^{TM} disk, used as a receiving phase in this Chemcatcher prototype, has been shown to have a high affinity and capacity for many organic pollutants. The octadecyl functional groups bonded to the silica surface provide mainly non-polar interactions with hydrophobic molecules. However, a fraction of the silica material has non-substituted silanol groups with a high affinity for molecules with polar functional groups. These interactions involve mainly hydrogen bonding or dipole–dipole interactions. Thus, this sorbent disk exhibits can retain analytes with a broad range of physicochemical properties.

As described earlier, PES is a porous membrane with a high permeability for polar organic chemicals. This material has also been used in other passive samplers, e.g. polar organic chemical integrative samplers (POCIS) [15] (also see Chapter 8).

Retention of some polar compounds on C_{18} Empore^{TM} disks is stronger than one would expect from their hydrophobicity. This high receiving phase affinity permits the sampling of pollutants over a prolonged period without reaching the saturation of the sorbent material. On the other hand, this high affinity complicates the selection of compounds with a medium sampler fugacity that could be used as PRCs, since offloading rates are extremely low and it is not possible to measure *in situ* analyte exchange kinetics. This is shown in Fig. 9.6. Linear uptake of atrazine (a compound with relatively low hydrophobicity: log $K_{OW} = 2.61$) into the Chemcatcher was observed during a period of 14 days under a range of exposure conditions. No significant elimination of D_5-atrazine, loaded onto the Empore^{TM} disk prior to exposure, was observed over this period. This demonstrates an ideal performance of this variant of Chemcatcher as an integrative sampler for polar compounds. However, it is impossible to see whether the uptake kinetics of atrazine was correlated with the elimination kinetics of D_5-atrazine. Thus this compound cannot be used as a PRC in the time scale of a typical field exposure. Several other compounds, including D_5-atrazine, D_{10}-chlorpyrifos, D_8-naphthalene, D_{10}-simazine and D_{14}-trifluralin, were tested and none was identified to be suitable as a potential PRC.

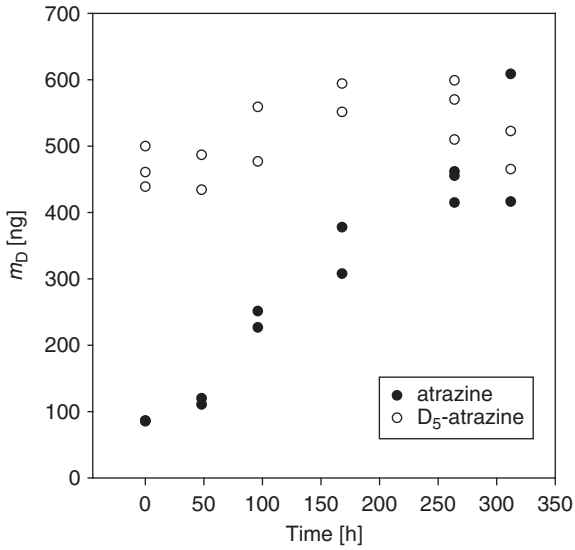

Fig. 9.6. Uptake of atrazine in the Chemcatcher prototype fitted with C_{18} Empore^{TM} disk and a polyethersulfone membrane in a flow-through laboratory exposure (14 days). No significant elimination of D_5-atrazine, loaded onto the Empore^{TM} disk prior to exposure was observed. Data are presented from an exposure conducted at 4°C in turbulent water (rotation speed 70 rpm). The aqueous concentration of atrazine was held constant at 1 μg L^{-1}, and the water-exchange rate in the flow-through system was 50 L day^{-1}.

Calibration data for the polar variant of Chemcatcher were obtained in laboratory experiments in a similar experimental set up as described in Section 9.5.1. Experiments were designed to determine sampling rates R_S of a selected number of triazine and phenylurea herbicides for various combinations of temperature and hydrodynamic conditions. An example of sampling rates of the triazine herbicides is shown in Fig. 9.7.

The sampling rates increase with increasing temperature, and the activation energy for the triazine herbicides under investigation (simazine and atrazine) was 130 kJ mol^{-1}. This would correspond to an increase in R_S of nearly a factor 10 over the temperature range 6–18°C. Thus, the temperature dependence of sampling rate for devices fitted with PES membranes seems to be greater than for those fitted with LDPE membranes. On the other hand, the observed effect of hydrodynamic conditions on sampler performance was only moderate.

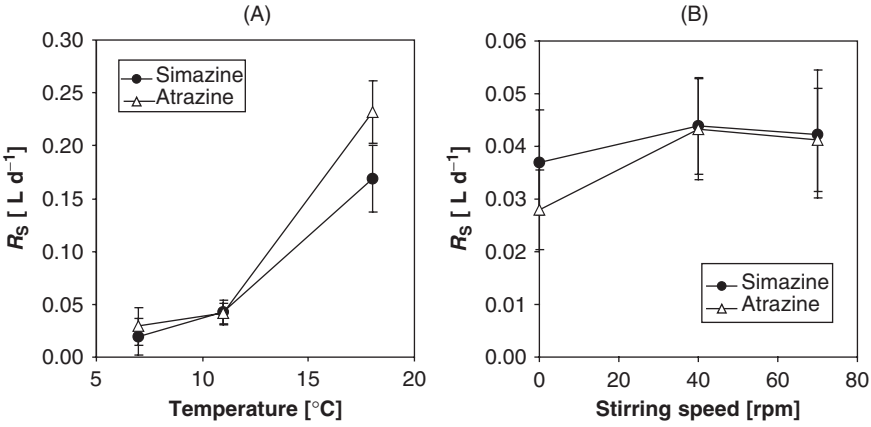

Fig. 9.7. Effect of temperature (A: measured in turbulent water) and water turbulence (B: expressed as rotation speed of a carousel device loaded with samplers; measured at 11°C) on the sampling rate of the polar Chemcatcher for triazines.

9.6.2 Short pollution event detector

Many pesticides, some of which are polar molecules, are released at high concentrations into streams and rivers in episodic events, such as field runoff after pesticide spraying, heavy rain and storm events, or during wastewater discharge. These events usually last only a few hours and in order for these compounds to be detected by passive samplers, a device with a short response time is required. However, the device fitted with a PES membrane, although ideal for long-term monitoring, has a lag phase of several hours that represents the time necessary for the analytes to diffuse through the membrane to reach the receiving phase. The lag phase of the device can be predicted using a theoretical model for the mass flux through a plane sheet with constant concentration on both sides of the sheet, as outlined in Chapter 7. Since the PES membrane is discarded before analysis (only the receiving phase is analysed), the lag time for passage through the membrane has to be taken into account.

Shaw and Müller [16] suggested the use of a device fitted with only an Empore^{TM} disk receiving phase (without a diffusion membrane) to reduce the response time and make the sampler more reactive to accidental pollution events. The naked Empore^{TM} disks deployed in stainless steel cages secured between two squares of wire mesh that

allowed the disks to be exposed on both surfaces. Later, Stephens *et al*. [17] used a device with a naked Empore™ disk fitted in the Chemcatcher PTFE body, and accumulation in such a device is shown in Fig. 9.1. Such samplers have a very short lag phase that represents only the time taken for the analyte to diffuse across the aqueous boundary layer. The analyte sampling rates are higher than in devices fitted with PES membranes as the resistance to mass transfer is lower in absence of the membrane. The disadvantage of such device is a fast equilibration of the sampling device with the water phase, which restricts to a few days the time over which the sampler operates in time-integrative mode. Moreover, because the main barrier to the mass transfer is the aqueous boundary layer, the sampling kinetics of such devices are sensitive to changing hydrodynamic conditions [18,19]. Potentially, problems may arise with sample clean-up due to fouling of the receiving phase during a direct contact with sampled water in the field. More work is required to minimise the uncertainty caused by sampling rate fluctuations with degree of water turbulence. Nevertheless, this approach is very useful for detecting and semi-quantitative evaluation of short pollution events.

9.7 SAMPLING OF METALS

A Chemcatcher variant based on diffusion through a porous CA membrane to a receiving phase, where the analyte is removed by chelation in a chelating Empore™ disk has been developed for monitoring metals [19]. Uptake rates to the receiving phase were determined in both batch and flow-through laboratory exposures for different metal ions. Sampling rates were found to be diffusion controlled and inversely related to pH. The uptake rate can be used for calculating the diffusion coefficients for specific compounds under defined laboratory conditions [19]. *In situ* deployment of the passive sampler was demonstrated to provide metal concentrations, corresponding to the electrochemically available fraction of total metal [20].

Laboratory handling procedures were developed that enabled a direct analysis of the accumulated metals on the receiving membrane by laser ablation inductively coupled plasma mass spectrometry [20]. In a later study, a calibration database of R_S values for five metals for independently varied temperature and turbulence conditions was established in an experimental setup similar to that described in Section 9.5.1 [6]. R_S for cadmium, copper, nickel and zinc were within

the same order of magnitude (50–150 mL day^{-1}) and showed similar variations with temperature and turbulence. Somewhat lower sampling rates (12–17 mL day^{-1}) were measured for lead. Both changes in temperature and turbulence were shown to have a significant effect on sampling rates of metal ions [6].

9.8 SAMPLING OF ORGANOMETALLIC COMPOUNDS

Another version of Chemcatcher has been developed for the measurement of the TWA concentrations of organotin compounds (monobutyltin, dibutyltin, tributyltin and triphenyltin) in water. The receiving phase is a C_{18} Empore^{TM} disk and the diffusion membrane is CA. The effects of environmental variables (pH, salinity and biofouling) that could influence accumulation in receiving phase have been evaluated in the laboratory. Linear uptake was observed for at least for 14 days of exposure at constant aqueous concentration of analytes. Compound-specific sampling rates varied between 0.063 and 0.038 L day^{-1} [7].

9.9 FIELD APPLICATIONS

9.9.1 Pan-European field trials to compare the performances of the Chemcatcher and spot sampling in monitoring the quality of river water

In 2004, field performance of the non-polar Chemcatcher was tested in a field trial in rivers in four European countries (the Czech Republic, Finland, The Netherlands and Norway). The sampler exposure was repeated twice at each of the four sampling sites, once in spring and once in autumn. The uptake of selected organic priority pollutants (PAHs and OCPs) in the Chemcatchers during deployment periods up to 28 days were compared with the contaminant levels found in extracts from filtered spot samples of water collected regularly over the exposure period. The resulting dataset provides a solid basis for the evaluation of the passive sampling method for hydrophobic chemicals with log K_{OW} from 3 to 7. The main objective of the study was to evaluate the ability of non-polar Chemcatcher samplers to estimate TWA concentrations of selected PAHs and OCPs under various exposure conditions (contaminant spectrum, temperature, water turbulence and fouling).

For practical estimation of the chemical exchange kinetics between Chemcatcher and water, the PRC approach was successfully applied and validated. The coefficients of variation of the two-point estimate of

the PRC overall exchange rate constants k_e ranged from 1% to 34% and the precision was sufficient to allow significant k_e estimates for a number of PRCs in each of the individual field studies. The PRC offload data confirmed that the chemical exchange kinetics are site specific and depend significantly on exposure conditions, including temperature, turbulence and biofouling. The knowledge of PRC offload kinetics in combination with laboratory-derived Chemcatcher calibration data enabled estimation of *in situ* sampling rates for the whole range of target analytes that were expected to be found in the monitored rivers. The compound-specific sampling rates ranged from 0.003 to 0.424 L day^{-1}. Maximum *in situ* sampling rates were measured for compounds with moderate hydrophobicity (log K_{OW} 4–6). The method sensitivity decreased for very hydrophobic (log $K_{OW} > 6$) compounds. The examination of the site-specific exchange kinetics of PRCs indicated in eight field exposures for European rivers that the uptake remained linear for up to 28 days for compounds with log $K_{OW} > 4.3$ at all sampling sites.

Heavy biofouling of the samplers was observed at all four sampling sites. This may be the reason for the deterioration of the exchange kinetics of the samplers with increasing time. Confocal laser microscopy was used to obtain semi-quantitative measure (film thickness and density) of the biofilm layer.

Method detection limits of target analytes in sampler extracts ranged from 0.2 to 10 ng per sampler. Instrumental method detection limits can be translated into site-specific minimum detectable water concentrations of 0.1–138 ng L^{-1} on the basis of compound-specific *in situ* sampling rates over a 14- or 28-day exposure period. The lowest detection limits were achieved for compounds with a favourable combination of a low instrument detection limit and high sampling rate. This was the case for the OCPs including dieldrin, α-endosulfan, hexachlorobenzene, lindane and pentachlorobenzene, as well as for PAHs with less than five aromatic rings.

Mean masses of PAHs found in Chemcatchers exposed in the field ranged between one and tens of ng per sampler. Compounds with two, three and four aromatic rings per molecule dominated the PAH spectrum. These are more water soluble than the heavier PAHs, and are thus likely to be present in water at higher concentrations. Moreover, the sampling performance characteristics of the Chemcatcher favour the uptake of compounds with moderate hydrophobicity. The concentrations of analytes found in Chemcatcher extracts were converted into the corresponding TWA aqueous concentrations, using the calculated *in situ* sampling rates. The estimated TWA concentrations of individual

truly dissolved PAHs at the sampling sites ranged between the detection limit and 60.3 ng L^{-1}. The estimated TWA concentrations of individual truly dissolved OCPs ranged between the detection limit and 3.4 ng L^{-1}.

The TWA concentrations estimated from the passive sampler data were compared with concentrations of analytes determined from filtered water samples to assess the performance of Chemcatcher. When comparing the TWA concentrations calculated from spot samples and passive samplers, it is important to consider the differences in contaminant fractions in water that are measured using the two methods. TWA concentrations estimated using passive samplers reflect the truly dissolved concentrations and do not account for the pollutants bound to particles and colloids in water. Water samples filtered through 0.45-μm pore size filters still contain a contaminant fraction that is bound to dissolved organic material (DOM) present in water. The truly dissolved fraction of hydrophobic analytes in water will depend on the level and quality of DOM, which may fluctuate during the sampling period. Unfortunately, there is a lack of equipment that is suitable for routine measurements of dissolved concentrations at a reasonable cost. The comparison was limited to cases where a particular analyte was detected in both the spot samples and the passive samplers. With a few exceptions (namely hexachlorobenzene and lindane) a comparison with spot samples was possible for the pesticides and for the PAHs with a maximum of four aromatic rings per molecule. The difference in water concentrations calculated using both methods never exceeded one order of magnitude.

9.9.2 Monitoring pesticide runoff in Brittany, France

In 2005, Schäfer *et al*. [21] used Chemcatcher fitted with naked SDB-XC Empore™ disks to investigate whether they can be applied to monitor field runoff of ecotoxicologically relevant pesticides in current use. The field study was performed in Brittany, in the North-western France, a region with intensive agriculture and pesticide usage. Between 1 and 3 samplers were deployed for 10–13 days at each of the 16 small streams. The target analytes were mainly polar or moderately polar pesticides with log K_{OW} values between 1.4 and 4.13. These belonged to multiple classes of pesticides: chloracetanilide herbicides (alachlor, acetochlor), the phenylurea herbicide linuron, the oxadiazolone herbicide oxadiazon, carbamate insecticides (pirimicarb, carbofuran), the organophosphate insecticide chlorfenvinphos, the organochlorine insecticide

endosulfan, the pyperidine fungicide fenpropidin and the conazole fungicide tebuconazole. A significant accumulation of all compounds except fenpropidin, chlorfenvinphos and α-endosulfan was observed in the devices. These results indicate the potential utility of these samplers in providing semi-quantitative or qualitative data on compounds present in episodic events, and the utility of the SDB-XC Empore™ disks for sequestering polar compounds. This phase may be more useful than the C_{18} disks described for the polar variant of the Chemcatcher, and further work in this area is ongoing.

9.9.3 Field trial in the River Meuse in The Netherlands

A field test of the wide range of passive sampling devices presently available was conducted at RIZA's monitoring station at Eijsden (NL) in April 2005 as part of the Screening method for Water data InFormation in support of the implementation of the Water Framework Directive (SWIFT-WFD) project. The aim of this trial was to evaluate the suitability of passive samplers for monitoring water quality to meet the requirements of the European Union's Water Framework Directive (WFD) legislation. The trial was designed to provide data on the robustness and utility of this technology in order to strengthen the case for its introduction into monitoring programmes.

Passive samplers for metals, polar and non-polar organic pollutants were deployed for overlapping periods of 7, 14 and 21 or 28 days in the River Meuse. Chemcatchers with different configurations were tested alongside SPMD, membrane-enclosed sorptive coating (MESCO), POCIS and DGT. TWA concentrations obtained were compared with those obtained from conventional spot sampling and analysis by an accredited laboratory. In addition, since the field deployment was undertaken at RIZA's monitoring station, concentrations from continuous monitoring for organic contaminants and composite sampling for metals were available for further comparisons.

It was therefore possible to evaluate information provided by the passive samplers alongside that from *in situ*, spot and composite sampling for the monitoring of metals in water. TWA zinc concentrations measured with Chemcatcher were calculated from the masses of zinc accumulated over exposures of 7, 14 and 21 days and available calibration data. These were compared with spot sampling and weekly composite sampling conducted to determine total and filtered (0.45 μm) fractions of zinc (Fig. 9.8). TWA concentrations measured with the Chemcatcher for 7-, 14- and 21-day exposures are generally in good

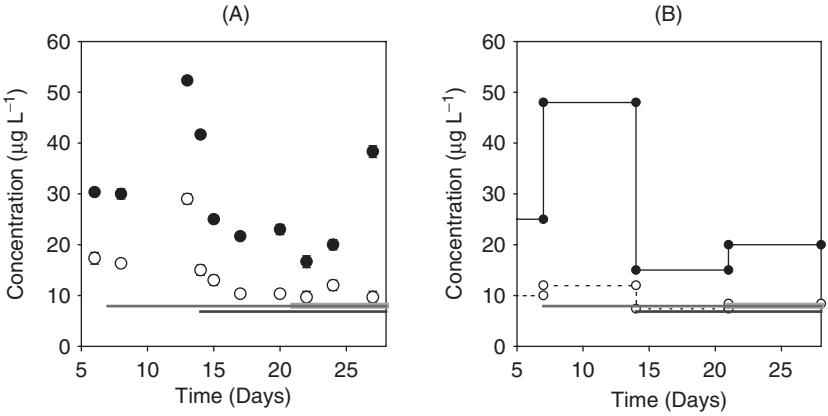

Fig. 9.8. Comparison of TWA zinc concentrations obtained for exposures of 7, 14 and 21 days of the Chemcatcher in the River Meuse with spot sampling (A) and composite sampling (B). Both sets of water samples were analysed without (•) and with filtration (o) to 0.45 μm.

TABLE 9.2

Comparison of mean zinc concentrations measured with the Chemcatcher and spot sampling (with and without filtration) for exposure times of 7, 14 and 21 days

Exposure (days)	TWA concentration (μg L^{-1})		Spot sampling dissolved concentration (μg L^{-1})	
	Mean	Std dev.	Mean	Std dev.
7	8.0	1.8	10.5	1.3
14	6.9	1.7	10.9	1.4
21	7.9	2.4	13.9	6.2

agreement with those determined by spot and composite sampling. While Chemcatcher-measured zinc concentrations are similar to mean dissolved concentrations from spot sampling for 7- and 14-day exposures, the precision of the measurement appears lower (Table 9.2). Higher fluctuations in concentrations observed during the 21-day exposure resulted in a significant loss of precision for spot sampling, while lower precision for Chemcatcher may have resulted from environmental impacts such as biofouling. However, it remains difficult to judge the accuracy of each of these methods in determining the TWA labile fraction of zinc. Slight underestimation of time-integrated filtered concentration

of zinc by the Chemcatcher may be the result of the uncertainty or bias from the calibration data used or due to a fraction of filtered zinc not available for uptake by the Chemcatcher. The time-integrated nature of *in situ* sampling is likely to offer more representative information than that provided by infrequent spot samples, and should be useful in assessing long-term trends in contaminant levels.

9.9.4 Field trial in the estuary of the River Ribble in the United Kingdom

A field trial was conducted as part of the SWIFT-WFD project in the United Kingdom Pilot River Basin, the Ribble catchment. Pressure points along the Ribble estuary were identified, and a risk assessment was then effected. A trial was then designed to be carried out in October 2005, and passive samplers were selected to monitor some of the contaminants that might be present as a result of past and present industrial activity, including boat building, shipping and oil drilling. These pollutants potentially included metals (e.g. cadmium and mercury), organotin compounds (MBT, DBT and TBT) and PAHs. Chemcatchers for polar, non-polar organic pollutants, metals and organotins were deployed along with other sampling devices over a 5-week period. A number of sampling sites was selected along the estuary including Preston docks and a control site upstream of the tidal area. One aim of this trial was to demonstrate the value of these tools in comparison with standard monitoring methods used in the estuary. The estuary was an aggressive environment with high tidal flows, and episodic storm events carrying debris down the river. Some of the sampling devices were lost because of physical damage in which the moorings were dislodged and swept away. However, sufficient deployment rigs survived to allow the measurement of pollutants at four sites over the deployment period. An example that illustrates the utility of the samplers is provided by the measurements of TWA concentrations of cadmium along the estuary (Fig. 9.9). Masses of cadmium accumulated in the Chemcatchers were generally low. Concentrations upstream of the tidal area, in Preston docks and downstream of the dock appeared similar while the concentration in one sampler from the site in mid-estuary was significantly higher. Despite possible error in the estimation of uptake rates, R_S due to the uncertainty in the levels of turbulence at the different sites, the Chemcatcher samplers yielded more useful information than that provided by the routine spot sampling carried out over the period of the trial.

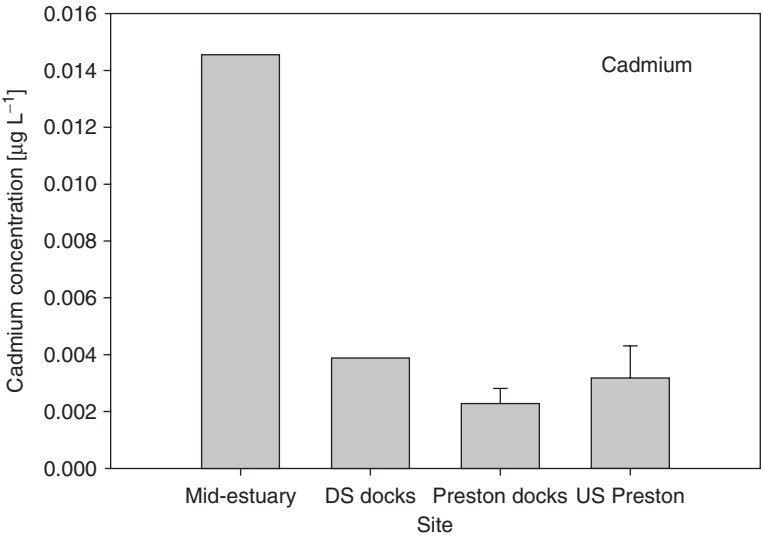

Fig. 9.9. TWA cadmium concentrations measured using the Chemcatcher passive sampler at various sites along the Ribble estuary. Data for the mid-estuary and DS docks sites are from a single sampler and data shown for Preston docks and upstream of Preston are the mean of two measurements (DS: downstream; US: upstream).

The standard monitoring by the Environment Agency for England and Wales was conducted on two occasions during the trial. Cadmium concentrations were found below limits of detection (LOD: 0.04 $\mu g\,L^{-1}$) for all sites monitored. This is in agreement with concentrations measured with Chemcatcher and emphasises the advantage of *in situ* time-integrative sampling over spot sampling in term of detection limits, since useful data that could be used in determining trends were obtained. This contrasts with the spot sampling where only categorical information (not detected) was obtained.

9.10 COMPARISON OF THE PERFORMANCE OF THE CHEMCATCHER WITH THAT OF OTHER SAMPLING DEVICES

The performances of passive samplers can be compared for a range of classes of pollutants, and evaluated alongside other methodologies. For example, calibration data for hydrophobic organic pollutants are available in the literature for SPMDs [22] and the MESCO sampling devices [23,24]. These devices differ in their design geometry and the materials

used in their construction. However, the sampling rate is directly proportional to the sampler functional surface area. Consequently, the highest sampling rates will be achieved with passive samplers having the largest surface area, such as the standard size SPMDs (450 cm^2 in comparison to 17.5 cm^2 for the Chemcatcher). It is therefore necessary to compare the performances on a surface area specific basis, i.e. with sampling rates expressed as volume of water cleared for a chemical, per unit time and unit surface area ($L\,day^{-1}\,cm^{-2}$). In making this comparison it is necessary to take into account reported variations in sampling rates with exposure conditions. Although the most calibration studies reported in the literature were performed in flow-through systems, they were not all conducted under identical conditions (temperature and turbulence). However, if these limitations are taken into account an approximate comparison of sampling rates can be made. The surface-specific sampling rates of three passive sampling devices (MESCO, SPMD and non-polar Chemcatcher) are similar for PAHs compounds with three and four aromatic rings, and range from 5 to 13 $mL\,day^{-1}\,cm^{-2}$. This indicates that the uptake of these compounds by the three different samplers is governed overall by a similar mass transfer process; this is most likely to be diffusion across the aqueous boundary layer.

A similar comparison can be made for the polar variant of Chemcatcher and the POCIS. The surface area of the standard configuration of POCIS is 41 cm^2 (see Chapter 8), in comparison with 17.5 cm^2 for the Chemcatcher. The two samplers are fitted with similar diffusion membrane materials, both are made of PES. The surface-specific sampling rates at room temperature for atrazine and simazine were approximately a factor 2 higher for the Chemcatcher than those reported by Alvarez (Table 8.4 in Chapter 8). This is a reasonable agreement, and the observed difference may be caused by differences in the calibration conditions for the two sets of samplers.

While for the metal version of Chemcatcher, uptake is limited by diffusion in water across the boundary layer and the CA membrane, for the DGT it is restricted by metal diffusion across the hydrogel and only minor effects of the boundary layer are reported [25]. For both samplers, free ions and organic/inorganic metal complexes are able to dissociate within the time required to cross the diffusion layers will accumulate and therefore the TWA concentration will be representative of these fractions. A major difference between these devices is the procedure for the calculation of TWA concentrations. While laboratory-based calibration data are used to calculate TWA concentrations with

the Chemcatcher, concentrations for DGT are obtained using known metal diffusivities for the hydrogel layer measured in the laboratory.

In order to evaluate the performance of the Chemcatcher and the DGT when responding to simulated peaks of metal concentrations, a 5-day tank experiment was conducted using Meuse river water. TWA concentrations were measured and compared with the equivalent concentrations from unfiltered, filtered (0.45 μm) and ultra-filtered (5 kDa) spot samples. Figure 9.10 shows a comparison of TWA concentrations measured by the Chemcatcher and the DGT, relative to spot sampling concentrations. While for Cd and Ni, the Chemcatcher slightly underestimates TWA concentrations, the DGT is in better agreement with filtered fractions of these metals. Similar results are obtained for both samplers for Zn and closest agreement is with the filtered fraction. For Cu, both samplers underestimate the filtered concentration while clearly overestimating the ultra-filtered fraction. Generally, results appear in agreement with the speciation of these metals under those conditions. Overall, TWA concentrations obtained using the Chemcatcher appear to have a slight bias as most data points are below the 1:1 relationship. This may be related to the selection of laboratory

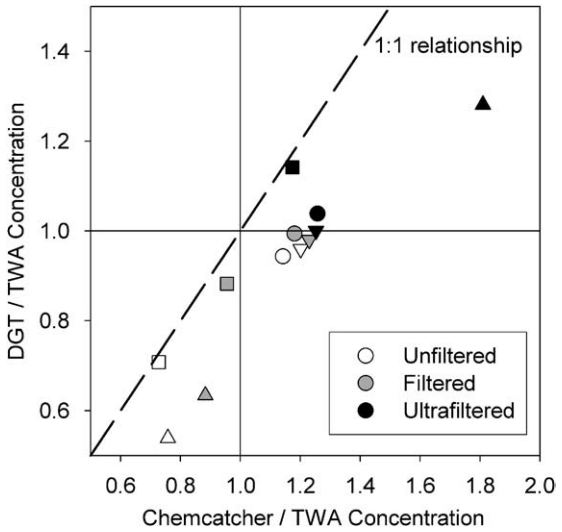

Fig. 9.10. Comparison of TWA Cd (O), Cu (Δ), Ni (▽) and Zn (□) concentrations measured by Chemcatcher and DGT relative to TWA concentrations (unfiltered, filtered (0.45 μm) and ultra-filtered (5 kDa)) measured by spot sampling during a 5-day long tank experiment with spiked metals simulating fluctuating concentrations in natural Meuse river water.

calibration data for set levels of temperature and turbulence that differ slightly from conditions observed during the experiment.

9.11 FUTURE TRENDS

The advantage of passive sampling over classical spot sampling is that it provides a measure of average conditions in a body of water over extended periods of time. This gives a more representative picture of water quality than a few instantaneous measurements of pollutant levels taken at intervals over a year. Monitoring programmes based on passive sampling will therefore provide better information on which to assess long-term trends in pollutant concentrations. For metal samplers, it is possible to obtain extra information on speciation that is pertinent to their bioavailability and potential toxicity [26,27] and hence underpin robust risk analysis. In order to facilitate recognition of the value of passive sampling, and its potential for underpinning legislation it is essential to demonstrate the validity of the method, and to develop standards for use in this field. One national standard (BSI PAS 61) [28] is available, and this covers the preparation, field deployment in surface waters and preparation for analysis of passive samplers. It is also important, however, to recognise the limitations of passive samplers, and to address some of the challenges laid down by these. One important challenge is the assessment of the impact of biofouling of the diffusion membrane on uptake rates. A further challenge is to develop sampler designs that can be used to detect and quantify peaks of concentrations during short but significant pollution events. This may be especially important for the measurement of, for example, intermittent industrial releases that may otherwise not be detected. Currently, it is difficult to assess whether an observed accumulation in a sampler is the result of a transient event or a lower but more constant concentration. In order to be able to interpret passive sampler data, particularly over the short-term deployments needed to detect peak episodic events, a better knowledge of observed lag phases between the appearance of a peak of contaminant concentration in water and its detection by a passive sampling device will be required to allow a clearer interpretation of passive sampling data.

ACKNOWLEDGMENTS

We acknowledge the financial support of the European Commission (Contracts EVK1-CT-2002-00119; http://www.port.ac.uk/stamps/ and

SSP1-CT-2003-502492; http://www.swift-wfd.com) for this work. We thank Arne Holmberg (Alcontrol, Sweden) and Miro Vrana for providing the technical drawing of the Chemcatcher prototype (Fig. 9.3).

REFERENCES

1 B. Vrana, G.A. Mills, E. Dominiak and R. Greenwood, Calibration of the Chemcatcher passive sampler for the monitoring of priority organic pollutants in water, *Environ. Pollut.*, 142 (2006) 333.
2 J.K. Kingston, R. Greenwood, G.A. Mills, G.M. Morrison and B.L. Persson, Development of novel passive sampling system for the time-averaged measurement of a range of organic pollutants in aquatic environments, *J. Environ. Monit.*, 2 (2000) 487.
3 J.N. Huckins, G.K. Manuweera, J.D. Petty, D. Mackay and J.A. Lebo, Lipid-containing semipermeable membrane devices for monitoring organic contaminants in water, *Environ. Sci. Technol.*, 27 (1993) 2489.
4 G.D. Johnson, Hexane-filled dialysis bags for monitoring organic contaminants in water, *Environ. Sci. Technol.*, 25 (1991) 1897.
5 B. Vrana, G.A. Mills, M. Kotterman, P. Leonards, K. Booij and R. Greenwood, Modelling and field application of the Chemcatcher passive sampler calibration data for the monitoring of hydrophobic organic pollutants in water, *Environ. Pollut.*, 145 (2007) 895–904.
6 K. Runeberg, S. Rauch, B. Vrana, G.A. Mills, R. Greenwood, M. Kotterman, S. Herve, M. Weideborg, V. Kocourek and G.M. Morrison, Assessment of the performance of the Chemcatcher sampler for the monitoring of metals in water (2006, in preparation).
7 R. Aguilar, R. Greenwood, G.A. Mills, B. Vrana, M.A. Palacios and M. Gómez, Development of a passive sampling system for the time weighted average monitoring of mercury and organotin species in water (2006, in preparation).
8 B. Vrana, G. Mills, R. Greenwood, J. Knutsson, K. Svensson and G. Morrison, Performance optimisation of a passive sampler for the monitoring of hydrophobic organic pollutants in water, *J. Environ. Monit.*, 7 (2005) 612.
9 J.N. Huckins, J.D. Petty and K. Booij, *Monitors of Organic Contaminants in the Environment: Semipermeable Membrane Devices*, Springer Verlag, New York, 2006.
10 R.J. Scheuplein, On the application of rate theory to complex multibarrier flow co-ordinates: membrane permeability, *J. Theor. Biol.*, 18 (1968) 72.
11 G.L. Flynn and S.H. Yalkowsky, Correlation and prediction of mass transport across membranes. I. Influence of alkyl chain length on flux-determining properties of barrier and diffusant, *J. Pharm. Sci.*, 61 (1972) 838.

12 B. Vrana and G. Schüürmann, Calibrating the uptake kinetics of semipermeable membrane devices in water: impact of hydrodynamics, *Environ. Sci. Technol.*, 36 (2002) 290.
13 D.W. Connell, *Bioaccumulation of Xenobiotic Compounds*, CRC Press, Boca Raton, FL, 1990.
14 J.N. Huckins, J.D. Petty, H.F. Prest, R.C. Clark, D.A. Alvarez, C.E. Orazio, J.A. Lebo, W.L. Cranor and B.T. Johnson, A guide for the use of semipermeable membrane devices (SPMDs) as samplers of waterborne hydrophobic organic contaminants. Report for the American Petroleum Institute (API), API publication number 4690, API, Washington, DC, 2002.
15 D.A. Alvarez, J.D. Petty, J.N. Huckins, T.L. Jones-Lepp, D.T. Getting, J.P. Goddard and S.E. Manahan, Development of a passive, *in situ*, integrative sampler for hydrophilic organic contaminants in aquatic environments, *Environ. Toxicol. Chem.*, 23 (2004) 1640.
16 M. Shaw and J.F. Müller, Preliminary evaluation of the occurrence of herbicides and PAHs in the Wet Tropics region of the Great Barrier Reef, Australia, using passive samplers, *Mar. Pollut. Bull.*, 51 (2005) 876.
17 B.S. Stephens, A. Kapernick, G. Eaglesham and J. Müller, Aquatic passive sampling of herbicides on naked particle loaded membranes: accelerated measurement and empirical estimation of kinetic parameters, *Environ. Sci. Technol.*, 39 (2005) 8891.
18 C.E. Green and M.H. Abraham, Investigation into the effects of temperature and stirring rate on the solid-phase extraction of diuron from water using a C_{18} extraction disk, *J. Chromatogr. A*, 885 (2000) 41.
19 L.B. Persson, G.M. Morrison, J.U. Friemann, J. Kingston, G. Mills and R. Greenwood, Diffusional behaviour of metals in a passive sampling system for monitoring aquatic pollution, *J. Environ. Monit.*, 3 (2001) 639.
20 L.B. Blom, G.M. Morrison, J. Kingston, G.A. Mills, R. Greenwood, T.J.R. Pettersson and S. Rauch, Performance of an *in situ* passive sampling system for metals in stormwater, *J. Environ. Monit.*, 4 (2002) 258.
21 R. Schäfer, R. Mueller, A. Paschke, B. Vrana, L. Lagadic and M. Liess, Comparison of three methods for determination of moderately polar pesticides in small streams in agricultural areas (2006, in preparation).
22 J.N. Huckins, J.D. Petty, C.E. Orazio, J.A. Lebo, R.C. Clark, V.L. Gibson, W.R. Gala and K.R. Echols, Determination of uptake kinetics (sampling rates) by lipid-containing semipermeable membrane devices (SPMDs) for polycyclic aromatic hydrocarbons (PAHs) in water, *Environ. Sci. Technol.*, 33 (1999) 3918.
23 B. Vrana, P. Popp, A. Paschke and G. Schüürmann, Membrane-enclosed sorptive coating. An integrative passive sampler for an integrative passive sampler for monitoring organic contaminants in water, *Anal. Chem.*, 73 (2001) 5191.

24 B. Vrana, A. Paschke and P. Popp, Calibration and field performance of membrane-enclosed sorptive coating for integrative passive sampling of persistent organic pollutants in water, *Environ. Pollut.*, 25 (2006) 296.
25 K.W. Warnken, H. Zhang and W. Davison, Accuracy of the diffusive gradients in thin-films technique: diffusive boundary layer and effective sampling area considerations, *Anal. Chem.*, 78 (2006) 3780.
26 I.J. Allan, B. Vrana, R. Greenwood, G.A. Mills, B. Roig and C. Gonzalez, A ''toolbox'' for biological and chemical monitoring requirements for the European Union's Water Framework Directive, *Talanta*, 69 (2006) 302.
27 S.C. Apte, G.E. Batley, K.C. Bowles, P.L. Brown, N. Creighton, L.T. Hales, R.V. Hyne, M. Julli, S.I. Markich, F. Pablo, N.J. Rogers, J.L. Stauber and K. Wilde, A comparison of copper speciation measurements with the toxic responses of three sensitive freshwater organisms, *Environ. Chem.*, 2 (2005) 320.
28 British Standards Institute (BSI), Publicly Available Specification: Determination of priority pollutants in surface water using passive sampling (PAS-61), May 2006.

Chapter 10

Membrane-enclosed sorptive coating for the monitoring of organic compounds in water

Albrecht Paschke, Branislav Vrana, Peter Popp, Luise Wennrich, Heidrun Paschke and Gerrit Schüürmann

10.1 INTRODUCTION

Membrane-enclosed sorptive coating (MESCO) denotes the recently developed miniaturised passive sampling devices consisting of a membrane which encloses polydimethylsiloxane (PDMS) coatings or coarse silicone material (embedded in a fluid) as the collecting phase for organic compounds.[1] The general advantages of the MESCO samplers are (i) the simple and loss-free separation of the collector phase; (ii) its processing without further clean-up steps by direct thermal desorption or solvent microextraction; (iii) the possibility to spike the collecting phase before deployment with so-called performance reference compounds (PRCs) and (iv) that, in addition to chemical target or non-target analysis, the collecting phase can also be subject to biological effect screening (after digestion using an appropriate solvent).

In our work we took advantage of commercially available PDMS coatings or silicone materials as the collecting phase. PDMS is recommended as a receiving phase in extraction and thermodesorption as it has a number of benefits compared with other sorbents [1]. The predominant mechanism of analyte extraction into PDMS/silicone phase is absorptive partitioning which has the advantage that displacement effects of the analytes (competitive enrichment), characteristic for adsorbents, play no role.

[1]When neat silicone material is used as collecting phase instead of a sorptive coating, one can take the abbreviation MESCO also for membrane-enclosed silicone collector.

Comprehensive Analytical Chemistry 48
R. Greenwood, G. Mills and B. Vrana (Editors)
Volume 48 ISSN: 0166-526X DOI: 10.1016/S0166-526X(06)48010-7

The chapter gives an overview of theoretical aspects and design of the different MESCO sampler formats for water monitoring[2] and summarises our efforts to calibrate the samplers for several priority pollutants in laboratory studies and to test them under field conditions.

10.2 PASSIVE UPTAKE MODEL FOR MESCO SAMPLER

It has been shown that the amount of the chemical accumulated in the MESCO sampler from water with constant chemical composition can be described by the following equation [2]:

$$m_S(t) = m_0 + (C_W K_{SW} V_S - m_0)\left[1 - \exp\left(-\frac{k_{ov} A \alpha}{K_{SW} V_S} t\right)\right] \tag{10.1}$$

where m_S is the mass of analyte in the receiving phase (PDMS), m_0 is the amount of analyte in the sampler at the start of the exposure, C_W represents the water concentration during the deployment period, K_{SW} is the receiving phase/water distribution coefficient, V_S is the volume of the receiving phase, k_{ov} is the overall mass transfer coefficient, A is the membrane surface area, α is the pore area of the membrane as fraction of total membrane area (membrane porosity) and t equals time. α will be set to 1 for non-porous membranes. The coefficient in the exponential function is referred to as the overall exchange rate constant k_e:

$$k_e = \frac{k_{ov} A \alpha}{K_{SW} V_S} = \frac{R_S}{K_{SW} V_S} \tag{10.2}$$

where R_S is the sampling rate, expressing equivalent volume of water cleared of chemical per unit of time in the linear (integrative) uptake phase.

Adding standards (i.e. PRCs) to the receiving phase prior to exposure of the passive sampler has been suggested as a means to calibrate the exchange rates *in situ* [3,4]. When PRCs are used that are not present in water ($C_W = 0$), Eq. (10.1) reduces to

$$m_S(t) = m_0 \exp(-k_e t) \tag{10.3}$$

which is a one-parameter equation, because the amount of PRC added to the MESCO sampler (m_0) is known.

[2]Some other MESCO variants designed for monitoring semi-volatile organic compounds in air are described in Chapter 5.

10.3 DESIGN OF THE DIFFERENT MESCO FORMATS

10.3.1 PDMS-coated fibre enclosed in an LDPE membrane

As a precursor of the MESCO [5] we tested membrane bags (13×2.5 cm) of 100 μm thick low-density polyethylene (LDPE) tubing (Polymer-Synthesewerk Rheinberg, Germany), heat-sealed at both ends, in combination with a 100 μm PDMS-coated SPME fibre (Supelco, Deisenhofen, Germany) as collector phase ($V_S = 0.68$ μL) and 25 mL of a 40/60 isopropanol/water mixture (v/v) as inner fluid. LDPE is the membrane material also used in construction of SPMDs [6] and the PDMS-coated fibre is a rational tool for solid-phase microextraction of analytes from aqueous samples, and provides high enrichment factors for more hydrophobic substances [7]. Figure 10.1 shows the design of this permeation sampler. The coil spring (of stainless steel) prevents the fibre coating from a direct contact with the membrane. A serious shortcoming of this sampler is that the polymer-coated quartz glass fibre tip is fragile and difficult to handle during removal from and re-inserting into the steel needle of the commercial SPME syringe device.

10.3.2 PDMS-coated stir bar enclosed in a dialysis membrane bag (MESCO I)

This type, first described by Vrana *et al*. in 2001 [2,8], uses the PDMS-coated stir bar as collector phase. The stir bar is known under the trademark Twister^{TM} (Gerstel, Mülheim/Ruhr, Germany) and is commonly used for solvent-free microextraction using the same principle as

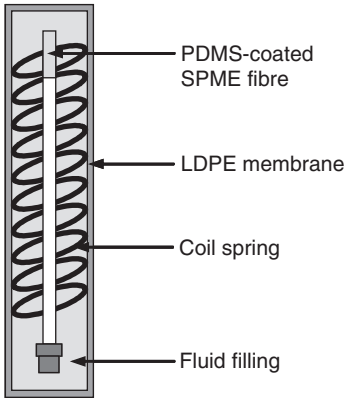

Fig. 10.1. Construction of MESCO precursor [5].

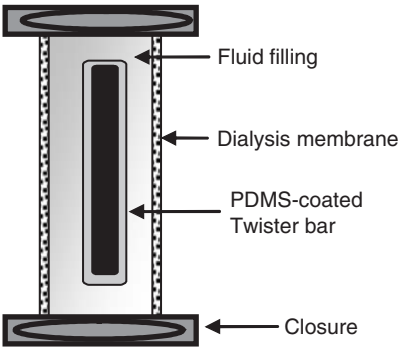

Fig. 10.2. Diagram of MESCO I [2].

an SPME fibre, but with a larger extraction capacity. Figure 10.2 shows a diagram of the sampler. Specifically, we tested dialysis membrane bags made of regenerated cellulose (Spectra/Por 6) with molecular weight cut-off of 1 kDa (3×1.8 cm), sealed at each end with a 35 mm Spectra/Por closure, in combination with Twister bars of 15 mm length coated with a 500-μm-thick layer of PDMS ($V_S = 24\,\mu L$) and 3 mL bi-distilled water as membrane bag filling. Regenerated cellulose is a porous hydrophilic membrane material that enables widening the applicability to a broader polarity range of pollutants, including low-hydrophobic substances ($\log K_{OW} < 4$). Unfortunately, this material has relatively low chemical and thermal stability and is subject to microbial degradation, which potentially leads to the damage of the sampler in natural surface waters during prolonged exposure of several weeks.

10.3.3 Silicone material enclosed in an LDPE membrane (MESCO II)

This sampler type combines [8,9] the advantages of a high-capacity collector phase with that of a more stable membrane material, LDPE. These membranes are hydrophobic, resistant to solvents and biodegradation and they can be heat-sealed. Furthermore, the relatively expensive and fragile Twister bar is substituted by a cheap silicone material (pieces of a tube or rod) as collector phase. Figure 10.3 shows the schematic design of the sampler. Additional investigations have shown the usefulness of these materials for an effective pre-concentration of several classes of persistent organic pollutants from water samples and the applicability of thermodesorption–GC–MS analogously to the processing of Twister bars [9,10]. The significantly enhanced volume of the collector phase

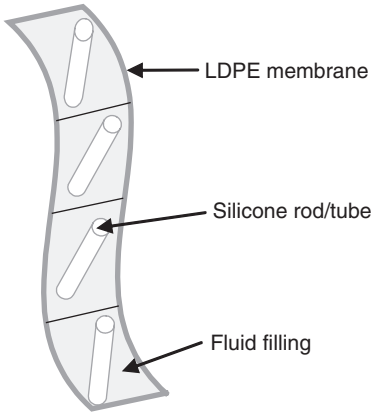

Fig. 10.3. Schematic design of MESCO II [8].

($>100\,\mu L$) increases the maximum exposure time of the passive sampler in the field. A practical drawback of silicone tubes, when used as collecting phase in combination with water as fluid filling, is that remaining water droplets (inside the tube) can disrupt the GC–MS analysis.

Since 2004 we have focused our work on improvement of the promising MESCO II format with silicone rods enclosed. Several thicknesses of LDPE membrane were tested as well as other membrane materials, such as the dense polypropylene bag, usually used for membrane-assisted solvent extraction of water samples in the laboratory [11]. Interestingly, it turns out in a preliminary laboratory study that this latter material is not useful for MESCO devices because it obviously prevents the transfer of substances to the inner receiving phase (silicone rod).

10.4 LABORATORY-DERIVED SAMPLING RATES OF THE VARIOUS MESCO FORMATS

The performance of the PDMS-coated fibre in LDPE membrane bag (MESCO precursor) was tested by time-dependent exposure in a flow-through system [2] at 19°C (upstream flow: 36 $L\,h^{-1}$; nominal water concentration for each test substance: 50 $ng\,L^{-1}$; exposure times: up to 360 h). The sampling rates obtained are summarised in the second column of Table 10.1 (for details of SPME fibre desorption and gas chromatographic analysis see Ref. [7]).

MESCO I samplers were also tested in this flow-through apparatus (under the same conditions as above; see Ref. [2] for experimental

TABLE 10.1

Sampling rates (R_S) of the two early MESCO formats in comparison with that of a standard SPMD for selected priority pollutants

Substance	R_S of SPMD ($mL\,h^{-1}$)[a]	R_S of MESCO precursor ($mL\,h^{-1}$)[b]	R_S of MESCO I ($mL\,h^{-1}$)[b]
α-HCH[c]	108	0.0005	0.40
Hexachlorobenzene	58	0.0022	0.25
Anthracene	150	0.0014	0.22
Fluoranthene	188	0.0015	0.25
Pyrene	217	0.0012	0.27
Benzo[a]anthracene	133	0.0009	0.37
PCB 28[c]	350	0.0070	0.15
PCB 52	258	0.0088	0.15
PCB 101	258	0.0063	0.13
PCB 138	200	0.0046	0.09
PCB 153	133	0.0031	0.10

[a]At 18°C for α-HCH, hexachlorobenzene and the polyaromatic hydrocarbons, at 12°C for PCBs; taken from Ref. [12].
[b]At 19°C.
[c]Substance abbreviations: HCH—hexachlorocyclohexane; PCB—polychlorinated biphenyl.

details). The determined sampling rates are given in the last column of Table 10.1.

Due to its much larger sampling capacity, the standard SPMD (of 450 cm^2 surface area) has up to five orders of magnitude higher sampling rates than the MESCO formats tested. But one should bear in mind that the substances trapped in the PDMS coating (of an SPME fibre or a Twister bar) are, in contrast to that sampled using an SPMD, transferred quantitatively to the injector of the analytical instrument. This prevents, at similar sampling sensitivity, possible volumetric dilution errors but has on the other hand the disadvantage of having only ''one shot'' per sampler specimen that can be overcome only by multiple exposure of samplers (as a MESCO string). Further flow-through calibration experiments showed that the sampling rates in MESCO I were not significantly affected by the flow velocity, within the tested range of exposure conditions [2,13].

Different configurations of the MESCO II sampler were exposed to spiked water in a similar flow-through system at 14°C (upstream flow: 60 $L\,h^{-1}$; nominal concentration: 50 $ng\,L^{-1}$ for each test chemical; exposure times: up to 176/236 h). The membrane bags (5 cm × 3 cm) consisted of 100 μm thick LDPE tubing (Polymer-Synthesewerk Rheinberg,

Germany). Four cm long pieces of silicone tube (with 3.6 mm O.D., 3.0 mm I.D.; Reichelt, Heidelberg, Germany) or 4-cm-long pieces of silicone rod (2.0 mm O.D., Goodfellow, Bad Nauheim, Germany) were used as collector phase. The silicone material was embedded in 8 mL water in one series of experiments or in air for another series (see Ref. [9] for further experimental details). The sampling rates calculated from the accumulated analyte mass are given in Table 10.2. Remarkably higher R_S values (in the same order of magnitude as those obtained for MESCO I) were obtained with air as fluid filling of the membrane bags. This can be explained by a detailed consideration of the mass-transfer resistances [9]. Tube and rod material yielded similar results but the variances in R_S were lower for the tube-containing sampler.

Recently, we determined preliminary sampling rates for new MESCO II sampler formats in rapid semi-continuous batch extraction tests [14]. These consisted of lay-flat membrane strips, 15×3 cm of the 100 μm thick membrane or 8×4 cm of that with 50 μm wall thickness. The strips were segmented by heat-sealing into four or two uniform parts, respectively. Each segment (2 cm long) contained a 15 mm long piece of pre-conditioned SR ''embedded'' in air. Such an SR piece is equivalent to 47 μL of receiving phase. These data are given in Table 10.2. There is a reasonably good agreement with R_S values obtained in the previous study. Additional flow-through experiments are in progress to investigate the influence of temperature and water flow on the sampling rates of these inexpensive MESCO variants and to test the applicability of the PRC concept for R_S adjustment to varying sampling conditions.

10.5 FIELD APPLICATION OF MESCO SAMPLERS

10.5.1 A case study with MESCO I for monitoring of persistent organic pollutants in surface water

10.5.1.1 Sampling site

To assess the performance of MESCO for monitoring persistent organic pollutants (POPs) in the field, samplers were exposed in water at a site located in the river Weisse Elster at the locality Halle-Burgholz in Saxony-Anhalt, Germany, close to the confluence of the River Weisse Elster with the River Saale (51°25′10″N; 11°59′47″E, estimated using Google Earth). Three MESCOs were deployed at the sampling site for 28 days during summer 2002 (24th July–21st August). The last two weeks of sampler exposure coincided with the major flood that occurred

TABLE 10.2

Sampling rates (R_S) of different MESCO II configurations (SR—silicone rod; ST—silicone tube) for selected priority pollutants determined in various laboratory experiments

Substance	R_S of SR+water in 100 μm LDPE[a] ($mL\,h^{-1}$)	R_S of ST+water in 100 μm LDPE[a] ($mL\,h^{-1}$)	R_S of ST+air in 100 μm LDPE[a] ($mL\,h^{-1}$)	R_S of SR+air in 100 μm LDPE[b] ($mL\,h^{-1}$)	R_S of SR+air in 50 μm LDPE[b] ($mL\,h^{-1}$)
α-HCH[c]	0.28	0.18	0.14	0.031[d]	0.039[d]
1,2,3,4-TCB[c]	*not det.*[e]	*not det.*[e]	*not det.*[e]	1.47	0.61
Pentachlorobenzene	0.21	0.19	4.30	1.30	2.24
Hexachlorobenzene	0.09	0.06	0.90	0.65	0.87
Naphthalene	*not det.*[e]	*not det.*[e]	*not det.*[e]	0.13[d]	*not det.*[e]
Acenaphthylene	0.51	0.73	1.40	0.07[d]	*not det.*[e]
Acenaphthene	0.48	0.67	2.23	0.35	*not det.*[e]
Fluorene	0.75	1.34	1.88	0.49	*not det.*[e]
Phenanthrene	0.26	0.27	0.93	0.63	0.72
Anthracene	0.13	0.26	0.99	0.40	0.83
Fluoranthene	0.04	0.06	0.12	0.33	0.26
Pyrene	0.03	0.03	0.10	0.26	0.23
PCB 28[c]	0.06	0.06	0.92	0.74	0.63
PCB 52	0.03	0.04	0.62	0.66	4.12[f]
PCB 101	0.004	*not det.*[e]	*not det.*[e]	0.39	*not det.*[e]
PCB 138	*not det.*[e]	*not det.*[e]	*not det.*[e]	0.14	0.05
PCB 153	*not det.*[e]	*not det.*[e]	*not det.*[e]	0.15	0.05

[a]Determined in a flow-through apparatus with a nominal analyte concentration of $50\,ng\,L^{-1}$ at 14°C [9].
[b]Determined in serial batch extraction tests with a nominal analyte concentration of $25\,ng\,L^{-1}$ at room temperature [14].
[c]Substance abbreviations: HCH—hexachlorocyclohexane; TCB—tetrachlorobenzene; PCB—polychlorinated biphenyl.
[d]Distribution constant ($K_{SW} = C_{MESCO}(eq.)/C_{W}(eq.)$) calculated by assuming that $C_{W}(eq.) = 25\,ng\,L^{-1}$.
[e]Not determined.
[f]Potential outlier.

in the river basins of Elbe and Danube in Central Europe in August 2002. A local flood event was observed also at the Weisse Elster, accompanied with the rise in water level up to 2 m against the typical summer average. The samplers were retrieved after the flood wave retreated. During the exposure, the water temperature at the sampling site varied from 19 to 22°C.

10.5.1.2 Target pollutants

The analytes included several groups of POPs: γ-hexachlorocyclohexane (γ-HCH), hexachlorobenzene (HCB), 2,2′-bis(4-chlorophenyl)-1,1′-dichloroethylene (DDE), selected polycyclic aromatic hydrocarbons (PAHs) and polychlorinated biphenyls (PCBs). The K_{SW} values, needed in further data evaluation, were approximated by PDMS/water distribution coefficients from the literature and were reported previously [13].

10.5.1.3 Sampler preparation

MESCO I preparation has been described in detail elsewhere [2,13]. Briefly, the cleaned and conditioned Twister stir bar was pre-loaded with six PRCs: $^2H_{10}$-biphenyl (D_{10}-BIP), $^2H_{10}$-phenanthrene (D_{10}-PHE), $^2H_{10}$-anthracene (D_{10}-ANT), $^2H_{10}$-fluoranthene (D_{10}-FLT), $^2H_{10}$-pyrene (D_{10}-PYR) and $^2H_{12}$-benzo[a]anthracene (D_{12}-BaA). This was performed by stirring the Twister bar for 30 min at 1000 min^{-1} at room temperature in 25 mL of solution containing 1 $\mu g L^{-1}$ of each PRC. For sampler assembly, the Twister bar was placed inside a dialysis membrane bag. The bag was filled with 3 mL of bi-distilled water and sealed at each end with 35 mm Spectra Por closures.

Four control samplers were prepared together with the three field-deployed samplers; these were stored in the laboratory at −20°C until analysis. Controls were processed exactly as deployed samplers and were used to define contamination during preparation and storage, and to determine nominal PRC concentrations in MESCO samplers.

10.5.1.4 Sampler deployment and retrieval

On the day of deployment, MESCOs were freshly prepared in the laboratory and transported to the field in amber glass jars filled with bi-distilled water to prevent drying of the dialysis membrane during transport. At the sampling site, MESCOs were removed from the jars and placed into a protective deployment device designed for sampling using SPMDs. The deployment device was a canister made of perforated stainless steel sheet (5 mm openings), containing five racks designed for holding standard length SPMDs. One of these carriers was used to hold

the MESCOs. Three SPMDs with standard configuration (2.54 × 91.4 cm, 75–90 μm membrane thickness, total mass 4.3 g each) were exposed next to MESCOs, in the same deployment device. Before exposure, SPMDs were spiked with PRCs (10 μg/SPMD of each standard) as described earlier [15]. The deployment device protected MESCOs and SPMDs from abrasion and the sequestered pollutants from sunlight. The canister was held at depth of approximately 1 m below surface using a buoy, rope and anchor, and was secured to the shore with a rope.

On day 28, samplers were removed from the deployment device and checked visually for mechanical damage. Although disintegration (mechanical or biological degradation) of the cellulose bags occurred during the exposure of MESCOs, the Twister bars were found to be intact, sticking by their magnets to the inner surface of the deployment canister. The Twister bars were dried using a soft paper tissue, transferred using clean forceps to GC vials (2 mL), sealed and transported to the laboratory in a portable icebox (on ice and in darkness) and stored at −20°C till analysis. Field exposed samplers were analysed together with the control samplers.

10.5.1.5 Sampler processing and analysis

The quantification of the compounds accumulated during field exposure on Twister bars of the MESCO samplers was carried out as described previously [2,13]. Briefly, analyses were performed on an Agilent Technologies (Palo Alto, CA, USA) GC 6890 with MSD 5973N system equipped with a Gerstel (Mülheim/Ruhr, Germany) thermodesorption system TDS A and a cold injection system CIS-4 from Gerstel with an empty liner that was used for cryofocusing the analytes prior to the transfer onto the analytical column. The single ion monitoring (SIM) mode of the mass selective detector applying one or two characteristic ions per compound was chosen for the detection. Quantification of target substances sorbed on Twister bars was accomplished using a five-point external standard curve. Method quantification limit for the analytes under investigation ranged from 1 to 5 pg per Twister.

Details of SPMD processing were described earlier [15,16]. SPMD data evaluation was performed using the empirical uptake model derived by Huckins *et al*. [17].

10.5.1.6 Accumulated amount of water pollutants

Table 10.3 shows the mass of each target analyte accumulated in the MESCOs during a 28-day field deployment. Quantifiable amounts of all target analytes were found in field-exposed samplers. Control blanks

TABLE 10.3

Average mass of pollutants (in pg per Twister bar) determined in the control MESCOs (m_0) and in the field-exposed MESCOs (m_S; $n = 3$), and *in situ* aqueous concentrations of organic analytes estimated from MESCO (C_W)

Compound	m_0 (pg)	CV[a] ($n = 4$) (%)	m_s (pg)	CV ($n = 3$) (%)	k_e (day^{-1})	C_W ($ng\,L^{-1}$)
HCB	1	13	79	2	0.085	0.14
γ-HCH	1.8		1695	27	0.130	182
p,p'-DDE	<1		132	8	0.069	0.03
PCB 28	1	16	62	7	0.077	0.05
PCB 52	<1		43	6	0.072	0.02
PCB 101	<1		27	12	0.065	0.004
PCB 138	<1		33	5	0.062	0.003
PCB 153	<1		22	9	0.062	0.002
PCB 180	<1		8	10	0.064	0.001
Acenaphthylene	4	45	124	11	0.107	2.16
Acenaphthene	10	10	1172	3	0.102	12.2
Fluorene	18	9	1128	4	0.100	9.76
Anthracene	8	30	1494	9	0.094	7.03
Phenanthrene	62	30	3128	7	0.094	15.4
Fluoranthene	13	30	3135	8	0.079	2.86
Pyrene	13	15	3302	8	0.076	2.16
Benzo[a]anthracene	2	76	1185	3	0.069	0.32
Chrysene	4	42	967	2	0.063	0.10
Benzo[b]fluoranthene	<5		450	1	0.071	0.15
Benzo[k]fluoranthene	<5		244	3	0.068	0.06
Benzo[a]pyrene	<5		455	4	0.067	0.09
Indeno[1,2,3-cd]pyrene	<5		121	7	0.087	0.29
Dibenzo[a,h]anthracene	<5		46	10	0.084	0.03
Benzo[g,h,i]perylene	<5		115	10	0.076	0.20

The samplers were exposed 28 days in August 2002 at a site in the river Weisse Elster in Saxony-Anhalt, Germany.
[a]CV, coefficient of variation or relative standard deviation of multiple samples.

contained quantifiable amounts of lindane, PCB 28 and PAHs with up to four aromatic rings. Nevertheless, analyte levels found in field exposed samplers were in all cases significantly higher than those in control blanks. The variation of the masses recovered from three replicate field exposed devices ranged from 1% (benzo[b]fluoranthene) to 27% (lindane). This is an excellent precision despite the degradation of the protective cellulose membranes of the MESCOs during exposure.

10.5.1.7 In situ exchange kinetics from PRC offload

Our previous investigations have shown that both uptake and elimination of a particular compound in MESCO I are characterised by the same exchange rate constant k_e, according to Eq. (10.1) [13]. The use of PRCs allowed a two-point estimation of the first-order exchange rate constants k_e. These were calculated from the rearranged Eq. (10.3) using mean values (from replicate samples) of the PRC amounts found in field exposed samplers (m_S) and in the controls (m_0) and exposure time of 28 days:

$$k_e = \frac{\ln(m_0/m_S)}{t} \tag{10.4}$$

The calculated k_e values ranged from 0.072 day^{-1} (D_{10}-PYR) to 0.126 day^{-1} (D_{10}-BIP). Student's t-test ($\alpha = 0.05$) was performed to ensure that changes in PRC residue concentrations were statistically significant, according to the law of error propagation. This was the case for all PRCs excepting D_{12}-BaA with no significant offload during exposure.

The field-derived k_e values were two to three times higher than those reported in a laboratory calibration study [13]. This indicates faster exchange kinetics at the sampling site than those observed under laboratory conditions. The temperature at the sampling site during the field study was similar to that in the calibration study. Although this investigation [13] indicated that the flow velocity had no significant effect on the exchange kinetics, this was tested only at low velocities. The flow around the cage with samplers in the field was much faster than the simulated flow in the calibration apparatus, and the increased water turbulence might have affected the analyte mass transfer between water body and samplers, despite the buffering effect of the protective cage. The elevated exchange kinetics can also be explained by degradation of cellulose membranes during the field exposure, resulting in a significant loss of resistance to analyte exchange between Twister and water.

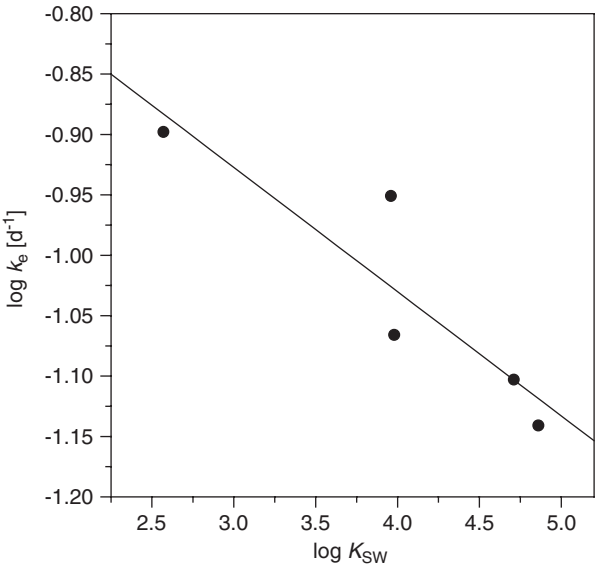

Fig. 10.4. Correlation between estimated *in situ* exchange rate constants k_e and PDMS/water distribution constant K_{SW}. The sampling using MESCO I was performed in August 2002 in the river Weisse Elster near confluence with River Saale.

The substance-specific k_e values were estimated from the linear correlation between log k_e and log K_{SW} (Fig. 10.4):

$$\log k_e = -0.6187 - 0.1029 \log K_{SW}$$
$$(n = 5, s = 0.05, r = 0.904) \qquad (10.5)$$

The estimated *in situ* k_e values of target analytes are shown in Table 10.3.

10.5.1.8 Sampling-mode considerations

The knowledge of *in situ* k_e values enables to estimate the percentage of sampler saturation with target analytes after 28 days of exposure, when a constant pollutant concentration in the river water is assumed. This can be calculated as $(1-\exp(-k_e\ t)) \times 100\%$ and shows that the accumulated concentrations of target analytes approached 83–97% of partitioning equilibrium, determined by the magnitude of the PDMS/water distribution constant K_{SW} (Fig. 10.5). The sampler exposure seems to have exceeded the maximum time period allowing time-weighted average (TWA) sampling, which lasts approximately until the sampler approaches

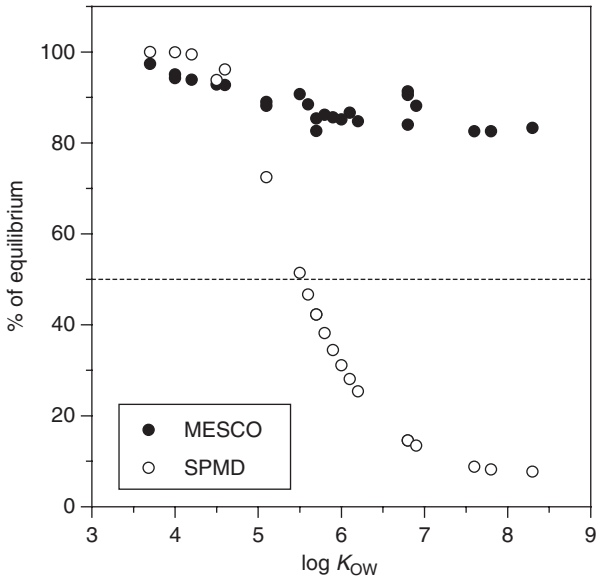

Fig. 10.5. Percentage of target–analyte equilibration between passive samplers and water as dependent from their hydrophobicity (expressed as log K_{OW}) after 28 days of field exposure in the river Weisse Elster. The dashed line indicates the maximum limit of saturation (50%) permitting a time-integrative sampling.

half-saturation. The prolonged field exposure was due to the flood event that made it impossible to retrieve the samplers any earlier.

A comparison of percentage of sampler saturation with target analytes in MESCO and a standard-size SPMD shows that after 28 days of exposure, partitioning equilibrium was reached in both samplers for compounds with log $K_{OW} < 4.5$ (Fig. 10.5). Compounds with log $K_{OW} > 5.5$ have not exceeded half-saturation in SPMDs. This indicates that SPMDs sampled those compounds in time-integrative mode.

In contrast, all compounds have likely exceeded the half-saturation in MESCO samplers (Fig. 10.5). Thus, after 28 days, MESCO was in the curvilinear or equilibrium sampling phase. This is caused by the fact that MESCO has much lower absorption capacity than SPMD, due to its very small receiving-phase volume. The calculation of saturation halftime $t_{1/2} = \ln 2/k_e$ shows that the MESCO remained in the linear or integrative uptake phase during the first two weeks of exposure for most of the analytes under investigation. This information is valuable for further method validation, indicating that field exposures using MESCO I in warm and turbulent water should not exceed two weeks,

if the study is aimed the estimation of TWA concentrations. Two weeks seems to be also a compromise time period during which no degradation of the cellulose membrane is expected.

10.5.1.9 Estimate of ambient aqueous concentrations

As a consequence of the different exchange kinetics between the field study and laboratory experiments, a direct application of laboratory-derived calibration data for calculation of ambient aqueous concentrations of target analytes was not appropriate in this particular case. Nevertheless, the calculation of aqueous concentrations was performed using Eq. (10.1), knowing the necessary substance-specific parameters k_e and K_{SW}:

$$C_W = \frac{m_s - m_0}{K_{SW} V_S [1 - \exp(-k_e t)]} \tag{10.6}$$

The estimated aqueous concentrations are shown in Table 10.3. They range from $1\,\mathrm{pg\,L^{-1}}$ (PCB 180) to more than $180\,\mathrm{ng\,L^{-1}}$ (lindane), demonstrating that MESCO allows for *in situ* measurement of very low contaminant levels. It is important to stress that the calculated aqueous concentrations are an estimate of the truly dissolved fraction present in water as shown by Garcia-Falcon *et al*. [18]. The sampling-mode considerations indicate that the calculated values in this particular study did not provide an accurate TWA concentration estimate, nevertheless, MESCO I has a great potential for time-integrative sampling, provided the deployment period is restricted to a shorter time.

10.5.1.10 Comparison of MESCO I with SPMD

Figure 10.6 shows a comparison of aqueous concentrations of PAHs estimated from analyte amounts accumulated in MESCOs and SPMDs during a 28-day field deployment. Both methods provide information on a dissolved fraction of analytes, enabling a direct comparison of results obtained using the two approaches. Aqueous concentrations estimated using both methods showed similar patterns, with higher levels of less hydrophobic light PAHs (with four and less aromatic rings) and low concentrations of more hydrophobic, heavy (less water soluble PAHs with five and more aromatic rings). MESCO-derived aqueous concentrations of light PAHs were higher than those derived from SPMDs. The opposite trend was observed for heavy PAHs.

There may be various sources of differences in absolute values calculated using the two methods. First, neither of the two methods provided accurate estimates of TWA concentrations for light PAHs, because both samplers nearly approached partitioning equilibrium. Thus, values

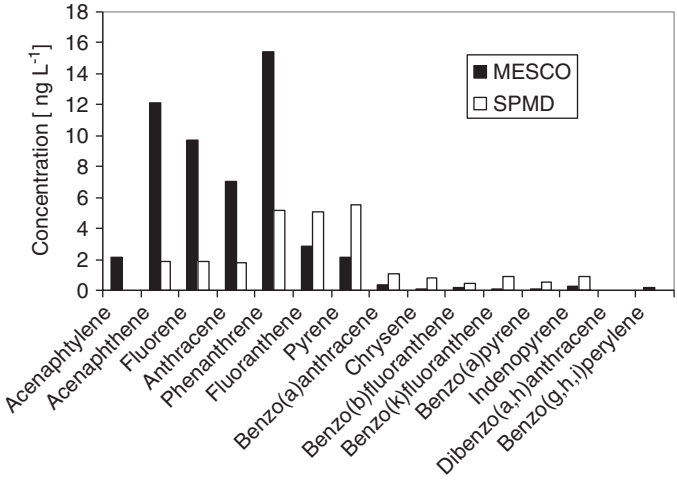

Fig. 10.6. Comparison of aqueous concentrations of PAHs at the sampling site in the river Weisse Elster (August 2002), estimated using two passive sampling approaches.

calculated for these compounds reflect also short-term (from the last week of exposure or so) fluctuations in concentrations, rather than the representative time-weighted mean. Further, SPMD-derived concentrations of heavy PAHs provide a qualitatively better estimate of TWA than those derived from MESCO (see Section 10.5.1.9). Finally, calculations of MESCO-derived concentrations relied on accuracy of K_{SW} values reported in literature. There is only a limited number of studies that provide these values and relatively high risk that some of them may be biased.

Nevertheless, we believe that the two passive sampling methods provide a more representative picture of the water quality than occasional spot sampling. Moreover, with the use of MESCO II devices some disadvantages of the foregoing MESCO format (underestimation of very hydrophobic compounds, possible disintegration of sampler due to membrane degradation during longer exposure) can be prevented although this, in turn, sets other restrictions, especially with respect to more polar target substances which will not be accumulated due to their low permeability in the non-porous and hydrophobic LDPE membrane envelope.

10.5.2 Field trials with MESCO II—first results

Since 2004, water monitoring using MESCO II strips (SR+air) alongside other passive samplers (SPMDs, bare silicone rods and Chemcatcher)

was carried out at several sites in three rivers in Germany (Elbe, Saale, Mulde) and additionally in the Spittelwasser creek, a tributary to the Mulde river near Bitterfeld, an area heavily polluted by chemical industry during the last 100 years. The major goal of these trials was to test the field performance of MESCO II devices under different ambient conditions (regarding water flow and temperature, hydrochemistry and biological activity). Similar to the Twister bars, the silicone rod pieces were spiked with PRCs before sampler assembly in order to adjust the laboratory-derived sampling rates to *in situ* conditions. The data evaluation for these field campaigns is still under way.

As an example we present results obtained for HCB in the Spittelwasser near Jessnitz (at the site 51°41′28″N; 12°17′25″E, estimated using Google Earth) during Summer 2005. MESCO II strips with 50 and 100 μm LPDE membrane thickness, respectively, were tested in two different deployment devices, i.e. in a wide-mesh protective grid and in a long narrow perforated cage as used for SPMDs. The samplers were exposed for 28 days and TWA concentrations were estimated from the amounts accumulated using the sampling rates listed in Table 10.2. Figure 10.7 shows the TWA concentrations against snapshot results obtained every two weeks from grab samples pre-concentrated by SPME and analysed using GC-MS (for analytical details see Ref. [14]). The correspondence between the results of the different sampling strategies is remarkable, especially if one bears in mind that the evaluation of MESCO data is based on preliminary sampling rates from a rapid semi-continuous laboratory calibration test. Figure 10.7 also shows a slight influence of hydrodynamics on the HCB accumulation. Reduced flow in the cage seemed to have lowered the substance uptake into MESCO samplers. This aspect is currently under investigation in flow-through experiments.

Also from another monitoring exercise, the field trial in the Meuse river in Eijsden (The Netherlands) which was organised in April–May 2005 within the framework of the EU project SWIFT-WFD [19], interesting results are expected on the field performance of MESCO I and II devices in comparison to other passive sampler formats that were applied [20].

Currently, field trials are in progress in the region of Bitterfeld (Saxony-Anhalt, Germany) with miniaturised MESCO II strips for time-integrative and depth-oriented monitoring of groundwater wells. The first results show that silicone rods enclosed in LDPE membrane are even able to accumulate volatile organic compounds such as 1,4-dichlorobenzene over several weeks. A comparison of substance amounts accumulated with the water concentrations obtained from parallel exposed passive diffusion

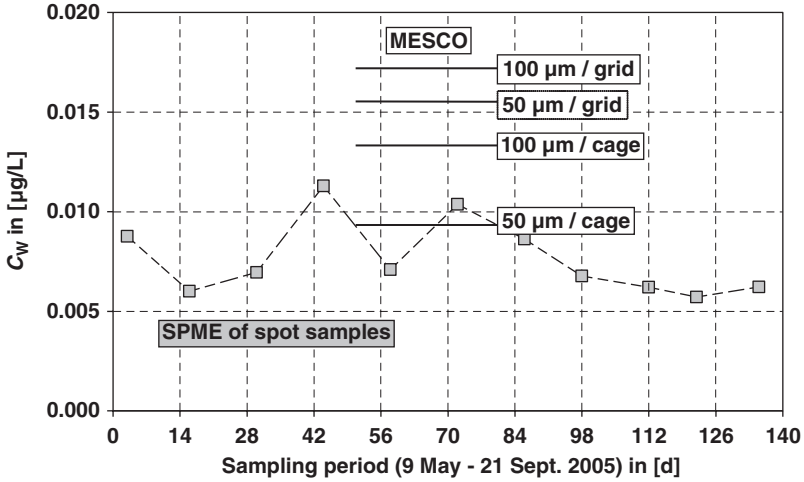

Fig. 10.7. Comparison of aqueous concentrations of HCB in the Spittelwasser creek (Summer 2005), obtained from analyses of snapshot samples and from passive sampling with MESCO II samplers made using different LDPE membranes (either 100 or 50 µm thick), deployed in wide-mesh protective stainless steel grids or in perforated cages as usually used for SPMDs, respectively.

bags [21] will allow the estimation of *in situ* sampling rates and/or distribution constants for such analytes with the MESCO II sampler. More work is needed, both in field and laboratory, to screen the spectrum of more volatile compounds to be monitored and to determine the period for time-integrative sampling.

ACKNOWLEDGMENTS

We thank Petra Keil and Uwe Schröter for their help with sample preparation and instrumental measurements. We acknowledge the financial support of the British Council and the German Academic Exchange Service (Academic Research Collaboration project No. 1239) for this work.

REFERENCES

1 E. Baltussen, C.A. Cramers and P.J.F. Sandra, *Anal. Bioanal. Chem.*, 373 (2002) 3.
2 B. Vrana, P. Popp, A. Paschke and G. Schüürmann, *Anal. Chem.*, 73 (2001) 5191.

3 K. Booij, H.M. Sleiderink and F. Smedes, *Environ. Toxicol. Chem.*, 17 (1998) 1236.
4 J.N. Huckins, J.D. Petty, J.A. Lebo, F.V. Almeida, K. Booij, D.A. Alvarez, W.L. Cranor, R.C. Clark and B.B. Mogensen, *Environ. Sci. Technol.*, 36 (2002) 85.
5 B. Vrana, P. Popp, A. Paschke, B. Hauser, U. Schröter and G. Schüürmann, Patentschrift DE 100 42 073 C 2, Deutsches Patent- und Markenamt, München, 2002.
6 J.N. Huckins, M.W. Tubergen and G.K. Manuweera, *Chemosphere*, 20 (1990) 533.
7 A. Paschke and P. Popp, *J. Chromatogr. A*, 999 (2003) 35.
8 P. Popp, B. Hauser, A. Paschke and B. Vrana, Gebrauchsmuster Nr. 200 23 183.9, Deutsches Patent- und Markenamt, München, 2003.
9 L. Wennrich, B. Vrana, P. Popp and W. Lorenz, *J. Environ. Monit.*, 5 (2003) 813.
10 L. Montero, P. Popp, A. Paschke and J. Pawliszyn, *J. Chromatogr. A*, 1025 (2004) 17.
11 B. Hauser, M. Schellin and P. Popp, *Anal. Chem.*, 76 (2004) 6029.
12 J.N. Huckins, J.D. Petty, H.F. Prest, R.C. Clark, D.A. Alvarez, C.E. Oranzio, J.A. Lebo, W.L. Cranor and B.T. Johnson, *A Guide for the Use of Semipermeable Membrane Devices (SPMDs) as Sampler of Waterborne Hydrophobic Organic Contaminants*, API Publication 4690, American Petroleum Institute, Washington, DC, 2000.
13 B. Vrana, A. Paschke and P. Popp, *Environ. Pollut.*, 144 (2006) 296.
14 A. Paschke, K. Schwab, J. Brümmer, G. Schüürmann, H. Paschke and P. Popp, *J. Chromatogr. A*, 1124 (2006) 187.
15 B. Vrana, H. Paschke, A. Paschke, P. Popp and G. Schüürmann, *J. Environ. Monitor.*, 7 (2005) 500.
16 B. Vrana, A. Paschke, P. Popp and G. Schüürmann, *Environ. Sci. Pollut. Res.*, 8 (2001) 27.
17 J.N. Huckins, J.D. Petty and K. Booij, *Monitors of Organic Chemicals in the Environment: Semipermeable Membrane Devices*, Springer, New York, 2006.
18 M.S. Garcia-Falcon, C. Perez-Lamela and J. Simal-Gandara, *Anal. Chim. Acta*, 508 (2004) 177.
19 http://www.swift-wfd.com/Local/swift/dir/doc/newsletter3.pdf
20 I.J. Allan *et al*. (2007), in preparation.
21 D.A. Vroblesky and W.T. Hyde, *Ground Water Monit. Remediat.*, 17 (1997) 177.

Chapter 11

In situ monitoring and dynamic speciation measurements in solution using DGT

Kent W. Warnken, Hao Zhang and William Davison

11.1 INTRODUCTION

Diffusive gradients in thin-films (DGT) was first used in the mid-1990s as an *in situ* technique for dynamic trace metal speciation measurements [1,2]. It has since been developed as a general monitoring tool for a wide range of analytes in addition to the transition and heavy metals originally measured, including the major cations, Ca and Mg [3], stable isotopes of Cs and Sr [4], radionuclides of Cs [5] and Tc [6], phosphate [7] and sulphide [8]. In a comprehensive study, Garmo *et al*. [9] demonstrated the capabilities of DGT to measure 55 elements with a Chelex® 100-based resin-gel.

As its name implies, DGT relies on the quantitative diffusive transport of solutes across a well-defined gradient in concentration, typically established within a layer of hydrogel and outer filter membrane. The filter membrane is exposed directly to the deployment solution and acts as a protective layer for the diffusive gel. Once diffusing through these outer layers, solutes are irreversibly removed or chelated at the back side of the diffusive gel by a selective binding agent, typically Chelex 100, which is immobilized in a second layer of hydrogel. The hydrogels used in DGT are typically made of polyacrylamide, which can be fabricated with a range of properties, including almost unimpeded diffusion due to the gel having a water content as high as 95% [10].

The pre-filter, diffusive gel and binding-gel layers are assembled into an all plastic sampling device comprised of a base and cap (Fig. 11.1). The cap is push-fit onto the base to provide a water-tight seal and has an opening or 'viewing window' that exposes a known area of the filter to the deployment solution. The theoretical basis for the use of DGT

Comprehensive Analytical Chemistry 48
R. Greenwood, G. Mills and B. Vrana (Editors)
Volume 48 ISSN: 0166-526X DOI: 10.1016/S0166-526X(06)48011-9

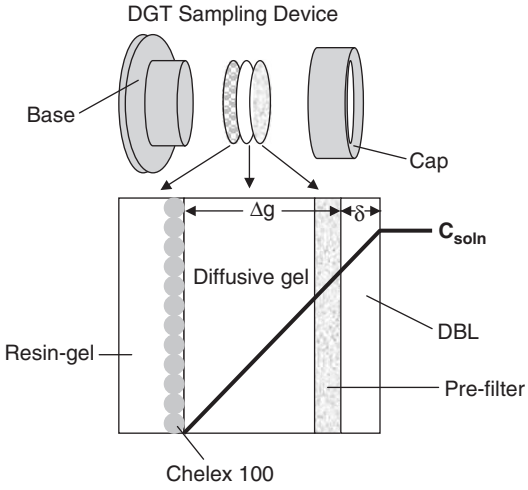

Fig. 11.1. The DGT sampling device is composed a base and cap, which contains the pre-filter, diffusive gel and resin-gel layers. The DBL extends out from the device face into the bulk water with a concentration (C_{soln}).

in aqueous solutions has been systematically developed over the past decade [1,7,11–14].

Transition and heavy metals have usually been measured using a binding layer of Chelex 100, known as the resin-gel layer. To lay the groundwork for their measurement by DGT, initial experiments were carried out to establish performance characteristics, including the capacity of the resin layer [2,15], the diffusion coefficients of metals and their complexes [16,17], pH dependence [2,15,18], the elution factor of metal ions from the resin-gel [2,9,10,19–21] and the effects of solution composition, flow and deployment time [18,21]. Effects of waters with very low ionic strength (<1 mmol L^{-1}) on DGT measurements reported by several workers [19,20,22] have been shown to be largely due to incomplete washing of the gels [23].

DGT has been deployed *in situ* in a wide range of natural waters, including fresh-waters, such as soft Canadian shield lakes [19], a eutrophic hard-water lake [24] and several rivers [16,25–28], coastal sea-water [29] and open ocean sea-water [1,2]. The early development of DGT, including applications in waters, soils and sediments, has been reviewed [30]. Here, we focus on its further development and applications in aqueous systems, which include its use (1) for speciation measurements [12,16,24–29,31–35] and kinetic tools [11], (2) for bioavailability studies [36–40] and (3) for routine environmental monitoring [41–44].

11.2 METHODOLOGY

11.2.1 Gel preparation

Details of the procedures for preparing the diffusive gel and the resin-gel used for trace metal measurements are well documented [2,30] and can be obtained directly from DGT Research Ltd. (Lancaster, UK). Procedures for preparing specific binding gels for other solutes can be found in the individual scientific publications. The diffusive gel most commonly used is prepared from a polyacrylamide gel cross-linked with an agarose derivative and is referred to as APA2 [17]. It is prepared by mixing 3.75 mL of acrylamide solution (40%) and 4.75 mL of deionized water with 1.50 mL of DGT cross-linker (DGT Research Ltd.) (0.3%, measured by weighing 1.50 g). This 10 mL of gel solution is well mixed using a pipette and to it a further 70 μL ammonium persulphate solution (10%, 0.1 g in 1 g of H_2O) and 25 μL of *N*,*N*,*N*′*N*′-tetramethylethylenediamine (TEMED) (99%) are added and well mixed using a pipette. The solution is then cast between two acid-cleaned glass plates, separated by a 0.5 mm plastic spacer (for 0.08 cm diffusive gels), and immediately placed into a 45°C oven for 1 h. Once the gels are completely set, they are removed from the glass plates and placed into a deionized water bath (two gel sheets per litre of deionized water), which is changed repeatedly until all the excess polymerization products are removed, i.e. the pH of the wash solution is equal to that of the deionized water it is stored in. Finally, the diffusive gels are conditioned in a separate solution of 10–30 mmol L^{-1} $NaNO_3$ before use.

The Chelex® 100 resin-gel used for measuring trace metals is prepared by mixing 3–4 g of Chelex® 100 (200–400 mesh), available from Bio-Rad Laboratories (USA), with 10 mL of gel solution consisting of 3.75 mL of acrylamide (40%) (BDH Electran®), 1.5 mL of DGT cross-linker (DGT Research Ltd.) and 4.75 mL deionized water. To this solution, 50 μL of ammonium persulphate (BDH Electran®) and 15 μL of *N*,*N*,*N*′*N*′-TEMED (BDH Electran®) are added. The resin-gel solution is immediately cast between two glass plates, which are separated by a 0.025 cm acid-cleaned plastic spacer and held together with plastic clips. Once cast, the glass plate assembly containing the gel with incorporated resin, known as resin-gel, is placed into an oven set at 45°C for ~1 h. Once the gel sheets are set, they are placed into ultra-pure water and allowed to hydrate before use by repeatedly changing the wash solution until all the excess polymerization products are completely washed from the gel. As with the diffusive gels, the resin-gels are also placed into

10–30 mmol L^{-1} $NaNO_3$ before use. For low-level trace metal work, all handling and processing of gels, up until the time of deployment, should be carried out in a laminar flow Class-100 clean bench using 'ultra-clean' trace metal techniques.

11.2.2 Diffusive gel variants

DGT has generally used a diffusive hydrogel prepared from an acrylamide monomer cross-linked with a patented agarose derivative (DGT Research Ltd.). Originally, the diffusion coefficients of metal ions in this gel (D_{Gel}), known as APA1, were found to be very similar to their diffusion coefficients in water (D_w). However, changes in the manufacturing process of the cross-linker resulted in a gel with a slightly smaller pore size, which is now referred to as APA2. These two gels are notionally the same, i.e. 15% acrylamide with 0.3% agarose cross-linker, but the diffusion coefficients of metal ions in APA2 are approximately $0.85 \times D_w$. A third type of gel in common use, APA3, uses a reduced amount of cross-linker (0.12%) and has a pore size closer to the original APA1 gel. Additional gel types include a restricted gel (RG) with a much smaller pore size that appreciably retards the diffusion of complexes with fulvic and humic acids [10,17]. It uses bis-acrylamide (BDH Electran®) as the cross-linker (0.8%) and 7 μL of ammonium persulphate and 2 μL TEMED per mL of gel solution.

DGT holders have also been used with a chromatographic paper as a diffusion layer [45], but required individual calibration at ionic strengths $\leqslant 5$ mmol L^{-1} due to increased effective diffusion coefficients, likely due to the paper having a negative charge. The authors found them easy to prepare and handle. DGT has also been successfully used with a membrane filter as the diffusion layer [1,21].

11.2.3 Alternative binding agents

Numerous variants on the diffusive and resin-gel types originally used in DGT have been used, including poly(acrylamideoglycolic acid-*co*-acrylamide) for selective binding of Cu^{2+} [46]. Under competitive binding conditions, this resin showed a stronger binding affinity for Cu. When tested as a binding agent for the DGT technique, it was shown to have a linear mass response with respect to time, with C_{DGT}/C_{soln} ratios of approximately 1.

An alternative approach to using ion-specific resins is the use of co-polymer hydrogels composed of polyacrylamide–polyacrylic acid [47]. These gels selectively bind Cu^{2+} and Cd^{2+}, over alkali and alkaline earth metals, within the hydrogel structure. DGT devices containing a liquid binding phase, poly(4-styrenesulphonate) (PSS) aqueous solution and a cellulose dialysis membrane (CDM) as a diffusive layer, have also been proposed [48,49], with the intent of excluding the availability of copper–organic matter complexes to the device.

A commercially available strong cation exchange membrane (Whatman P81) has also been used as the binding layer in DGT [50]. Like Chelex 100, it preferentially binds transition metals over competing divalent matrix cations such as Mg and Ca. DGT devices with this binding layer showed good agreement with theory and its performance was not degraded even after four consecutive uses. A systematic comparison of DGT sampling devices containing different binding agents showed that DGT concentrations measured by the different binding agents can be significantly different and suggests that DGT labile concentrations may depend on the binding strength of the binding agent [51]. However, as above a low threshold, the binding strength would not be expected to affect measurement of a complexed metal, further work is required to establish this observation [2].

DGT has been used to measure phosphate in natural waters using a binding layer of ferrihydrite embedded in gel [7]. This binding layer has also been used for the measurement of As [52]. Mason *et al*. [53] have used a mixed binding layer (MBL), consisting of both Chelex 100 and ferrihydrite, to measure both cations (Mn, Cu, Zn and Cd) and anions (molybdate and phosphate) in a single measurement. As all elements were measured by ICP-MS, including ^{31}P, 1 mol L^{-1} HCl was used for elution to minimize interferences from $^{14}N^{16}OH$ and $^{15}N^{16}O$. Measurements of both cations and anions by devices with a MBL were similar to those made using standard DGT resin-gels containing either Chelex 100 or ferrihydrite. An alternative binding agent, suspended particulate reagent-iminodiacetate (SPR-IDA) available from CETAC Technologies Inc. (USA) with similar iminodiacetate functionality to Chelex 100, has been used [30]. While a systematic characterization of its performance has been carried out [15], due to the elevated cost of this resin type and its smaller bead size, it is most appropriate for laser ablation inductively coupled plasma mass spectrometry (LA-ICP-MS) for determining trace metal distributions in sediments at high spatial resolutions in 2D [54].

11.3 DGT THEORY

11.3.1 DGT principles

At steady-state, the diffusive flux (F) of an ion is given by Fick's first law of diffusion where dC/dx is the change in concentration (g cm^{-3}) occurring over the distance x (cm):

$$F = D_0 \frac{dC}{dx} \tag{11.1}$$

The diffusion coefficient measured at infinite dilution and a reference temperature of 25°C, D_0, can be corrected to any *in situ* temperature, D_t, by applying the Stokes–Einstein equation, where T_0 and T_t are in Kelvin (K):

$$\frac{D_0\eta_0}{T_0} = \frac{D_t\eta_t}{T_t} \tag{11.2}$$

The viscosity of water can be expressed by the following equation [55] where η_0 is the viscosity of water at the reference temperature of 25°C and η_t is at the *in situ* temperature t (°C):

$$\log\frac{\eta_0}{\eta_t} = \frac{1.37023(t-25) + 8.36e^{-04}(t-25)^2}{109+t} \tag{11.3}$$

In DGT with the commonly used APA2 gel, the diffusion coefficient of divalent metal cations in the diffusive gel layer, D_{Gel}, can be approximated by $0.85 \times D$ [17]. At steady-state, the concentration gradient, dC/dx, is the difference between the concentration in the bulk solution and the concentration at the interface between the diffusive and resin-gel layers, C', which is 0 if the resin-gel layer is a rapid and effective sink. The distance x is the diffusional path length, which is the combined thickness of the diffusive gel layer, the protective membrane filter and the diffusive boundary layer in solution, DBL (see Fig. 11.1 and later). Here we simplify the system by assuming that the thickness of the DBL is negligible and the diffusion coefficient for the other two layers, with a combined thickness of Δg, is the same:

$$F = \frac{D_{Gel}(C - C')}{\Delta g} \tag{11.4}$$

The flux (F) is equal to the mass (M, in g) of metal through an area (A, in cm^2) per unit time (t, in s):

$$F = \frac{M}{At} \tag{11.5}$$

The mass of metal, M, accumulated by the resin-gel layer is calculated after placing it into a known volume of elution acid (V_e). V_{Gel}, the volume of the gel layer, is generally taken to be 0.16 mL for an 8 mm thick gel and f_e is the elution efficiency:

$$M = \frac{C_e(V_{Gel} + V_e)}{f_e} \tag{11.6}$$

Substituting for F in Eq. (11.6), the bulk solution concentration as measured by DGT (C_{DGT}) can be calculated by the following equation:

$$C_{DGT} = \frac{M\Delta g}{D_{Gel}tA} \tag{11.7}$$

11.3.2 Potential sources of error when using DGT

When using DGT, errors can arise from a number of sources including (1) changes in the temperature of the deployment solution, (2) variation in the thickness of the diffusive gels used, (3) resin-gel blank variability, (4) the elution factor (f_e) used to calculate M, (5) measurement of the diffusion coefficients (D_{Gel}) and (6) the existence of a DBL at the solution interface with the device. When performing DGT measurements under controlled conditions in the laboratory, the DGT measurement of concentration, C_{DGT}, is often compared with the concentration measured directly in solution, C_{soln}. A further error is then the accuracy of the measurement of C_{soln}. Several of these sources of error can be greatly reduced or even eliminated altogether under controlled laboratory conditions. For example, a stable temperature can be established by stirring the solution overnight prior to DGT deployment. Elevated labile metal concentrations (e.g. 10 μg L^{-1}) for elements such as Cd, which exhibit very low DGT blank levels (~0.3 pg per disc), can be used to reduce the analytical uncertainty associated with the determination of C_{soln}. Casting the diffusive gels using spacers with a uniform thickness throughout their length should eliminate variations in the

thickness of the diffusive gels used. Thus, the primary sources of error still remaining are uncertainties associated with the resin-gel elution efficiency, the value of the diffusion coefficient used for D_{Gel}, and the thickness of the DBL, δ.

11.3.2.1 Diffusion coefficients

Several studies have tried to determine accurately the diffusion coefficients of metal ions in gels and metal–ligand complexes such as fulvic and humic acids [10,56,57]. Recently, Scally *et al*. [17] investigated the effect of a DBL within the stirred, two-compartment cell used to estimate diffusion coefficients and examined the effect of ionic strength (0.1–100 mmol L^{-1}) on the diffusion coefficient of Cu and Cd in three different gel types (APA2, APA3 and RG). A similar diffusion coefficient was measured with 0.4, 0.8 and 1.6 mm gel thicknesses, suggesting that the DBL within the stirred cell device was negligible. The diffusion coefficients of these two metals in the APA2 diffusive gel and pre-filter were indistinguishable. However, when using the RG, it may be necessary to consider the gel layer and pre-filter separately, as diffusion coefficients determined with the RG and pre-filter were higher than those obtained with the RG alone. At very low ionic strengths ($I = 0.1$ mmol L^{-1}), the diffusion coefficients of Ni, Cu, Cd and Pb were 50% lower than those measured at $I \geqslant 1$ mmol L^{-1}, in agreement with the results of Warnken *et al*. [23]. The diffusion coefficients of Pb complexes decreased with increasing molecular weight, in the order DGA > NTA > FA > HA.

11.3.2.2 Elution efficiency

The elution efficiency, or the recovery of metal ions from the resin-gel, was first measured by Zhang and Davison [2] using 2 mol L^{-1} HNO_3 concentrations and elution times ranging from 1 h to 1 week. These initial experiments were contrived to ensure that all the metal added was taken up by the resin and consequently metal loadings on the resin-gel were moderate to high. They reported values of 0.81 $\pm$ 0.022 for Mn, 0.82 $\pm$ 0.069 for Ni, 0.79 $\pm$ 0.064 for Cu, 0.80 $\pm$ 0.055 for Zn and 0.84 $\pm$ 0.027 for Cd. Thus, an elution factor (f_e) of 0.80 was adopted for DGT resin-gels containing Chelex 100.

Alfaro-De la Torre *et al*. [19] determined elution efficiencies by adding resin-gel discs to solutions of known volume containing 7.8–234 nmol L^{-1} $NiCl_2$, 3.2–225 nmol L^{-1} $CuCl_2$ and 0–232 nmol L^{-1} $CdCl_2$. The 5 mL Teflon vials were then shaken for 24 h. Upon recovery of the resin-gels, they were placed in 4 mL polyethylene vials containing

1 mL of 1 mol L^{-1} HNO_3 and shaken for 12 h. The elution efficiencies of 0.83 ± 0.06, 0.83 ± 0.04 and 0.78 ± 0.04 determined for Ni, Cu and Cd, respectively, led to these authors adopting a mean value of 0.80 for these metals. Sangi *et al*. [20] reported that there was no significant difference in the amount of metal leached from a resin-gel disc over a time period of ~0.2–8 h using volumes of 1–50 mL and HNO_3 concentrations of 1–2.5 mol L^{-1}. For ease of use, they chose an elution period of 0.5 h with addition of 10 mL of 2 mol L^{-1} HNO_3.

Garmo *et al*. [9] used double elution of Chelex 100 resin-gels with concentrated HNO_3. It was found that the elution efficiency increased to values of 0.97–0.99 for most of the metals measured. The elution efficiency was lower for the metals Al, Ni and Cr, with values of 0.94, but still higher than the values determined using 1–2 mol L^{-1} HNO_3. In addition, a complete acid digestion of the resin-gel was performed using hot concentrated HNO_3 and microwave digestion (170°C at elevated pressure). However, poorer blank values offset any gains in elution efficiency and the cold concentrated HNO_3 elution method was recommended for routine work.

Warnken *et al*. [21] have recently simulated metal elution as it would occur after a standard 4 h deployment in the laboratory, by deploying DGT devices into solutions containing metals in the 2–10 μg L^{-1} range, i.e. low resin-gel metal loadings. Elution of the resin-gels was carried out using 1 mL of 1 mol L^{-1} HNO_3 for 24 h. They reported values of 0.86 ± 0.029 for Co, 0.87 ± 0.016 for Ni, 0.85 ± 0.014 for Cu, 0.85 ± 0.023 for Cd and 0.83 ± 0.013 for Pb. While the mean elution efficiency of 0.85 ± 0.023 (2.7% RSD) was higher than the commonly accepted values, it was within the metal-specific errors reported by Zhang and Davison [2] and could reflect the difference in resin-gel metal loadings, the elution acid strength used or a combination of the two.

11.3.2.3 Ionic strength

There has been much contention in the literature over the use of DGT in low ionic strength solutions of < 1 mmol L^{-1}, with some studies reporting enhanced solute diffusion rates or poor DGT measurement precision. At and above this ionic strength, DGT measurements in synthetic solutions are quantitative, i.e. a value of 1 is obtained for C_{DGT}/C_{soln}. However, below this ionic strength, the performance of DGT has been inconsistent. For instance, values of $C_{DGT}/C_{soln} > 1$ were reported by Alfaro-De la Torre *et al*. [19] when they made measurements in solutions with ionic strengths of 0.2 mmol L^{-1} using DGT with a APA diffusive gel. They suggested that, to preserve electro-neutrality,

the diffusion of displaced Na from the Chelex resin-gel through the diffusive gel was balanced by counter-diffusion of metal ions at an enhanced rate.

Irregular DGT results were also reported by Peters *et al*. [22] using APA gels at low ionic strength, with values of C_{DGT}/C_{soln} ranging from 0.5 to 3. They attributed this behaviour to local charges at the surface and within the interior of the gel, suggesting that the sporadic behaviour was due to an insufficient amount of excess cations. Their findings were not consistent with either simple DGT theory established for higher ionic strengths ($\geqslant 1$ mmol L^{-1}) by Davison and Zhang [1] or with enhancement in diffusion as suggested by Alfaro-De la Torre *et al*. [19]. Using a bis-acrylamide cross-linked (BPA) gel, Sangi *et al*. [20] showed enhanced diffusion of Cd in low ionic strength $NaNO_3$ solutions. While they could not explain their results completely using the model proposed by Alfaro-de la Torre *et al*. [19], they did acknowledge that electro-neutrality considerations were probably of some importance. They also suggested that irreversible cation binding by the diffusive gel occurred prior to irreversible binding by Chelex 100.

Recent work by Yezek and van Leeuwen [58] using a similar BPA gel has shown that at low ionic strength these gel types can have a negative charge, due to the initiation chemicals used during their polymerization. They presented a systematic theory that accounts for apparent increased rates of diffusion of metal ions in terms of partitioning of metals at the gel/solution interface, according to the Donnan potential that is developed. Fatin-Rouge *et al*. [59] also attributed apparent elevated diffusion coefficients at low ionic strengths in a pure agarose (AGE) gel to a negative charge. The smaller than expected elevation was thought to be due to specific binding between metal ions and the agarose gel.

Warnken *et al*. [23] showed DGT devices made from gels that were poorly washed of polymerization products gave erroneously high values of C_{DGT}/C_{soln} when deployed at low ionic strengths (0.1 mmol L^{-1}), while gels that were completely washed of initiation products gave values of ~0.5 for C_{DGT}/C_{soln} (Fig. 11.2). This apparent decrease in the diffusion coefficient at very low ionic strengths is in agreement with independent diffusion cell experiments [17]. It can be explained by a net positive charge on the gel changing the concentration of metal ions at the interface between the gel and the bulk solution through Donnan partitioning. These authors also showed that low-capacity binding sites within the diffusive gel were capable of binding trace metals irrespective of ionic strength. The only substantial effect on most DGT

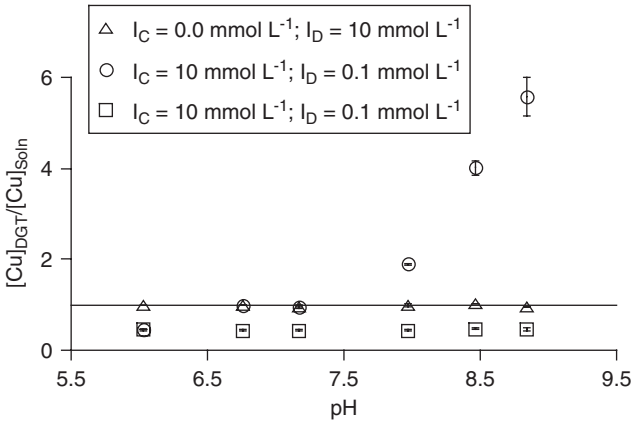

Fig. 11.2. The ratio C_{DGT}/C_{soln} plotted as a function of the final pH of gel wash solution. IC and ID are the ionic strengths of the conditioning and deployment solutions, respectively (reprinted from Ref. [23]. Copyright (2005), with permission from American Chemical Society).

measurements is likely to be an increase in the time taken to establish a steady-state gradient, but there was no observed effect on DGT measurements for 4 h laboratory deployments.

11.3.2.4 Diffusive boundary layer

In the simplest case, the diffusive boundary layer (DBL) adjacent to the DGT sampling device can be ignored if it is sufficiently thin compared with the total thickness of Δg, allowing the standard DGT equation (Eq. (11.1)) to be used. However, when the DBL is sufficiently thick that it can no longer be ignored, such as in quiescent lake waters or when using very thin diffusive gels, the following equation must be used [30]:

$$C_{DGT} = \frac{M(\Delta_{Gel}/D_{Gel} + \Delta_f/D_f + \delta/D_w)}{At} \tag{11.8}$$

Δ_{Gel} is the thickness of the gel, Δ_f is the thickness of the pre-filter, δ is the thickness of the DBL and D_f and D_w are the diffusion coefficients in the pre-filter and DBL, respectively. Since $D_{Gel} = D_f$, for a typical filter and APA2 gel, the Δ_f term can be incorporated into Δg. On rearrangement, this gives

$$\frac{1}{M} = \frac{1}{C_{DGT}At}\left(\frac{\Delta g}{D_{Gel}} + \frac{\delta}{D_w}\right) \tag{11.9}$$

If simultaneous measurements are made with DGT devices with different gel layer thicknesses, a plot of $1/M$ versus Δg is a straight line with a slope (m) of $1/(C_{DGT}D_{Gel}At)$ and a y-intercept of $\delta/C_{DGT}D_{w}At$. The thickness of the DBL, δ, and the concentration in the solution, C_{DGT}, can therefore be calculated:

$$\delta = \frac{y_{int}}{m}\left(\frac{D_w}{D_{Gel}}\right) \tag{11.10}$$

By measuring Ca and Mg using DGT devices loaded with three different gel layer thicknesses, Alfaro-De la Torre *et al*. [19] calculated a DBL thickness in an acidic (pH 5.3–5.6) and oligotrophic, Precambrian Shield lake. A mean value of $\delta = 0.031 \pm 0.022$ cm was obtained for the whole water column, since no trend was observed with depth. Zhang *et al*. [7] used a combination of nine DGT devices (three diffusive gel layer thicknesses in triplicate) to measure phosphorus in a shallow quiescent eutrophic pond and estimate a DBL thickness of 0.039 cm. Similarly, Zhang [16] estimated a DBL thickness of 0.038 ± 0.005 cm for a humic-rich stream, from measurements of Ni, Cu and Zn.

The calculated δ might not only represent the thickness of the DBL, but could incorporate a term due to biofouling as mucilaginous bacterial biofilms can form in <2 days [7,60]. The assumption that biofouling affects all DGT devices equally, irrespective of their gel layer thicknesses, is likely valid as they all have the same geometry and pre-filter. In this case, the effect of biofouling on DGT can be calculated using the same approach as for estimating δ (Eqs. (11.9) and (11.10)), but δ now becomes the mean thickness of the biofilm during the deployment time plus the thickness of the DBL. Where only two gel layer thicknesses with accumulated masses M_1 and M_2 are available, following equation can be used:

$$\delta = \left(\frac{D_w}{D_{Gel}}\right)\frac{M_1(\Delta g_1 - M_2)\Delta g_2}{M_2 - M_1} \tag{11.11}$$

Warnken *et al*. [21] found when making very precise measurements in the laboratory under well-controlled stirring regimes at different gel layer thicknesses that the above procedure for estimating DBL had problems. They concluded that the effective area of resin-gel that accumulates metal is larger than the geometric area of the window of the DGT device. This effective area of 3.8 cm^2 for a standard solution device should be used when measurements are made at a range of gel layer

thicknesses. They also found that in most reasonably well-stirred solutions, the thickness of the DBL is 0.23 ± 0.023 mm.When DGT is used with a 0.8 mm thick diffusive gel layer, the geometric area can be used in Eq. (11.7) with reasonable accuracy, as the error introduced by ignoring the DBL cancels the error introduced by using the geometric rather than effective area.

11.4 NOVEL APPLICATIONS

11.4.1 Analytes

DGT has been used for a wide range of analytes, in addition to the transition and heavy metals (Al, Cd, Co, Cu, Fe, Mn, Ni, Pb and Zn) that were originally measured, and been applied to many different natural water types. Dahlqvist *et al*. [3] showed that Ca and Mg, which are bound less selectively than trace metals to Chelex, can be measured by DGT, although care must be taken to establish that saturation of the resin is not approached. They compared DGT measurements of Ca and Mg in filtered and modified lake-water with results obtained from ultra-filtration. The fraction of Mg measured by DGT was similar to the fraction of Mg residing in the <1 kDa ultra-filtration fraction.

To measure mercury in river-water using DGT, Docekalova and Divis [61] found it necessary to use an agarose diffusive gel layer, since the polyacrylamide gel type normally used binds Hg covalently via the amide nitrogen groups. A Spheron-Thiol resin as well as Chelex 100 was used. These two resins provided different measurable fractions of Hg, with DGT containing the Spheron-Thiol resin measuring 11.6 ± 0.9 ng L^{-1} Hg and Chelex 100 measuring 4.2 ± 0.50 ng L^{-1} Hg. It appeared that the difference in the Hg-resin stability constants enabled discrimination between the Hg complexes bound by DGT. Concentrations of Hg measured by DGT (with either resin-type) were significantly lower than the measured total concentrations (88 ± 12 ng L^{-1} Hg), indicating the presence of organic colloids or complexes that were not measured.

Ernstberger *et al*. [62] showed that DGT with a Chelex resin could be used to measure Cr(III) but not Cr(VI). The laboratory performance of DGT for the measurement of chromium speciation was further evaluated by Barakat and Giusti [63] prior to its use in natural river-water [64]. The isotopic composition of Zn in the binding layer of DGT was measured using a multi-collector inductively coupled plasma mass spectrometer (MC-ICP-MS) [65]. Provided quantitative elution was

achieved, DGT did not fractionate Zn compared with the bulk isotopic signature of the deployment solution.

Stable Cs and Sr were measured using DGT containing AG50W-X8 resin as the binding agent [4]. As this resin was not as selective as Chelex 100, it was more prone to saturation by major cations, which limited its use for Cs and Sr to relatively short deployment times ($\leqslant$20 h) in soft-waters. The species of Cs and Sr measured by DGT in fresh-water were completely labile, indicating a lack of stable complexes or colloidal forms. The rare earth element, Nd, was measured by Dahlqvist *et al*. [66] across a salinity gradient using DGT. The proportion of Nd measured by DGT increased from 9% in fresh-water to 40% in sea-water. The isotopic signature of Nd, as sampled by DGT was unchanged from that sampled in the bulk water, indicating that there was complete exchange of Nd with the colloidal/particulate fraction. These results suggest that Nd isotope ratios measured in foraminiferans and Fe–Mn crusts have an isotopic signature similar to that of bulk sea-water.

Radiocesium has been measured using DGT containing an ammonium molybdophosphate (AMP) binding agent [5]. Field trials in a fresh-water lake receiving direct inputs from a nuclear power station, conducted over a 5 day to 1 month period, resulted in mean concentrations of ^{137}Cs to be 47–61 mBq L^{-1}, in general agreement with grab-sample measurements. The DGT technique provided several advantages over traditional sampling methods, such as its relative simplicity, provision for time-averaged concentrations and *in situ* pre-concentration onto a medium with an ideal sample geometry for gamma spectrometry. The relatively long-lived radioisotope ^{99}Tc was measured in sea-water using DGT with a trialkyl methylammonium nitrate or TEVA resin (Eichrom Technologies) [6]. The DGT response for ^{99}Tc was independent of pH (3–8) and ionic strength (0.01–1.3 mol L^{-1}). Using quadrupole ICP-MS, a detection limit of 0.125 mBq L^{-1} was obtained for a 4 week deployment period, sufficiently low for use in contaminated waters such as the Irish Sea. This technique represents a simple, fast method of obtaining time-integrated data for ^{99}Tc.

Zhang *et al*. [7] used DGT with a gel impregnated with ferrihydrite as the binding layer to measure phosphate by elution with 0.25 mol L^{-1} H_2SO_4 and colorimetric analysis as phosphomolybdenum blue. *In situ* DGT measurements of reactive phosphorus in a eutrophic pond agreed well with replicate measurements of filterable reactive phosphorus, with limits of detection for 24 h and 1 week deployments of 0.07 μg L^{-1} and 0.01 μg L^{-1}, respectively.

11.4.2 Kinetics

It has been suggested that before metal ions react with the binding layer, they must first dissociate from their complexes [2]. As the binding layer of DGT continually removes metal, it perturbs the equilibrium condition of the solution in the diffusion layer and DBL. Metals in these layers that rapidly dissociate from complexes are measured along with the metal present at equilibrium as the free ion.

The time available for metal complexes to dissociate is the time required to traverse the diffusive gel layer. In principle, the kinetic window of the technique can be adjusted by varying Δg. Scally *et al*. [11] examined the lability of complexes of Cu and Ni with nitrilotriacetic acid (NTA) and determined their dissociation rate constants using a simplified theory. In water, metals exist as either free metals, M, or as inorganic and organic metal complexes, ML.

$$\mathrm{ML} \Leftrightarrow \mathrm{M} + \mathrm{L} \tag{11.12}$$

When a metal–ligand complex (ML) enters the diffusion layer, it will, in principle, be measured if it dissociates in the time (t_d) it takes to diffuse through the layer at a rate determined by the diffusion coefficient of the complex, D_ML:

$$t_\mathrm{d} = \frac{(\Delta g)^2}{2D_\mathrm{ML}} \tag{11.13}$$

Thus, the mass of metal accumulated by the DGT resin-gel layer will be the sum of the contributions from the free metal ions in solution, M, and the free metal ions dissociated from the complex, ML, M′ (concentration $C_{\mathrm{M}'}$).

$$M = \frac{(C_\mathrm{M} D_\mathrm{M} + C_{\mathrm{M}'} D_\mathrm{ML}) A t}{\Delta A + \delta} \tag{11.14}$$

The first-order dissociation of ML is given by

$$C_{\mathrm{M}'} = C_\mathrm{ML}(1 - \exp^{-k_{-1}\tau}) \tag{11.15}$$

Since ML can only be measured if it dissociates in the time required to traverse Δg, it is a reasonable approximation to set $\tau = t_\mathrm{d}$. Thus, combining Eqs. (11.13)–(11.15) gives the full equation for predicting the mass of metal accumulated by DGT:

$$M = \frac{[C_\mathrm{ML} D_\mathrm{ML}(1 - \exp^{(-k_{-1}(\Delta g + \delta)^2)/2D_\mathrm{ML}}) + C_\mathrm{M} D_\mathrm{M}] A t}{\Delta g + \delta} \tag{11.16}$$

Complexes of Cu–NTA were found to be fully labile with respect to DGT, with $k_{-1} > 0.012\ s^{-1}$. The measured mass of the Ni–NTA complex, however, increased with increasing gel thickness, indicating kinetic rather than diffusion control, with a k_{-1} value of $3.6 \times 10^{-5}\ s^{-1}$, in good agreement with the limited rate data in the literature. This work provided the first direct evidence that only the free metal ion, and not the metal complex, reacts with the resin binding layer. This gives DGT the potential to distinguish between adjunctive and disjunctive dissociation mechanisms and opens the possibility of using DGT to obtain kinetic information directly in natural and contaminated environmental systems.

The above equations represent a simplification of the true situation, as they are based on several assumptions [11]. A full dynamic model of the time dependence of concentrations of each component at various positions in the diffusion layer was developed [12]. Galceran *et al*. [13] have also used a more complete modelling approach to consider how lability affects the DGT measurement. More recently, the influence of binding strength and slow diffusion of complexes has been modelled [14].

Garmo *et al*. [67] used DGT to investigate the effects of complexation in solutions containing the lanthanide series elements (except Pm) and the ligand 8-amino-2-[(2-amino-5-methylphenoxy)methyl]-6-methoxyquinoline-*N*,*N*,*N*′,*N*′-tetraacetate quin2. The mass measured by DGT was fitted using two recently proposed models [11,12]. While uptake rates were dependent on the dissociation constants of the complexes, the kinetically limited lanthanides showed no dependence on Δg. Instead it was found that increasing the thickness of the resin-gel layer increased the mass uptaken by DGT, especially for the less labile complexes. Finally, the measured uptake rate was found to decrease significantly with increasing deployment times.

11.4.3 Speciation

Recent research on trace metal chemistry in natural waters has focused on chemical speciation, bioavailability and toxicity to aquatic organisms. Methods such as anodic stripping voltammetry (ASV) and competitive ligand exchange adsorptive stripping voltammetry (CLE-AdSV) have revealed a complex distribution of ligand binding strengths. DGT is sensitive to the chemical speciation in solution, as it will measure only those complexes that can dissociate (labile) and diffuse through the gel (mobile). It has been classified as a dynamic speciation technique because of these properties [68].

Concentrations of Cd, Cu and Mn measured *in situ* by DGT in river- and lake-waters was first compared with the total dissolved concentrations measured in filtered samples in four Australian waters [25]. Over a 72 h deployment period, the mass of Cd and Cu in two rivers increased linearly with time and matched the total dissolved concentrations. This indicated that biofouling was not a concern and that concentrations of strong complexing ligands were negligible in these waters. However, in two other rivers, the fraction of Cu and Cd measured by DGT was only 30% and 50% of the total dissolved concentration. DGT was used to obtain an *in situ* depth-profile of Mn in a stratified estuary, which showed a pronounced concentration maximum associated with redox-associated, reductive mobilization.

Zhang and Davison [26] were able to obtain more quantitative speciation information. They made the simplifying assumption that natural waters can be regarded as having two classes of compounds that can be measured by DGT (a) labile inorganic species, including the free ion, of total concentration C_i with a mean diffusion coefficient D_i and (b) labile organic species of total concentration C_o with a mean diffusion coefficient D_o. This assumption is reasonable in humic-rich fresh-waters where the metal speciation is dominated by complexes with fulvic acid.

The mass of metal (M_{DGT}) accumulated by a DGT device is then the sum of the contributions from both labile inorganic (M_i) and organic complexes (M_o).

$$M_{DGT} = M_i + M_o \tag{11.17}$$

According to Fick's first law of diffusion, the inorganic and organic contributions to M_{DGT} are given by Eqs. (11.18) and (11.19), respectively.

$$M_i = \frac{D_i C_i A t}{\Delta g} \tag{11.18}$$

$$M_o = \frac{D_o C_o A t}{\Delta g} \tag{11.19}$$

Combining Eqs. (11.17)–(11.19) gives

$$M_{DGT} = \frac{(D_i C_i + D_o C_o) A t}{\Delta g} \tag{11.20}$$

It can be rearranged to

$$\frac{M_{DGT} \Delta g}{D_i A t} = C_i + \frac{D_o}{D_i} C_o \tag{11.21}$$

A plot of $M_{DGT}\Delta g/D_i At$ versus D_o/D_i yields a straight line with a slope equal to C_o and a y-intercept equal to C_i. To make use of this equation to determine C_i and C_o, measurements must be made with DGT devices having two or more gel compositions and values of the mean effective diffusion coefficients of inorganic and organic complexes must be determined in each gel type.

Zhang and Davison [26] used this approach to measure the inorganic and organic components of Cu species in a humic-rich stream. They found that DGT labile organic species accounted for ~60% of the total species measured by DGT, which was 90% of the total dissolved Cu concentration. This difference was thought to be due to the presence of larger organic colloidal forms not available to the DGT device. Further *in situ* measurements of Ni and Zn in this same water showed that 45% of the Zn was present as inorganic complexes with the remaining 55% present as organic complexes. Inorganic complexes of Ni (Fig. 11.3) accounted for 68% of the total DGT measurable fraction with the remaining (32%) present as organic complexes [16].

Twiss and Moffett [29] used DGT and competitive ligand exchange adsorptive cathodic stripping voltammetry (CLE-ACSV) to measure the speciation of Cu in various marine systems with different degrees of pollution. The substantial differences in the very reproducible amounts of metal accumulated by DGT at contaminated and pristine sites suggested that DGT could be used to detect episodic contaminant inputs. Ten to thirty-five percent of the Cu determined by CLE-ACSV

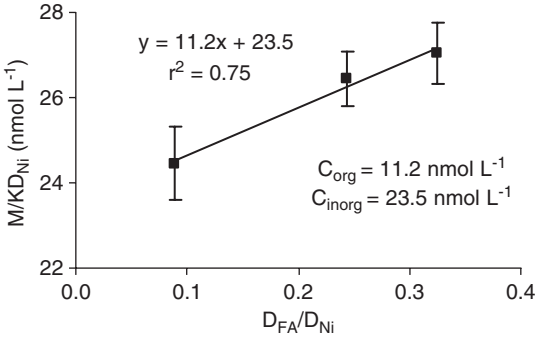

Fig. 11.3. *In situ* results for DGT sampling devices containing three distinct diffusive gel compositions plotted as mass (converted to the y-axis function where $K=At/\Delta g$) versus the ratio of the diffusion coefficients of fulvic acid (FA) and Ni. The slope (m) and y-intercept (b) of the lines gives the organic and inorganic concentrations, respectively. Reprinted from Ref. [16]. Copyright (2004), in part with permission from American Chemical Society.

to be organically bound was measured by DGT. The effective diffusion coefficients for these complexes ranged from 0.77×10^{-6} to 2.2×10^{-6} cm^2 s^{-1}, in broad agreement with the values for complexes with fulvic acid [10].

A comparison of the lability of Al and Cu fulvic acid complexes was carried out by Downard *et al*. [32] using DGT and flow injection analysis (FIA), where the time available for complex dissociation was restricted to 1–3 s. Independent measurements of the Al–FA and Cu–FA diffusion coefficients confirmed that the metal complexes diffuse at the same rate as FA. The DGT measured Al was equal to the sum of the labile and moderately labile fractions determined by FIA, but this was not the case for Cu. These authors concluded that the value of D_{FA} measured in a diffusion cell may not be appropriate for use in DGT.

Gimpel *et al*. [33] compared the metal speciation measured in several lakes, using *in situ* DGT, *in situ* dialysis and on-site filtration, with the speciation predicted using the humic ion binding model VI incorporated in the WHAM software [69]. In the most acidic lake (pH 4.7) all measurement techniques agreed, indicating negligible complexation or colloid formation. In circum-neutral waters, Mn concentrations were similar for each of the three measuring techniques indicating it was free from complexation. Zn concentrations determined by DGT, dialysis and filtration (0.45 μm) were in agreement when considering the uncertainty in the measurements (Fig. 11.4).

Significant differences between dialysis and DGT measurements of Cu were consistent with complexation by fulvic and humic substances. The greatest difference between the three measurement

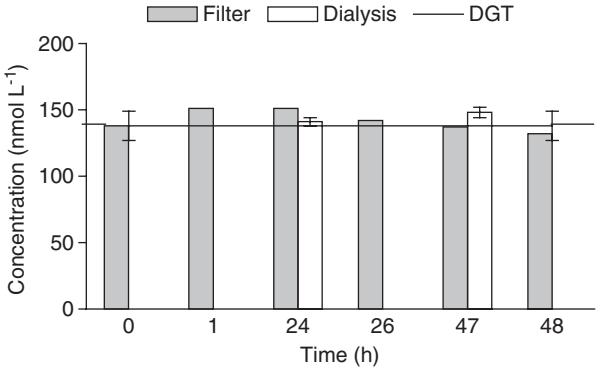

Fig. 11.4. Concentrations of Zn in Levers Water (pH 4.7) measured by DGT, dialysis and filtration through 0.45 μm filters (reprinted from Ref. [33]. Copyright (2003), with permission from American Chemical Society).

techniques, apparent for Fe, was attributed to organic complexation and the presence of large colloidal oxyhydroxides and lower molecular weight hydrolysis products.

The speciation of Cu and Zn was measured in two Swiss hard-waters and compared with results from competitive ligand exchange (CLE) experiments [34]. In mesocosms, both CLE and DGT measured a similar fraction of Zn, $76 \pm 9\%$ and $61 \pm 4\%$, respectively. For Cu, the addition of a strong synthetic ligand NTA, which can compete with the weakest binding sites of natural organic ligands, increased the fraction measured by DGT from $34 \pm 1\%$ to $57 \pm 1\%$. The result was similar for the CLE experiments conducted in the presence of NTA with a ratio of Cu_{DGT} to Cu_{CLE} of $81 \pm 6\%$. This result indicates that Cu–NTA complexes are fully measurable by DGT, in agreement with previous work [11,39]. Odzak *et al*. [24] measured the speciation of Cu, Mn and Zn in a Swiss lake using DGT and CLE. The concentrations of Cu and Ni measured by DGT amounted to only 15–25% of the total concentrations. Measurements by CLE showed these two metals to be almost entirely organically complexed. These results are consistent with the complexes being DGT labile, but their diffusion coefficients being about 20% of those for simple inorganic species [26]. For Zn and Mn, the fraction measurable by DGT was 36 to $>90\%$ and 50–100%, respectively, indicating that these two metals are much less organically complexed than Cu.

Scally *et al*. [70] investigated the distribution of Pb between inorganic and organic forms using synthetic solutions containing fulvic acid, humic acid and NTA over a pH range of 4–8. Diffusive gels with three different compositions, APA2, APA3 and restricted (RG), were used. When the appropriate diffusion coefficient for each diffusing species in each gel type was considered, the species distribution measured by DGT was in a good agreement with the predictions made using the speciation model *ECOSAT* [71]. Measurements made using only the RG gel provided good estimates of the inorganic species in solution, provided complexation by organic ligands was not dominant.

DGT has also been used by Unsworth *et al*. [72] to measure cadmium speciation in solutions with both synthetic and natural ligands and compared the results with model outputs. Cd was found to be fully labile in its free state and as complexes of $CdC1_2$, $Cd(NO_3)^+$, Cd–NTA and Cd–DGA, but the appropriate diffusion coefficients for the organic complexes, which were 25–30% lower than D_{Gel}, must be used in the calculation. To estimate the proportion of Cd complexed by fulvic acid (FA), DGT devices containing a RG were used. Again, *ECOSAT*

predicted the correct magnitude and pH dependence of the complexation by FA.

A rigorous comparison of trace metal speciation techniques involving several laboratories using several independent speciation techniques and modelling approaches has recently been reported [27,28]. The techniques investigated included DGT, ASV with a gel-integrated microelectrode (GIME), permeable liquid membrane (PLM) and the Donnan membrane technique (DMT). The concentrations of Cd, Cu and Pb decreased in the order DGT $\geqslant$ GIME-VIP $\geqslant$ PLM $\approx$ DMT, consistent with the known properties of the techniques. The results were compared with speciation calculations performed with WHAM VI and Visual MINTEQ modelling software, the latter incorporating the Non-Ideal Competitive Adsorption (NICA)-Donnan model for ion binding to humic substances. The dynamic fraction of species measured by DGT and ASV includes several species that contribute to the signal in different proportions according to their diffusion coefficients. Previous comparison with model predictions has taken this into account [33,68], but this paper provided new terminology. The concentration measured by the technique assuming no kinetic limitations was defined as $c_{\mathrm{max}}^{\mathrm{dyn}}$, the maximum dynamic concentration. When fulvic acid is the only ligand present, the following equation applies:

$$c_{\mathrm{max}}^{\mathrm{dyn}} = \sum (C_{\mathrm{i}} + xC_{\mathrm{o}}) \tag{11.22}$$

The ratio x, given by the diffusion coefficient of metal fulvic acid complexes, D_{o}, divided by the diffusion coefficient of simple inorganic metal species, D_{i}, has a value of 0.2 to a good approximation. For the hard-water Furtbach stream, metals Ni, Cu and Cd, dynamic speciation measurements agreed well with model predictions of $c_{\mathrm{max}}^{\mathrm{dyn}}$ calculated from total dissolved concentrations (Fig. 11.5).

In general, GIME measured less metal than DGT, consistent with the smaller time window available for metal uptake. For Pb in the River Wyre, a soft-water with high dissolved organic carbon (DOC), DGT and GIME agreed well, but were an order of magnitude lower than model predictions. These results suggest that most metal complexed by humic substances in the environment is labile within the timescale of DGT.

11.4.4 Bioavailability

Webb and Keough [36] have investigated whether DGT could be used as a surrogate for the bioaccumulation of trace metals (Cu, Cd, Pb and Zn)

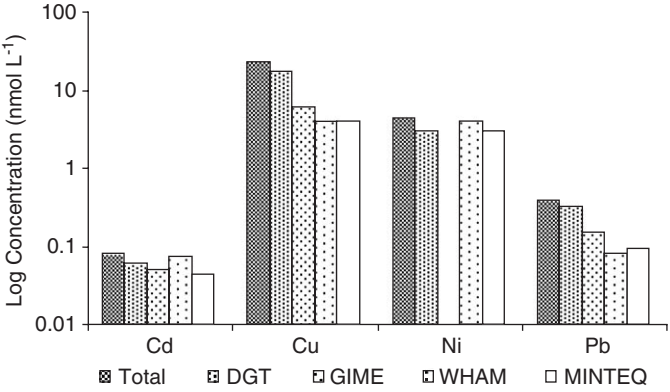

Fig. 11.5. Concentrations measured by different speciation techniques compared to total measurements and speciation calculations by WHAM VI and Visual MINTEQ (reprinted from Ref. [27]. Copyright (2006), in part with permission from American Chemical Society).

by mussels. Over the 1 year study period, mussel concentrations of Zn and Cd were similar at the four stations (two inside and two outside an enclosed marina), while Cu and Pb showed significant temporal and spatial variations. While DGT also showed significant temporal variations, there were more defined differences between sites. It was suggested that bio-fouling effects on the DGT sampling devices need to be quantified or avoided by using multiple short-duration deployments.

The accumulation of Cu by the gills of Rainbow Trout (*Oncorhynchus mykiss*) was compared with measurements of Cu speciation by DGT and ion selective electrodes (ISE) [38]. Natural organic matter (NOM) decreased the uptake of Cu by trout gills and the concentrations measured by both DGT and ISE. The source of NOM also seemed to affect the free ion concentration and the amount of Cu taken by the trout gills and DGT, with allochthonous (terrestrially derived) NOM decreasing uptake more effectively than autochthonous (algal-derived) NOM.

Tusseau-Vuillemin *et al*. [39] used DGT to evaluate the toxicity of Cu to *Daphnia magna* in solutions containing EDTA, NTA and glycine. DGT could not predict the influence of NTA, as Cu–NTA complexes were completely labile. However, as Cu–EDTA complexes were completely inert, Cu toxicity could be predicted by the DGT measurement. Cu–glycine complexes were both partially measurable and toxic. Humic acids and aged and fresh algal exudates all appeared partially labile and non-toxic when using APA2 gels. The contribution to the DGT-measured mass was greatly reduced when a restricted gel was used, as complexes

with humic material and aged algal exudates were largely excluded. It was concluded that DGT with a RG is a powerful tool for assessing the bioavailable fraction of Cu in natural waters. A bioavailable fraction was calculated in English and Italian rivers by Garofalo *et al*. [37] as the DGT-measured concentration divided by the total dissolved concentration. The percentage of bioavailable fractions of Ni, Cu, Zn, Cd and Pb were 14–51%, 5–52%, 2–66%, 0.4–16% and 9% to completely labile, respectively.

Al measured by DGT was found to predict the gill uptake of Al more accurately than conventional column measurements of Al, as evidenced by strong linear correlations with the fish physiological responses, increased blood glucose levels and decreased plasma chloride [40]. The better prediction by DGT was attributed to the measurement being *in situ*.

11.4.5 The use of DGT as a routine monitoring tool

As an alternative to logistically demanding and expensive discrete sampling, routine monitoring of estuarine waters was carried out using DGT [41]. Time-integrated DGT concentrations showed good correlations with composite total dissolved concentrations (<0.45 μm), sampled at 4 h intervals over 24 h period. The following correlation coefficients were obtained: Ni, $r = 0.92$; Cu, $r = 0.97$; Zn, $r = 0.91$ and Pb, $r = 0.80$. Using free metal diffusion coefficients, corrected to the *in situ* temperature, DGT concentrations as a fraction of the total dissolved (<0.45 μm) were $21 \pm 2\%$, $29 \pm 11\%$, $28 \pm 5\%$ and $27 \pm 12\%$ for Cu, Pb, Zn and Ni, respectively. Interestingly, the Cu results correspond exactly with the predicted $c_{\max}^{\mathrm{dyn}}$ for 100% complexation by fulvic acid. While it was acknowledged that the fraction measured was operationally defined, the overall conclusion was that DGT is a very promising *in situ* monitoring tool for these dynamic estuarine waters. Munksgaard and Parry [42] found sufficient sensitivity, accuracy and precision for the measurement of Mn, Cu, Cd, Co and Pb in nearly pristine, but turbid coastal sea-water. The DGT measured fraction was 44–63% for Cu but was close to 100% for both Co and Cd.

A study was conducted in Queensland's Gold Coast Broadwater area, Australia, to determine whether anti-biofouling paints used on small recreational boats lead to increased levels of Cu in and around recreational boat anchorage sites [43]. While total dissolved Cu concentrations were above the 1.3 μg L^{-1} guideline value when the number of boats in the vicinity exceeded 30, DGT concentrations were well below

this value at all of the boat numbers observed. DGT results showed a strong linear correlation ($n = 14$; $r = 0.82$; $p < 0.001$) with the number of recreational boats in the vicinity of the anchorage sites, while total dissolved Cu concentrations were less significantly correlated ($n = 14$; $r = 0.70$; $p < 0.01$). This was the first study to show a clear correlation between recreational boat numbers and available Cu concentrations.

Cleven *et al*. [44] used DGT for routine monitoring of Ni, Cu and Pb concentrations in the rivers Meuse and Rhine. They concluded that while DGT was suitable as a robust tool for routine monitoring, the associated errors were greater (~20–30%) than those observed under controlled laboratory conditions (<10%), due partly to variations in some of the constants (e.g. temperature) used in the DGT calculations.

11.4.6 Metal remobilization from settling particles

DGT has been used to measure metal remobilization from settling particles in a lake-water column. The DGT device formed the base of a cylindrical sediment trap. Any remobilization of trace metals from particles was measured as an increase in mass taken up by DGT [73]. Laboratory tests indicated that there was negligible turbulence near the bottom of the trap, where the particles are collected and consequently uptake is likely to be diffusion controlled. Control devices, deployed upside down and thus, not in contact with settling particles, were used to measure metal uptake in the absence of settling particles. Remobilization of Al, Ba, Co and from settling particles significantly increased the DGT accumulated masses over the controls, with the release being attributed to reductive dissolution of Mn oxides.

11.5 CONCLUSION

DGT has been used to measure a wide range of analytes (transition and heavy metals, rare-earth elements, radioisotopes and anionic species) in natural waters simply by varying the binding agent used within the resin-gel layer. While DGT is simple to use and the interpretation in terms of concentration is straightforward in most cases, the exceptions are being increasingly explored. The exact dependence of the DGT measurement on ionic strength and diffusive layer thickness has increased our detailed understanding of the processes involved. DGT's capability to discriminate solution species, based on their diffusion coefficients in the diffusion layer, has been explored in the laboratory

and successfully applied to fresh-waters. This rigorous foundation has provided a better appreciation of what DGT measures when it is used as an *in situ* passive sampler for monitoring purposes. The dependence of the DGT measurement on the kinetics of free metal release from solution complexes and colloids is beginning to emerge. Advances in understanding these challenging systems require both dynamic models of the DGT–natural water system and better treatments of the kinetics of supply from natural complexes formed with ligands that often contain a spectrum of binding sites with differing conditional constants. These complexities, which are advancing our understanding of natural waters, should not obscure the fact that there is a continuous stream of publications that demonstrate diverse applications of DGT as a measurement tool in natural waters.

REFERENCES

1 W. Davison and H. Zhang, *Nature*, 367 (1994) 546.
2 H. Zhang and W. Davison, *Anal. Chem.*, 67 (1995) 3391.
3 R. Dahlqvist, H. Zhang, J. Ingri and W. Davison, *Anal. Chim. Acta*, 460 (2002) 247.
4 L.Y. Chang, W. Davison, H. Zhang and M. Kelly, *Anal. Chim. Acta*, 368 (1998) 243.
5 C. Murdock, M. Kelly, L.Y. Chang, W. Davison and H. Zhang, *Environ. Sci. Technol.*, 35 (2001) 4530.
6 M.A. French, H. Zhang, J.M. Pates, S.E. Bryan and R.C. Wilson, *Anal. Chem.*, 77 (2005) 135.
7 H. Zhang, W. Davison, R. Gadi and T. Kobayashi, *Anal. Chim. Acta*, 370 (1998) 29.
8 P.R. Teasdale, S. Hayward and W. Davison, *Anal. Chem.*, 71 (1999) 2186.
9 Ø.A. Garmo, O. Røyset, E. Steinnes and T.P. Flaten, *Anal. Chem.*, 75 (2003) 3573.
10 H. Zhang and W. Davison, *Anal. Chim. Acta*, 398 (1999) 329.
11 S. Scally, W. Davison and H. Zhang, *Environ. Sci. Technol.*, 37 (2003) 1379.
12 M.H. Tusseau-Vuillemin, R. Gilbin and M. Taillefert, *Environ. Sci. Technol.*, 37 (2003) 1645.
13 J. Galceran, J. Puy, J. Salvador, J. Cecilia, F. Mas and J.L. Garces, *Phys. Chem. Chem. Phys.*, 5 (2003) 5091.
14 N. Lehto, W. Davison, H. Zhang and W. Tych, *Environ. Sci. Technol.*, 40 (2006) 6368.
15 K.W. Warnken, H. Zhang and W. Davison, *Anal. Chim. Acta*, 508 (2004) 41.

16 H. Zhang, *Environ. Sci. Technol.*, 38 (2004) 1421.
17 S. Scally, W. Davison and H. Zhang, *Anal. Chim. Acta*, 558 (2006) 222.
18 J. Gimpel, H. Zhang, W. Hutchinson and W. Davison, *Anal. Chim. Acta*, 448 (2001) 93.
19 M.C. Alfaro-De la Torre, P.Y. Beaulieu and A. Tessier, *Anal. Chim. Acta*, 418 (2000) 53.
20 M.R. Sangi, M.J. Halstead and K.A. Hunter, *Anal. Chim. Acta*, 456 (2002) 241.
21 K.W. Warnken, H. Zhang and W. Davison, *Anal. Chem.*, 78 (2006) 3780.
22 A.J. Peters, H. Zhang and W. Davison, *Anal. Chim. Acta*, 478 (2003) 237.
23 K.W. Warnken, H. Zhang and W. Davison, *Anal. Chem.*, 77 (2005) 5440.
24 N. Odzak, D. Kistler, H.B. Xue and L. Sigg, *Aquat. Sci.*, 64 (2002) 292.
25 S. Denney, J. Sherwood and J. Leyden, *Sci. Total Environ.*, 239 (1999) 71.
26 H. Zhang and W. Davison, *Anal. Chem.*, 72 (2000) 4447.
27 E.R. Unsworth, K.W. Warnken, H. Zhang, W. Davison, F. Black, J. Buffle, J. Cao, R. Cleven, J. Galceran, P. Gunkel, E. Kalis, D. Kistler, H.P. van Leeuwen, M. Marin, S. Noel, Y. Nur, N. Odzak, J. Puy, W. van Riemsdijk, E. Temminghoff, M.-L. Tercier-Waeber, S. Toepperwien, R.M. Town, L. Weng and H. Xue, *Environ. Sci. Technol.*, 40 (2006) 1942.
28 L. Sigg, F. Black, J. Buffle, J. Cao, R. Cleven, W. Davison, J. Galceran, P. Gunkel, E. Kalis, D. Kistler, M. Marin, S. Noel, Y. Nur, N. Odzak, J. Puy, W. van Riemsdijk, E. Temminghoff, M.-L. Tercier-Waeber, S. Toepperwien, R.M. Town, E. Unsworth, K.W. Warnken, L. Weng, H. Xue and H. Zhang, *Environ. Sci. Technol.*, 40 (2006) 1934.
29 M.R. Twiss and J.W. Moffett, *Environ. Sci. Technol.*, 36 (2002) 1061.
30 W. Davison, G. Fones, M. Haper, P. Teasdale, H. Zhang. In: J. Buffle and G. Horvai (Eds.), *In situ Monitoring of Aquatic Systems: Chemical Analysis and Speciation*, Wiley, Chichester, 2000.
31 H. Zhang and W. Davison, *Pure Appl. Chem.*, 73 (2001) 9.
32 A.J. Downard, J. Panther, Y.C. Kim and K.J. Powell, *Anal. Chim. Acta*, 499 (2003) 17.
33 J. Gimpel, H. Zhang, W. Davison and A.C. Edwards, *Environ. Sci. Technol.*, 37 (2003) 138.
34 S. Meylan, N. Odzak, R. Behra and L. Sigg, *Anal. Chim. Acta*, 510 (2004) 91.
35 E.R. Unsworth, H. Zhang and W. Davison, *Environ. Sci. Technol.*, 39 (2005) 624.
36 J.A. Webb and M.J. Keough, *Mar. Pollut. Bull.*, 44 (2002) 222.
37 E. Garofalo, S. Ceradini and M. Winter, *Ann. Chim.*, 94 (2004) 515.
38 C.D. Luider, J. Crusius, R.C. Playle and P.J. Curtis, *Environ. Sci. Technol.*, 38 (2004) 2865.
39 M.H. Tusseau-Vuillemin, R. Gilbin, E. Bakkaus and J. Garric, *Environ. Toxicol. Chem.*, 23 (2004) 2154.
40 O. Røyset, B.O. Rosseland, T. Kristensen, F. Kroglund, Ø.A. Garmo and E. Steinnes, *Environ. Sci. Technol.*, 39 (2005) 1167.

41 R.J.K. Dunn, P.R. Teasdale, J. Warnken and R.R. Schleich, *Environ. Sci. Technol.*, 37 (2003) 2794.
42 N.C. Munksgaard and D.L. Parry, *J. Environ. Monit.*, 5 (2003) 145.
43 J. Warnken, R.J.K. Dunn and P.R. Teasdale, *Mar. Pollut. Bull.*, 9 (2004) 833.
44 R. Cleven, Y. Nur, P. Krystek and G. Van den Berg, *Water Air Soil Pollut.*, 165 (2005) 249.
45 B.L. Larner and A.J. Seen, *Anal. Chim. Acta*, 539 (2005) 349.
46 W. Li, H. Zhao, P.R. Teasdale and R. John, *Polymer*, 43 (2002) 4803.
47 W. Li, H. Zhao, P.R. Teasdale, R. John and S. Zhang, *React. Funct. Polym.*, 52 (2002) 31.
48 W.J. Li, P.R. Teasdale, S.Q. Zhang, R. John and H.J. Zhao, *Anal. Chem.*, 75 (2003) 2578.
49 W.J. Li, H.J. Zhao, P.R. Teasdale and F.Y. Wang, *Talanta*, 67 (2005) 571.
50 W. Li, H. Zhao, P.R. Teasdale, R. John and S. Zhang, *Anal. Chim. Acta*, 464 (2002) 331.
51 W.J. Li, H.J. Zhao, P.R. Teasdale, R. John and F.Y. Wang, *Anal. Chim. Acta*, 533 (2005) 193.
52 S. Mason, R. Hamon, A. Nolan, H. Zhang and W. Davison, *Anal. Chem.*, 77 (2005) 6339.
53 S. Mason, R. Hamon, A. Nolan, H. Zhang and W. Davison, *Anal. Chem.*, 77 (2005) 6339.
54 K.W. Warnken, H. Zhang and W. Davison, *Anal. Chem.*, 76 (2004) 6077.
55 P.W. Atkins, *Physical Chemistry*, Oxford University Press, Oxford, 1982.
56 J.R. Lead, K.J. Wilkinson, K. Starchev, S. Canonica and J. Buffle, *Environ. Sci. Technol.*, 34 (2000) 1365.
57 J.R. Lead, K. Starchev and K.J. Wilkinson, *Environ. Sci. Technol.*, 37 (2003) 482.
58 L.P. Yezek and H.P. van Leeuwen, *J. Colloid Interface Sci.*, 278 (2004) 243.
59 N. Fatin-Rouge, A. Milon, J. Buffle, R.R. Goulet and A. Tessier, *J. Phys. Chem. B*, 107 (2003) 12126.
60 J.A. Webb and M.J. Keough, *Sci. Total Environ.*, 298 (2002) 207.
61 H. Docekalova and P. Divis, *Talanta*, 65 (2005) 1174.
62 H. Ernstberger, H. Zhang and W. Davison, *Anal. Bioanal. Chem.*, 373 (2002) 873.
63 S. Barakat and L. Giusti, *J. Phys. IV*, 107 (2003) 111.
64 L. Giusti and S. Barakat, *Water Air Soil Pollut.*, 161 (2005) 313.
65 D. Malinovsky, R. Dahlqvist, D.C. Baxter, J. Ingri and I. Rodushkin, *Anal. Chim. Acta*, 537 (2005) 401.
66 R. Dahlqvist, P.S. Andersson and J. Ingri, *Earth Planet. Sci. Lett.*, 233 (2005) 9.
67 Ø.A. Garmo, N. Lehto, H. Zhang, W. Davison, O. Røyset and E. Steinnes, *Environ. Sci. Technol.*, 40 (2006) 4754.

68 H.P. van Leeuwen, R.M. Town, J. Buffle, R. Cleven, W. Davison, J. Puy, W.H. van Riemsdijk and L. Sigg, *Environ. Sci. Technol.*, 39 (2005) 8545.
69 E. Tipping, *Aquat. Geochem.*, 4 (1998) 3.
70 S. Scally, H. Zhang and W. Davison, *Aust. J. Chem.*, 57 (2004) 925.
71 M.G. Keizer and W.H. van Riemsdijk, *ECOSAT*, Department of Soil Science and Plant Nutrition, Wageningen Agricultural University, Wageningen, The Netherlands, 2002.
72 E.R. Unsworth, H. Zhang and W. Davison, *Environ. Sci. Technol.*, 39 (2005) 624.
73 J. Hamilton-Taylor, E.J. Smith, W. Davison and H. Zhang, *Limnol. Oceanogr.*, 44 (1999) 1772.

Chapter 12

Use of ceramic dosimeters in water monitoring

Hansjörg Weiß, Kristin Schirmer, Stephanie Bopp and Peter Grathwohl

12.1 INTRODUCTION

Passive sampling with ceramic dosimeters allows for time-integrated monitoring of dissolved chemicals in ground and surface water. The purely diffusion controlled device is based on a porous ceramic membrane. This membrane is in the shape of a tube. The ceramic tube functions as a diffusion barrier and at the same time serves as a container to hold a solid sorbent. The latter can be selected according to compounds of interest and time scale needed for monitoring. The sorbents are required to have a high affinity and capacity for the uptake of the chemicals of concern combined with an easy extraction at high analyte extraction recovery rates. As long as such sorbents can be found, ceramic dosimeters fit any analytical need.

Diffusive transport of chemicals across the ceramic membrane at steady state can be described by Fick's first law. Thus, the accumulated mass of a chemical at the end of an exposure period can be used to calculate the time-weighted average (TWA) concentration at which this chemical was present over the entire sampling time. Based on this, the ceramic dosimeter allows for quantification of chemical concentrations over extended periods, without the need for calibration or frequent snapshot sampling.

The idea of the ceramic dosimeter was first conceived by Grathwohl [1] and by now, a number of laboratory experiments as well as explorations in the field have proven the suitability of ceramic dosimeters for time-integrated, long-term monitoring. Applications to date include the sampling of polycyclic aromatic hydrocarbons (PAHs) using Amberlite IRA-743 sorbent (available from Sigma-Aldrich) as solid receiving

Comprehensive Analytical Chemistry 48
R. Greenwood, G. Mills and B. Vrana (Editors)
Volume 48 ISSN: 0166-526X DOI: 10.1016/S0166-526X(06)48012-0

phase [2–4] as well as the sampling of benzene, toluene, ethylbenzenes and xylenes (BTEX) [5], naphthalenes [5] and chlorinated hydrocarbons (CHCs) [5,6] using Dowex Optipore L-493 sorbent (available from Supelco). Furthermore, the ceramic dosimeter provided the basis for the development of the Toximeter, the first passive sampler that is directly compatible with toxicological tests. Biosilon polystyrene beads (available from Nunc) were used as the sorbent material in the initial development of the Toximeter, which focused on PAH sampling and subsequent testing in a bioassay measuring responses elicited in vertebrate cells (see also Chapter 18).

The goal of this chapter is to provide details on the functioning of ceramic dosimeter sampling devices with particular focus on the role of the ceramic membrane and requirements regarding the solid receiving phase. Additionally, a number of practical considerations will be discussed to highlight strengths and limitations of ceramic dosimeters in the field.

12.2 CERAMIC DOSIMETER DESIGN

The ceramic dosimeter consists of a ceramic tube with a diameter of 1 cm and a wall thickness of 1.5 mm (manufactured by UFS Schumacher, Crailsheim, Germany). The pore size of the inner wall coating of the tube is 5 nm. The length of the tube can be varied, but in most applications so far a length of 5 cm was used. The tube is filled with water-saturated sorbent and closed at either end with caps made of, e.g., polytetrafluoroethylene (PTFE) (Fig. 12.1).

12.2.1 Ceramic membrane

The ceramic membrane serves both as a diffusion barrier and as a container to hold the sorbent material. Key characteristics of this membrane with regard to quantitative time-integrated passive sampling are its porosity and inertness, its inner pore size and its thickness.

12.2.1.1 Porosity and inertness

The porosity (ε) of the ceramic membrane was measured by Piepenbrink [4] by means of a capillary pyknometer and determined to be 0.305 (or 30.5%). The membrane can easily be saturated with water. Water saturation does not lead to swelling that can occur with some organic polymers. With the high porosity and water saturation, a steady-state concentration profile of chemicals within the membrane

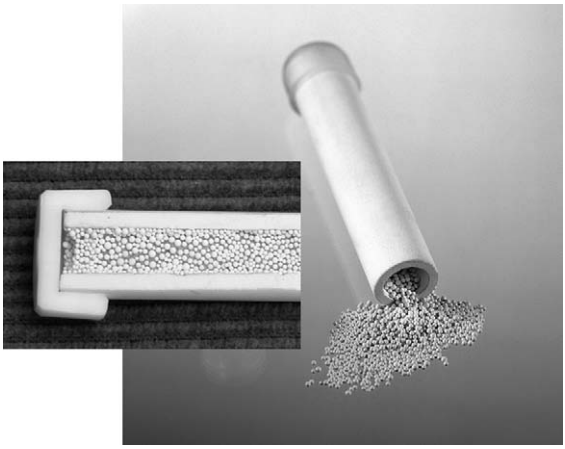

Fig. 12.1. Dosimeter design and cross section through the ceramic tube filled with sorbent material.

can be accomplished quickly with no significant lag times relative to the usual sampling periods, which are typically several weeks to months. This is also related to the inertness of the membrane, which is typical for ceramics in general. Piepenbrink [4] modeled the breakthrough of phenanthrene through the ceramic membrane and found a quasi–steady-state to develop within an hour of exposure.

12.2.1.2 Pore size

The inner wall of the ceramic membrane has a pore size of 5 nm. With this characteristic, the ceramic membrane prevents microorganisms from entering the interior of the ceramic tube (cut-off for microorganisms is a pore size of about 200 nm). The small pore size also minimizes flow of water and limits solute transfer to diffusion only.

12.2.1.3 Thickness

The wall of the ceramic tube is 1.5 mm thick. With this thickness, the ceramic tube forms a rate-limiting diffusion barrier because it is larger than any diffusion boundary barrier so far described under environmentally relevant conditions. Thus, even under low-flow conditions, where a significant boundary layer may form outside of the sampling device, the sampling behavior can be assumed to be determined by diffusion through the ceramic membrane alone. Gale [7], for example, reported an aqueous boundary layer thickness of 100–400 μm in a quiescent aqueous system. This is about 1/15 to 1/4 of the thickness of the

ceramic membrane. The great advantage of the ceramic membrane therefore is that uptake of chemicals is predictable based on its characteristics. Along these lines, uptake of chemicals is independent of hydrodynamic flow because effects of flow velocity on the diffusion boundary layer around the sampling device have no impact on the diffusion barrier formed by the ceramic membrane. Taken together, the thickness of the ceramic membrane forms the basis for quantitative analysis of TWA contaminant concentrations without the necessity to calibrate for chemical uptake in the laboratory or otherwise account for varying exposure conditions.

12.2.2 Sorbent material

Upon diffusion of solutes through the ceramic membrane, they need to be trapped onto a receiving phase. This step removes the chemical from the aqueous phase inside the ceramic tube. The role of this is to maintain a steep concentration gradient between the exterior and the interior of the sampler in order to ensure continuous diffusion along the gradient into the sampling device. Thus, the sorbents need to have a high affinity as well as a high capacity for the uptake of the chemicals to be sampled. In the ceramic dosimeter, this is accomplished by means of solid sorbent beads. In as much as the ceramic dosimeter is used under water-saturated conditions, the beads need furthermore to be easily wetted by water and non-swelling. Additionally, in order to allow for chemical analysis after sampling, they are required to yield high recovery rates of the target chemicals by means of solvent extraction or, potentially, thermo-desorption.

Three different bead materials have thus far been identified to fulfill these criteria. These are Amberlite IRA-743, which has proven suitable for sampling of PAHs [2–4], Biosilon, which has been applied in the ceramic membrane-based Toximeter for sampling PAHs (see Chapter 18), as well as Dowex Optipore L-493, the sorbent material of choice for BTEX, naphthalenes [5] and CHCs [5,6]. In contrast, activated carbon (F100) as well as XAD resin (XAD8), which sorb many organic chemicals very well, showed either very low recovery rates or cannot easily be handled in water [8].

For chemical analysis of the sorbent materials after sampling, a simple solvent extraction is desired. The materials mentioned above can be extracted two to three times using acetone. The pooled acetone extracts are subsequently spiked with deuterated internal standards for a direct GC–MS analyses [2,4,5]. Based on this method, recovery rates

for Dowex Optipore L-493 upon 2 weeks of contact with the chemicals in mixture were 92%, 95% and 96% for BTEX, naphthalenes and CHSs, respectively [5]. Recovery rates for Amberlite IRA 743 upon 4 months of contact with a mixture of PAHs were 101% for naphthalene, 98% for acenaphthene, 100% for fluorene, 97% for phenanthrene, 94% for fluoranthene, 83% for benzo[a]anthracene and 63% for benzo[a]pyrene ($n = 3$ for each PAH; [3]). Although recovery rates have not explicitly been tested in the laboratory upon exposures beyond 4 months of contact time, the results obtained in field exposures, using Dowex Optipore L-493 for 3 months [5] or Amberlite IRA 743 for up to 12 months [2], are in support of the high extraction efficiency and recovery rates obtained in the laboratory.

12.2.3 Determination of time-weighted average chemical concentrations

The diffusive flux of chemicals across the ceramic membrane is defined by Fick's first law of diffusion [9]. This law states

$$F = D\frac{\Delta C}{\Delta x} \tag{12.1}$$

F (g s^{-1} cm^{-2}) describes the mass flux, i.e., the accumulated mass M (g) of a certain chemical per area A (cm^2) available for diffusion throughout a certain time t (s):

$$\frac{M}{At} = D\frac{\Delta C}{\Delta x} \tag{12.2}$$

With reference to ceramic dosimeters, M is what is being measured upon solvent extraction of the sorbent material and subsequent chemical analysis. The term Δx (cm) describes the diffusion path length, which, in the case of the ceramic membrane, equals the thickness of the membrane, i.e., 1.5 mm. The term ΔC (g cm^{-3}) is the difference in aqueous chemical concentration between the sampling environment C_W (g cm^{-3}) and the inner part of the ceramic tube C_I (g cm^{-3}). The difference $C_W - C_I$ must be kept at its maximum during the whole monitoring period (quasi–steady-state diffusion rate) (Fig. 12.2).

This is accomplished by the solid sorbent material inside the ceramic membrane. Given a high affinity of the chemicals of concern to the sorbent (for selection see Section 12.2.2), the aqueous concentration of the chemicals in the inner part of the sampler can be assumed to approach zero. Thus, ΔC can be re-written as C_W, the term sought for

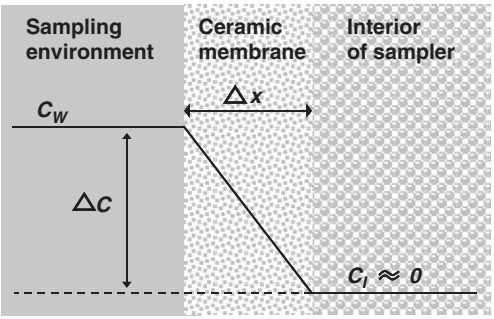

Fig. 12.2. Concentration gradient across the ceramic membrane.

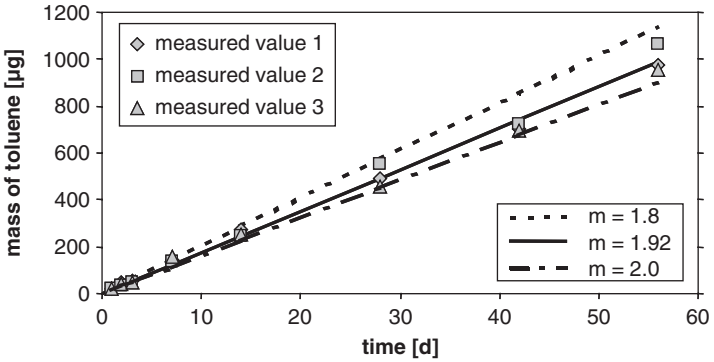

Fig. 12.3. Uptake of toluene in the ceramic dosimeter measured over 8 weeks. A constant aqueous toluene concentration was obtained and maintained by pre-loaded Dowex Optipore L-493 serving as a reservoir. The measured values 1 to 3 represent three replicates that were taken from the same batch container at each time point. Lines represent the calculated cumulative mass uptake (Eq. (12.2)) for different Archie's law exponents m. The best fit was obtained for $m = 1.92$ ($\varepsilon = 0.305$, $\Delta C = 4.100\,\mu g\,L^{-1}$, $D_e = 9.58 \times 10^{-6}\,cm^2\,s^{-1}$ for 20°C, $\Delta x = 0.15\,cm$, $A = 7.6\,cm^2$).

quantification of TWA chemical concentration:

$$C_W = \frac{M\Delta x}{AtD_e} \tag{12.3}$$

The term D_e ($cm^2\ s^{-1}$) in this equation stands for the effective diffusion coefficient. It accounts for the altered diffusion of chemicals in the porous membrane compared to water according to Archie's law:

$$D_e = D_w \varepsilon^m \tag{12.4}$$

where D_w ($cm^2\ s^{-1}$) is the diffusion coefficient of the selected chemical in water, ε (–) is the porosity of the ceramic membrane (i.e., 0.305) and m (–) is Archie's law exponent, which in porous media generally ranges from 1.5 and 2.5 [10]. For the ceramic membrane specifically, the Archie's law exponent ranged from 1.8 to about 2.0 in calibration experiments in the laboratory [3,4,6] and was used at a value of 2.0 for applications in the field [2,3]. Figure 12.3 shows the determination of m for toluene according to Blos [6].

The diffusion coefficient in water, D_W, can be calculated for various organic compounds according to Worch [11] (see Section 12.2.4). One determinant of D_W is temperature, the other molecular weight and viscosity of the water. The only parameter that needs to be accounted for field applications is therefore the average temperature.

12.2.4 Effect of temperature

The temperature influences the diffusion coefficient of chemicals in water, D_W, and therefore the mass of chemicals taken up by the ceramic dosimeter during the monitoring period. According to Worch [11], D_W can be calculated as

$$D_W = 3.595 \times 10^{-7} \frac{T}{\eta \cdot M^{0.53}} \tag{12.5}$$

where T (K) is the absolute temperature, η (mPa s) the dynamic viscosity and M ($g\ mol^{-1}$) the molecular weight of the chemicals. On account of this, the average temperature should be known during sampling. A rise in temperature leads to an increase in the diffusion coefficients and thus in a higher mass uptake. If this is not accounted for, the calculation of TWA aqueous concentrations of the chemicals would lead to an underestimation of water concentration. Overall, however, the influence of temperature is moderate. A temperature increase of 1 K corresponds to an increase of the diffusion coefficients of about 3–4% in the range of 8–20°C.

12.3 PRACTICAL CONSIDERATIONS

12.3.1 Preparation of the ceramic dosimeter for field application

In order to prevent background contamination, the sorbent materials have to be cleaned with acetone prior to use. The acetone is decanted and the washing step repeated until the solvent stays clear with no

Fig. 12.4. Illustration of a stainless steel cage used in application of the ceramic tube in the field.

discoloration. The sorbents are then stored dry or under water until application. Prior to use, the sorbents are wetted with distilled water. About 1.5 g is placed into each ceramic tube, e.g., with the aid of a glass pipette. The tube is closed with the caps and mounted into a stainless steel holder put together by screws. An additional option is to place the ceramic tube into a stainless steel cage for protection from physical damage, impurities (dirt etc.) and easy access of water (Fig. 12.4).

The device is then placed into a bottle filled with distilled water and evacuated in an exsiccator to remove any air within the tube and to ensure a complete water saturation of the ceramic membrane. The prepared ceramic dosimeters can be stored in amber glass bottles filled with distilled water in the dark at 4°C for at least 4 weeks until deployment.

For deployment in the field, the ceramic dosimeter is tied by means of a polyethylene or nylon string to the stainless steel holder. The length of the string is chosen such that the samplers can be placed in the middle of the screened portion of a groundwater well or at the depth of interest in rivers and lakes. After the termination of sampling, the ceramic dosimeters are removed and placed in bottles with distilled water, or wrapped in tissue soaked in distilled water, and packed in zip plastic bags for transportation back to the laboratory.

12.3.2 Sampling rates

Sampling rate is a frequently used parameter for passive sampling devices. It describes the volume of water that is extracted with regard to

the chemical of concern within a certain time. In the case of the ceramic membrane, sampling rates (R in mL day^{-1}) are defined by Fick's first law according to the following equation [12]:

$$R = \frac{D_e A}{\Delta x} \tag{12.6}$$

Based on the relatively small area (A) and large diffusion path (Δx), sampling rates of ceramic membrane-based devices are relatively low. For example, sampling rates for commonly monitored PAHs were calculated to be between 1.5 and 2.5 mL day^{-1} at 14°C [2]. For comparison, sampling rates of semipermeable membrane devices (SPMDs) for PAHs have been measured to comprise up to several liters per day [12]. The low sampling rates of ceramic membrane-based devices emphasizes their suitability for long-term, time-integrated monitoring. Based on the low sampling rate, steep concentration gradients can be maintained for many months or even years. Furthermore, low sampling rates provide sufficient time for delivery of chemicals from the surrounding water toward the sampling device. This is particularly important for low-flow sampling environments, such as groundwater, where limitations due to high sampling rates have been observed at least for SPMDs [13]. The downside of the low sampling rate is that extended times are required to reach detection limits in the sampling devices (see Section 12.3.3). Thus, ceramic dosimeters are generally not well suited for sampling periods of less than 1 month in a low concentration environment (depending on the compounds to be assessed), where the mass collected would be below the detection limit. Because of their design, however, they are well equipped for long-term sampling in environments that would be otherwise difficult to probe.

12.3.3 Detection limits

In order to analyze the chemicals adsorbed by passive sampling, the mass of the chemicals needs to be above the detection limit of the extraction and analysis method. Thus, some preliminary information on chemical concentration is necessary if TWA chemical concentrations shall be determined by means of passive sampling. Based on the expected aqueous concentration of the chemicals, a minimum sampling time can be calculated prior to deployment of the sampling devices. Examples of this are provided in Table 12.1. As expected from the low sampling rates of the ceramic membrane (see also Section 12.3.2), sampling times to reach detection limits could range from a few months

TABLE 12.1
Minimum sampling times required to reach detection limits for selected chemicals in the ceramic dosimeter[a]

	PAHs		BTEX		CHCs	
	Naphthalene	Phenanthrene	Benzene	Toluene	TCE[c]	PCE[d]
Minimum mass (μg)[b]	0.09	0.12	1.2	1.35	6	6.3
Assumed aqueous concentration	Predicted required sampling times					
0.1 ($\mu g\,L^{-1}$)	330 d[e]	1.4 a[f]	9 a	11 a	61 a	73 a
1 ($\mu g\,L^{-1}$)	33 d	53 d	341 d	1.1 a	6.1 a	7.3 a
10 ($\mu g\,L^{-1}$)	3 d	5 d	34 d	41 d	224 d	267 d
100 ($\mu g\,L^{-1}$)	0.3 d	0.5 d	3.4 d	4.1 d	22.4 d	26.7 d

[a]Calculations are based on Eqs. (12.3) and (12.4) with $T = 10^{\circ}C$, $m = 2$, $\varepsilon = 0.305$, $\Delta x = 0.15\,cm$, $A = 8.4\,cm^2$.
[b]Minimum analyte mass detectable in the ceramic dosimeter by the method described in Bopp *et al*. [2]. The extraction volume in this method is 30 mL, which could be significantly reduced to improve sensitivity if needed. Detection limit is set to three times the detection limit of standard instrumental analytical methods.
[c]Trichloroethylene.
[d]Tetrachloroethylene.
[e]d = days.
[f]a = years.

to years. This supports the suitability of the ceramic membrane for sampling in highly polluted environments or for long-term monitoring.

12.3.4 Long-term stability

Once collected, chemicals do not significantly diffuse out of the ceramic dosimeter back into the water when the concentration in the surrounding water declines. To validate this type of long-term stability, ceramic dosimeters loaded with a specific mass of chemicals on Amberlite were immersed into a flow-through system with clean distilled water for different periods. The mass accumulated within the dosimeters was followed over time and compared with the initial accumulated mass. As illustrated in Fig. 12.5, little change in the accumulated masses was observed.

Another example of the long-term stability of ceramic dosimeters is presented by Martin *et al*. [5] for benzene and naphthalene extracted from Dowex Optipore L-493-filled devices over a period of 4 weeks. These results not only demonstrate the suitability of the sorbent materials but also the stability of sorbed chemicals within the sampling devices with no apparent biotic or abiotic degradation.

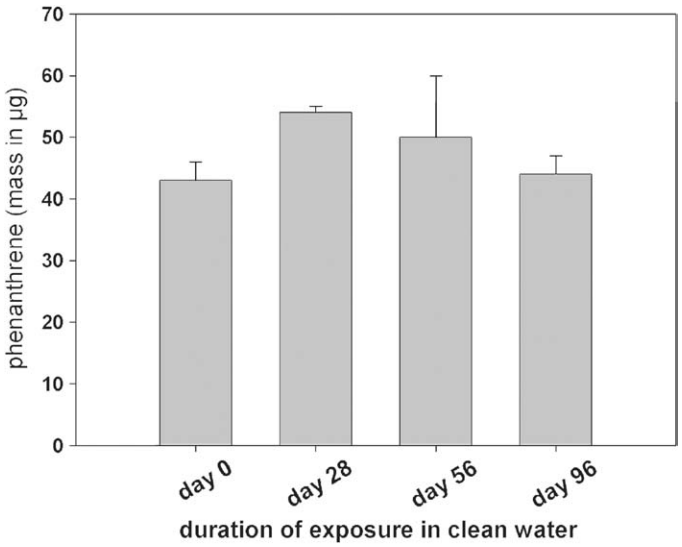

Fig. 12.5. Mass of phenanthrene extracted from ceramic dosimeters after purging in a flow-through system with clean water for up to 96 days [3]. Bars represent the average of three samplers with vertical lines representing the standard deviation.

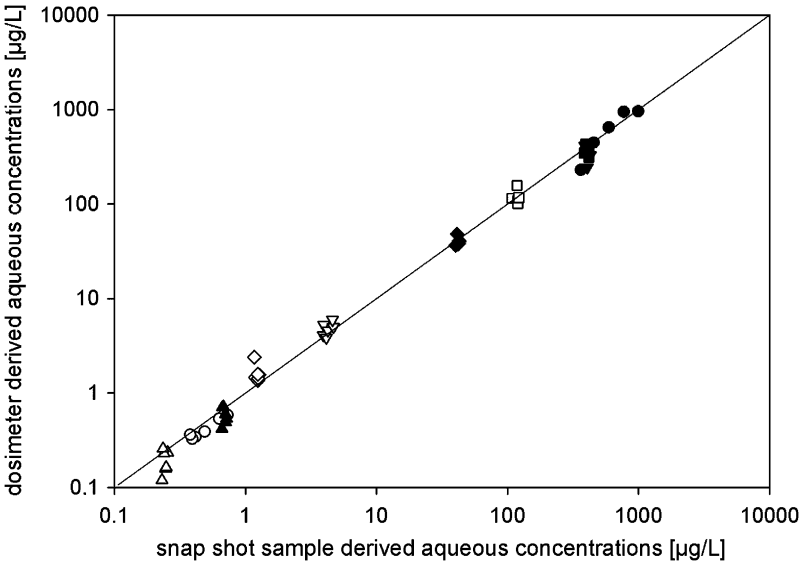

Fig. 12.6. Comparison of ceramic dosimeter derived and time-averaged snap-shot sample determined aqueous PAH concentrations for six sampling times over the course of 1 year in one groundwater borehole. For absolute agreement between the two sampling methods, symbols should lie on the diagonal line. Reprinted from Bopp *et al*. [2] with permission from Elsevier.

12.4 EXAMPLE OF FIELD RESULTS AND FUTURE WORK

So far, the ceramic dosimeter has been employed in the field for sampling a number of organic chemicals under various sampling conditions with a main focus on groundwater. Figures 12.6 and 12.7 are taken from Bopp *et al*. [2] where groundwater boreholes at a former gas works site were sampled for PAHs over the course of 1 year. They illustrate the sampling behavior of Amberlite IRA-743-filled ceramic dosimeters in a harsh environment: the borehole was found to contain an unexpected tar oil phase.

Because of its robustness and flexibility, many different sampling applications for the ceramic dosimeter can be envisaged. The robustness stems from the ceramic membrane. The flexibility is due to the possibility of filling the ceramic tube with any sorbent material to accumulate a chemical or chemical group of choice. Along these lines, extensive research was performed by Martin [14] in order to identify suitable sorbents and extraction methods for anions (nitrate) and cations (Cu, Zn). Additionally, applications for sampling different

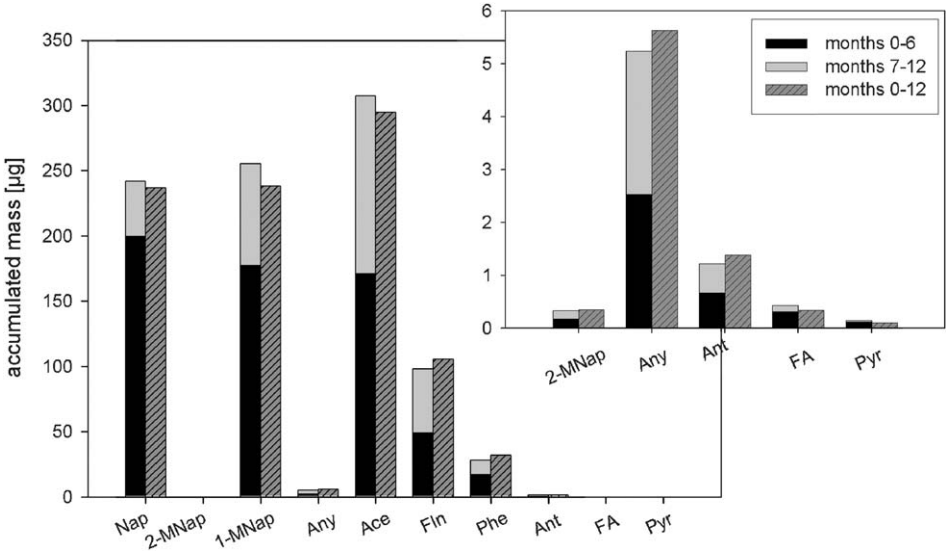

Fig. 12.7. Comparison of accumulated PAH masses collected over the whole exposure period in 12 months exposed ceramic dosimeters and the sum of accumulated masses in samplers exposed for the first (month 0–6) and the second 6 months (months 7–12) of a 1-year sampling campaign. Reprinted from Bopp *et al*. [2] with permission from Elsevier.

pharmaceuticals are also underway. The link of ceramic dosimeter derived samples to bioassay analysis, as initiated with the development of the Toximeter (see Chapter 18), is of particular value if the presence of toxicologically relevant chemical contaminants is unknown.

Taken together, any chemical can be collected in any aqueous environment by means of the ceramic dosimeter as long as a solid receiving phase with a high affinity and capacity for the chemical of concern can be found. Therefore, further research is also undertaken to explore the use of ceramic dosimeters as a monitoring instrument in surface waters (rivers, lakes) and sediments. One vision is to provide to authorities the ceramic dosimeters in a sealed cage for time-integrated monitoring at industrial sites with potentially problematic discharges into a river or lake. In principle, even single, temporary events can be detected by the dosimeters because of the long-term stability of once trapped compounds (see Section 12.3.4). Likewise, industrial chemical site owners could use the device as a reassurance that they release only wastewaters according to the quality required by law.

ACKNOWLEDGMENT

We would like to thank Dr. Matthias Piepenbrink (now University of Darmstadt, Germany) and Dr. Holger Martin (now ''Hydroisotop'' company, Germany) for continued discussions on ceramic membrane based passive sampling devices. Annegret Walz and Dr. Thomas Wendel (both University of Tübingen, Germany) are thanked for their help in chemical analysis.

REFERENCES

1 P. Grathwohl, Dosimeter, Deutsches Patent [DE 198 30 413 A1]. (30.10.2003).
2 S.K. Bopp, H. Weiß and K. Schirmer, Time-integrated monitoring of PAHs in ground water using the ceramic dosimeter passive sampling device, *J. Chromatogr. A*, 1072 (2005) 137.
3 H. Martin, Dissertation: *Entwicklung von Passivsammlern zum zeitlich integrierenden Depositions- und Grundwassermonitoring: Adsorberkartuschen und Keramikdosimeter*, University of Tübingen, 2000.
4 M. Piepenbrink, Master Thesis: *Entwicklung von Passivsammlern zur Grundwasserbeprobung*, University of Tübingen, 1998.
5 H. Martin, B.M. Patterson, G.B. Davis and P. Grathwohl, Field trial of contaminant groundwater monitoring: comparing time-integrating ceramic dosimeters and conventional water sampling, *Environ. Sci. Technol.*, 37 (2003) 1360.
6 M. Blos, Master Thesis: *Nachweis flüchtiger organischer Schadstoffe im Grundwasser anhand von Keramikdosimetern: Evaluierung von Adsorbermaterialien und vergleichende Felduntersuchungen*, University of Tübingen, 2003.
7 R.W. Gale, Three-compartment model for contaminant accumulation by semipermeable membrane devices, *Environ. Sci. Technol.*, 32 (1998) 2292.
8 P. Grathwohl and T. Schiedek, *Passive Sampler as a Long-Term Monitoring System for Hydrophobic Organic Contaminants*. In: International Conference Field Screening Europe, 1997, 29.09.–01.10.1997, Karlsruhe, Germany, 1997.
9 A. Fick, On liquid diffusion, *Philos. Mag.*, 294 (1855) 30.
10 P. Grathwohl, *Diffusion in Natural Porous Media: Contaminant Transport, Sorption/Desorption and Dissolution Kinetics*, Kluwer Academic Publishers, Boston, 1998, p. 224S.
11 E. Worch, Eine neue Gleichung zur Berechnung von Diffusionskoeffizienten gelöster Stoffe, *Vom Wasser*, 81 (1993) 289.

12 J.N. Huckins, J.D. Petty, C.E. Orazio, J.A. Lebo, R.C. Clark, V.L. Gibson, W.R. Gala and K.R. Echols, Determination of uptake kinetics (sampling rates) by lipid-containing semipermeable membrane devices (SPMDs) for polycyclic aromatic hydrocarbons (PAHs) in water, *Environ. Sci. Technol.*, 33 (1999) 3918.
13 B. Vrana, H. Paschke, A. Paschke, P. Popp and G. Schüürmann, Performance of semipermeable membrane devices for sampling of organic contaminants in groundwater, *J. Environ. Monit.*, 7 (2005) 500.
14 H. Martin, *Entwicklung von Keramikdosimetern zum zeitlich integrierenden Monitoring von Natural Attenuation für leicht-flüchtige organische und anorganische Schadstoffe im Grundwasser*. Abschlussbericht zum Forschungsstipendium der DFG MA 2365/1-2 von Dr. H. Martin, 2003.

Chapter 13

Passive diffusion samplers to monitor volatile organic compounds in ground-water

Don A. Vroblesky

13.1 INTRODUCTION

Diffusion samplers (DSs) have been used since at least the 1990s to sample volatile organic compounds (VOCs) in ground-water [1,2]. DSs can be advantageous for sampling VOCs in ground-water primarily because they have the potential to reduce costs substantially compared with pumping approaches to well sampling. The depth-specific characteristic of the samples can also be advantageous in certain investigations. In general, the types of DSs used to examine VOCs in ground-water can be divided into sorption devices and equilibrium DSs. Sorptive devices are discussed briefly in the following paragraph; however, this chapter concentrates on equilibrium DSs.

Sorption devices for measuring VOC concentrations in ground-water typically consist of a semi-permeable membrane enclosing a sorptive medium, such as hydrophobic carbonaceous resins or polymeric resins. In this type of sampler, dissolved VOCs partition into a vapor phase in order to cross the hydrophobic membrane (examples include low-density polyethylene (LDPE) and Gore-Tex®[1]) to the internal sorption material in an air space. A simple example consists of an air-filled glass vial containing a wire coated with activated carbon. The vial is enclosed in a plastic zip-lock bag and buried in the bottom sediment in a pond. This type of inexpensive DS has been used successfully to map the zone of VOC-contaminated ground-water beneath a tidal pond where the contaminated ground-water was discharging to surface-water [1]. Because sorptive-type samplers continue to sorb analytes until the sorptive

[1]The use of trade names does not imply endorsement by the U.S. Geological Survey.

Comprehensive Analytical Chemistry 48
R. Greenwood, G. Mills and B. Vrana (Editors)
Volume 48 ISSN: 0166-526X DOI: 10.1016/S0166-526X(06)48013-2

medium is saturated, the samplers are highly sensitive, and some analytes can be measured to the parts per trillion level.

Equilibrium-type DSs typically consist of a closed receptacle composed of a semi-permeable or permeable membrane containing vapor or water free of the target analytes. When these types of DSs are deployed in VOC-contaminated water, equilibrium begins to develop between VOC concentrations in the ambient water and in the water or air of the DS. Once the VOC concentrations attain equilibrium, the VOC concentrations within the DS maintain equilibrium with the concentrations in the ambient water and can be used to track changes in the ambient water [3]. The equilibrated DS can be recovered, and the sample can either be sealed in the DS or transferred to sealable sample vials, depending on specific sampler requirements.

An equilibration time of 1–7 days is typical for equilibrium-based membranes [4–7]. To allow the deployment disturbance to dissipate, however, most equilibrium-based samplers are usually left in place for at least 2 weeks prior to recovery. In poorly permeable sediments, longer times may be required [8].

Semi-permeable or permeable membranes used for this application include LDPE [9,10], regenerated cellulose [11], polysulfone [12], silicone polycarbonate [13], porous polyethylene [14,15], and others. LDPE membranes have been tested extensively for monitoring VOCs in ground-water at wells and at the ground-water/surface-water interface [9,16–20]. The pore size of LDPE membranes is about 1 nm. The samplers constructed from these membranes for use in ground-water applications typically are either a water-filled LDPE lay-flat tube sealed at both ends, or a vapor-filled vial with the membrane covering one end. The water-filled samplers are called polyethylene or passive diffusion bag (PDB) samplers and typically hold about 220–350 mL (Fig. 13.1). The vapor-filled vials are called polyethylene or passive vapor diffusion (PVD) samplers, and typically are constructed of an open 20 mL vial containing air and sealed in two LDPE bags (Fig. 13.2). The samplers are deployed at the target horizon in a well or in stream-bottom sediment and allowed to equilibrate. During the equilibration period (typically about 2 weeks), aquifer VOCs diffuse through the LDPE membrane and into the sampler in accordance with the principles of Fickian diffusion. Fick's first law states that the flux of solute movement is directly proportional to the concentration gradient and inversely proportional to the resistances to flow. At the end of the deployment period, water-filled samplers contain the same dissolved-phase VOC concentrations as the ambient water, and

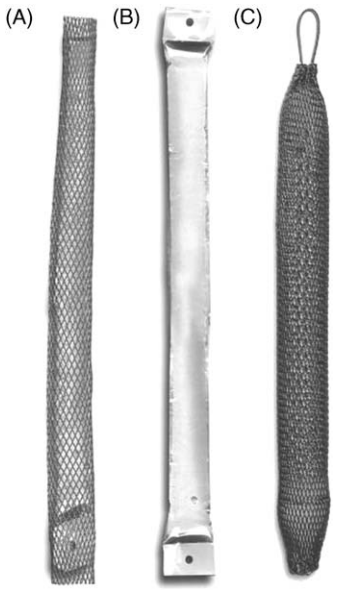

Fig. 13.1. Typical water-filled polyethylene diffusion bag (PDB) samplers used in wells, including (A) a diffusion bag with polyethylene protective mesh, (B) a diffusion bag without mesh, and (C) a bag and mesh attached to a bailer bottom.

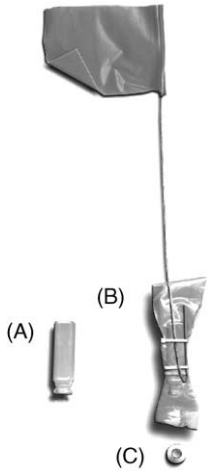

Fig. 13.2. Passive vapor diffusion (PVD) sampler showing (A) an empty vial, (B) a completed sampler consisting of the open vial enclosed in two polyethylene bags and attached to a survey flag, and (C) a crimp cap.

vapor-filled samplers contain headspace concentrations in equilibrium with ambient water.

The polyethylene samplers are not permeable to water, but are permeable to many VOCs that constitute some of the most common priority contaminants. These VOCs include chlorinated ethenes and ethanes, benzene, toluene, ethylbenzene, and others [10]. The samplers are also suitable for monitoring helium, neon, hydrogen, oxygen, and nitrogen [6]. Some very soluble VOCs, such as methyl-*tert*-butyl ether (MTBE) do not move through the LDPE rapidly enough to be effective target analytes. Polar molecules, such as most inorganic solutes, do not diffuse through the membrane. In some cases when sampling for VOCs, this may be an advantage. For example, PDB samplers may be particularly practical in carbonate environments where alkalinity can be high enough to cause effervescence when an acid preservative is added. The effervescence results in loss of VOCs by volatilization. Collection of VOCs without addition of acid preservative prevents volatilization loss, but significantly shortens the sample holding time. An investigation by Vroblesky and Pravecek [21] in an alkaline aquifer in Hawaii showed that the PDB sampler membranes transmitted VOCs, but not alkalinity. Therefore, they collect VOCs in a non-alkaline matrix and allow for the addition of an acid preservative even when sampling from a highly alkaline aquifer. Technical and regulatory guidance documents are available for monitoring VOCs with the PDB [10,21,22] and the PVD [18] samplers.

Regenerated cellulose dialysis samplers are equilibrium-based DSs that have been used in a variety of investigations for VOCs and inorganic constituents in ground-water [2,7,11,23]. The nominal pore size of cellulose-based membranes used for DSs in environmental studies for VOCs ranges from about 1.8 nm [7,11,23] to about 4.0 nm [24,25]. Cellulose-based membranes tend to biodegrade once deployed [23,26] so the sample deployment time needs to be minimized. Harter and Talozi [27] found that regenerated cellulose DSs could be deployed in warm, bioactive ground-water monitoring wells with sufficient ambient advective exchange for up to 4 days without being compromised by biodegradation.

Rigid porous polyethylene samplers (RPPSs) are equilibrium-based devices that have been used to sample VOCs in wells and also are capable of sampling inorganic constituents. RPPSs are porous polyethylene tubes filled with water. Pore size is approximately 6–15 μm. A field study in 2004 of wells showed that the RPPS produced VOC and 1,4-dioxane concentrations similar to low-flow sampling results [15]. A recent

laboratory study of RPPSs showed that they produced accurate concentrations of most VOCs [14].

13.2 APPLICATIONS

Passive DSs have been used to examine ground-water VOCs primarily in two types of applications. The first type of application involves obtaining VOC concentrations in ground-water immediately prior to its discharge to surface-water. This application is of interest because dilution of VOCs in surface-water and lateral transport by currents make contaminant-discharge zones difficult or impossible to locate by examining surface-water samples. The second type of application involves deploying DSs in wells for well monitoring. In wells having saturated screen intervals longer than 1.5 m, multiple DSs typically are deployed to investigate the entire screen length. This application is of interest in appropriate wells because it has the potential to greatly reduce sampling costs by eliminating purge requirements and the need for expensive well pumps, and by decreasing the manpower and time normally required for sampling. A series of investigations in 2002–2003 [19] examined the potential for application of PDB samplers for use in monitoring wells at 14 Air Force bases. Data from these studies showed an average cost savings of 75% when switching from conventional sampling to PDB samplers. An additional advantage of DSs is the potential to delineate VOC stratification in the screened or open interval of the well.

13.2.1 VOCs in ground-water at the ground-water/surface-water interface

VOCs in ground-water at the ground-water/surface-water interface have been used for several years as a tool for examining contaminant-discharge zones. Because VOCs are volatile, there is a tendency for VOCs moving through pore water to partition into any vapor phase, such as a gas bubble, that they contact. VOCs in ground-water discharging to surface-water through organic-rich bed sediments can come into contact with methane bubbles forming as the bed sediments decay by methanogenesis. Thus, some VOCs partition into the methane bubbles and are released to the overlying water and atmosphere during ebullition (bubble emission). One study found that the VOC content of methane gas bubbles in bottom sediment could be used to identify discharge zones of VOC-contaminated ground-water [28]. In a like

manner, PVD samplers provide a vapor phase for VOC partitioning at the ground-water/surface-water interface. This type of sampler has been used widely to identify VOC-contamination zones in ground-water beneath surface-water (e.g. [3,16–18,29,30]). In one study, data from the samplers were used to identify specific fracture zones contributing contamination to a stream [16]. PVD samplers provide a vapor concentration in equilibrium with the environmental aqueous concentration of VOCs. In some cases, water-filled PDB samplers have been deployed in bed sediments to obtain direct aqueous concentrations of VOCs in pore-water [29,31].

The PVD sampler, an empty, uncapped vial (Fig. 13.2A) enclosed in two LDPE bags (Fig. 13.2B), is buried approximately 18–45 cm in the bottom sediment of gaining reaches in surface-water bodies and allowed to equilibrate. The sampler is attached to a wire surveyor flag for sampler identification and recovery. Sampler deployment often can be done by wading and using a shovel. In some circumstances, however, deployment and recovery may involve divers or other means of deep-water emplacement. The samplers are allowed to remain in place for at least 2 weeks for the samplers to equilibrate and for the pore-water to recover from the environmental disturbances caused by sampler deployment.

During sampler recovery, the outer LDPE is removed from the vial opening to prevent entrained sediment from interfering with the seal. The inner LDPE bag is left intact, and the vial is sealed by capping over the inner bag. A septated cap (Fig. 13.2C) is used to allow the trapped vapor to be sampled by a syringe.

An example of a study using PVD samplers in deep water is at Johns Pond, Western Cape Cod, MA, USA [29]. PVD samplers were deployed in Johns Pond to confirm that VOCs in a ground-water plume emanating from the Massachusetts Military Reservation were discharging into the pond. An array of 134 PVD samplers was buried by divers about 15 cm below the pond bottom in the presumed discharge area and allowed to equilibrate for about 2 weeks. At selected sites, water-filled PDB samplers also were buried.

Two areas of high VOC concentrations were identified by the PVD samplers (Fig. 13.3). One area was a broad discharge zone (about 335 m wide) approximately 30–106.5 m offshore, having trichloroethene (TCE) and tetrachloroethene (PCE) with vapor concentrations as high as 890 and 667 parts per billion (ppb) by volume, respectively [32]. This zone represented the discharge area of a plume moving toward the pond from the northwest, identified as the Storm Drain-5 plume. Samples from the second area were located closer to shore than the larger

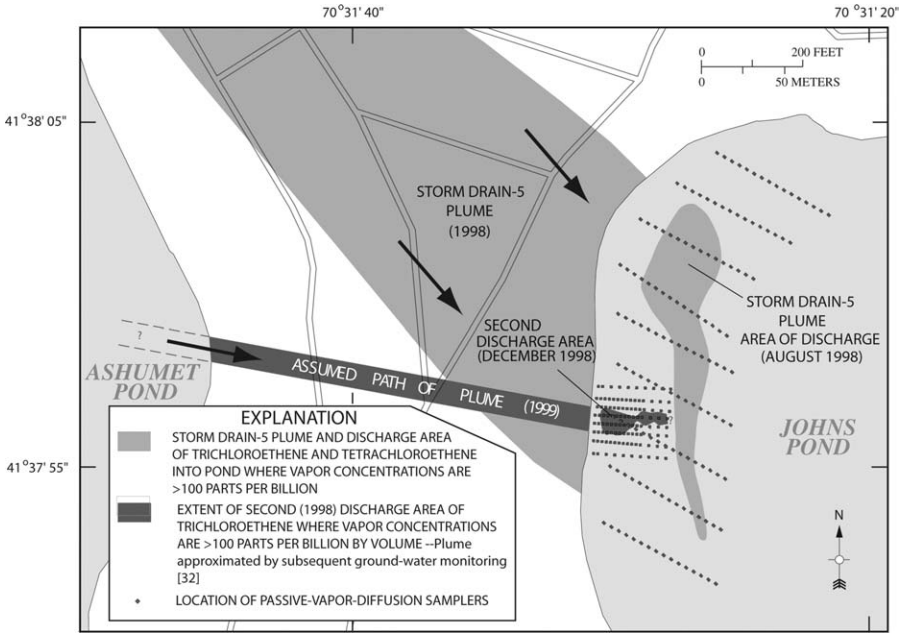

Fig. 13.3. Discharge areas of TCE plumes, as identified by passive vapor diffusion (PVD) samplers, August and December 1998, Johns Pond, Massachusetts (modified from Ref. [29]).

contamination zone and contained unexpectedly high concentrations of TCE ($>40{,}000$ ppb by volume in a PVD sampler and $1200\,\mu g\,L^{-1}$ in an adjacent water-filled PDB sampler). Confirmatory ground-water samples collected with a drive-point sampler near the second area had aqueous TCE concentrations as high as $1100\,\mu g\,L^{-1}$.

Following the initial investigation, a more closely spaced array of 110 PVD samplers was installed to map the second area of elevated TCE concentrations (Fig. 13.3). The discharge area detected with the samplers was about 22.9 m wide and extended from about 7.6 to 60 m offshore. Subsequent drilling into the pond bottom and onshore confirmed that the second area was the discharge zone of a distinct TCE plume not associated with Storm Drain-5 plume discharging in the first area. The second plume discharged closer to shore because it was shallower than the Storm Drain-5 plume. Further investigation showed that the second plume was related to a ground-water contamination plume west of Ashumet Pond that had flowed under Ashumet Pond and was discharging into Johns Pond [33] (Fig. 13.3). Thus, in this investigation, PVD samplers confirmed the suspicion that the Storm Drain-5

plume was discharging to Johns Pond, and were used to map the discharge zone and to detect and map a previously unsuspected discharge zone of a ground-water plume from the opposite side of an adjacent pond.

13.2.2 VOCs in ground-water in monitoring wells

Investigations have found that in permeable formations, under natural gradient conditions, there can be sufficient flow through the screened interval of a monitoring well to maintain water isolated from the overlying stagnant water stored in the unscreened part of the well (e.g. [34]). In permeable formations, the general consensus is that flow through the screen is expected to occur, with most of the flow coming from the most permeable strata in the screened interval. Where such through-flow is occurring and there is no mixing with the overlying stagnant water in short-screened wells (3.05 m or less), DSs placed in the screened interval have the potential to provide VOC concentrations comparable with those obtained by traditional pumping methods. Several field investigations have shown good agreement between pumped-sample and DS VOC concentrations in wells (see Ref. [22] for examples).

A number of factors should be considered when using DS in wells. These factors include the potential for contaminant stratification and the potential for in-well mixing.

Contaminant stratification is commonly seen in aquifers when multilevel short-screened wells are utilized [35]. In the absence of in-well mixing, this stratification can manifest itself within the screened interval of the well, as shown by investigations of standing water in monitoring wells using dialysis cells isolated between baffles to limit in-well mixing and vertical flow [24,36].

In the absence of the flow-limiting baffles in the well, in-well mixing can obscure or eliminate the development of chemical stratification within the screened or open intervals of wells. A variety of factors can facilitate the mixing in boreholes. These factors include thermally driven convection cells [37], diffusive mixing [38], and vertical in-well flow [39]. A field test conducted by Church and Granato [40] found that well screens can act as conduits for vertical flow because they can connect zones of differing head and transmissivity, even in relatively homogeneous aquifers. They found that vertical flow can mask the presence of discrete contaminated horizons in the screened interval and can contaminate zones of the aquifer that would not otherwise become contaminated. In these situations, little vertical variation in VOC

concentrations is observed across the length of the screened interval or the zone undergoing vertical flow.

Even in wells without flow-limiting baffles, however, solute stratification can sometimes be seen by using multiple DSs. Harter and Talozi [27], using regenerated cellulose membranes, found large contrasts in salinity and nitrate concentrations over approximately 3 m intervals in 40 wells. They found non-uniform nitrate profiles in 80% of the wells they examined. Stratification of inorganic solutes in the screened intervals of wells has been observed in a variety of open-screened intervals using multiple regenerated cellulose passive samplers [23,41].

Stratification of VOCs has also been observed in the screened intervals of monitoring wells by using multiple PDB samplers at a variety of sites [41–44] (Fig. 13.4). The source of this stratification may include

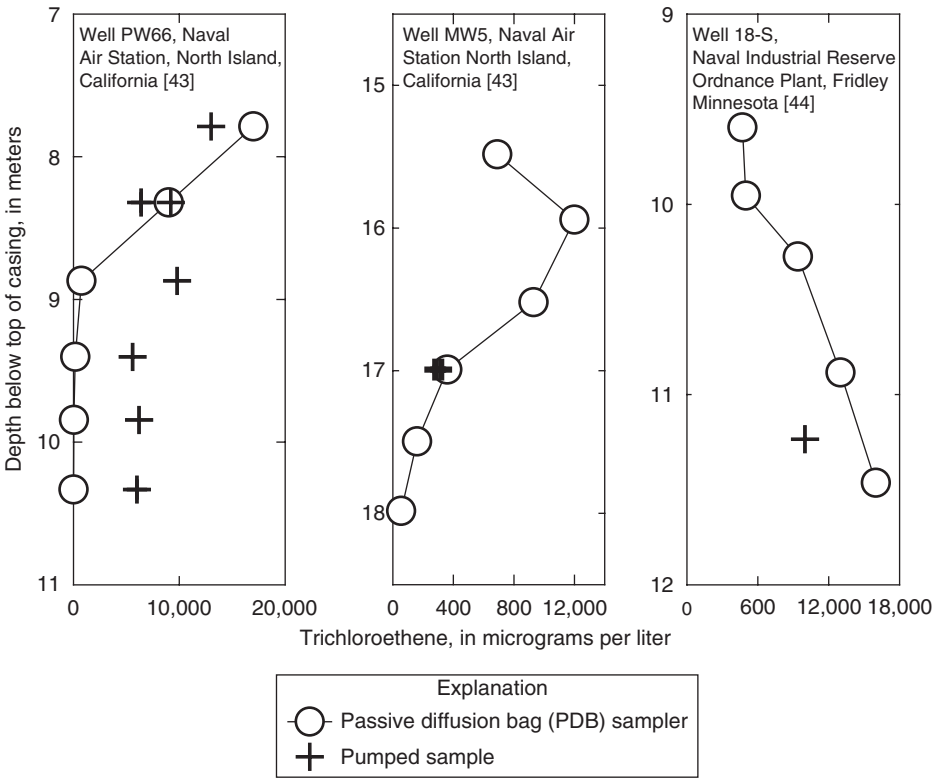

Fig. 13.4. Comparison of diffusion and pumped samples in ground-water showing vertical stratification of TCE in the screened interval (modified from Refs. [43,44]).

such factors as vertical differences in contaminant concentrations outside the well screen, vertical flow through a portion of the screen, density contrasts, or, in wells screened at the water table, volatilization loss at the air/water interface.

In situations where there is vertical stratification of contaminants in the well bore, the use of a borehole flow-meter can sometimes aid in understanding the distribution of contamination and the relation between the pumped-sample concentrations and the DS concentrations, particularly when the pumped-sample and DS VOC concentrations disagree. For example, borehole flow-meter testing in well IRP-31 at Andersen Air Force Base, Guam, showed little or no vertical movement of water within the limits of the flow-meter under ambient conditions (Fig. 13.5A) [41]. Under pumped conditions, most of the water entered the well near the top of the screen (Fig. 13.5B). PDB samplers in the open screen (without flow-limiting baffles) showed substantial stratification of TCE (Fig. 13.5C). The TCE concentration was about 211–218 $\mu g L^{-1}$ at a depth of 136.2 m and only 20 $\mu g L^{-1}$ at a depth of 141.2 m. The upward increasing concentration in well IRP-31 implies that there may be higher concentrations at shallower depths than the uppermost zone sampled by the PDB samplers (Fig. 13.5C). Because during pumping, most of the water in this well is derived from a horizon shallower than the PDB samplers (Fig. 13.5B), it is probable that the PDB samples represent local concentrations, and the pumped sample primarily represents water derived from a more contaminated zone at a depth of about 135–136 m, slightly shallower than the PDB samplers (Fig. 13.5C). Therefore, it is not surprising that the uppermost PDB sample TCE concentration is slightly lower than the adjacent pumped sample.

The TCE concentration in well IRP-31 at the depth from which pumped samples typically were collected (about 139.5 m) was higher in the pumped samples (150–153 $\mu g L^{-1}$) than in the PDB samples (57–63 $\mu g L^{-1}$). Examination of the flow-meter data and the vertical distribution of contamination, however, show that the difference does not mean that the PDB concentrations are inaccurate. The vertical concentration and flow-meter profiles in the well show that most of the water during pumping is derived from a shallower zone having higher TCE concentrations than the typical pumped-sample collection depth (Fig. 13.5C). Therefore, the most probable explanation for the difference is that the pumped sample represents a higher concentration in the water from a shallower horizon transported downward in response to pumping.

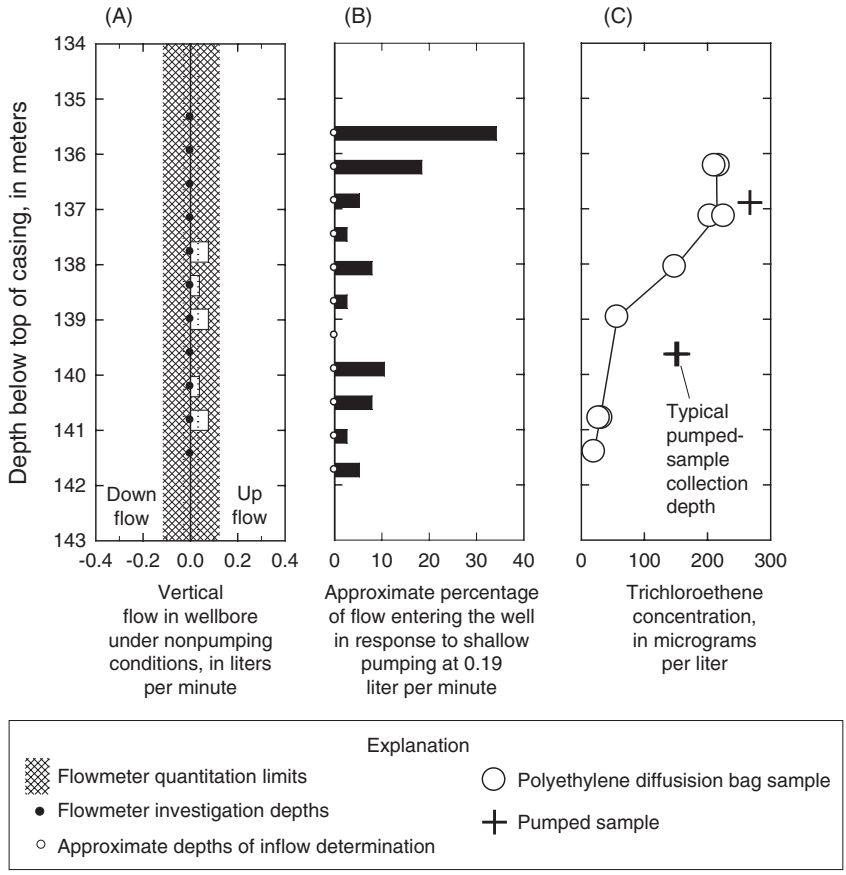

Fig. 13.5. (A) Borehole flow-meter data under non-pumped conditions, (B) approximate water-yielding zones during pumping, and (C) TCE concentrations in polyethylene diffusion bag samples and pumped samples at well IRP-31, Andersen Air Force Base, Guam, April 2002 (modified from Ref. [41]).

The PDB data show that the typical pumping depth in well IRP-31 is deeper than the zone of maximum contamination and maximum yield, and in the shallower, more contaminated part of the well screen, the PDB and pumped-sample concentrations more closely correspond (Fig. 13.5C). At a depth of 136.2 m, the TCE concentration in the pumped sample was 267 $\mu g\,L^{-1}$, and the average TCE concentration in the PDB samples was 214 $\mu g\,L^{-1}$. It is highly probable that the PDB samples would more closely correspond to the pumped sample if they were placed at a depth of about 135.6 m, corresponding to the zone of maximum water movement into the well during pumping.

As in the previous example, a common approach used to determine whether the use of DSs is appropriate at a particular well is to do a side-by-side comparison with a conventional sampling method, such as pumping. In wells where there is little or no temporal variation in VOC concentrations, it may be acceptable to compare the DS VOC concentrations with historical records. In general, if the two approaches produce VOC concentrations that are within a range deemed acceptable by the applicable regulatory agencies, then use of DSs will provide data consistent with the historical record. If the DS VOC concentrations are higher than the conventional results, then the DSs probably adequately represent the ambient conditions because the mixing during collection of pumped samples may dilute the pumped-sample VOC concentration. If, however, the DS VOC concentrations are substantially lower than concentrations in the pumped sample, then the DSs may or may not adequately represent local ambient conditions. In this case, the difference may be due to a variety of factors, including pump-induced movement of contaminants into the well, mixing or translocation resulting from hydraulic and chemical heterogeneity of the aquifer within the screened or open interval of the well, a poorly permeable well screen that limits through flow under ambient conditions, or possibly inherent differences between whole-water pumped samples and samples obtained by diffusion (e.g. colloidal transport of analytes present in the pumped sample, but excluded from the DS). Different VOC concentrations in the pumped sample relative to the DS sample do not necessarily indicate that the DS misrepresents local concentrations, as illustrated in the above example (Fig. 13.5).

As shown above, DSs can be an inexpensive and effective tool for monitoring VOC concentrations in wells. The appropriate depth for DS placement in wells should be determined based on knowledge of the potential for contaminant stratification in the well. A variety of techniques can be used to determine the presence of contaminant stratification. One approach involves using multi-level DSs. When multi-level DSs are used, a single DS with a nominal length of about 0.46 m should not represent more than about 1.5 m of screened interval [21]. Depth-specific data also may be available from discrete-depth sampling during well installation or other sources.

13.3 CONCLUSIONS

DSs can be useful in examining VOC concentrations at the groundwater/surface-water interface and in monitoring wells. When used at the

ground-water/surface-water interface, they have the potential to map contaminant-discharge zones by intercepting discharging ground-water before it is diluted and laterally transported by surface-water. When used in monitoring wells, they have the potential to provide VOC concentrations in ground-water without the need for purging. The primary application in wells is for long-term monitoring of VOCs where significant cost savings over conventional methodologies can be achieved. The cost savings usually result from a combination of decreased material costs, decrease or elimination of contaminated purge-water, and reduced time onsite associated with use of DS relative to pumping methods. Confirmation of the appropriateness for use of DSs in particular wells is typically done by comparing DS results with historical or with pumped sample results collected soon after recovering the DSs.

ACKNOWLEDGMENT

Funding for the production of this chapter was provided by the U.S. Geological Survey Toxic Substances Hydrology Programme.

REFERENCES

1 D.A. Vroblesky, M.M. Lorah and S.P. Trimble, *Ground Water*, 29 (1991) 7.
2 E. Kaplan, S. Banerjee, D. Ronen, M. Magaritz, A. Machlin, M. Sosnow and E. Koglin, *Ground Water*, 29 (1991) 191.
3 D.A. Vroblesky and J.F. Robertson, *Ground Water Monit. Remediat.*, 16 (1996) 196.
4 P.W. Hare, R. Cohen, J. Forsell and M. Gefell, *Ground Water Monit. Remediat.*, 20 (2000) 127.
5 D.A. Vroblesky and T.R. Campbell, *Adv. Environ. Res.*, 5 (2001) 1.
6 C.E. Divine and J.E. McCray, *Environ. Sci. Technol.*, 38 (2004) 1849.
7 T.A. Ehlke, T.E. Imbrigiotta and J.M. Dale, *Ground Water Monit. Remediat.*, 24 (2004) 53.
8 G.A. Harrington, P.G. Cook and N.I. Robinson, *Ground Water Monit. Remediat.*, 20 (2000) 60.
9 D.A. Vroblesky and W.T. Hyde, *Ground Water Monit. Remediat.*, 17 (1997) 177.
10 D.A. Vroblesky, U.S. Geological Survey Water Resources Investigations Report 01-4060, 2001, 18 pp.
11 T.E. Imbrigiotta, T.A. Ehlke, P.J. Lacombe and D.M. Dale, *Third International Conference on Remediation of Chlorinated and Recalcitrant Compounds, Battelle*, May 20–23, 2002, Monterey, CA.

12 M.M. Lorah, L.D. Olsen, B.L. Smith, M.A. Johnson and W.B. Fleck, U.S. Geological Survey Water Resources Investigations Report 97-4171, 1997, 95 pp.
13 R.D. Blanchard and J.K. Hardy, *Anal. Chem.*, 56 (1984) 1621.
14 D. O'Neill, *Proceedings of the 21st Annual National Environmental Monitoring Conference*, July 25–27, 2005, Washington, DC, Paper 8–5, 2005, 11 pp.
15 Parsons, Results report for the demonstration of no-purge groundwater sampling devices at former McClellan Air Force Base, California: Consultant's report to U.S. Army Corps of Engineers (Omaha District), the Air Force Center for Environmental Excellence, and the Air Force Real Property Agency, 2005, 83 pp.
16 D.A. Vroblesky, L.C. Rhodes and J.F. Robertson, *Ground Water*, 34 (1996) 223.
17 D.A. Vroblesky, *Proceedings of the Ground Water/Surface Water Interactions Workshop*, January 26–28, 1999, U.S. Environmental Protection Agency, Denver, Colorado, 2000, 143 pp.
18 P.E. Church, D.A. Vroblesky, F.P. Lyford and R.E. Willey, United States Geological Survey Water Resources Investigations Report 02-4186, 2002, 79 pp.
19 Parsons, Final comprehensive results report for the passive diffusion bag sampler demonstration: Consultant's report to the Air Force Center for Environmental Excellence, the Air Force Environmental Directorate, the Air Force Real Property Agency, and the Defense Logistics Agency, August 2003, 205 pp.
20 L.V. Parker and C.H. Clark, *Ground Water Monit. Remediat.*, 24 (2004) 111.
21 Interstate Technology and Regulatory Council (ITRC) Technical and Regulatory Guidance for Using Polyethylene Diffusion Bag Samplers to Monitor Volatile Organic Compounds in Groundwater, February 2004, 40 pp.
22 D.A. Vroblesky, U.S. Geological Survey Water Resources Investigations Report 01-4061, 2001, 102 pp.
23 D.A. Vroblesky and T. Pravecek, U.S. Geological Survey Water Resources Investigations Report 02-4159, 2002, 38 pp.
24 D. Ronen, M. Magaritz, H. Gvirtzman and W. Garner, *J. Hydrol.*, 92 (1987) 173.
25 M. Magaritz, M. Wells, A.J. Amiel and D. Ronen, *Appl. Geochem.*, 4 (1989) 617.
26 R. Dasika and J. Atwater, *Water Res.*, 29 (1995) 2609.
27 T. Harter and S. Talozi, *Ground Water Monit. Remediat.*, 24 (2004) 97.
28 D.A. Vroblesky and M.M. Lorah, *Ground Water*, 29 (1991) 333.
29 J.G. Savoie, D.R. LeBlanc, D.S. Blackwood, T.D. McCobb, R.R. Rendigs and S. Clifford, U.S. Geological Survey Water Resources Investigations Report 00-4017, 2000, 30 pp.

30 J.P. Campbell, F.P. Lyford and R.E. Willey, U.S. Geological Survey Open-File Report 02-143, 2002, 33 pp.
31 D.A. Vroblesky, C.T. Nietch, J.F. Robertson, P.M. Bradley, J. Coates and J.T. Morris, U.S. Geological Survey Water Resources Investigations Report 99-4071, 1999, 43 pp.
32 Air Force Center for Environmental Excellence, SD-5 South plume and adjacent TCE plume design and data-gap technical memorandum: Jacobs Engineering Group, Inc. (July 1999) various pagination.
33 Air Force Center for Environmental Excellence, Groundwater plume maps and information booklet, Massachusetts Military Reservation, Cape Cod, Massachusetts: Air Force Center for Environmental Excellence, May 2005, 35 pp.
34 R.M. Powell and R.W. Puls, *J. Contam. Hydrol.*, 12 (1993) 51.
35 S.M. Dean, J.M. Lendvay, M.J. Barcelona, P. Adriaens and N.D. Katopodes, *Ground Water Monit. Remediat.*, 19 (1999) 90.
36 D. Ronen, M. Magaritz and I. Levy, *Water Res.*, 20 (1986) 311.
37 J.M. Martin-Hayden, Poster 175–0 Geological Society of America, Annual Meeting, November 5–8, 2001, Boston, MA.
38 S.L. Britt, *Ground Water Monit. Remediat.*, 25 (2005) 73.
39 A. Elci, G.P. Flach and F.J. Molz, *J. Hydrol.*, 281 (2003) 70.
40 P.E. Church and G.E. Granato, *Ground Water*, 34 (1996) 262.
41 D.A. Vroblesky, M. Joshi, J. Morrell and J.E. Peterson, U.S. Geological Survey Water Resources Investigations Report 03-4157, 2003, 29 pp.
42 R.L. Huffman, U.S. Geological Survey Water Resources Investigations Report 02-4203, 2002, 24 pp.
43 D.A. Vroblesky and B.C. Peters, U.S. Geological Survey Water Resources Investigations Report 00-4182, 2000, 27 pp.
44 D.A. Vroblesky and M.D. Petkewich, U.S. Geological Survey Water Resources Investigations Report 00-4246, 2000, 10 pp.

Chapter 14

Field study considerations in the use of passive sampling devices in water monitoring

Per-Anders Bergqvist and Audrone Zaliauskiene

14.1 INTRODUCTION

Semipermeable membrane devices (SPMDs) are passive monitors that are being increasingly used by monitoring agencies and wastewater dischargers to measure the contents of lipophilic organic chemicals that may adversely affect water quality. Passive sampling devices can monitor most 75% of the organic pollutants included in the EU Water Framework Directive (WFD) priority pollutant list as well as many other compounds. Furthermore, applications and the theory underlying the use of SPMDs have been described in over 200 peer-reviewed scientific publications during the last two decades, making them the most comprehensively studied type of passive sampler for semivolatile organic pollutants in water.

The most frequently asked questions regarding the use of SPMDs for water monitoring are the following. What compartments of the environment do the SPMD extracts represent? Have lowest environmental concentrations of concern (C_c) been established for the compounds of interest? How many SPMDs are needed to detect these concentrations? What are the ranges of, and the most suitable, SPMD exposure times? What additional information should be collected about the site to enhance the interpretation of SPMD results? What quality control (QC) measures are needed for SPMD sampling? Are SPMD calibration data available for the compounds of interest? What constitutes good SPMD practice in terms of storage, transportation, deployment, retrieval and analytical procedures?

This chapter addresses these and other questions related to the field application of SPMDs (many of which are also relevant to other types of

Comprehensive Analytical Chemistry 48
R. Greenwood, G. Mills and B. Vrana (Editors)
Volume 48 ISSN: 0166-526X DOI: 10.1016/S0166-526X(06)48014-4

passive water samplers). In so doing, we aim to provide a sound understanding of the applicability and limitations of SPMDs for obtaining reliable monitoring data.

14.1.1 SPMD rationale and applicability

Standard, commercially available SPMDs consist of a layflat 92 × 2.5 cm virgin, low-density, 75–90 μm thick, low-density polyethylene (LDPE) tube containing 1 mL of pure (>95%, >99% or >99% and cleaned) pure triolein (Fig. 14.1). The last of these three types is mainly used for toxicity testing. The surface area-to-volume ratio (A/V) is about 90 cm^2 mL^{-1} of SPMD (membrane plus triolein) or about 460 cm^2 mL^{-1} of triolein. A device with these dimensions weighs approximately 4.50 g, of which triolein accounts for about 20%. However, an SPMD of any length with an A/V ratio of about 460 cm^2 mL^{-1} of triolein, a lipid-to-membrane mass ratio of approximately 0.25, and a 70–95 μm wall thickness is considered to be a standard SPMD. In order for an SPMD to function correctly, nearly 100% of the targeted compounds taken up should partition into the device and no additives with adsorptive properties should be present in it.

Standard, commercially available SPMDs are modeled on an original United States Geological Service (U.S.G.S.) design (Fig. 14.1) [1]. Use of SPMDs with a standard design and quality ensures that published SPMD sampling rate calibration data are applicable for estimating ambient water concentrations of analytes. Use of standard SPMDs also allows data obtained in different studies to be validly compared, since such SPMDs are used globally in most applications [2]. Recently, alternative device called the polar organic chemical integrative sampler (POCIS) has been developed for sampling polar compounds. In the USA, these devices are called ''Aquasence-P'' and in Europe ''Expos-Meter Hydrophilic'' samplers.

Standard SPMDs are designed to sequester and concentrate bioavailable dissolved aqueous-phase hydrophobic organic contaminants (HOCs) with $3 < \log K_{ow} < 8$ and molecular weights of approximately <600 Da such as polyaromatic hydrocarbons (PAHs), non-polar pesticides, polychlorinated biphenyls (PCBs), polychlorinated naphthalenes, polychlorinated dibenzofurans, polychlorinated dibenzodioxins, polybrominated diphenyl ethers, polychlorinated benzenes and alkyl phenols (nonyl phenols).

HOCs in the water are carried to the SPMD by convection or eddy diffusion. Molecular diffusion is the dominant transport process in the

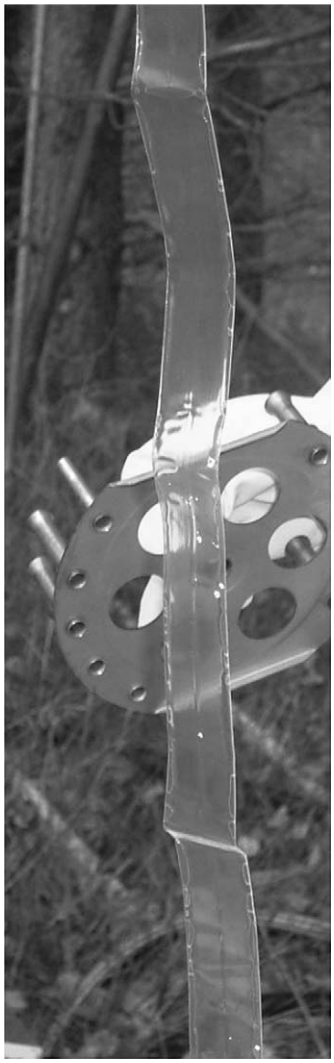

Fig. 14.1. A standard SPMD and commercially available stainless steel deployment spider.

layer extending a few millimeters from the surface of the membrane. HOC molecules of appropriate sizes move through the transient membrane pores and accumulate in the triolein and partly in the polymer itself.

SPMDs are not suitable for sampling ionic species such as metal ions, ionized forms of organic acids or polar organic chemicals. The suitability of SPMDs for monitoring chlorinated phenols is an issue

that is frequently raised by wastewater dischargers. The environmental pH determines the ratio of ionized to neutral species for such compounds as chlorinated phenols and, thus the capacity of SPMDs to sample them since only the neutral species are available for accumulation. Table 14.1 shows the applicability of SPMDs to target compounds included in the EU WFD priority pollutant list [3].

TABLE 14.1
Compounds identified in the European Union's Water Framework Directive that can be monitored by SPMD or POCIS samplers

Compound	Sampler
Alachlor	POCIS
Anthracene	SPMD
Atrazine	POCIS
Benzene	SPMD
Brominated diphenylethers	SPMD
C_{10}-$_{13}$-chloroalkanes	SPMD
Chlorfenvinphos	SPMD
Chlorpyrifos	POCIS
1,2-Dichloroethane	not yet
Dichloromethane	not yet
Di(2-ethylhexyl)phthalate (DEHP)	SPMD
Diuron	POCIS
Endosulfan	SPMD
Fluoranthene	SPMD
Hexachlorobenzene	SPMD
Hexachlorobutadiene	SPMD
Hexachlorocyclohexane	SPMD/POCIS[a]
Isoproturon	POCIS
Naphthalene	SPMD/POCIS[a]
Nonylphenols	SPMD/POCIS[a]
Octylphenols	SPMD/POCIS[a]
Pentachlorobenzene	SPMD/POCIS[a]
Pentachlorophenol	SPMD/POCIS[b]
Polyaromatic hydrocarbons	SPMD
Simazine	POCIS
Tributyltin compounds	SPMD
Trichlorobenzenes	POCIS/SPMD[a]
Trichloromethane (Chloroform)	not yet
Trifluralin	SPMD

[a]Compounds that can be sampled by both SPMDs and POCIS.
[b]Ionized species.

SPMDs are meant to provide complementary information to that provided by grab sampling, but not always to substitute it in water monitoring projects (Table 14.2). However, in some cases, SPMDs have advantages over manual grab or automatic composite sampling.

SPMDs can be used in the following broad applications:

- Determination of the presence, sources, transport and fate of HOCs.
- Estimation of time-weighted average (TWA) dissolved-phase chemical concentrations.
- Determination of the fluxes of bioavailable residues in aquatic systems.
- *In situ* biomimetic concentration of bioavailable chemicals for bioindicator or immunoassay tests.
- Contaminant sequestration in toxicity identification and evaluation (TIE) procedures.
- Estimation of organisms' exposure and the chemicals' bioconcentration potential.
- *In situ* pre-concentration and clean-up.

14.2 FIELD STUDY CONSIDERATIONS

14.2.1 Pre-exposure considerations

Prior to the start of a study with SPMDs, a number of issues should be considered, including the following. Firstly, sufficient SPMDs should be used to ensure that the target compounds can be analyzed if present at their respective levels of concern at each site. Secondly, information on turbulence-flow rates, temperature, conductivity, water depth, biofouling potential and turbidity at the exposure sites should be available (or acquired), and used to decide if published SPMD calibration data for target compounds can be used, or if *in situ* calibration data should be obtained using performance reference compounds (PRCs). Thirdly, the possibility that target compounds may undergo photolysis should be considered and, if so, whether deployment devices and site conditions (e.g. turbidity, natural shading and albedo or light reflectance from site surfaces) will adequately protect the SPMD contents from photodegradation. If not, further measures to avoid photolytic degradation may need to be implemented. Fourthly, the risks that SPMDs may be vandalized, stolen or otherwise interfered with need to be assessed. Finally, the accumulation kinetics of residues sequestered by the SPMDs must

TABLE 14.2

Examples of field applications of SPMDs for monitoring organic contaminants from Vrana *et al*. [4] and experience of the authors

Application	Environment	Analytes
Screening of contaminants for presence or absence	River	HOCs
Monitoring of temporal pollution trends	Seawater	Organochlorine pesticides, PCB
Monitoring of spatial distribution and tracing pollution sources	River	PCBs, dioxins, PAHs, pesticides, HxCBz, PBDEs
	Surface water	UV filter compounds
	Discharge from wastewater treatment plants	Alkylphenol ethoxylates
	Seawater contaminated by discharged oilfield produced water	PAHs
Assessment of contaminant fate and distribution between environmental compartments	Irrigation water canal	PAHs
	Discharges from industrial sources to seawater	PCBs, chlorophenols, chlorobenzenes
	Freshwater, wastewater treatment plants	Triclosan
	River	PCBs, PAHs, PCDDs, PCDFs and substituted benzenes
Biomimetic extraction for toxicity assessment of aqueous contaminants	Effluents of wastewater treatment plant	Organochlorine pesticides, PCBs, PAHs

be considered, i.e. whether they will display linear (integrative), curvilinear or equilibrium uptake kinetics, which depends on sampling conditions and the compounds concerned.

In order to estimate the number of SPMDs required at a specific site Huckins *et al*. [2] suggested that the following estimated relationship between forecast sampling parameters and the analytical outcome should be applied:

$$R_s t n C_c P_r E_t > \mathrm{MQL} V_i \tag{14.1}$$

where R_s is the sampling rate (L day^{-1}), t is days of exposure, n the number of SPMDs, C_c the lowest environmental concentration of concern, P_r the method recovery for the analyte as a fraction of one, E_t the fraction of the total sample injected into the analytical instrument, MQL the method quantitation limit and V_i the volume of the standard injected.

For example, to design a program for monitoring anthracene in a river with a flow rate of 50 cm s^{-1} and average temperature of 25°C the following considerations would apply. Our concentration of concern C_c is 10 ng L^{-1}, since this is the detection limit for anthracene required in the EU quality criteria for the aquatic environment. Using the above relationship we can forecast that a single standard SPMD exposed to 10 ng L^{-1} of aqueous anthracene would sample around 987 ng of the compound during 21 days. The anthracene uptake rate by an SPMD is 4.7 L day^{-1} at 25°C and a flow rate 50 cm s^{-1} [5]. Assuming a P_r of 0.7, and an E_t of 0.001, the analytical result (i.e. left side of the above equation) would be 690 pg. Clearly this would be much more than the MQL (690 times more, assuming an MQL of 1 pg μL^{-1} and a V_i of 1 μL), so one SPMD would be enough to obtain sufficient anthracene to analyze the compound at the level of concern stipulated by the EU quality criteria.

Practical applications have proved that one standard SPMD is enough for the concentration and subsequent analysis of a range of PAHs, PCBs and pesticides during 21 days. However, separate standard SPMDs should sometimes be used when determining the concentrations of dioxins, depending on the target detection limits.

Assessments of the study site conditions are also important when interpreting SPMD sampling and analysis results. Data on temperature, water body flow and turbidity should be available for the period of exposure when standard SPMDs are used without PRCs. All the above-mentioned factors, together with the potential for biofouling, will influence the uptake rate by the membrane. Uptake rates for many

classes of compounds at various temperatures and flow rates have been established under both field and laboratory conditions and are presented in Huckins *et al*. [2].

Since environmental variables affect the SPMD uptake of all types of chemicals, it is very important to collect as much data as possible regarding each deployment site and field conditions during deployment and retrieval. When standard SPMDs are being deployed at multiple sites for comparative purposes, investigators should select sites with similar flow regimes or use uptake rates for different flows when calculating ambient concentrations at the respective sites. Uptake rates for low flow and different temperature regimes have been published by Huckins *et al*. [2]. Another approach would be to use SPMD PRCs to compensate for differences in the environmental conditions at each deployment site. Temperatures (at very least at the beginning and end of the exposure period), visual assessments of the extent of biofouling (e.g. light, medium, heavy and none) and estimates of flow rates should all be noted and recorded [6].

Surface water bodies are often stratified, i.e. often have layers with differing temperatures, densities and chemical compositions. Waters (even oceans) also have high degrees of patchiness that can be manifested (*inter alia*) in highly localized variations in the density of algal blooms. In various water bodies, the stratum from which the sample is collected is a very important consideration in chemical monitoring programs. Stratification can often be neglected in lakes shallower than 5 m [7]. However, in larger enclosed water bodies, such as lakes, lagoons and epicontinental seas such as the Baltic Sea, boundary layers like the thermocline and halocline in seawater profiles act as ''glide surfaces'' for water and pollutants carried by it. As shown in Fig. 14.2, there can

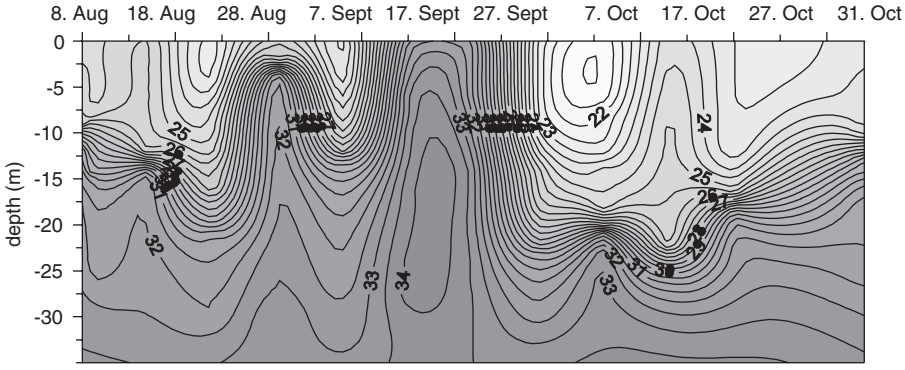

Fig. 14.2. Example of a salinity profile in Gullmar Fjord 2001 [9].

be substantial temporal variations in the salinity profiles of seawater bodies. These variations should also be taken into account when investigating phenomena such as the transport of pollutants by floodwaters, which usually consist of freshwater. For this reason, oceanographic data on the floodwater distribution were used in a temporal monitoring program of organochlorine compounds close to the Swedish coast following a flooding episode in Western Europe [8]. Oceanographic investigations confirmed that floodwater moved toward the Swedish coast from the North Sea and began to reach the coast in the second half of March 1995. The freshwater current in the North Sea was mixed with the seawater mass during a storm and descended below the halocline (at approximately 20-m depth) just before reaching the Swedish coast. Strong winds at the end of March caused substantial turbulence in the water and temporary movement of the floodwater masses away from the coast. After considering this information, SPMDs were deployed at two stations at 24-m depth a few miles off the coast where floodwater masses were expected to be found. SPMDs were changed every 12–16 days during the 12-week study period. Time trends were detected in which, *inter alia* contents of DDTs and (to lesser degrees) PCBs, dieldrin, chlordane and HCHs were high during the first two sampling periods when the floodwater arrived, and subsequently declined [8].

When sampling river water, we must also consider the heterogeneity of the system, because the common assumption that running water environments are generally homogeneous in composition, due to mixing by the current, may be erroneous. For example, sum PCBs obtained from two SPMD sampling points (St5 and St5a) situated 15 m apart across the River Umeå were found to differ 60-fold, as shown in Fig. 14.3. The average flow of the River Umeå is 340 m^3 s^{-1} [10]. Later, a source was found approximately 500-m upstream from sampling sites St5 and St5A, causing the near-shore (10 m) sampling site St5 to be much more polluted than the other.

Lounch *et al*. have investigated the influence of the spatial variability of the target chemical within the water column on the interpretation of SPMD results [11]. This is particularly important when considering the impact of point sources. They placed three sets of SPMD along a transect across the small river (25 m wide at the deployment site) to investigate if one membrane is sufficient to characterize the cross-section of the river, or a specific river mile or water column at a specific point along the river by measuring PAHs with log K_{ow} values ranging from 4.08 to 5.61. The results showed that we should not assume even a

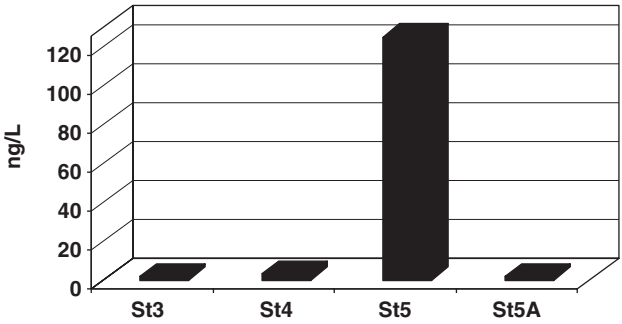

Fig. 14.3. Sampling results of sum PCB from River Umeå; St3 was located upstream of the city, St4 in the city center and St5 downstream of an old industrial area. St5A was located at the same point along the river as St5, but 15 m further toward the middle of the river [10].

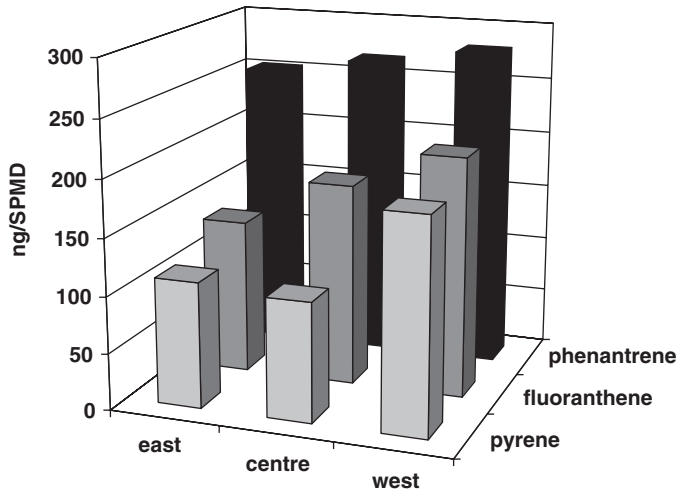

Fig. 14.4. Influence of spatial variability on sampling by SPMDs during sampling across a cross-section of the river. Three sampling sites across the river (east, centre and west) were chosen [11].

small canalized river to be homogeneous or ''well-mixed'', even if the river sampling point is relatively distant from point sources of contaminants (in the cited case the nearest point source was 10.4 km away) (see Fig. 14.4). Thus, the spatial variability in water column concentrations needs to be taken into account when interpreting the results from SPMD sampling. Gradients of increasing SPMD residues were

found for most of the analyzed PAHs from east to west across the river cross-section [11].

Samples must be taken sufficiently far downstream of effluent discharges and other potential sources of contamination to be sure that the waters have been thoroughly mixed; otherwise samples should be taken from the same side of the stream as the effluent/contamination source.

By choosing SPMDs with PRCs that do not interfere with the analysis, such as perdeuterated PAHs, with low-to-moderate SPMD fugacity, that have been added to the SPMD lipid prior to deployment, most of the field interactions discussed above can be corrected for. Currently, commercially available SPMDs (ExposMeter AB, Sweden) contain a PRC mixture of four deuterated PAH compounds, four C^{13}-labeled PCB compounds and one chlorinated naphthalene.

SPMDs should be sheltered from direct sunlight. Orazio *et al.* [12] showed that PAHs spiked into SPMDs deployed in a protective cage at 1-m depth (clear pond) were not influenced by photolysis. However, PAHs in naked SPMDs (with no protective cage) deployed under the same conditions did undergo photolysis.

The potential for vandalism and theft should also be taken into account when selecting the deployment site. In shallow waters, the devices can be deployed under various shelters that may be present, e.g. bridges or trees, which can protect membranes from direct sunlight and make them less readily visible to people who may interfere with them. In deeper waters, SPMDs are usually attached to an anchor line and float, which can be kept just below the water surface. To illustrate the possible risks, in a monitoring project in Nicaragua POCIS were deployed at four locations and local people were hired for 3 weeks to guard them. During the deployment period, one sampler disappeared and the woman hired to guard this sampler went upstream and retrieved another sampler, with which she replaced the lost one. Luckily each device was numbered, so the replacement was discovered, the woman was not paid, but her actions resulted in the loss of data from two, instead of just one, sampling sites.

Due to the integrative nature of the sampling process, SPMDs can be deployed for sampling intervals ranging from days to months depending on the expected levels of contaminants and their properties. Generally, we have found deployments of 14–30 (routinely 21) days to be sufficient to sequester quantifiable levels of most environmentally relevant hydrophobic contaminants. During the 21 days in normal surface conditions, the sequestered amounts of only a few of the normally

targeted lipophilic organic compounds exceed the linear sampling range, and thus the possibility for TWA concentration calculations. However, several factors should be taken into account when selecting an appropriate interval for integrative sampling with SPMDs, including the linear uptake time, the types of analytes targeted and the analytical sensitivity (i.e. method detection and method quantification limits) required, the time resolution needed for defining changes in waterborne chemical concentrations and environmental variables (e.g. flow-rate, temperature, expected level of biofouling, potential for vandalism or other damage to SPMDs).

In order to predict the time that SPMDs can be deployed while retaining the ability to calculate TWA values, the following equations can be used:

$$t_{1/2} = -\frac{\ln\ 0.5K_{\mathrm{sw}}V_{\mathrm{s}}}{R_{\mathrm{s}}} \approx \frac{0.693K_{\mathrm{ow}}\,V_{\mathrm{s}}}{R_{\mathrm{s}}} \tag{14.2}$$

$$t_{95} = -\frac{\ln\ 0.05K_{\mathrm{sw}}V_{\mathrm{s}}}{R_{\mathrm{s}}} \approx \frac{2.99K_{\mathrm{ow}}\,V_{\mathrm{s}}}{R_{\mathrm{s}}} \tag{14.3}$$

where $t_{1/2}$ and t_{95} are the times required to reach 50% and 95% of the equilibrium concentrations, respectively, and V_{s} is SPMD volume. Returning to the previous example of a program for monitoring anthracene in a river with a flow rate of 50 cm s^{-1} and average temperature of 25°C, the following considerations would apply. The anthracene uptake rate by a standard SPMD is 4.7 L day^{-1} at 25°C and a flow rate of 50 cm s^{-1} [5], while the log K_{sw}, log K_{ow} and V_{s} values are 4.67, 4.54 and 4.9 cm^3, respectively. Using the above relationship [3], we can forecast that the $t_{1/2}$ for anthracene would be 25 days, or in other words, uptake of anthracene by SPMDs should remain integrative for 25 days.

14.2.2 SPMD storage considerations

SPMDs exposed to air will concentrate/sample vapor-phase chemicals, therefore care must be taken to prevent their contamination during storage prior to, during and after the deployment. SPMDs must be stored in the vapor-tight, solvent-rinsed sealed metal cans provided by the supplier, and ideally should be kept frozen (< -15°C) until deployment. If PRCs are used in any of the SPMDs, the PRC-containing SPMDs must be kept separate from the others. Furthermore, although it may not be completely essential to transport SPMDs to the field at low temperatures (the SPMDs are in a clean atmosphere until the seal

on the can is broken), it is always preferable to maintain them at freezing or near-freezing temperatures; especially SPMDs with PRCs, during transport to and from the sampling sites to minimize losses of the PRC compounds. A variety of coolants can be used for shipping SPMDs, including ice, blue ice and dry ice. However, some commercial cooling blocks may contain bactericides, e.g. triclosan, which may contaminate the samples during transport.

14.2.3 Precautions/procedures during deployment and retrieval of SPMDs

Sampling will start once the SPMD has been removed from its airtight can. Therefore, the deployment area should be examined for potential sources of contamination. Since there are many sources of vapor phase contaminants, including *inter alia* engine exhaust gases, gasoline, diesel fuel, oils, wheel dust, tars, paints, solvents and cigarette smoke. It is essential to avoid exposing the samplers to the atmosphere for longer than necessary before they are deployed in the water. Samplers containing PRCs should be protected from UV light (sunlight) during the handling procedure since just 1–2 min exposure can alter the PRC concentration. Hand lotions, cologne, perfume, powered gloves, etc. must not be used because these materials can contain target chemicals. After the SPMD has been deployed, the lids are resealed on the shipping cans and the empty cans are stored refrigerated until the SPMDs are retrieved, when the same cans should be re-used.

SPMDs are deployed in the field in deployment devices that minimize abrasion of the membrane in the turbulent environment, buffer external flow, protect them from mechanical damage caused by sharp items in the water and/or living organisms and minimize their exposure to sunlight. The commercially available stainless steel deployment canisters, such as the one shown in Fig. 14.5, hold two to five standard SPMDs mounted on spider racks. The perforated surface of the device permits adequate water exchange rates and the rack design prevents SPMD both from coming into contact with the canister walls and from self-adherence, which would reduce the diffusion surface area. The robust construction of the device allows membranes to be deployed in such highly turbulent environments as oceans, industrial pipes and rivers.

In highly polluted environments, when chemicals are visible on the surface of the water (for example oil films), it is recommended to minimize their exposure to the surface when the sampler is submerged.

Fig. 14.5. A commercially available stainless steel deployment canister that holds a maximum of two SPMD racks and an airtight tin can for storage of membranes.

When the SPMDs are retrieved their exposure to sunlight must also be minimized, since some target analytes may be rapidly photodegraded.

Experienced or trained technicians should be assigned the tasks of deploying and retrieving SPMDs in order to avoid questions such as the one I was asked by a consultant, ''I just received your membranes and took them out from the cans to examine them in my office. How do I mount them on the rack?'' Personnel with accreditation based on the BSI PAS 61:2006 standardization protocol should be used if possible [13].

As mentioned previously in this chapter, environmental conditions affect the sampling rates of SPMDs, so data on relevant variables such as temperature (ideally obtained using temperature loggers that can measure and record temperatures every 10 min during the deployment, down to 200-m depth) should be acquired; a minimum requirement is to record the temperature at the beginning and end of the exposure. Flow rates and the extent of biofouling on the membrane surface should also be recorded, even if PRCs are used in the membranes to provide compensatory factors for the influence of environmental variables. Sometimes it is useful to take notes on additional phenomena such as visible discoloration of the triolein, visible damage to the membrane and the ''feel'' of the surface of the membrane (e.g. if it feels ''fatty''). Johnson *et al*. [14] performed a study on hazard assessment of oil spills and they noticed that extracts from membranes retrieved during the first 2 weeks had distinctive chocolate colors. However, the colored residues were no longer visible in the extracts from SPMDs retrieved in weeks 4, 6, 8 and 12.

Global positioning systems (GPS) devices are recommended for identifying SPMD deployment sites. Following retrieval from the exposure medium, SPMDs should be immediately dried with tissue paper, sealed inside the same labeled metal cans and transported (frozen or near frozen) back to the analytical laboratory in a cooler. Biofouling or layers of dirt must be carefully removed from the SPMDs directly after retrieval of the membrane, using tissue paper and maybe gentle wetting with hexane-extracted water. Removing salty water is also important since it will cause corrosion of the inside of the tin can, which can cause increased numbers of particles in the can and thus reduce the measured amounts of target compounds inside the membranes. Marl deposits within the biofilm may lower the dialytical recovery unless an acid wash is included in the precleaning procedure. Harsh cleaning should always be avoided since it can harm the membrane, especially if calcitric biofouling has occurred, since the calcitric deposits may tear the membranes during handling. Small losses of triolein from a membrane during sampling or after cleaning may be detectable only if membranes with an appropriate PRC (e.g. octachloronaphthalene) have been used. However, large losses of triolein can also be measured gravimetrically.

If it is necessary to delay the shipping of exposed SPMDs more than a few hours they should be stored frozen at -15°C in their sealed metal cans. Failure to maintain exposed SPMDs under freezing conditions can result in losses of analytes with relatively high fugacity (e.g. naphthalene). However, no measurable losses of 2,4,5-trichlorophenol (which has high fugacity from SPMDs at room temperature) were observed from SPMDs stored at –15°C for 6 months in sealed cans in a study by Huckins *et al.* [2].

14.3 QUALITY CONTROL

In environmental monitoring projects using SPMDs, QC procedures for sampling and analysis must be applied to ensure that the data are of high quality. Appropriate QC samples should be prepared to quantify possible sampler contamination during transport, deployment, retrieval, storage, processing, enrichment, fractionation operations and analyte recovery. A formal set of quality assurance parameters are defined in BSI PAS 61:2006 [13].

In general, two groups of quality assurance measures must be implemented: replicate QC and sampling device control.

Three to five SPMDs for each group of compounds are recommended to be deployed per sampling site to replicate QC. If, according to detection limit calculations, more than one membrane should be used to sample group(s) of compounds of interest at their respective levels of concern, the number of replicates should be increased accordingly. For example, if one set of SPMDs is used to sample sum PCBs, 16 PAHs and pesticides and another to sample dioxins the number of SPMDs should be increased to 6–10 per site. However, the difference in concentration between the replicates is usually less than 20%.

The number of control SPMDs that should be used depends on the required level of confidence. Usually, fabrication quality data for the batch of SPMDs are provided by the manufacturer. Field controls (FCs) are used to account for contamination during transport, deployment and retrieval of the SPMDs. For SPMDs with PRCs, FCs (or sometimes fabrication controls) will also provide data on the initial concentration of PRCs in the SPMDs. It is recommended that at least one FC per sampling site should be used if the sites are far apart. FCs should be taken out from the can at the place of deployment, handled and exposed to the air for the same period as it takes to deploy one sampler. Afterwards, the FC SPMDs should be resealed and stored frozen at < -15 °C until the exposed SPMDs are retrieved. The same procedure should be repeated during the retrieval of the membranes since the FC should reflect all contamination and losses during deployment and retrieval. FCs should be processed and analyzed in exactly the same way as deployed SPMDs. The commercially available SPMDs contain measurable amounts of some contaminants. For example, naphthalene is found in FCs at levels of 230–280 ng $SPMD^{-1}$. However, this compound migrates from the samplers during the sampling period, and thus equilibrium sampling levels are approached after just a few days. The UV filter ethylhexyl methoxycinnamate (EHMS) has been reported to be present at concentrations of approximately 60 ng $SPMD^{-1}$ in FC SPMDs exposed at a remote mountain lake [15]. In our consultancy work, FC SPMDs have been found to contain up to 1080 ng $SPMD^{-1}$ of the C_{17-24} fraction of oil compounds and 150–518 ng $SPMD^{-1}$ of the turpentine substance limonene. Fabrication blanks, which never leave the laboratory, are seldom reported to have been analyzed. Shipping controls are used to account for the possible leakage of air to the air-tight cans during transportation. This control is optional, but if the project's quality assurance scheme requires shipping control it is recommended to use at least one SPMD per sampling site. Reagent blanks (at least one per sample set) consisting of equivalent portions of all

solvents used during the processing, enrichment and analysis of SPMD samples, should be analyzed in the same way as the retrieved SPMDs. Such blanks provide information regarding the laboratory and reagent background associated with the entire analytical process. It is recommended that three SPMDs per sample set are used as recovery spikes. Control SPMDs are spiked with a target compound mixture and processed in the same way as the rest of the exposed SPMDs.

It is also recommended that SPMDs spiked with PRCs should be deployed in cases where *in situ* compensation is likely to be necessary or calibration data for the compounds of interest are not available. As a general precaution an extra membrane can also be deployed and stored frozen as a backup (or saved in a deep freezer by a suitable sample banking organization) in case the analysis of one of the controls fails for any reason or proves to have leaked or to be corrupted in some other way.

General recommendations for the sampling and handling processes set by ISO 5667-14 also apply to SPMDs [16]. Specific details of recommended procedures for sampling using SPMDs have been presented in the previous subchapters.

REFERENCES

1 J.N. Huckins, M.W. Tubergen and G.K. Manuweera, Semipermeable membrane devices containing model lipid—A new approach to monitoring the bioavailability of lipophilic contaminants and estimating their bioconcentration potential, *Chemosphere*, 20 (1990) 533.

2 J.N. Huckins, J.D. Petty and K. Booij, *Monitors of Organic Chemicals in the Environment*, Springer Science+Business Media, LLC, New York, NY, 2006.

3 EU, December 2001. Decision no. 2455/2001/EC of the European Parliament and of the Council of 20 November 2001 establishing the list of priority substances in the field of water policy and amending Directive 2000/60/EC. Official Journal of the European Communities 15.

4 B. Vrana, G.A. Mills, I.J. Allan, E. Dominiak, K. Svensson, J. Knutsson, G. Morrison and R. Greenwood, Passive sampling techniques for monitoring pollutants in water, *Trends Anal. Chem., TrAC*, 24 (2005) 845.

5 D. Luellen and D. Shea, Calibration and field verification of semipermeable membrane devices for measuring polycyclic aromatic hydrocarbons in water, *Environ. Sci. Technol.*, 36 (2002) 1791.

6 J.D. Petty, C.E. Orazio, J.N. Huckins, R.W. Gale, J.A. Lebo, J.C. Meadows, K.R. Echols and W.L. Cranor, Considerations involved with the use

of semipermeable membrane devices for monitoring environmental contaminants, *J. Chromatogr. A*, 879 (2000) 83.
7 L.H. Keith, *Principles of Environmental Sampling*, ACS Professional reference book: American Chemical Society, Washington, DC, 1996.
8 Å. Granmo, R. Ekelund, M. Berggren, E. Brorström-Lunden and P.-A. Bergqvist, Temporal monitoring of organochlorine compounds in seawater by semipermeable membranes following a flooding episode in Western Europe, *Environ. Sci. Technol.*, 32 (1998) 3887.
9 O. Lindahl, Salinity profile from Gullmar fjord in 2001. *Toxicity of* Dinophysis *spp in relation to population density and environmental conditions on the Swedish west coast*, Harmful algae, Personal communication, 2006.
10 P.-A. Bergqvist and L. Strandberg, Organic pollution in water samples taken in Umeå river near rain water and industry discharge places by SPMD technique in September 1997, Umeå University, Sweden; Report to the County environmental office; Umeå, Sweden, 1998.
11 J. Louch, G. Allen, C. Erickson, G. Wilson and D. Schmedding, Interpreting results from field deployments of semipermeable membrane devices, *Environ. Sci. Technol.*, 37 (2003) 1202.
12 C. Orazio, S. Haynes, J. Lebo, J. Meadows, J.N. Huckins and J. Petty, Potential for Photodegradation of Contaminants During SPMD Sampling. Poster P192. SETAC meeting Salt Lake City, 2002.
13 British Standards Institute Publicly Available Specification PAS 61:2006, Determination of priority pollutants in surface water using passive sampling (2006).
14 B.T. Johnson, J.D. Petty, J.N. Huckins, K. Lee and J. Gauthier, *Hazard Assessment of a Simulated Oil Spill on Intertidal Areas of the St. Lawrence River with SPMD-TOX*, Wiley InterScience, *Environ. Toxicol.*, 19 (2004) 329.
15 T. Poiger, H.-R. Buser, M.E. Balmer, P.-A. Bergqvist and D.M. Muller, Occurence of UV filter compounds from sunscreens in surface waters: regional mass balance in two Swiss lakes, *Chemosphere*, 55 (2004) 951.
16 ISO 5667-14, Water quality—Sampling—Part 14: Guidance on quality assurance of environmental water-sampling and handling.

Chapter 15

Techniques for quantitatively evaluating aquatic passive sampling devices

B. Scott Stephens and Jochen F. Müller

15.1 INTRODUCTION

As the suite of available devices for passively sampling aquatic environmental pollutants has grown in recent years, groups wishing to make quantitative measurements with them have been met with similar challenges. Perhaps the most pressing is the need for large amounts of publicly available, accurate, device-specific validation data for each compound of interest. With the continual advance of separation and analytical methods, the emergence of novel sequestration phases and membranes and the prioritisation of new pollutants, generating meaningful sampler validation databases will remain an ongoing problem.

While a number of international standards have been developed specifying criteria and a set of experiments for quantitative validation of workplace passive dosimeters [1–3], validation of their aquatic environmental variant has remained the work of researchers. A number of innovative approaches have been devised and several standardised devices have been presented, each with its own set of validation/calibration data.

The aim of this chapter is to illustrate the methods workers have employed for generating these different datasets and to review the techniques that have been applied to validate them in the laboratory and *in situ*. It should be useful to students wishing to research the techniques underlying the validation and calibration of passive sampling devices, particularly those considering the logistics of their own aquatic passive sampler validation studies.

Comprehensive Analytical Chemistry 48
R. Greenwood, G. Mills and B. Vrana (Editors)
Volume 48 ISSN: 0166-526X DOI: 10.1016/S0166-526X(06)48015-6

15.2 KEY PARAMETERS

What does it mean to quantitatively validate a passive sampling device? The answer depends to a large extent on the researchers' intention for it, and which mathematical model does the best job of approximating its behaviour.

There are two modes of quantitative passive sampler operation: equilibrium and kinetic. This section briefly outlines the key parameters that play a role in each mode. The reader is encouraged to inspect the other chapters in this book and the references within this chapter for detailed theoretical considerations.

15.2.1 Equilibrium partitioning

The 1970s saw the *n*-octanol–water equilibrium partition coefficient emerge as a powerful parameter for predicting the potential for contaminants to concentrate in aquatic organisms [4]. More recently, the passive sampling literature introduced the concept of a sampler–water partition coefficient, K_{SW}, defined as the ratio of sampler to water concentration of the compound of interest at thermodynamic equilibrium. Although several pitfalls may exist in using this parameter [5], the approach has proved fruitful, allowing the development of a number of functional equilibrium sampling devices, perhaps most notably the solid-phase microextraction (SPME) technique, pioneered by Pawliszyn *et al.* [6].

Validation of aquatic equilibrium samplers typically aims to determine K_{SW} for the compound of interest and to investigate its integrity in environmental deployments. The other key parameter is the time needed to reach an approximate equilibrium state, and it is important to know this in order to ensure that the assumption of equilibrium applies.

15.2.2 Time-integrated sampling

Uptake with time of pollutants into a passive sampler has been modelled at several levels of complexity [7]. In practice, a one-dimensional first-order diffusion model, invoking Fick's first law underlies the time-weighted averaging (TWA) approach. In this simple kinetic model, resistance at either (1) the hydrodynamic boundary layer or (2) within the sampler membrane/sequestering phase acts to control pollutant flux into the sampler. The classical first-order solutions for each scenario

introduce a hydrodynamic diffusive mass transfer coefficient k_f ($m\,s^{-1}$), or a membrane diffusion coefficient D_{AB} ($m^2\,s^{-1}$), respectively [5]. Huckins *et al.* [7] and a number of subsequent workers have also expressed the limiting kinetic parameter in terms of an overall device ''sampling rate'', R_S ($L\,day^{-1}$).

The objective of workers seeking to validate time-integrated sampling behaviour has typically been to obtain values for R_S, k_f or D_{AB} for the compound of interest. More detailed validation studies then seek to investigate the problems of measuring these parameters, and determining their variability in a range of conditions taking into account water flow, temperature and surface fouling of the diffusion membrane. In most cases, a combination of work both in the laboratory and field has been undertaken.

15.3 LABORATORY METHODS

15.3.1 The concentration problem

Much of the appeal of synthetic aquatic passive devices arises from the difficulties inherent in conventional methods of measuring true dissolved concentrations. It is thus understandable that some of the greatest challenges in designing experiments for validating passive sampling devices relate to regulating and monitoring concentration in the exposure vessel. Measurement is particularly difficult for hydrophobic organic contaminants, which exist naturally at low levels in the aquatic environment. In many cases, the amount of water necessary for an accurate measurement may be a significant portion of, if not greater than, the amount practicable for the experiment. Taking several samples to confirm exposure concentrations during an experiment is therefore often not possible. Furthermore, with potential loss routes through sorption to the vessel walls, volatilisation, degradation and uptake by the sampling devices, accepting a nominal concentration can be erroneous. A large number of innovative approaches to these problems have been taken.

15.3.2 Batch techniques

Batch experiments typically allow for a greater number of replicates and are generally much simpler and less expensive to implement than flow-through based experiments. They are therefore very attractive to researchers.

15.3.2.1 C_w depletion

In 1974, Benes and Steines [8] placed dialysis membranes filled with distilled water into 1-L beakers containing a solution of radioactively labelled metals. Water was analysed from both the samplers and the beaker over the course of a week, revealing the differences in uptake kinetics as well as equilibration concentrations of the spiked compounds in these early aquatic passive sampling devices. This simple batch depletion experimental design has been applied as a useful starting point for testing numerous passive sampler designs.

Södergren's [9] *n*-hexane-filled dialysis bags were exposed to PCB, HCB and DDT in the same fashion in 1987 and two years later the first work on SPMD kinetics by Huckins *et al*. [7] followed suit, exposing prototype SPMDs to 1-L well water spiked with radiolabelled PCBs, mirex and fenvalerate. Additionally, Huckins' study exposed spiked SPMDs to clean well water, providing kinetics data for diffusion in both directions. For Benes and Steines' and Huckins' work, the radiolabelled compounds could be detected in both the passive samplers and the water phases via scintillation counting. Thus, simple mass balances were possible, as was the first calculation of equilibrium coefficients between the two phases at the experimental temperatures.

Given that the aqueous concentration is depleted, calculation of kinetic sampling rates, or mass transfer coefficients, is complicated—although not precluded—with such batch depletion techniques. Providing degradation and/or loss through sorption and volatilisation can be minimised, or at least measured so that the aqueous concentration over time is known, then Fick's law can be solved computationally for both K_{SW} and R_S [10,11] simultaneously. However, the problem of how to measure water concentration continuously in such low volume experiments remains. Detection limits for conventional techniques at environmental concentrations typically require much larger volumes of water.

This simple batch depletion method is amenable to both stagnant and stirred exposures and has been applied repeatedly in subsequent kinetic studies [12–14]. Despite its drawbacks, it is the most easily applied technique for investigating the affinity of a device for the compound of interest, and where water concentration is monitored, has the potential to determine both kinetic and equilibrium parameters.

15.3.2.2 Negligble C_w depletion

For samplers with low mass transfer rates, such as SPME, depletion due to sampler uptake during the experiment becomes less an issue,

even for small water volume batch experiments. Here a single spike batch method has been used with a much higher confidence of a stable exposure concentration [15]. Similarly, a very large water volume may be employed to achieve virtual non-depletive uptake [11] for high R_S samplers. The drawbacks of this approach may be the need for an expensive large vessel, significant laboratory space and energy input to control temperature. Unfortunately, although working with small pieces of larger passive sampling devices (e.g. standard SPMDs) may allow for non-depletive uptake, it is seldom a useful way of attaining quantitative measurements. The aim is typically to measure the kinetic parameters for the real-world device and the hydrodynamics of the standard device are very difficult to replicate using smaller pieces.

15.3.2.3 Batch renewal

The formative work investigating SPMD sampling rates by Huckins and co-workers at the laboratories of the U.S.G.S. [13,14] employed a system based on 30-L aquaria. In their early studies, the full aquarium volume was exchanged every 30 min, in a batch like fashion. In the later work, $6\,L\,h^{-1}$ of water containing nominal concentrations of polycyclic aromatic hydrocarbon (PAH) was pumped into the aquaria at intervals of 10 min, displacing depleted water. Although the water concentration was not independently validated, the frequency of freshly prepared and spiked water additions should have ensured a roughly constant concentration for the duration of exposure studies. In the original publications this was called a flow-through system, but it might also be termed a large volume batch renewal system.

In a more typical batch renewal system for polar compounds, Alvarez *et al.* [16,17] maintained roughly constant water concentration by replacing exposure water in 1-L chambers at carefully determined renewal intervals. Firstly, a rough estimate of sampling rate was obtained in a static exposure over a few days. More accurate calibrations over periods up to 56 days were then conducted by completely replacing the exposure water with freshwater of the original concentration at the predefined renewal intervals. The intervals were selected to maintain a water concentration greater than half the equilibrium concentration, and to allow the chemical concentration to decrease by no more than one-eighth of the original value. A significant advantage of the method is a high level of certainty in the C_w value, with the obvious drawback being the laborious preparing and changing of water on a daily basis.

15.3.2.4 Diffusion cells

If the limiting resistance to flux into the passive sampler is known to be a homogeneous diffusion layer, such as the hydrogel for diffusion of metals in diffusion gradient thin-film devices (DGTs), determination of the diffusion coefficient, D_{AB}, of this layer becomes the focus of validation work. A variety of diffusion cells have been developed for D_{AB} measurement.

The developers of the DGT technology at the University of Lancaster employed a diaphragm cell operating in *pseudo*-steady-state mode to determine D_{AB} for their devices [18,19]. Their setup comprised two 70-mL perspex compartments, each with a stirrer and connected to the other by a small opening. The diffusive gel was fitted in between the openings of the two chambers and 50 mL of spiked water was introduced into one cell while pure water was placed in the adjoining cell. The diffusion gradient between the cells results in flux through the gel. As the DGT sequesters metal species, the analyte concentration in the cell was measured throughout the course of the experiment by taking small samples (200 μL) during the experiments and analysing these by atomic absorption spectroscopy (AAS). The setup is considered *pseudo*-steady-state as the concentration changes in both compartments throughout the course of the experiment.

15.3.2.5 Partition-controlled delivery

A useful approach to the problem of maintaining constant concentration in a batch system has been demonstrated in the form of partitioning delivery administering (PDA) also referred to as partition-controlled delivery (PCD). The basic principle of PCD is to introduce into the system a third phase, typically a solid-phase sorbent, which contains a high concentration of the test compound that is able to rapidly equilibrate with the aqueous phase. Mayer *et al*. [20] noted that in such systems, the aqueous concentration should remain virtually constant if (1) the amount in the PCD phase remains nearly unaffected by the partitioning process and (2) the loss kinetics from PCD phase are sufficiently fast to keep up with the depletion processes of the test compound in the vessel. A third criterion would be to ensure the exposure experiment does not commence until the PCD phase has equilibrated with the aqueous phase.

Clearly, a high partitioning coefficient is a desirable characteristic of the PCD phase if criterion (1) is to be met. The key parameters controlling criterion (2) are the thickness of the laminar boundary layer adjacent to the surface of the PCD phase—governed by the degree of

turbulence in the system—as well as the total exposed surface area of the PCD phase. Thus, in addition to employing a PCD phase with a high partition coefficient for the compound of interest, a good PCD system will incorporate a relatively high surface area in contact with a high flow-rate solution (Table 15.1). Such systems that have been demonstrated to maintain constant concentrations of a range of hydrophobic organic chemicals have employed as the PCD phase: strips of C_{18} Empore™ disk [20]; poly(dimethylsiloxane) (PDMS) films [21,22] and intriguingly Teflon® [23], which has been incorrectly considered by many workers to be a non-adsorptive substrate.

15.3.3 Flow through techniques

15.3.3.1 Injection delivery

Further work effect of hydrodynamics on mass transfer in SPMDs was conducted by Vrana *et al.* [31] in a system comprising a 1-m high vertical column flow-through system, containing the SPMDs. Water was continuously pumped from the bottom to the top of the column over the samplers at a rate of $180\,L\,h^{-1}$ with water leaving the top of the column and going to waste. Constant concentration was maintained in the column by peristaltic injection of spike compounds into a 1-L mixing chamber at the bottom of the column. Another flow-through system was devised by Vrana *et al*. [32] for exposure of the Chemcatcher Empore™ disk based passive samplers. This consisted of a 20-L glass tank inside of which was a rotating carousel containing the smaller passive samplers. Water was pumped into the tank at a rate of $2\,L\,h^{-1}$ with addition of a solution containing the spike compounds (e.g. PAHs) added directly to the tank via a peristaltic pump at a rate of $100\,\mu L\,min^{-1}$. Rotation of the carousel provided mixing in the exposure vessel. This system was specifically designed to be small and simple enough for other workers to set up for calibration of these passive samplers for other compounds of interest. It is small enough to be moved and can be installed in temperature-controlled room.

Huckins *et al*. [34] also developed an injection flow-through system that accommodated SPMDs and oysters.

15.3.3.2 Partition-controlled delivery in a flow-through vessel

In early work investigating the kinetics of performance reference compounds (PRCs) in SPMDs, Booij *et al*. [28] presented a flow-through exposure system, which incorporates the same principles used in partition delivered control for batch systems. They employed 5.5 kg of

TABLE 15.1
Aquatic laboratory calibration systems

Type	Advantages	Disadvantages	Examples
Batch depletion	Simplest and earliest exposure method; only single spike addition required. Suitable for low R_S samplers.	For high R_S samplers concentration will typically decrease significantly, but models may be able to account for this if loss through volatilisation and degradation are small. Volume likely to be insufficient to allow confirmation of water concentration for many compounds.	[8,9,13,16,24–26]
Negligible depletion batch exposure	Simple. Single spike addition. Higher volume: R_S ratio allows more stable water concentration; enables a series of samplers to be exposed to the same water throughout experiment; water samples may be taken to verify concentration.	May require large-volume vessel/aquarium for high R_S samplers such as SPMDs; other loss routes such as volatilisation, degradation and sorption to vessel walls are still potentially important.	[11,15,27]

Batch renewal	High level of reliability maintaining constant concentration.	Very labour intensive, often requiring daily preparation and transfer of solutions. High level of waste solution generated.	[16,17]
Batch partition-controlled delivery	Simple design. Ease of use. A few validation studies for low R_S samplers such as SPME fibres exist.	Few validation studies exist for high R_S samplers and secondary confirmation of stable concentrations will likely be necessary.	[20–23]
Diffusion cell	Simple system offering precise measurement of D_{AB} for membranes and gels.	Suitable only for systems in which the resistance to flux is a diffusive membrane or gel (not hydrodynamically limited).	[18,19]
Flow-through –partition-controlled delivery	Similar advantages to batch PCD, with the addition of control of flow that may improve the efficiency of delivery.	Same caveats as with PCD above. Note an increase in exposure concentration with time has been observed [30] in this type of system.	[28–30]
Flow-through –injection-controlled delivery	Traditional method, with greatest number of validation studies.	Most wasteful of water and spike compounds. Most complicated and expensive to operate.	[13,14,31–34]

sediment that was spiked with 2–5 $\mu g\,kg^{-1}$ of chlorobenzenes and PAHs as a PCD phase. This sediment was immersed in a 10-L chamber of water. SPMDs were deployed in a connected 200-L stirred vessel and the water circulated through the system at a flow rate of $24\,L\,h^{-1}$ by means of a pump. Flow velocity was estimated with a float and stopwatch and by the volumetric flow rate in the large and small vessel, respectively.

Rantalainen *et al*. [29] used a similar approach for PCDDs, PCDFs and PCBs. This system, however, employed a single much larger stirred vessel (900 L) that contained both the spiked sediment and the passive samplers. The spiked sediment was held in place inside the vessel on top of a mat of glass fibre in a 4-cm deep perforated steel tray. In order to assess both direct sediment and aqueous exposure, eight SPMDs were buried inside this tray and eight were suspended in water. A custom filter unit was connected to the system, inside of which was placed a further 500 g of the delivery sediment. A circulation rate of $10\,L\,h^{-1}$ was achieved via an in-line pump. This system also had the advantage of circulating water through an adjacent cooling and heating unit, allowing internal system temperature control.

In later work, investigating the effects of temperature on PAH uptake into SPMDs Booij *et al*. [30] used a pair of ''generator columns'' each containing 1 kg of spiked (with 3 chlorobenzenes and 10 PAHs) silica bonded C_{18} as the PCD phase. These columns were installed in series on either side of a 200-L round bottom exposure vessel, each with its own attached pump. The vessel itself was immersed in a 750-L temperature-controlled water bath. Inside, SPMD membranes were mounted and rotated in the solution, which was pumped through the system at approximately $900\,L\,day^{-1}$. Batch analyses of water samples taken throughout the exposure period indicated that despite a combined SPMD sampling rate of $60\,L\,day^{-1}$, the water concentration remained relatively stable for most compounds in this system. An *increase* in concentration was observed in several cases, which was attributed to the removal of samplers over the duration of the experiment, and the subsequent decrease in overall extraction from the system. The main advantage over the injection system is the circulatory nature of such a flow-through system, which in itself should improve the efficiency of the PCD process.

15.4 *IN SITU* METHODS

While a laboratory exposure experiment may provide the potential to control concentration, flow conditions, temperature, pH and salinity, it

often fails to address other factors that are equally—or quite likely more—important in evaluating a passive sampling design. The real value of a field validation is that it allows the developer to experience the process that users will need to go through in deploying the devices in a real-world situation. These include storage, refrigeration and transport issues; deployment and retrieval processes at the site; cleaning up a sampler after deployment; assessment of degradation of the sampler surface housing; and extraction, clean-up and analysis of a contaminated passive sampler extract. Laboratory studies seldom address these issues, which may indeed prove to be crucial in adoption of a technology.

In situ validation also obviates the requirement for maintaining an exposure concentration in the laboratory. However, here the problem becomes independently validating the exposure concentration, particularly for hydrophobic compounds distributed in both the dissolved and particulate associated phases. The purpose of this section is to review briefly the methods that have been employed in the limited simultaneous active and passive field deployments to date. It covers both high-volume sampling for hydrophobic organics and high-frequency grab sampling for hydrophilics and inorganics.

15.4.1 High-volume solid-phase extraction

Solid-phase extraction (SPE) has become the preferred method for separation of organics from water in recent decades. This is due to the widespread availability of SPE phases with an affinity for a broad spectrum of compounds; lower solvent requirements (compared with liquid–liquid extraction), relatively high recovery rates and ease of use. Although SPE is typically performed under vacuum in the laboratory, a number of mechanical systems have been developed for its application in the field, in particular for extracting hydrophobics from large volumes of water. Several devices such as the Infiltrex, and Kiel *in situ* pump are available commercially, but the basic elements of these systems may be put together by any laboratory. They are hosing, filter(s), sorbent column(s), pump, power supply, flow meter and an optional electronic controller.

15.4.1.1 Pumping systems

Typically, water pumps are designed to be placed such that they are ''pushing'' water through the greatest resistance; however, it is desirable to prevent contact between the mechanical components of the

pump and the water prior to extraction, which means the pump usually needs to be operating in suction mode. In the field, this requires that the device is not situated too high above the water level because suction is limited to 1 atm of negative pressure, beyond which the pump pulls a perfect vacuum. Practically, a metre or two is the maximum, depending on the resistance in the rest of the system. An alternative is to make the pump and the batteries submersible, although this significantly increases the cost of the system.

15.4.1.2 Filters

Passive samplers theoretically sample only the dissolved phase fraction of pollutants, meaning that thorough filtration of the particulates from high-volume water samples is required prior to passing it through the sorbent (Table 15.2). As can be seen in Table 15.3, most workers opt for glass fibre filters with a maximum cut-off of 1 μm. To improve throughput, the overall filter diameter should be as large as possible, although this can require more expensive filter housings and filter paper. Flow-through centrifuges have also been used prior to filtration to reduce the load on the filter [58].

15.4.1.3 Sorbents

One of the earliest publications of *in situ* SPE for environmental sampling dates to 1972 when the long-term decline of PCB concentrations

TABLE 15.2

Compounds detected with mechanical high-volume SPE field samplers

Compound group	Refs.	
	Infiltrex XAD-2	Other systems/sorbents
Alkanes	[35–37]	[35]
PAHs	[36–43]	[44]
PCBs	[35,38,41–48]	[44,49–52]
PCDD/Fs	[41,43,47,53]	
PBDEs/flame retardants	[42,54]	
Pesticides	[42,55]	[52,56,57]
Herbicides	[38,42]	
Pharmaceuticals	[42]	
Fragrances and PCPs	[42]	[58]
Plasticisers	[42]	
Alkylphenols	[42,59]	
Other organics	[60]	[57]

in North Atlantic was observed by extraction of 60-L seawater samples using XAD-2 [61]. Although the XAD polymeric sorbents have remained the most commonly used phase for these systems, they require time-consuming and solvent-intensive cleaning and extraction procedures. Contamination, particularly in transport and handling has been shown to be very challenging with these sorbents. Other polymeric sorbents such as SDB-1 or LiChrolut EN have been reported to be less susceptible to contamination [47,49]. Another potential problem with high-volume SPE is the formation of water channels in the sorbent column, leading to premature breakthrough. More modern sorbent products such as particle-loaded Empore™ disks [62] and Bakerbond Speedisks® go some way to addressing this, although the breakthrough volume of the former is typically much smaller than a sorbent column. Recently, Speedisks® have exhibited excellent recovery of a broad spectrum of compounds for high-volume water extractions of lake water in the field [38].

Breakthrough is typically prevented by maximising the contact time in the sorbent column, which requires minimising the overall flow rate through the system. As can be seen from Table 15.3 most workers have limited flow rate to less than 1 L min^{-1}. The use of two columns in parallel can reduce the overall sampling time while maintaining low flow conditions [53]. There are a number of excellent summaries of the properties of both modern and classical sorbents and their application in high- and low-volume extractions from surface waters [57,63]. Undoubtedly, novel SPE products will continue to become available in the future and detailed information about the properties of these as well as existing sorbents can often be obtained directly from the manufacturer.

Table 15.4 lists the few reported studies in which high-volume SPE systems have been deployed in conjunction with passive samplers.

15.4.2 Grab sampling validation methods

With more polar chemicals, the traditional approach to water sampling is taking small ‘‘grab’’ or ‘‘spot’’ samples. The standard volume for many organic spot sampling methods, such as those incorporated in the US EPA 500 (drinking water) and 600 (wastewater) series of protocols, is 1 L. It is typically less for inorganics. A high-frequency grab sampling programme may be facilitated with automated and refrigerated mechanical sampling devices. Enough samples can provide temporal information that can be used in passive sampler validation in the field.

TABLE 15.3
High-volume solid-phase extraction configurations

Media	Adsorbent	Filter		Flow rate (mL min^{-1})	Column	Volume extracted (L)	Refs.
		Cut-off (μm)	Diameter (cm)				
Arctic	Isolute Env+	GF/F			200 mg	20	[56]
High elevation lake water	XAD-2 and Speedisks®	GF/F		200		50	[38]
Mountain lake	XAD-2	1.0	14.2	300	75 g	100	[48]
Lake Superior	XAD-2	GF/F	29.3	<600	75 g		[37]
Lake Michican	XAD-2	0.7	29.3	1000 (filter), 250 (column)		65	[45]
Seawater	XAD-2 and PUF	GF/C, 0.5	14.2	100–1900	PUF: 5 cm × 30.5 cm; XAD: 2.7 cm × 20 cm	42–1000	[35]
Ohio River	XAD-2	140	14	1600	2 × 75 g in parallel	1000	[53]

Milli-Q and seawater	XAD-2 and C_{18} Empore™	0.7 GF/F		400 (XAD-2), 50 (C_{18})	50 g XAD-2, 90-mm diam. disk	50 (XAD), 10 (C_{18})	[49]
Ocean outfalls, California	XAD-2	Not filtered		50–200	37-cm long, 2.5-cm diam.		[51]
Reef platform and seawater basins	XAD-2	Gelman AE GFF	14.9	500	100 mL	221–435	[36]
Aluminium reduction plant discharge	PUF	0.7 GF/F	14.2	1000	30-mm diam., 45-mm long	30–40	[39]
Oceanic	XAD-2	Not filtered		<300	300 mm long., 22-mm diam.	150–400	[52]
San Francisco Estuary	XAD-2	1		1400	250 g and 2×75 g	400	[41]
Deep Atlantic	XAD-2	GF/F		5 bed volumes			[50]

TABLE 15.4
Simultaneous passive and high-volume validation studies

Passive samper	Site	Target compounds	Refs.
SPMD	Lower Fraser River, British Colombia	PCBs, PCCD/Fs	[47]
SPMD	Aluminium Smelter Norway	PAHs	[39]
SPMD	North Sea, Norway	PAHs	[43]
SPMD	Upper Misissippi River	OCs	[64]
SPME	Coastal California	Pesticides	[55]

OCs = Organo-chlorine compounds

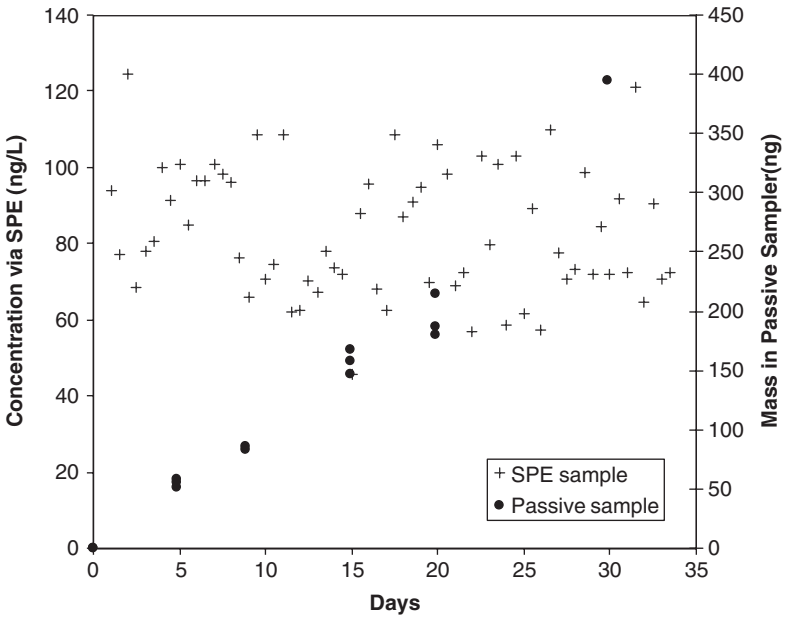

Fig. 15.1. Field validation for the herbicide Simazine in a modified Chemcatcher passive sampler (using an SDB-RPS sequestering phase), Brisbane River Australia.

Figure 15.1 shows the results from a field validation study using modified Chemcatcher passive samplers conducted in the Brisbane River, Australia, by the authors. In this case, spot samples of water were taken twice daily over the course of the deployment and passive samplers were deployed in series to investigate uptake kinetics. Figure 15.1 shows reasonably high short-term variation in spot measurements,

TABLE 15.5
Some simultaneous passive and grab field validations

Location	Type	Sites	Passive samples[a]	Grab samples[a]	Exposure duration	Comments	Refs.
Menai Straits, UK	DGT	1	6	6	5–6 h		[27]
Ephraim Island, Australia	DGT	13	24	24	Up to 72 h	Numerous deployment periods and sampling regimes.	[65]
Gold Coast Broadwater, Australia	DGT	8	1/1	6/2	24 h/72 h	Entailed two field exposures. Grab samples were composited for second.	[66]
Thames Tideway	POCIS		7				[16]
Constructed Wetlands, Missouri	POCIS	3	1	1	28 d	Only single water samples taken at each of five sites.	[17]
Portsmouth Harbour	Empore™	2	2	10	14 d		[33]

[a]Not counting replicates.

but like many environmental systems, the medium-term trend is for a relatively stable mean concentration. Thus, the kinetic sampling rate can be calculated using the standard laboratory calibration methods. Indeed, as mentioned before, sampling rates can be derived even from a variable C_w exposure, as long as C_w can be described mathematically [11].

Several other simultaneous grab-passive field evaluations are listed in Table 15.5. In many cases, grab samples have been taken at regular intervals during the deployment, but it is often practicable to obtain grab samples only at the deployment and/or retrieval time of the passive samplers. It is up to the worker to determine the extent of variation in water concentration, taking into consideration periodic point source discharges, tidal and flow variation and rain events.

The danger with field validations is that each deployment will expose the sampler to a fluctuating mixture of potentially hundreds of compounds at concentrations that are likely to span several orders of magnitude, with various bound and dissolved fractions. There will also be variation from site to site in temperature, flow velocity, acidity and salinity. The question arises as to how these variable conditions affect the kinetic and equilibrium parameters of the sampler.

If a passive sampling technology is to be adopted in routine monitoring programmes, there needs to be a robustness or at least a measurable responsiveness (such as with PRCs) to these factors. A much larger database of field exposures than exists today is necessary for each of the currently available passive sampler designs. It is the hope of the authors that the techniques outlined in this chapter can assist continuing contributions to this important resource.

REFERENCES

1 E.R. Kennedy, T.J. Fischbach, R. Song, P.M. Eller and S.A. Shulman, Guidelines for Air Sampling and Analytical Method Development and Evaluation. NIOSH technical report. Available online: http://tinyurl.com/72nj2
2 ISO 16107: 1999 Workplace Atmospheres—Protocol for evaluating the performance of diffusive samplers.
3 ASTM D6246-02 Standard Practice for Evaluating the Performance of Diffusive Samplers.
4 C.T. Chiou, *Partition and Adsorption of Organic Contaminants in Environmental Systems*, Wiley, NJ, 2002, Chapter 5.

5 R. McGregor, *Diffusion and Sorption in Fibres and Films*, Academic Press, New York, 1974, Chapter 12.
6 University of Waterloo, Waterloo, Canada, SPME Bibliography. Available online: http://tinyurl.com/d2bfc
7 J.N. Huckins, J.D. Petty and K. Booij, *Monitors of Organic Chemicals in the Environment: Semipermeable Membrane Devices*, Springer, New York, 2006.
8 P. Benes and E. Steinnes, *Water Res.*, 8 (1974) 947.
9 A. Södergren, *Environ. Sci. Technol.*, 9 (1987) 21.
10 J. Crank, *The Mathematics of Diffusion*, Oxford University Press, London, 1975.
11 B.S. Stephens, A.P. Kapernick, G. Eaglesham and J. Müller, *Environ. Sci. Technol.*, 39 (2005) 8891.
12 J.N. Huckins, M.W. Tubergen and G.K. Manuweera, *Chemosphere*, 20 (1990) 533.
13 J.N. Huckins, G.K. Manuweera, J.D. Petty, D. Mackay and J. Lebo, *Environ. Sci. Technol.*, 27 (1993) 2489.
14 J.N. Huckins, J.D. Petty, C.E. Orazio, J.A. Lebo, R.C. Clark, V.L. Gibson, W.R. Gala and K.R. Echols, *Environ. Sci. Technol.*, 33 (1999) 3918.
15 R Ferrari, *J. Chromatogr. A*, 795 (1998) 371.
16 D.A. Alvarez, J.D. Petty, J.N. Huckins, T.L. Jones-Lepp, D.T. Getting, J.P. Goddard and S.E. Manahan, *Environ. Toxicol. Chem.*, 23 (2004) 1640.
17 J.D. Petty, J.N. Huckins, D.A. Alvarez, W.G. Brumbaugh, W.L. Cranor, R.W. Gale, A.C. Rastall, T.L. Jones-Lepp, T.J. Leiker, C.E. Rostad and E.T. Furlong, *Chemosphere*, 54 (2004) 695.
18 J. Gimpel, H. Zhang, W. Hutchinson and W. Davison, *Anal. Chim. Acta*, 448 (2001) 93.
19 H. Zhang and W. Davidson, *Anal. Chim. Acta*, 398 (1999) 329.
20 P. Mayer, J. Wernsign, J. Tolls, P.G.-J. de Maagd and D.T.H.M. Sijm, *Environ. Sci. Technol.*, 33 (1999) 2284.
21 Y. Kiparissis, P. Acktar, P.V. Hodson, R. Brown and S. Brown, *Environ. Sci. Technol.*, 37 (2003) 2262.
22 S.R. Brown, P. Akhtar, J. Åkerman, L. Hampel, I.S. Kozin, L.A. Villerius and H.J.C. Klamer, *Environ. Sci. Technol.*, 35 (2001) 4097.
23 A. Gerofke, P. Kömp and M. McLachlan, *Water Res.*, 38 (2004) 3411.
24 C.E. Green and M.H. Abraham, *J. Chromatogr. A*, 885 (2000) 41.
25 B. Vrana, P. Popp, A. Paschke and G. Schüürman, *Anal. Chem.*, 73 (2001) 5191.
26 P. Mayer, W.H.J. Vaes and J.L.M. Hermens, *Anal. Chem.*, 72 (2000) 459.
27 H. Zhang and W. Davison, *Anal. Chem.*, 67 (1995) 3391.
28 K. Booij, H.M. Sleiderink and F. Smedes, *Environ. Toxicol. Chem.*, 17(7) (1998) 1236.
29 A.-L. Rantalainen, W.J. Cretney and M.G. Ikonomou, *Chemosphere*, 40 (2000) 147.

30 K. Booij, H.E. Hofmans, C. Fischer and V.E.M. van Weerlee, *Environ. Sci. Technol.*, 37(2) (2003) 361.
31 B. Vrana and G. Schüürmann, *Environ. Sci. Technol.*, 36 (2002) 290.
32 B. Vrana, G.A. Mills, E. Dominiak and R. Greenwood, *Environ. Pollut.*, 142 (2006) 333.
33 J. Kingston, R. Greenwood, G.A. Mills, G.M. Morrison and L. Björklund Persson, *J. Environ. Monit.*, 2 (2000) 487.
34 J.N. Huckins, H.F. Prest, J.D. Petty, J.A. Lebo, M.M. Hodgins, R.C. Clark, D.A. Alvarez, W.R. Gala, A. Steen, R. Gale and C.G. Ingersoll, *Environ. Toxicol. Chem.*, 23 (2004) 1617.
35 J.I. Gómez-Bellinchón, J.O. Grimalt and J. Albaigés, *Environ. Sci. Technol.*, 22 (1988) 677.
36 M.G. Ehrhard and K.A. Burns, *J. Exp. Marine Biol. Ecol.*, 138 (1990) 35.
37 Minnesota Pollution Control Agency. Lake Superior/Duluth-Superior Harbor Toxics Loading Study. USA EPA Grant #X995402-01 Septermber 1999.
38 S. Usenko, K. Hageman, D.W. Schmedding, G.R. Wilson and S.L. Simonich, *Environ. Sci. Technol.*, 39 (2005) 6006.
39 J. Axelman, K. Naes, C. Näf and D. Broman, *Environ. Toxicol. Chem.*, 18 (1999) 2454.
40 K. Tran and E. Zeng, Laboratory and Field Testing on the Infiltrex 100 Pump. Southern California Coastal Water Research Project. Annual Reports 1996/1997. Available online: http://www.sccwrp.org/
41 San Francisco Estuary Institute. South Bay/Fairfield-Suisun Trace Organic Contaminants in Effluent Study. March 28, 2001. Available online: http://www.sfei.org/cmr/TOESv5.pdf
42 D.R. Oros, W.M. Jarman, T. Loweb, N. David, S. Lowe and J.A. Davis, *Mar. Pollut. Bull.*, 46 (2003) 1102–1110.
43 T.I. Utvik, G.S. Durell and S. Johnsen, *Mar. Pollut. Bull.*, 38 (1999) 977.
44 D.E. Schulz-Bull, G. Petrick, R. Bruhn and J.C. Duinker, *Mar. Chem.*, 61 (1998) 101.
45 D. Achman, R.K. Hornbuckle and C.S. Eisenreich, *Environ. Sci. Technol.*, 27 (1993) 75.
46 D. Muir and W. Strachan, Contaminant Levels, Trends and Effects in the Biological Environment. Canadian Arctic Contaminants Assessment Report II. Northern Contaminants Program. Indian and Northern Affairs Canada. Available online: http://www.ainc-inac.gc.ca/ncp/index_e.html
47 A.-L. Rantalainen, M.G. Ikonomou and I.H. Rogers, *Chemosphere*, 37 (1998) 1119.
48 R. Vilanova, P. Fernández and J.O. Grimalt, *Sci. Total Environ.*, 279 (2001) 51.
49 J. Dachs and J.M. Bayona, *Chemosphere*, 35 (1997) 1669.
50 D.E. Schulz, G. Petrick and J.C. Duinker, *Mar. Pollut. Bull.*, 19 (1988) 526.

51 D. Green, R.J. Stull and K.T.C. Heesen, *Mar. Pollut. Bull.*, 17 (1986) 324.
52 H. Iwata, S. Tanabe, N. Sakai and R. Tatukawa, *Environ. Sci. Technol.*, 27 (1993) 1080.
53 S.A. Dinkins, Quantification of Dioxin Concentrations in the Ohio River Using High Volume Water Sampling. Available online: http://tinyurl.com/9valj
54 D.R. Oros, D. Hoover, F. Rodigari, D. Crane and J. Sericano, *Environ. Sci. Technol.*, 39 (2005) 33.
55 E.Y. Zeng, D. Tsukada and D.W. Diehl, *Environ. Sci. Technol.*, 38 (2004) 5737.
56 T. Harner, H.H. Kylin, T.F. Bidleman and W.M.J. Strachan, *Environ. Sci. Technol.*, 33 (1999) 1157.
57 S. Weigel, K. Bester and H. Hühnerfuss, *J. Chromatogr. A*, 912 (2001) 151.
58 M. Winkler, G. Kopf and T. Hauptvogel, *Chemosphere*, 37 (1998) 1139.
59 D.A. Van Ry, J. Dachs, C.L. Gigliotti, P.A. Brunciak, E.D. Nelson and S. Eisenreich, *Environ. Sci. Technol.*, 34 (2000) 2410.
60 K.A. Burns, J.K. Volkmann, J.-A. Cavanagh and D. Brinkmann, *Mar. Chem.*, 80 (2003) 103.
61 G.R. Harvey, W.G. Steinhaver and H.P. Miklas, *Nature*, 252 (1974) 387.
62 T. McDonnell and J. Rosenfield, *J. Chromatogr. A*, 629 (1993) 41.
63 Perry's Chemical Engineers' Handbook, 7th ed., McGraw Hill, New York, 1997, Chapter 16.
64 G.S. Ellis, J.N. Huckins, C.E. Rostad, C.J. Schmitt, J.D. Petty and P. MacCarthy, *Environ. Toxicol. Chem.*, 14 (1995) 1875.
65 R.J.K. Dunn, P.R. Teasdale, J. Warnken and R.R. Schleich, *Environ. Sci. Technol.*, 37 (2003) 2794.
66 J. Warnken, R.J.K. Dunn and P.R. Teasdale, *Mar. Pollut. Bull.*, 49 (2004) 883.

Chapter 16

Theory and applications of DGT measurements in soils and sediments

William Davison, Hao Zhang and Kent W. Warnken

16.1 INTRODUCTION

The technique of diffusive gradients in thin-films (DGT) was first used for the measurement of trace metals in sea-water [1]. However, within a year it was used to measure trace metals in sediments at high spatial resolution [2]. Its use in sediments was a natural extension of the technique of diffusive equilibration in thin-films (DET), which had been developed a few years earlier [3]. With DET, a strip of hydrogel, which typically comprises 95% water, is held in a plastic supporting probe, which is inserted into the sediment. Solutes equilibrate between the pore-water of the sediment and the water of the hydrogel. After a typical equilibration time of 24 h, the probe is removed and the solutes in the gel are back-equilibrated and analysed [4]. Initially, DET was used for the measurement of solutes present at relatively high concentrations, including Fe and Mn [5], major anions [6] and major cations [7], as analysis of eluent solutions from small volumes of gel was challenging. The continued improvement in analytical techniques, particularly inductively coupled plasma mass spectrometry (ICP-MS), made it possible to measure trace metals by DET in some studies [8–11], but care must be taken to verify that binding of trace components to the hydrogel does not bias the results [12].

In DGT, a layer of binding agent is introduced behind the diffusive layer of hydrogel. This allows trace solutes such as metals to accumulate progressively with time, greatly improving the detection limits compared to DET. However, the basis of the technique is fundamentally changed from the simple equilibration of DET to a dynamic measurement of a flux of the solute. DGT perturbs the environment into which it is introduced by removing solute. The subsequent analysis

Comprehensive Analytical Chemistry 48
R. Greenwood, G. Mills and B. Vrana (Editors)
Volume 48 ISSN: 0166-526X DOI: 10.1016/S0166-526X(06)48016-8

provides a measure of the amount of solute that has been supplied for a given exposure area for a given deployment time. This is the time-averaged flux to the device. The magnitude of this flux depends on the dynamic response of the medium to the perturbation of solute removal. Consequently, when DGT is deployed in sediments or soils, it provides information on the supply of solute. The dynamic interactions of DGT with a sediment or soil have been represented by numerical models, which provide a fuller, quantitative understanding [13,14]. Depending on the conditions of the sediments or soils, it may be possible to interpret the measurements in terms of localised or bulk concentrations.

Sediments are usually anoxic and highly structured and therefore cannot be homogenised without severely compromising their chemistry. It is partly because of this that DGT measurements have focussed on obtaining information at high spatial resolution [2,15,16]. Homogenised soils can represent *in situ* conditions reasonably well, largely due to them being oxygenated. This simpler deployment environment has facilitated rapid progress, since the first use of DGT in soils [17], in understanding the soil response to the DGT perturbation [18,19]. Moreover, the recognition that DGT mimics the dynamic uptake of metals by plants has led to it being used to provide new insights into plant–soil interactions and as a risk assessment tool [20–22].

The principles and early applications of DGT in soils and sediments have been reviewed previously [23], while a review of more recent publications is available [24]. This chapter sets out the developing theoretical basis for the use of DGT in soils and sediments and appraises the key applications that have advanced understanding of chemical interactions occurring in these complex media.

16.2 PRINCIPLES IN SOILS AND SEDIMENTS

The theory for measurements by DGT in solution is presented in Chapter 11 of this book [25]. The complications introduced there, with respect to the effects of gel pore size, pH, ionic strength and the measurement of labile species, apply to the use of DGT in sediments and soils. For simplicity they are not treated here where the focus is on the influence of the solid-phase adjacent to the device.

The key effects of the solid-phase were recognised in the first publication on the use of DGT in sediments [2]. The continual removal of metal from the pore-water to the resin sink induces a concentration

gradient within the diffusion layer. If the only transport mechanism for solutes in sediment pore-waters is diffusion, the metal becomes depleted in the pore-waters adjacent to the device. This lowering of the solute concentration can mobilize metal from the solid-phase. Therefore, the mass of solute accumulated by the DGT device depends on the initial concentration in the pore-water, the rate of diffusional supply and the extent and rate of release of solute from the solid-phase. Rather than being a simple device for measuring solute concentrations in the bulk pore-water, DGT is best regarded as a tool for conducting *in situ* perturbation experiments by introducing a localized solute sink. The amount of solute that accumulates in a given time depends on the extent of the perturbation of the soil or sediment dynamics.

Harper *et al*. [13] have developed a full mathematical treatment of these processes. Initially, there is no concentration gradient at the surface of the binding layer, as the diffusion layer does not contain solute. The gradient increases as the diffusion layer is supplied with metal from the soil or sediment, with a linear gradient being established in the diffusion layer in a few minutes [2]. A typical profile of the concentration of solute, C, through the diffusion layer of thickness Δg and the pore-waters, at time t, is shown in Fig. 16.1.

The large concentration of binding agent with strong binding sites ensures that the concentration of solute at the surface of the binding layer is effectively zero. There is depletion of solute in the pore-waters, with the concentration at the interface between the DGT surface and the pore-waters, C_i, being less than the concentration in the bulk solution of the pore-waters, C_{soln}. The concentration gradient through the diffusion layer is linear, allowing calculation of the flux of solute, $F(t)$,

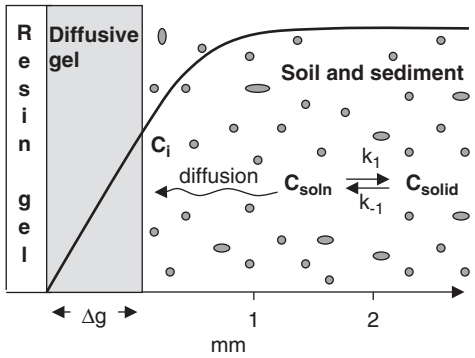

Fig. 16.1. Schematic representation of the concentration gradient through a DGT device and the adjacent soil or sediment.

towards the resin at this instance of time:

$$F(t) = D\frac{C_{\mathrm{i}}(t)}{\Delta g} \tag{16.1}$$

D is the effective diffusion coefficient of labile solute species in the diffusion layer. With increasing deployment time, solutes in the porewater become progressively depleted, tending to lower C_{i}. The supply of solutes from the solid-phase to solution counteracts this depletion, slowing down the decline in C_{i}. A *pseudo*-steady-state can be achieved for relatively short (~day) deployment times, but the progressive depletion of solute associated with the solid-phase adjacent to the device ensures that C_{i} declines at longer deployment times. The concentration gradient in the diffusion layer, and consequently the flux, therefore changes with time. The total mass of solute accumulated per unit area of the DGT device, M_{a}, is given by integrating the flux over the deployment time (T):

$$M_{\mathrm{a}} = \int_{t=0}^{T} F(t)\,\mathrm{d}t \tag{16.2}$$

M_{a} is the directly measured quantity that is obtained from a DGT deployment by eluting a known area of the binding gel and measuring the concentration in the eluent. The time-averaged interfacial concentration during the deployment time (C_{DGT}) is given directly by

$$C_{\mathrm{DGT}} = \frac{\int_{t=0}^{T} C_{\mathrm{i}}(t)\,\mathrm{d}t}{T} \tag{16.3}$$

Combining Eqs. (16.1)–(16.3) gives Eq. (16.4), which is the soil or sediment equivalent to the standard DGT equation used for solution [23,25].

$$C_{\mathrm{DGT}} = \frac{M_{\mathrm{a}}\Delta g}{DT} \tag{16.4}$$

This derivation does not consider the conditions at the onset of a DGT deployment, i.e. before the linear concentration gradient is established within the gel. Depending on the thickness of the diffusion layer, this could take 1–10 min [2], which is negligible compared to a typical deployment time of 1 day. Therefore, except for short deployment times, Eqs. (16.1)–(16.4) are good approximations of the *in situ*

conditions. For metals, the presence of slowly diffusing complexes in solution can extend the time required to reach the *pseudo*-steady-state.

DGT measurements in soils and sediment can be reported either as the mean flux to the device during the deployment time, calculated simply from M_a/T, or as the mean interfacial concentration, C_{DGT}. The ratio of the average concentration at the DGT surface to the concentration in the bulk pore-waters, C_{soln}, measured by other techniques, is given as R:

$$R = \frac{C_{DGT}}{C_{soln}} \tag{16.5}$$

Like C_{DGT}, R is initially zero and quickly reaches a maximum value as solute enters the diffusion layer and establishes a linear gradient. A maximum value of R would be maintained if there was an infinitely large reservoir of solute in the solid-phase, which could be supplied very quickly. In practice, the rate of release from the solid-phase can limit supply, resulting in a lower value of R. Even if this rate is very fast, R will gradually decline as the reservoir of solute in the solid-phase in close proximity to the DGT device is consumed, extending the concentration gradient further into the soil or sediment. For a given deployment time, R provides an assessment of how well the soil or sediment is able to supply solute from the solid-phase as it is consumed from solution by DGT. In general, for a typical 24 h deployment time, three scenarios of sediment supply have been proposed [2,13]:

1. Rapid and sustained supply from the solid-phase that is maintained ($R > 0.8$).
2. Virtually no release of solute from the solid-phase, such that diffusion is the only supply ($R < 0.1$).
3. An intermediate case ($0.1 < R < 0.8$) with some supply, but insufficient to sustain R.

16.3 MODELLING INTERACTIONS OF DGT WITH SOILS AND SEDIMENTS

When DGT is deployed in soils or sediments, a steady-state condition is never truly reached. Thus, time-dependent models are required to quantify the contribution of diffusional supply and release from the solid-phase to the accumulated mass of solute. The DGT-induced fluxes in soils and sediments (DIFS) model developed by Harper *et al*. [13,26]

provides a numerical simulation of the interaction between the DGT device and its deployment medium. It quantifies the dependence of R on the supply of trace metals from solid-phase to solution, coupled to diffusional supply to the interface and across the diffusion layer, by solving a pair of linked partial differential equations describing dissolved and sorbed solute concentrations in the soil or sediment and the DGT device. The model assumes that all pore spaces are filled with solution, which restricts its use to sediments and soils with moisture content at or above field capacity.

Initial calculations, based on a finite difference approach, considered two-dimensional diffusion and release processes in the soil perpendicular to the plane of the DGT device [13]. A simplified version of the original model, which considered only one dimension along the axis perpendicular to the DGT device, was made generally available [14]. The exchange of solute between solid-phase and solution is described by the first-order rate constants for binding, k_1, and release, k_{-1} (Fig. 16.1). Although these constants are sometimes referred to as sorption and desorption rate constants, no mechanism, other than exchange between the solid-phase and solution, is assumed. A distribution coefficient for the labile solute, K_{dl}, is used to define the ratio of the concentration of exchangeable solute in the solid-phase, C_{ls}, to that in solution:

$$K_{\mathrm{dl}} = \frac{C_{\mathrm{ls}}}{C_{\mathrm{soln}}} \tag{16.6}$$

Another key parameter is the response time, T_{c}, which is the time needed for the disequilibria of solute induced by DGT to revert to 63% of the equilibrium value [27]. T_{c} is the reciprocal of the sum of the rate constants, which for most situations approximates to the inverse of the rate given by the product of k_{-1} and K_{dl}:

$$T_{\mathrm{c}} = \frac{1}{k_1 + k_{-1}} \approx \frac{1}{k_{-1} K_{\mathrm{dl}}} \tag{16.7}$$

The model has been used to generate concentration profiles of solute in solution, in the solid-phase, through the soil or sediment, and within the diffusion layer (Fig. 16.2) [13,18,20]. The dependence of these profiles on the values of K_{dl} and T_{c} provides insight into their controlling influence on the DGT measurement. Generally, the concentration in solution within 1 mm of the DGT surface is sustained at high values for several days when K_{dl} is large and T_{c} is small, with little depletion of the solid-phase. However, when K_{dl} is small and T_{c} is large, the depletion of

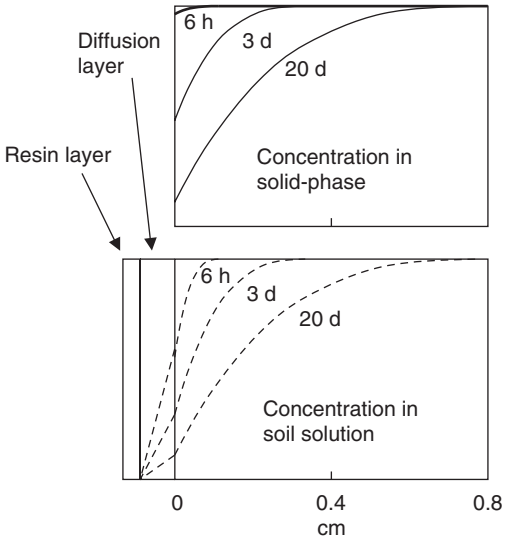

Fig. 16.2. Dependence of the normalized concentration of a DGT active component, in the solution and solid-phase of a soil (with reported characteristics [18]), on time and distance from the surface of the diffusion layer. Simulated using DIFS with $K_d = 150\,mL\ g^{-1}$ and $T_c = 300\,s$. At long times, the concentration in solution is determined by K_d, as kinetic effects become negligible. Thus, the normalized 20 days lines for both solution and solid-phase are identical.

the concentration in both solution and solid-phase rapidly extends away from the device. For the more common intermediate case, a rapid response (small T_c) helps to sustain the interfacial concentration, but only for relatively short deployment times (hours). The interfacial concentration's fraction of its initial value, R, is determined exclusively by K_{dl} at long deployment times (several days), when the controlling effect on the solution concentration is the extent of depletion of solute associated with the solid-phase.

The one-dimensional model is accurate for short deployment times or for cases when there is rapid and sustained supply from the solid-phase. However, the model is less accurate when concentration gradients extend appreciably into the soil or sediment. Supply solely by diffusion represents the worst case and corrections based on a fuller two-dimensional calculation were provided with the model. To overcome these problems, the model has been reformulated within a mathematical framework that uses the finite element method (FEM) [28]. Significant advances include (a) a two-dimensional solution, (b) full

flexibility in selection of DGT geometry and parameters, (c) incorporation of two-dimensional (*planar*) microniche sources of solutes and (d) an interactive, user-friendly interface. The accuracy of this new model, called 2D-DIFS, was tested using a three-dimensional solution and correction equations derived for the diffusion-only case. The performance and sensitivity of the model has been evaluated systematically using available DGT data [29].

16.4 SOILS

16.4.1 Practicalities for deployments in soils

DGT measurements in soils initially used the standard piston assembly supplied by DGT Research Limited (Lancaster, UK) that is regularly used for solution measurements [17,30,31]. More recently, a device specially designed for soils has become available [32]. It is similar in appearance to solution devices, but it has an improved seal between the cap and pre-filter to prevent soil particles from entering the device and biasing measurements. Its exposure window consequently has a smaller area (2.54 cm^2). Initially, soils are dried and sieved to remove particles larger than 2 mm. Hydration is carried out in two stages, which allows time for equilibration and avoids anoxic conditions. Typically, the soils are hydrated to 60% of the maximum water holding capacity, well mixed and left to stand for 2 days. They are further hydrated to 80–100% maximum water holding capacity, mixed to a smooth paste or slurry and left for an additional 24 h. Prior to deployment, a small amount of soil paste is gently smeared onto the surface of the exposure window (filter membrane) of the DGT unit, to ensure no pockets of air exist between the DGT sampling face and the soil. It is then gently pressed into the soil surface, using a slight turning action to ensure good contact between the soil and the DGT unit. Upon removal of the DGT device, adhering soil particles are washed off by rinsing with a stream of high-purity water from a wash bottle. Obvious surface water is then removed by blotting with a clean tissue. If the soil paste is very sticky, and it is difficult to rinse the DGT unit with water, it can simply be wiped with clean tissue paper. The subsequent procedures are similar to those used for solution, with the caveat that the derived concentration, C_{DGT}, will be the mean concentration at the surface of the device during the deployment time.

The suitability of these procedures has recently been systematically investigated [32]. Extending the soil hydration times did not affect the

DGT measurement and acceptable results were obtained by sieving a field soil and simply estimating the water needed to bring the soil to a smooth paste. Direct DGT measurements on soils hydrated *in situ* were acceptable, but less reproducible than measurements on soils returned to the laboratory where they were sieved, homogenised and hydrated prior to deployment [32,33].

16.4.2 Soil dynamics

The first use of DGT in soils measured R values for Cd and Zn in homogenised soils contaminated with sewage sludge and interpreted them directly in terms of the kinetics of the metal's release from the solid-phase to solution [17]. The authors concluded that Cd and Zn each had two pools of metal, characterised by different rate constants for release to solution, but that Cu and Ni each had only one kinetically defined pool. The dependence of the DGT flux on the diffusion layer thickness, used in the above study, has been used more generally to investigate the dynamic availability of metals [34,35]. Another study showed that the amount of metal accumulated by DGT was dependent on the moisture content of the soil [36]. Metal uptake increased with increasing moisture content, reaching a broad maximum corresponding to field capacity, and declined at higher moisture contents. The lower accumulations at low moisture contents were attributed to the more tortuous diffusion path, while the decline at higher values was due to dilution of the concentration of metal in the soil solution. Docekal *et al.* [34] have confirmed some of these effects of soil moisture on the DGT measurement.

Ernstberger *et al.* [18] deployed DGT in homogenised slurries from a single soil for various times (4 h to 20 days) and obtained time-dependent values of R for Cd, Cu, Ni and Zn. The 1D DIFS model provided good fits of the plots of R versus time, using K_{dl} and T_c as adjustable parameters. The work was extended to five soils in a later study, where good fits were also obtained [19] (Fig. 16.3). Cd and Zn showed similar behaviour, with fast supply from the solid-phase of all soils being reflected by relatively high rate constants, while the release of Ni was kinetically limited. Distribution coefficients for labile Cd and Zn agreed well with those measured by isotopic exchange. While they were very dependent on the pH of the soil, the K_{dl} values for Ni were generally lower and more dependent on soil texture (low in sandy soils) than pH. The good fit to experimental data and agreement between K_{dl} values determined by different techniques provided validation of the DIFS

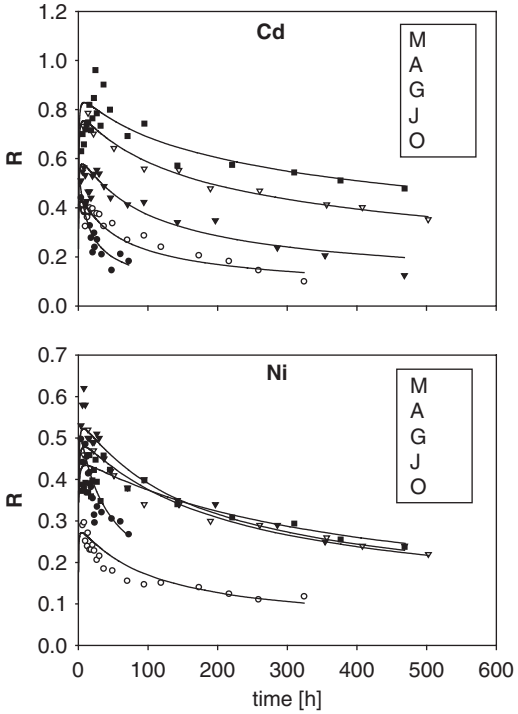

Fig. 16.3. Measured values of the ratio, $R = C_{DGT}/C_{soln}$, for different deployment times in five soils labelled M, A, G, J and O. The lines show fits to the data using the DIFS model (adapted from Ref. [19]).

model. It was considered that this methodology was unsuitable for Cu, due to pronounced complexation in solution that biased the estimation of R [19]. Nowack *et al*. [33] used a similar approach to determine K_{dl} and T_c for Cu and Zn in a contaminated field soil. Best fits of their data were obtained by assuming there were two pools of metal, characteristic of fast and slow release. Ernstberger *et al*. [18] showed that, as model fits are not very sensitive to the values of T_c and K_{dl}, the values of these parameters cannot be obtained very accurately. A full sensitivity analysis has defined the precision available for a wide range of parameter values [29].

Degryse *et al*. [37] used the DIFS model to obtain R values from estimated values of T_c and K_{dl} and then calculated C_{soln} for Zn from the measured C_{DGT}. The prediction was generally good, except at very high Zn concentrations, where it failed due to the resin-gel approaching saturation.

Some studies have used values of K_{dl} determined by comparing solution and extracted concentrations. If this value is combined with a single determination of R, the kinetic parameters T_c and k_{-1} can be calculated using DIFS. Using this approach, Zhang *et al*. [38] found that the rate of supply of Zn from solid-phase to solution is much higher in soils freshly spiked with Zn than in contaminated field soils with similar total concentrations of Zn. The rate constant (k_{-1}) for release of As in rhizosphere soil was smaller than in the bulk soil, presumably due to plant roots preferentially removing the most readily available fraction in the rhizosphere [39]. A systematic study of 14 freshly contaminated soils showed that the rate of supply of Zn from the solid-phase was too fast to measure in all except three soils, which had fairly low pH and a silt-sand texture [40]. Rates of supply of Cd could be measured in all except six clay soils.

Several studies have used DGT in soils to measure the flux and interpret it in terms of available metal. Comparisons to conventional leaching procedures were used to aid the interpretation of data on Cd, Cr, Cu, Ni and Pb from three contaminated sites [35]. Rachou *et al*. [41] focussed on the dependence of available Cd on pH, while Lombi *et al*. [42] used DGT to demonstrate the *in situ* fixation of metals in soils treated with a bauxite residue. The mobilisation of metals in organically contaminated soils with high microbial activity has been demonstrated in a series of papers [43–45]. A further series of papers has used DGT to investigate the speciation of Al, Cu, Fe and Zn in solutions extracted from soils [46–50].

Phosphorus has been determined in soils using DGT with ferrihydrite in the binding layer, either as a pure phase or mixed with Chelex for the simultaneous determination of metals [51]. DGT-measured P correlated better with P in soil solution than with the standard Colwell and Bray extracts [52], suggesting that the extractions measured more P than that measured by DGT.

16.4.3 Biological mimicry

Like DGT, plants accumulate metals by removing them from soil. The perturbation of the soil is similar if the rate of removal by the plant and DGT is similar. Lehto *et al*. [53] have modelled the uptake of metals by plants and DGT and shown that fluxes to plants and DGT are generally similar for values of diffusion layer thicknesses typically used in DGT devices. Hyper-accumulator plants will tend to have slightly higher uptake fluxes than DGT.

Processes that are not mimicked by DGT can also affect the supply of metals to plants, including convective transport, the root encountering fresh surfaces as it grows through the soil and the influence of root exudates and microenvironments. For DGT to be effective in predicting plant uptake, the contribution from each of these processes must be small compared with supply by diffusion and associated release from the solid-phase. According to the accepted ranges of mass flow [54], modelling indicates that supply by convection is usually negligible compared with diffusive supply, especially when release from the solid-phase is also considered [55]. It is more difficult to model the other terms that are not mimicked by DGT. When good relationships between metal accumulated by DGT and plants are obtained, it is reasonable to suggest that these other terms do not contribute appreciably to metal supply to the plant. Their possible significant contribution to supply may be one of the reasons for such relationships breaking down.

In the first comparison of DGT measurements with metal uptake by plants (*Lepidium sativum* L.), DGT was deployed and plants were grown in the same soil, but at different moisture contents, representing 50–90% of the maximum water holding capacity [56]. The concentration of Cd, Co, Cu, Ni, Pb and Zn in the plant herbage and the flux of metals to the DGT device both increased systematically with moisture content, while the concentration of the metals in soil solution declined. As only the water content of the soil was varied, the concentration of metals in the soil solution can be expected to be proportional to the free ion activity. The results showed that neither the free ion activity nor the concentration of metal in the soil solution could predict metal uptake by the plants. The fact that DGT could predict plant uptake was attributed to supply by mass transport and associated release from the solid-phase being dominant and a similar dependence for both DGT and the plants on soil moisture content.

In the second comparison, an indicator species for Cu (*Lepidium heterophyllum* Banth.) was grown in 29 different soils with a range of Cu concentrations [20]. Copper was measured by four methods: DGT, in soil solution, as free ion activity and by EDTA extraction. The concept of effective concentration, C_E, was introduced. Diffusional supply of a metal to a plant or DGT device is augmented by release from the solid-phase. Therefore, the effective concentration that the plants experience, C_E, is larger than the concentration in solution. The DIFS model was used to convert the DGT measured concentration, C_{DGT}, to the effective concentration, C_E. Essentially, the flux for the diffusion-only case is compared to the DGT measured flux. A good correlation

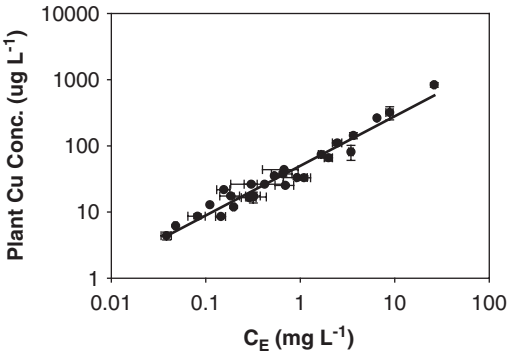

Fig. 16.4. Cu measured in plants grown on 29 different contaminated soils plotted against the Cu measured by DGT, C_E, on the same soils after harvesting (adapted from Ref. [20]).

was obtained between the Cu concentration in the herbage and C_E, whether plotted on a logarithmic ($r^2 = 0.95$) or linear ($r^2 = 0.98$) scale (Fig. 16.4). Poor correlations were obtained for the free ion activity of Cu and the EDTA extractable Cu, but a reasonable logarithmic relationship was found for Cu in soil solution. The good correlation for C_E, as measured by DGT, for this very wide range of soils, suggested that the processes mimicked by DGT, namely supply of Cu by diffusion and release from the solid-phase, dominated supply of metal to the plant for a wide range of conditions.

This type of experiment, where the concentration of metal in herbage is correlated with metal measured by DGT, has been replicated by several laboratories using a wide variety of soils, metals and plants. *Elsholtzia splendens* and *Silene vulgaris* were grown on essentially the same set of contaminated soils [57]. Reasonable correlations were obtained between the concentration of Cu in the herbage and C_E, measured by DGT. Although these relationships were not significantly better than the corresponding ones for extractable Cu (1 M NH_4NO_3) or soil solution Cu, they were better than those for total soil Cu, EDTA extractable Cu or free Cu^{2+} activity.

Lepidium sativum was grown in four different soils with various levels of Zn contamination collected near busy roads and close to galvanized pylons [38]. Similar soils, with low background Zn, were amended with Zn to similar concentrations to the contaminated samples. Zn in the herbage correlated more closely with C_E (for field contaminated and amended soils) than with Zn in soil solution or total Zn in the soil. Above a threshold concentration, Zn in the plants increased

systematically with C_E. This observation was attributed to homeostatic processes controlling internal Zn concentrations at optimal levels until supply from the soil, as indicated by C_E, is large enough to override this control. DGT was used to show that the rate of release of Zn from the solid-phase was faster in the amended soils.

Koster *et al*. [58] measured Zn in grass, lettuce and lupine grown in 28 soils with various textures and amended amounts of Zn. Good correlations were found between Zn concentrations in grass and lettuce and C_E, Zn extracted with $CaCl_2$ and soil solution Zn, but the correlation between Zn in lupine and C_E was not significant.

Nowack *et al*. [33] found non-linear relationships between Cu and Zn in the herbage of *Lolium perenne* (ryegrass) and C_E measured by DGT. The source of metal contamination was filter dust from a brass smelter. The same relationships were observed for freshly amended soils and field contaminated soils, regardless of whether or not the soils were homogenized, showing the robust nature of the predictive capability of DGT. The non-linear relationship was attributed to saturation type behaviour, which is appropriate for a metal excluder plant, such as ryegrass, where there is limited translocation between roots and shoots. These workers also measured Cu and Zn uptake by ryegrass and DGT directly in the field. Some deviations from the relationship obtained in the laboratory were observed and attributed to local variations in microsite conditions.

The toxicity of Zn to *Sorghum vulgare* grown in sand amended with $ZnSO_4$ and mine wastes, assessed as 90% of the control yield, was well predicted by both DGT measured Zn and Zn extracted using $CaCl_2$ [21]. The toxicity response of barley (root elongation) and tomato (shoot growth) to Cu additions was assessed on 18 European soils representing a wide range of soil types and soil properties [22]. The concentrations of Cu in soil solution, free Cu^{2+} activities and DGT measurements were compared with the plants' toxicity response. The DGT measurement was found to lessen the inter-soil variation in EC_{50} considerably, and to be a better predictor of plant Cu concentrations than either soil solution Cu or free Cu^{2+} activity.

The most extensive comparison of different measurements of metals in soils, which includes C_E and metal concentrations in plants, was undertaken using wheat (*Triticum aestivum* L.) grown in 13 metal-contaminated soils [59]. In addition to C_E, Cd, Cu, Pb and Zn were measured as total concentrations, total dissolved metal, free metal ion activities in soil solution, $CaCl_2$ extractable metal and E values (exchangeable labile metal) measured by isotopic dilution. Zn concentrations

in wheat correlated best with C_E, Cd equally well with C_E and $CaCl_2$ extractable Cd, and Pb equally well with C_E and total dissolved Pb. Surprisingly, for Cu, the total concentration gave the best correlation.

While a number of studies have shown that DGT is generally a good predictor of metals in plants, it is not infallible. For Cd and Zn, the concentration of metal extracted by $CaCl_2$ often appears to match the predictive capability of DGT. The available pool of labile solid-phase metal, which is involved in both the DGT measurement and the $CaCl_2$ extraction, appears to contribute significantly to the metal supplied to the plants. This finding agrees with DGT studies of the kinetics of release of Cd and Zn from the solid-phase, which generally indicate a fast supply [18,19,40]. The similar performance of C_E and the concentration of metal in soil solution for predicting the behaviour of Pb is, so far, restricted to one study. However, the finding is consistent with the known strong sorptive properties of Pb, which are unlikely to result in substantial and fast supply from the solid-phase. Without this supply, metal accumulated by both plants and DGT are likely to be related directly to the total labile species in solution, which usually approximates to their total dissolved concentration.

DGT has also been used to study phosphorus uptake by plants. The rates of accumulation of P by DGT were comparable with the uptake rates of tomato plants that were adequately supplied with P [52], again demonstrating DGT's potential to mimic uptake processes of plants. Preliminary findings suggest that DGT is not the best indicator of the toxic response of soil micro-organisms to Cd and Zn [60]. Although correlations of LC_{50} values with C_E were better than for total metal, they were not as good as correlations with metal in soil solution.

16.5 SEDIMENTS

Sediment heterogeneity arising from steep gradients in solute concentrations associated with the well-known sequence of redox reactions prevents accurate replication of measurements at high spatial resolution. Moreover, efforts to homogenize sediments are generally unsuccessful and new structure in solute distributions develop within hours as local redox gradients are re-established. Consequently, it has not been possible to apply and test the DIFS models on simple homogenised sediment systems. From the outset, the primary use of DGT in sediments has been to investigate the distribution of solutes at high spatial resolution [2].

16.5.1 Practicalities for deployments in sediments

DGT sediment probes have been designed to be pushed into the sediment, so the binding gel, diffusive gel and filter are held in a slim probe, typically 5 mm thick (Fig. 16.5). To ensure a tight seal between the frame and the front pre-filter, a second pre-filter membrane is usually placed behind the 0.4 mm binding gel and 0.8 mm diffusive gel. It also serves as a support for the binding gel when it is removed. The probes have a large window area to allow the binding layer to be sliced prior to analysis. Before they are deployed in anoxic sediment, probes must be deoxygenated by immersing them in a container of 0.01 M NaCl solution, which is moderately bubbled with oxygen-free nitrogen or argon gas for 24–48 h. The container should be either closed except for a small vent or housed in a glove bag. For low-level trace metal work, care must be taken at this stage to prevent contamination and probes that serve as blanks should follow the same procedure. Once removed from the oxygen-free solution, probes should be deployed in the sediment as quickly as possible (seconds), using a smooth insertion action to minimize sediment disturbance and avoid any cavitation, which could allow solution to flow along the probe face. Upon retrieval from the sediment, the surface of the probe is rinsed using a wash bottle of high-purity water, ensuring that there are no particles remaining on the window

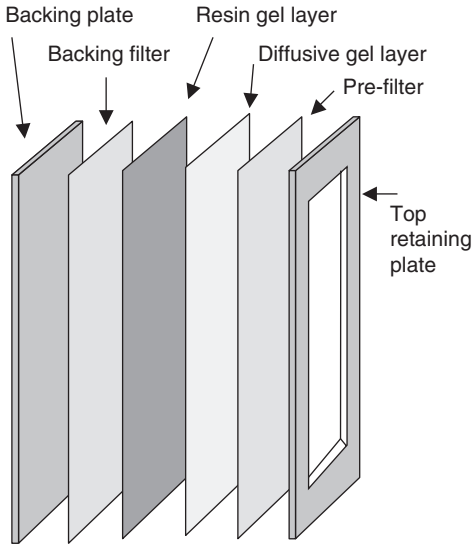

Fig. 16.5. Schematic depiction of the layers of a DGT sediment probe.

area. The sediment–water interface can usually be seen at this stage as a stain on the filter and should be marked.

Using the sampling window as a guide, a Teflon-coated razor blade can be used to cut through the gel and the filter membrane layers, which can then be carefully removed from the device and placed on a clean flat surface. The top filter membrane and the diffusive gel can then be removed and discarded leaving only the binding gel layer and the supporting filter membrane. The binding gel can then be sliced to the desired resolution using a new, rinsed Teflon-coated razor blade. The smallest practical gel slices that have been used have either been 1 mm wide by ~1–2 cm long [2,16] or 3×3 mm squares [11]. Even at this size, it is difficult to slice accurately, and there is a risk that the Chelex 100 resin beads are not distributed uniformly within the resin-gel layer. For trace metal analysis, each gel strip is placed into a micro-centrifuge tube (0.5 or 1.5 mL) and the gel is eluted using an appropriate volume of 1 M HNO_3. The gel should be left in the dilute acid for at least 24 h, to ensure complete elution and diffusional mixing.

16.5.2 Analyte distributions from gel slicing

The first DGT measurements made in sediments using this gel-slicing approach showed steep vertical gradients of metals in the surface sediments of a productive lake [2]. The DGT measurements were reported both as localized fluxes to, and as concentrations (C_{DGT}) at, the interface of the device. The pronounced maxima of metals, particularly Cu and Zn, immediately below the sediment–water interface, were attributed to release from rapidly oxidized organic material. While the various maxima were interpreted in terms of local supply processes, comparisons between interfacial concentrations measured by DGT and concentrations in the bulk pore-waters were made using a theory of supply from the solid-phase, which later formed the basis of the DIFS model [13]. Model calculations for the diffusion-only and well-buffered cases were performed in this early paper. From measurements made using different diffusive gel layer thicknesses, it was concluded that the supply of Zn was fully sustained (rapid) while that of Ni was only partially sustained (slow). These results agree well with conclusions drawn from more recent measurements made on soils, where the dependence of the DGT measurement on deployment time was interpreted using the DIFS model [19].

In view of the significant advances made by this first use of DGT in sediments, it is surprising how few subsequent studies have been

carried out using this rather simplistic slicing approach. Zhang *et al*. [61] used the slicing approach to show pronounced localized features in DGT measurements of As, Co, Fe, Mn and Ni in a marine sediment, with good correspondence between Co and Mn, and Co and Ni. DGT measurements of Fe in this same sediment were interpreted in terms of production rates and used to infer a significant recycling of Fe within the sediment through interactions with sulphide [62,63]. The vertical distributions of Fe and Mn measured by DGT have also been compared with the presence of particular species of micro-organisms [64].

DGT devices were also deployed in Black Sea sediments using an autonomous benthic lander [65]. Distinct maxima in Co and Cd at 4 and 6 cm depth in the sediment coincided precisely with maxima in Mn, whereas Fe maxima were offset by several millimetres (Fig. 16.6). Fones *et al*. [16] also performed DGT measurements on North Atlantic sediments using both a lander and deployments in retrieved cores. Their data showed highly localised features superimposed on the usual redox-associated gradients. Coincident maxima of Cd, Cu, Ni and Zn were not directly linked to the redox-sensitive elements Co, Fe and Mn.

The difficulties of precise interpretation were considered for measurements of Cd, Fe, Mn and Pb in a lake sediment using diffusion layer thicknesses of 0.4 and 1.2 mm [66]. Reproducible results for Cu and Fe measured close to the sediment–water interface have been reported [67]. When Roulier and Motte [68] compared DGT measurements of Cu with concentrations in the pore-waters, they deduced that there was a good supply of Cu from the solid-phase in one reservoir, but not in

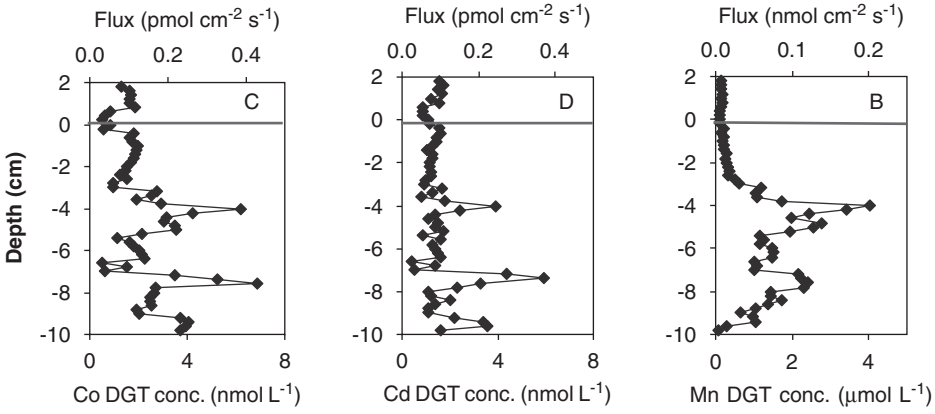

Fig. 16.6. Co, Cd and Mn measured *in situ* in sediment of the Black Sea by DGT (adapted from Ref. [65]).

another. In their comprehensive study of river sediment using DGT, Leermakers *et al.* [10] found that Pb and Zn were well supplied and that Co, Cu, Ni and Zn were only partly supplied. There was also very little supply of Fe and Mn, in contrast to previous work [2]. Strong geochemical linkages were apparent between As and Fe, and Co and Mn. Pronounced surface maxima of Cd, Cu, Ni, Pb and Zn were similar to previous observations [2] and attributed to release from fresh supplies of organic matter. Pronounced DGT maxima of Cd in the top 3 cm of sediment of a contaminated marine lagoon were also attributed to mineralization of organic matter, but generally this sediment acted as a strong sink for Cd, due to the formation of CdS [69].

The two-dimensional distribution of trace metals was measured in contaminated, marine, harbour sediment, by slicing the resin-gel into 3×3 mm squares [11]. All features in the sediment were horizontally uniform, suggesting that localized features were absent in this sediment, which had been incubated for more than a year in a flume. Maxima of Cd, Cu and Ni observed within the surface centimetres of sediment were above the maxima in Co and Fe, suggesting that the primary source of these trace metals was release from freshly decomposing organic material.

Mercury was measured in river and marine sediments using DGT with an agarose diffusive gel and either Chelex 100 or Spheron-Thiol as the binding agent [70]. Measurements made using the thiol binding agent agreed well with Hg measured in pore-waters, indicating that total dissolved Hg was measured and that there was a good supply from the solid-phase. The lower concentrations measured using Chelex 100 suggested that only inorganic ions and weak complexes were measured.

16.5.3 Direct measurements of analytes in the binding layer

Metals have also been measured by DGT at much higher spatial resolution using a beam technique to analyse the binding layer, which is first dried onto a filter support using a gel drier. In the first application, proton-induced X-ray emissions (PIXE) was used for the analysis [15]. A resin with a very small bead size (0.2 μm) was used to ensure an effectively homogeneous, but immobilised binding layer. With the use of ceramic rather than plastic supports, it was possible to keep the total thickness of the DGT sediment probe to less than 1 mm. Images of concentrations, obtained in two dimensions by rastering the 1 μm proton beam, showed similar pronounced vertical gradients of Mn and Zn in a fresh-water sediment and overlying microbial mat. There was

evidence of coincident release of As and Fe from an approximately spherical source. However, caution should be exercised when interpreting these very small scale features, as numerical simulations have shown that lateral diffusion within the diffusion gel will cause broadening of sharp peaks [71].

The same resin type and gel drying procedures have also been used to obtain 2D images of metal concentrations with analysis by laser ablation inductively coupled plasma mass spectrometry (LA-ICP-MS) being used as the beam technique [72,73] (Fig. 16.7). While LA-ICP-MS has higher sensitivity than PIXE, data acquisition, which is based on a series of individual analyses, is tedious. The problems associated with internal standardization and energy stability at low power settings, to avoid penetration through the filter and the possibility of contamination, have been systematically investigated [73]. Once these issues are overcome, very precise quantitative measurements can be made. Early work without such good calibration procedures was still able to provide 2D images of metal concentrations in fresh-water [72] and marine [16] sediments.

A technique for measuring total dissolved sulphide by DGT was first developed for sediments by Teasdale *et al*. [74]. It uses a binding layer of AgI, which reacts with sulphide to form Ag_2S. Quantification has been achieved in three ways: (1) the sulphide has been liberated with acid and measured colorimetrically [74], (2) it has been measured directly on the dried gel using LA-ICP-MS [75] and (3) by using the colour

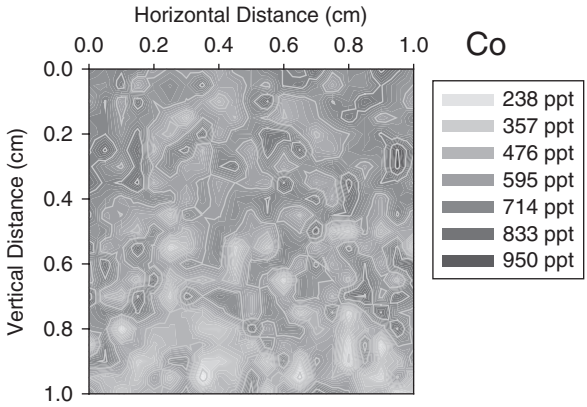

Fig. 16.7. Two-dimensional image of Co in a fresh-water sediment measured by DGT with laser ablation ICP-MS of the resin-gel at 200 μm spatial resolution (adapted from Ref. [73]).

change that occurs when pale yellow AgI is converted to black Ag_2S [74,76]. The grey scale intensity is simply measured on a flat bed scanner and calibrated against measurements on binding gels from DGT devices exposed to standard solutions for known periods of time. Using this approach, 2D images of concentration are obtained simply and automatically. They have revealed localised areas of elevated sulphide production, 1–5 mm in diameter, in fresh-water sediments [74,76]. Teasdale *et al.* [74] used ground AgI crystals, while DeVries and Wang [76] considered that forming the AgI directly in the gel from $AgNO_3$ and KI improved homogeneity.

Metals and sulphide have been measured together by using DGT devices with two binding layers, one containing a metal chelating resin and the other containing AgI [72,77,78]. These two types of binding layers have been used either with the AgI layer as the backing layer or with it sandwiched between the chelating and diffusive gel layers. The metals appear to diffuse through the AgI layer and the sulphide through the chelating layer as if they were simple diffusive gels. Using this combined technique, metal liberation at the same location as sulphide has been observed in a fresh-water sediment [72]. The rapid removal of metals, as insoluble metal sulphides, produces well-defined local maxima. Similar, but broader features were observed in a marine sediment [77]. When these combined DGT measurements have been compared with more traditional techniques that measure acid volatile sulphide and simultaneously extracted metals, they have highlighted the dynamics of the interactions of metals and sulphides [78].

Jézéquel (pers. comm.) used a DGT device with PVC tape as the binding layer to obtain two-dimensional images of the supply of S(-II). Phases comprising both S and Fe are believed to form on the tape catalytically. Two-dimensional images of Fe(II) were obtained with the same probe using a variant of DET with colorimetric detection.

16.5.4 Sources of localised maxima

The very sharp features in the fluxes or interfacial DGT concentrations of metals and sulphides observed in sediments indicate that there are local, approximately spherical, sources. Localised distributions of reactive organic matter have been suggested as the most likely cause, with redox-sensitive metals and sulphate acting as oxidants [2,15,16]. Trace metals can be released from the decomposing organic material and from Fe and Mn oxides. The steep solute gradients that occur in the porewaters are recorded as accumulated distributions by DGT, as shown by

simple models of the system [71]. Further modelling has shown that maxima resulting from solute generation at localised sources were much steeper than those arising from a source where diffusion occurred only in one dimension [79].

As release from the solid-phase can augment the supply of solute to the DGT device, local maxima can also arise from heterogeneous distributions of the solid-phase. This effect has been modelled by considering a solid sphere adjacent to the DGT device, which had a different distribution coefficient, K_{dl}, and response time, T_c, from the surrounding sediment [14]. Thus, localized regions of high K_{dl} and low T_c can produce local maxima, depending on the value of these parameters in the surrounding medium, but they are unlikely to be more than a factor of 3 greater than the background. Recently, however, localised maxima of Cu have been attributed to release from chalcopyrite that was identified in the solid-phase adjacent to the DGT surface where the maxima were observed (unpublished data).

16.5.5 Advances in understanding of soils and sediments using DGT

DGT has provided new information in both soils and sediments and therefore has made important contributions to advancing understanding of processes in these systems. Three main features facilitated these advances: the capability for making measurements at high spatial resolution, interpretation of the dynamics of the processes through modelling and the DGT mimicry of plant uptake. There is great scope for further advances. Combination of DGT with other techniques capable of providing two-dimensional information, such as planar optodes, will provide comprehensive information on localised processes in sediments. Progress in soils is likely to come from improvements in modelling to account for dynamics of interactions in solution and solid-phases linked to systematic measurements with devices with varied binding and diffusive layers. More comparative measurements between DGT and plant uptake is likely to provide the scientific rigour and confidence to develop DGT as a routine soil-testing tool.

REFERENCES

1 W. Davison and H. Zhang, *Nature*, 367 (1994) 546.
2 H. Zhang, W. Davison, S. Miller and W. Tych, *Geochim. Cosmochim. Acta*, 59 (1995) 4181.

3 W. Davison, G.W. Grime, J. Morgan and K. Clarke, *Nature*, 352 (1991) 323.
4 M.P. Harper, W. Davison and W. Tych, *Environ. Sci. Technol.*, 31 (1997) 3110.
5 W. Davison, H. Zhang and G.W. Grime, *Environ. Sci. Technol.*, 28 (1994) 1623.
6 M.D. Krom, P. Davison, H. Zhang and W. Davison, *Limnol. Oceanogr.*, 39 (1994) 1967.
7 H. Zhang, W. Davison and C. Ottley, *Aquat. Sci.*, 61 (1999) 354.
8 H. Docekalova, O. Clarisse, S. Salomon and M. Wartel, *Talanta*, 57 (2002) 145.
9 J. Morford, L. Kalnejais, W. Martin, R. Francois and I.M. Karle, *J. Exp. Mar. Biol. Ecol.*, 285 (2003) 85.
10 M. Leermakers, Y. Gao, C. Gabelle, S. Lojen, B. Ouddane, M. Wartel and W. Baeyens, *Water Air Soil Pollut.*, 166 (2005) 265.
11 S. Tankere-Muller, H. Zhang, W. Davison, N. Finke and O. Larsen, *Mar. Chem.*, (2007), in press.
12 K.W. Warnken, H. Zhang and W. Davison, *Anal. Chem.*, 77 (2005) 5440.
13 M. Harper, W. Davison, H. Zhang and W. Tych, *Geochim. Cosmochim. Acta*, 62 (1998) 2757.
14 L. Sochaczewski, W. Davison, W. Tych and H. Zhang, in preparation.
15 W. Davison, G.R. Fones and G.W. Grime, *Nature*, 387 (1997) 885.
16 G.R. Fones, W. Davison and J. Hamilton-Taylor, *Continent. Shelf Res.*, 24 (2004) 1485.
17 H. Zhang, W. Davison, B. Knight and S.P. McGrath, *Environ. Sci. Technol.*, 32 (1998) 704.
18 H. Ernstberger, H. Zhang, A. Tye, S. Young and W. Davison, *Environ. Sci. Technol.*, 39 (2005) 159.
19 H. Ernstberger, W. Davison, H. Zhang, A. Tye and S. Young, *Environ. Sci. Technol.*, 36 (2002) 349.
20 H. Zhang, F.J. Zhao, B. Sun, W. Davison and S.P. McGrath, *Environ. Sci. Technol.*, 35 (2001) 2602.
21 O. Sonmez and G.M. Pierzynski, *Environ. Toxicol. Chem.*, 24 (2005) 934.
22 F.J. Zhao, C. Rooney, H. Zhang and S.P. McGrath, *Environ. Toxicol. Chem.*, 25 (2006) 733.
23 W. Davison, G.R. Fones, M. Harper, P. Teasdale and H. Zhang, *In situ* environmental measurements using dialysis, DET and DGT. In: J. Buffle and G. Horvai (Eds.), *In situ Monitoring of Aquatic Systems: Chemical Analysis and Speciation*, Vol. 6, IUPAC Series on Analytical and Physical Chemistry of Environmental Systems, Wiley, New York, NY, 2000, pp. 495–569.
24 P. Divis, H. Docekalova and V. Smetkova, *Chem. Listy*, 99 (2005) 640.
25 K.W. Warnken, H. Zhang and W. Davison, *In-situ* monitoring and dynamic speciation measurements in solution using DGT, in this volume.

26 M.P. Harper, W. Davison and W. Tych, *Environ. Modell. Software*, 15 (2000) 55.
27 B.D. Honeyman and P.H. Santschi, *Environ. Sci. Technol.*, 22 (1988) 862.
28 L. Sochaczewski, W. Tych, W. Davison and H. Zhang, *Environ. Modell. Software*, 22 (2007) 14–23.
29 N.J. Lehto, Ph.D. thesis: *Developing a Theoretical Base for Interpreting DGT Measurements of Bioavailability and Lability*, Lancaster University, Lancaster, 2006.
30 H. Zhang and W. Davison, *Anal. Chem.*, 67 (1995) 3391.
31 K.W. Warnken, H. Zhang and W. Davison, *Anal. Chem.*, 78 (2006) 3780.
32 K. Owen, Ph.D. Thesis, University of Lancaster, UK, 2006.
33 B. Nowack, S. Koehler and R. Schulin, *Environ. Sci. Technol.*, 38 (2004) 1133.
34 B. Docekal, V. Smetkova and H. Docekalova, *Chem. Papers Chem. Zvesti*, 57 (2003) 161.
35 V. Rezacova-Smetkova, B. Docekal and H. Docekalova, *Chem. Listy*, 99 (2005) 594.
36 P.S. Hooda, H. Zhang, W. Davison and A.C. Edwards, *Eur. J. Soil Sci.*, 50 (1999) 285.
37 F. Degryse, E. Smolders, I. Oliver and H. Zhang, *Environ. Sci. Technol.*, 37 (2003) 3958.
38 H. Zhang, E. Lombi, E. Smolders and S. McGrath, *Environ. Sci. Technol.*, 38 (2004) 3608.
39 W.J. Fitz, W.W. Wenzel, H. Zhang, J. Nurmi, K. Stipek, Z. Fischerova, P. Schweiger, G. Kollensperger, L.Q. Ma and G. Stingeder, *Environ. Sci. Technol.*, 37 (2003) 5008.
40 H. Zhang, W. Davison, A.M. Tye, N.M.J. Crout and S.D. Young, *Environ. Toxicol. Chem.*, 25 (2006) 141.
41 J. Rachou, W. Hendershot and S. Sauve, *Commun. Soil Sci. Plant Anal.*, 35 (2004) 2655.
42 E. Lombi, F.J. Zhao, G. Zhang, B. Sun, W. Fitz, H. Zhang and S.P. McGrath, *Environ. Pollut.*, 118 (2002) 435.
43 M.A. Amezcua-Allieri, J.R. Lead and R. Rodriguez-Vazquez, *Chemosphere*, 61 (2005) 484.
44 M.A. Amezcua-Allieri, J.R. Lead and R. Rodriguez-Vazquez, *Soil Use Manag.*, 21 (2005) 337.
45 M.A. Amezcua-Allieri, J.R. Lead and R. Rodriguez-Vazquez, *Biometals*, 18 (2005) 23.
46 B. Jansen, M.C. Kotte, A.J. van Wijk and J.M. Verstraten, *Sci. Total Environ.*, 277 (2001) 45.
47 B. Jansen, K.G.J. Nierop and J.M. Verstraten, *Anal. Chim. Acta*, 454 (2002) 259.
48 B. Jansen, J. Mulder and J.M. Verstraten, *Anal. Chim. Acta*, 498 (2003) 105.

49 B. Jansen, K.G.J. Nierop, J.A. Vrugt and J.M. Verstraten, *Water Res.*, 38 (2004) 1270.
50 K.G.J. Nierop, B. Jansen, J.A. Vrugt and J.M. Verstraten, *Chemosphere*, 49 (2002) 1191.
51 S. Mason, R. Hamon, A. Nolan, H. Zhang and W. Davison, *Anal. Chem.*, 77 (2005) 6339.
52 N.W. Menzies, B. Kusumo and P.W. Moody, *Plant Soil*, 269 (2005) 1 (Sp. Iss. SI).
53 N.J. Lehto, W. Davison, H. Zhang and W. Tych, *J. Environ. Qual.*, 35 (2006) 1903.
54 S.A. Barber, *Soil Nutrient Bioavailability. A Mechanistic Approach,*, Wiley, New York, NY, 1995.
55 N.J. Lehto, W. Davison, H. Zhang and W. Tych, *Plant Soil*, 282 (2006) 227.
56 W. Davison, P.S. Hooda, H. Zhang and A.C. Edwards, *Adv. Environ. Res.*, 3 (2000) 550.
57 J. Song, F.J. Zhao, Y.M. Luo, S.P. McGrath and H. Zhang, *Environ. Pollut.*, 128 (2004) 307.
58 M. Koster, L. Reijnders, N.R. van Oost and N.R. Peijnenburg, *Environ. Pollut.*, 133 (2005) 103.
59 A.L. Nolan, H. Zhang and M.J. McLaughlin, *J. Environ. Qual.*, 34 (2005) 496.
60 A.R. Almas, L.R. Bakken and J. Mulder, *Soil Biol. Biochem.*, 36 (2004) 805.
61 H. Zhang, W. Davison, R.J.G. Mortimer, M. Krom, P.J. Hayes and I.M. Davies, *Sci. Total Environ.*, 296 (2002) 175.
62 M.D. Krom, R.J.G. Mortimer, S.W. Poulton, P.J. Hayes, I.M. Davies, W. Davison and H. Zhang, *Aquat. Sci.*, 64 (2002) 282.
63 R.J.G. Mortimer, M.D. Krom, S.J. Harris, P.J. Hayes, I.M. Davies, W. Davison and H. Zhang, *Mar. Ecol. Prog. Ser.*, 236 (2002) 31.
64 S.P.C. Tankere, D.G. Bourne, F.L.L. Muller and V. Torsvik, *Environ. Microbiol.*, 4 (2002) 97.
65 G.R. Fones, W. Davison, O. Holby, B.B. Jorgensen and B. Thadrup, *Limnol. Oceanogr.*, 46 (2001) 982.
66 P. Divis, H. Docekalova and V. Smetkova, *Chem. Listy*, 97 (2003) 1184.
67 J. Pizarro, M.A. Rubio and G. Lira, *Bol. Soc. Chil. Quim.*, 46 (2001) 281.
68 J.L. Roulier and B. Motte, *J. Phys. IV*, 107 (2003) 1161.
69 E. Metzger, C. Simonucci, E. Viollier, G. Sarazin, F. Prévot, F. Elbaz-Poulichet, J.-L. Seidel and D. Jézéquel, *Est. Coastal Shelf Sci.*, (2007), doi: 10.1016/j.ecss. 2006.11.016
70 P. Divis, M. Leermakers, H. Docekalova and Y. Gao, *Anal. Bioanal. Chem.*, 382 (2005) 1715.
71 M.P. Harper, W. Davison and W. Tych, *Aquat. Geochem.*, 5 (1999) 337.
72 M. Motelica-Heino, C. Naylor, H. Zhang and W. Davison, *Environ. Sci. Technol.*, 37 (2003) 4374.

73 K.W. Warnken, H. Zhang and W. Davison, *Anal. Chem.*, 76 (2004) 6077.
74 P.R. Teasdale, S. Hayward and W. Davison, *Anal. Chem.*, 71 (1999) 2186.
75 D. Bellis, G.M. Nowell, C.J. Ottley, D.G. Pearson and W. Davison. In: J.G. Holland and D.R. Bandura (Eds.), *Plasma Source Mass Spectrometry, Current Trends and Future Developments*, Royal Society of Chemistry, Cambridge, 2005, pp. 268–283.
76 C.R. Devries and F.Y. Wang, *Environ. Sci. Technol.*, 37 (2003) 792.
77 C. Naylor, W. Davison, M. Motelica-Heino, G.A. Van Den Berg and L.M. Van Der Heijdt, *Sci. Total Environ.*, 328 (2004) 275.
78 C. Naylor, W. Davison, M. Motelica-Heino, G.A. Van Den Berg and L.M. Van Der Heijdt, *Sci. Total Environ.*, 357 (2006) 208.
79 M.P. Harper, W. Davison and W. Tych, *Environ. Sci. Technol.*, 33 (1999) 2611.

Chapter 17

Passive sampling devices for measuring organic compounds in soils and sediments

Gangfeng Ouyang and Janusz Pawliszyn

17.1 INTRODUCTION

Monitoring of organic pollutants in the environment is an ongoing challenge for the analytical chemist [1]. As for water and air sampling techniques, there are two basic types of soil/sediment sampling methods: active and passive. The active sampling approach is time-consuming and can be very costly, due to the need for the collection of a large number of samples from the given sampling location for the duration of the monitoring period. The passive sampling approach is more attractive, especially for long-term monitoring programmes, because it is economical and easy to perform and time-weighted average (TWA) concentrations of target analytes can be obtained with one sampler. Some passive samplers can be analysed directly, therefore no complicated sample preparation treatment is required [1].

The monitoring of volatile organic compounds (VOCs) and semivolatile organic compounds (SVOCs) in soil is normally done by measuring the concentrations of target analytes in soil gas. Passive soil gas sampling technology was developed in the early part of 20th century [2], when investigators used a variety of methods to collect near-surface samples of petroleum-derived hydrocarbon gases diffusing upwards from subsurface reservoirs. The passive soil gas sampling techniques, such as the PETREX sampling system [3], the GORE^{TM} module [4] and the Emflux® passive sampling system [5] can be completed in several days or weeks and are most useful for monitoring field sampling sites contaminated with SVOCs or where soils prevent sufficient air flow for active sampling.

Comprehensive Analytical Chemistry 48
R. Greenwood, G. Mills and B. Vrana (Editors)
Volume 48 ISSN: 0166-526X DOI: 10.1016/S0166-526X(06)48017-X

The monitoring of organic pollutants in sediments is usually achieved by measuring the concentrations of contaminants in the sediment vapour or pore-water. The PETREX sampling system can be used for measuring VOCs and SVOCs in sediment vapour [3,6]. Semipermeable membrane devices (SPMDs) have been employed for monitoring polycyclic aromatic hydrocarbons (PAHs) in sediment pore-water [7–9].

Newly developed polydimethylsiloxane (PDMS)-rod and PDMS-membrane [10–12] samplers are based on the solid-phase microextraction (SPME) technique [13]. These passive sampling devices are suitable for measuring organic pollutants in water and air, including soil gas and sediment pore-water.

17.2 PETREX PASSIVE SOIL GAS AND SEDIMENT VAPOUR SAMPLING SYSTEM

The PETREX sampling system is a soil gas/sediment vapour sampling technology developed by Northeast Research Institute (NERI) Limited Liability Corporation (San Diego, CA, USA) [3]. The PETREX system is a near-surface monitoring method that collects contaminant vapours migrating to the surface from the soil and groundwater beneath each collection point. Soil gas is collected by the diffusion of the contaminant vapour into the PETREX sampler. The sediment vapour is collected by the diffusion of dissolved contaminants through a watertight, gas-permeable container.

The sampling system uses PETREX tubes to collect VOCs and SVOCs in the soil gas or sediment vapour that emanates from subsurface sources. The PETREX tubes consist of two or three activated carbon adsorption elements fused to ferromagnetic wire in a glass tube. They are typically buried 30–45 cm deep with the open end down, and left in place for various periods of time, from overnight to two or three weeks [6]. Soil gas samples are collected by unsealing the sampler and exposing the collector to the soil gas at the bottom of a shallow borehole. Sample collection proceeds via free vapour diffusion through the opening of the uncapped sample container. For sediment vapour sampling, the PETREX samplers are placed in watertight gas permeable containers, such as polyethylene bags, before they are placed in the sediment using a drive shoe [3].

After a controlled period of time, sufficient to allow for the loading of gases onto the activated carbon adsorbent wires, the sampler is

retrieved from the borehole, resealed and transferred to the laboratory for analysis. The wire with the adsorbed sample is thermally desorbed directly into a mass spectrometer (MS) for analysis. The results are reported in ion flux counts and the flux counts are proportional to contaminant concentrations in the soil or sediment.

The PETREX sampling system can collect a broad range of VOCs and SVOCs. The system can provide site reconnaissance data regarding the presence of VOCs and SVOCs emitting from subsurface sources. Passive surveys of soil gas and sediment vapour with PETREX samplers cause minimal site disruption, and require minimal mobilization and demobilization. This type of passive sampling device has been successfully used for surveys of soil gas and sediment vapours at contaminated sites in San Diego Bay [6] and Brazil [14].

There are some limitations of the PETREX passive soil gas and sediment vapour sampling system. First, the ion count cannot be directly correlated to the contaminant concentrations in the soil gas or sediment pore-water and the ion count of a compound at one sampling location cannot be compared with that of another compound because of the differences in physicochemical properties between individual compounds, including their ability to both adsorb and desorb from the charcoal PETREX collector elements. In addition, the effectiveness of the PETREX system for site screening and characterization will be influenced by irregularities in the near-surface and subsurface environment, such as man-made structures, groundwater and surface water, the free carbon content of soil, etc. A quality assurance program for the placement of the sampling devices in the soil must be rigorously followed and it should be noted that the moisture will affect the sampling because the activated carbon adsorbents exhibit a high affinity for water vapour.

17.3 GORE^{TM} MODULES FOR PASSIVE SOIL GAS COLLECTION

In 1992, W.L. Gore pioneered the use of expanded polytetrafluoroethylene (ePTFE) for environmental site-characterization applications, using a patented passive sampler called the GORE^{TM} module, formerly known as the GORE-SORBER® module for sampling air, soil gas and water. GORE-SORBER® was evaluated by the U.S. Environmental Protection Agency's (EPA) Superfund Innovative Technology Evaluation Program in 1998 [15].

Inside the GORE^{TM} module is the granular sorbent material, which consists of various polymeric and carbonaceous adsorbents selected for their affinity to a wide variety of volatile inorganic and organic compounds ranging from C_2 (ethane) to C_{20} (phytane). The adsorbents are hydrophobic, to minimize the uptake of water vapour. These adsorbents are protected by a microporous tube of polytetrafluoroethylene (PTFE) or GORE-TEX® membrane. The membrane has pores 1000 times larger than the target molecules to be collected and these hydrophobic pores are small enough to reject soil and water to a depth of over 10 m, which helps to keep the adsorbents clean [4].

The GORE-TEX® membrane is also used as a cord for insertion and retrieval of the sampler. The membrane cord is about 1.3-m long and contains enough adsorbent for two samples. This enables duplicate analyses or can be used as a backup for one sampling location.

The GORE^{TM} modules are installed into a small-diameter hole, typically about 1–2 cm with depths of 50–100 cm.The hole can be dug with simple hand tools, such as a hammer, screwdriver, tile probe, slam bar or battery-operated drill. The GORE^{TM} module is stored and transported in a glass vial. Once the hole is formed, a stainless steel insertion rod, which is supplied by Gore, is placed into the pocket in the end of the module and then inserted into the pilot hole. A cork is tied to the surface end of the cord. The cork will seal the hole and the cord will allow for retrieval of the sampler. The sample location is marked and the coordinates are recorded using a global position system (GPS) hand unit for subsequent retrieval.

The adsorbents inside the module are analysed by a thermal desorption apparatus using gas chromatography–mass spectrometry (GC–MS). The analysis generates a mapped interpretation [21]. Several applications of this technique were reported after the passive sampling system was initially developed [16–20]. Most recently, this technique has been used in environments ranging from the frozen soil zone in Russia and Canada to deserts in Egypt and Libya [21].

17.4 EMFLUX® PASSIVE SOIL GAS SAMPLING SYSTEM

In 1988, Beacon Environmental Services, Inc. (formerly Quadrel Services, Inc.) developed the Emflux® passive soil gas sampling system [5]. The Emflux® soil gas sampling system had been verified through the EPA's Environmental Technology Verification (ETV) Program in 1998 [22].

The Emflux® soil gas collector consists of 100 mg of hydrophobic adsorbents sealed in a fine mesh screen. The adsorbent is placed in a 7-mL screw top glass vial. When sampling, the solid plastic cap of the vial is removed and replaced with a sampling cap. The sampling cap is made of plastic and has a hole covered with a mesh screen. A wire is secured around the vial for later retrieval. The collector is installed in a small diameter hole, 2-cm wide and 10-cm deep. After an Emflux® collector has been installed, the top of the hole will be completely sealed by collapsing the soils above the collector, which ensures that the collector will not be susceptible to the influences of surface water or the escape of subsurface gases. The sampling system also includes a computer model to predict the optimal sampling times for specific geographic locations and sample analyses. This software model can therefore optimize the sampling time. After the sampling is completed, the collector is retrieved. Analysis of the samplers is completed by thermal desorption with gas chromatography–flame ionization (GC–FID) or GC–MS analysis, using EPA methods. Optimum results are achieved when the analytical procedures match the data quality objectives (DQOs) of the project [5]. Each Emflux® collector contains two adsorbent cartridges to allow for duplicate analyses from one sample location.

Compared with other sampling systems, the Emflux® soil gas sampling system uses hydrophobic adsorbent materials that have a strong affinity for the targeted compounds. The hydrophobic adsorbents have no affinity for water vapour; therefore, all receptors are available to adsorb the contaminants without having to compete with water molecules. However, the Emflux® soil gas sampling system does not use a waterproof membrane to prevent the uptake of water vapour. It reduces the resistance of the flow of subsurface vapours to the adsorbent.

17.5 SEMIPERMEABLE MEMBRANE DEVICES FOR PASSIVE SAMPLING IN SEDIMENT PORE-WATER

The SPMD was first introduced by Huckins *et al*. in 1990 [23]. SPMDs can also be used for passive sampling in sediment pore-water. Williamson *et al*. employed SPMDs for sampling sediment pore-water in static exposure studies under controlled laboratory conditions, using sediments fortified with 15 priority pollutant PAHs [7,8]. Zhu *et al*. also used SPMDs for passive sampling, to concentrate and identify 16 PAHs in coastal sediment pore-water [9]. Further details about the sampling, analysis and calibration methods for SPMDs are described in Chapters 2, 7 and 14 of this book.

17.6 SOLID-PHASE MICROEXTRACTION DEVICES FOR PASSIVE SAMPLING IN SOIL AND SEDIMENT

The SPME technique was first introduced by Pawliszyn *et al.* in 1990 [24]. Since then, the SPME technique has been widely applied to the sampling and analysis of environmental, food and pharmaceutical samples [25]. Nilsson *et al*. introduced an SPME device for *in situ* sampling of groundwater and soil gas [26]. In this device, the SPME fibre was protected with a cap and a number of holes were drilled into the cap for liquid exchange or gas flow. The analytes passed through the holes and were then extracted by the SPME fibre. This SPME device was placed in the headspace to monitor underground soil gas or was lowered into a well for direct groundwater sampling. Toluene and naphthalene were detected by underground soil gas sampling and their presence was confirmed by extractions using Tenax® tubes. This type of SPME device requires a sampling time that is long enough to reach equilibrium. The results obtained by this device are the concentrations of analytes at the time the samplers were retrieved, not the TWA concentrations of the analytes in the sampling period.

It has also been demonstrated that SPME can be used as a TWA passive sampling technique. SPME TWA passive samplers for air and water sampling have been developed by Pawliszyn *et al*. between 1999 and 2005 [27–29]. Such devices are referred to as fibre-in-needle SPME devices [29]. For these devices, the SPME fibre is retracted a known distance into its needle during the sampling period. Analyte molecules access the fibre coating only by means of diffusion through the static air or water gap between the opening and fibre coating. The face velocity of air or water across the needle opening will not affect the sampling, due to the extremely small inner diameter of the fibre needle. The mass uptake can therefore be predicted by Fick's law of diffusion. This type of SPME device was also designed for field sampling. Figure 17.1 illustrates an SPME diffusive sampler for air sampling designed by Chen and Pawliszyn [30] and then modified by Supelco Company. Figure 17.2

Fig. 17.1. Supelco® SPME TWA air sampler.

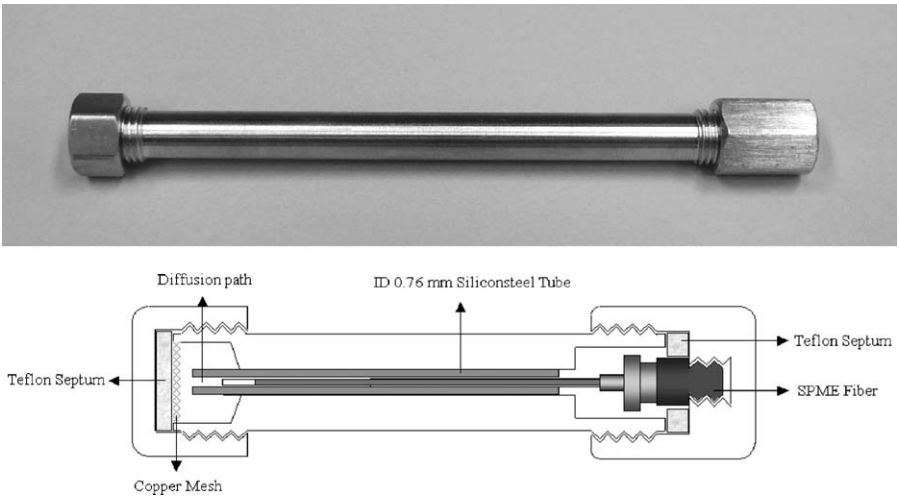

Fig. 17.2. SPME TWA water sampler.

illustrates a SPME diffusive sampler for water sampling designed by G. Ouyang *et al.* [31]. This type of SPME device can also be used for measuring organic pollutants in soils and sediments.

Recently, more sensitive, convenient and low-cost TWA passive samplers based on the SPME technique have been developed. These new samplers are referred to as PDMS-rod [10] and PDMS-membrane [11] passive samplers (Fig. 17.3). The device on the left is a PDMS-rod passive sampler, composed of a pure PDMS rod, 1-mm wide and 1-cm long, with a volume of 7.85 μL. The device on the right is a PDMS-membrane passive sampler. It is a piece of pure PDMS membrane, 125-μm thick with a volume of 62.5 μL. The volumes of the PDMS-rod and the PDMS-membrane samplers are much larger than commercial PDMS fibres (0.61 μL). This increases the sensitivity of the passive samplers. The simple use of a PDMS rod and membrane as a TWA passive sampler is based on the newly developed kinetic calibration method for SPME [32]. This kinetic calibration method, also called the on-fibre standardization technique, uses the desorption of the standards, which are pre-loaded in the extraction phase, to calibrate the extraction of analytes.

The kinetic process for the absorption of analytes into a PDMS rod or membrane from a medium with constant analyte concentration can be described by [33]

$$\frac{n}{n_e} = 1 - \exp(-at) \tag{17.1}$$

Fig. 17.3. PDMS-rod and membrane samplers.

where n is the amount of analyte in the extraction phase at time t, a is a first-order exchange rate constant that is dependent on the volumes of the extraction phase, headspace and sample, mass transfer coefficients, distribution coefficients and the surface area of the extraction phase. The kinetic process of the desorption of the internal standard from the extraction phase to a medium with negligibly low internal standard concentration is defined by [32]

$$q = q_0 \frac{V_s}{K'_{es} V_e + V_s} [1 - \exp(-at)] \tag{17.2}$$

where V_e and V_s are the volumes of the extraction phase and the sample, respectively. K'_{es} is the distribution coefficient of the internal standard between the extraction phase and the sample, q is the amount of standard lost from the extraction phase at time t and q_0 is the amount of pre-loaded standard in the extraction phase. Let $Q = q_0 - q$, and Q is the amount of the standard remaining in the extraction phase after exposure of the extraction phase to the sample matrix for the sampling time, t. Thus, for the desorption process, Eq. (17.2) can be

expressed by [34]

$$\frac{Q - q_e}{q_0 - q_e} = \exp(-at) \tag{17.3}$$

where q_e is the amount of standard remaining in the extraction phase at equilibrium. If the desorption and absorption processes occur simultaneously, the constant a should be similar for the analytes and the internal standard, if their physicochemical properties are similar. Then, Eqs. (17.1) and (17.3) can be combined to form

$$\frac{n}{n_e} + \frac{Q - q_e}{q_0 - q_e} = 1 \tag{17.4}$$

As q_e and n_e can be calculated with the distribution coefficient between extraction phase and sample:

$$q_e = \frac{K'_{es} V_e q_0}{K'_{es} V_e + V_s} \tag{17.5}$$

$$n_e = \frac{K_{es} V_e V_s}{K_{es} V_e + V_s} C_0 \tag{17.6}$$

where K_{es} is the distribution coefficient of the analyte between extraction phase and sample. As $K'_{es} \approx K_{es}$, then Eq. (17.4) can be expressed by [10]

$$C_0 = \frac{q_0 n}{K_{es} V_e (q_0 - Q)} \tag{17.7}$$

Equation (17.7) indicates that the sample volume and sampling time will not affect the determination of C_0, the initial concentration of the analyte in the sample. When the extraction of the analytes and the desorption of the internal standard are isotropic, environmental factors, such as temperature and turbulence, will not affect the determination of the concentrations of the organic pollutants in the original sample.

The samplers and pre-loaded standards are protected with copper mesh bags and are put in the sample matrix for a certain time, and subsequently retrieved and sealed in a glass vial. Analysis of the samplers is completed by direct thermal desorption with GC–MS analysis; no further sample preparation treatment is required. The injection of the sample is automatically performed by the ATAS (a total analytical solution) system. The middle of Fig. 17.3 illustrates a liner for the automated injection of the sample. The initial amount of standard

loaded on to the rod (or membrane), the remaining standard and the amount of analytes extracted by the sampler is used to calculate the TWA concentration of the target analytes, using Eq. (17.7) [10].

The PDMS-rod and PDMS-membrane passive samplers are based on the in-fibre standardization technique and exhibit all of the advantages of the SPME technique: they are simple, convenient, combine both the sampling and sample preparation in one step and can transfer analytes directly into a standard gas chromatograph (GC). They also address the needs of all passive sampling techniques: they are highly sensitive, inexpensive, easy to deploy, and the TWA concentrations of the target analytes can be obtained by one sampler and can be analysed directly, eliminating the need for further sample preparation treatment.

The PDMS-rod and PDMS-membrane samplers are suitable for TWA passive sampling in water and air, including soil gas and sediment pore-water. The usefulness of these samplers has been demonstrated experimentally, both under laboratory conditions and under field conditions, in Hamilton Harbour, Hamilton, Ontario [10,11]. The effect of environmental factors, such as temperature, turbulence, etc., was successfully calibrated in the field studies. Till now, this in-fibre standardization technique is limited to calibrate the analytes with similar physicochemical properties to the pre-loaded standards.

Similar method, called performance reference compound (PRC), were used for the calibration of SPMD, in which an internal standard was first introduced for SPMD to monitor the biofouling effect [35,36]. The exposure adjustment factor (EAF) can be used to adjust the sampling rate of SPMD [37]. In this case, separate studies needed to be performed in the laboratory to derive EAF before applying the SPMDs in real sampling. The PRC-based method for SPMD is normally limited to the linear chemical uptake into SPMD and the PRC is only used to estimate *in situ* SPMD sampling rate. The concentration of analyte in water can not be directly calculated with the loss of PRC in the field sampling.

17.7 CONCLUSION

Passive sampling techniques for measuring organic compounds in soils and sediments should be rapid, low cost and provide a high yield of information. Most developed soil gas sampling techniques, such as the PETREX sampling system, the GORE^{TM} module and the Emflux® passive sampling system, are used only for site screening. The

concentration of analytes in the sample cannot be quantitated. The SPMDs and the samplers based on SPME technique can obtain the TWA concentrations of analytes in the sample, by using PRCs or in-fibre standardization technique. But these techniques are being developed to get more accurate calibration result.

REFERENCES

1 J. Namieśnik, B. Zabiegala, A. Kot-Wasik, M. Partyka and A. Wasik, *Anal. Bioanal. Chem.*, 381 (2005) 279.
2 http://www.epa.gov/nerlesd1/factsheets/soil-gas.pdf.
3 http://www.nasni.navy.mil/nelp/nelpfs-7.pdf.
4 http://www.gore.com/en_xx/products/geochemical/petroleum/surveys_petroleum_modules.html.
5 http://www.emflux.com.
6 M. Anderson and G. Church, *J. Environ. Eng.*, 124 (1998) 555.
7 K.S. Williamson, J.D. Petty, J.N. Huckins, J.A. Lebo and E.M. Kaiser, *Chemosphere*, 49 (2002) 703.
8 K.S. Williamson, J.D. Petty, J.N. Huckins, J.A. Lebo and E.M. Kaiser, *Chemosphere*, 49 (2002) 717.
9 Y. Zhu, Y. Zhang, J. Zhang, Y. Zhuang, K. Poon, M. Lam, H. Hong and R. Wu, *Chin. J. Oceanol. Limnol.*, 19 (2001) 382.
10 W. Zhao, G. Ouyang, M. Alaee and J. Pawliszyn, *J. Chromatogr. A*, 1124 (2006) 112.
11 L. Bragg, Z. Qin, M. Alaee and J. Pawliszyn, *J. Chromatogr. Sci.*, 44 (2006) 317.
12 G. Ouyang, W. Zhao, L. Bragg, Z. Qin, M. Alaee and J. Pawliszyn, *Environ. Sci. Technol.*, 2006, submitted for publication.
13 J. Pawliszyn, *Solid Phase Microextraction—Theory and Practice*, Wiley-VCH, New York, 1997.
14 D.C. Gomes, M. Alarse, M.C. Salvador and C. Kupferschmid, *Water Sci. Technol.*, 29 (1994) 161.
15 USEPA, EPA/600/R-98/095, 1998.
16 M.J. Wrigley, *Hazard. Ind. Wastes*, 27 (1995) 909.
17 P. Kless, *Soil Environ.*, 5 (1995) 509.
18 C. Mehltretter and H. Sorge, *Soil Environ.*, 5 (1995) 523.
19 W.M. Wells and S.G. Mcmahon, *Princ. Pract. Diesel Contam. Soils*, 5 (1996) 59.
20 A.D. Hewitt, *Am. Environ. Lab.*, 10 (1998) 14.
21 http://www.gore.com/en_xx/products/geochemical/petroleum/index.html.
22 USEPA, EPA/600/R-98/096, 1998.
23 J.N. Huckins, M.W. Tubergen and G.K. Manuweera, *Chemosphere*, 20 (1990) 533.

24 C.L. Arthur and J. Pawliszyn, *Anal. Chem.*, 62 (1990) 2145.
25 J. Pawliszyn (Ed.), *Applications of Solid Phase Microextraction*, RSC, Cambridge, UK, 1999.
26 T. Nilsson, L. Montanarella, D. Baglio, R. Tilio, G. Biodoglio and S. Facchetti, *Int. J. Environ. Anal. Chem.*, 69 (1998) 1.
27 P.A. Martos and J. Pawliszyn, *Anal. Chem.*, 71 (1999) 1513.
28 Y. Chen and J. Pawliszyn, *Anal. Chem.*, 75 (2003) 2004.
29 G. Ouyang, Y. Chen and J. Pawliszyn, *Anal. Chem.*, 77 (2005) 7319.
30 Y. Chen and J. Pawliszyn, *Anal. Chem.*, 76 (2004) 6823.
31 G. Ouyang, W. Zhao, M. Alaee and J. Pawliszyn, *J. Chromatogr. A*, 1138 (2007) 42.
32 Y. Chen and J. Pawliszyn, *Anal. Chem.*, 76 (2004) 5807.
33 J. Ai, *Anal. Chem.*, 69 (1997) 1230.
34 Y. Wang, J. O'Reilly, Y. Chen and J. Pawliszyn, *J. Chromatogr. A*, 1072 (2005) 13.
35 H.F. Prest, W.M. Jarman, S.A. Burns, T. Weismuller, M. Martin and J.N. Huckins, *Chemosphere*, 25 (1992) 1811.
36 K. Booij, H.M. Sleiderink and F. Smedes, *Environ. Toxicol. Chem.*, 17 (1998) 1236.
37 J.N. Huckins, J.D. Petty, J.A. Lebo, F.V. Almeida, K. Booij, D.A. Alvarez, W.L. Cranor, R.C. Clark and B.B. Mogensen, *Environ. Sci. Technol.*, 36 (2002) 85.

Chapter 18

Use of passive sampling devices in toxicity assessment of groundwater

Kristin Schirmer, Stephanie Bopp and Jacqueline Gehrhardt

18.1 INTRODUCTION

Groundwater is one of our most vital resources. Approximately 90% of all readily available fresh water (that is excluding glaciers and icecaps) is stored as groundwater. Groundwater is a major source for drinking water in many parts of the world and it provides baseflow and recharge to streams and lakes. For these reasons, groundwater requires protection and appropriate ways to assess its quality.

Groundwater quality can be impaired by basically two types of contamination—microbial or chemical. Both can occur due to point or non-point sources. With regard to chemical contamination, substances such as organic chlorinated compounds, polycyclic aromatic hydrocarbons (PAHs) or nitrate have been, and continue to be, of frequent concern. More recently, pharmaceuticals and personal care products had to be added to the list of chemicals of concern. For example, Heberer *et al.* [1,2] reported several human pharmaceuticals at $\mu g\ L^{-1}$ concentrations in groundwater at a drinking water production site located downstream of a sewage treatment facility and a pharmaceutical production plant. Thus, there is growing awareness that we need to improve our ability to assess groundwater quality and that more effective ways of groundwater monitoring are essential to protect its vital role.

Effective groundwater monitoring requires that site- and problem-specific characteristics are taken into account. Traditional ways of groundwater monitoring are often limited in their suitability to accomplish this. Several innovative monitoring approaches have been developed over the past years and these promise to overcome a number of shortcomings of conventional monitoring strategies. For example, long-term surveillance to monitor the success of remediation measures

Comprehensive Analytical Chemistry 48
R. Greenwood, G. Mills and B. Vrana (Editors)
Volume 48 ISSN: 0166-526X DOI: 10.1016/S0166-526X(06)48018-1

has been shown to be achievable with very little effort by means of time-integrating sampling devices, such as the ceramic dosimeter [3,4] (see Chapter 12). Sampling devices are installed for months and with only one sampling event, time-weighted average contaminant concentrations can be calculated. This approach is far superior to conventional snapshot sampling, which requires time- and labour-intensive field trips but still does not provide any information about contaminant concentrations between sampling events. Another limitation of conventional approaches to monitoring contaminants is the focus on chemical analysis alone. If contamination is known to be caused by one or few well-described chemicals, this approach is adequate. However, a multitude of chemicals is often present at contaminated sites with the identity of most of the chemicals being unknown. Toxicological analysis can greatly aid in the monitoring of such complex contaminations because it accounts for groundwater in its entirety. It has indeed been repeatedly shown that chemicals assumed to be a priority did not explain the toxicity, and thus the reduced quality observed in groundwater samples [5–7]. If toxicological and chemical analyses are combined, the identity of relevant chemicals may be deciphered and remediation measures adopted accordingly.

It can be concluded that the challenge of measuring groundwater quality can best be met if a wide spectrum of methodologies is considered and applied according to needs. Passive samplers as well as toxicity tests comprise two methodologies that have been shown individually to be promising additions to conventional assessment schemes. To further extend their applicability, we propose that passive sampling and toxicity tests can also be combined. Thus, this chapter will illustrate the concepts and examples available to date on the use of passive sampling devices in assessing the toxicity of groundwater. We will also discuss how additional groundwater-compatible passive sampling devices could be used in the future to derive information on the toxic potency of groundwater.

18.2 CONCEPTS AND EXAMPLES FOR LINKING PASSIVE SAMPLING OF GROUNDWATER WITH TOXICOLOGICAL ANALYSIS

There are currently two approaches to linking passive sampling of groundwater with toxicological analysis (Fig. 18.1). The first is to build a passive sampler in such a way that it is directly compatible with toxicological tests. This has been accomplished in the toximeter, which

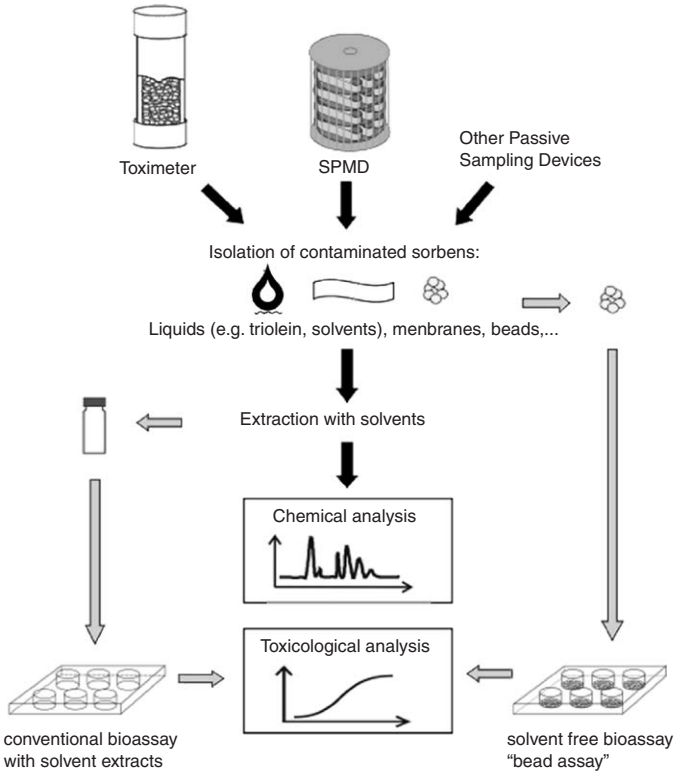

Fig. 18.1. Schematic representation of the two approaches currently available to link passive sampling and toxicological analysis. Any sampler can initially be applied as long as solvent extracts can be derived, which are subsequently applied in bioassays (left-hand side). The beads used in the toximeter are chosen such that they can directly be used in the specifically developed solvent-free bead assay (right-hand side) so that a chemical extract is not required for bioassay analysis.

is based on adherence-dependent vertebrate cells to detect a toxicological response (see Section 18.2.1). The second approach is to employ a passive sampler commonly used for monitoring groundwater contaminants based on chemical analysis alone, prepare an extract of sampled contaminants and apply this extract in a toxicity test (see Section 18.2.2). The advantage of the first approach is that chemical contaminants present in the groundwater can be explored without the need for solvent extraction and the use of organic solvents in toxicity tests. The advantage of the second approach is that any passive sampler suitable for groundwater can be applied as long as an extract of the sampled chemicals can be derived. Inasmuch as passive sampling devices

generally report on the fraction of chemical contaminants that is freely dissolved, both approaches have the advantage that sampled contaminants reflect the bioavailable fraction present in the groundwater. In many cases, this fraction may only be detectable by time-integrating (i.e. non-equilibrium) passive sampling devices because it is too small to be detectable both chemically as well as toxicologically by equilibrium or snapshot sampling.

18.2.1 The toximeter

The toximeter is a recently developed passive sampling device. It is the first passive sampler to allow direct bioassay analysis of accumulated chemicals. It is also possible, by means of simple solvent extraction, to carry out a chemical analysis and link the information obtained on concentrations of chemicals present to the results of toxicity tests [8]. The underlying principle of the toximeter is that sorbents used for sampling can be applied directly in toxicity tests [9]. Although, technically, the design of the toximeter pertains to surface or pore-water sampling, its first development and application were focused on groundwater.

The toximeter is a solid sorbent sampler, which uses loose beads as receiving phase. It builds on the ceramic dosimeter developed by Grathwohl [10] (see also Chapter 12). The toximeter uses the same ceramic tube design, which is 5 cm long and 1 cm in diameter and serves both as a container for the solid sorbent material and as the diffusion barrier. Based on the thickness of the membrane and the small inner pore size (pore size 5 nm), the ceramic tube comprises a robust barrier that limits uptake into the inner part to diffusion alone. The small pore size also prevents microorganisms from entering the sampling device. The key difference from the ceramic dosimeter is the choice of bead material: in addition to a high affinity to target analytes, it is non-toxic by itself and supports the viability and responsiveness of toxicity reporting entities. In the current toximeter design, adherence-dependent vertebrate cell lines are used as versatile reporters of toxicity. Toxicological analysis of toximeter samples is performed in a specifically developed solvent-free, solid-phase bioassay, called the bead assay [11]. The bead assay is performed by first inserting contaminant-loaded sorbent beads (i.e. beads from the toximeter after sampling) to multiwell plates. Subsequently, vertebrate cells are added to the plates in which the beads act as a surface for the cells to attach and grow. Due to the direct contact of the vertebrate cells with the contaminant-loaded sorbent beads, contaminants are able to enter the cells (Fig. 18.2). We

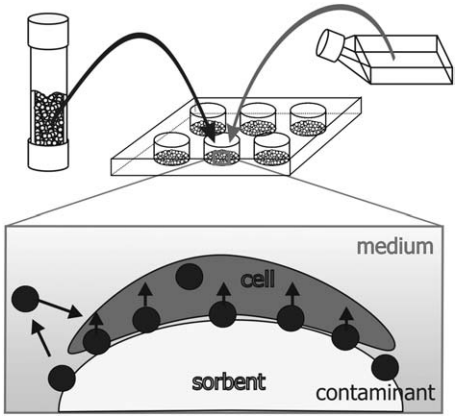

Fig. 18.2. Principle of the bead assay to assess the toxicity of toximeter-derived samples. Sorbent beads from the toximeter passive sampler are transferred to multi-well plates and used as cell culture surface after field exposure. Adherence-dependent vertebrate cells, used as biological indicators, are added to the sorbent-containing wells. Cells attach onto the contaminated surface (magnified insert) and by the direct contact are able to easily take up the sorbed contaminants. After incubation of cells for a pre-determined time, toxicological effects in the cells can be assessed.

have shown that indeed, the direct contact of the cells to the contaminant-coated bead surface greatly facilitates the cellular transfer of contaminants and a biological response [11].

The bead assay as a pre-requisite for the toximeter was developed using permanent cell lines from rainbow trout (*Oncorhynchus mykiss*) liver (RTL-W1 and R1) [11]. PAHs were used as model compounds. Biological effects elicited by the PAHs were detected based on cell viability assays and the induction of cytochrome CYP1A, an aryl hydrocarbon receptor mediated (dioxin-like) response, measured as 7–ethoxyresorufin-*O*-deethylase (EROD) activity [12]. The sorbent bead material found to be most suitable for the application in the toximeter for PAH sampling as well as for use in the bead assay was Biosilon (Nunc). Biosilon consists of beads of 160–300 μm diameter made of polystyrene. Among 10 tested materials with a known or suspected high affinity for PAHs, it was the one that best enabled cell attachment and the detection of dose–response curves elicited by sorbed PAHs in adhering fish liver cells [11]. Figure 18.3 illustrates the appearance of cells upon attachment onto Biosilon beads. An example of a dose–response curve for EROD induction elicited in RTL-W1 cells by benzo[k]fluoranthene sorbed to Biosilon is shown in Fig. 18.4.

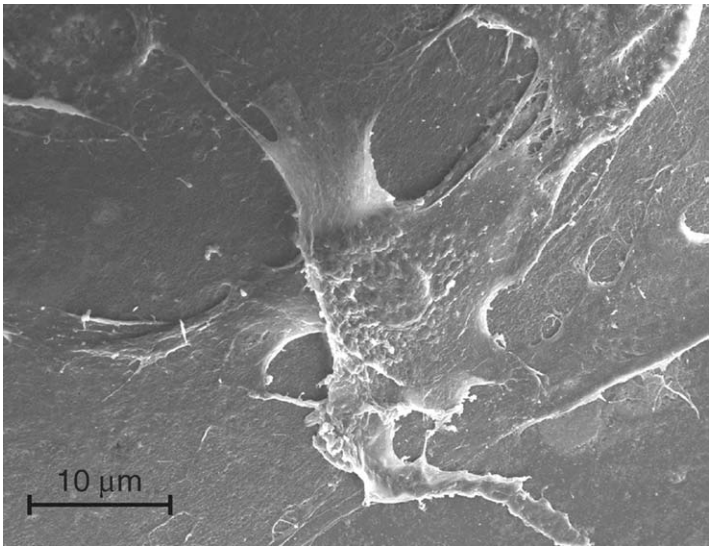

Fig. 18.3. Appearance of RTL-W1 cells grown for 4 days on a Biosilon bead. Photo was kindly provided by Dr Michael Gelinsky, Max Bergmann Center of Biomaterials, University of Technology Dresden. [SEM: Zeiss DSM Gemini 982, working distance 9 mm, acceleration voltage 5 kV; the sample was critical point dried and carbon coated].

The toximeter was evaluated for PAH sampling and combined toxicological and chemical analyses in several laboratory experiments and an extensive, 1–year field study at a contaminated gas works site [8]. Both laboratory experiments in semi-static exposure systems as well as the field study showed the general suitability of the Biosilon-filled toximeter for PAH sampling. The toximeter accumulated PAHs with a $\log K_{ow}$ between 4.5 and 6 as predicted based on Fick's first law. Thus, it allowed the calculation of time-weighted average aqueous PAH concentrations (see also Chapter 12). The lower predictability for PAHs with $\log K_{ow}$ values lower than 4.5 and higher than 6 was assumed to be due to lower binding affinities to Biosilon as receiving phase for the less hydrophobic PAHs (naphthalene, acenaphthene, acenaphthylene and fluorene) and hindrance in passing the ceramic membrane for the higher hydrophobic ones (dibenzo[a,h]anthracene, benzo[ghi]perylene and indeno[1,2,3–cd]pyrene). An example of accumulated masses obtained by the toximeter compared with the masses predicted based on conventional water analysis is depicted in Fig. 18.5.

The field study also confirmed the long-term stability of the toximeter sampling device even under extreme conditions. One of the three

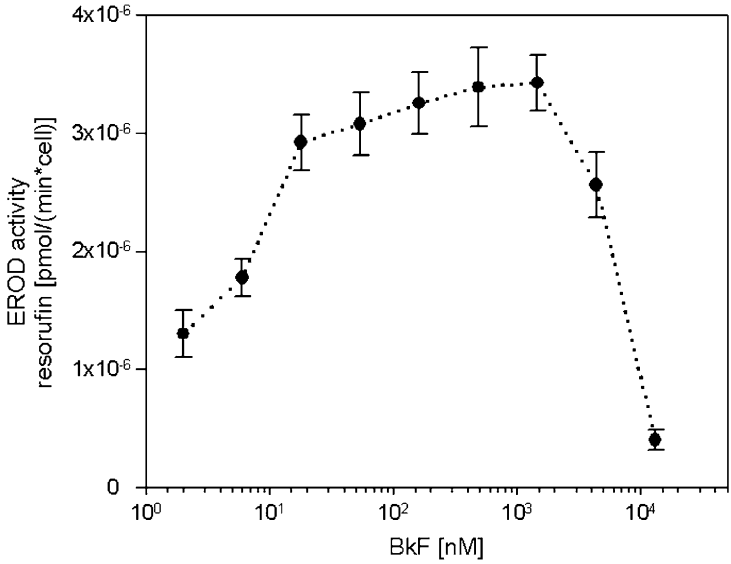

Fig. 18.4. Induction of EROD activity elicited in RTL-W1 cells after 24 h of exposure to benzo[k]fluoranthene (BkF) in the bead assay. Biosilon beads were coated with BkF prior to the testing by adding methanolic BkF solutions and allowing the methanol to evaporate. Biosilon with the sorbed BkF was transferred to 96–well plates at 30 mg Biosilon per well. A total of 200 µL of an RTL-W1 cell suspension with 30,000 cells/well was then added to the beads. After 24 h of exposure, EROD induction, measured as resorufin produced per minute per cell, was determined using a fluorescence plate reader according to the method described by Ganassin *et al.* [13]. BkF concentrations on the *X*-axis were calculated based on the total amount of BkF sorbed to the beads of one well divided by the volume of the medium in one well. The response curve detected in the bead assay was similar in shape to that typically observed in the standard assay. This similarity is reflected in the bell-shape of the curve as well as in the EC_{50} values, which were, respectively, about 9 nM (see the figure) in the bead assay and 8 nM (Bopp, unpublished) in the standard assay.

boreholes investigated for 1 year was filled up to half of its depth with a tar oil phase, which occurred unexpectedly upon constructions at the test site. Despite surface discolorations of toximeters hanging directly in the tar oil phase, sampling behaviour was not impaired. This was similar to the results obtained for ceramic dosimeters [11] (see also Chapter 12), which were simultaneously employed under identical conditions. Toxicological responses elicited by the field-exposed toximeters in the bead assay could be explained, in part, by the chemically detected PAHs but indicated the presence of other relevant contaminants not detected in routine chemical analyses [8].

In summary, the toximeter opens new avenues in the application of passive sampling devices. Because of its immediate compatibility with cultured vertebrate cells, a solvent extraction is not required and toxicity of the sampled groundwater contaminants is assessed quickly

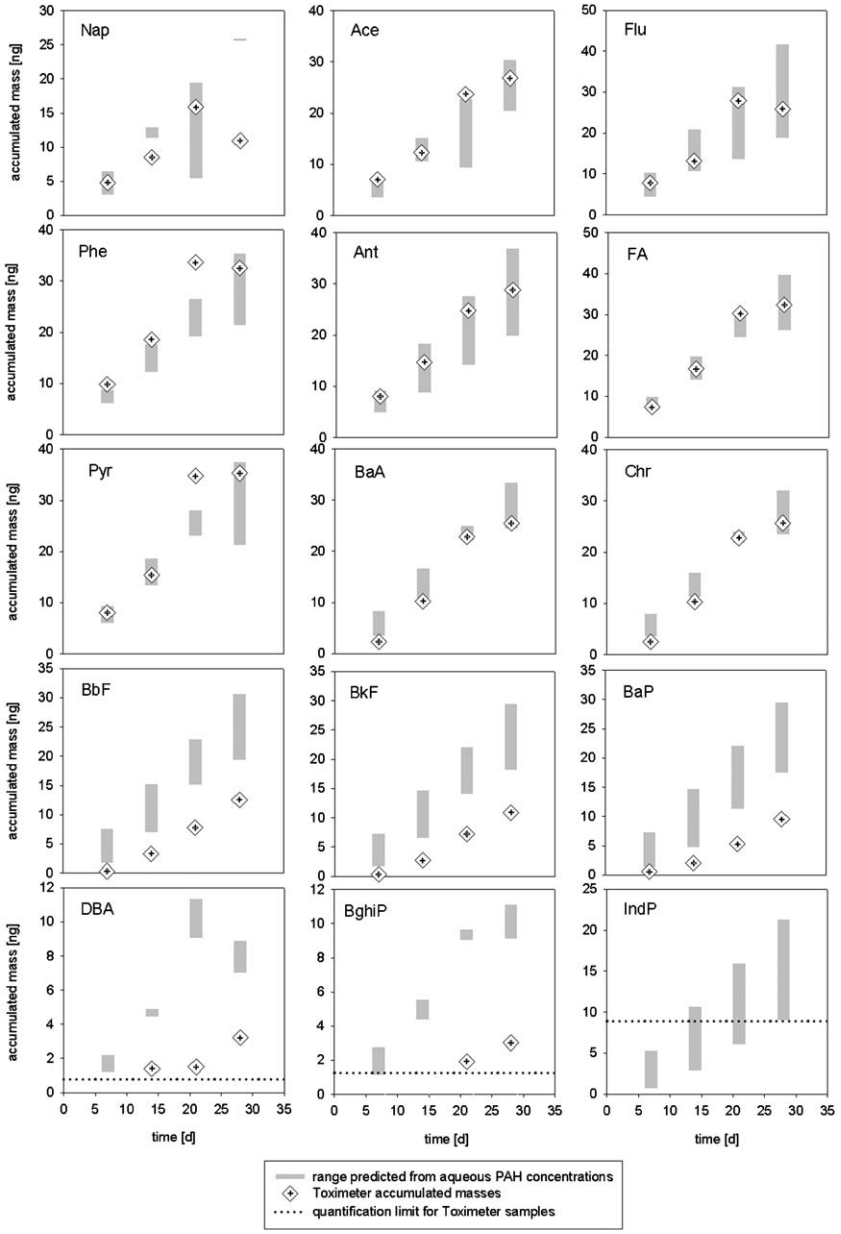

with minimal preparation. Rainbow trout liver cells were chosen as reporters of toxicity by PAHs in the first toximeter design because of their applicability to monitoring water quality in general. However, the cell line used could be from any species. Indeed, cell lines could be from any tissue or organ of origin, depending on the toxicological response of interest. Along these lines, we are currently applying the human breast cancer cell line, MCF-7, in order to detect cell proliferation and/or altered gene expression due to estrogenic compounds. Additional research is underway to apply the toximeter to surface- as well as pore-water.

18.2.2 Toxicological analysis of solvent extracts obtained from passive sampling devices

Passive samplers not directly designed for toxicological investigations have rarely been used to study groundwater toxicity. The methodology for using these is to obtain a solvent extract of the groundwater contaminants sampled by the chosen passive sampler and apply this extract to toxicity reporting entities. At least three interrelated aspects need to be considered in this approach. The first is that the solvent used for extraction and chemical analysis may not be compatible with application to a toxicity test. Thus, solvent exchange may comprise a necessary additional step. This may potentially lead to the loss of contaminants, particularly volatile and sparingly soluble compounds. Secondly, the extraction procedure itself may yield toxic compounds. An example was reported by Sabaliunas *et al*. [14] where oleic acid, a potential impurity of the triolein (the receiving phase material used in semi-permeable membrane devices (SPMDs)), was concentrated during extraction and found to be toxic toward luminescent bacteria. Thirdly, it is necessary to dilute the solvent extract in order to avoid interference with the toxicological reporters and/or the conditions of the toxicity tests. This may

Fig. 18.5. Comparison of accumulated amounts in the toximeters and accumulated amounts predicted from aqueous concentrations for each PAH over a 28-day exposure period in a semi-static exposure scenario. Toximeters were exposed in a semi-static system, exchanging exposure solutions every 24 h, in order to counteract sorptive losses of PAHs to test vessels. Squares depict the average accumulated mass from three toximeters. Bars represent the range of accumulated masses predicted from average aqueous concentrations with initial measured concentrations as basis for upper limits and concentrations of exchanged water after 24 h for lower limits. Abbreviations for the PAHs are as described in Ref. [3]. Indeno[1,2,3-cd]pyrene (IndP) concentrations were below the quantification limit for the toximeter samples.

limit the concentration range that can be applied. Despite these limitations, extracts of passive samplers, particularly SPMDs, have been applied successfully in a number of studies in surface water. Yet for groundwater, the potential of this approach has not been widely realized and only two examples can be provided at this point.

The first example is the use of extracts obtained from the ceramic dosimeters, exposed at a former gas works site, which were otherwise used for chemical analysis of PAHs [11]. The extracts, prepared in acetone, were applied to RTL-W1 cells at a 200–fold dilution in order to limit the acetone content to 0.5% per culture well (Bopp and Schirmer, unpublished). These extracts were found to be less potent in eliciting an EROD response when compared with the bead assay of toximeter-derived samples. One likely cause of this was the several-fold lower initial contaminant load in the acetone extract compared with that available in the bead assay. Up-concentration of the acetone extract prior to addition to the cells would have been possible but not to the same level of contaminant load as with the toximeter-derived beads. The second example is the use of extracts from SPMDs applied in groundwater in the industrial area of Bitterfeld (Germany). In addition to chemical analysis [15], SPMD extracts were applied to three organisms and one cell line-based bioassay (Altenburger and Schirmer, UFZ Centre for Environmental Research, Germany, personal communication). The cell line-based test was the induction of CYP1A in the rainbow trout liver cell line, RTL-W1. None of the extracts elicited this response, which led to the conclusion that dioxin-like compounds were not present at the site. The three organism-based toxicological tests comprised the inhibition of luminescence in *Vibrio fischeri* (the acute Microtox test), the *Daphnia magna* immobilization test as well as the inhibition of reproduction of the unicellular green alga *Scenedesmus vacuolatus*. All three tests showed that the samples most toxic were those from the sampling well GWM 19/91, which was the one most directly affected by seepage of spilled chemicals [15]. Toxicity of the extracts declined with increasing distance from this source, which well reflected the detected chemical load. Yet, further analysis revealed that toxicity could only partly be explained by the chemicals analysed. Thus, a combination of the bioassays and chemical fractionation and analysis could be used in the future to identify the chemicals that were sampled by the SPMDs but are not yet known to contribute to toxicity.

Taken together, these examples show that extracts obtained from passive samplers can be used in toxicity tests to investigate the potential of groundwater to be toxic. Combination with chemical

analysis enables the identification of possible links between contaminants analysed chemically and the observed toxicity. A particular strength of time-integrative passive samplers is that they accumulate the bioavailable contaminants from groundwater so that they can be detected both chemically as well as biologically even at concentrations that would be too low to be identified with conventional snapshot sampling.

18.3 POTENTIAL FUTURE APPROACHES

Passive sampling and toxicological analysis of groundwater quality are not yet routinely applied but the examples provided above illustrate the potential usefulness of this approach. The combination of the two techniques is advantageous and extra benefits are obtained from the interaction between the two methodologies. For the passive sampling, the advantages are the ability to carry out undisturbed, resource-efficient water sampling and, in the case of time-integrated sampling, the ability to calculate time-weighted average contaminant concentrations based on only one sampling event. For the toxicological tests, the advantage is that it accounts for the groundwater sample overall, rather than being focused on individual contaminants known or assumed to be present. If combined, the toxicity of the bioavailable fraction in the groundwater can be assessed and the toxicologically relevant contaminants be identified. Finally, if time-integrated sampling devices are applied, the toxicity of contaminants can be assessed even if their fraction is too low to be detectable on the basis of snapshot sampling.

Based on these advantages, a more widespread use of combined passive sampling and toxicological analysis can be foreseen. In addition to the examples provided above, there are simple means to advance this approach with the methods available to date. In principle, any extract obtained from a passive sampling device can be explored in toxicological tests. Equilibrium-based passive samplers, such as the passive diffusion bag samplers [16,17] or the diffusive multi-layer samplers [18,19] could also be applied to toxicological tests without additional steps. These samplers use water as the receiving phase and this water could be used to expose organisms typically occurring in groundwater or other test systems with relevance to human and/or ecosystem health. For example, the organism *Tetrahymena pyriformis* [20], or cell-based systems, such as cultured gill cells [21], can be exposed directly to water using microtitre plates. Methods are also available to apply such groundwater

samples to vertebrate cells that cannot sustain direct exposure to pure water [7,22,23]. In many cases, these assays not only add important information with regard to groundwater quality but they also comprise a cost- and time-efficient addition or alternative to chemical analysis. For example, the analysis of CYP1A induction, measured as EROD activity, requires about 24 h and approximately €30 of material costs for a full dose–response analysis [23]. In this respect, the combination of passive sampling and toxicological analysis can be regarded an early warning instrument to initiate more in-depth analyses of the causes of toxicity and the identification of relevant chemicals for better risk assessment and optimized remediation measures.

ACKNOWLEDGMENTS

We are grateful to Professor P. Grathwohl and Dr H. Weiß for continued discussions on ceramic-membrane-based passive sampling devices. Dr M. Gelinsky is thanked for the provision of electronmicrographs of fish liver cells adhering to Biosilon beads. We also thank Dr B. Vrana and Dr R. Altenburger for their cooperation in the bioassay analysis of SPMD extracts derived upon groundwater sampling. The work presented herein was financially supported by the German Federal Ministry of Education and Research (Project RETZINA, 02WT0041), the Saxonian Ministry of Environment and Geology (GenTec-Toximeter, 13–8811.61/184) and the Ontario Centre for Research in Earth and Space Technology (CRESTech).

REFERENCES

1 Th. Heberer, K. Reddersen, D. Feldmann and Th. Zimmermann, From municipal sewage to drinking water: fate and removal of pharmaceutical residues in the aquatic system of Berlin. In: *Proceedings of the 11th Annual Meeting of the American College of Toxicology (ACTox)*, San Diego, USA, November 2000.
2 Th. Heberer, U. Dünnbier, Ch. Reilich and H.-J. Stan, *Fresenius Environ. Bull.*, 6 (1997) 438.
3 S.K. Bopp, H.-J. Weiß and K. Schirmer, *J. Chromatogr. A*, 1072 (2005) 137.
4 H. Martin, B.M. Patterson, G.B. Davis and P. Grathwohl, *Environ. Sci. Technol.*, 37 (2003) 1360.
5 A. Baun, A. Ledin, L.A. Reitzel, P.L. Bjerg and T.H. Christensen, *Water Res.*, 38 (2004) 3845.

6 C. Helma, P. Eckl, E. Gottmann, F. Kassie, W. Rodinger, H. Steinkeller, C. Windpassinger and R. Schulte-Hermann, *Environ. Sci. Technol.*, 32 (1998) 1799.
7 K. Schirmer, S. Bopp, S. Russold and P. Popp, *Grundwasser*, 9 (2004) 33.
8 S.K. Bopp, Ph.D. thesis: *Development of a Passive Sampling Device for Combined Chemical and Toxicological Long-term Monitoring of Groundwater*, University of Rostock, Germany, ISSN 0948-9452, 2000.
9 K. Schirmer, N.C. Bols and M. Schirmer, U.S. patent application No. 09/908,690 (2001).
10 P. Grathwohl, Deutsches Patent [DE 198 30 413 A1]. 30.10.2003 (1999).
11 S. Bopp, N.C. Bols and K. Schirmer, *Environ. Toxicol. Chem.*, 25(5) (2006) 1390–1398.
12 N.C. Bols, K. Schirmer, E.M. Joyce, D.G. Dixon, B.M. Greenberg and J.J. Whyte, *Ecotoxicol. Environ. Safety*, 44 (1999) 118.
13 R.C. Ganassin, K. Schirmer and N.C. Bols. In: G.K. Ostrander (Ed.), *The Laboratory Fish*, Academic, San Diego, CA, USA, pp. 631–651.
14 D. Sabaliunas, J. Ellington and I. Sabaliuniene, *Ecotoxicol. Environ. Safety*, 44 (1999) 160.
15 B. Vrana, H. Paschke, A. Paschke, P. Popp and G. Schüürmann, *J. Environ. Monit.*, 7 (2005) 500.
16 D.A. Vroblesky and T.R. Campbell, *Adv. Environ. Res.*, 5 (2001) 1.
17 D.A. Vroblesky and W.T. Hyde, *Ground Water Monit. Remed.*, 17 (1997) 177.
18 R.W. Puls and C.J. Paul, *J. Contam. Hydrol.*, 25 (1997) 85.
19 D. Ronen, M. Magaritz and I. Levy, *Ground Water Monit. Rev.*, 7 (1987) 69.
20 V.R. Dayeh, S. Grominsky, S.J. DeWitte-Orr, D. Sotornik, C.R. Yeung, L.E. Lee, D.H. Lynn and N.C. Bols, *Res. Microbiol.*, 156 (2005) 93.
21 L.E.J. Lee, S.J. Van Es, S.K. Walsh, D.J. Rainnie, N. Donay, R. Summerfield and R.J. Cawthorn, *J. Fish Dis.*, submitted for publication.
22 V.R. Dayeh, K. Schirmer and N.C. Bols, *Water Res.*, 36 (2002) 3727.
23 K. Schirmer, V.R. Dayeh, S.K. Bopp, S. Russold and N.C. Bols, *Toxicology*, 205 (2004) 211.

Chapter 19

Monitoring of chlorinated biphenyls and polycyclic aromatic hydrocarbons by passive sampling in concert with deployed mussels

Foppe Smedes

19.1 INTRODUCTION

Passive sampling has been used for more than a decade for the sampling of hydrophobic contaminants in water. Since 1990, the number of publications has increased exponentially each year. Huckins, Prest and co-workers first introduced the semi-permeable membrane devices (SPMDs), a polyethylene membrane filled with lipid (triolein) in 1990 [1–3]. Subsequently, several modifications have been introduced to improve the performance of the design and field use of SPMDs. One of these was the introduction of performance reference compounds (PRCs) used to correct for differences in uptake rate caused by locally different flow conditions, temperatures or biofouling. PRCs are spiked in the sampler before deployment and their release rate supplies information on the uptake rate, corrected for the local conditions [4,5]. Uptake rate has been optimised by increasing the ratio of surface area of polyethylene to mass of lipid. The increased mass of polyethylene makes a significant contribution to the uptake of pollutants. About half of the mass of compounds taken up are accumulated in the membrane [6]. The percentage of lipid in an SPMD was standardised to 20% [7]. For very hydrophobic contaminants polyethylene on its own behaves similar to that observed from the SPMD [4]. Basically, any material with a non-polar structure can function as a passive sampler (PS). In this monitoring programme, PSs made from polydimethylsiloxane (PDMS) sheets, better known as silicon rubber, were deployed. PDMS

Comprehensive Analytical Chemistry 48
R. Greenwood, G. Mills and B. Vrana (Editors)
Volume 48 ISSN: 0166-526X DOI: 10.1016/S0166-526X(06)48019-3

is also used for coating solid-phase microextraction (SPME) samplers [8] and stir bar sorptive extraction (SBSE) [9].

SPMDs have been widely used in passive sampling campaigns, and these have been reported in numerous publications. However, so far passive sampling has not been applied in routine monitoring. After several years of testing, the National Institute for Coastal and Marine Management included passive sampling in their monitoring programme. The trials revealed that silicone rubbers were excellent samplers that were strong, chemically resistant and robust in use. Only a few disadvantages are known. An additional theoretical reason for choosing silicone rubber as a sampler construction material is that for a single phase a single partition coefficient applies instead of two such as the lipid and polyethylene used in SPMDs. Furthermore, spiking with PRCs is easier and samplers can be reused. To investigate the validity of passive sampling the sampling was performed in concert with the existing ''mussel watch'' programme.

19.2 MONITORING

19.2.1 General

In The Netherlands a number of important European rivers enter the North Sea, often via an estuarine area. Contaminants are transported to downstream areas in variable quantities depending on the pollution level up stream and the river flow. Precipitation of particulate matter in the mixing zone with saline water causes the accumulation of particle bound contaminants in the estuaries of The Netherlands. Marine particulate matter is also deposited in the Dutch estuaries. Turbulence caused by storms and elevated river flows can result in re-suspension and transport of particulate matter to the North Sea. In general the precipitation is larger than the erosion. It is therefore necessary to dredge the waterways to maintain a sufficient depth for ships to pass. Low contaminated dredged material is deposited in the sea and material that causes a risk is collected in a special storage place. The particulate material entering the North Sea is slowly transported north by the Gulf Stream. Part of the material that is entering in the south North Sea is deposited in the Wadden Sea. The Wadden Sea is very shallow and, because of the numerous tidal flats, it is an important ecological area. Another important ecological area is the delta of Zeeland in the southernmost area of The Netherlands. This area is threatened by the Scheldt as well as the Rhine River. Intensive and

complex environmental policy is protecting the aqueous environment of The Netherlands. To support this, and to indicate the positive effects, a monitoring network has been installed. This includes all kinds of programmes for different parameters and matrices. One of those is the ''mussel watch'' programme.

19.2.2 History of musselwatch programme

The National Institute of Coastal and Marine Management (RIKZ) in The Netherlands has maintained a ''mussel watch'' programme since 1990. The intention of the programme was to follow the water quality for compounds that have a low solubility in the water phase, e.g., polychlorinated biphenyls (PCBs), polycylic aromatic hydrocarbons (PAHs) and heavy metals. Mussels were expected to accumulate these compounds during the deployment, and to provide a measure of the water quality integrated over time. Initially, the programme contained 17 stations that were measured three times a year, in winter, summer and autumn. Spring was omitted as this would include the spawning period which was considered to add an uncontrollable variation to the data. In two evaluation rounds the programme was reduced to eight stations with deployment in only winter and autumn [10]. The evaluations had shown that the time-integrating properties of the mussels were limited and in some cases elimination of contaminants occurred when compared with the levels before deployment. This indicated that the area where the mussels were collected had a higher level of contamination than some of the stations. This moved the programme towards trend monitoring, and the summer deployments showed such a large variation that acceptable trend detection was impossible. The stations monitored in the present programme are all situated in the central area of receiving water systems. Deployment directly in the water flows is not possible as the mussels (*Mytilus edulis*) do not survive at lower salinity. A description of sampling stations is given in Table 19.1 and their positions are shown in Fig. 19.1.

19.2.3 Passive samplers

Since 2001, PSs have been deployed in parallel with the mussels. PSs were made of silicone rubber PDMS sheeting to create a robust sampling system. PSs were expected to give a good reflection of the level for hydrophobic contaminants to which the mussels were exposed.

TABLE 19.1
Sampling stations descriptions

Station name	Description
Dantziggat	This station is situated in the middle of the Wadden Sea. The area is highly influenced by tidal movement resulting in frequent sedimentation and re-suspension.
Malzwin	Situated in the west part of the Wadden Sea. This part is under frequent influence of North Sea water entering the Wadden sea at high tide, followed by a return stream.
Slijkgat	This is the only station in the North Sea, although close to the coast. The station is influenced to a varying extent by the outflow of Rhine and Meuse water discharged from the Haringvliet Sluices.
Vlissingen	Station in the mouth of the Western Scheldt. Almost fully marine with influence of the Western Scheldt outflow.
Hansweert	Upstream in the Western Scheldt. Salinity is still sufficiently high for mussels to survive.
Bommenede	De Grevelingen is the largest marine water lake in Europe. Since it is a lake it has no tidal current. The station Bommenede is situated in the central part of De Grevelingen.
Wissekerke	The Eastern Scheldt is essentially a lagoon. It is connected to the North Sea by an open dam that can be closed when necessary because of a spring tide or storm. The station Wissekerke is situated on the west side not far from the dam.
Yerseke	This station is also situated in the Eastern Scheldt but in the eastern part. Several mussel farms are situated in the surrounding area.

Moreover, monitoring by PSs has some advantages over the use of living organisms:

- initial concentration of contaminants is negligible;
- PSs do not metabolise pollutants;
- are not mortal and can be deployed in all salinities;
- the uptake process is simple compared with that found in organisms.

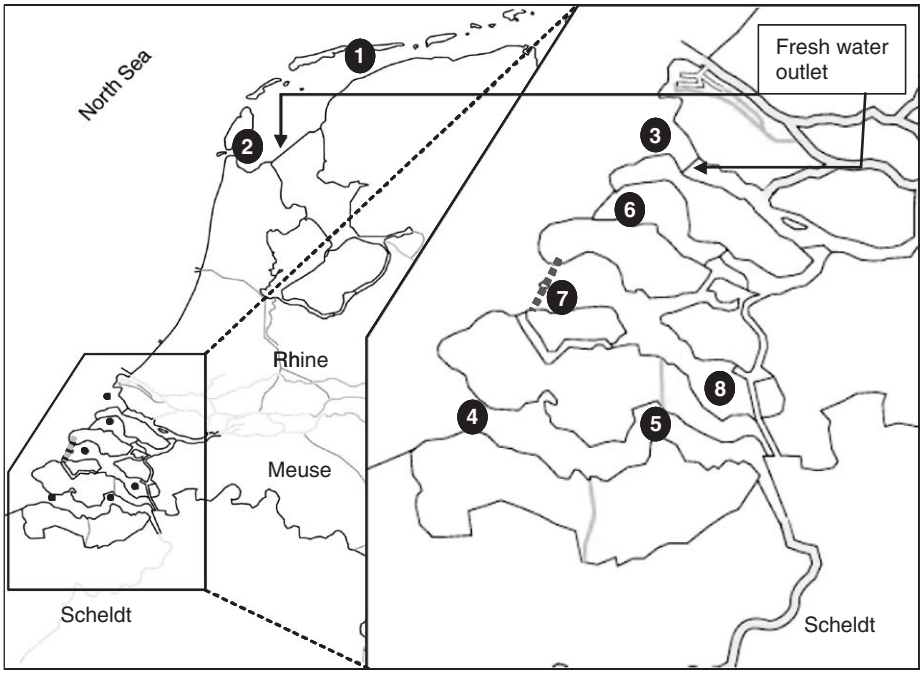

Fig. 19.1. Position of sampling stations in the marine waters of The Netherlands. For sampling site names and description see Table 19.1.

The contaminant uptake, or exchange, process of PSs has been widely investigated and can be better analytically quantified than for mussels. Organisms have several uptake/release routes and the exchange rate depends heavily on environmental variables such as temperature, food availability, stress factors, etc. which influence the activity of the mussels [11]. While PSs take up from only the freely dissolved phase, mussels may also take contaminants through feeding. However, in spite of the better-defined uptake of PSs, the field conditions also may have a considerable influence on the results. Temperature, hydrodynamic conditions and biofouling are factors that influence the uptake rate and may cause different concentrations in the sampler for equal contamination levels. The resulting variability may still be lower than data influenced by biological factors but much higher than common quality assurance targets for analytical variability. This is not an issue when applying PSs to compare heavily contaminated sites with reference areas, e.g., differences in contaminant level of a factor 10 or more. However, in the case of monitoring the quality of (marine) surface waters in order to detect changes in contaminant levels, e.g., as result of

measures to reduce pollution, it is of utmost importance to reduce variability to a minimum. This can be done in different ways:

- ''Isolate'' the sampler from external turbulences using an increased layer of stagnant water by installing a cover of a more or less hydrophilic material. Diffusion through this layer is then the uptake rate-limiting step [12,13]. A disadvantage is that the uptake rate is considerably reduced and consequently the detection limits will increase substantially. Moreover, a hydrophilic layer could also act as a substrate for biofouling more than a strongly hydrophobic surface.
- Another possibility is correcting for the influence of current and waves instead of regulating the uptake rate. This is performed through the use of PRCs that are spiked in the sampler and are released to the water phase by the same processes by which uptake occurs [4,5]. In that way the uptake is not limited and a maximum sensitivity is obtained.
- Booij *et al*. investigated a third method by mechanically rotating the sampler or creating a large flow that could overrule the differences in local hydrodynamic conditions [14]. Basically, this would be the ideal approach as a very high sampling rate is obtained giving high sensitivity and the influence of local flow conditions is strongly reduced if not excluded. Moreover, when using rotating or otherwise moving samplers the risk of biofouling also diminishes. However, the large amount of energy needed for such non-passive sampling approach is generally not available at sampling stations.

Thus, for correcting the influence of hydrodynamic conditions the use of PRCs is preferred over isolation. It allows a simpler sampler design and sample processing, and results in higher uptake, i.e., better sensitivity.

19.2.4 Objectives

Passive sampling in aquatic environments has been proposed as a promising technique since before 1990. The large amount of literature on passive sampling is mainly research orientated, and comprises data from one time/year and a few sites with special pollution histories. So far passive sampling has not been widely applied in routine water quality monitoring programmes. The objectives of the trial implementation of the passive sampling monitoring programme reported here were:

- to build experience and to optimise the procedure through ''learning by doing'';

- that application alongside mussels should validate the environmental relevance of the results obtained;
- to obtain practical data that allow evaluation of the suitability for routine monitoring.

In routine monitoring the methodology must be robust, repeatable and accompanied by a sufficient level of quality assurance. Over the years the sampler design has been adapted, extraction procedures have been improved and clean-up simplified. Several PRCs have been applied and evaluated.

Validation of passive sampling methods is not as straightforward as for classical analytical methods. Further a distinction must be drawn between analytical and environmental validation. For classical analyses of water usually only analytical validation is considered, meaning that a true concentration is determined with a known uncertainty. However, due to sorption of contaminants to, e.g. suspended matter, such a concentration does not necessarily reflect the (bio)available fraction. The conversion into an environmental risk is generally accompanied by a huge uncertainty and is hard to validate. A sound analytical procedure does not automatically mean that environmentally relevant data are obtained [16].

Passive sampling is a chain of actions and calculations using various constants (all with their uncertainty) that yields an estimate of the freely dissolved aqueous-phase concentration. From an analytical point of view this will end in a higher uncertainty than a classical analytical method. However, one should be aware that a more environmentally relevant result is obtained as the freely dissolved concentration is directly proportional to the environmental threat for that contaminant. Moreover, the concentration obtained reflects the exposure over a long period of time. Therefore, in a risk assessment the result of passive sampling is likely to provide a better reflection of the risk than that of a classical analysis of a total water sample. Validation of passive sampling using whole or filtered water analyses will always suffer from the inability to isolate the freely dissolved fraction, especially for hydrophobic compounds [15]. Testing different filtration systems revealed that part of the free dissolved fraction is affected by sorption to the filter material and contaminants bound to dissolved organic matter pass through the filter to a different extent depending on the extent of clogging of the filter [16]. Therefore, instead of trying to show agreement with large volume grab sampling followed by classical analyses, the validation of passive sampling would be better achieved by demonstrating that exposure concentrations experienced by organisms can be predicted sufficiently accurately.

19.3 METHODS

19.3.1 Materials

Silica chromatography powder (SiO_2), acetone, ethyl acetate, *n*-hexane, isooctane (Mallinckrodt Baker), methanol (Lab-Scan) aluminium oxide (Al_2O_3) (ICN Biomedicals, Boom BV, Meppel, The Netherlands) and C_{18}-silica (Bakerbond, 40 μm, PrepLCpacking) were all obtained from Boom BV, Meppel, The Netherlands. All standard compounds used were obtained from different manufacturers, all ordered through Boom BV, Meppel. A list of compounds and their abbreviations is given in the Glossary. Thimbles for Soxhlet extraction were from Schleicher & Schuell MicroScience GmbH (Dassel, Germany). Sampler frame and other materials were tailor-made by a local workshop. Translucent silicone rubber sheeting (0.5 mm) was obtained from Technirub Vizo (Zeewolde, The Netherlands).

19.3.2 Mussels

19.3.2.1 Deployment of mussels

Mussels were obtained from a local mussel farm in the Eastern Scheldt. They were selected from a set of the same age and shell length (typically 45–50 mm). The selected 1100 mussels were randomly distributed into 40 subsets of 25 mussels (4 times 25 mussels are used for one station). Two samples of 100 mussels were frozen immediately to determine the concentrations of pollutants in the test organisms before deployment. The other portions were placed in holding nets and kept in aerated North Sea water until transport for deployment. For all stations an extra set of 10 mussels was packed to replace any mussels that died before deployment. During transport, the live mussels were placed in an isolated box with cooling elements maintaining adequate distance between mussels and cooling elements. When the deployment was delayed, e.g., in case of unsuitable weather, the mussels were stored in aerated seawater. The deployment frames were constructed from 12 mm stainless steel rod capable of mounting four mussel cages (Fig. 19.3). A mussel cage consists of two baskets, each containing 25 mussels, which were both mounted on a disc as shown in Fig. 19.2. Two cages were mounted at the lower position of the large frame using screws and safety nuts. Frames were fixed to a buoy or to the chain of the buoy at about 2 m below water surface.

After a period of 6 weeks the mussels were recovered. Any visible fouling was removed from the mussels and any mortality was recorded.

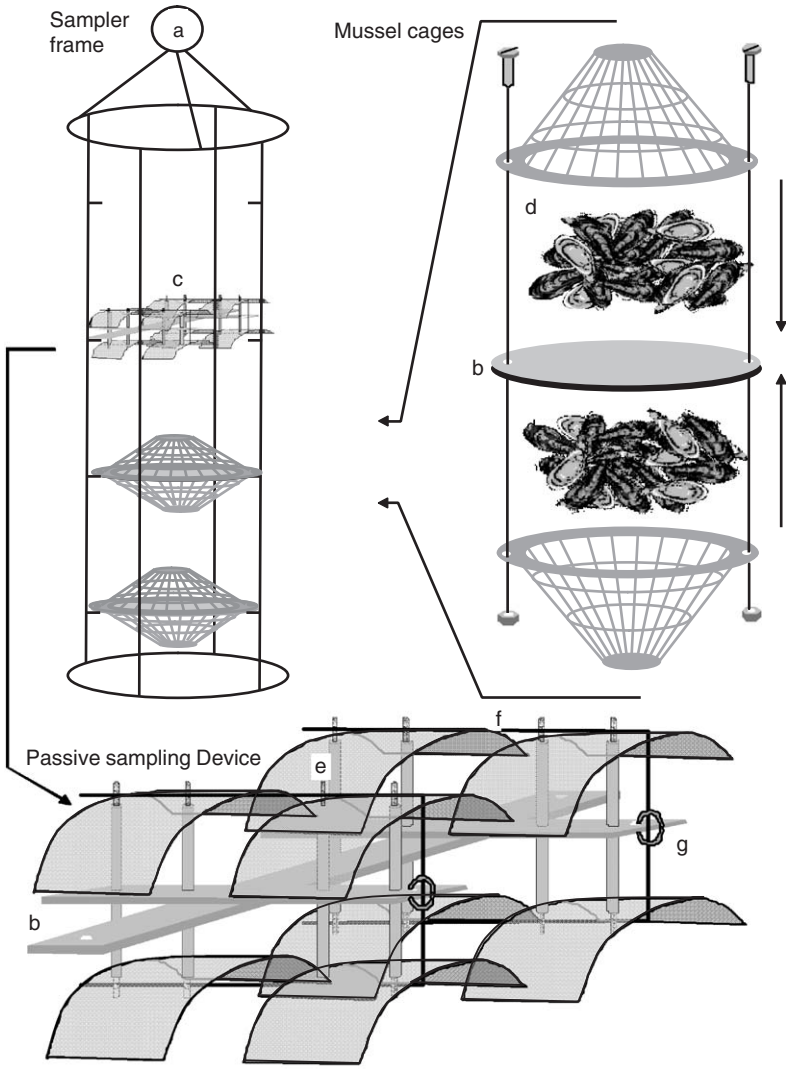

Fig. 19.2. Sampler frame for mussels and passive samplers. (a) fastening ring; (b) fixing eyes for and on samplers; (c) passive sampler; (d) mussels; (e) silicone rubber sheets; (f) U-shaped fixing rod; (g) cable strap, fixing the U-shaped fixing rod.

Dead mussels were not included in the sample. After collection the mussels were packed in bags, frozen immediately and transported to the laboratory. Until analysis, that usually took place within 6 weeks, samples were stored at -20°C. Water temperature was recorded at the start and end of the exposure.

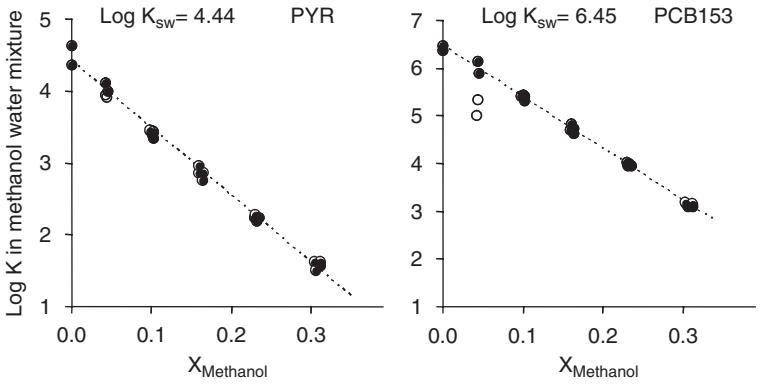

Fig. 19.3. Log K_{SW} ($L\,kg^{-1}$) versus the methanol content. Regression is used to estimate the log K_{SW} for pure water. Only closed symbols were used for regression.

19.3.2.2 Sample processing

Mussels were taken from the freezer and washed with Milli-Q water while still frozen. The shell length of each individual mussel was measured using a calliper. The average length and standard deviation were recorded. The adductor muscle was cut with a titanium knife, and during thawing the shells open and the mussels were placed with the internal surface facing downwards on a sheet of glass placed on a slight slope. In this way the water was drained from the soft tissue. The soft tissue was cut from the shell with the titanium knife and collected in a weighed glass beaker. The total mass and the number of mussels were used to calculate the average individual wet weight. A Büchi mixer (B400, Mettler-Toledo, Tiel, The Netherlands) equipped with ceramic knives was used to blend the combined mussel tissue to obtain a fully homogeneous sample. From this sample a sub-sample was taken for determination of dry weight (1 h at 105°C) and ash content (4 h at 450°C). The mussel tissue was freeze-dried and homogenised using a ball mill (Retsch PM-400, Ochten, The Netherlands). The dried tissue was stored at < -20°C.

For the extraction of lipids, chlorinated biphenyls (CBs) and PAHs separate subsamples were identically extracted. An aliquot (2 g) of dry mussel tissue was weighed in a pre-extracted glass fibre thimble and extracted in a ''hot'' Soxhlet [17] extractor for 8 h with acetone–hexane mixture (1:3 v/v) (50 mL) on a water bath. Prior to extraction, CB 29 (50 ng) and CB 155 (50 ng), or D12-perylene (100 ng) was added to the sample for CB or PAH analyses, respectively. The resulting extract was

evaporated in a modified Kuderna-Danish (KD) apparatus to 1 mL using a water bath (85°C). For determination of extractable lipid the extract was evaporated to dryness for 1 h at 105°C.

For CB analyses the sample extracts were cleaned up by elution with 25 mL *n*-hexane over a pre-eluted (30 mL *n*-hexane) column containing 1 g of SiO_2 (dried overnight at 180°C) and topped with 8 g Al_2O_3 (deactivated with 10% water). An aliquot of isooctane (1 mL) and 50 ng of CB 143 (internal standard for quantification) were added to the eluate. After this the extract was evaporated in a KD followed by blowing down with nitrogen to obtain a volume of 1 mL. An aliquot (2 μL) of this extract was analysed using a gas chromatograph fitted with electron capture detector (GC-ECD) equipped with an auto-sampler (Perkin-Elmer Autosystem, Wellesley, MA, USA). Hydrogen was used as carrier gas and for separation of CBs two columns were connected to the injection port; an SE-54 and a CPSil 19CB column, both 50 m × 0.15 mm; 0.22 μm film (Chrompack, Middelburg, The Netherlands). Detection was performed by ECD and data processing by using Turbochrom software (Perkin-Elmer, Wellesley, MA, USA).

An extract produced as above was used for PAH analysis and eluted through a pre-eluted (30 mL *n*-hexane) column containing 8 g Al_2O_3 (deactivated with 10% water) with 30 mL *n*-hexane. The eluate was evaporated using KD on a water bath (85°C) to less than 2 mL, an aliquot (10 mL) of acetonitrile and 1 μg of 2-methylchrysene (IS for quantification) were added. The *n*-hexane was removed by evaporation on a water bath (100°C) using acetonitrile as an azeotrope. The resulting acetonitrile solution was further evaporated to a volume of 1 mL with the assistance of a nitrogen flow in the final stage. The extract was analysed by HPLC (Model 1100, Agilent, Amstelveen, NL) using a methanol/water gradient on a Dionex Vydac 201TP54 HPLC column (4.6 mm × 25 cm, 5 μm C_{18} stationary phase). Two fluorescence detectors, Jasco FP920 (Jasco Benelux BV, IJsselstein, The Netherlands) were used in series running different sets of excitation and emission wavelengths. Data were processed as for GC.

19.3.3 Passive sampling

19.3.3.1 Deployment of passive samplers

The silicone rubber sheeting (1 m wide and several meters long with 0.5 mm thickness) was washed with water and soap, cut into pieces. Holes for fixing were made using a perforator. In the first design (not shown) the sheets were stretched over hooks in the sampler. However,

because of the vigorous hydrodynamic conditions in the marine environment samplers were torn and sometimes lost. Although with another more robust fixing system sheets occasionally broke loose on one side but were not lost as they remained fixed on one side. Therefore, in the next generation of samplers sheets were fixed only in the middle as shown in Fig. 19.2. Sheets were made shorter to prevent them from folding double but at the same time more sheets could be mounted on a given frame. In total, eight sheets of 9.5 cm × 5.5 cm (104 cm^2) were used in each sampler. This last design has been used for the last 3 years of monitoring.

Prior to deployment, sheets were pre-extracted to remove any uncrosslinked oligomers that could interfere with later analyses. Initially, this was done by Soxhlet extraction with acetone/*n*-hexane (1:3 v/v). Later it was found that ethyl acetate was more efficient, while the swelling was much less. Silicone rubber can take up *n*-hexane to about twice its volume and is very vulnerable in that condition. Soxhlet extraction with ethyl acetate for 100 h ensured that the silicone rubber did not release any oligomers in the analytical process.

At least 100 pre-extracted sheets were placed in a 2-L-wide-mouth dark glass bottle and washed twice with methanol (300 mL) to remove the ethyl acetate (in the cases where *n*-hexane was used in the extraction, the methanol washing was preceded by a rinse with acetone (300 mL)). An aliquot (300 mL) of methanol and a spike solution containing the PRCs were added to the washed sheets [18]. After shaking for 1 h, an aliquot (60 mL) of water was added followed by another 250 mL after 4 h of shaking. This mixture was shaken overnight after which water (400 mL) was added to reach a final methanol concentration of 30%. Shaking then continued for a further 24 h. Samplers were stored in this condition at room temperature until deployment or analysis.

Sheets from only a single batch of spiking were used and at least eight were stored for reference. Not more than 1 week before deployment nine samplers were prepared with eight sheets each. Samplers were placed in a stainless steel container, the lid was taped down, the container packed in a double polyethylene bag and kept in the freezer or frozen condition continuously except during deployment. One container remained in the freezer and eight containers were sent to be deployed. For the deployment the samplers were mounted above the mussels in the sampler frame as illustrated in Fig. 19.3. After exposure samples were packed again, returned to the laboratory and extracted within 1 week.

19.3.3.2 Processing of passive samplers

After deployment samplers were unpacked and from the eight sheets, two composite analytical samples of four sheets (~400 cm^2) were provided by combining the extracts of the four sheets. Sheets were cleaned with water and dabbed dry with a tissue. The sheets were ''hot'' Soxhlet extracted for 8 h with acetone–*n*-hexane (1:3 v/v) (60 mL). The sheets swelled markedly, and therefore the volume of the sheets did not take up more than 25% of the volume in the Soxhlet extractor. The extract was concentrated by KD to less than 2 mL and quantitatively transferred to a column with 2 g Al_2O_3 (deactivated with 10% water) that was pre-eluted with *n*-hexane (25 mL). The compounds were eluted with *n*-hexane (25 mL). After KD evaporation down to 1 mL, acetonitrile (10 mL) was added, followed by KD evaporation down to 1 mL. This extract was loaded on a column containing 300 mg C_{18} modified SiO_2 that was pre-rinsed with acetonitrile (5 mL). After transfer of the extract to the column, it was eluted with acetonitrile (5 mL) and the eluate was KD evaporated to 1 mL. Then CB 143 (50 ng) and 2-methylchrysene (1 μg) were added. After this the extract was split by taking 300 μL for analyses of PAHs by HPLC with fluorescence detection, as described for mussel analysis. To the remaining portion, *n*-hexane (10 mL) was added and then reduced by KD evaporation to a volume of 1 mL to complete the transfer back to *n*-hexane. This extract was further purified using a column containing 2 g SiO_2. After pre-elution with *n*-hexane (25 mL) the extract was transferred to the column and eluted with *n*-hexane (25 mL). Subsequently, isooctane (1 mL) was added and the extract was KD evaporated to less than 2 mL. Using a nitrogen flow the extract was further concentrated to 0.5 mL in which CBs were analysed by GC–ECD as described for the mussel analysis.

19.3.4 QA data

Several factors influence variability and uncertainty:

- analytical process,
- sampling,
- natural variability of mussels,
- accuracy of partition coefficients,
- correction procedure for external factors influencing the sampling rate.

The first three points are more of analytical aspects and are discussed in this section. Other aspects are more related to the interpretation of

TABLE 19.2
Quality assurance data from mussel and passive samplers (PS)

Par	Mussel RM (CB $n = 37$, PAH $n = 26$)				Passive sampling duplicates		
	DL	S_A	CV	CV-S	DL	S_A (n)	CV (n)
Phenanthrene	3	[4]	8	3	3	Nd	7 (84)
Anthracene	1	0.2	[33]	7	1	0.7 (40)	14 (36)
Fluoranthene	3	[4]	6	2	3	nd	6 (84)
Pyrene	3	[2]	6	1	3	nd	6 (84)
Benz(a)anthracene	3	0.8	[28]	4	3	0.9 (22)	7 (60)
Chrysene	3	1.1	[16]	4	3	0.6 (4)	7 (76)
Benz(e)pyrene	3	1.1	[11]	5	3	1.0 (32)	8 (48)
Benz(b)fluoranthene	3	0.8	[12]	5	3	0.8 (22)	7 (56)
Benz(k)flyoranthene	4	0.4	[15]	6	4	1.7 (84)	nd
Benzo(a)pyrene	3	0.6	[60]	5	3	0.4 (66)	8 (10)
Benz(ghi)perylene	3	0.5	[14]	7	3	1.2 (84)	nd
Dibenz(ah)anthracene	3	0.4	[65]	8	3	0.3 (86)	nd
Indeno(1,2,−c,d)pyrene	3	0.5	[21]	8	3	1.0 (86)	nd
Hexachlorobenzene	0.2	0.04	[11]	10	0.3	0.1 (8)	10 (76)
CB 18	0.4	0.1	[26]	11	0.3	0.1 (30)	14 (54)
CB 28	0.3	0.2	[26]	5	0.3	0.2 (12)	7 (70)
CB 31	0.3	0.2	[23]	3	0.3	0.2 (20)	8 (62)
CB 44	0.2	[0.2]	8	10	0.3	0.1 (22)	9 (58)

CB 49	0.4	[0.6]	28	3	1.3	0.4 (54)	10 (30)
CB 52	0.2	[0.2]	12	4	0.2	0.03 (4)	6 (62)
CB 101	0.1	[0.5]	6	3	0.2	0.1 (6)	9 (74)
CB 105	0.1	[0.1]	8	3	0.2	0.1 (60)	5 (14)
CB 118	0.1	[0.4]	6	3	0.2	0.1 (22)	7 (62)
CB 138	0.1	[1.1]	8	3	0.2	0.1 (20)	7 (62)
CB 153	0.1	[1.1]	5	2	0.2	0.03 (4)	8 (80)
CB 156					0.2	0.03 (68)	nd
CB 170	0.1	0.03	[11]	16	0.2	0.1 (64)	6 (12)
CB 180	0.1	[0.1]	9	6	0.2	0.06 (52)	10 (28)
CB 187	0.1	[0.5]	7	4	0.2	0.05 (40)	8 (34)
Anthracene-D10					1	0.6 (72)	9 (6)
Fluoranthene-D10					3	3 (6)	9 (16)
Pyrene-D10					3	nd	6 (48)
Chrysene-D12					3	nd	5 (84)
Perylene-D12-					3	nd	7 (84)
Coronene-D12					6	nd	5 (48)
CB 4					2	3 (24)	8 (10)
CB 29					0.2	nd	6 (68)
CB 155					0.2	nd	5 (68)
CB 204					1.2	nd	3 (84)

Mussel data are from the period of 1999–2004. Standard deviation (S_A) is calculated from data less than 10 times DL and the CV from data higher than 10 times DL. Results for mussels from data outside that range are also given and are identified by square brackets. S_A and DL for mussel in μg kg^{-1} dw and for PS in ng per sampler (12 g and 400 cm^2 surface area). CV-*S* is within-batch variability. See text for further explanation and Table 19.5 for full compound names.

data and are discussed later (Section 19.4.2) based on the analytical variability estimated here.

19.3.4.1 Mussels

Mussel analyses were performed in batches that contain 6–15 samples, a blank, a standard solution for testing the recovery efficiency of the procedure, a reference sample and a duplicate from another batch. The yield of the recovery internal standards added to each individual sample before analysis is used as an indicator of whether the analytical process was performed correctly for an individual sample. Typical recoveries in samples are 99% ($\pm$4%) for CB 29, 97% ($\pm$4%) for CB 155 and 98% ($\pm$6%) for D12-perylene. From standard solutions processed and analysed as samples an average recovery of 95% ($\pm$5%) was measured for CBs as well as PAHs. It should be noted that for anthracene, benzo(a)pyrene and the D12-perylene the recovery from standard solutions was always the lowest and sometimes below 80%. It is suspected that this is an effect of photo-decomposition and occurs only when no light-absorbing matrix is present. This was supported by the observation that the recovery of D12-perylene from standard solutions is 88% ($\pm$8%) while for samples 98% ($\pm$6%) is found. The final analytical variability for the individual parameters was calculated from the repeated analyses of the reference sample. Detection limits (DL) are defined as three times the variability of long-term blank levels and subsequently rounded upward (Table 19.2). Analytical variability is calculated as standard deviation (S_A) for compounds with a concentration level less than 10 times the detection limit and as coefficient of variation (CV) when the average exceeded the level of 10 times detection limit. The results are listed in Table 19.2. In order to complete the information, CV was also calculated for values less than 10 times DL, and S_A for values higher than 10 times DL. These data are given in square brackets. For several higher PAHs S_A values lower than 1/3 of the DL are found, and this indicates that the DL is set at a conservative level for those compounds. When values are above 10 times DL the CV ranges from 5 to 9%, with the exception of CB 49 and CB 52.

19.3.4.2 Passive sampling, analytical aspects

The QA for passive sampling is still in development. It is evident that the analytical variability of the actual analysis of the sampler is equal or better than that associated with matrices like mussel or sediment. Often better, because the sampler has a constant composition and

consequently constant sorption properties. Furthermore, the sampling approach already includes an extraction step performed in the field and therefore the final extract contains only a minimal amount of matrix, where biotic samples contain large and sometimes variable amounts of lipids. The analytical QA for passive sampling is focused on blanks and duplicate samplings. From duplicates analyses of reference samplers stored in the freezer, differences of the PRCs were occasionally higher than could be explained solely by analytical variation. At the same time the ratios between the individual PRCs were remarkably constant. Initially it was feared that this was due to variation in sorption properties of the silicon rubber material but later it was concluded that this was due to swelling of the material with the extraction solvent and that this hindered the solvent flow in the Soxhlet extractor in some individual cases. In later samplings measures were taken to prevent this. A step to reduce the effect of this problem was to normalise all results using the CB 204 content. This is possible as CB 204 does not significantly deplete. Analytically there is no interference from any co-eluting compounds for CB 204 in the GC analyses as compounds with equal hydrophobicity are present in the water phase at very low concentrations and consequently only a small amount will be taken up by the PSs. The procedure, using CB 204 as internal standard was continued even after the extraction problems were solved.

The blanks were used to set the DL listed in Table 19.2 for passive sampling. The duplicate results that are less than 10 times the detection limit are used to calculate the absolute standard deviation (S_A) using

$$S_A = \sqrt{\frac{\sum (N_1 - N_2)^2}{2k}} \tag{19.1}$$

where N_1 and N_2 are the duplicates and k the number of duplicates. Similarly the results higher than 10 times DL are used to calculate the CV (%) from the relative difference between the duplicate results:

$$\mathrm{CV} = \sqrt{\frac{\sum \left[(N_1 - N_2)/(N_{\mathrm{avg}})\right]^2}{2k}} \tag{19.2}$$

In the equation, N_{avg} is the average of the duplicate samples.

The S_A values for passive sampling agree well with what would be expected from the DL. Furthermore the CVs are very similar to those calculated for the reference mussel tissue. It should be noted that this variability for passive sampling also includes the sampling repeatability.

For the PRCs spiked to the samplers similar CVs were observed. Only CB 204 stands out because of its low value of 3%.

19.3.4.3 Representivity of mussel samples

Mussels are living material with natural variation. For an accurate average a certain number of mussels is required. When deploying the mussels two samples of 100 mussels are kept in the freezer as a representation of the starting situation. These are both analysed and the duplicate results allow the calculation of a CV-S using Eq. (19.2). The resulting CV-S (see Table 19.2) comprises the representivity and the analytical variation. A lower value for CV-S than the CV for the reference material is explained by the fact that here only the within-batch variability is involved which is apparently substantially lower than the long-term variability. It can be concluded that sample variability using 100 mussels does not contribute to the overall variability.

19.3.5 Partition coefficients

The sampler/water partition coefficients K_{SW} are the driving force for the uptake of compounds by PSs. The K_{SW} describes the relation between the concentrations in the sampler (C_S) and the water phase (C_W) at equilibrium:

$$K_{SW} = \frac{C_S}{C_W} \tag{19.3}$$

Determination of K_{SW} for highly hydrophobic compounds is easily biased through the overestimation of the concentrations in the water phase. The strong sorption of these compounds to any material like suspended particulate matter (SPM), stirring bars, wall of containers, etc., causes an overestimation of the concentration in the water phase when included in the analysis. To exclude these factors the determination of the K_{SW} was performed using the co-solvent approach [19,20]. Compounds are equilibrated with samplers in a range of water–methanol solutions. The presence of methanol reduces the K_{SW} and subsequently sorption to any solid-phase. Since the log K_{SW} is inversely related to the mole fraction methanol extrapolation to a pure water situation is possible. Briefly, solutions from 0 to 50% methanol in steps of 10% are equilibrated with a sampler spiked with the target compounds by shaking. After 20 days, sampler and aqueous phase are extracted with n-pentane or n-hexane and the extracts analysed. Where necessary, samples are diluted with water to reduce the methanol

TABLE 19.3
Applied log K_{SW} values in $L\,kg^{-1}$

Name	Log K_{SW}	Name	Log K_{SW}	Name	Log K_{SW}
HCB	4.87	CB 18	4.99	Ant-D10	3.95
		CB 28	5.22	Flu-D10	4.33
Phen	3.89	CB 31	5.23	Pyr-D10	4.39
Ant	4.00	CB 44	5.56	Chr-D12	4.91
Flu	4.38	CB 49	5.66	Pe-D12	5.38
Pyr	4.44	CB 52	5.57	Cor-D12	6.35
BaA	5.06	CB 101	6.03		
Chr	4.97	CB 105	6.17	CB 4	4.38
BeP	5.45	CB 118	6.20	CB 29	5.18
BaP	5.52	CB 138	6.53	CB 155	6.67
BbF	5.51	CB 153	6.45	CB 204	7.46
BkF	5.51	CB 156	6.58		
BghiP	5.92	CB 170	6.90		
DbahA	6.04	CB 180	6.84		
InP	5.99	CB 187	6.77		

See Glossary for full compound names.

content to 25% prior to extraction. Results are used to calculate the K_{SW} and the log K_{SW} is plotted versus the methanol content. Using linear regression the intercept (the value corresponding to pure water) is determined. To increase the precision multiple equilibrations are performed. In Fig. 19.3, two examples of the results with applied regression are given for pyrene and CB 153. The open symbols are data that could be affected by SPM and were not included in the regression. For all compounds such a graph is constructed and a log K_{SW} is calculated. The K_{SW} values are given in Table 19.3.

19.4 DATA HANDLING AND CALCULATION

19.4.1 Mussels

The concentrations in the mussels were expressed as $\mu g\ kg^{-1}$ dry weight. Lipid contents were used to calculate lipid-based concentrations. Knowing the starting concentration in the deployed mussels the uptake can be calculated taking into account the growth of the mussels during deployment.

19.4.2 Calculation of sampling rate

The sampling rate can be calculated from the release of the PRCs that were spiked on the sampler before exposure [4]. The release of compounds from the PS follows:

$$N^t = N^0 \cdot \mathrm{e}^{-k_e t} \tag{19.4}$$

where N^0 is the mass of PRC measured in reference samplers that were not deployed, N^t is the mass of PRC remaining in the PS after deployment, k_e (day^{-1}) is the first-order dissipation constant that rules the release process and t is the sampling time (days). After rewriting k_e is calculated from

$$k_e = -\frac{\ln(N^t/N^0)}{t} \tag{19.5}$$

From Eq. (19.5), the mass of the sampler (m) (kg) and the K_{SW} ($\mathrm{kg\,L^{-1}}$), the sampling rate R_S ($\mathrm{L\,day^{-1}}$) is calculated through

$$R_S = k_e\, m\, K_{SW} = -\frac{\ln(N^t/N^0)}{t} m\, K_{SW} \tag{19.6}$$

For calculation of the R_S the measured values for the PRCs are normalised to CB 204 to reduce the variability due to analysis and differences between individual samplers.

19.4.3 Analytical precision of sampling rate

As multiple values for R_S are obtained from the different PRCs used these values were merged to give the best estimate of the sampling rate. However, this should apply only to the R_S values that have adequate precision. Assessing the error that can occur in R_S it can be noted that contribution of t and m will be negligible (Eq. (19.6)). The uncertainty in K_{SW} will be directly reflected in R_S and will introduce a systematic error that contributes to the uncertainty but will not influence the variability. In other words it does not affect relative comparisons of data. Thus, the major variability arises from the ratio of N^t and N^0. It must be noted that there is no suitable mathematical solution known to propagate the errors in the individual results in order to express the error in R_S. An estimate of the precision in R_S was therefore deduced only for the ratio of N^t and N^0. This ratio ranges from 0 to 1 and implies that $-\ln(N^t/N^0)$ ranges from ∞ to 0, which are both irrelevant solutions. To calculate a measure for the significance of $-\ln(N^t/N^0)$ it is rewritten to $+\ln(N^0/N^t)$ for mathematical convenience. This factor

N^0/N^t is 1 if no depletion occurs and increases to ∞ for total depletion of PRCs. Consequently ln (N^0/N^t) equals 0 without depletion and rises with increasing release of PRC. Therefore the significance of the extent N^0/N^t is moving away from 1 is a measure for reliability of ln (N^0/N^t). At the other limit N^t will approach the detection limit and the variability of N^0/N^t will increase dramatically. It will result in a large but non-significant number for N^0/N^t. The CV of $(N^0/N^t - 1)$ was selected as a parameter to assess the quality of the R_S measurement from analytical perspective. This CV for $(N^0/N^t - 1)$ is calculated by summing the variances of the error components:

$$\mathrm{CV}_{(N^0/N^t-1)} = \frac{N^0/N^t\sqrt{(S/N_t)^2 + \mathrm{CV}_{N^t}^2 + (S/N_0)^2 + \mathrm{CV}_{N^0}^2}}{(N^0/N^t - 1)} \tag{19.7}$$

where S is the absolute component of the error, dominating close to the DL, and CV the relative component dominating at higher values. However, because S is not known for most of the PRCs the numeric value of DL was used instead. The values DL and CV were taken from Table 19.2 and apply for N^0 as well as N^t. In practice only those R_S values for which the result from Eq. (19.7) was lower than 0.2 (20%) were used.

Both error profiles are plotted as a function of N^t for a hypothetical PRC with a spike level of ''1'' in Fig. 19.4. The right-hand graph indicates the importance of sufficiently low CV. Where the measuring error exceeded 12% no values would meet the criteria. The left-hand graph shows how better sensitivity extends the range where the precision meets the assessment criterion of 0.2. When the detection limit is

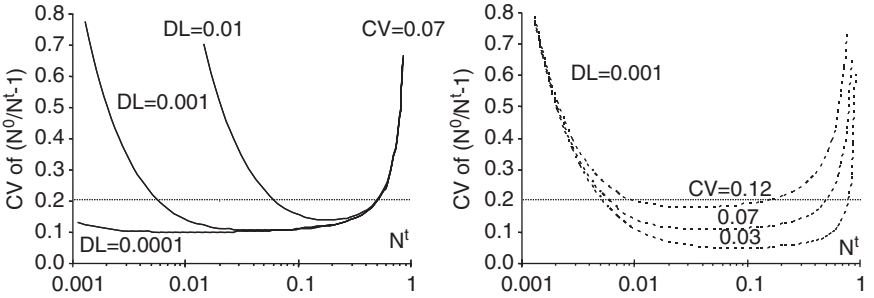

Fig. 19.4. Error profiles for $(N^0/N^t - 1)$ versus N^t. Left graph shows the dependence on the DL and the right graph the CV of the measurement. The horizontal line at 0.2 (20%) indicates the assessment criteria for use or not use of the corresponding R_S.

10 times lower the range extends by almost a full order of magnitude. An effect similar to that observed with reduced DL can be achieved by increasing the amount of PRC spiked. The maximum amount of PRCs that can be added is governed by the linear range of the analytical method, but environmental factors should also be considered as the PRCs will deplete to the environment. During the monitoring programme, the number of PRCs used was increased, and higher concentrations were spiked. Thus as the programme continued, more PRCs fell more frequently in the application range.

19.4.4 Artefacts in sampling rates

In addition to inaccurate analytical performance, sample properties and sampling processes may also affect the reliability of the estimates of sampling rate. As for internal standards used in analytical chemistry, it is important that PRCs do not occur in environmental samples. In the left-hand graph in Fig. 19.5 the R_S calculated for D10-fluoranthene is plotted versus the one for D10-pyrene. The bubble diameter represents the amount of pyrene that was collected by the sampler. The majority of the R_S values show an excellent agreement with a slope not distinguishable from 1. However, the R_S values from samplers where the pyrene levels, and all other PAHs, are rather high show a much lower R_S for D10-pyrene. A likely explanation is that the D10-pyrene

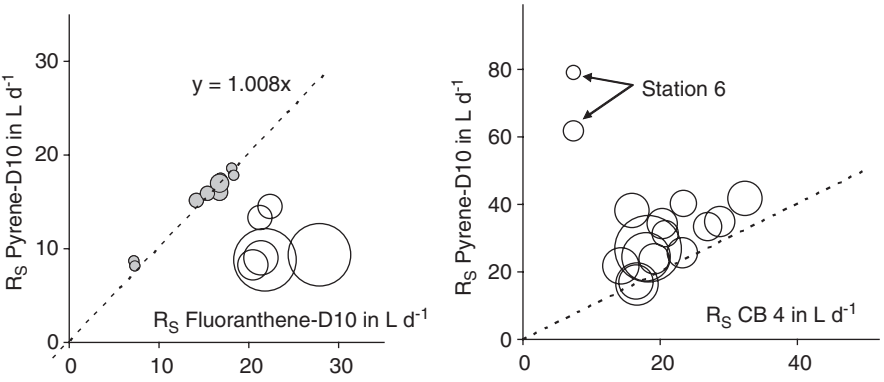

Fig. 19.5. Relation between sampling rates calculated from different PRCs. The left-hand graph shows the R_S of Pyr-D10 versus that of Flu-D10 (L day^{-1}). The bubble diameter represents the pyrene content on the sampler. The regression line applies only to the grey shaded bubbles. In the right graph the R_S from Pe-D12 is plotted versus that from CB 4. The bubble diameter is the CV for (N^0/N^t–1). Data from Winter 2005.

signal was elevated by co-eluting compounds. This can be partly explained by the area from which the samples came; stations 3, 4 and 5 are directly influenced by Western Scheldt, Meuse and Rhine rivers. A further factor is that a high sampling rate gives a high uptake that coincides with a large dissipation of PRCs. For D10-fluoranthene 5% or less was retained. So if analytes are at high level the PRCs are at low level. This increases the chance that interferences elevate the signal for the PRC and lead to anomalously low R_S values that will pass the assessment described in the previous section. There is no simple objective way to detect these anomalies, except parallel exposure of unspiked samplers. Questionable values may be found by plotting and comparing R_S values. A further warning sign is the existence of a positive relationship between a contaminant and a PRC. The influence of interferences can be reduced by (1) increasing the spike level of the PRCs, (2) use of slower samplers (made of thicker silicone rubber) that will dissipate less during the same sampling period and (3) increasing the selectivity. With respect to the latter more selectivity may be obtained by GC–MS. The HPLC-fluorescence method used here is well applicable for the parent PAHs but has limited selectivity.

In some cases unexpected high values for R_S can be observed for other reasons. This is the case for D12-perylene. In the right-hand graph of Fig. 19.5 the R_S calculated from D12-perylene is plotted versus that from CB 4. The bubble diameter represents the assessment parameter (4.3) for D12-perylene and in fact most do not comply ($CV > 0.2$), explaining the larger variation. However, the duplicate samples from station 6 amply comply with this criterion but are way out of range. Outlying high R_S values for D12-perylene were observed at station 6 for each sampling. Smaller deviations occasionally occurred at some other sampling stations. Station 6 is a salt water lake where sampling rate is up to four times lower than in other stations. In addition, the biological activity at this station is likely to be very high as the growth of the mussels is higher than at any other station. A possible explanation is that biodegradation at the surface of the sampler causes this effect. If bacteria live at the surface of the sampler they may be able to receive the compounds without a rate-limiting diffusion through the water phase. Normally it only replaces the diffusion process to the outside of the bacteria but if degradation occurs this does not apply. Clearly the disappearance was not caused by analytical error. For the last two samplings the outlying data were confirmed by GC–MS analyses.

19.4.5 Results for R_S

The findings above support the necessity for including several PRCs for both analytical reasons, to improve the reliability of the R_S values and backup for unexpected environmental processes. During the monitoring programme, the number of PRCs used was increased, and higher concentrations were spiked. Thus as the programme continued, more PRCs fell more frequently in the application range. The target set described above does not apply for the first 2 years of sampling where only few PRCs were applied and at relatively low concentrations. For those years the assessment criteria were less stringently applied to allow the inclusion of more data.

The variability of R_S values obtained through the different PRCs were in good agreement with the proposed assessment target of 20% and consequently are not distinguishable. As far as the variability allows there is slight tendency for R_S to increase for more hydrophobic compounds. To confirm this measurements are required over a larger K_{OW} range. Nevertheless, for this work a single R_S value was taken for calculation of the sampler equilibrium concentration and the free dissolved concentration in the water phase. Because of the unpredictable nature of interferences the median of the values that applied to the, some times adjusted, assessment targets were used.

The resulting median R_S values are plotted versus time in Fig. 19.6. Although there is some crossing over of the lines the general profile is that the estimated sampling rate is higher in autumn than in winter and this is especially clear for the last years where the reliability of the measurements increased. The difference is, however, not very large, 20–30% on average, and only significant because it occurs at all stations simultaneously. Obviously in winter the water temperature is lower as is shown in the right-hand graph. Lower temperature leads to a decrease of the first-order rate constant k_e [14] and an increase in the K_{SW} which may partly offset each other. The k_e is determined in situ by using the PRCs and a decrease, already taken into account, in the sampling rates in winter. The 30% decrease of R_S for 10°C temperature change is in agreement with the observations by Booij *et al.* [21] who found a 100% increase in R_S with a 30°C increase in temperature for silicon rubber. For SPMDs a twofold increase was reported for a 10°C rise in temperature [6].

Other variables are the flow regime, SPM content and salinity (Fig. 19.6). Generally in winter there is a higher fresh water flow which at some stations lowers the salinity considerably (station 5 and to a

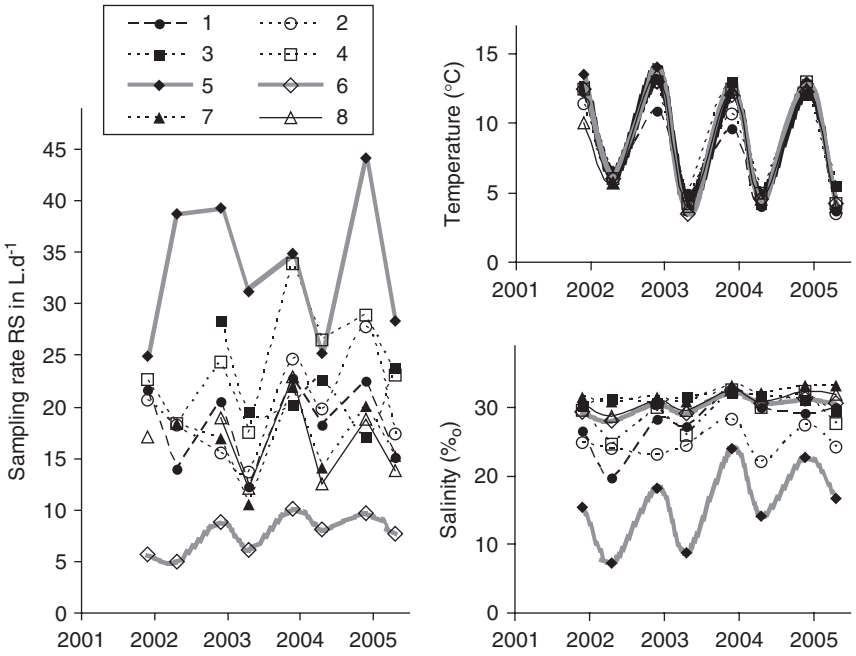

Fig. 19.6. Seasonal variation of median sampling rates, temperature and salinity for different stations.

lesser extent 1, 2 and 4). All of these factors may influence the R_S. At this stage it was assumed that these factors are accounted for by applying PRCs, and no further attempt was made to correct any of these variables. Furthermore, a correction of K_{SW} has not been considered to date and this parameter has not been observed to be influenced consistently by temperature [14]. It is reasonable to use uncorrected data when comparisons are being made with uptake by mussels since this may be affected in a similar way by the variables described above.

19.4.6 Passive sampling and aqueous concentrations

For estimation of the freely dissolved concentration (C_W) in the water phase the full uptake model that is valid for equilibrium and non-equilibrium situations is applied. The uptake is described by the following equation that includes the sampling rate (R_S):

$$N^t = N^\infty \left(1 - e^{-\frac{R_S t}{m K_{SW}}}\right) \tag{19.8}$$

Here N^t is the amount of compound in the sampler after deployment for time t and corrected using the internal standard CB 204. R_S is the sampling rate and N^∞ is the final amount taken up in the equilibrium situation. N^∞ can essentially be estimated from Eq. (19.8) when R_S and K_{SW} are known. Using the mass of the sampler the equilibrium concentration in the sampler C_S^∞ can be calculated, and consequently C_W can be determined using Eq. (19.3):

$$C_S^\infty = \frac{N^\infty}{m} = C_W K_{SW} \quad \text{that gives} \quad C_W = \frac{N^\infty}{K_{SW}\, m} \tag{19.9}$$

Combining Eqs. (19.8) and (19.9) the concentration in water (C_W) is given by

$$C_W = \frac{N^t}{mK_{SW}} \frac{1}{1 - e^{\left(-\frac{R_S t}{mK_{SW}}\right)}} \tag{19.10}$$

The last term is important only when equilibrium is not reached. In the exponent $R_S t$ is the number of sampled litres and mK_{SW} the ''volume'' of the sampler. When that ratio ($R_S t/mK_{SW}$) exceeds 2.4 equilibrium is approached within 10%. When R_S is 10 or 40 L day^{-1} equilibrium is obtained up to $K_{SW} = 4.1$ or 4.7, respectively.

The R_S values used were the median from the different PRCs added using the criteria and observations described above. For this work a single R_S value was taken for calculation of the freely dissolved concentration (C_W) in the water phase.

19.5 RESULTS AND DISCUSSION

19.5.1 Concentrations in water and mussels

For all target compounds concentrations could be determined in mussels and PSs. Most compounds were well above DL in the majority of the samplings. For mussels lower CBs are mostly below the detection limit and while in PS they are generally easily detected. Higher PAHs are regularly close to the DL for mussels as well as for PS. At station 6 where the sampling rate was about four times lower than that at most other stations the results for these compounds were more often close to or below DL. To give an impression of the concentrations obtained, the 10% and 90% percentile of C_M and C_W are listed in Table 19.4. The relative range for mussel and PS are in reasonable agreement and are not skewed by to many values below DL (CB 18). An exception is

TABLE 19.4
Concentration ranges and BAF values for a set of organic pollutants

Compound	C_M (μg kg^{-1})		C_W (pg L^{-1})		Log K_{OW}[c]	Log BAF[d]	s	n[e]
	Low[a]	High[b]	Low[a]	High[b]				
Phen	15	36	962	8001	4.57	3.92	0.26	60
Ant	1	5	62	168	4.54	4.50	0.28	34
Flu	32	100	1379	4476	5.22	4.42	0.14	60
Pyr	24	138	811	3289	5.18	4.49	0.12	60
BaA	5	34	45	214	5.91	5.15	0.17	46
Chr	9	40	66	229	5.86	5.14	0.20	56
BeP	11	78	39	162	6.04	5.58	0.16	58
BbF	11	55	50	118	5.80	5.51	0.23	58
BkF	5	19	16	42	6.00	5.66	0.18	35
BaP	4	24	7	38	6.04	5.79	0.20	38
BghiPe	6	28	8	23	6.50	6.01	0.20	49
DBahA	3	7	1	4	6.75	(6.21)[f]	0.22	16
InP	4	17	6	14	6.50	6.06	0.23	34
HCB	0.3	1	9	29	5.50	4.41	0.15	20
CB 18	0.4	2	4	46	5.24	4.53	0.32	11
CB 28	0.4	2	8	28	5.67	4.84	0.18	31
CB 31	0.3	2	6	20	5.67	4.90	0.21	16
CB 44	1	5	4	34	5.75	5.14	0.12	49
CB 49	2	8	4	51	5.85	5.25	0.16	26[g]
CB 52	1	11	8	76	5.84	5.18	0.16	60
CB 101	7	27	7	54	6.38	5.84	0.16	60
CB 105	1	4	1	4	6.65	5.99	0.15	60
CB 118	5	16	4	17	6.74	6.05	0.12	60
CB 138	13	40	4	24	6.83	6.36	0.15	60
CB 153	22	58	8	39	6.92	6.36	0.14	60
CB 170	0.3	2	0.4	3	7.27	5.89	0.13	37[g]
CB 180	1	7	1	6	7.36	6.16	0.15	59
CB 187	8	19	2	6	7.17	6.60	0.15	54[g]

[a]Low means 10% percentile.
[b]High means 90% percentile.
[c]K_{OW} values as collected by Booij *et al.* [25]
[d]Only data twice the detection limit were used.
[e]Less than 60 datapoints generally means that other data are below twice DL.
[f]Also data lower than twice DL were used to calculate the BAF for DBahA.
[g]CB 49, CB 170 and CB 187 were not always analysed.

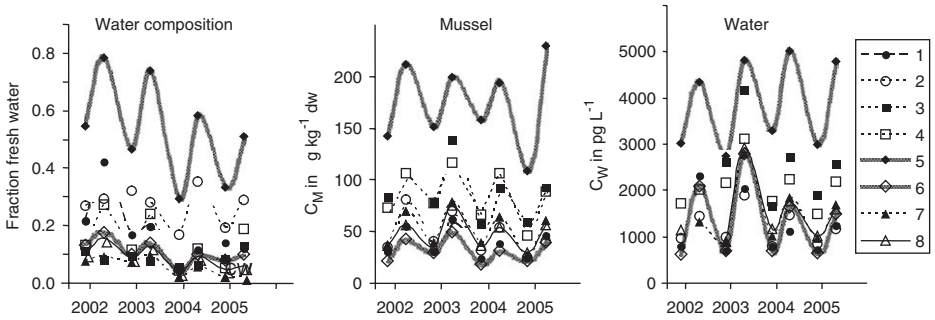

Fig. 19.7. Seasonal variability of freshwater fraction and pyrene concentrations in mussel ($\mu g\,kg^{-1}$) and water ($pg\,L^{-1}$). Freshwater fraction is calculated as (1−salinity/34). Data points are connected by lines to make profiles more clearly visible but do not necessarily represent the concentration between sampling.

phenanthrene where the relative range for C_W is over three times larger than that of the equivalent range for mussels. Over the set of compounds investigated there is a strong decrease in freely dissolved concentration as hydrophobicity increases.

A simple comparison of mussel and water phase concentrations illustrated in Fig. 19.7 shows that the seasonal variation observed for pyrene in the water phase also occurs in mussels. A first glance suggests that the seasonal profile is related to the salinity, i.e., the freshwater fraction. However, the variation also occurs where there is little variation in salinity. Note that it is not a log scale and that the relative abundance for lower concentrations is of the same order of magnitude as the higher concentrations. A profile similar to that observed for salinity is seen for temperature across all stations. Furthermore the sampling rate tends to have, with some scatter, a similar profile. However, the sampling rate would not affect the pyrene concentration as pyrene almost reached equilibrium for all stations except station 6. In this work no corrections were made for temperature. A correction would imply that a higher K_{SW} should apply at lower temperature, leading to lower concentrations in the aqueous phase for winter periods and would indeed flatten the profile.

19.5.2 Equilibrium or uptake phase

Passive sampling monitoring was introduced to measure the pollution as experienced by organisms, in this case mussels. The reasoning was that it would be possible to predict uptake by or concentrations in

mussels (C_M) from PS data. Passive sampling results are expressed as freely dissolved aqueous phase concentrations; the driving force for uptake by mussels. On this basis just as PS does not reach equilibrium for the more hydrophobic compounds it is also possible that the mussels are still in the uptake phase for these compounds when sampled after 6 weeks. Though equilibrium is more likely than for PS since when the mussels are in good shape, they actively pump water over the respiratory surface, and also take up pollutants through the food [11]. Moreover mussels do not start from zero concentration but already contain contaminants at the start of deployment. A factor that works against the achievement of equilibrium is the growth of mussels during deployment. In order to assess contaminant levels in mussel in relation to PS results it is important to know whether the mussel was in the uptake phase or whether approached equilibrium or steady state. When both mussels and samplers are in the uptake phase this would mean that the uptake of mussels may be related to the uptake of the PS. Where equilibrium is achieved the final concentration is a function of the concentration in the water phase. To explore this, the uptake by mussels is plotted versus the uptake of the PS for the winter and autumn samplings of 2003 (left-hand graphs in Fig. 19.8). These samplings were selected because of the large variation in growth and include a situation with only 28% survival. A non-equilibrium situation will be more prominently visible for hydrophobic compounds and therefore CB 153 was selected for illustration. For the PS this compound is far from equilibrium and clearly still in the linear uptake phase. The measured (uncorrected) PS concentrations were used as a measure of the PS uptake. The uptake for mussels is calculated as the difference between the final concentrations minus the start concentration, i.e., the concentration the mussel would have had without uptake but corrected for growth. This is essentially a measure for the difference in body burden before and after exposure. In the graphs the bubble size represents the growth factor in relation to the initial size which is also indicated. The left-graphs of Fig. 19.8 shows that the amount taken up by the mussels correlates well with uptake by the PS, with the exception of station 5. For this station only 28% of the mussels survived and the remaining mussels had lost 25% weight. In this condition the uptake is limited. However, in the right-hand graph the same sample fits well when C_M is plotted versus the C_W. Another observation in the left graph is that there is a slight tendency for mussels that grow strongly to also have a higher than average uptake; especially visible in autumn data. This, however, does not lead to larger concentrations as

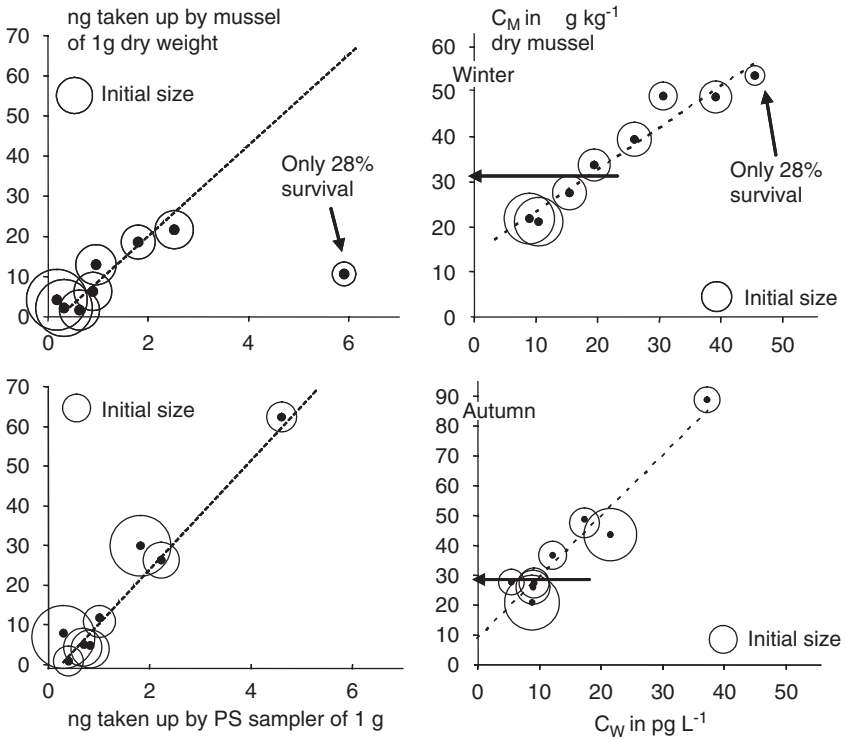

Fig. 19.8. Uptake of CB 153 by mussel in addition to the start body burden plotted versus the uptake of PS (left-hand graph). The bubble diameter indicates the growth compared with the initial size. Concentration of CB 153 (C_M) in mussel versus the concentration in the water phase (C_W) estimated from PS (right-hand graph). The arrows in the right-hand graph indicate the concentration of CB 153 at the start of the exposure. The upper graphs show winter 2003 data and the lower those from autumn 2003.

shown in the right-hand graphs where they appear on the low side of the line. Nevertheless, the results are encouraging, especially when considering that they are from living material that had grown by a factor 2 and still not become outliers.

Further it is notable that relations for the absolute uptake graphs go through the origin while for the relation between C_W and C_M a positive intercept is present. In equilibrium the slope of such a line equals the bioaccumulation factor (BAF) and should go through the origin. Examining all the data the following observations were made:

- the intercepts were higher for more hydrophobic compounds;
- in winter higher intercepts occur than in autumn;

- initial concentrations were generally higher in winter than in autumn;
- although concentrations fell from the starting level (the arrow in Fig. 19.8 indicates the initial concentration), in only a few cases was an actual loss of compounds observed.

The above observations apply especially to CBs ranging from CB 52 and higher. The most logical conclusion is that for highly hydrophobic contaminants an intercept coincides with the initial concentration and indicates that mussels seem to have limited capabilities to eliminate those compounds and actually may not be in full equilibrium with the surroundings. Elimination does occur because when animals grow by a factor of 2, contaminants will also be taken up with the food and so when the body burden remains roughly constant this implies that mussels do eliminate contaminants. It is likely that uptake is from both food and by diffusion from the water whilst elimination (in the absence of significant metabolism) is mainly through exchange with the water phase, and this is a slow process for more hydrophobic contaminants [11]. Since food for the mussel will have a pollution level representative of the environment that is monitored it is possible that equilibrium is attained faster when only uptake is involved; i.e., in the more polluted areas.

For PAHs such a data analysis is not possible. The lower PAHs are no longer in the uptake phase in PS and a comparison of PS uptake and mussel uptake is not informative. Higher PAHs are quite scattered and show both positive and negative intercepts and a poorer correlation. For PAHs the compounds and stations seem to behave in a more independent manner.

This evaluation shows that:

- clear relations exist between the PS and mussel concentrations;
- the issue of whether equilibrium is attained for the mussels or not is very complex;
- growth did not result in outlying results.

For assessment of the mussel data the concentration in mussels is a better parameter than the uptake during deployment. A strong indication that equilibrium is obtained or approached is found in the observation that for about the same C_W similar concentrations in the mussel occur for stations with a large growth compared with stations where only limited growth took place. This was valid even for most hydrophobic compounds. This statement applies when uptake is

required to reach an equilibrium situation. In cases where elimination would be required to obtain equilibrium no concise conclusion can be drawn from these data. Literature observations indicate that equilibrium is usually attained after the 6 weeks deployment period that is used routinely [11,22]. Offloading experiments showed half-life times for lower PAHs up to pyrene of only a few days [23].

19.5.3 BAF values

For hydrophobic contaminants freely dissolved concentrations in the water phase act as an indicator of the contamination level in the environment [24] and the concentrations found in mussels are considered to be related to C_W. Such a relationship is represented by the BAF. The BAF is the ratio between C_M and C_W, and is analogous to the K_{SW} for PSs. However, where K_{OW} and K_{SW} are thermodynamic properties, i.e., have a constant value the BAF is obviously dependent on the species and possibly environmental variables like growth, reproductive status, food availability and pollution. In addition to temporal and spatial differences the variables temperature, salinity and growth were measured. Temperature variability is sufficiently reflected by the season and the extent of variation in salinity (station 5) was also associated with the season. In Fig. 19.9 C_M is plotted versus C_W for benzo(a)pyrene and CB 52 to illustrate the observed variability. For benzo(a)pyrene the data are identified per station and it is clear that data from within one

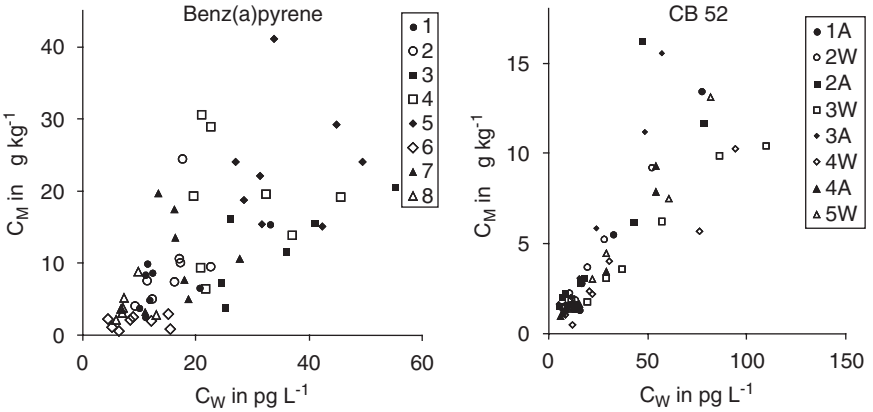

Fig. 19.9. Relationship between C_M and C_W for benzo(a)pyrene marked according to station (left). The right graph shows the same for CB 52 but symbols identify the sampling event. In the legend the number is the year after 2000 and the letter the season (A is autumn, W is winter).

station are rather wide spread, for both more polluted stations as well as those with lower concentrations. Concentrations in mussels do not always give a good reflection of concentrations in the water phase, and this is especially marked in station 6. For CB 52 (right-hand graph in Fig. 19.9) the relationship is clearer. In terms of concentration the stations are equally spread as for benzo(a)pyrene, and so the data points were marked by sampling event. There is better relationship between C_M and C_W compared with that observed for benzo(a)pyrene, especially near the origin. In autumn the C_M values seem a little higher than those in winter periods. An examination of the regression parameters revealed in general that where they were based on data for all stations for a single sampling period very good correlations were observed between the concentrations of a pollutant in mussels and the concentration in the water. For some PAHs, an R^2 in the range of 0.70–0.95 was observed with the exceptions of anthracene, chrysene, and of low values for higher PAHs. The correlations were always better in autumn samplings. For CBs an R^2 of 0.95 was very common and the decrease in this for winter samplings was less than observed for PAHs. Investigating the correlations within a single station for all sampling periods generally shows no or little correlation. This is due to there being only a narrow range of concentrations and any correlation is overwhelmed by the larger seasonal variation in uptake by the mussels. A remarkable exception was fluoranthene. Within one station good correlations were found between the concentrations of fluoranthene in mussels and that in water over time, including samples in autumn and winter, with an average R^2 for eight stations of 0.82. However, the data within one sampling were usually very scattered.

To give equal importance to situations with lower and higher concentrations all BAF values were calculated by the ratio of C_M to C_W. BAF values were averaged for all data and for each station for autumn and winter separately, excluding data below DL.

19.5.3.1 Variability for station and season

In Fig. 19.10, BAF values are plotted for all stations for a number of compounds. The profile of fluoranthene clearly indicates that BAF values are different for the separate stations, whereas for pyrene there is relatively less variation between stations both in autumn and in winter, with the exception of station 6 where the level is lower in winter. The BAF values for benzo(a)pyrene are markedly higher in winter than in autumn for all stations. This large variability is typical for most of the PAHs, including anthracene. Excluding fluoranthene and pyrene, BAF

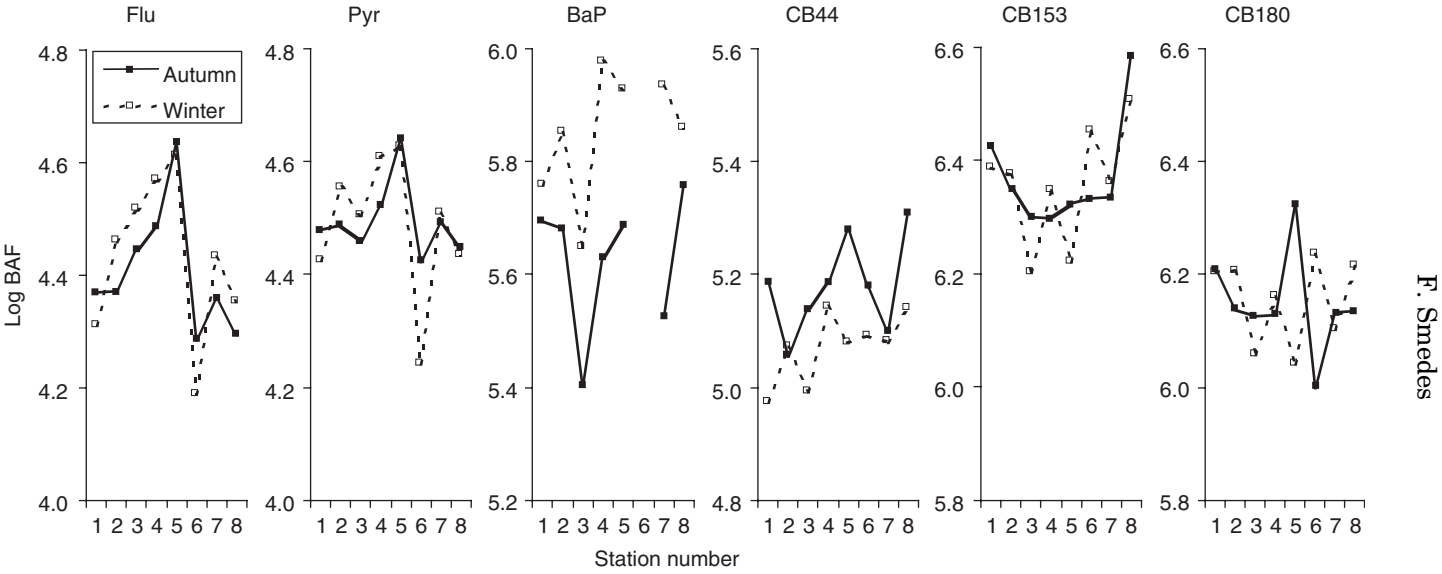

Fig. 19.10. Relation of log BAF for a range of pollutants with station for autumn and winter sampling periods. The lines connecting data points have no meaning other than visual convenience.

values for PAHs were all found higher in winter than in autumn with a an average difference of 0.2 log units (60%). The average within-station standard deviations of the BAF for PAHs were 0.13 and 0.18 for autumn and winter, respectively.

Average BAF values of CB 44 for all stations were 0.1 log units (25%) lower in winter than in autumn. This is also the case for CB 52. For higher CBs the difference slowly declines with increasing molecular size to become negligible around CB 118. The higher CBs show little variation with only station 8 slightly standing out. This is the only station where release of, e.g., CB 153 from mussels is observed and the station has the lowest C_W values for CB 153. It is possible that C_W is even lower than in the area from which the mussels originated. Since release is slow the mussels may still not have reached the lower equilibrium concentration than belongs to that station. The average within-station standard deviations of the BAF values for CBs were 0.11 and 0.09 for autumn and winter, respectively, quite lower variation than observed for PAHs.

19.5.3.2 Variability over time

Following the above analysis of the data for the separate seasons and stations, the average BAF values based on all stations combined were investigated for the same set of compounds, and the data are shown in Fig. 19.11. For both fluoranthene and pyrene, although the BAFs vary markedly between stations, the average across all stations varies little between both seasons year on year. For benzo(a)pyrene and the CBs there is a marked variation visible in Fig. 19.11, which cannot be linked

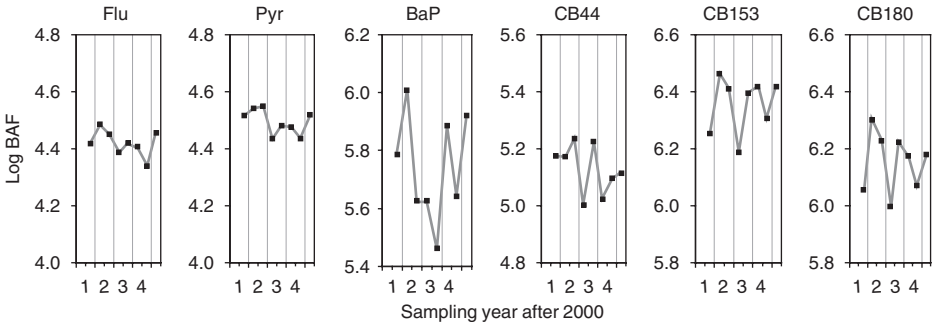

Fig. 19.11. Average log BAF through seasons for a range of organic pollutants. The *x*-axis denotes the year after 2000. Lines connecting data points have limited meaning as no samples were taken in spring and summer. (See Glossary for full compound names.)

to season and there are no visible trends. Although around winter 2003 there is a minimum that coincides for all three CBs, the overall variation is likely to be considered as natural variability.

19.5.3.3 Average BAF values

In spite of differences between stations and between seasons overall average BAF values and associated standard deviations were calculated, excluding values below two times the detection limit. The data are listed in Table 19.4. The highest standard deviations coincide with compounds (e.g., anthracene, indeno(1,2,3-cd)pyrene, CB 18 and CB 31) that are mainly present in concentrations close to the DL, i.e., of which the 90% percentile was only five times the DL.

The uptake into mussels is by a partition process and the BAF is therefore expected to be related to the K_{OW}. In the right-hand graph of Fig. 19.12 all the obtained log BAF values are plotted versus the log K_{OW}. In the left-hand graph of Fig. 19.12 the relationship between the average log BAF and the log K_{OW} (data listed in Table 19.4) is plotted. Three compounds were not included in the regression. Anthracene was excluded since there was no correlation between C_M and C_W, and a negative slope was observed. Furthermore two of the higher CBs, 170 and 180 were outliers. It is known that higher CBs often show a lower uptake than can be explained by the K_{OW}. It has been suggested that

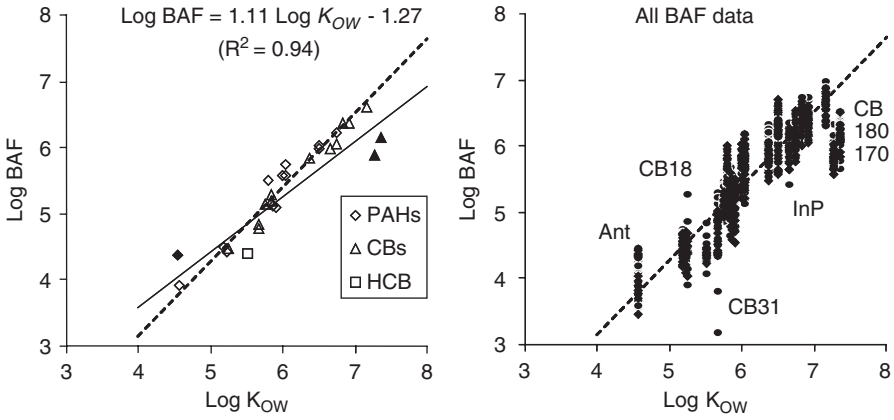

Fig. 19.12. Relationship of BAF with K_{OW} values. In the right graph the average for each compound is plotted versus the K_{OW}. The relationship of the regression (dotted line) is given above in the graph. Filled symbols were not used in regression. The solid line is the relationship given by Booij *et al*. [25] recalculated to dry weight. The left graph is similar to the right but contains all data above DL. (See Glossary for full compound names.)

the size hinders passage through the membrane. However, it is not clear why CB 187 does not show a similar deviation.

No statistically significant differences were found between slopes or intercepts for PAHs and CBs when calculated separately for autumn or winter data. The differences in BAF values between autumn and winter discussed earlier do not have a significant effect on slope and intercept. The natural variation of the data as shown in the right-hand graph of Fig. 19.12 highlights the fact that small differences will not be statistically significant. In the graph some outliers are identified. The deviations of indeno(1,2,3-cd)pyrene and CB 18 probably result from analytical variability and that of CB 31 from chromatographic co-elution with an unknown compound.

The average concentration of lipid in the mussels was 81 mg kg^{-1} and showed little variation ($\pm 11\%$). As a consequence the uncorrected and the lipid-based BAF values showed exactly the same slope with the K_{OW}. Only the intercept increased from -1.27 to -0.30. Similarly, expressing C_M in terms of wet weight will affect only the intercept, and results in a decrease to -2.14.

The observed relationship was compared with the common slope and intercept from different studies in literature as combined by Booij *et al.* [25]. This average relationship became after recalculation to dry weight:

$$\log \mathrm{BAF}_{dw} = 0.840 \log K_{OW} + 0.2 \qquad (19.11)$$

This relation is shown as a solid line in Fig. 19.12. For compounds with lower K_{OW} values there is agreement between the observed and average literature BAF values but for those with higher K_{OW} the BAF values were higher by up to a half order of magnitude. Given the variation in literature data the present results would fall in the upper range but not really be outliers. For example the obtained slope and intercept for lipid-based log BAF were in close agreement with Hofelt and Shea [26]. BAF reported in literature are generally based on classical methods to determine the concentration in the water phase and this may easily lead to an overestimation of the freely dissolved concentration in the water phase due to the presence of particulate and dissolved organic carbon [16]. In this data set the C_W is derived from PS data that moves the uncertainty of the BAF to the K_{SW} and the R_S. For this work the determination of the K_{SW} is much less sensitive to overestimation of aqueous-phase concentrations (see Section 19.3.5) and the K_{SW} is generally higher than reported in the literature for similar materials. This higher K_{SW} values lead to higher calculated sampling rates (R_S) and consequently lower C_W, particularly for the more hydrophobic

compounds that are in the linear uptake phase, so the C_W depends entirely on the estimated sampling rate. This may explain why BAF values from compounds that generally reach equilibrium have closer agreement with average literature values.

19.6 USEFULNESS OF PS IN MONITORING

The ultimate aim of passive sampling is to obtain a measure of the level of pollution that gives a representative measure of the exposure of organisms. In order to demonstrate the capabilities of PS for that purpose the calculated BAF values were used to estimate the expected concentration in the mussel (C_{M-W}). However, in fact that is only a comparison with C_W that has been recalculated to give the concentration in the mussels. One effect of this is that the values to be compared have the same units (μg kg^{-1}). This is illustrated in Fig. 19.13 for a number of compounds where the time-averaged C_M and the calculated C_{M-W} are plotted for the different stations. The overall results agree quite well,

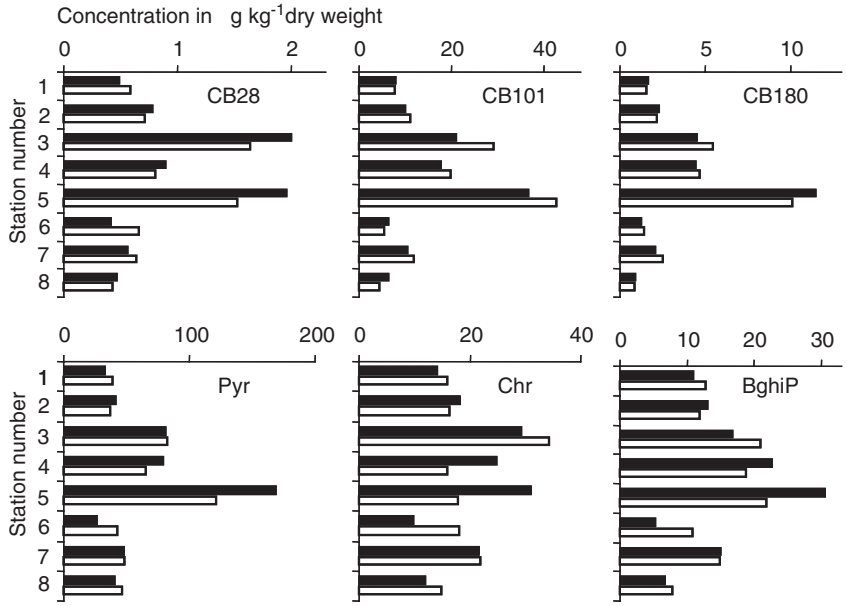

Fig. 19.13. Comparison of measured and calculated concentrations in mussels for all stations and a range of organic pollutants. Black bars are average concentrations measured in mussels and open bars represent the average concentrations calculated from C_W and BAF values. (See Glossary for full compound names.)

but better for CBs than for PAHs. The latter tend to behave individually and vary between stations and between seasons. For example at station 6 the mussels always showed lower concentrations of PAHs than calculated, and this is likely to be a result of the very high biological activity with consequently more potential for metabolism. Separating the seasons the PAHs show better agreement in autumn samplings where mussels commonly were more active. Furthermore, for compounds that achieved equilibrium changes in mussel concentrations were often very closely followed by the PS throughout the seasons.

Also the patterns for the different compounds are in good agreement with those found in the PS. The spatial distribution is similar to that observed in the CBs. For example at station 3 there is a dependence on the pattern of the outflow of the Rhine/Meuse that resulted in an enhanced presence of lower CBs (Fig. 19.13). This is observed in both mussels and PS.

It is notable that the concentration of pyrene is elevated at station 5 while chrysene is more evenly distributed. These differences in pattern are sometimes very distinct and allow the identification of sources of pollution. The ratio between pyrene and fluoranthene is very high (2.2) at station 5 indicating changes to the pattern introduced by the Scheldt River. Further down stream the ratio reduces to about 1.0 for station 4. At station 3 that is influenced by the Rhine/Meuse River outflow a similar value was found. At stations like 6 and 7 without direct flow from the rivers, the pyrene is even lower than fluoranthene and the ratio becomes 0.4. Ratios for other stations are in the range between 0.4 and 1. These ratios are strikingly similar in both mussels and PS. When the two sets of ratios are as close as this it indicates that the residual differences between concentrations in mussels and PS are probably not caused by sampling and measuring variability of the passive sampling process, but are more likely to be a consequence of variations in the behaviour of the mussels due to changing environmental conditions such as availability of food, temperature and salinity. This is in spite of the uncertainty that is inseparably connected with the estimates of sampling rate.

Finally, the following conclusions can be drawn from the monitoring reported here:

- the programme provided a very useful learning experience, and a foundation for future work;
- close relationships between concentrations found in mussels and those derived from passive sampling confirm the environmental relevance of passive sampling;

- not only were the differences in pollution level reflected by the two methods but seasonal variations were often followed in the same way by both mussels and PS;
- PS and mussels show the same detailed changes in the ratios of the various compounds.

Passive sampling may be an even better tool for measuring bioavailability than the mussels themselves. As discussed earlier (Section 19.2.3) in PS there is no initial concentration (as confirmed by construction and field blanks), no metabolism and no mortality and these are all valid reasons for using passive sampling. In addition there is still a degree of uncertainty associated with the achievement of equilibrium, especially for the more hydrophobic compounds. One solution would be the inclusion of PRCs in mussels if it were not unethical. In PS the PRCs essentially give information on the equilibrium level. More accurate determination of the sampling rates over a wider K_{OW} range could further improve the accuracy of results obtained using passive sampling.

GLOSSARY: Compounds short and full names

Short	:	**Name**
Ant	:	Anthracene
Ant-D10	:	D10-Anthracene
BaA	:	Benz(a)anthracene
BaP	:	Benzo(a)pyrene
BbF	:	Benz(b)fluoranthene
BeP	:	Benz(e)pyrene
BghiP	:	Benz(ghi)perylene
BkF	:	Benz(k)fluoranthene
CB 101	:	CB 101
CB 105	:	CB 105
CB 118	:	CB 118
CB 138	:	CB 138
CB 153	:	CB 153
CB 155	:	CB 155
CB 156	:	CB 156
CB 170	:	CB 170
CB 18	:	CB 18
CB 180	:	CB 180
CB 187	:	CB 187

CB 204 : CB 204
CB 28 : CB 28
CB 29 : CB 29
CB 31 : CB 31
CB 4 : CB 4
CB 44 : CB 44
CB 49 : CB 49
CB 52 : CB 52
Chr : Chrysene
Chr-D12 : D12-Chrysene
Cor-D12 : D12-Coronene
DBahA : Dibenz(ah)anthracene
Flu : Fluoranthene
Flu-D10 : D10-Fluoranthene
HCB : Hexachlorobenzene
Ind : Indeno(1,2,-c,d)pyrene
Pe-D12 : D12-Perylene
Phen : Phenanthrene
Pyr : Pyrene
Pyr-D10 : D10-Pyrene

REFERENCES

1 J.N. Huckins, M.W. Tubergen and G.K. Manuweera, *Chemosphere*, 20 (1990) 533.
2 H.F. Prest, W.M. Jarman, S.A. Burns, T. Weismüller, M. Martin and J.N. Huckins, *Chemoshere*, 25 (1992) 1811.
3 J.N. Huckins, G.K. Manuweera, J.D. Petty, D. Mackay and J.A. Lebo, *Environ. Sci. Technol.*, 27 (1993) 2489.
4 K. Booij, H.M. Sleiderink and F. Smedes, *Environ. Toxicol. Chem.*, 17 (1998) 1236.
5 J.N. Huckins, J.D. Petty, J.A. Lebo, F.V. Almeida, K. Booij, D.A. Alvarez, W.L. Cranor, R.C. Clark and B.B. Mogënsen, *Environ. Sci. Technol.*, 36 (2002) 85.
6 A. Rantalainen, W.J. Cretney and M.G. Ikonomou, *Chemosphere*, 40 (2000) 147.
7 J.N. Huckins, J.D. Petty, H.F. Prest, R.C. Clark, D.A. Alvarez, C.E. Orazio, J.A. Lebo, W.L. Cranor and B.T. Johnson, *A Guide for the Use of Semipermeable Membrane Devices (SPMDs) as Samplers of Waterborne Hydrophobic Organic Contaminants*. API publication 4690. American Petroleum Institute, Washington, DC, 2002.
8 C.L. Arthur and J. Pawliszyn, *Anal. Chem.*, 62 (1990) 2145.

9 E. Baltussen, P. Sandra, F. David and C. Cramers, *J. Microcolumn Sep.*, 11 (1999) 737.
10 A.C. Belfroid, W. Lise and G.J. Stromberg, *Interpretation of Musselwatch Results*. Report Nr. O-00/20, IVM/VU Boelelaan 1115, 1081 HV, Amsterdam, 2000.
11 M. Björk and M. Gilek, *Aquat. Toxicol.*, 38 (1997) 101.
12 J.K. Kingston, R. Greenwood, G.A. Mills, G.M. Morrison and L.B. Persson, *J. Environ. Monit.*, 5 (2000) 487.
13 H.M. Paterson, G.B. Davis and P. Grathwohl, *Environ. Sci. Technol.*, 37 (2003) 1360.
14 K. Booij, H.E. Hofmans, C.V. Fischer and E.M. Van Weerlee, *Environ. Sci. Technol.*, 37 (2003) 361.
15 F. Smedes, *Int. J. Environ. Anal. Chem.*, 57 (1994) 215.
16 J.H. Hermans, F. Smedes, J.W. Hofstraat and W.P. Cofino, *Environ. Sci. Technol.*, 26 (1992) 2028.
17 F. Smedes and J. de Boer, *Trends Anal. Chem.*, 16 (1997) 503.
18 K. Booij, F. Smedes and H.M. Sleiderink, *Chemosphere*, 46 (2002) 1157.
19 W.J.M. Hegeman, C.H. Van Der Weijden and J.P.G. Loch, *Environ. Sci. Technol.*, 29 (1995) 363.
20 M.T.O. Jonker and F. Smedes, *Environ. Sci. Technol.*, 34 (2000) 1620.
21 K. Booij, E.M. van Weerlee, C.V. Fischer and J. Hoedemaker, NIOZ report 2000-5, NIOZ, PO Box 59, 1790 AB, Den Burg, Texel, The Netherlands.
22 C.S. Peven, A.D. Uhler and F.J. Querzoli, *Environ. Toxicol. Chem.*, 15 (1996) 144.
23 P. Rantamäki, *Chemosphere*, 35 (1997) 487.
24 P. Mayer, J. Tolls, J.L.M. Hermens and D. Mackay, *Environ. Sci. Techol.*, 37 (2003) 184A.
25 K. Booij, F. Smedes, E.M. Van Weerlee and P.J.C. Honkoop, *Environ. Sci. Technol.*, 40 (2006) 3893.
26 C.S. Hofelt and D. Shea, *Environ. Sci. Technol.*, 31 (1997) 154.

Subject Index